Copper and bloomery iron smelting in Central China

Technological traditions in the Daye County (Hubei)

David Larreina-García

Thesis submitted to

University College London

for the Degree of

Doctor of Philosophy (PhD)

UCL Institute of Archaeology

January 2017

I, David Larreina-García, confirm that the work presented in this thesis is my own. Where information has been derived from other sources, I confirm that this has been indicated in the thesis.

Date: 5 January 2017

Signature:

Abstract

This project investigates the copper and iron producing industries of Daye County, a substantial mining and smelting area in the Hubei Province (China) with activities well documented from the early 1st millennium BC. In particular, this study aims to characterise the engineering parameters of the primary smelting of copper and bloomery iron at eight metal production sites located in the proximity of the prominent ancient mine of Tonglushan, in an area of ~1300 km^2.

The thesis is focused on the materials science analyses of surface collected technical material such as slags, furnace remains, and ores of eight archaeological sites located in close proximity of each other in the Daye County. The methods include optical microscopy, scanning electron microscopy coupled with energy dispersive X-ray spectroscopy (SEM-EDS), and wavelength dispersive X-ray fluorescence (WD-XRF), to characterise their microstructure, mineralogy and chemical composition.

The copper-smelting technologies reconstructed here – broadly framed in the Western Zhou period by ceramic typology – seemingly correspond to modest size workshops, thus different from the large scale production centres involving numerous workers, resources and infrastructures typically described in the literature. Moreover, and exceptionally for most of Eurasia, extensive evidence of large-scale production of bloomery iron at the core of the Chinese Empire is documented, with radiocarbon dates placing the activity in the 18th century AD, thus in the Qing Dynasty and over 2000 years after the production of copper. This finding challenges traditional generalisations whereby bloomery iron smelting is widely deemed to be a rarity in China, due to the early development of the blast furnaces; when identified, bloomeries are usually presented as isolated examples of limited scale, mostly in marginal areas to the Central Plains.

The reconstruction of the various smelting processes in a relatively small region illustrates different technological adaptations to natural resources and socio-technological contexts, which are discussed using conceptual frameworks of *technological choices* and *regionalism.*

Table of contents

List of Figures

List of Tables

Acknowledgements

There are many people I would like to thank for the support and help through this research, in the time spent in (and out) the field, in the lab, and in reading and writing.

In the academic part, I'm more than obliged to Marcos Martinón-Torres and Thilo Rehren – principal and secondary supervisor of this thesis – for their support, stimuli and confidence in this project. I cannot imagine better Professors to learn from. They offered me the drug of archaeological sciences in the year of MSc 2008/9 that ended in the fantastic experience of researching Chinese archaeometallurgy during two years in Beijing. There I met the other academic pillar of this thesis: Professor Yanxiang Li from the Institute of Historical Metallurgy and Materials, University of Science and Technology Beijing (USTB 北京科技大学) who accepted the challenge of taking me as student; enable the fieldwork and trusted a wonderful collection within my hands. The other person from the Beijing team I need to thank specially is Kunlong Cheng, who guided me throughout the Chinese culture and gave me uncountable useful advices during all these years of friendship. Equally grateful to Jianxi Li for his help in the laboratory and in the library.

Still in China, many thanks to all the members of the archaeological group of Daye city and Tonglüshan Ancient Metallurgy Museum, especially to Professor Chen Shuxiang and Dr. Qu Yi, for hosting and guiding me throughout both archaeological sites and severe intoxications with the local spirits.

The Institute for Archaeo-Metallurgical Studies (IAMS), and the Rio Tinto Group are acknowledged for providing the financial support necessary to carry on this research.

Thanks to John Moffett, in Cambridge, for welcoming me at the Needham Institute Library to explore the potential of the 'old' papers.

Back to London, I want to recognise the support staff at the institute. In particular to Keevin Reeves at the SEM-lab; Harriet White at the sample preparation lab; Philip Austin for analysing the charcoal samples; and George Davies, the building manager, because it feels very good to be greeted everyday with such positive energy. Special thanks to

Tom Gregory, technician at the SEM-lab, who did much more than assisting with instruments, but he is also the foundational stone of our morning ‘coffee club’. The 20 minutes tasting the excellent coffee of Mounia – the only decent coffee that you can find in London – sharing conversation and laughs with the original members Charlie Bashore, Mike Charlton, Peter Schauer, and lately also with Philip Riris, boosted me with energy for the rest of the day, and made the work much easier. Many thanks to Mike Charlton in particular for his extraordinary enthusiasm, kindness and suggestions.

Million thanks to all the “basement people”. In particular to Jonathan Woods, Loic Boscher, Anastasya Cholakova, Hanna Page, Hayley Simons, Carlotta Farci, Nohora Bustamante, Yaxiong Liu, Ana Franjick, Umberto Veronessi, Marianne Hem Eriksen, Lente Van Brempt, Katharina Smith, Matt Phelps, Yi-Ting Hsu and Carlotta Gardner.

A special mention must be made here for Mainardo Gaudenzi Asinelli, Teresa Plaza, Pira Venunan and Frederick Rademakers for their friendship, the lunch time conversations, and the endless discussions about metallurgy and analytical techniques, which frequently ended in coffees, pints and dinners.

There are two people that I do not know how to thank them enough, but I do know that I would not have finished this thesis without them. These are Siran Liu and Agnese Benzonelli. We shared much happiness, but also frustration and hard moments which is when human quality is really appreciated, and they were always there for me, never failed. I'm truly grateful to share such a solid friendship with so extraordinary people.

Next part is for my colleagues at the University of Basque Country (UPV-EHU) in Vitoria. Especially to Pedro Lobo, Andoni Tarriño, Ana Polo, Luis Eguiluz and Javier Fernández Eraso because they introduced me first in the archaeological world and walked with me the first steps into archaeometry.

Finally, I cannot forget my parents and brothers since they offered me unconditional support that never went down. They understood that archaeology, to learn and to research is so important to me, and they not only respect it but encouraged me in the pursuit even if this implied to stay out of home for eight years now, between Scotland, London and Beijing.

The lovely metal is used for casting of swords and pikes; it is used in company of dogs and horses (for profitless hunting). The ugly metal is used for casting of hoes which flatten (weeds) and axes which fell (trees); it is used upon the fruitful earth.

(Dialogue between the philosopher Guan Zhong and the Duke Huan of Qin, 7th century BC)

1 Introduction

1.1 The significance of metals in China

Scholars and the public alike have a long-standing fascination with the singularities of early Chinese metallurgy, as exemplified in the conspicuous bronze ritual vessels (Figure 1.1) or the remarkable fact that China produced cast iron more than two millennia earlier than the rest of the world. As a matter of fact, metal has for a long time been a vital ingredient of the Chinese identity (Ko 2000). As proof of how intrinsically engrained metal is in its technological history, trade, art and symbolic behaviour, suffice to remember that the first political state in China, the Xia Dynasty (2070-1600 BC) and the succeeding ones (Shang and Zhou, 1600-256 BC, see Appendix I) obtained legitimacy to rule the country by means of the possession of nine large bronze tripod cauldrons; these came to symbolise the power and authority of the ruling dynasty, with strict regulations imposed as to their use (Fong 1980). The secular capitals moved constantly as part of the search for copper and tin, and bronze naturally became associated with sovereignty, rulership and even testimony of Heaven's Mandate for the royal house (Wang, A. 2000). The individual states during the Warring States period (476-221 BC) had administrative entities to manage bronze production, and it is supposed that a similar involvement by the administration existed during the previous periods (Chang 1983; Liu, L. & Chen 2001; Wagner 2001a, 4). The symbolic power of metal was perpetuated over the centuries: still during the Tang Dynasty (618-906 AD) the most important attributes of the lifestyle of the aristocracy were made of metal, with the singularity that there is virtually no association of precious metals – silver and gold – with the elite (Marshak 2004), since wealth, prosperity and cultural traditions were reflected in the use of bronze – the *lovely* metal – and jade.

Figure 1.1: *You* bronze vessel with a phoenix from the Western Zhou period (9th century BC).
Cast in one piece, 37 cm high and 4.3 kg weight. From Li, C. et al. (2004, Fig. 48).

As a result of this strong association – *'*bronze was political power*'* (Chang 1980a) –, this copper alloy was employed for very specific objects, such as ritual vessels or musical instruments, normally aimed to be exhibited (Chengyuan 1980; Linduff 2000; Sun, S. & Han 2000; Wang, Q. 2002; Lu & Yan 2005). Conversely, agricultural implements and tools were made of the *ugly* metal (Taylor & Shell 1988, 207), with iron utensils becoming indispensable for every aspect of daily life and productive activities (Wang, Z. 1982), (Figure 1.2).

Iron filled the utilitarian gap left by the 'luxury' bronze, covering a large range of implements and tools: ploughs, scissors, spades, sickles, knives, chisels, cooking pots, etc., and ultimately steel weapons; even constructions – statues, pagodas, bridges, etc. – made extensive use of iron during late imperial times (Needham 1958; Wagner 2000).

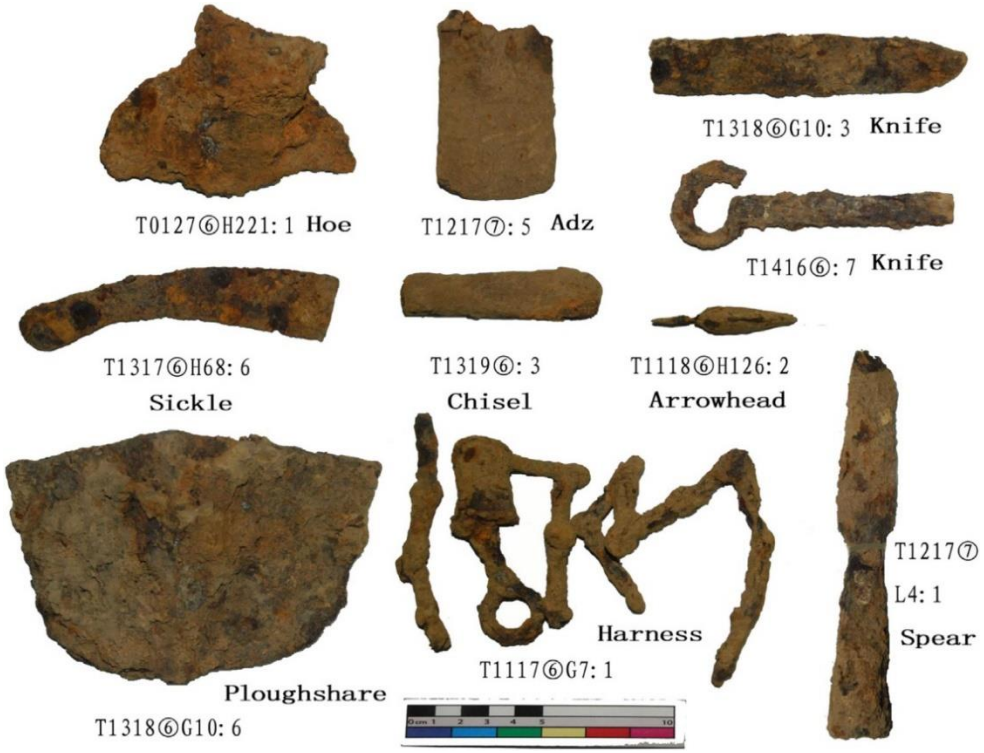

Figure 1.2: Selection of iron objects dating to the Warring States period (476-221 BC) and Western Han Dynasty (206 BC-AD 9).
Unearthed in Dongheisan (Hebei Province). From (Liu, Haifeng et al. 2014a).

Another peculiarity of early Chinese metallurgy is that the transition between the two metals 'was not so much from bronze to iron as from bronze to steel' (Needham 1958, 2). Bloomery iron is known in Central China from the 9th century BC at least (Han 2013), and five centuries earlier in regions to the northwest of the Central Plains (Chen, J. et al. 2012) (Figure 1.6). However, in a relatively short period, China developed blast furnaces capable of producing cast iron (Figure 1.4) – the earliest object, found in the Central Plains, dated to the 8th century BC (Han & Chen 2013). The new technology spread rapidly across the Central Plains and neighbouring areas by the 6th–4th centuries BC (Wagner 2008; Liu, Haifeng et al. 2014a), and virtually displaced completely the production of bloomery iron by the early Han Dynasty (3rd-2nd century BC) (Wagner 1996, 2008). Since then, bloomery iron smelting is widely deemed to have been a rare, residual practice, with only a single bloomery iron production site dated to the Western Han Dynasty (206 BC-9 AD) documented within the extensive territory of China (Huang, Q. 2008; Han & Duan 2009; Huang, Q. & Li 2013). The metallographic study of iron implements reveals a 'clear

dominance of cast and cast iron over forged iron, wrought iron and steel in China' (Taylor & Shell 1988, 215).

Moreover, the technological invention was not limited to the blast furnaces but extended to a series of advanced treatments to convert cast iron into diverse alloys of iron and carbon, creating a broad assortment of steels with different properties that could be adjusted depending on the intended use (Han & Chen 2013). Iron 'became the workhorse metal in China' (Hua 1983, 122), and its production was established from early on (6th-5th centuries BC) as large-scale industrial complexes where the iron ore was reduced, and foundries in which the objects – coins, woks, buckles, ploughs, etc. – were mass-produced by stack-casting in moulds (Hua 1983; Li, J. 1994, 1997) (Figure 1.3). Soon enough – probably by the end of the Warring States and the rise of the Qin Dynasty, the first imperial dynasty (221-206 BC) –, the political administrations were closely involved in the iron factories (Wagner 1999). By the year 117 BC the Han emperor Wudi imposed a monopoly on the salt and iron industries. In order to ensure better control of the production, ironworks were moved (as put by an imperial counsellor in 81 BC) 'from deep mountains and remote marshes' to be concentrated next to the urban centres (Wagner 2001a, 38). The new complexes – so far 45 offices are documented archaeologically – worked as small cities with a population around one thousand people and frequently of several thousands, mostly formed by convict labourers commanded by a whole range of imperial officials of different rank; production was strongly regularised establishing quotas and controls of quality, standardising the end products, specialisation of personnel, etc. From that moment onwards, the production of iron outside the imperial ironworks was forbidden and prosecuted (Wagner 2001a, 2008).

> Anyone who dares privately to cast iron implements or to boil salt should (be sentenced to) wear a fetter on his left foot, and his equipment should be confiscated[1].

The successive dynasties are supposed to have followed similar policies concerning iron production although in general there is a lack of historical references to it – in contrast to

[1] Proposal for a state monopoly on salt and iron presented to the throne in 117 BC by Dongguo Xiangyan （東國咸陽） – great salt boiler – and Kong Jin （孔僅） – great smelter – as recorded by Han historian Sima Qian (Wagner 2001b, 10).

the abundance of bureaucratic documents for the Han Dynasty –, and the archaeological evidence is also far more sparse (Wagner 2001a, 2008). The exception is the Northern Song Dynasty, around 1000 years after the Han, with well-documented large-scale capital intensive production monopolised by the imperial administration, reaching a peak of production of 1.2 kg of iron per capita in the year AD 1078. This figure is equal to England's production in the first phase of the Industrial Revolution at the beginning of the 19th century (Hartwell 1966; Wagner 2008, 35). Another exception may have occurred during the Ming Dynasty, when this large-scale model of production supervised by the state may have existed briefly during the 15th century (Wagner 2005).

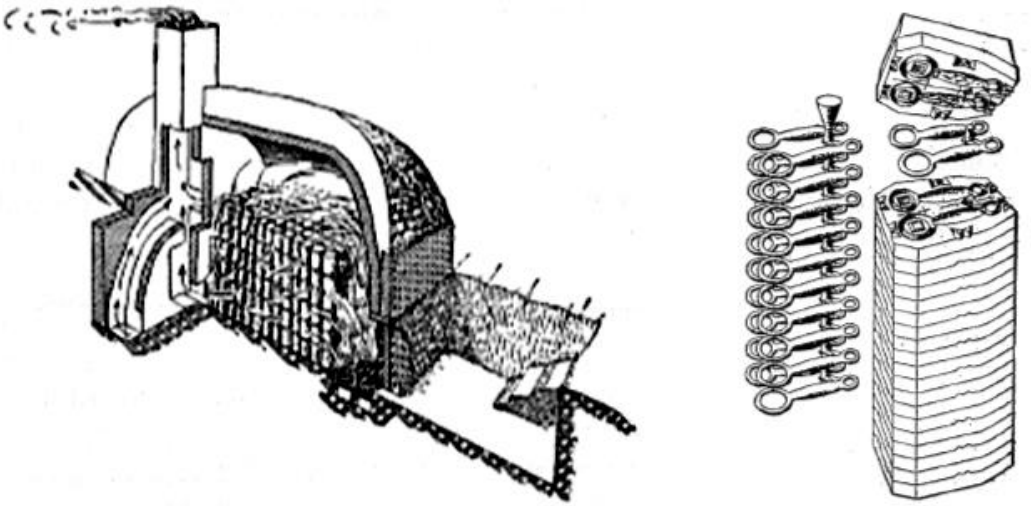

Figure 1.3: Section of a kiln for moulds production and diagram of a stack-mould for 20 horse bits.
From Li, J. (1996, Fig. 29 and Fig. 30).

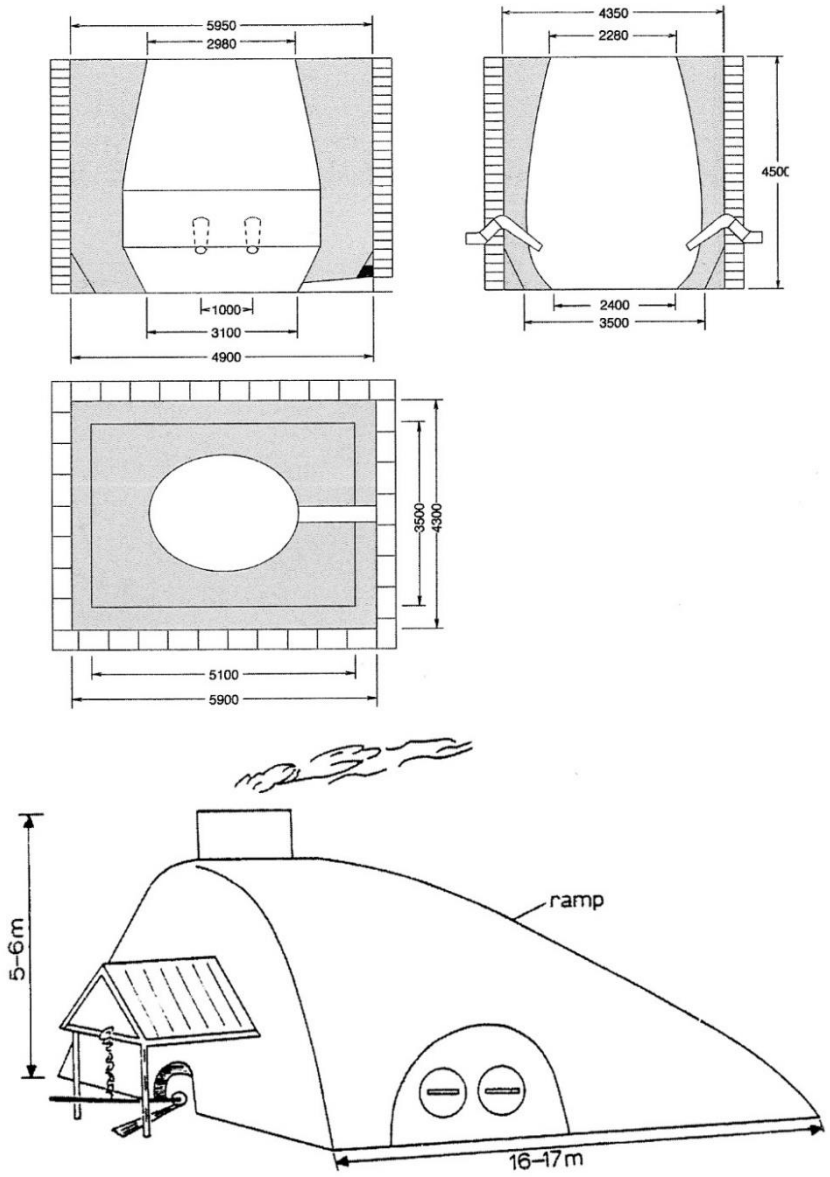

Figure 1.4: Reconstruction of a Han blast furnace at Guxingzhen (Henan province) and sketch of the operation of a Han blast furnace.
Scale (up) is given in cm. After Wagner (2008, Fig.100 and Fig. 101).

1.2 The study of Chinese archaeometallurgy, research gaps

The history of metallurgy in China has experienced a profound revision over the past few decades. Initially the Chinese Bronze Age seemed so unique that it was believed that metallurgists started directly producing tin bronze alloys without native or arsenical copper stages preceding the Bronze Age (Yan 2000). The discussion was focused largely on the origins of Chinese metallurgy, and whether this was the result of diffusion or

indigenous invention, concerning both copper and iron. At some point the debate became 'arguably irrelevant' (Taylor & Shell 1988) since – regardless the pure origins – it became clear that even though Chinese metallurgy shared traits with those observed elsewhere in the world (Muhly 1988), it maintained at least three idiosyncratic characteristics (Han 1998; Linduff 2000; Mei 2004; Chen, J. & Han 2005; Han & Ke 2007; Mei 2009a, 2009b; Han 2013; Linduff & Mei 2014; Mei et al. 2015):

1) The development of the sophisticated piece-mould method to reproduce complex shapes in one single casting (Figure 1.5).
2) The invention of the blast furnace to reduce iron, and a clear preference for cast over bloomery iron, following the bronze casting tradition.
3) The dominant position of the Central Plains (in contact with the Steppe) in the innovation and development of metallurgy, and control of the (large-scale) production by the administration from early times.

The consumption of metals appears to have been always extraordinary in scale, as shown by examples such as the Houmuwu (后母戊), a prehistoric bronze vessel (~1100 BC) that weights 833 kg (Jiang et al. 2011); the quantity of 1000 tonnes of copper necessary per year to produce coins during the reign of the Emperor Xuanzong (唐玄宗, AD 742-756) (Sadao 1986); or the production of 125,000 tonnes of iron annually by the year AD 1078 (Hartwell 1966, 33, this number has been questioned as overestimated by other scholars, e.g. Wright 2007).

Significantly, the above statements as well as most of the studies regarding ancient Chinese metallurgy (e.g. Needham 1958; Needham 1970; Barnard & Tamotsu 1975; Fong 1980; Bagley 1987; Li, X. & Liang 1996; Hua 1996-97; Craddock et al. 2003; Han & Sun 2004; Scott & Ma 2006; Wayman & Michaelson 2006; Han & Li 2009; Liu, S. et al. 2013; Liu, Haifeng et al. 2014a) are largely based on the study of finished objects, and they also rely on historical sources written in very distant periods to the ones described, with very little research done on the underlying primary production of metal, or the *chaîne opératoire* prior to the mould making and casting stage for bronze and cast iron.

Chernykh (2009) notes the 'explosion' of metals during the Shang Dynasty, to point to the same research lacuna: metal plays a crucial role in the whole process of cultural and

ideological development and harmonisation of a Chinese cultural identity, but most research efforts are so far focused on the study of finished objects (Liu, L. & Chen 2001).

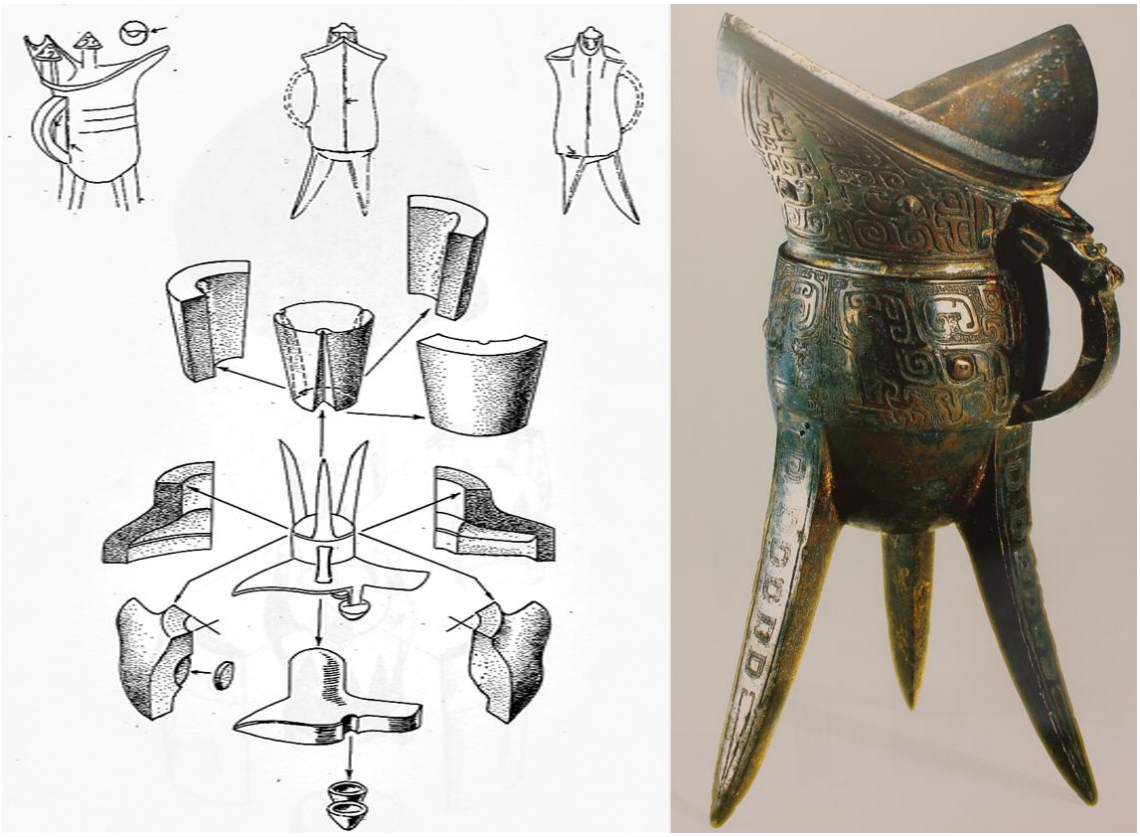

Figure 1.5: Scheme of the piece-mould casting technique and *Jue* for drinking or pouring liquors (1600-1100 BC) produced by this technique.
From Fong (1980, Fig. 4) and Li, C. et al. (2004, Fig. 8).

The case of the bloomery iron study is even in a more deficient situation since, as mentioned above, China is widely accepted as the birthplace and shrine of the blast furnace, with bloomery iron technology largely believed to be scant before the Han Dynasty and abandoned afterwards (Wagner 2008). This accepted paradigm is perpetuated as it is repeated by students and researchers. As a matter of fact, the existence of a bloomery iron production tradition was a surprise discovery when analysing supposed copper slags for the case studies investigated here, but it was subsequently documented in four additional sites.

A further issue with regards to the cultural and technological preponderance of the Central Plains over the rest of China (Linduff 2000) is raised by Gernet (1999, 31),

concerning the common misconception of Chinese history as an homogenous package: in reality, this is a very complex mixture of realities developed within a colossal territory. The uniform model of expansion of a single culture has been recently questioned for the early stages of the Chinese history (2nd millennium BC), and making particular reference to metallurgy (e.g. Chen, K. et al. 2016); nevertheless, this simplified picture of an enormous area without internal notable diversity, united under one political entity, has remained largely unchallenged for Imperial China (221 BC-AD 1912) (Liu, S. 2015, 327).

As an illustrative counterpoint, recent studies on African ferrous metallurgy (Humphris et al. 2009; Humphris 2010) has described the changing nature of iron production and the variable technological approaches that can be observed over the 18th and 19th centuries AD of metallurgical history of the kingdom of Buganda region. How likely is it then that blast furnaces exported from the Central Plains operated in identical conditions for centuries across the vast landscape of different natural resources, climate, changeable borders and political situations that was China? Moreover, the model of large-scale production exclusively controlled by a single entity requires large investment, good transportation, technical knowledge – the Han iron monopoly was directed by iron industrialists – and, perhaps the most important fact, a large and stable market (Wagner 2001a, 14). Such a model can hardly be operative in times of crisis, with contraction of the economy, famine, war, and general instability; this unfavourable scenario occurred repeatedly in all Dynasties (e.g. Huang, R. 1981; Gernet 1999; Benn 2004; Loewe 2006; Rowe 2009). Bloomery smelting, despite being considerably less efficient in terms of iron yield than the blast furnace, is a useful small-scale process which can be economical in many circumstances (Wagner 2001a, 65), and thus the disappearance of the bloomery smelting is 'odd' (Wagner 2001c, 3), even though it might appear to be supported by the absence of archaeological evidence.

As a result of these two complementary approaches – the focus on artistic and art historical aspects of artefact production, and the assumption of a uniform and unalterable model to explain too many realities –, the knowledge of Chinese ancient metallurgy is still in its 'infancy' (Linduff 2000, 3) in terms of primary production of metals, the literature on iron industry is full of 'misunderstandings and contradictions' (Taylor & Shell 1988, 205),

and the technological variability of metallurgical practices across China remains largely undescribed.

Figure 1.6: Map showing the location of the Chinese Central Plains.
The red star shows the location of Daye County. The Central Plains covers modern-day Henan, the southern part of Hebei, the southern part of Shanxi, and the western part of Shandong province (shown in the map in yellow). A broader interpretation of the Central Plains' extent would add the Guanzhong plain of Shaanxi, the north-western part of Jiangsu, and parts of Anhui and northern Hubei, basically the space between the middle and low basins of the Yellow and Yangtze rivers (approx. dotted line). Image courtesy of http://www.ssqq.com

1.3 Aim and research questions

This thesis focuses on the smelting process – an unexplored yet fundamental step to obtain the raw metals necessary to be transformed into metal items. For a country where both iron and copper are an inherent part of its identity, it is surprising that such limited research has been done on the primary production of base metals.

Against this background, the study of the Daye County assemblages constitutes only a first but significant step in a larger long-term research agenda. This project investigates the

copper and iron producing industries of Daye County, a substantial mining and smelting area in Hubei Province (China) with activities well documented from the late 2nd and early 1st millennium BC (Huangshi Municipal Museum 1999) (see section 2.5). In particular, this study aims to reconstruct the engineering parameters of the primary smelting of copper and bloomery iron of eight production sites located in the proximity to the prominent ancient mine of Tonglüshan (Huangshi Municipal Museum 1980), and to place them on a chronological and historical framework. These production sites present remains of smelting activities of a substantial scale, likely obtained throughout several centuries, therefore a crucial research point is to discern between different technological trajectories for both metals and their possible interplay. It is hoped that their initial study, based on surface materials recovered during survey, can shed light on technological traditions and variability of technology as much as on trends in social organisation and economics.

Moreover, Hubei province – although not strictly located within – has always been very close to the cultural sphere of the Central Plains during pre-imperial times, and was part of the core of the empire from the foundation of the Imperial Dynasty, in the 3rd century BC. Therefore, Daye County is not only suitable for this archaeometric study because of its mineral richness and volume of metallurgical activities, but also because the relation with the Central Plains and with the posterior imperial administration avoid the characterisation as 'exceptional', 'marginal', 'influenced by external factors to the Chinese culture', etc. described in other metal productions (e.g. Mei & Li 2003; Chen, K. et al. 2012; Huang, Q. & Li 2013), since Daye County was always a fundamental part of territory for both political and cultural Chinese identity (Zhang & Fan 2003).

Some particular research strands to which it hopes to make a relevant contribution include:

I. To reconstruct the engineering parameters of both copper and iron production. This is not well recorded in historical documents nor has it received much attention by archaeometallurgists. Base metal production is a flexible process, leaving much space to develop different technological trajectories to achieve the same goal. Therefore, this dissertation investigates the types of technology being employed to smelt the ores in each of the sites and compares the results in order to identify technological traditions within them. Aspects investigated for each site include the types of ores and furnaces, operating conditions, temperatures and redox, inter-smelt standardisation and technical efficiency of the process.

II. To provide a chronological framework for the smelting sites as far as allowed by the evidence, to better demarcate chronologically the smelting activities, which before this research were assigned loosely to a long period from the early 1st millennium BC to the 11th century AD. A series of charcoal samples were recovered for direct dating, in addition to information obtained from associated pottery and other field observations. The new data is contrasted with the existing information for Tonglüshan (Wagner 1986; Huangshi Municipal Museum 1999) and with the chronological frameworks proposed for some of the sites within Daye County (Wei et al. 2008; Hubei Provincial Institute 2006). The objective is to understand the chronological relationships between the smelting sites under investigation, with a particular focus on ascertaining whether the two technologies (copper and bloomery iron) were diachronic or synchronic and to assess if the copper productions are comparable to the main centre of Tonglüshan, which equally has a very long period of activity framed between the early 1st millennium BC and the 1st century BC.

III. To understand why a specific technology and/or model of production was used. The concepts of *chaîne opératoire*, *technological choice*, and *technological change* are employed to investigate technologies in their broader contexts, considering in particular the influence of production organisation, degree of specialisation and ecological conditions. This information also allows an assessment of the technologies in terms of cost/benefit.

IV. The last objective of this project is to document the existence of bloomery iron in China and to investigate how 'marginal' this technology was in its context, reviewing the classical scenario of abandonment of a 'simple' bloomery technology in favour of a 'sophisticated' one by means of blast furnaces and iron refining. The sociotechnical context of the bloomery versus cast iron is explored in terms of technical variants, specific cultural traditions and socioeconomic contexts, combining all the data from the previous objectives.

From a broader perspective, and considering the methods and historical frameworks necessary to undertake this research, it is hoped that this thesis will make a contribution to two wider fields of scholarship in China: first, the use of materials science and

instrumental analyses of metallurgical production debris to provide high-resolution characterisation of ancient technologies; second, the incorporation of regional perspectives in the historiography of China, which account for its social and ecological diversity.

1.4 Thesis outline

This introductory chapter is followed by Chapter 2, which provides the necessary background in two sections: a brief general outline of the technical parameters in copper extraction and iron reduction, and a summary of current knowledge on how these base metals were smelted in the study area, presenting the technical, historical and archaeological aspects.

Chapter 3 introduces the archaeological background to the eight case studies concerning copper and bloomery iron smelting in the Daye County: Hongfengshuiku (洪枫水库), Mianyangdi (眠羊地), Maochengnao (茅城脑), Wangyuecun (王月村), Xiyuqiao (栖杅桥), Lidegui (李德贵), Yanwopu (燕窝铺) and Cangxiawu (仓下吴). The chapter includes the description, state of preservation and available archaeological data, as well as detailing the sampling strategy and the nature of the studied assemblage.

Chapter 4 presents the conceptual and methodological framework adopted as the backbone of this PhD thesis. The chapter has two main parts, the first providing the theoretical frameworks employed to investigate technology in archaeology, and the second focused on the analytical methods utilised to investigate the assemblage. This chapter also includes the results of the ^{14}C radiocarbon measurements.

Chapters 5 and 6 constitute the core of the dissertation, presenting the analytical results of metal production technical materials – slag, ceramics and ores – from the sites in Daye. Chapter 5 concerns the production of copper, and details the analysis of each specific debris type and the arising interpretation, with emphasis given to the kinetics of the primary smelting. Chapter 6 is similarly organised but concerns to the reduction of bloomery iron.

Chapters 7 and 8 address the research questions of the thesis and seek a more contextualised understanding of the technical data. Each chapter presents a synthesis of the evidence building an understanding of smelting as a whole in Daye, and uses the *chaîne opératoire* structure to answer a number of the subsidiary questions more specific to each metal production, such as chronology, efficiency and cost/benefit, regionalism vs centralised model of production, economy of scale vs rational economy, etc. Subsequently, the other aims of this project are addressed, and thus Chapter 7 attempts to establish a chronological framework for the copper smelting activities while Chapter 8 investigates the technological choices employed by the smelters in Daye in the reduction of iron by the bloomery method instead of using blast furnaces to produce cast iron.

Conclusions are presented in Chapter 9, where the main findings are summarised according to the research questions posed, and potential lines for future research are outlined.

Appendix I provides a timeline of Chinese history. Appendix II presents analytical data on certified reference materials (CRMs). Appendices III-V present raw analytical data on archaeological samples. Appendix VI presents chemical composition of Cu-rich particles trapped in the copper slag and, finally, Appendix VII presents XRD diffractograms not included within the text.

In the first month of the second year of emperor Heping 河平 (27 BC), in the spring, the Iron Office in Pei Commandery was casting iron. The iron did not leave the furnace and come down into the moulds. There was a roaring sound, as of thunder, and also the sound of drums, and the thirteen workmen fled in alarm.

(Book of Han, 汉书, AD 111)

2 The practicalities of base metal production

The first part of this chapter provides brief technical background in the form of an overview of pre-modern copper and iron smelting technologies, with particular reference to archaeological sites. The aim is to provide a generalised explanation of the various stages of copper and iron production considering the key steps required to extract metal from an ore, by-products generated in each stage, etc. While a necessarily simplified picture, this will provide a basic framework that may facilitate the contextualisation of more detailed analyses and discussion presented later in this thesis.

The second part focuses on the smelting of copper and iron in the area of study – the Daye County in Hubei province –, and summarises current knowledge on the technical procedures used to smelt base metals in the county in pre-modern times, based on information from archaeology and written sources.

2.1 Copper metal smelting

With the exception of the very early use of native copper during the inception of metallurgy (Tylecote 1992, 1-17), ancient extraction of copper in its early stages relied on secondary deposits of Cu-rich minerals – carbonates or silicates such as malachite, azurite, chrysocolla, etc. (Hauptmann 2007, 69). As summarised by Bachmann (1982, 21), a copper carbonate ore heated above 500 °C decomposes as follows:

$CuCO_3Cu(OH)_2 \rightarrow 2CuO + CO_2 + H_2O$

Copper oxide, separate from hydrogen and carbon, is obtained and can then be reduced to metallic copper, by reaction with carbon monoxide obtained through the combustion of fuel:

$2CuO + CO \rightarrow Cu_2O + CO_2$

$Cu_2O + CO \rightarrow 2Cu + CO_2$

As ores typically contain significant amounts of other materials (mainly silica and iron oxides), slag will also form during the process:

$SiO_2 + 2FeO \rightarrow 2FeO.SiO_2$ (fayalite)

Early slags are often referred to as 'primitive' or 'immature', as they are made of rather viscous conglomerates of semi- or unreacted materials and scant molten phases (Figure 2.1). These are the result of subideal conditions such as weak air flows, short smelting cycles or variable redox conditions. These can result in large heat losses, low temperatures, and significant loss of copper into the slag, reaching up to 20-40% (e.g. Levy et al. 2002; Liu, S. 2002; Hanning et al. 2010).

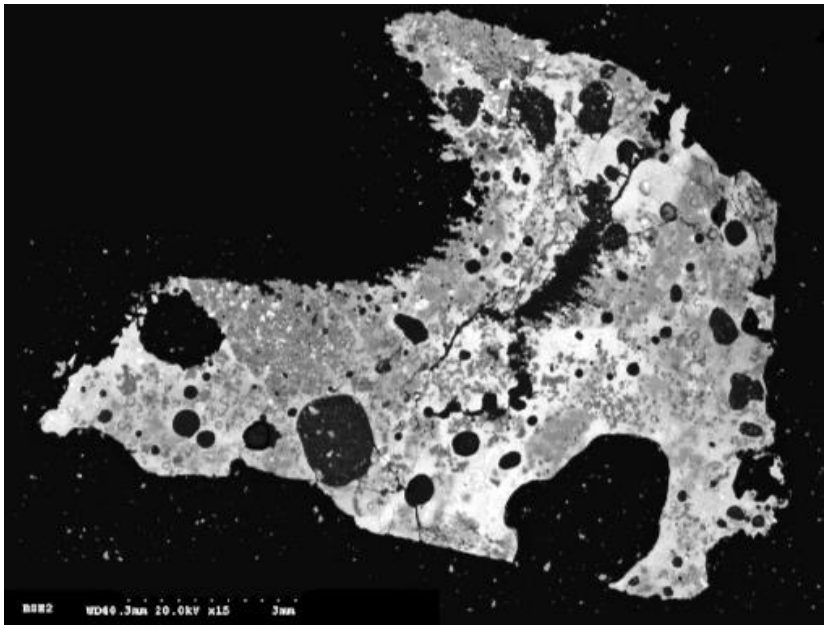

Figure 2.1: BSE micrograph of a copper slag from Laoniupo (Shaanxi, China) showing the typical appearance of an early smelting slag.
Large gas bubbles, numerous partially decomposed constituents (grey colours) and metal agglomerations (bright). Scale is 3 mm. Micrograph courtesy of Dr. Kunlong Chen.

The process of smelting copper from oxidic ores usually employed bowl and low shaft furnaces (Figure 2.2) operating around 1100 °C with charcoal as reducing agent. Often, the complete process occurred in a single step. The resulting copper could include impurities such as iron, requiring additional refining to purify the product (Rothenberg 1990, 14) – but with suitable control of the engineering parameters it is also possible to produce metal of sufficient purity directly.

Figure 2.2: Han shaft furnace with stone walls in Beiliu-Tongshiling (Guangxi province, China).
From Li, Y. (2009, Fig. 2-2). Scale is 10 cm.

Prior to smelting, a beneficiation process was used to prepare ores that were heterogeneous in both metal content and physical properties (Craddock 1995, 156-166). By selecting and crushing the ore, the smelter could remove significant amounts of gangue. This facilitated the smelting process by allowing the charging of a reasonably standard amount of ore, which had similar grain size (Figure 2.3). Gradually the smelting mechanisms were improved through advances in ore beneficiation, furnace geometry, addition of flux and use of bellows. Separation between slag and clean copper metal became more efficient by generating sufficiently fluid slag, in adequate amounts, which established the foundations of a more systematic smelting procedure (e.g. Merkel & Rothenberg 1999; Abd El-Rahman et al. 2013) (Figure 2.4).

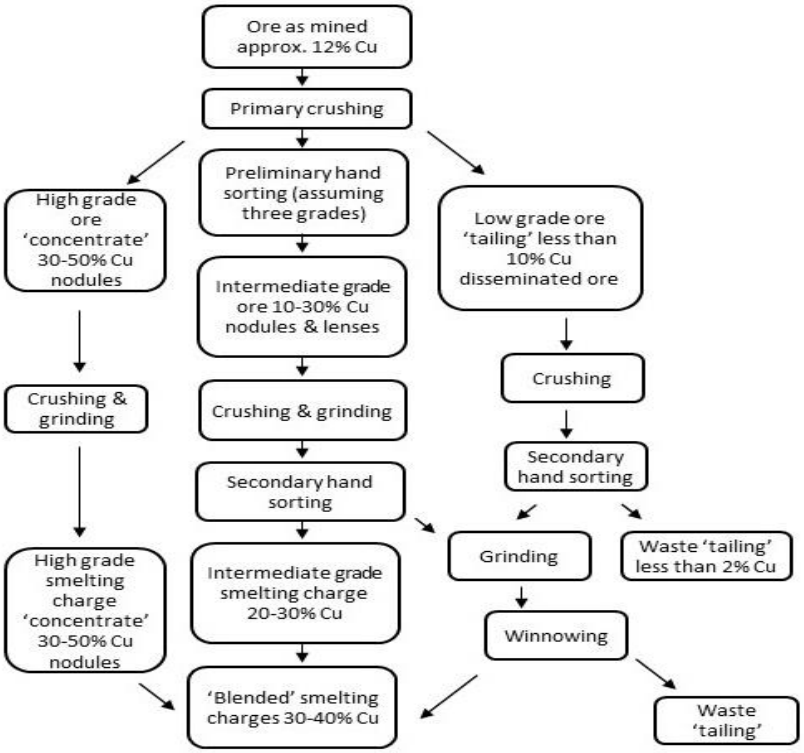

Figure 2.3: Flow chart summarising the beneficiation of copper ores at Timna in the Late Bronze Age.
After (Craddock 1995, Fig. 5.1).

With some notable exceptions such as the Chinese mine of Tonglüshan, (Wagner 1996, 44) (section 2.5), most of the copper in antiquity was produced from sulphidic ores (Rehder 2000, 115). This is because oxidic copper ore deposits on the Earth's crust are limited and were depleted during the early stages of metallurgy (Killick 2014), hence forcing metallurgists to begin exploiting sulphidic deposits. The reduction of sulphidic ores is a more complex process (Rostoker et al. 1989) that requires several stages, and is often assumed to require a higher level of expertise.

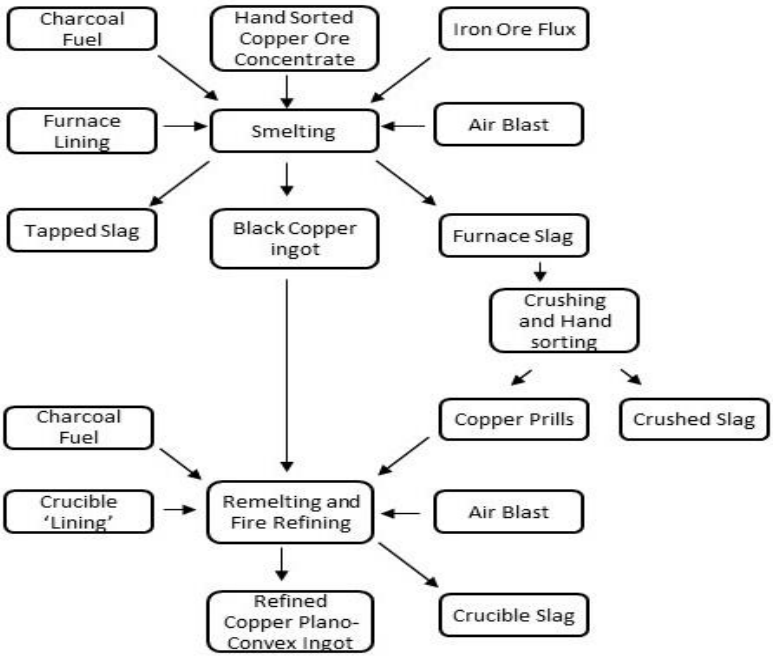

Figure 2.4: Flow chart of copper smelting at Timna during the Late Bronze and Early Iron Age.
After (Merkel 1990, Fig. 107).

2.2 Matte smelting

The main difficulty in dealing with primary ores lies in that it is necessary to remove the sulphur as sulphur dioxide, to convert copper and iron sulphides into oxides, and subsequently remove the iron from the copper. Matte smelting is a process for treating the low-grade primary sulphidic ores by successive transformation and concentration operations, culminating in a rather impure metal that then requires refining (Craddock 1995, 149). Relevant reactions can be summarised as follows (Bachmann 1982, 22):

(Partial roasting)	$4\ CuFeS_2 + 7O_2$	→	$2Fe_2O_3 + 4CuS + 4SO_2$
(Smelting)	$CuFeS_2 + 5O_2 + 2FeS_2$	→	$FeS + CuS + 2FeO + 4SO_2$
(Roasting)	$CuS + FeS + 3O_2$	→	$CuO + FeO + 2SO_2$
(Reducing)	$CuO + CO$	→	$Cu + CO_2$

This reaction chain is hardly going to occur in a single smelting cycle with clean separation slag/metal; furthermore, it is likely that several reactions will occur simultaneously during each stage of the smelting process, leading to multiple phases and unreacted materials

(Rostoker et al. 1989). Another complication lies in the challenge of completely removing sulphur from copper, as sulphides tend to combine within the furnace and form another material: matte (metal sulphides) (Figure 2.5). Higher temperatures and pressure are required to separate copper from sulphur, and even under such conditions, Cu metal and Cu_2S phases may still co-exist without separation (Elliot 1976). Frequently, the ingot obtained by the smelting of sulphidic ores contains a certain amount of sulphur (~1-3%) that needs to be removed through refining, in order to avoid metal embrittlement (Romanow 1995; Goldenberg 1998).

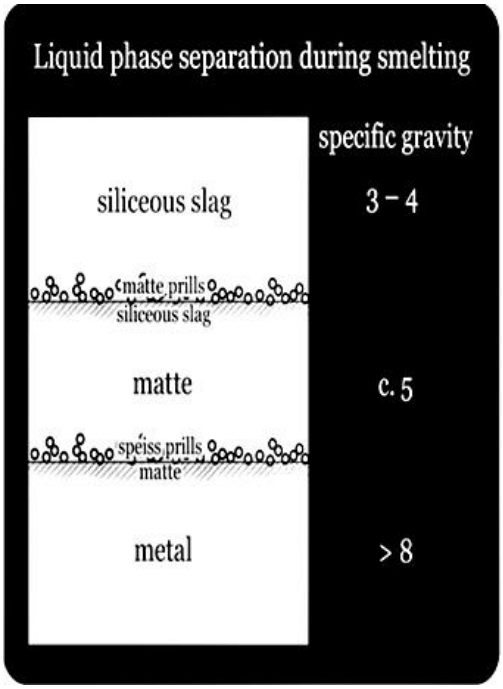

Figure 2.5: Ideal near-perfect segregation between three major phases involving complex sulphidic ores, according to their respective specific gravities.
Modified from Thornton et al. (2009, Fig. 1).

To achieve a successful reduction, a common solution in ancient times was to submit the ore to a multiple-step process, alternating oxidising roasting and reducing smelting stages until usable copper metal was obtained (Craddock 1992), in a process typically lasting for more than one day (Goldenberg 1998). In general, the roasting of ore increases its friability, porosity and reducibility before smelting (Rehder 2000, 115). Roasting involves heating at a temperature far below the smelting temperature – ~600 °C – in an oxidising

environment with the double aim of volatilising sulphur and concentrating the iron by partial oxidation, which can be later slagged during smelting to obtain enriched Cu–S matte from the original Cu–Fe–S phase (Marechal 1985).

A good example of the complexity and sophistication of matte smelting is provided by the Song's Dynasty official Hong Zikui (1176-1236) who in his prose poem *'Rhapsody of the Great Smelting'* (*Daye fu* 大冶赋) describes a method of smelting sulphidic ores practiced during his time (Figure 2.6). As shown in the flow chart in Figure 2.6, the process is both time and resource-intensive, particularly with regard to energy (fuel) consumption. An entry from the 1244 '*Song dynasty manuscript compendium*' (*Song huiyao jigao* 宋會要輯稿) provides specific information (Jost 2014, 47-48):

> For every one thousand jin of copper ore, several hundred dan of firewood and charcoal are needed [1 dan = ~100 jin = ~66.1 kg]

According to this source, the ratio of ore to charcoal would be of 1:10, i.e. an extremely fuel-consuming process employing a large labour force. Due to the important investment required by the enterprise, as well as the strategic importance that copper metal had in China as the base of the monetary system, the smelting of copper was typically carried on in large workshops licensed by the administration, and in close relation with mint and coinage offices. Even though the poem was written in 1210, it contains several references to a possible origin of the smelting procedure during the Western Han Dynasty – some 1200 years before. There is historical and archaeological evidence for the application of the model – with some modifications – at least during Tang (618-907), Song (960-1279) and Ming (1368-1644) Dynasties (Li, Yanxiang 1993b, 1998b, 2000; Cao 2012; Jost 2014). A simpler but similarly sophisticated, multi-stage process for the reduction of sulpharsenide ores has been documented in 1st millennium BC Xingjiang, the westernmost province of China (Mei & Li 2003). In general, the sequence roasting → smelting under reducing conditions → roasting → reduction, was widely used throughout Asia, 'which itself suggests that the process is of considerably antiquity' (Craddock 1995, 150).

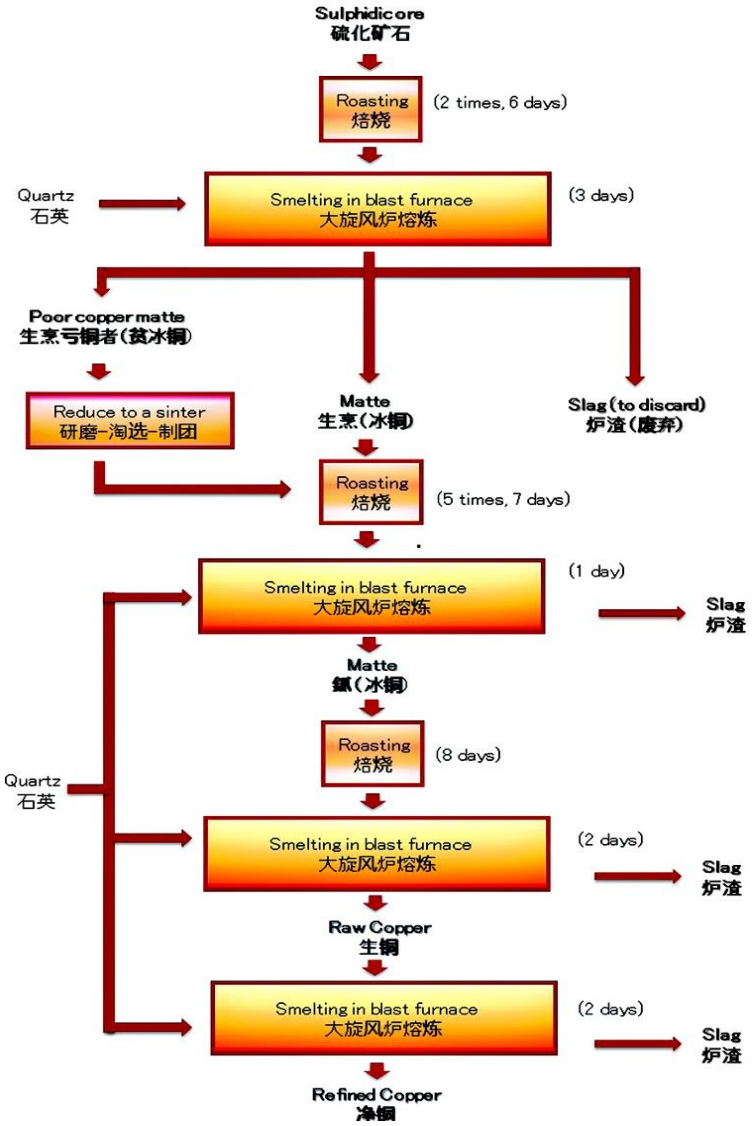

Figure 2.6: Flow chart showing the smelting process stages described in the Daye fu (大冶赋).
Modified after Li, Yanxiang (1993, 1998, 2000). Translation into English is mine.

Another solution to smelt sulphidic ores is co-smelting, which consists of charging the furnace with a mixture of oxidic and sulphidic ores. The main advantage of this solution is that it allows usable copper metal to be obtained after the first smelting, as in the direct reduction from oxidic ores. Rostoker et al. (1989) demonstrated that during co-smelting sulphur acts as the reducing agent, extracting oxygen from the oxide ore to reduce the metal. Furthermore, a substantial amount of sulphur is released as gas (SO_2), reducing copper from the sulphidic ore. The Chalcolithic co-smelting process of Cabrières (France) has been described as a 'extraordinarily simple' process without roasting or fluxing to

smelt fahlore copper ores (Bourgarit et al. 2003, 431), with many other examples of co-smelting in archaeology (e.g. Pryce et al. 2010) and also in experimental archaeology (e.g. Lechtman & Klein 1999).

2.3 Bloomery iron

The temperature at which iron melts (1550 °C) was unattainable for most of the ancient smelting furnaces; consequently, the extraction of iron was typically achieved in the solid state. In simplified terms, this involved reducing part of the iron oxides of the charge to metal particles that coalesced to form a bloom, consisting of iron uniformly mixed with slag that required hammering and annealing (smithing) to be refined and shaped. Iron produced by this method is called bloomery iron and the method itself is known as the direct method. The direct method was the only way to reduce iron in most of the Western countries until the 13^{th}-14^{th} centuries, and only declined significantly – but did not disappear – after the Industrial Revolution in the 19^{th} century (Rostoker & Bronson 1990; Craddock 1995; Pleiner 2000; Rehder 2000; Buchwald 2005; Veldhuijzen 2005).

Several processes take place simultaneously during a smelt, in different areas of the furnace. As a result, furnace design is a crucial parameter to consider during the iron reduction processes (Figure 2.7). The mainstay of the process is the reduction of ore by carbon from the fuel at a sufficient temperature. A key aspect is the appropriate circulation of the furnace gases produced from the combustion of the fuel (charcoal) – carbon monoxide (CO reducing) and carbon dioxide (CO_2 not reducing). CO is transformed to CO_2 near the air inlets and rises up through the furnace. The rising CO_2 encounters unburnt fuel and is converted into CO, making the atmosphere reducing.

At the same time, the ore travels down and is gradually reduced by CO gas and solid carbon in the form of charcoal, converting the iron oxides into iron metal by extracting oxygen. As the ore descends, it goes through various temperature zones. The efficiency and nature of the reduction is not homogeneous. In each stage the ore progressively breaks down and is reduced until it reaches the combustion zone. Close to the combustion zone the non-reduced iron oxides react with siliceous components from the gangue and technical ceramics – and flux if added – to form a fluid fayalitic slag. The generation of a

sufficiently fluid slag is fundamental since: 1) it provides a medium for the coalescence of the solid iron metal reduced particles into a bloom that will often form opposite the tuyere; 2) it prevents re-oxidation of the reduced metal particles; and 3) it effectively separates the metal from the other components of the charge.

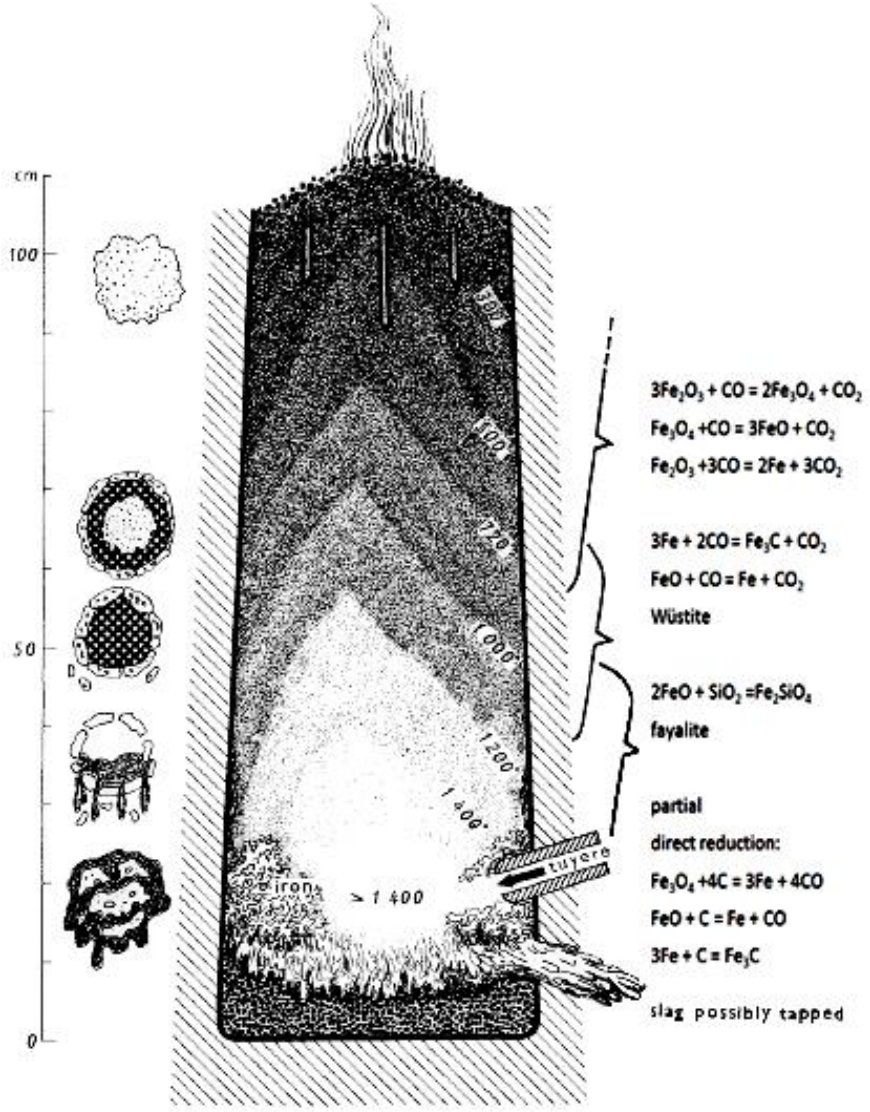

Figure 2.7: The principle of the bloomery process in a shaft furnace.
Ranges of temperatures and chemical reactions are showed on the right. The position of the iron sponge in the furnace hearth is marked at the tuyere level. Liquid slag penetrates the pores down and may be tapped. On the left the drawing shows schematically the various stages of the smelting process from the original ore, the formation of slag, reduction of metal particles and the transportation of metal particles by the slag. After Pleiner (2000, Fig. 33).

The direct method is complex and the internal dynamics were only partially controlled by the smelter; as a result there was a risk that the smelting could be unsuccessful, either producing only slag with no bloom if the reduction was insufficient, or molten, unusable over-carburised iron if the reduction was too high (Rehder 2000, 123). A furnace capable of reducing iron demands specific conditions to maintain high temperatures under a stronger reducing atmosphere than required for copper.

Roasting the ore before smelting is a convenient step in iron smelting, as it dries it, makes this more porous and concentrates the iron oxides; and thus facilitates crushing and separation of the gangue. Ultimately, the roasting makes easier the reduction because the hot gases in the reaction have access to a greater surface area of contact with the mineral. Roasting also removes water from hydrated ores (Rostoker & Bronson 1990, 52; Gordon & Killick 1993).

The four major problems which need to be overcome in bloomery smelting are summarised by Espelund (1997): 1) reduction of the iron oxides in a carbon-rich environment; 2) sintering of the iron particles under reducing conditions and high temperatures; 3) correct amount of carbon to create a sufficiently reducing atmosphere but not so high to produce an unworkable alloy too rich in carbon; 4) slag must be fluid enough to separate from the bloom (Figure 2.8).

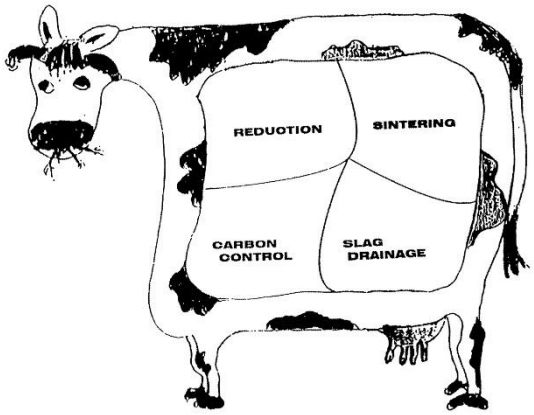

Figure 2.8: The cow with its four stomachs, representing four problems in bloomery ironmaking.
The cow has a combustion system (which needs oxygen from the air and produces CO_2) and delivers milk and dung, equivalent to iron and slag. No milk without dung, no iron without slag! After Espelund (1997, Fig. 1).

Bloomery iron has tensile strength and good toughness, and the ability to be readily shaped by forging and forge-welding (Wayman & Michaelson 2006), although it can be internally heterogeneous because of its formation in the solid state.

2.3.1 Bloomsmithing

Though the method is called *direct*, the bloom obtained after the smelting is not directly workable, and needs to be consolidated. The bloom is a porous conglomerate of fibres, sheets, and globules of iron roughly sintered together and permeated with slag and charcoal. Consolidation of a bloom involves hammering while the bloom is still hot. Hammering on the spongy, raw bloom compresses the iron metal and squeezes out the slag, which is expelled out of the bloom (Figure 2.9). The heating of the bloom for smithing was performed in shallow hearths at temperatures of ~1100 °C. Frequently, iron oxidised on the surface of the bloom which could be slagged by the addition of sand. This operation may or may not have occurred at the smelting place. The process produced an iron bar or billet ready to be forged to manufacture items. Producing an iron implement by the *direct* method therefore involved four main stages: roasting (ore), smelting (bloom), consolidation (bar or billet), and manufacture (item) (Craddock 1995; Pleiner 2000, 2006; Buchwald 2005).

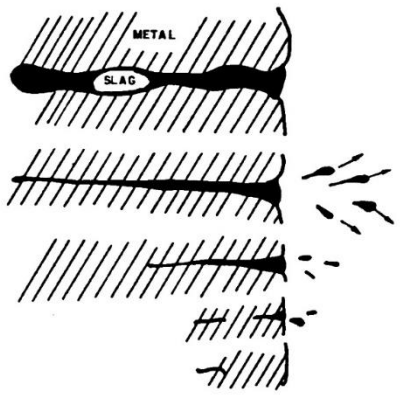

Figure 2.9: Expulsion of slag from a bloom.
The bloom is a sponge represented by two interpenetrating networks, one of iron and one of slag. If the hot bloom is rapidly hammered on an anvil, the slag is viscous but the force of the hammer ejects it like toothpaste squeezed from a tube. After Rostoker & Bronson (1990, Fig. 9.5).

2.4 Cast iron

The other main method used to smelt iron, known as the indirect process, produces a liquid state iron-carbon alloy in a blast furnace. Before the 2nd millennium AD only China had developed blast furnace technology (Wagner 2008). While the reduction process is not too dissimilar to the direct method – CO reacts with the iron oxides to produce CO_2, which reacts with carbon to produce CO in a cycle until Fe_2O_3 is reduced to Fe – the blast furnace considerably increases the temperatures attainable and also the CO/CO_2 ratio in the gas, to the point that it is capable of reducing most of the iron oxides present in the charge. A flux (normally limestone, $CaCO_3$) needs to be added to form slag (Figure 2.10), which is therefore lime-rich in contrast to the iron-rich slag from the bloomery process. Blast furnaces reach easily 1300-1400°C and are more efficient than the bloomery furnace in terms of yield, since more metal is extracted per ore unit, although they also consume more fuel – from 3 to 10 times more (Rostoker & Bronson 1990, Table 6.3). Blast furnaces require taller shafts to produce the highly reducing atmosphere, and a constant and powerful blast of air. They can be kept running uninterrupted operation for months until repairs are necessary (Wagner 2008, 14-15).

The product obtained from a blast furnace is liquid iron, known as pig iron or raw cast iron, which is a ferrous alloy with a high carbon content – ~4-5% – and a lower melting point than the pure metal; the metal has good casting properties and is very hard although it also shows poor resistance to crack growth (Wayman & Michaelson 2006).

Although it may have been possible to produce steely blooms in bloomery furnaces (Merwe & Avery 1982), neither the direct nor the indirect method would easily produce steel in a single step – both require more actions after the smelting. As a matter of fact, 'the difficulty with iron lay not in obtaining high temperatures but in developing the new techniques necessary to hot-forge the bloom or, in China, […], to decarburize the brittle cast iron to produce a usable material' (Taylor & Shell 1988, 206). It is therefore the post-smelting treatment that actually defines the final product, which depending on the iron-carbon ratio in the alloy, will lead to widely variable mechanical properties, e.g. hardness, toughness, castability, malleability. In addition to many other differences, however, there is a key difference in the output between both production models: bloomery iron is

inherently a small-scale system since each artefact has to be manufactured individually by forging, whereas cast iron is suitable for large-scale production, allowing continuous production of standardised items (Wagner 2001a, 85-87); the differences between the models of production of bloomery and cast iron are later discussed in this thesis (chapter 8).

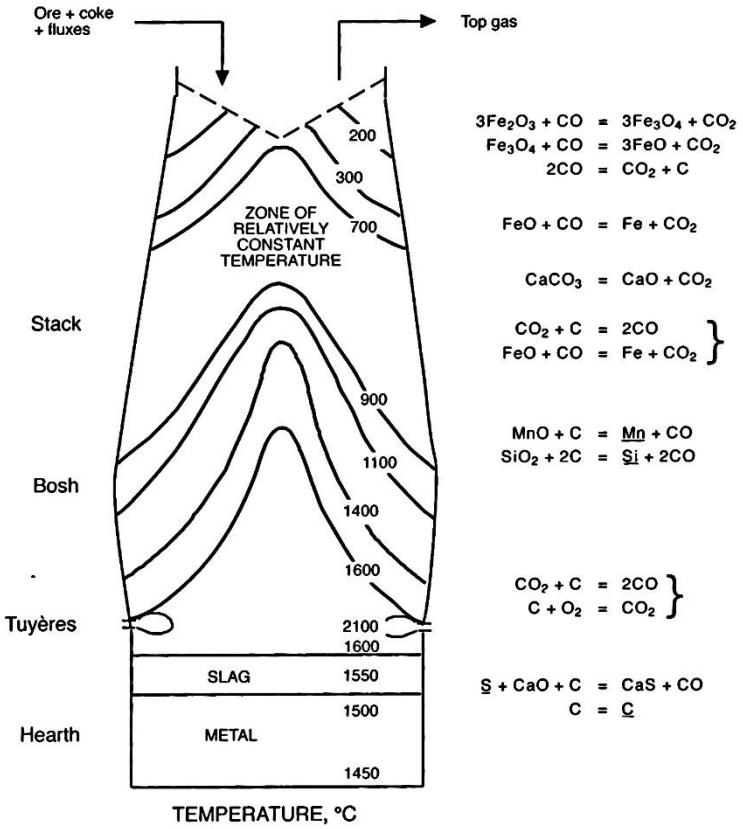

Figure 2.10: Diagram of a modern large-scale coal-fuelled iron blast furnace.
The height is typically 20-30 m. The reactions are indicated at the right, underlined elements are in solution in iron. After (Wagner 2008, Fig. 10).

2.4.1 Refining of raw cast iron

Cast iron is very different from bloomery iron and steel because its high carbon content (~4-5%) means that it is too brittle to be hot or cold forged. Though it has been demonstrated that cast iron with up to 3% carbon can be hot forged (Wadsworth & Sherby 1980 in Redher 2000, 141) this does not seem to have been common practice in ancient

times. In China, a wide range of techniques to handle cast iron were known since relatively early dates, allowing metallurgists to remove carbon from the alloy down to the desired level. As such, craftsmen reserved different types of iron alloy depending on the final product (e.g. agricultural implements, tools and weapons): 'raw' cast iron, malleable cast iron, wrought iron (decarburised cast iron) by forgery, and steel by wrought or cast iron (Taylor & Shell 1988; Han & Chen 2013; Liu, Haifeng et al. 2014a), (Figure 2.11).

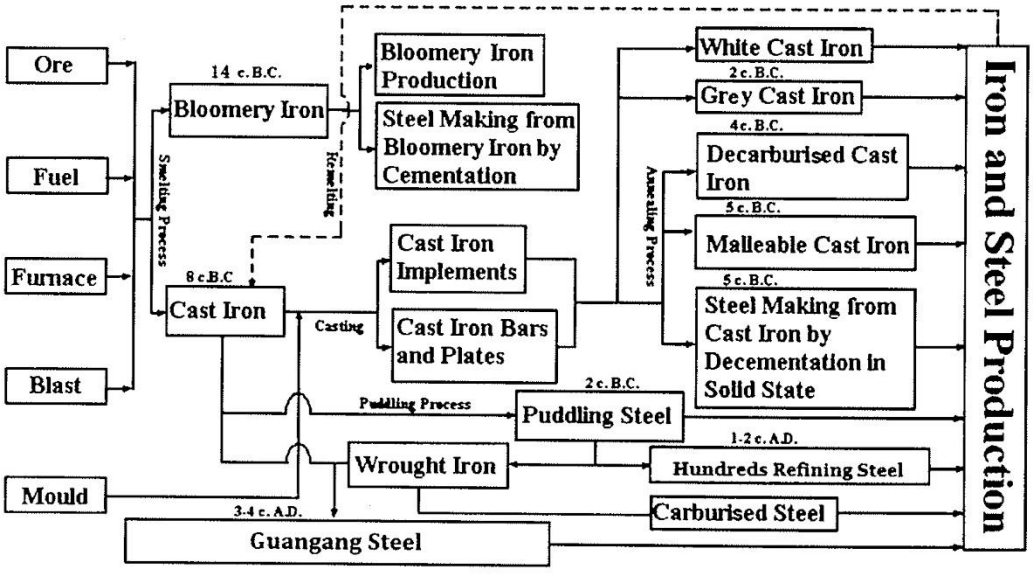

Figure 2.11: Chronological scheme of iron and steel production techniques in ancient China. After Han & Chen (2013, Fig. 14).

It is not within the scope of this thesis to analyse in detail the different iron alloys and their production. Relevant detailed information is available in other publications (e.g. Wagner 1996; Han 1998; Wayman & Michaelson 2006). However, it is worth pointing out that although raw cast iron can be directly used by a foundry, most of the iron would be further processed and converted into a different material. In China, the iron from blast furnaces was typically either converted to wrought iron in a fining hearth or cast into useful products in a cupola furnace. There are several possible translations into English of these practices such as 'roasting', 'refining, 'converting', 'puddling', etc., and the terms are frequently equivocal since they do not exactly refer to the same technique conveyed in English. Therefore, following Wagner (2008, 16), this dissertation used the term 'fining'

for 'the operation of converting cast into malleable iron in a hearth or open fire, urged by a blast of fuel' – as opposed to 'puddling' which is in essence the same operation but in which fuel is not mixed directly with the iron, requiring the use of a more sophisticated device than a pit on the ground.

The traditional Chinese iron industry, still in production during the 20th century, used a fining process to convert pig iron from the blast furnace into low-carbon wrought iron. The fining hearths were relatively simple structures consisting of a shallow pit, rarely more than ~90 cm in depth, charged with wood, charcoal and pieces of cast iron (Figure 2.12). The charge was ignited and left for a short period of time (~20 minutes) until white flames appeared. Air was then pumped in from the top and the iron violently stirred with an iron or wooden rod. Occasionally sand or clay was added to the charge to slag the oxidised iron. It is estimated that temperatures of 1400 °C could be reached in these devices, though the iron would typically remain somewhat viscous rather than fully liquid. When the iron was sufficiently decarburised and converted to wrought iron, it was removed from the furnace to be immediately hammered on an anvil, to squeeze the slag in an identical way as from a bloom from bloomery smelting. Typically, the whole operation would last for about 60 minutes and obtained forgeable wrought iron with very low levels of impurities: C was reduced from >4% to <0.1%; Si, Mg and S to <0.1% and P to 0.1-0.2% (Wagner 1985, 2001c, 2008).

The other treatment of pig iron did not thoroughly decarburise the metal, but instead converted it into *white* or *grey* cast iron, which has a carbon content of ~2-3.5%, i.e. ~1% less carbon than pig iron (Scott 1991, 37-42). Roughly, these two iron types are hard but brittle, and have very good fluidity and casting properties, particularly the latter. Most of the agricultural implements in China such as ploughshares or spades, and quotidian utensils such as cooking pots or ladles were made of white or grey cast iron, with many other applications such as statues, coins or guns (Needham 1958; Hua 1983; Wagner 1996).

Pig iron was remelted using a device known as cupola furnace. This is basically a shaft furnace with resemblance to a blast furnace but much smaller (Figure 2.13). The fuel and the iron were charged into the top, and a blast of air is blown through one or more tuyeres near the bottom where there is also a taphole to tap the molten iron. Typically, cupolas

are built in sections and have a total height of ~3m. The walls were built with refractory materials and were thick (~20-30 cm) to provide thermal insulation (Wagner 2001a, 75). The molten iron can be poured directly into moulds or handled from the bottom section of the cupola, used like a crucible (Wagner 2001b; 2008).

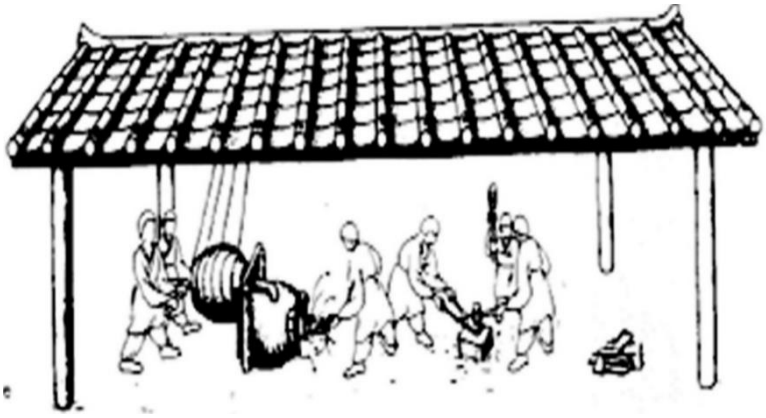

Figure 2.12: Speculative reconstruction of a Han-period fining hearth.
The bellows that directed the blast on top are based on a tomb-relief of the same period**.** After Hua (1983, Fig. 11).

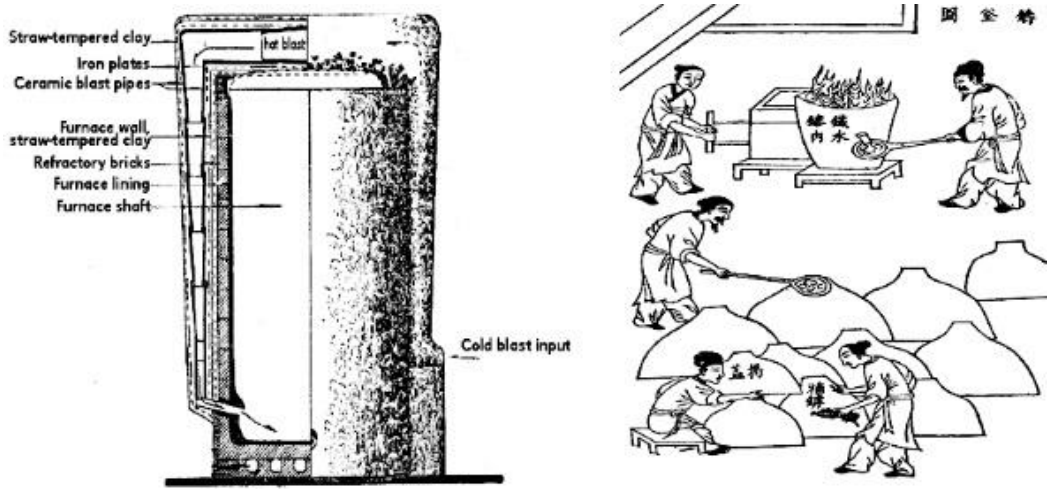

Figure 2.13: Reconstruction of a Han-period cupola furnace and casting cooking pots from a cupola furnace in the 17th century.
Original illustration of casting pots from AD 1637 (Sung 1966, Fig. 8.4), and Han cupola from Wagner (2001a, Fig. 6).

2.5 Background to the research area

2.5.1 Tonglüshan Mine

The area of Daye County in Hubei province has long been an important site of metal production due principally to its geological mineral richness in copper and iron, but also in other metals, with a massive reserve of high grade copper ore which was exploited in ancient times (Xie et al. 2011; Zhao et al. 2012). The Tonglüshan ancient mine was rediscovered in 1965 and excavated between 1974-1985, revealing a sophisticated complex of underground operations as well as a large number of mining tools (Xia & Yin 1982; Wagner 1986; Huangshi Municipal Museum 1999) (Figure 2.15). Radiocarbon dates indicate that the mining activities took place during a long period spanning at least from the Shang period (*c.*1600 BC) to the Han dynasty (1st century AD), leading to their recognition as *'undoubtedly the biggest and the one [mine] with longest service life'* (Huangshi Municipal Museum 1980, unpaged) (Table 2.1). The earlier dates, however, are questioned by some scholars and in fact there is disagreement between the different calibrations published (Wagner 1986; Huangshi Municipal Museum 1999); the later publication indicates Shang chronology which is not indicated in the first one. The earlier date which is widely accepted is that mine exploitation was initiated during the Western Zhou Period (AD 1046-771). Nonetheless, Barnard (1986, in Reinhardt 1997, 51) reports the existence of many ancient mines also located in the vicinity of Tonglüshan, and Zhu, S. (1986, 6) that 'there existed a rather long period of open-cut mining before underground mining in Tonglüshan', both scholars leaving open the possibility of an earlier initiation date.

The excavation campaigns revealed an extensive area (~2x1 km) of mining and smelting remains; a total of seven mining sites and three smelting sites were excavated. In total, 231 old timbering shafts and 10 copper smelting furnaces were unearthed, and nearly 300 mining tools were found (Huangshi Municipal Museum 1999) (Figure 2.15). The archaeologists defined XII different ore bodies, consisting of plentiful mineral aggregates with a great reserve of high grade copper ore, of which the more intensely exploited were the bodies I, II, IV, VII and XI (Huangshi Municipal Museum 1999, 29-31). These ore bodies – frequently referred as 'veins' in the Chinese literature – are at the contact zone between granite and granodiorite-porphyry, where the rock is friable and easy to mine although

for the same reason extensive timbering was necessary to prevent collapse (Wagner 1996, 42) (Figure 2.14).

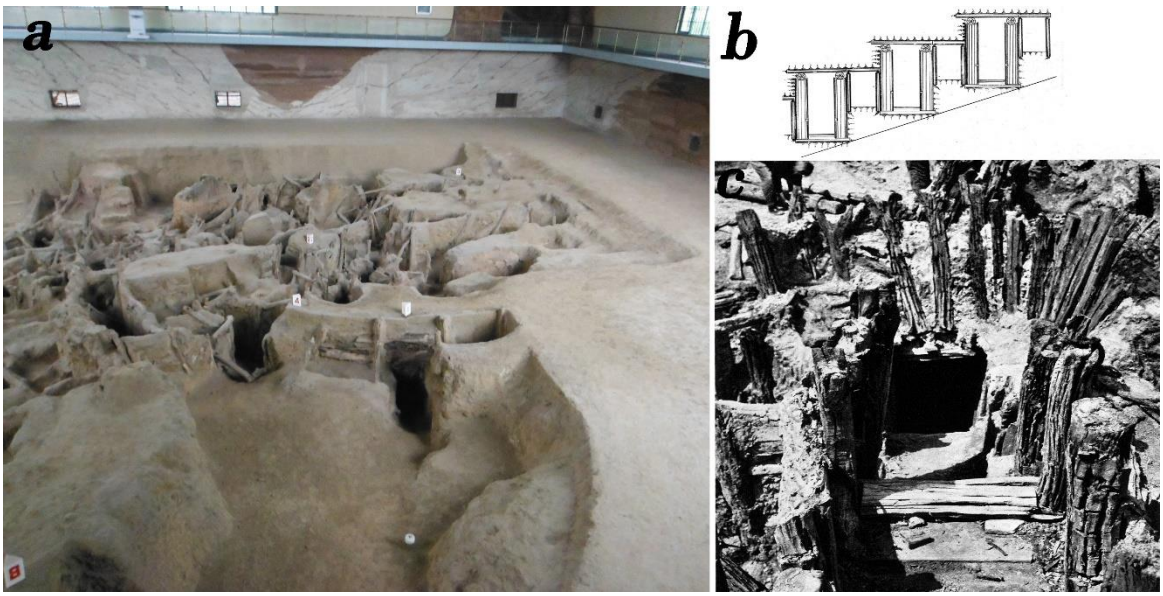

Figure 2.14: Tonglüshan mine as currently preserved and during excavation.
a) Tonglüshan mine as preserved in the Tonglüshan Ancient Metallurgy Museum in Daye; **b)** plan of a crosscut connecting drifts; **c)** shafts during the excavation in 1975. The preserved part of the mine correspond to the Warring States-Han Period, as well as the crosscut section. Left picture by the author, b) and c) from Huangshi Municipal Museum (1980, unpaged).

It is observed that there was a gradual evolution in the complexity of the extraction which, at the beginning (~1100-800 BC), consisted of shallow shafts following the outcrops, whereas later (~800-500 BC) the ore mineralisation was also followed by vertical shafts and underground tunnels. Finally, from the 500 BC onwards, a complex process of extraction was developed whereby the outcrop was followed until the base and the ore was extracted in stair-crosscut galleries (Figure 2.14).

Through time, shafts and tunnels showed enlargement in both cross section and depth whereas timbering structures, drainage mechanisms and windlass hoisting systems to lift the ore also evolved from 'simple and crude' to 'solid and secure' (Xia & Yin 1982; Zhou, B. et al. 1988; Huangshi Municipal Museum 1999, 252). The activity of the mine increased dramatically by the beginning of the Warring States period (first half of the 5th century BC) directly related to the rise of one of the main state contenders – the state of Chu – and kept the high level of exploitation until the 1st century BC, when it was abandoned because

the ingress of water made digging impossible (Huangshi Municipal Museum 1980, unpaged; Xia & Yin 1982; Zhou, B. et al. 1988, 127; Reinhardt 1997, 97; Huangshi Municipal Museum 1999, 252; Zhu, J. & Xiong; 2006, 305-312; Coulson 2012, 13).

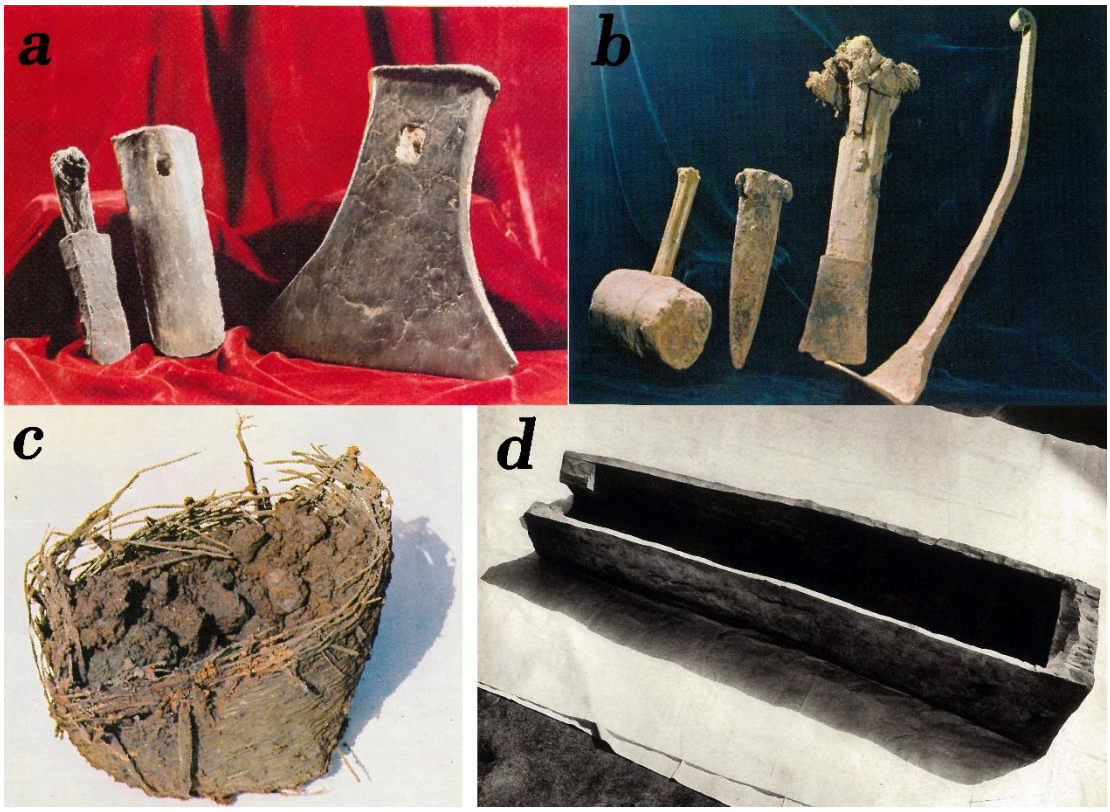

Figure 2.15: Mining tools unearthed in Tonglüshan.
a) Copper Adze (height 25 cm, weight 3.5 kg) and chisels before 5th century BC; **b)** Iron implements of Han Dynasty: Sledge-hammer (13x11 cm, 6 kg), Square chisel (22 cm long), Rake (50 cm long), Adze inscribed 'Ho·3' (manufactured in Iron Office 3 from Henan, not unearthed in Tonglüshan): **c)** Bamboo basket (18-25 cm diameter) containing chunks of high grade malachite ore (~50% Cu); **d)** Wooden trough for ore dressing from the Warring States-Han period. The trough is 116 cm long, 36 cm wide at one end and 31 at the other, and 20 cm deep. It would separate the ore by gravity, the ore was put into the trough and stirred about in water, and then the blocking board at the lower end was taken off releasing the muddy water with fine sediment and leaving inside the heaviest (high grade) ore chunks. (Huangshi Municipal Museum 1980, 1999).

Notably, all the copper ore extracted throughout the wide timespan in which Tonglüshan was active corresponds to secondary deposits of which the main minerals are chrysocolla ($CuSiO_3.2H_2O$), malachite [$Cu_2CO_3(OH)_2$], azurite $Cu_3(CO_3)_2(OH)_2$, native copper (Cu), cuprite (Cu_2O) and tenorite (CuO); other minerals include haematite (Fe_2O_3), magnetite (Fe_3O_4) and andradite [$Ca_3Fe_2(SiO_4)_3$] (Wagner 1986). There is no matte smelting

documented in Tonglüshan with the exception of one possible deposit in the ore body XI, in which is argued that matte smelting was performed during the Warring States period (Li, Yanxiang 1998b; Li, Yanxiang et al. 1999). However, other scholars claim that the smelting of sulphidic ores occurred very late and that the profitable extraction of copper from lean sulphidic ores was not practiced in Daye until the imperial period (Zhu, S. 1986; Hong et al. 1996).

ample	*Description*	*Location*	*Uncalibrated date (BP)*	*Calibrated date (BC)*
ZK-559	Charcoal (close to furnace)	Ore body XI	3205±400	1880- 840
ZK-758	Timber	Ore body VII	3260±100	1530-1325
unlabelled	?*	?*	3265±100	1521-1317
WB 80-44	Timber	Ore body VII	3150±80	1424-1225
BK945058	Timber	Ore body VII	3185±70	1422-1263
WB 80-40	Timber	Ore body VII	3140±80	1420-1220
XJX2	Timber	Ore body XI	3140±80	1046-1139
WB 80-39	Timber	Ore body VII	2810±80	986-813
WB 79-35	Timber	Ore body VII	2810±80	986-813
ZK-560	Timber	Ore body VII	2795±75	972-810
unlabelled	?*	?*	2795±75	972-810
BK95056	Timber	Ore body VII	2750±75	892-798
WB 80-42	Timber	Ore body VII	2680±75	829-662
WB 79-36	Timber	Ore body VII	2600±80	800-446
WB 79-37	Axe handle (iron head)	Ore body VII	2575±135	800-400
XJ46	Timber	Ore body XI	2750±70	788-415
ZK-297	Axe handle (bronze head)	Ore body XI	2485±75	761-399
WB 80-43	Timber	Ore body VII	2470±75	758-397
WB 80-6	Timber	Ore body VII	2430±65	512-391
ZK-561	Timber	Prospection	2075±30	167-AD 58

Table 2.1: Radiocarbon dates for the ancient copper mine at Tonglüshan.
From Huangshi Municipal Museum (1999, 192). *information not given.

2.5.2 Tonglüshan copper smelting furnaces

A total of 10 smelting furnaces were found associated with the mine. There is only one radiocarbon date, obtained from a piece of charcoal collected close to a furnace structure. Unfortunately this is the least credible date, showing a very large standard deviation (ZK-559, Table 2.1). All the furnace structures were found in stratigraphic levels of the late Spring and Autumn, and Early Warring States period (6^{th}–5^{th} century BC) based on material typology (Wagner 1996, 44; Huangshi Municipal Museum 1999). As will be later substantiated in this thesis (chapter 7), the technological process fits much better in the Warring States Period than in the Shang or Western Zhou periods that indicates the radiocarbon measure.

Figure 2.16: Model showing workers operating the Tonglüshan copper furnace, and scale reconstruction of the furnaces at Tonglüshan Ancient Metallurgy Museum.
A furnace would be operated by four or five workers: two to pump the accordion bellows, one or two to prepare the charge and fill the furnace, and one to open/close the tap-hole and facilitate the tapping. Note the large working platform of the reconstructed model.

These consisted of large structures integrating a characteristic hollow base to preserve the heat and insulate the hearth from moisture; a hearth with taphole for the tapping of both molten copper and slag, with two tuyeres arranged at the same level; a relatively high conical shaft (1.5 m); and large working platforms for crushing and screening materials (Figure 2.16). The different parts of the furnace were built with a combination of different materials: red clay, iron ore powder, quartz fragments and kaolin (Figure

2.17). It is estimated that they operated at 1200-1300 °C reducing a mix of copper ores with iron oxides fluxes, and that the reduction of non-sulphidic ores in these powerful furnaces was straightforward, with each furnace easily producing 300 kg of copper per day. It was also suggested that, if operated differently, the same furnaces would have been capable of reducing iron, functioning as blast furnaces and generating molten iron (Wagner 1986, 1996), although no evidence of early iron smelting was found in Tonglüshan (Xia & Yin 1982; Zhu, S. 1986; Zhou, B. et al. 1988; Huangshi Municipal Museum 1999).

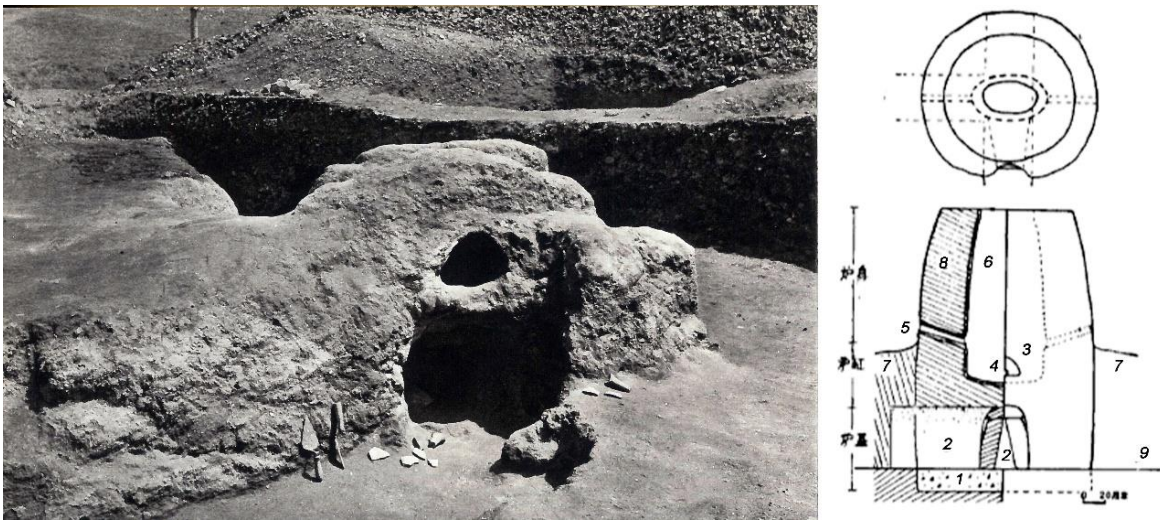

Figure 2.17: Tonglüshan copper smelting furnaces.
Remains of a smelting furnace during the excavation of 1975-1985 with a large heap of slag visible at the back (Huangshi Municipal Museum 1980, unpaged), and generalised reconstruction from Wagner (1996, Fig. 1.15): 1. Base, 2. Wind channel, 3. Tapping arch, 4. Taphole, 5. Tuyere, 6. Inner lining, 7. Working area, 8. Furnace wall, 9. Ground surface. Scale is 20 cm.

Plano-convex ingots weighing 1.5 kg were found in the vicinity of the furnaces; the crude metal smelted in Tonglüshan contained around 93% Cu and 5.4% iron. There are several estimates about the total volume of copper metal extracted from Tonglüshan calculating a production of 40,000, 80,000, 100,000 or even, most optimistically, 120,000 tonnes (summarised by Wagner 1986; see also Coulson 2012, 13).

Several heaps of slag up to 3 m high appeared associated to the furnaces and spread within an area of ~140,000 m^2 with a total estimated volume of around 400,000 tonnes

of slag. In spite of its historical relevance, only scant archaeometric research has been devoted to the smelting furnaces and slag from Tonglüshan in order to understand the nature and evolution of the production technology. The slag has been described as flat thin and flow cakes (Figure 2.18) with less than 0.7% Cu content, and it is mentioned that 'over 100 slags were analysed by chemical analyses' (Zhou, B. et al. 1988, 129).

Figure 2.18: Several fragments of tap slag from Tonglüshan. Exhibited at the Tonglüshan Ancient Metallurgy Museum. The largest fragment is ~9 cm long.

To my knowledge – excepting the 64 analyses that were published in 1999 (Li Yanxiang et al.) to investigate matte smelting – these analyses are limited to bulk chemical composition, which is fayalitic, and the published samples are exactly 25 in number (in English by Wagner 1986, 1996). There is no microstructural and mineralogical description except for the mentioned possible evidences of matte smelting of vein XI, which only includes six very high magnification micrographs of the copper particles; these images are repeated in the various publications (Li, Yanxiang 1998a; Huangshi Municipal Museum 1999; Li, Yanxiang et al. 1999). Overall, the technical information is rather vague – e.g. 'successful control of the temperature in the furnace with the smelting technique at rather high level' (Huangshi Municipal Museum 1999, 253) or 'the basicity $CaO/(SiO_2+FeO)$ lies between 1.0 and 1.3' (Zhou et al 1988, 129) –, and the same basic parameters summarised here are repeated multiple times in the different publications

without adding new information (Huangshi Municipal Museum 1980, unpaged; Xia & Yin 1982; Wagner 1986; Zhou, B. et al. 1988, 127; Wagner 1996; Huangshi Municipal Museum 1999, 252; Zhu, J. & Xiong; 2006). Equally, the archaeological description is ambiguous, and sampling strategies are not clear, with slags randomly recovered from 'inside, beside, in the vicinity, from surface' etc. of veins. Moreover, virtually no research has been conducted on the approximately 50 smelting sites documented around the main mining area (Wagner 1986, 1996), including some with tonnes of metallurgical residues and evidence of prolonged settlement (Hubei Provincial Bureau of Cultural Heritage 2002). Some of these sites constitute the core focus of the current project.

2.5.3 Iron smelting in the Daye County

Iron smelting has not been archaeologically documented in Daye prior to this work, nor there is any smelting activity recorded in the written sources consulted. Presumably, the bloomery activities documented in this dissertation (chapter 6) were deemed unimportant and thus overlooked in the official imperial records – although there may be some references in the local gazettes. Likewise, any earlier activities would not be recorded, perhaps because the scale of the activity was too small to be noticed. Nonetheless, Daye is listed as an iron resource in documents of the Yuan (AD 1271-1368), Ming (AD 1368-1644) and Qing (AD 1644-1911) Dynasties, and the first modern Chinese ironworks – *Hanyeping Coal and Iron Company* (1889) – utilised ore from the Daye iron mines (Feuerwerker 1958, 87; Golas 1999, 153-163; Wu 2015, 106).

However, although there is no evidence of smelting, there is archaeological evidence of iron production in the area. Several of the references that reported the excavation of Tonglüshan give brief notice to the 1977 find of 17 furnace structures not related to copper extraction, and framed chronologically in the Song Dynasty around 1000 years after the cease of the activity in the mine (Huangshi Municipal Museum 1980, 1999; Wagner 1986; Zhou et al. 1988). These structures were found lined up in a 320m^2 workshop and correspond to small bowl furnaces – ~40 cm in diameter – with one tuyere at the rear opposite the tap-hole. The only picture published (also repeated in several papers and reproduced in Figure 2.19) seems to illustrate a kind of free-standing vessel

with several instances of relining of the walls, and has a large squared 'tablet' of slag attached to the tap-hole (Zhu, S. & Zhang 1986).

Next to the aligned furnaces were located several heaps of slag which are briefly described as displaying irregular shapes and having a highly viscous appearance (Zhu, S. & Zhang 1986, 470). The chemical composition of the slag cake trapped in furnace 14 (Figure 2.19) is 0.04% Cu, 60.98% FeO, 7.51% Fe_2O_3, 21.28% SiO_2, and 1.04% CaO, but the type of analyses is not given. The main minerals in the microstructure are identified as fayalite laths and magnetite, with frequent haematite, wüstite and calcium ferrite. Iron particles trapped in the slag melt appeared much more rarely, corresponding to small particles of ferrite of sub-angular or sub-rounded forms, and occasionally larger rounded prills. The larger metallic grains were identified as steel after etching (Zhu, S. & Zhang 1986, 471-3). There are several mentions concerning the complicated interpretation of these by-products, since in principle these were expected to be copper smelting debris, but Cu is only present as a trace element and thus this possibility was discarded; iron smelting was also discarded due to the high amount of iron lost into the slag (Zhu, S & Zhang 1986, 474). Lead or silver smelting were considered a likely possibility but were finally discarded as well since the Pb and Ag content in slag was too low (~100 ppm Pb, 1-2 ppm Ag).

Figure 2.19: Remains of a bowl furnace of Song Dynasty (AD 960-1276) found in Tonglüshan.
From Huangshi Municipal Museum 1980, unpaged.

The final conclusion is that since the slag 'was formed under an oxidising atmosphere and contains particles of steel' (Zhu, S. 1986, 8), the furnaces correspond to *puddling* furnaces to produce steel from cast iron (Zhu, S. & Zhang 1986, the italics are mine). The puddling process is what in this dissertation is named as 'fining' i.e. the constant blow of air whilst stirring cast iron in an open fire, in order to burn off some of the carbon. The authors show their perplexity and remark upon the significance of these furnaces for the Chinese history of metallurgy, as they are very different from the traditional puddling furnaces known for the period (Figure 2.20). Scholars also highlighted that in spite of the fining process being long known in China this is the first time that the 'furnaces appeared in groups like this with so much slag' (Zhu, S. 1986, 8).

Significantly, in the year AD 1078, Daye (大冶) is explicitly mentioned in the *Collected documents of the Song Dynasty* (Song hui yao ji gao 宋會要輯稿) together with nine other places under the jurisdiction of the imperial iron prefecture of Xingguo jun (興國軍), within the circuit of the Jiangxi province, the province bordering Hubei to the southeast. The statistics given in the document concern both iron mines and smelters, as well as accounts of the production of the prefecture. The total was nearly 60 tonnes for the year 1078 for the case of Xingguo jun, but there is no breakdown among the various places listed (Wagner 2008, 294-305).

The blast furnaces of the Song-Yuan Dynasties were large structures with great capacity, reaching 6 m in height, which employed coal as fuel (Figure 2.21), although other smaller devices 2-3 m high built into a hillside and fuelled with charcoal were also utilised in this period. The examination of remains of blast furnaces from late Tang to Jing Dynasties revealed that by this period the furnace design was extremely powerful and efficient allowing an excellent control of the furnace atmosphere, and that these were capable to reach and maintain temperatures of ~1500°C (Huang, X. et al. 2015). Normally, these structures were installed in massive industrial complexes involving up to one thousand workers between mines and smelting sites, normally spreading out some kilometres from the mine to make more efficient use of forest resources for fuel or building purposes. (Wagner 2008, 305-311). Excavations of ironworks of the Song and Yuan periods have been reported in seven Chinese provinces – Anhui, Jiangxi, Fujian, Heilongjiang, Henan, Hebei, and Guangdong –, but not in Hubei (Wagner 2001b).

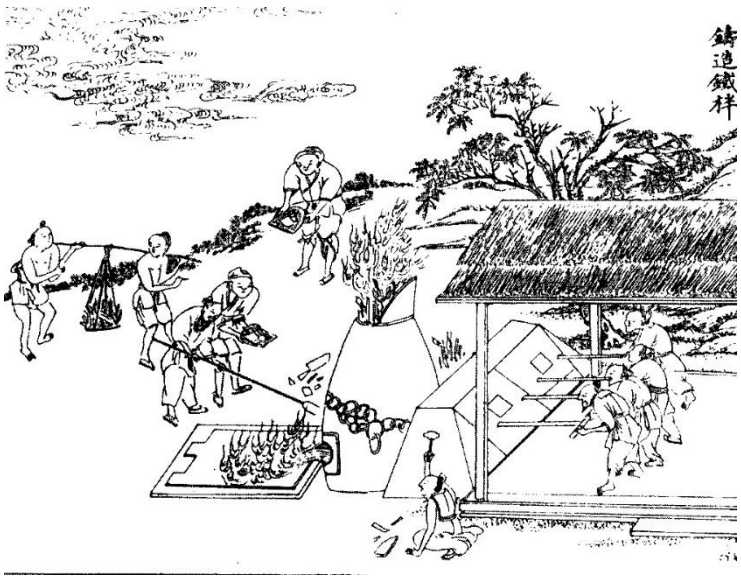

Figure 2.20: Chinese blast furnace of the Yuan Dynasty (~AD 1300).
Original illustration from the Ao bo tu (熬波圖) published in AD 1334. The cupola furnace is visible in the centre, to its right four workers operate the box-bellows to insufflate a constant blast of air. The liquid iron is directly poured into a large mould for a salt-boiling pan. From Wagner (2008, Fig. 130).

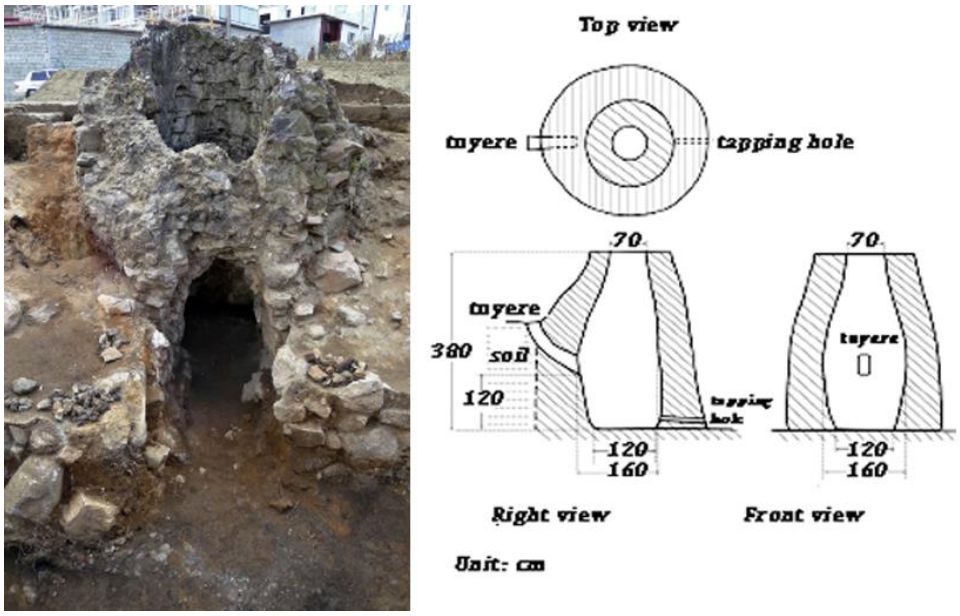

Figure 2.21: Blast furnaces from the Song-Yuan period.
Remains of a Song blast furnace (^{14}C cal. AD 970-1050) excavated in Shuiquangou (Yanqing County, approx. 40 km north of Beijing City). From Huang et al. (2015, Fig. 3 and Fig. 7).

2.6 Summary

This chapter overviews the main technical parameters in order to smelt copper and iron. A major point in copper extraction is the nature of the ore: secondary oxidised ores are less complicate to smelt than primary sulphidic ores, which typically required a multi-staged process and consumed more resources.

The reduction of iron, on the other hand, was achieved in the solid state by means of a technique known as the direct method the result of which was bloomery iron, i.e. a spongy material of iron mixed with slag. The bloom required smithing to obtain purer iron to be workable by forgery. The direct method was the main way to reduce iron in most countries until pre-modern times in which another method – the indirect method – was adopted.

Notably, China was the only country before the 2nd millennium AD that utilised the indirect method to reduce iron. This technique required more sophisticated technology – blast furnaces – to obtain cast iron – iron very rich in carbon very hard but brittle –, which typically also required a second stage – fining or puddling – to obtain iron of improved mechanical properties workable by forgery or casting.

Copper mining and smelting activities were generated at the large-scale in Daye County in Hubei province visible in the metallurgical complex of Tonglüshan, a huge deposit of secondary copper minerals active during the entire 1st millennium BC, if not earlier. While the mining is well documented for the entire period, the smelting has only been described for part of it, specifically at the beginning of the Warring States period (6th-5th century BC). In this time were used powerful furnace structures capable of producing 300 kg of copper per smelting cycle, and also capable of reducing iron if operated differently.

Iron smelting, however, is not archaeologically documented in Daye County, although there are abundant imperial written sources regarding the existence of iron mines. Few furnace structures of Song period (10th-11th centuries AD) were described as puddling furnaces, however, these do not correspond to the usual typology of fining devices and the volume of slag exceeds considerably the volume of by-products that a fining process generates.

After a torrential rain, beautiful verdigris and blue flowers blossom in the mountains.

(Annals of Daye County, edited in Qing Dynasty)

3 Case studies and material assemblage

Daye is at the south-eastern of Hubei province, east-central China. Administratively, Daye is nowadays a county-level city within Huangshi, a prefecture-level city along the southwestern bank of one of the major bends in the Yangtze river, about 90 km southeast of Wuhan, the provincial capital of Hubei. The difference between Daye and Huangshi is pertinent since Daye existed on and off per centuries and included much of today's prefecture-level city of Huangshi, and therefore, what is referred as Daye in written sources may not refer to the current Daye County (Figure 3.1), but to a larger surrounding area.

The economy of Daye County is historically marked by geography: fertile lands surfaced by many swamps and lakes that limited the agricultural use due to the permanent risk of floods – which nowadays are still a problem –, but that also provided fishing. However the richness of Daye remains in the belt of hills containing both ferrous and non-ferrous minerals, and coal deposits; these were known from early times (section 2.5). Ruins of an ancient copper smelter and mining site were found at the nowadays southwest of the city at Tonglüshan in 1974, indicating that there was continuous activity in the area during a 1000-year span throughout the entire 1st millennium BC, yet there are indicators of possible earlier exploitation; the metallurgical activities are evident even in the place name since Daye (大冶) literally means 'great smelting'. There are several references related to metallurgy in Daye in imperial documents from Tang to Qing Dynasties (AD 618-1912), however, most of them are too vague and it is not possible to determine the nature and level of activities developed there (Museum of Huangshi City 1984; Sadao 1986; Wagner 1996; Golas 1999; Huangshi Municipal Museum 1999; Coulson 2012)

The metallurgical importance of Daye is evident in the substantial volume of documentary and archaeological evidence from the 1st millennium BC to modern times, from the pre-imperial mine of Tonglüshan to the Hanyeping cartel, the first modern Chinese ironworks

(1889). Therefore, the suitability of Daye to investigate ancient metallurgical processes – which as mentioned are so far poorly described (chapter 1 and section 2.5) – is entirely justified. Furthermore, another powerful reason to choose Daye is because this is recognised as a birthplace of China's bronze culture, historically related with the Central Plains since Neolithic times and the natural territory of the Chu polity – nominally a tributary state to the Zhou administration –, which became one of the most powerful contenders in the conquest that ultimately lead to the unification of the first Chinese empire (Underhill 1996-97; Lian & Tan 2003; Hubei Provincial Institute 2006; Zhu, J. & Xiong; 2006; Yuan 2013; Wu 2015).

As introduced before, the core focus of the current project are the smelting sites around the main mining area of Tonglüshan which present on surface abundant metallurgical residues – mainly slag but also fragments of furnace wall, roasted ores, and remains of furnace structures are visible in some of them. The eight case studies are: Hongfengshuiku (HF), Mianyangdi (MY), Maochengnao (MC), Wangyuecun (WY), Xiyuqiao (XY), Lidegui (LD), Yanwopu (YW) and Cangxiawu (CX) (Figure 3.1).

The main reason for the selection of these eight sites in particular is basically pragmatic – the collection was immediately available for study. The current Chinese legislation over archaeological heritage is very strict; to receive approval to study archaeological materials is difficult and usually requires very long times. Nonetheless, exclusive permit from the Institute of Cultural and Historical Relics and Archaeology in Hubei Province (湖北省文物考古研究所, 湖北武汉) was given to Prof. Li Yanxiang, co-supervisor of this PhD, from the Institute of Ancient Metallurgy and Materials, University of Science and Technology Beijing (USTB 北京科技大学), who collected the archaeological materials with multiple restrictions and limited availability, to study an assemblage from these sites in 1993 as part of his own doctoral thesis. However, the materials were finally not used and remained unstudied since that date. When the current PhD project started in 2013, the permit to study was still in force and it was extended to HF and LD sites, discovered in 2005, where Prof. Li Yanxiang was also involved. Since no other archaeometric study was ever performed in the area and there is very scant archaeological information concerning any of the sites in Daye except Tonglüshan, at that stage it was decided that a random

selection of sites was actually a suitable sample to establish a preliminary characterisation of the metallurgical remains.

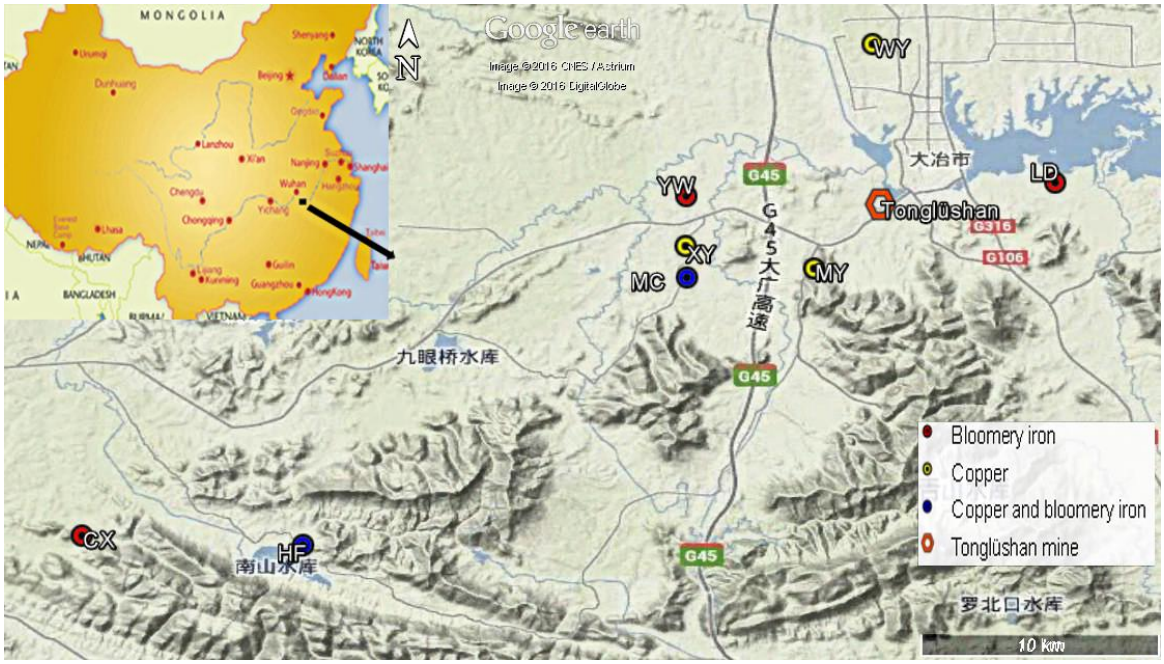

Figure 3.1: Location of the case study sites in Daye County in Hubei Province.

In general, these sites appear catalogued in the Chinese Heritage Atlas of Hubei Province (Hubei Provincial Bureau of Cultural Heritage 2002) as Neolithic (5000-2000 BC), Shang (~1600-1046 BC) or Zhou (1046-256 BC) in date, but there is barely a mention to any metallurgical activity. Typically, the smelting installations span over large areas (~10,000 m² or larger), even though today they are largely covered by crops, wild vegetation, buildings, utility poles and roads that threaten their integrity. An abundance of archaeological materials can be recorded on the surface, in addition to the predominant slag, and including pottery from Neolithic vessels to Ming Dynasty porcelain (Figure 3.2).

The lack of an inventory of the metallurgical activities and their heritage value impacts directly on the preservation of the sites which are severely threatened by four factors: a) houses and infrastructure building; b) agricultural use of the soil; c) spoilers that primarily destroy the slag heaps to re-smelt it; and d) floods and water reservoirs, to the extent that the site of Yanwopu (YW) has been destroyed completely, and the sites of Xiyuqiao (XY) and Wanyuecun (WY) have also practically disappeared.

Figure 3.2: Assorted materials recovered in several sites in Daye.
a) Large slag cakes found in LD; **b)** ceramic, porcelain, ore and slag found in HF; **c)** slag and technical ceramics recovered from all sites in Daye.

The majority of the sites remain unexcavated, and the assemblages studied here were recovered from surface deposits during survey. The only significant archaeological intervention for all the sites was a rescue excavation in Lidegui in 2005. Nevertheless, the excavation itself did not contribute to clarify the nature of the site, and starkingly conflicting interpretations have been presented: while the excavation report (2005 unpublished) states that the furnaces were likely employed to smelt copper and silver during late dynasties (Song and Ming, AD 960-1644), another paper (Wei et al. 2008) suggests that these were in use to smelt iron before the Han Dynasty (206 BC-AD 220), and a third one that the iron smelting activities occurred during mid Qing Dynasty (AD 1644-1800) (Hu et al. 2013). Such uncertainties illustrate the need of both technological and chronological analysis of the metallurgical remains.

3.1 Sampling strategy

Fieldwork in Daye was planned for May 2013, aiming at a reconnaissance survey of the sites; however, the permit was unexpectedly denied one day before the schedule, once the author was already in Beijing. Fortunately, a few samples collected during surveys in 1993 and excavations in 2005 by Prof Li Yanxiang were still available at the USTB Institute for Historical Metallurgy and Materials in Beijing, and these were consequently used as exploratory materials. The collected data was extremely helpful to design the fieldwork to visit the archaeological sites the following year, when the permit was granted by the Institute of Cultural and Historical Relics and Archaeology of Hubei Province, and the archaeological team in Daye directed by Prof. Chen Shuxiang and co-directed by Dr. Qu Yi arranged a date for the fieldwork.

The majority of the samples analysed were collected during a season of field walking and test excavation led by the author in May 2014. Field walking was possible in six of the eight scheduled sites: LD could not be visited since reportedly it was covered after the excavation and thus there was nothing to see on surface. YW was not visited because, as mentioned, the site does not exist anymore. Essentially, the sampling strategy designed together with Prof. Li Yanxiang was dictated by limitations in the permit: we requested a standard number of samples per site – specifically 12 samples of slag and, where available, two samples of furnace wall and one sample of ore. This number of 12 pieces of slag was granted for most of the sites, although a few are below that number since there were no more samples available (YW) or permit to sample more was not granted (WY); MY exceeded expectations with permission to sample 25 pieces of slag. Nonetheless, unexpectedly, two of these sites presented evidence of production of two metals – copper and iron –, and some of the bloomery iron sites also presented reduction and post-reduction slags. As a result, the final analysed assemblage per type of production or activity is different per site, and occasionally is of a rather small size (Table 3.1).

In addition to any human or instrumental errors, there are several factors derived from the nature of the dataset that limit this study, and which will inevitably add some uncertainty in the general characterisation of both metal production systems. These major limitations encountered refer to: 1) a general lack of archaeological context, since all the analysed materials are surface finds, and 2) an irregular number of the analysed

specimens per site, since I used material from past collections and had no input on the sampling strategy.

	HF	*MC*	*MY*	*WY*	*XY*	*CX*	*LD*	*YW*	*Total*
Copper slag	6	9	25	7	12	–	–	–	59
Bloomery iron slag	10	4	–	–	–	12	13	8	47
Furnace wall	3	3	–	2	1	1	2	2	14
Ore	7	1	–	–	–	–	–	2	10
Other by-products	2	–	–	–	–	–	–	–	2
Total	28	17	25	9	13	13	15	12	132

Table 3.1: Sampled specimens per material per site.

The lack of chronological resolution will to some extent be alleviated through comparison with excavated sites, particularly Tonglüshan for copper (Huangshi Municipal Museum 1999) and Lidegui for bloomery iron (Hu et al. 2013), as well as by considering the state of preservation of the sites, which often allows sampling from archaeological levels that are visible on soil sections, and thus facilitated a frame of reference for the sites without any stratigraphy. Even though the situation is far from ideal, the comparison between the studied assemblage and relevant materials together with the existing archaeological data, minimised the impact of a lack of a proper archaeological context and allowed for a coherent framework and sufficient chronological resolution – better defined by the radiocarbon measures (section 4.3.7) – to insert the archaeometric data into a wider historical and socio-economical context.

The second restriction, however, cannot be easily overcome. Access to archaeological materials is tightly controlled in China, and I had no permit to collect any materials from analyses. As such, the assemblages are those made available by Professor Li Yanxiang. As a result, the sampled assemblage per site is highly variable – e.g. 25 copper slags in one site against 6 specimens in another – and without clear criteria of archaeological significance. This limitation in sampling is emphasised in the relevant sections, while at the same time it is hoped that the very findings of the present research demonstrate the validity of this approach and the worth of making the most out of the samples available.

3.2 Site descriptions

The site descriptions are organised by the metal production type documented: the first two – HF, MC – present remains of copper and bloomery iron production. Then three copper production sites are presented – MY, WY and XY –, and finally the remaining three sites with only bloomery iron production remains – CX, LD, and YW.

3.2.1 Hongfengshuiku (HF), 洪枫水库

HF is not registered in the archaeologic Atlas of Hubei Province (2002) since the site was discovered in 2005 due to extraordinary circumstances. Around 90% of the area of Hongfengshuiku remains under the water of a reservoir. Abundant, relatively well preserved features are partially visible only during the summer or under extremely dry conditions, as was the summer of 2005 when the water level was low enough to allow archaeological works.

The 2005 campaign identified one heap of slag of considerable dimensions, ~2 m high and over 5 m long (Figure 3.3). Close to the slag heaps were identified several larger rounded structures associated, one of which was excavated revealing that these were porcelain kilns not associated to the metallurgical production. In a different area, approximately on the opposite bank of the reservoir, one shaft furnace was located as well. In 2014 none of these structures were visible, however new slag deposits were located on the banks as well as two new furnaces visible on the natural section. A sequence of four samples of charcoal was extracted from one of these furnaces and another five were found within slag cakes.

Due to the waterlogged circumstance it is very difficult to estimate the dimensions of the site, this seems to occupy an area of ~20,000 m^2, however, it is possible that the water had dispersed the materials on surface, thus giving a false impression of large dimensions. Also it needs to be considered that three different pyrotechnical industries – copper smelting, bloomery iron and porcelain – took place in the same area but the space delimitation per industry is not defined.

Figure 3.3: Archaeological remains visible in HF.
a) Large slag heap found in 2005; **b)** small deposit of slag, ore and ceramic found in 2014; **c)** tapping hole of a small furnace structure visible in section in 2014, the pen indicates the estimated position of the charging hole; and **d)** porcelain kiln excavated in 2005. 2005 images courtesy of Professor Chen Shuxiang.

3.2.2 Maochengnao (MC), 茅城垴

MC is catalogued in the Atlas of Hubei Province (2002, 43); estimated to have 30,000 m^2 of area and 0.8 m of stratigraphic deposit. It was first discovered in 1993 when several areas of rubefacted soil, slag, and one furnace structure were visible on surface. On surface was collected a large number of lithic and pottery materials dated from Neolithic to Western Zhou. The Neolithic pottery is coarse and grey with several distinct ware tripods whereas the Western Zhou Dynasty pottery is finer and displays red and orange colours.

In 2014 the terrain appeared heavily covered by vegetation that the locals use as pastureland to graze livestock, with a small part covered by a reservoir and a further

section affected by a graveyard or memorial (Figure 3.4). No materials were at sight except on one hill that contained several slag fragments at the bottom and a piece of furnace wall. On that same hill was located a furnace in 1993 when the site was identified for the first time as a smelting workshop, and a charcoal fragment was collected from the wall of the furnace. Unfortunately, the current conditions made it impossible to re-locate that structure or any other.

Figure 3.4: General view and detail of section of MC in 2014.

3.2.3 Mianyangdi (MY), 眠羊地

MY is catalogued in two different sources: Museum of Huangshi City (1984) and in the Atlas of Hubei Province (2002, 42), although the information included in the second is practically copied from the first source. According to these sources the site might be dated to the Neolithic and Shang-Zhou periods; the estimated total area is about 10,000 m^2; and the stratigraphic deposit is about 2 m deep. A large amount of slag could be found on surface, as well as abundant red and grey clays pottery sherds, and few lithic tools. In addition, two bronze artefacts (a spear head and a bell) were collected on the surface in 1984. Most of these finds can be dated to the Shang and Zhou periods (1600-256 BC) such as characteristic wares with ears, and pointed foots of Ding tripods some of which are inscribed on the foot with the character Li (鬲). A very distinct ware diagnostic of the Western Zhou period was found; this is a shallow square-shaped Dou (豆) plate with

radiating pattern. The two bronze artefacts are also supposed to date to these periods, more likely Western Zhou (1046-771 BC) than Shang.

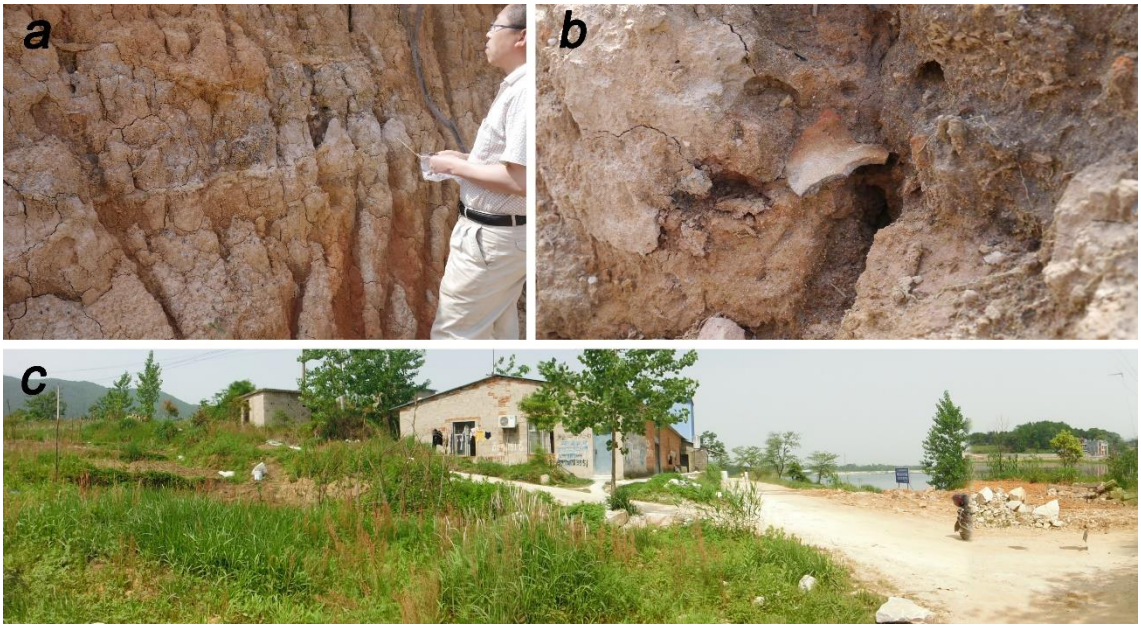

Figure 3.5: Archaeological remains in MY.
a) Archaeological deposit visible in section; **b)** detail of a large piece of ceramic protruding from the deposit; **c)** panoramic view of MY, the promontory is at the centre, the reservoir at the right and the section detail in a and b (not visible) is to the left.

In 2014 the large heap of slag was not visible and in all probability has been dismantled since the site has suffered several alterations. By then, the heap looked like a promontory cut by two roads, sloping down into a reservoir (Figure 3.5). An archaeological deposit of 1-2m deep was visible on the section open by the roads, and two samples of charcoal were taken from it. The slag appears preferentially close to the water mixed with abundant red clay pottery sherds. MY is the only site where fragments of furnace lining were not found (Table 3.1).

3.2.4 Wangyuecun (WY), 王月村

WY is succinctly mentioned in the Atlas (2002, 47). It is mentioned that the site is 350m to the northwest of Luojia village (罗家村) and that the total area is about 3000 m^2.

Pottery sherds – not described – were collected on the surface and roughly dated to the Zhou period. There is no mention of slag or other archaeological remains.

In 2014 the site was severely affected by constructions that had destroyed most of the archaeological deposit (Figure 3.6). Most of the soil was removed and levelled at ~2m of the original surface; several deeper trenches were being dug for pipelines and the foundations of a storehouse, and a pool and artificial canal for water drainage were already built up over the archaeological deposit. All the terrain displayed plenty of pieces of slag and ceramic sherds, mostly grey pastes that possibly date to the Shang period (1600-1046 BC) but also fragments of red vessels that possibly date to the Warring States period (475-221 BC) (Dr. Qu Yi personal communication).

Figure 3.6: View of WY in 2014, with construction works in progress, and detail of slag and ceramics visible on surface.

3.2.5 Xiyuqiao (XY), 栖杅桥

There is no published record of this site. In 1993 there were visible abundant pieces of slag, red clay fine ceramics and many pieces of furnace wall (Prof. Li Yanxiang personal communication). Unfortunately, the soil has been removed and levelled for agricultural use in the current times, and no traces of any archaeological deposit was found in stratigraphy, although the borders of the cultivated land still show abundant fragments of slag (Figure 3.7).

Figure 3.7: Current aspect of XY.
The original landscape was formed by hills like the ones visible in the background.

3.2.6 Cangxiawu (CX), 仓下吴

There is no archaeological information about this site although based on the appearance of slag it covers a large surface of ~3,000 m^2. Most of the site is covered within a small forest although pieces of slag are visible everywhere in the paths, and also as small heaps of ~1m high totally covered by soil and vegetation (Figure 3.8). No ceramic evidence was associated to the slag and thus there is no chronological information; however, the general opinion of most of the provincial archaeologists in Daye was that the site was dated to the Song Dynasty (AD 960-1279).

Figure 3.8: Current aspect of CX with all the features heavily covered by wild vegetation, and detail of pieces of slag embedded in the soil.

3.2.7 Lidegui (LD), 李德贵

LD is the only smelting site in Daye other than Tonglüshan that has been excavated. The following abstract has been extracted from Hu et al. (2013).

In May-July 2005, the Hubei Provincial Institute of Archaeology together with the Museum of Huangshi conducted a rescue excavation at Lidegui village, Chenguizhen, Daye County. The total excavation area was 160m^2. Six stratigraphic layers were identified; 2nd-6th are dated to the Qing Dynasty while the 1st one correspond to the current soil (Figure 3.9). Abundant slag ('hundreds of kilos of slag') is found in all layers. In addition, in the 3rd, 5th and 6th layers, were found 11, 10 and 1 furnaces respectively. The furnaces structures are small – shafts have ~40 cm of diameter and 50 cm high – with a "D" shape, and clustered closely. Each of them was only used for a short period and many of them were repaired several times (one was repaired 17 times); all the furnaces are entirely built up with clay, no other material – bricks, stone, etc.– was utilised. Apart from the furnaces and the slag: charcoal, iron ore powder, fragments of furnace base lining (is not clear if these are fragments of any of the 23 furnaces or if it refers to other structures), porcelain sherds; and two iron bars were found at this site.

The slag was analysed chemically revealing that this is fayalitic slag, and the microstructure was described as glassy matrix containing only fayalite crystals and wüstite (FeO). The Cu-content is very low (ppm) and therefore copper smelting was discarded while the discussion is focused in the comparison of the slag with cast iron slags, highlighting the extremely rich Fe-content and very low Ca-content of the LD slag in comparison, and suggesting that perhaps this was generated during a preliminary stage of cast iron production. The iron ore was analysed and found to be quartz, haematite and magnetite, with FeO content of ~50-60%.

The paper concludes that there are very few examples of bloomery iron smelting in China while there are many of puddling or fining process, and thus this may be the result of puddling. However, the Lidegui site has too much slag to be just an iron puddling site and, therefore, on the basis of the high Fe and low Ca content of Lidegui slag, they tentatively suggest that it may be a bloomery iron smelting site (Hu et al. 2013, 303).

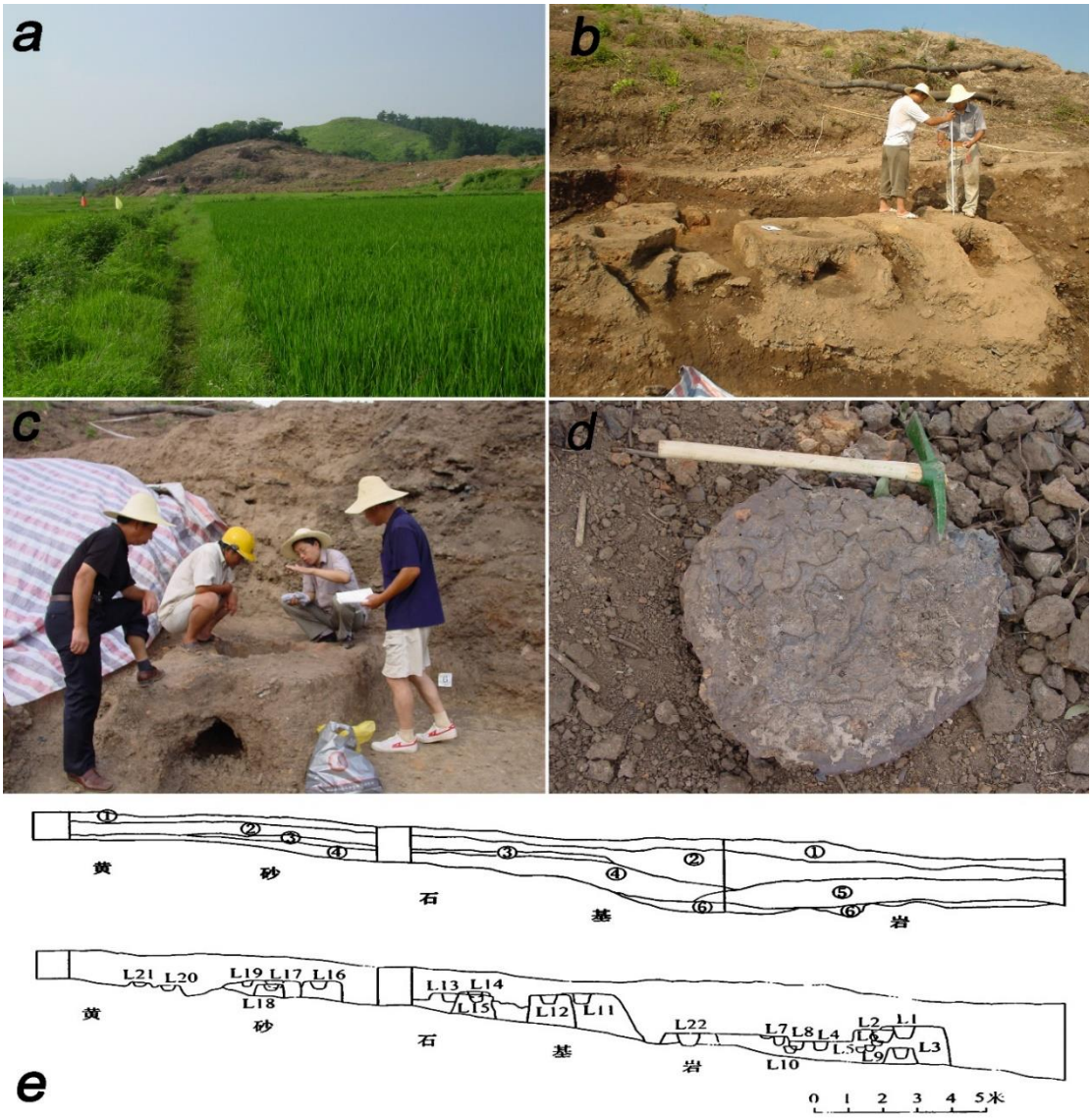

Figure 3.9 : Archaeological remains of LD.
a) Original landscape of LD in 2005, the excavated area is visible to the left of the hill; **b and c)** excavation of furnaces in progress, note the small size of the structures; **d)** complete slag cake; and **e)** stratigraphic profile of LD, detailing the layers (up) and the disposition of the furnaces, after Hu et al. (2013, Fig. 1-2). The five Chinese characters at the bottom mean approximately 'yellow sandstone bedrock'. Scale is in meters. Images courtesy of Prof. Chen Shuxiang.

3.2.8 Yanwopu (YW), 燕窝铺

The site is also called Yanwoshan (燕窝山), 200m to the northeast of Yanwopu village (Hubei Provincial Bureau of Cultural Heritage 2002, 48). This was a massive site (30,000 m^2) in principle dedicated exclusively to smelt mineral since no other materials were recovered, and is described a deposit of slag of about 1.2 m thick. It is mentioned that 'the date is not clear'.

All secrets can be fathomed in miniature.

(Rumo and his miraculous adventures)

4 Theoretical framework and methodology

The aim of this chapter is to provide an overview of the conceptual and methodological parameters adopted in this thesis to facilitate the study of technology within the *social construction of technology* framework. Technology is a term that has been revised constantly within different philosophical and historical contexts (e.g. Lemonnier 1992; Pfaffenberger 1992; Dobres 2000, 47-95; Charlton 2006; Miller, M.-L. 2007, 4). In this thesis technology is defined as a production process which involves knowledge and resources required to manipulate raw materials and create products. Traditional approaches to technology depict it as a circumstance external to society, whether it is seen as an anonymous collective phenomenon – e.g. the inception of metallurgy –, or as the personal achievement of certain individuals – e.g. Henry Bessemer and his process for steelmaking. It is only the consequences of technological inception and innovations that are considered as fundamental pieces of human history, receiving much attention from many scholars, and as such they have been approached from many different perspectives – e.g. historical, sociological, anthropological, political, environmental, etc. However, technology itself is only explained scientifically or, at most, as part of Economic History (e.g. Cipolla 1976; Hauptmann 2007). This study understands technology as an integral part of a system fully interactive with culture and society, not as an isolated phenomenon. In other words, the development of ancient technologies was not purely dominated by technical factors, but also strongly influenced by human factors (e.g. needs, cultural preferences, values, aesthetics, knowledge limitation, social structure, etc.) forming a 'seamless web' with society (Hughes 1986, 1987) in which political and cultural circumstances are as important as the natural environment or physical constraints.

Materials and technologies, as products and expressions of social and cultural phenomena, can inform on societies and cultures of reference, allowing a better understanding of past social and cognitive structures and reconstructing relationships between humans and environment (Dobres 2000, 164-211; Martinón-Torres 2008, 23), This approach is known

as *social constructionism* (Pfaffenberger 1992; Killick 2004; Martinón-Torres & Killick 2015).

4.1 Chaîne opératoire and technological choices

This research thus aims to investigate the *chaîne opératoire* for base metals production in Daye county (Hubei province, China). The *chaîne opératoire* is a conceptual framework (Figure 4.1) especially suitable to the reconstruction and interpretation of technical information in terms of artefact 'life-histories'. It seeks to describe and contextualise a number of events in the life of the artefact, including the sequential technical operations from raw material transformation into artefacts; the by-products generated and discarded on the process; and the relationship between design, raw material and end product; and allows the investigation of *technological choices* of artefact production, use, and repair (Pelegrin et al. 1988 in Dobres 2000, 167). The concept includes five elements (Lemonnier 1992): *matter* (raw material), *energy* (to transform the matter), *objects* (tools or means of work: e.g. adzes, furnaces), *gestures* (which 'move' the object, and are organised into linear operational sequences), and finally, specific *knowledge* or *know-how* (which refers to the specific shape that a technological action takes as a result of all different possibilities and choices). Perhaps the most powerful contribution of the *chaîne opératoire* to the study of technologies is that it has allowed scholars to move away from technological determinism, giving prominence to the many individual stages involved and the numerous choices that have to be taken in the entire sequence of production (Ottaway 2001). As put by the French prehistorian Leroi-Gourhan, who developed the concept in the 1960s century: 'without (human) gestures that move it, without matter on which it acts, without the knowledge involved in its use, an artefact is as strange as a fish without water' (in Lemonnier 1989, 156).

As is shown in Figure 4.1 the focus of a *chaîne opératoire* approach is wide and encompasses stages from the collection of raw materials to artefact use and ultimate destruction; it also includes the archaeological recovery and use of artefacts as research or educational material – thus potentially yielding a full 'life cycle'. As explained previously, most studies on ancient Chinese metallurgy are focused on finished objects and thus can

only contribute to reconstructing the cycle from the artefact fabrication step, failing to incorporate valuable information regarding technical dynamics, social structure and historical context. There is a clear gap that can be filled.

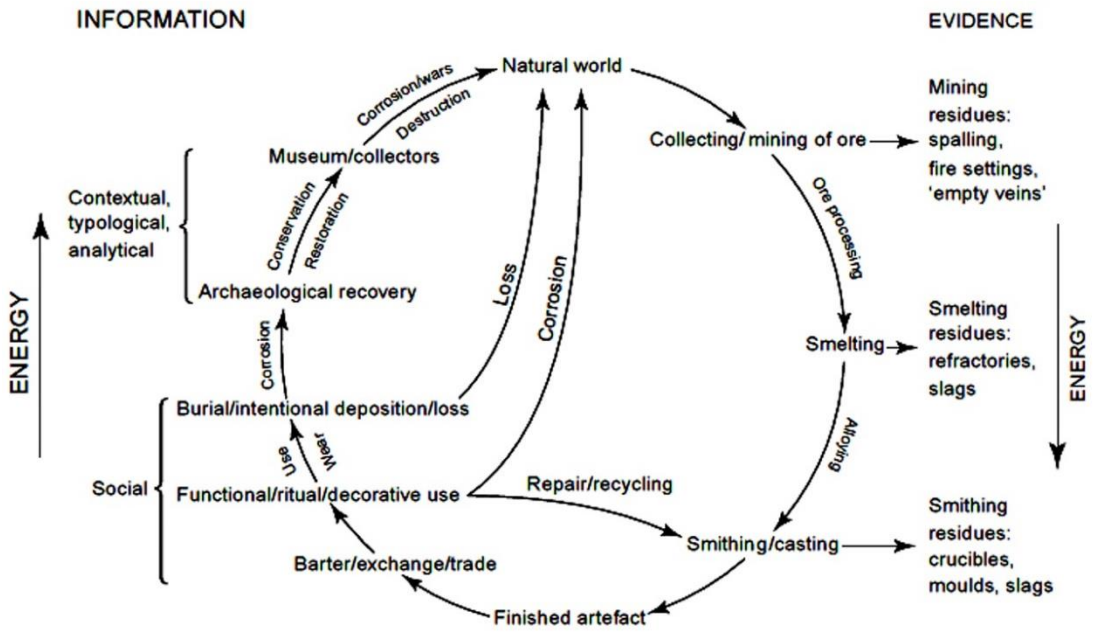

Figure 4.1: Metallurgical chaîne opératoire or 'Cycle of copper production and working'
After Ottaway (2001, Fig. 1).

In the past, most studies of Chinese metallurgy have been limited to art-historian, typological and metallographic studies. This information allows archaeologists to group the objects, and reveals details as to how they were constructed. However, this does not reveal a great deal about the transformation of raw materials into cultural objects or provide information about how the mining and smelting industries were organised. As a graphic example, many studies focus on slag inclusions in iron objects and struggle to determine whether they indicate that the object is product of bloomery iron or cast iron; the conclusion is frequently open and ambiguous 'they were produced either by bloomery iron or by cast iron' (Wayman & Michaelson 2006, 103, similar quotes can be found in e.g. Scott & Ma 2006 or Liu et al. 2014). Nonetheless, the comparison between slag by-products from the primary processes offers considerably more certainties and allows for a clear identification of how the metal was formed (Killick & Gordon 1987; Buchwald 2003).

4.2 Technological choices and technological change

Decisions made by workers in the production process are the backbone of the *chaîne opératoire*. These decisions are known as *technological choices*, which explain technological variation within specific socio-ecological environments as the result of complex interactions between techniques, tools, functional goals, and decisions between functional equivalents (Lemonnier 1993, 3). Technological choice is employed to investigate this decision-making process and implies that technology is an aspect of culture – not a consequence of it – (Sillar & Tite 2000), and ultimately refers to the selection of a particular technological solution over many other alternatives. For example, steel can be produced by carburisation of bloomery iron, decarburisation of cast iron, or by an intermediate approach to produce high carbon steel in bloomery furnaces (Merwe & Avery 1982) – in addition to a myriad of other subvariants and individual choices made within each of these pathways.

A particular technological choice will reflect social preferences or decision-making actions in order to meet with certain socioeconomic, political, and cultural needs (Figure 4.2). A very clear example of technological choice is the case of Chinese cast iron: cast iron technology was developed as opposed to the bloomery technique due to the interaction between the bronze piece-mould casting cultural tradition, and other associated technical and socio-political aspects – e.g. early invention of blast furnaces, strong political administrations, the necessity to develop economies of scale due to the large population which resulted in large demand, the availability of abundant labour force, etc. It is difficult to determine which of these arguments was the most decisive in the choice, but it is likely that they all played a part in shaping this technology in its context (Tylecote 1981; Hua 1983; Dai & Zhou 1995; Wagner 1996; Hua 1996-97; Han 1998, 2013).

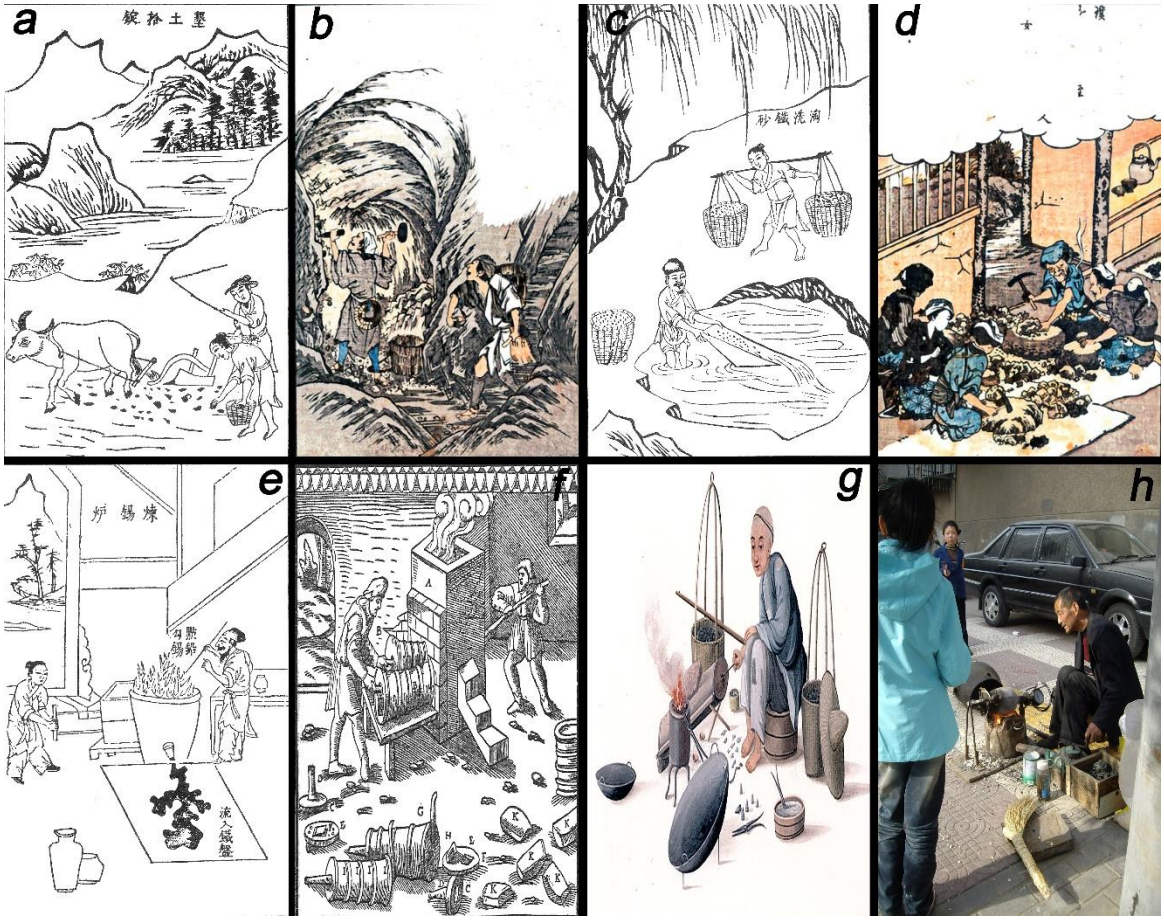

Figure 4.2: Variety of technological solutions applied to resolve the same problems.
Two strategies to collect the ore: by **a)** ploughing the soil (Sung 1966, Fig. 14-18, original illustration from AD 1637), and **b)** by deep mining (Tsuna 1983, Plate II, original illustration from 1801);
Two strategies to dress the ore: by **c)** concentration by washing (Sung 1966, Fig. 14-9) and **d)** by crushing and sorting (Tsuna 1983, Plate III);
Two strategies to smelt tin: e) in China using low shaft furnaces and box-bellows to obtain liquid tin and lead (Sung 1966, 14-13), and **f)** in Europe using tall shaft furnaces and accordion bellows to obtain tin ingots (Hoover & Hoover 1912, 421, original illustration from 1556);
Finally, g) street craftsmen using a portable stove in Guangzhou in the mid-19th century (Wagner 2008, Plate XI), and **h)** street seller in Xi'an in 2011 using a similar device. However, the difference between them is enormous since the first one is a wok repairman and the second is making popcorn!

Finally, the concept of technological choice acknowledges that decisions, whether individual or collective, conscious or unconscious, are influenced by cultural, economic, political and ideological systems within which the workers operate, as well as by environmental conditions, material properties and natural laws. Most of these factors are going to change throughout time, e.g. the prevailing taste is surpassed, technological discoveries are made, political systems adjust affecting transportation and the

accessibility of materials (new borders, taxes, etc.), population grows or declines affecting models of production, resources are depleted, etc. As a result we have *technological change*: technology is adapted to the new conditions typically through a sequences of modifications that result of rational choices – usually gradual rather than sudden or dramatic –, and inheriting all the previous background (Lemonnier 1992, 1993; Roux 2008; Charlton et al. 2010).

4.3 Slag as research material: laboratory methods

The choice of slag as the primary material for reconstructing the metallurgical process is well-established in the archaeometallurgical world (e.g. Rothenberg 1990; Pleiner 2000; Hauptmann 2007; Humphris and Rehren 2013). Slag is the waste resulting from metallurgical processes, and it traps information about all the elements that were part of the system. Therefore, chemical and microscopic analyses of slag are extremely informative about the smelting process, and can inform of facts such as the nature of raw materials (ore, fluxes, etc.); type of structures in which this was generated (crucibles, furnaces hearths, etc.); temperatures and atmosphere of the reduction; efficiency of the extraction; volume and standardisation of the process; etc. An important component of this archaeometric toolkit is the ontological perspective that chemical, microstructural and other kinds of data extracted by materials science methods are artefacts of human behaviour, but that these are bound within natural law. Rather than mere tools for classifying a technology or specifying the use of some natural resource, slag analyses may provide access to culture and decision-making in the past. High-resolution materials science allow empirical explorations of archaeological theory such as the study of materiality and the reconstruction of the *chaîne opératoire* (Charlton et al. 2010; Martinón-Torres & Killick 2015).

4.3.1 Laboratory-based analytical methods

The choice of analytical methods used in this thesis was primarily shaped by three major factors, which also apply to the sample preparation and presentation of results.

The first one is the appropriateness of the methods to the research questions. Given the concern with a full characterisation of base metal production, it was decided that chemical, microstructural and mineralogical data were needed. Therefore, the primary tools selected were: 1) optical microscopy (OM), and 2) scanning electron microscopy with an energy dispersive spectrometer (SEM-EDS) to describe and analyse mineral phases and internal microstructures; and 3) bulk chemical analysis by wavelength dispersive X-ray fluorescence (WD-XRF), following well established procedures (Bachmann 1982; Miller, D. & Killick 2004; Hauptmann 2007; Charlton et al. 2013). A further technique used for the characterisation of the ore samples is X-ray diffraction (XRD).

A second important parameter was access to equipment and consumables: the three main techniques are available at the Wolfson Archaeological Science Laboratories located at the UCL Institute of Archaeology – although in the course of this research it was decided to undertake the XRF analyses in a different laboratory, as reported below.

The third factor was to create new data that would fit in with existing and current work elsewhere, in order to make it easily comparable. This last factor supported the selection of WD-XFR – since most of the published copper and iron slag assemblages utilised XRF – as opposed to alternative bulk chemistry methods such as inductively coupled plasma atomic emission spectroscopy (ICP-AES).

4.3.2 Sample preparation

All the selected specimens from fieldwork were cut at the Institute of Ancient Metallurgy and Materials (USTB) in Beijing, and only the fragments were exported to London. In the majority of cases there was enough material to produce both a polished block – for OM and SEM-EDS analyses – and a pellet or powdered material – for WD-XRF and XRD. Occasionally, due to the original size of the sample or miscalculations, there was not enough material to perform all the analyses. In these cases, it was decided to utilise the available material in a polished block since this can be analysed by OM and SEM-EDS to describe microstructure and mineralogy, but also an indication of the bulk composition can be obtained by averaging chemical analyses of several areas per sample using SEM.

Prior to sampling, each specimen was recorded: this included dimensions, weight, macroscopic description, photographs and a magnetic test (performed on a fresh section after cutting, also tested on the powdered samples once in London). The magnetic test was particularly useful to roughly discern the copper and the iron slags since generally the former reacts strongly to the magnet whereas the latter weakly. The samples were mounted in using epoxy resin and prepared by grinding on successively finer abrasive paper – from P120 to P4000 – before being polished with diamond paste to a 1 µm finish. Only one sample – HF7, a piece of metallic iron – was polished to a 0.25 µm finish.

A second piece of the sample weighing 6 g – to ensure the necessary minimum of 4 g – was powdered for WD-XRF and XRD analyses, after removal of any adhered material (e.g. soil particles, corrosion). The samples were crushed by hammering a metal piston encased in a metal cylinder onto the sample, and the resulting fragments were then milled to a grain size of approximately 50 µm, using a tungsten carbide planetary mill. For the WD-XRF analyses the powder was dried for 24 hours to remove moisture, and finally mixed with 0.9 g of wax, heaped into an aluminium holder and pressed into a homogeneous pellet using 15 tonnes of pressure for 2.5 minutes.

4.3.3 Optical Microscopy (OM)

The optical microscope was used for preliminary examination of the sample in order to determine mineralogical composition, degree of homogeneity, shapes and sizes of crystals, as well as any possible features revealing characteristics of the production process or formation history of the material. The examination was undertaken on a Leica DM4500 P LED polarisation microscope, equipped with a Leica DFC 290 HD camera. Micrographs of interesting areas were systematically obtained throughout the analysis (200X, 100X and 50X magnification).

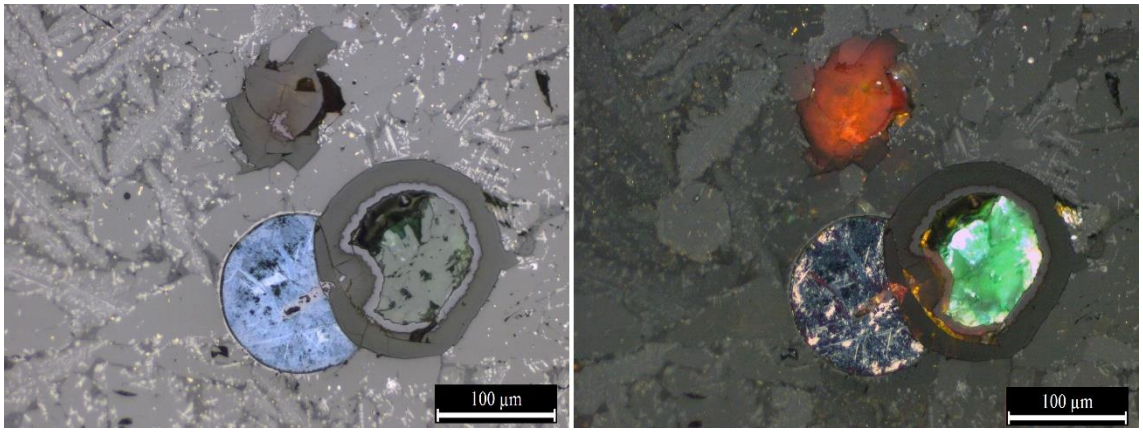

Figure 4.3: OM micrograph showing the same area under reflected PPL (left) and XPL light. The sample shows a multi-phased copper mineral grain (centre) attached to a gas bubble, and iron oxides (light grey) dispersed on glassy matrix. The blue sulphides in the left graph are much more easily recognisable as covellite (CuS, brass-yellow) and chalcocite (Cu_2S, indigo) in the right.

OM was also used in its own right to characterise certain minerals, particularly useful in the identification of metal-rich phases. Since many constituents of slag and ore are opaque, reflected polarised light was used, however, the combination of plane polarised light (PPL) and cross-polarised light (XPL) where appropriate, helped considerably in the diagnostic identification of some minerals by their optical properties such as crystal shape, colour or reflectivity (Figure 4.3); the last two properties not appreciable by SEM. Unless otherwise specified, all OM micrographs shown in this thesis are PPL images.

The terminology used to characterise the slag microstructure mineralogically borrows many terms from geological descriptions (Bachmann 1982). Some major references used are Miller and Killick (2004) for copper and bloomery iron slag; Hauptmann (2007) for the copper slags; and Buchwald (2005) and Selskiené (2007) for bloomery iron slag, although characterisations have been taken from many more sources which are referenced appropriately in the corresponding sections. Another technique borrowed from petrological studies is the frequency labels referring to concentration of minerals within the microstructure to estimate the percentage of area occupied in the polished block (Table 4.1). The labels described in the table are given as a guidance, since the original proposal is thought for thin sections, where the grains are counted rather than merely estimated (Whitbread 1995). However, the labels were found to be useful for the systematic description of the slag.

Predominant	Dominant	Frequent	Common	Few	Very few	Rare	Very rare
>70%	50-70%	30-50%	15-30%	5-15%	2-5%	0.5-2%	<0.5%

Table 4.1: Frequency labels estimating the percentage areas of concentration of features.

4.3.4 Scanning electron microscopy-energy dispersive spectrometry (SEM-EDS)

The SEM-EDS analysis was used to complement the information gathered during the optical microscopy sessions by the analyses of the average composition of small particles, and also to obtain a chemical composition of the bulk sample by averaging three to five area analyses of 1 mm by 0.8 mm each.

A JEOL 8600 Superprobe electron-probe microanalyser (EPMA) fitted with a back-scattered electron (BSE) and secondary electron (SE) detector for imaging, and energy-dispersive spectrometer (EDS) for compositional analysis was utilised for phase analysis. SE imaging was mainly used to check the focus of the electron beam. BSE imaging reflects variation of chemical composition among different microscopic phases, where phases with higher average atomic number are brighter in greyscale. All the SEM micrographs shown in this thesis are BSE images.

For analysis the electron beam of the JEOL was set to 20.0kV, and the beam current stabilised at 5.0 $x10^{-8}$ A. Oxford Instruments INCA software was used to interface with the EDS. All analyses were conducted with a working distance of 11 mm, an acquisition time of 50 seconds, and a beam current of 50nA, resulting in utilizing typical deadtimes between 26 and 34%. Oxygen was calculated by stoichiometry and the results, in both atomic and compound weight percent, normalised to 100% to facilitate comparability. Unless otherwise noted, all the results in this thesis are normalised and given as weight %.

The JEOL 8600 probe was fitted with a Faraday cup and a beam stabiliser which maintained the current of the electron beam, resulting in a higher accuracy and precision than typical of most SEM instruments; the analytical totals were checked routinely and these rarely ranged more than between 98-102% unless analysing corroded or very porous surfaces.

The precision and accuracy of the machine was monitored by repeatedly analysing homogeneous basalt and glass standards using the certified reference materials (CRMs) BCR-2, BHVO-2 b and NIST 1412; Swedish slag to evaluate slag samples; and NCS Clay DC60105 (China National Analysis Centre) and NIST76a burnt refractory were used or comparison with ceramic samples (Appendix II). Results show that precision errors are generally below 10% relative. The confidence limits of the JEOL Superprobe 8600 are established at 0.5 wt%, and analyses of CRMs demonstrate that when the concentration of a given element is lower than 0.5 wt%, accuracy decreases with relative errors higher than 10%. It must be noted that only basalt and glass standards were prepared as polished blocks, whereas the rest of the reference materials were only available as powders pressed in pellets. Precision and accuracy tests on these instruments show lower analytical totals as well as higher analytical errors, but these can be attributed to porosity and mineralogical effects rather than instrument performance, as demonstrated by the better results on polished blocks.

4.3.5 Wavelength dispersive-X-ray fluorescence spectrometry (WD-XRF).

WD-XRF was used to provide quantitative bulk chemical information for all samples except for the furnace ceramics since due to miscalculation during the sampling in 2014 there was not enough material to produce both a polished block and a pellet. Unfortunately, the assemblage was already sent back from the USTB in Beijing to Daye when I travelled to Beijing in 2015, and therefore there is no WD-XRF analyses for any of the 14 fragments of furnace wall.

This instrument has lower detection limits than a SEM-EDS for most elements and therefore is suitable for analysing minor and trace elements. Unlike SEM-EDS, where specific areas are analysed, bulk chemical information obtained from this methodology represents the mean composition of the sample.

The initial plan was to carry out bulk chemical analyses using a Spectro Lab XPro 2000 ED-XRF machine available at UCL; however, data quality on slag was found unsatisfactory and difficult to improve. Therefore, the samples were submitted for WD-XRF analyses to

Vincent Serneel's laboratory at the University of Fribourg, Switzerland. The same reference standards used for the SEM-EDS were used to assess the precision and accuracy of the WD-XRF in Fribourg. This was a Philips PW2400 sequential model, which used the UNIQUANT 5 analytical programme for quantification.

Overall, precision for the WD-XRF measurements of the standard materials was acceptable, as can be appreciated in the comparison of the same CRMs analysed on 10th April and 18th November 2014. In terms of precision, the CVs of most compounds calculated are below 5% whereas specifically the four major compounds present in the Daye slag FeO, SiO_2, Al_2O_3 and CaO are below 2%, therefore indicating that the results were precise and replicable compared with the same CRMs analysed on 10th April and 18th November 2014. Exceptions could be seen in the oxides with low concentrations: vanadium oxide (V_2O_5), chromium oxide (Cr_2O_3), lanthanum oxide (La_2O_3), and cerium oxide (CeO_2) where the CVs were above 15%. However, in this research trace elements are mostly irrelevant for all the interpretations except when using trace elements as a criteria to discern between smelting and smithing slag, and even in this case precision errors do not affect the interpretation (section 6.4.4.2). Like the SEM-EDS system, oxygen was not measured by the WD-XRF, so all elements were converted to oxides by stoichiometry and normalised by the laboratory as part of the quantification system employed. All iron is reported as FeO – converted and normalised from the original iron oxide reported as Fe_2O_3 (Appendices III-V). FeO was the most commonly occurring valency of iron in slag samples, as observed by OM and SEM-EDS – e.g. fayalite (Fe_2SiO_4). By default, FeO is reported for all iron oxides for simplicity and to facilitate comparisons between the materials and mass balance calculations, even though of course multiple oxidation states could occur.

4.3.6 X-Ray diffraction (XRD)

X-Ray diffraction is primarily a qualitative method, used to identify mineral phases that cannot be defined microscopically, by determining the nature of crystalline components and structures; SEM-EDS and XRF analyses can determine that the analysed sample has an iron content of xxx%, but cannot establish the iron oxide mineral – e.g. iron hydroxides

FeO(OH), magnetite (Fe_3O_4), etc. In this thesis XRD is used on the ore samples to identify the nature of the iron minerals.

The instrument used was Benchtop XRD Rigaku MiniFlex 600. A small quantity of milled sample (<1g) was placed on a small glass plate and installed into a clamp, and the analysis was run using the normal operating condition which is 40kV and 15mA; the measurement condition set up in 90 minutes. The interpretation of spectra was performed by the Rigaku PDXL application and despite of the reference library available was quite limited, yet it was sufficient to suggest the main minerals present in the sample (Appendix VII).

4.3.7 Radiocarbon dates

The chronological characterisation of the sites is of the upmost importance for this thesis since, as seen in chapter 3, the temporal framework was far too vague covering a period of ~2000 years. It was hoped that funding for radiometric dating would be found to date the material collected from Daye and provide as accurate a chronology as possible for the smelting events being studied. Funding was sought to date fifteen charcoal samples recovered from within smelting slag cakes, furnace base fills and stratigraphic deposits from four smelting sites across the area (Table 4.2). Funding was awarded on 22 December 2014 by the NERC radiocarbon facility of the University of Oxford but accepting only samples of short-lived identifiable materials. Therefore, a taxonomic study of the charcoal was performed by Phillip Austin, archaeobotanist at the UCL Institute of Archaeology. Finally, following both UCL and NERC criteria, eight samples were discarded and the NERC agreed to conduct seven measurements on the remaining samples; the results were sent to the author on 7 July 2015 (Table 4.2). Unfortunately, the three charcoal samples recovered from copper smelting sites were not recommended for analyses, and thus all the measured samples correspond to iron smelting remains only.

The calibration was done with OxCal 4.2 software (Bronk-Ramsey & Lee 2013). The results of all seven samples fall between the years AD 1646-1930, although the samples concentrate in the period 1650-1806 with a probability of 85%, with very scant possibilities of being later than 1806 and between 20-30% of being earlier than 1735 (Figure 4.4).

SAMPLE	PROCEDENCE	YEAR	FAMILY	GENUS/SPECIES	RING COUNT	COMMENTS	^{14}C	RESULTS*
LD001	Furnace fill	2005	ROSACEAE	cf Chaenomeles sp.	<10	Twig/small round wood	Recommended	**203±25**
HF2005	Slag cake	2005	MAGNOLIACEAE	cf Magnolia sp.	<15	Twig/small round wood	Recommended	**190±25**
HFC1	Furnace fill	2014	JUGLANDACEAE	cf Platycarya sp.	<10	Twig/small round wood	Recommended	**199±24**
HFC2	Furnace fill	2014	ROSACEAE	cf Chaenomeles sp.	<8	Twig-wood	Recommended	**213±25**
HFC3	Furnace fill	2014	JUGLANDACEAE	?	<7	Twig-wood	Recommended	**212±25**
YW13	Furnace fill	1993	FAGACEAE	*Quercus* sp. (x1)	<3	Twig-wood	Recommended	**239±25**
YW13b	Furnace fill	1993	RHAMNACEAE	*Rhamnus* sp. (x1)	<5	Twig-wood	Recommended	**213±24**
HFC4	Furnace fill	2014	Indeterminate	?	?	Hard-wood/Knot-wood	Not Recommended	
HF24	Slag cake	2014	Indeterminate	?	?	Fragments too small for ID	Not Recommended	
HF21	Slag cake	2014	PINACEAE	Pinus sp.	>5	Mature stem/branch wood	Not Recommended	
HF22	Slag cake	2014	FAGACEAE	?	?	?	Not Recommended	
HF20	Slag cake	2014	Indeterminate	Quercus sp. (x4)	?	?	Not Recommended	
MY22	Slag cake	2014	FAGACEAE	*Quercus* sp. (x4)	?	Mature stem/branch wood	Not Recommended	
MYC1	Stratigraphic deposit	2014	Indeterminate	[hardwood]	?	Poor condition; 'vitrified'	Not Recommended	
MC10	Stratigraphic deposit	2014	Indeterminate	?	?	No identifiable fragments	Not Recommended	
DLT1	Furnace fill (L23)	2005						**195±40**
DLT2	Stratigraphic level 3	2005						**170±40**
DLT3	Stratigraphic level 5	2005						**145±40**

Table 4.2: Characteristics and results of the charcoal samples recovered from four sites in Daye.
*Results in uncalibrated years BP. Daye sites are Lidegui (LD), Hongfengshuiku (HF), Mianyangdi (MY) and Yanwopu (YW). Last three measures are charcoal from the excavation of Lidegui (Hu et al. 2013).

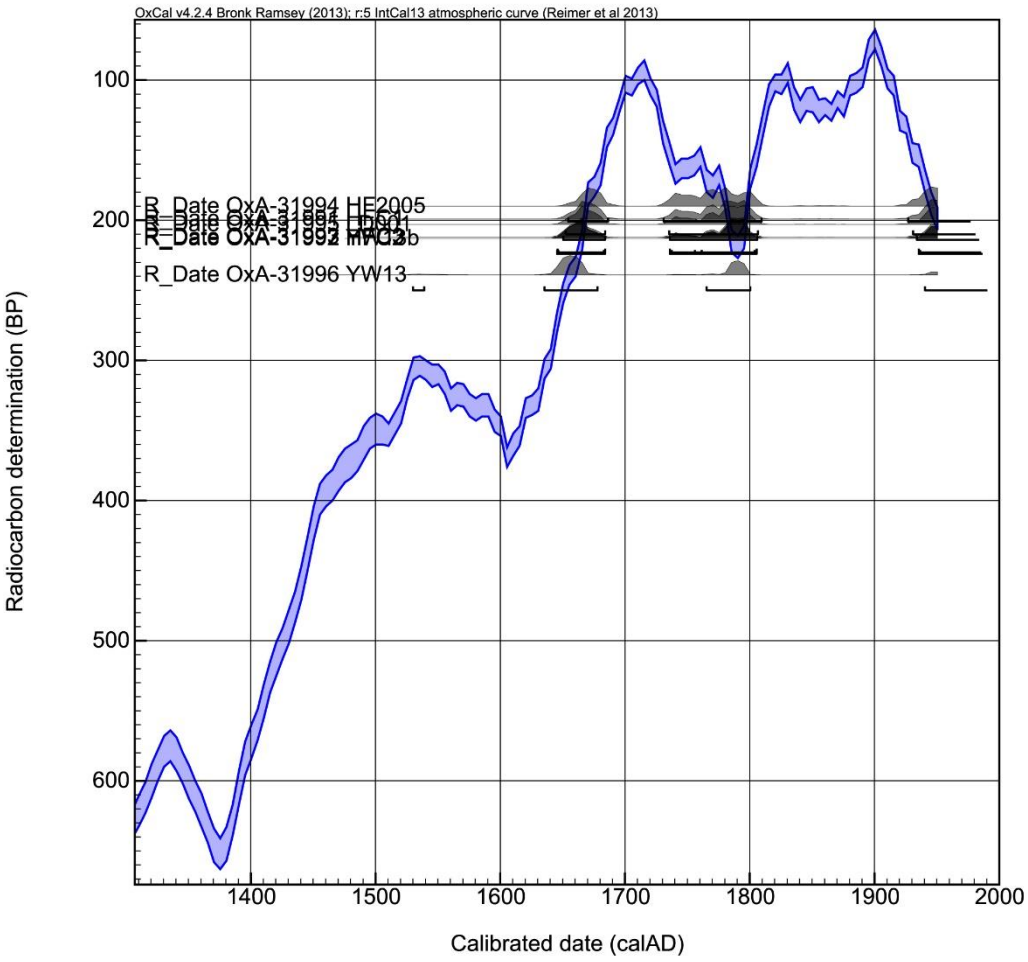

Figure 4.4: Calibration data for the seven charcoal samples of Daye.

"We are not that kind of masters who leave a bronze bell already made and run to toll another one which is only half-melt"

(Journey to the West, 西游记)

5 Analytical results I: extractive metallurgy of copper in the Daye County

Daye County yielded remains that are interpreted as related to copper smelting activities in five sites (Table 5.1): Honfengshuiku (HF), Mianyangdi (MY), Maochengnao (MC), Wangyuecun (WY) and Xiyuqiao (XY).

In general, and notwithstanding variations described in detail below, all the copper production sites show broadly similar by-products. The main features are outlined first here, before substantiating them and adding detail in the rest of this chapter. In general, the copper slag from Daye County is fayalitic tap slag, as indicated by the flow textures on surfaces, the magnetite skins visible under the microscope in between tapped layers, and the predominance of skeletal fayalite crystals. This is in agreement with their bulk chemical compositions, with 49-61% FeO and 27-34% SiO_2. Small Cu-rich sulphide inclusions and metallic copper particles are systematically present within the slag matrix, although the sulphur and copper content in the slag remains low – reported as 0.1-0.9% SO_3 and 0.7-1.7% CuO.

As a general rule, the slag appears broken as small fragments (~50 mm length, ~25 mm thickness, and range 50-100g of weight) normally keeping the original top and bottom surfaces. Some of the best preserved specimens in MC and MY suggest that a complete cake would form elongated lumps of small dimensions (~80x60x24 mm), however, it is not possible to reconstruct the total size of a cake based on the preserved samples since these are generally too fragmented to attempt a credible reconstruction. The fresh cut section invariably shows a dense, black-greyish homogeneous liquefied material with little porosity and free of unreacted inclusions.

	HF	*MY*	*MC*	*WY*	*XY*	*Total*
Copper slag	6	25	9	7	12	59
Furnace wall	3	–	3	2	1	9
Ore	3	–	1	–	–	4
Total	12	25	13	9	13	72

Table 5.1: Sampled specimens per site associated to copper production.

5.1 Characterisation of the Daye County copper slag

5.1.1 Slag morphology

The copper slag from the majority of the sites in Daye – MC, WY, XY, and MY – fits well the definition of tap slag: *'flat […], signs of ropey flow on one or more surfaces, and the impression of soil particles on the opposite side'* (Maldonado & Rehren 2009, 4) (Figure 5.1). These slags are of a thin type, very dense, and show an homogenous molten phase in section, overall quite similar to the platy slag – usually referred to by the German term *plattenschlacke* – characteristic of the Late Bronze Age in Central Europe, particularly within the Alpine region (Artioli et al. 2007; O'Brien 2015, 120, and literature therein), but also known from the Middle Ages. The *plattenschlacke* usually presents smooth upper surfaces with mild flow textures similar to the creases which develop on boiled milk, and smooth undersides as well, although these usually present many drop-shaped bumps corresponding typically to bubbles of gas. The main macroscopic features are summarised in Table 5.2.

The characterisation as platy slag is particularly well suited to WY, XY, some of the specimens of MY (MY1-MY10) and one of MC (MC4); these by-products are characteristically flat and even, and bear regular thickness of ~17, 13, 19 and 22 mm respectively. Although flowing patterns are much more conspicuous on the upper face, frequently they are evident on both of them whereas the underside of these cakes is usually quite smooth, and traces of hard layers of clay and/or soil particles are difficult to discern; this is in contrast to the MC slag where soil particles are conspicuous. Few specimens of XY present slightly twisted shapes and MC1 presents as well a ridge curved downwards. The curvature shown in these specimens is typical of liquids that solidify on

top of another liquid, which frequently occur when both metal and slag are tapped out of the furnace into a pit (Tylecote 1987, 206; Herdits 2003).

The six best preserved specimens are found in MY (MY20-MY25), measuring ~80x55x25 mm. One singularity is on MY20 and MY21 specimens which present accumulation of more than one tapping cycle; a feature that is absent in WY, XY, HF and the rest of specimens of MY (Figure 5.2).

In contrast, the copper slag of MC is frequently thick (~43 mm) with very strong flowing textures conferring the slag a bulbous appearance; often the cakes show distinct layers that appear as the result of two separate tapping cycles (Figure 5.2). The fresh cut section normally shows a dense, well-reacted molten phase. However, some unreacted chunks of quartz and/or clay are noted occasionally – including the very exceptional case of specimen MC14. MC14 together with other one sample from MC (MC8) stands out as slag with impressions of charcoal, a circumstance that is only repeated in two other samples (MY11 and MC15) within the Daye copper collection. MC8 is particularly bulky and its morphology does not fit into the tap slag description, this specimen could be furnace slag associated to the tap slag although does not present microstructural variations. The sample from MC includes the only specimen within all Daye County copper by-products with a macroscopic copper prill in the cross-section (Figure 5.3).

Only one (HF16) of the six samples of copper slag from HF correspond to the platy slag type. The rest correspond to bulky shapes with clear signs of flowing, but without clear evidence of tapping (Figure 5.3). These slag lumps did reach a liquid state but the term ‘flow slag’ was considered more appropriate for these because, in spite of the characteristic flowing texture, it is not clear that these slags were tapped out of the furnace since most of them seem to be complete small lumps of slag that could have solidified within the furnace, and also lack of magnetite bands associated indicative of rapid cooling outside the furnace (Georgakopoulou et al. 2011, 141). They are generally glossy and dark grey-greenish in colour – as most of the slags in Daye – and all of them respond strongly to the magnet. One specimen of WY (WY7) also fits broadly into these parameters although this case presents distinct surfaces and magnetite bands (Figure 5.3). Except HF17, which is an exceptionally bulky specimen with abundant soil particles attached and also seems more viscous, all HF specimens are considerably smaller in

comparison to the other copper slag from Daye (~20 mm length in HF to ~50 mm in the other sites).

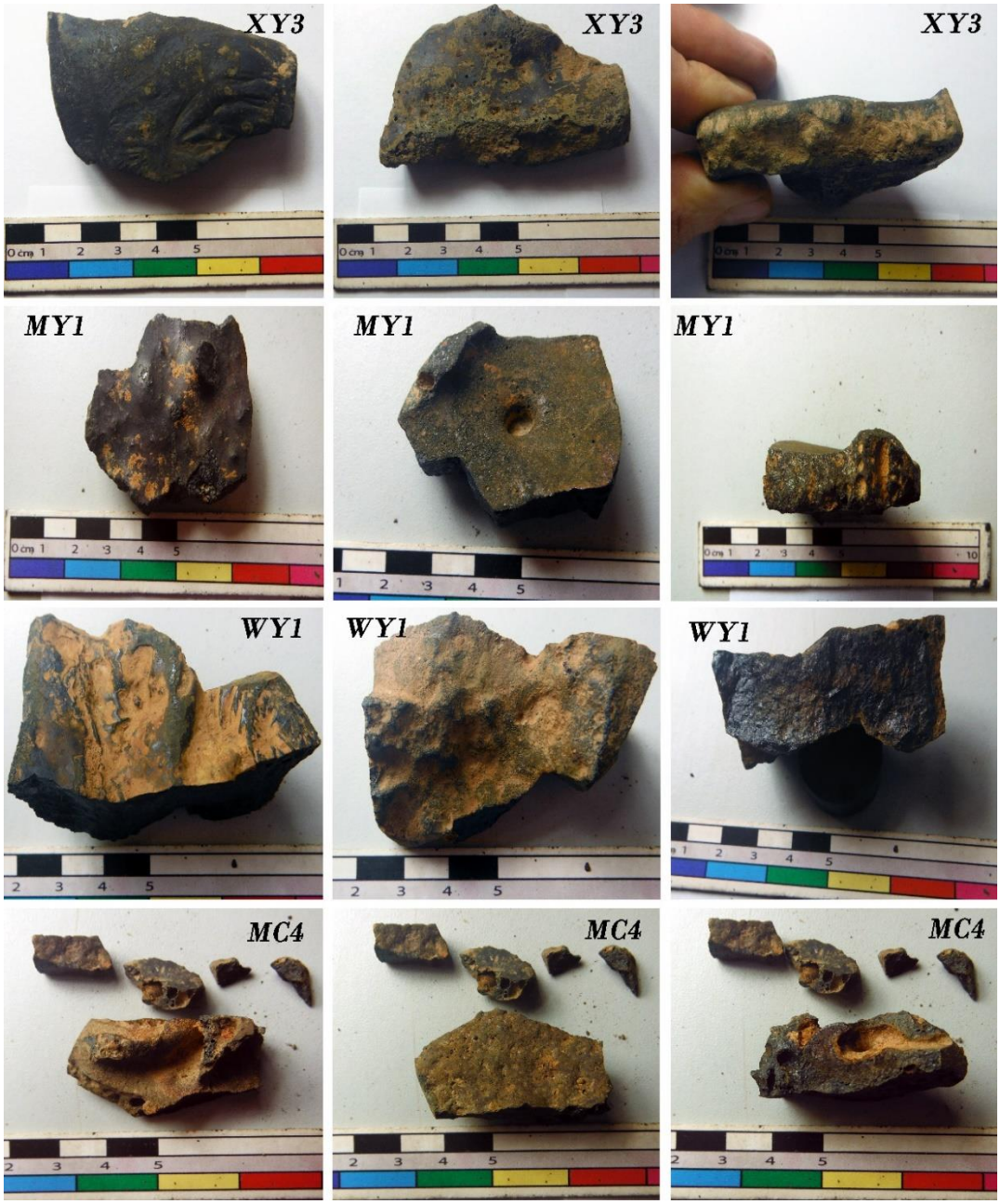

Figure 5.1: Typical appearance of the Daye copper smelting slag.
Top (left column), bottom (centre) and section (right) of different subtypes of tap 'platy' slag: **(XY3)** Very thin with smooth textures on both sides showing ridges on the top whereas the underside is slightly concave; **(MY1)** Thin with smooth glossy upper face and porous underside with a ridge curved downwards; **(WY1)** Slightly thicker and not so flat specimen with subtle differences between the opposite faces; **(MC4)** Thin cake with strongly marked bump due to a gas bubble.

	GENERAL MORPHOLOGY	*COLOUR*	*MAGNETISM*	*TEXTURE*	*SINGULARITIES*
HF	Flow slag lumps. Median thickness: 16 mm (6-65)	Dark greenish black or grey.	Strong	Flow molten textures and very smooth surfaces.	HF16 broken small fragment of tap slag. HF17 very thick and bulky.
MY	Tap platy slag. Median thickness: 19 mm (12-42)	Dark greenish grey or black, occasional reddish hues.	Strong	Smooth upper surface with ropey flow. Underside smooth and frequently free of soil particles. Thickest specimens occasionally show contorted lower surfaces.	MY26 bulky amorphous specimen heavily covered by a rusty tarnish. MY11 presents imprints of charcoal.
MC	Tap platy slag. Median thickness: 36 mm (22-40)	Dark greenish grey or black.	Strong	Contrasted smooth and rough surfaces typical of tap slag. Frequently the samples accumulate more than one tapping cycle.	MC2 shows a large prill on section (5 mm). MC14 contains abundant chunks of quartz. MC8, MC14 and MC15 present imprints of charcoal.
WY	Tap platy slag. Median thickness: 17 mm (12-23)	Dark greenish grey or black, occasional reddish hues.	Moderate	Smooth surfaces on both sides, mild flowing on the upper one.	WY7 mixture between tap and flow slag Types.
XY	Tap platy slag. Median thickness: 13 mm (11-29)	Dark greenish grey or black, occasional reddish hues.	Moderate	Smooth surfaces on both sides, mild flowing on the upper one.	Occasional twisted shape instead of flat (XY2, XY3, XY4 and XY12).

Table 5.2: Main macroscopic features of the Daye copper smelting slag by site.

The only exception to the described categories is MY26, which is a bulky amorphous specimen heavily covered by a rusty tarnish, also showing noticeable differences in bulk composition and microstructure (Figure 5.3).

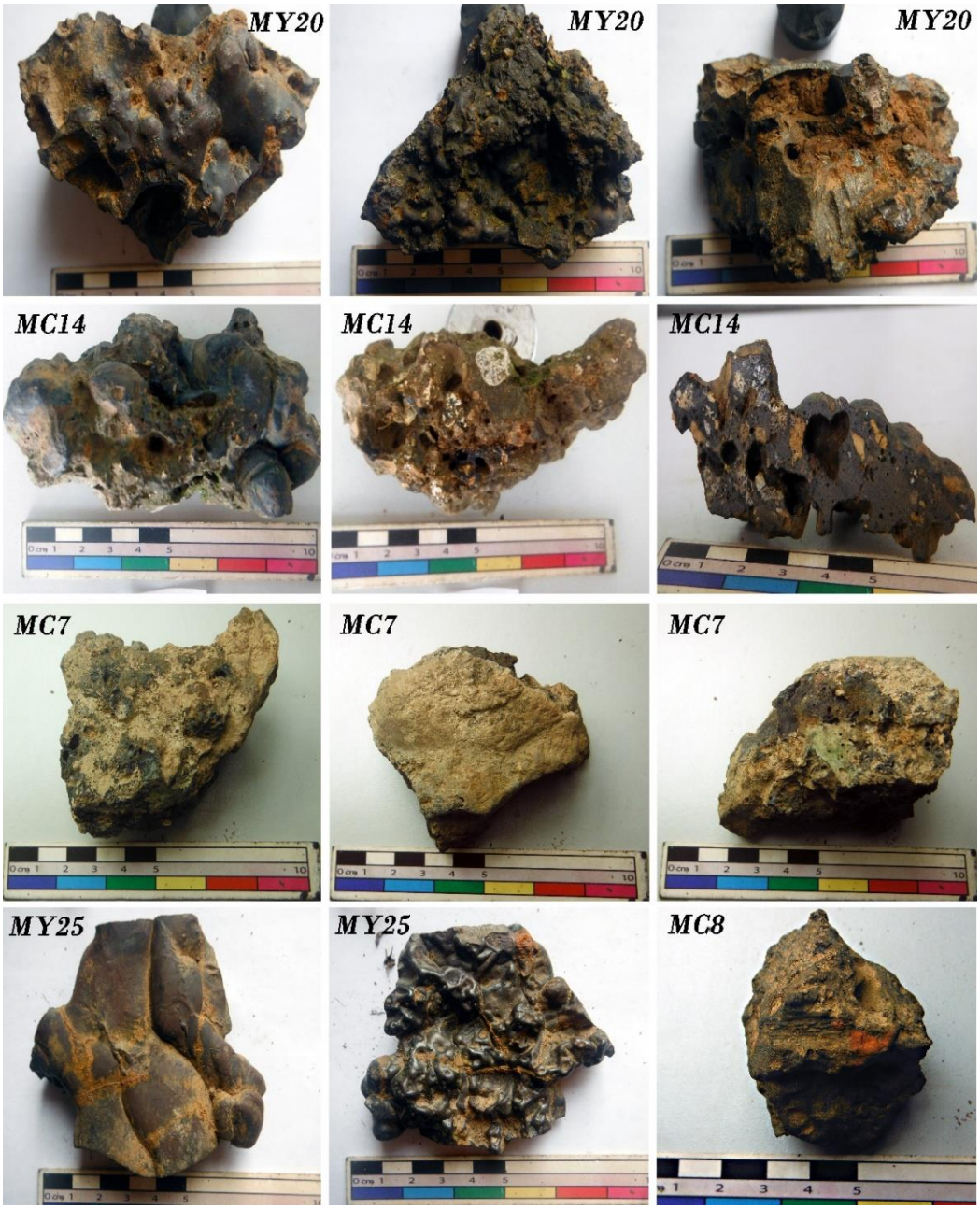

Figure 5.2: Thicker specimens of the Daye copper smelting slag.
(MY20) top (left column), bottom (centre) and section (right) of a thick mostly complete cake; **(MC14)** Bulky slag with chunks of quartz; **(MC7)** Thick specimen with less marked flowing on the upper face, a hard layer of earth at the bottom, and a join line of two different tapping cycles; **(MY25)** Cake showing strong flowing on the upper face and contorted texture on the underside; **(MC8)** Blocky specimen showing imprints of charcoal and a small patch of orange clay.

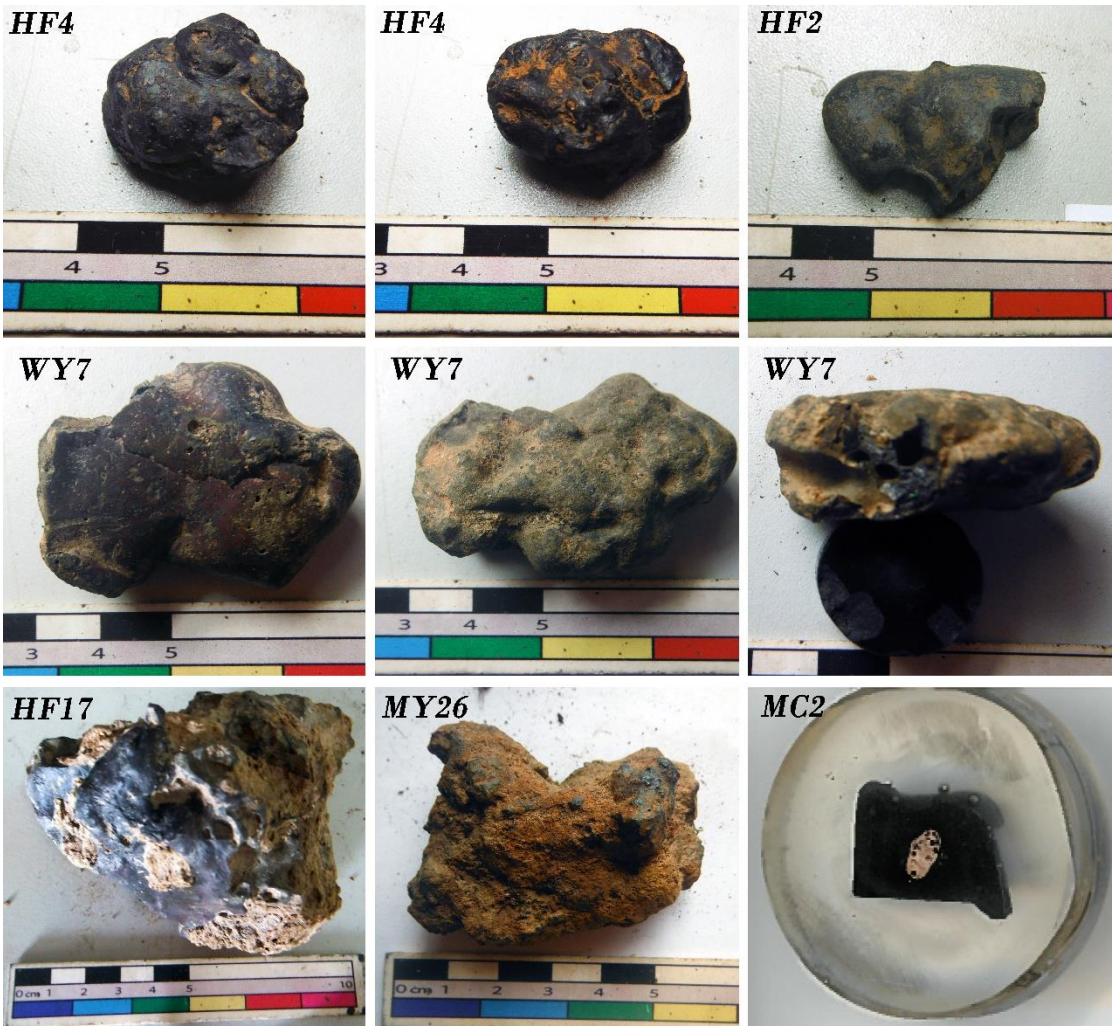

Figure 5.3: Morphology of the Daye 'flow' copper slag and atypical specimens.
(HF4) Top and bottom surfaces of a complete lump of flow slag; **(HF2)** Upper smooth face of a mostly complete fragment; **(WY7)** Top, bottom and section of a flow-tap slag; **(HF17)** Bulky version of flow slag; **(MY26)** Atypical specimen showing intense corrosion; **(MC2)** Polished block showing a large copper prill, the diameter of the block is 30 mm.

5.1.2 Bulk chemical composition

The bulk chemical composition of the samples is shown in Table 5.3. This consists primarily of FeO and SiO_2 totalling 84-90%. The third major compound is Al_2O_3 (5-8 %), with CaO (~2%) and MgO (0.5-2%) completing the composition. The rest of the oxides are typically under 1%. Figure 5.4 shows that the fluctuations between the three major oxides are relatively low (up to ~10% for FeO, ~6% SiO_2 and ~3% Al_2O_3), however, these changes are reflected in the microstructure. Therefore XY, which contains more silica and alumina displays a really glassy and lean cryptocrystalline microstructure while WY,

MC, MY and HF that are richer in iron oxides present a less glassy microstructure and packed textures (Figure 5.5). The main microscopic features of the slag per site are summarised in Table 5.4.

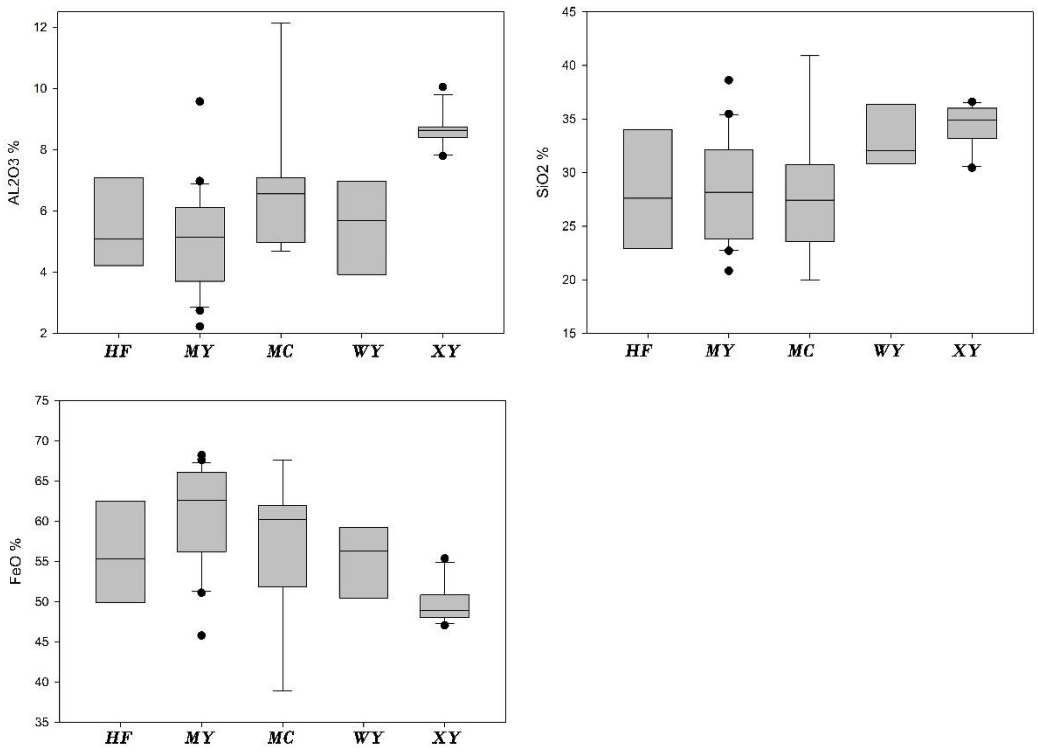

Figure 5.4: Box and whisker plot showing the average values for the main oxides in the copper slag from Daye.

Notwithstanding the broad similarities in bulk composition, a series of binary plots were generated to identify potential correlations between the composition and the sites (Figure 5.6). It is noticed that except XY, which tends to cluster together in every plot (mostly because of the slightly higher SiO_2 and Al_2O_3 and lower FeO), the rest of the sites do not present any clear pattern and frequently overlap with each other. As such, the majority of the specimens could be recognised as one single chemical group not clearly subdivided in most of the plots, except for a few outliers. The irregular lumpy specimen MY26 has a different composition: much richer in FeO (~85%, compared to an average of 55%) and poor in SiO_2 (9%) (Table 5.3).

SO_3 and CuO are the compounds that show the highest variation, the former from 0.08% in HF1 to 2.9% in MY6 and the latter from 102 ppm in HF1 to 4.1% in MC4. The majority

of the specimens contain levels under 1% each SO_3 and CuO; these levels are particularly low in XY (0.3 and 0.7%, respectively).

	MgO	*Al_2O_3*	*SiO_2*	*P_2O_5*	*SO_3*	*K_2O*	*CaO*	*TiO_2*	*MnO*	*FeO*	*CuO*
HF MEAN	2.1	5.5	28.7	2.1	0.2	0.8	2.6	0.2	0.6	56.1	1.2
MEDIAN	1.2	5.3	30.1	1.5	0.2	0.6	2.5	0.2	0.6	55.2	1.1
STD DEV	2.3	1.6	5.3	1.6	0.1	0.5	1.4	0.0	0.3	7.9	0.8
MAX	7.2	7.7	34.2	4.8	0.3	1.9	5.3	0.2	1.1	70.1	2.8
MIN	0.6	2.8	19.9	0.5	0.1	0.3	0.6	0.1	0.2	44.2	102^{ppm}
MY MEAN*	0.5	5.1	28.0	0.7	0.8	0.5	1.8	0.2	0.3	61.1	1.0
MEDIAN*	0.5	5.3	27.2	0.5	0.7	0.4	1.8	0.1	0.2	62.7	0.8
STD DEV*	0.2	1.7	5.1	0.5	0.6	0.3	0.6	0.1	0.1	6.3	0.4
MAX*	0.9	9.6	38.6	2.2	2.9	1.1	2.8	0.3	0.5	68.2	2.5
MIN*	0.2	2.2	20.0	0.2	0.3	0.2	0.9	0.1	0.2	45.8	0.6
MY26	0.5	2.3	9.3	0.6	0.8	0.1	0.5	0.1	0.3	84.8	0.8
MC MEAN	0.7	6.7	28.9	1.5	0.5	0.5	3.0	0.2	0.5	55.6	1.8
MEDIAN	0.5	6.4	27.9	1.3	0.3	0.5	2.2	0.2	0.5	58.6	1.3
STD DEV	0.3	2.2	5.3	0.8	0.6	0.1	2.0	0.1	0.2	7.8	1.1
MAX	1.4	12.1	40.9	2.6	2.2	0.7	7.8	0.3	1.0	62.4	4.1
MIN	0.4	4.7	23.4	0.5	0.2	0.4	1.5	0.1	0.2	38.9	0.8
WY MEAN	0.7	5.6	33.0	0.6	0.4	0.9	2.2	0.2	0.3	55.2	0.8
MEDIAN	0.8	5.8	30.9	0.5	0.4	0.9	2.0	0.2	0.4	56.5	0.8
STD DEV	0.2	1.7	3.4	0.3	0.3	0.2	0.6	0.1	0.1	4.7	0.2
MAX	0.9	7.7	39.5	1.2	0.9	1.2	3.1	0.3	0.5	61.3	1.2
MIN	0.4	2.4	30.7	0.4	0.1	0.5	1.5	0.1	0.2	47.1	0.7
XY MEAN	1.2	8.6	34.4	0.9	0.3	1.0	2.3	0.3	0.5	49.8	0.7
MEDIAN	1.1	8.6	34.9	0.9	0.2	1.0	2.3	0.3	0.5	48.9	0.6
STD DEV	0.1	0.6	1.9	0.1	0.1	0.1	0.4	0.0	0.0	2.4	0.2
MAX	1.4	10.0	36.6	1.1	0.5	1.1	2.9	0.3	0.6	55.4	1.3
MIN	1.0	7.8	30.4	0.5	0.2	0.6	1.4	0.3	0.5	47.1	0.5

Table 5.3: WD-XRF chemical composition of Daye slags.
*Excluding atypical specimen MY26.

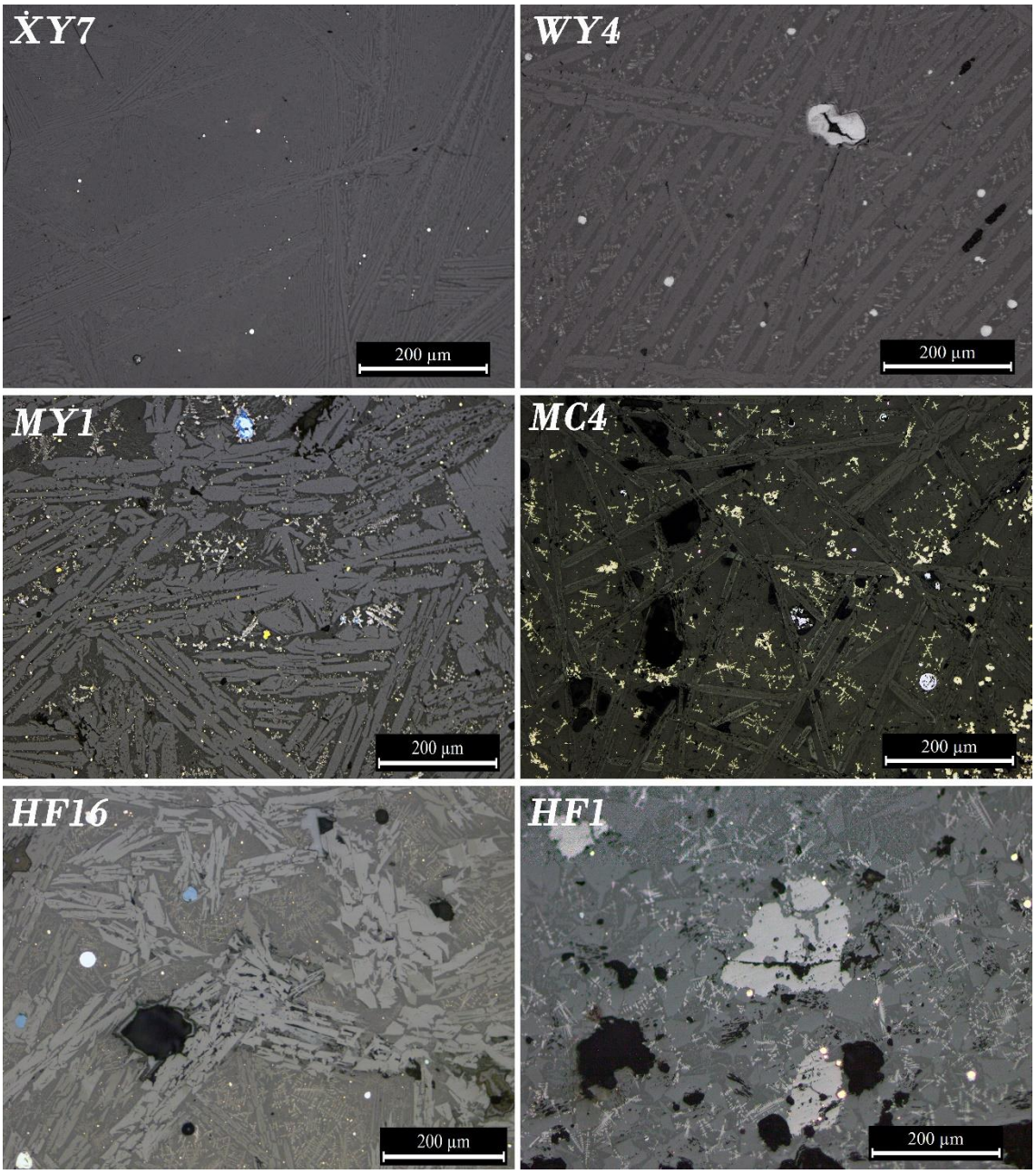

Figure 5.5: OM micrographs of glassy textures of thin 'tablet' specimens of tap slag compared to the typical microstructure of flow slag.
(XY7) Very glassy matrix with spinifex olivines; **(WY4, MY1, MC4, HF16)** Different versions of glassy matrix showing skeletal olivines (light grey) and free iron oxides (white grey). Note the difference in brightness between the dendritic structures within the olivine needles, the brighter crystals in MY1 and MC4 correspond to iron oxides whereas the pale grey ones in WY4 and HF16 to incipient fayalite crystals; **(HF1)** Typical glassy matrix of flow slag showing polygonal crystals and large clusters (light grey) of iron oxides. The droplets and round particles visible in all samples are copper or copper sulphide particles (yellow, indigo, and very pale blue).

The SO_3 versus CuO plot shows that in principle these are not correlated and that the bulk of the collection contains scant SO_3 (≤0.5%). Microanalyses confirmed that sulphur

typically occurs as small droplets of chalcocite. However, a substantial part of the MY assemblage contains between 0.5-1% or more SO_3. Significantly, the sulphides present in the microstructure of MY are always larger and frequently more complex – containing other phases different than chalcocite – than in any of the other sites (section 5.1.5). Very large sulphides are equally frequent in MC although in this case the binary plot does not show a clear pattern.

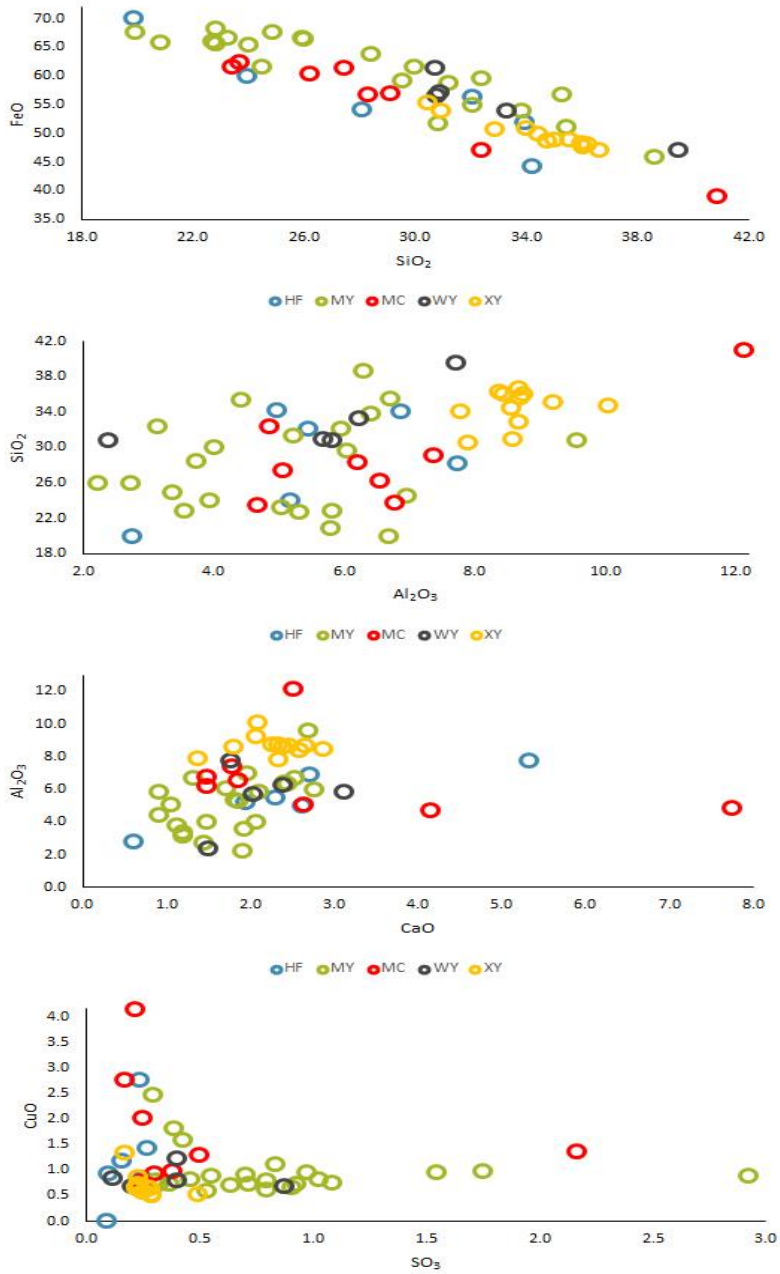

Figure 5.6: Binary plots of the bulk chemical composition of the Daye copper smelting slags.

	GENERAL CHARACTERISTICS	SILICATES	IRON OXIDES	METAL-RICH PARTICLES
HF	Molten and homogenised packed microstructure, frequently by large size minerals. Common residual iron oxides.	Predominant euhedral crystals of olivines, large (~200 µm) and close spaced. Exception is HF16 that presents laths instead of polygonal crystals.	Dominant sharp edged pseudomorphs of magnetite dispersed in the matrix. Occasional clusters and large agglomerations. HF16 is virtually free of iron oxides.	Few to very few copper prills of small size (10-40 µm) usually with a matte envelope. Granular shapes of matte (Cu_2S or CuS) are rare and smaller (10-20 µm). HF17 presents commonly copper prills of large size (100-200 µm and up to 500 µm).
MY	Molten and homogenised packed microstructure. Few residual iron oxides. Exception is MY11 with abundant chunks of residual quartz.	Predominant euhedral and thick skeletal olivines (~100-200 µm), close spaced.	Dominant skeletons or cubic shapes of magnetite dispersed in the matrix. Occasional very large grains (~300 µm) Occasional skins of magnetite. MY3 is virtually free of iron oxides.	Few to very few sulphides of generally large size grains (~50-100 µm). Occasionally presenting more complex phases than Cu_2S or CuS. Very few to rare small copper prills (10-30 µm).
MC	Molten and homogenised packed microstructure. Few residual iron oxides. Exception is MC14 with abundant chunks of residual quartz.	Predominant euhedral and thick skeletal olivines (100-200 µm), close spaced.	Dominant sharp edged pseudomorphs dispersed in the matrix. Occasional large clusters of magnetite. Common skins of magnetite.	Few to very few sulphides of medium size grains (~40-60 µm) occasionally presenting more complex phases than Cu_2S or CuS. Very few to rare small copper prills (10-30 µm). MC2 presents a large Cu prill (>500 µm).
WY	Molten and homogenised microstructure, generally uncongested and showing wide areas of glassy matrix. Very few residual iron oxides.	Predominant lath olivines, very large (~300) but narrow (~50 µm), close or single spaced depending on the specimen. Occasional massive crystals.	Common to few skeletons or cubic shapes of dendritic magnetite. WY5, WY7 and WY8 are virtually free of iron oxides.	Few to very few sulphides of medium to large size grains (~50-100 µm, up to 200 µm) typically Cu_2S. Rare copper prills, typically tiny (~10 µm). Exception is WY7 that presents large size copper prills (~50 µm, up to 200 µm).
XY	Molten and homogenised microstructure, lean and very glassy. Very few residual iron oxides.	Predominant laths olivines, very large (~300) and narrow (~50 µm), single spaced.	Few skeletons and cubic shapes of dendritic magnetite. 7 out of 12 sampled specimens are virtually free of iron oxides.	Few to very few sulphides of medium to large size grains (~50-100 µm, up to 200 µm) typically Cu_2S. Very rare and small (~10 µm) copper prills only present in XY5 and XY12.

Table 5.4: Main microscopical features of the Daye copper smelting slag by site.

5.1.3 Silicates

The slag microstructure is typically dominated by silicate crystals of the olivine group [Mg, Fe]$_2SiO_4$, namely fayalite (Fe_2SiO_4) with regular but scant MgO (~0.5-2%) which is slightly higher (~3-4%) within the olivines of HF (Table 5.5). In two of the sites – HF and MC – these olivines are commonly crystallised as euhedral crystals close or single spaced with an average diameter ranging 100-200 µm but occasionally forming larger crystals (up to 500 µm). Conversely, in WY and XY olivines are systematically lath crystals and plumes frequently arranged in the same direction. Lastly, olivines in MY are typically euhedral crystals or very thick skeletons but also laths in few specimens and is frequent to find a mixture of them within the same sample (Figure 5.8). Other silicate crystals are quite exceptional and consist of rare phases similar in composition to the mineral leucite ($KAlSi_2O_6$). Although small amounts of CaO and MnO (~0.5-2%) frequently complete the composition of the olivines (Table 5.5), pyroxenes are only present, and scantily, in MC slag as augite series [(Ca,Na)(Mg,Fe,Al,Ti)(Si,Al)$_2O_6$].

		MgO	*SiO2*	*CaO*	*MnO*	*FeO*			*MgO*	*SiO2*	*CaO*	*MnO*	*FeO*
HF	**MEAN**	4.2	30.3	0.5	1.2	57.4	***WY***	**MEAN**	2.2	31.0	0.6	0.7	64.4
	STD	1.5	1.1	0.4	0.3	6.4		**STD**	1.3	2.0	0.4	0.5	5.4
	MAX	7.2	33.3	1.3	1.8	64.1		**MAX**	6.9	37.4	2.3	2.7	69.9
	MIN	2.1	28.7	bdl	0.8	44.7		**MIN**	0.7	28.4	0.3	0.4	39.3
MY	**MEAN**	1.7	30.0	0.7	0.4	67.5	***XY***	**MEAN**	2.5	31.6	0.8	0.7	63.0
	STD	0.7	1.0	0.7	0.2	1.4		**STD**	0.9	1.9	0.5	0.1	3.9
	MAX	3.1	33.1	3.8	0.8	70.2		**MAX**	5.1	36.2	1.7	0.9	67.4
	MIN	0.5	27.9	bdl	bdl	64.8		**MIN**	1.0	29.1	0.3	0.5	53.8
MC	**MEAN**	1.4	29.7	1.6	4.2	63.8							
	STD	0.6	2.7	2.0	14.8	12.6							
	MAX	3.0	38.6	3.3	0.8	72.0							
	MIN	0.7	23.5	0.3	0.4	56.9							

Table 5.5: Average composition (SEM-EDS) of olivine crystals in the microstructure of the Daye copper smelting slag.
Average of 3-5 crystals per specimen.

Residual quartz and argillaceous materials are quite exceptional in all sites, with rare exceptions in specimens HF17, MY11 and MC14 (Figure 5.7). These residual materials normally show cracking, diffuse or merged boundaries in the matrix, showing some high-temperature reaction. Argillaceous materials are very rare and correspond to patches of clay attached to the surface that present sharp edges and little interaction with the slag, with a composition of ~12% Al_2O_3, 73% SiO_2, 8% FeO and 3% K_2O, similar to the composition of some red-wall furnace wall ceramics (Table 5.7).

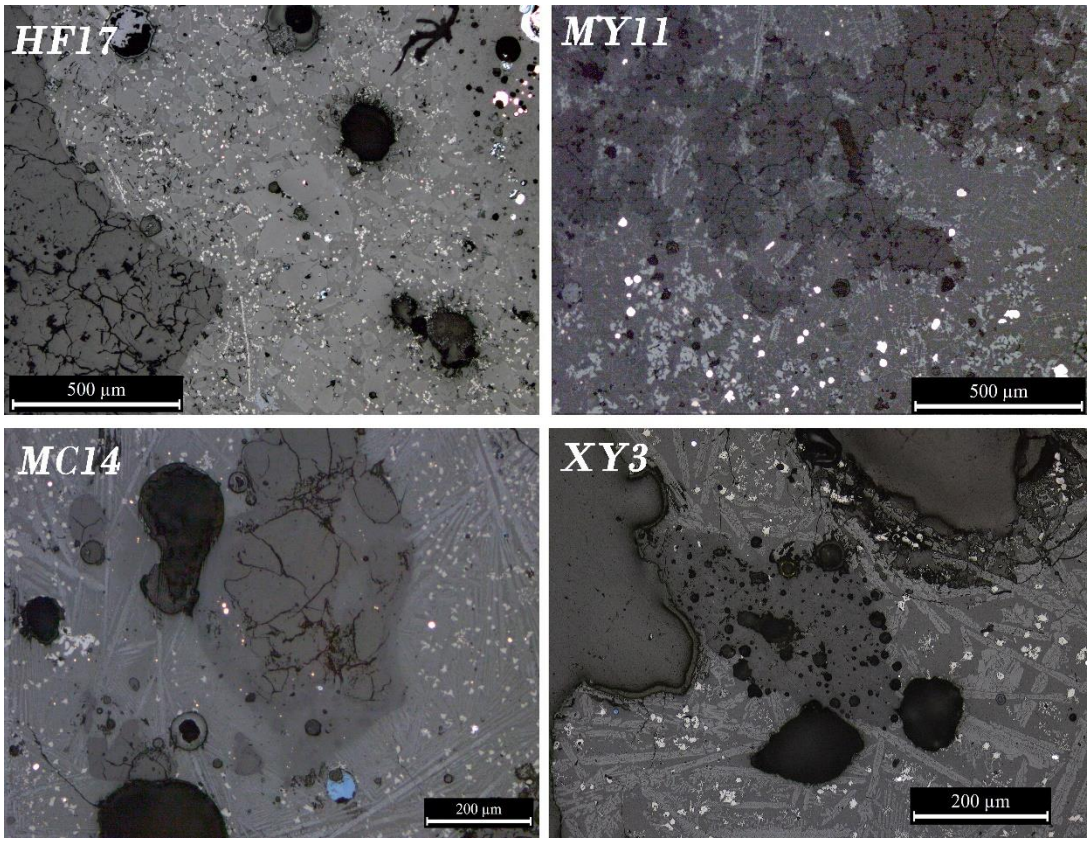

Figure 5.7: OM micrographs of unreacted quartz and argillaceous materials in the microstructure of the Daye copper smelting slag.
(HF17) Euhedral crystals of fayalite (pale grey) between two quartz inclusions, one mostly melted (top right) associated to scant copper particles (pale orange) and the other cracked (dark grey); **(MY11)** Chunks of semireacted quartz (dark grey), abundant copper prills (pale yellow) and pseudomorphs of iron oxides (light grey); **(MC14)** Detail of a embedded grain of quartz, sulphide (indigo), few copper prills (yellow) and pseudomorphs of iron oxides (light grey); **(XY3)** Detail of argillaceous material (dark grey) close to the surface nearly embedded in a glassy matrix with fayalite laths (light grey), and iron oxides (bright grey), some corrosion products are also visible close to the surface.

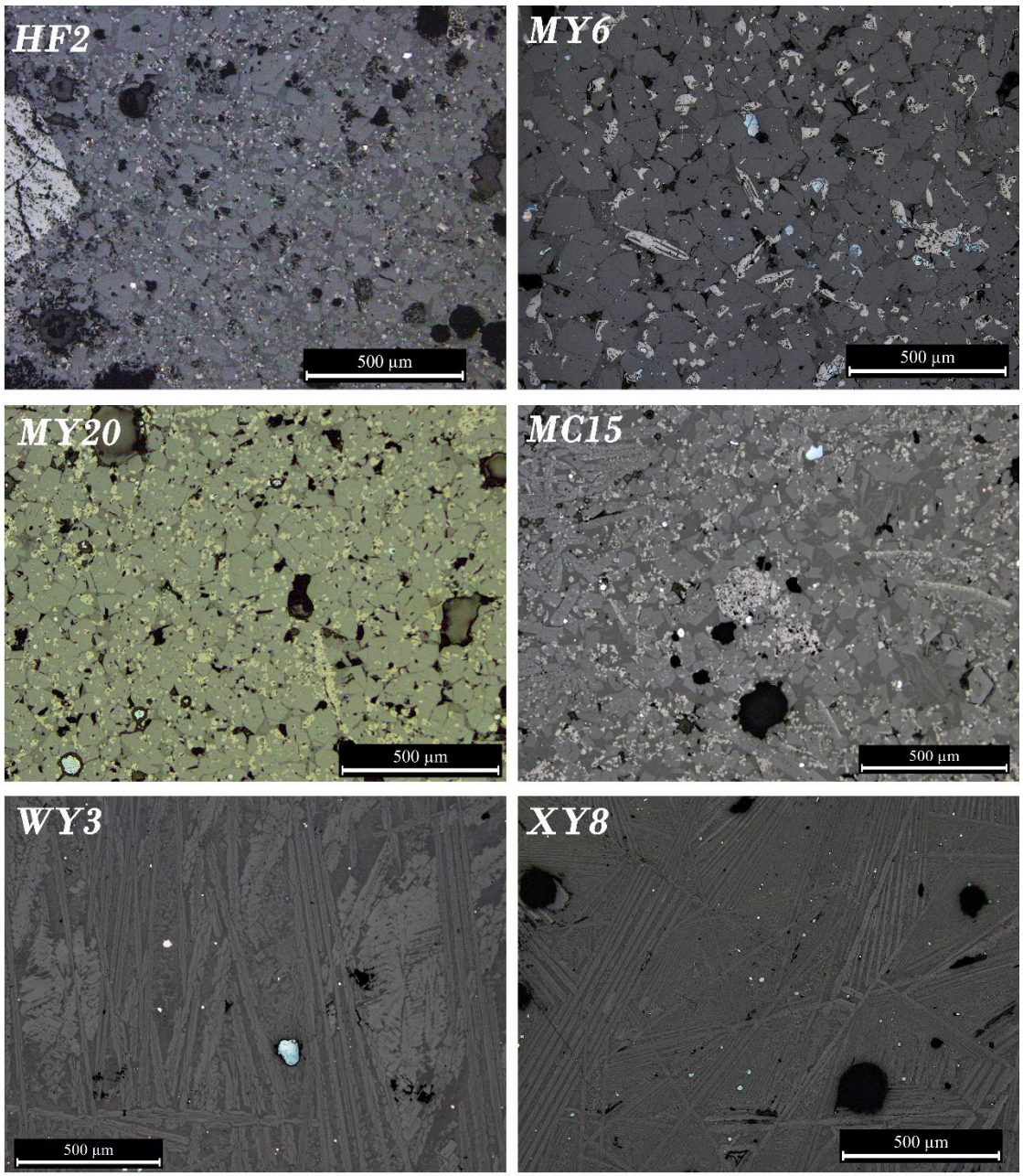

Figure 5.8: OM micrographs showing the typical microstructure and appearance of silicates in the Daye copper smelting slag.
(HF2) Example of flow slag in HF showing euhedral crystals of fayalite (medium grey), flakes of magnetite (bright white), scant copper particles (yellow), and a large chunk of haematite (bright grey); **(MY6, MY20)** Packed euhedral fayalite with large size cubic shapes of magnetite (bright grey) and scant sulphides (blue); **(MC15)** Euhedral crystals and large skeletal fayalite (light grey), dominant magnetite (bright grey), large cluster of semi-reacted iron oxides (bright grey, centre) and sulphides (blue); **(WY3)** Predominant thin laths of fayalite with occasional massive crystals (light grey) and few sulphides (blue); **(XY8)** Very thin fayalite needles (light grey) and sulphides (blue).

5.1.4 Iron oxides

Iron oxides are very frequent in the microstructure. They can be identified as magnetite, (Fe_3O_4) occurring typically as 'flakes' – skeletal or cubic shapes typical of this mineral –, but also frequently as nodular grains, occasionally forming large clusters or agglomerations that are likely pseudomorphs of the parent magnetite grains dispersed within the matrix (Figure 5.10). Normally, the flakes occur as small crystals of ~10 µm or less whereas the pseudomorphs are larger (~40 µm). In most of the specimens the magnetite appears scattered evenly within the matrix, and more occasionally arranged in dendritic formations. Wüstite is very rare in comparison, only identified in MY15, MY7 and in two specimens from MC – MC3 and MC12.

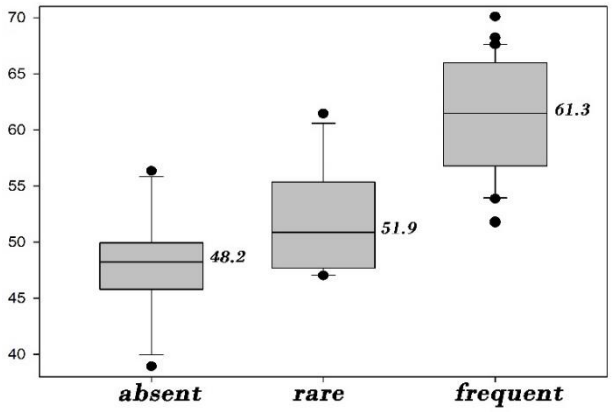

Figure 5.9: Box and whisker plot comparing the abundance of magnetite against the average bulk FeO in chemical composition in the Daye copper smelting slag.

In stark contrast with the abundance of iron oxides in HF, MY and MC (except specimens HF16 and MY3), the frequency of euhedral crystals of free iron oxides is considerably lower in WY, to the extent that three specimens (WY5, WY7, WY8) out of eight do not show any. This frequency is even lower in XY where magnetite is absent in seven out of twelve specimens. The abundance of iron oxide crystals seems to be correlated with the FeO content in the slag: Figure 5.9 classifies the abundance of free magnetite crystals as absent, rare or frequent and plots it against the bulk FeO content in slag, with the result

that the higher the FeO in chemical composition the higher frequency of magnetite crystals in the matrix regardless the site and type of slag.

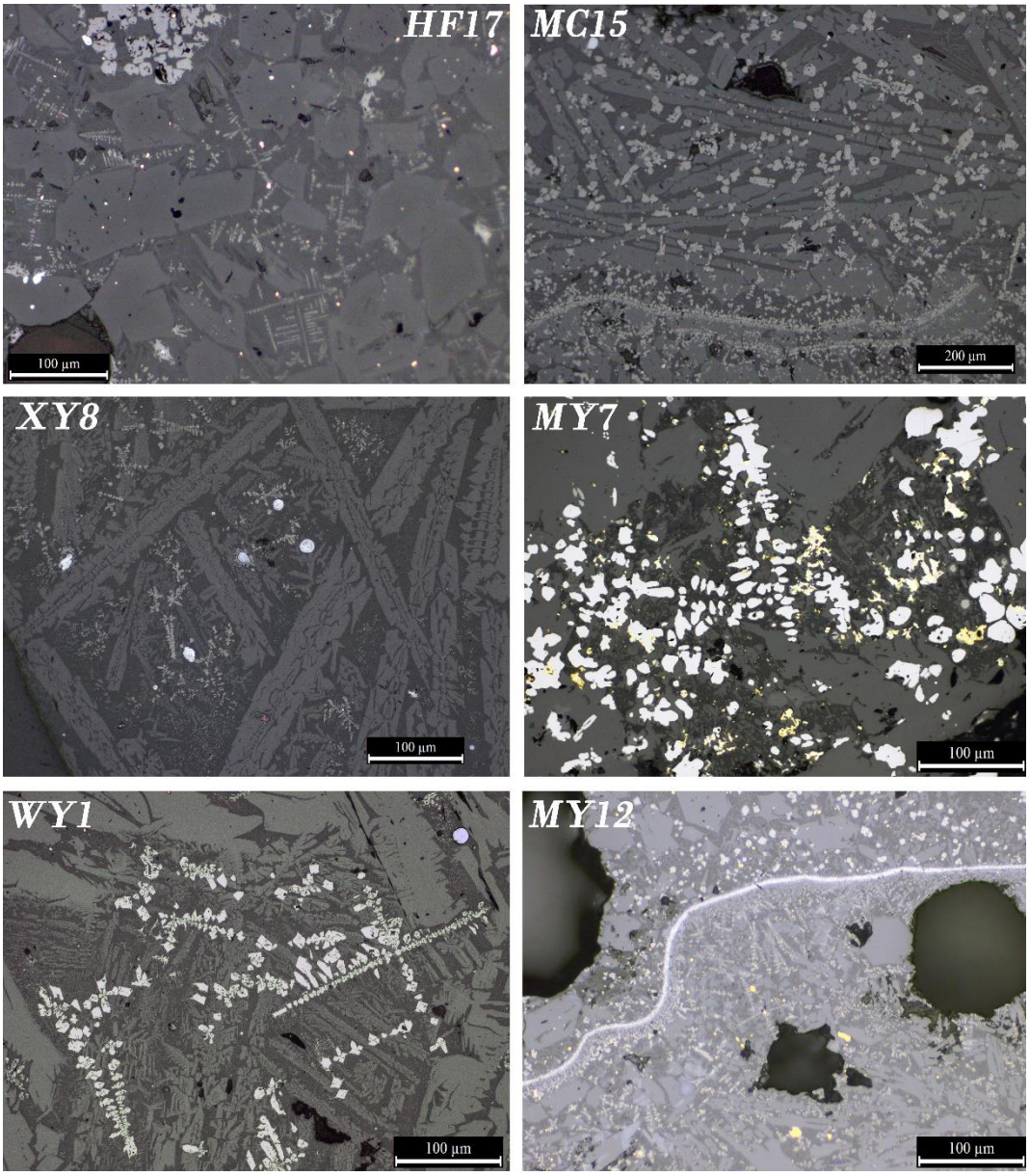

Figure 5.10: OM micrographs of iron oxides in the microstructure of the Daye copper smelting slags.
(HF17) Agglomeration of iron oxides (light bright grey) and tiny dendritic magnetite (light grey) within polygonal crystals of fayalite (dark grey) and few copper prills (yellow); **(MC15)** Pseudomorphs, cubic crystals and bands of magnetite (light grey), and fayalite laths (dark grey); **(XY8)** flakes of dendritic magnetite (light grey) within fayalite laths (dark grey and few sulphides (blue); **(MY7)** Dominant wüstite globules (bright white) and copper particles (yellow); **(WY1)** Dendritic magnetite (light grey) within fayalite crystals (dark grey); **(MY12)** Magnetite skin (bright) separating fayalite crystals (light grey), flakes of magnetite (bright) and droplets of copper (yellow).

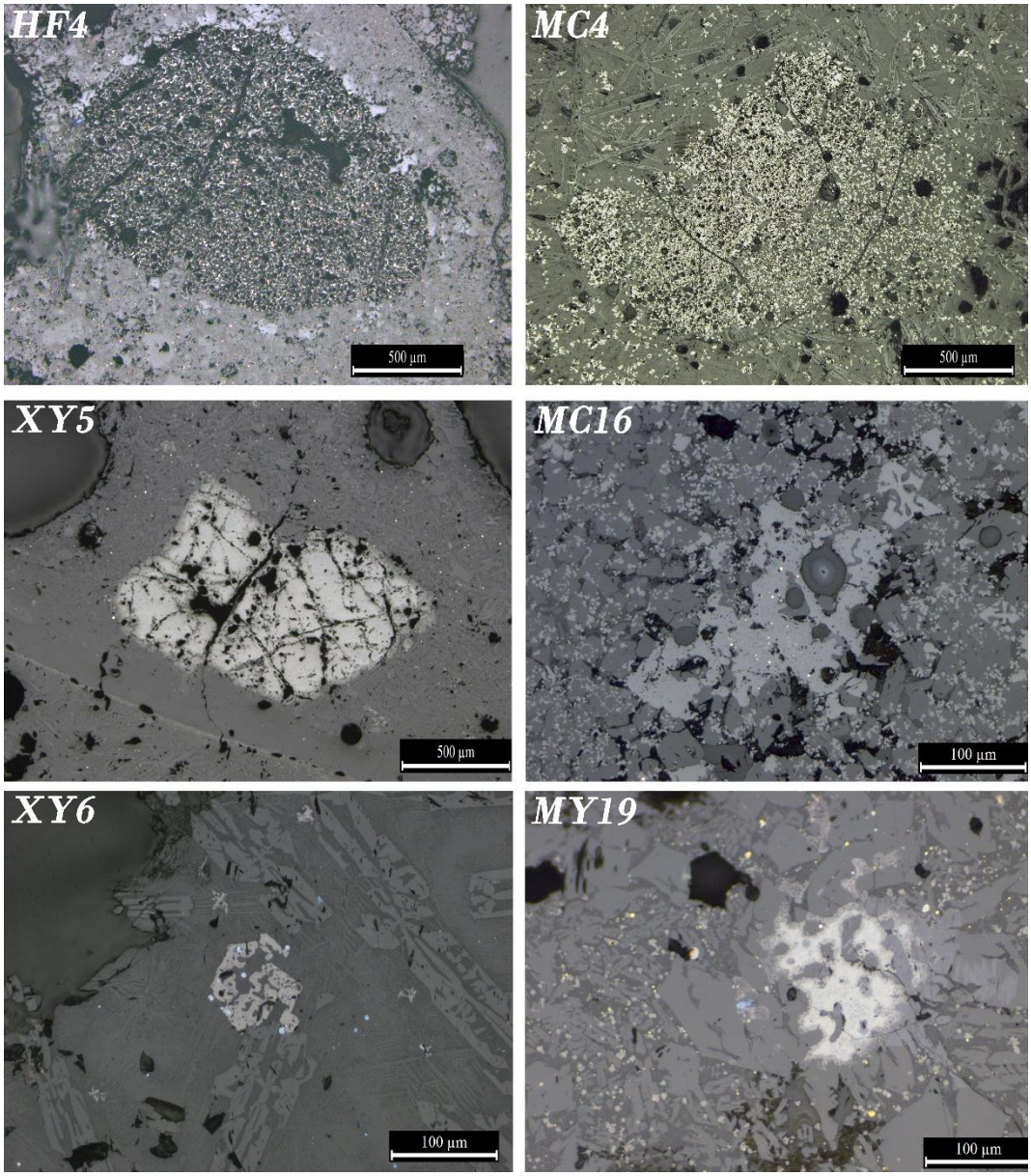

Figure 5.11: OM micrographs of residual iron oxides in the microstructure of the copper slag. **(HF4)** Large unreacted chunk on packed fayalitic microstructure; **(MC4)** Large chunk showing more advanced reactions than in the previous graph; **(XY5)** Semi-reacted enriched chunk (light grey) on a glassy microstructure; **(MC16)** Pseudomorph of the parent grain (light grey) associated to tiny copper prills and abundant smaller sharp edged pseudomorphs; **(XY6)** Same phenomenon associated to matte (blue) within a glassy matrix with laths of fayalite (dark grey); **(MY19)** Mostly dissolved agglomeration of iron oxides (bright), smaller cubic crystals, metal particles (yellow) and a sulphide droplet (blue).

One characteristic common to all sites in Daye is the recurrent presence of microscopic grains of residual iron oxide. In HF these appear as slightly reacted chunks – identified as haematite by the calculation of the Fe:O atomic ratio by SEM-EDS analyses – whereas generally in the other sites they show more advanced reactions with the surrounding melt,

usually as agglomerations of Fe-rich crystals arranged in pseudomorphs of the parent grains (Figure 5.11). The SEM area analyses of these phases revealed that these are very rich iron oxides (~95%) with minor levels of alumina, titania, and magnesia. Very occasionally, minor levels of copper oxide (<1%) are registered as well within the agglomerations.

5.1.5 Metal-rich particles

Cu-rich sulphides and matte prills are few to very few and even rare in the Daye slag, although their frequency varies. It is worth noting, however, that sulphides are the dominant Cu-bearing phase, while copper prills are even scantier in comparison. The matte particles consist typically of small (10-40 μm) grains of chalcocite (Cu_2S) and, less frequently, covellite (CuS), occasionally with tiny prills of metallic copper within. Also common is the appearance of chalcocite as an outer envelope of, or as discrete inclusions within, metallic copper prills (Figure 5.13). Typically, the sulphide droplets contain significant levels of iron (average of 3-7%) while copper fluctuates between ~53-73% (average) and sulphur between ~22-39% (Table 5.6 right) (Appendix VI).

Besides individual specimens MC5 and MY11, HF is exceptional as a site in that most of the sulphides occur as segregates within the metal prills, which are more abundant here than in slag from other sites. In general, Cu-rich particles contain significant amounts of S (up to 3%) and Fe (average of ~2-5%) (Table 5.6 left).

In contrast, MY and MC contain more abundant sulphides of more diverse types than the other three sites, with exceptionally large droplets exceeding 200 μm in diameter (Figure 5.13). Even though, like in the previous sites the predominant sulphides are chalcocite or covellite, MY and MC present a larger variety of Cu–Fe–S phases, which can be distinguished on the basis of their optical properties under the OM, and EDS-SEM phase analyses. The identified minerals are: chalcopyrite ($CuFeS_2$), bornite (Cu_5FeS_4), Cu_2FeS_3, and cubanite ($CuFe_2S_3$). However, in comparison with chalcocite and covellite that are present in all specimens, the rest of the S-rich phases are marginally present in less than one third of the samples. For the sake of simplicity, a few Cu–Fe–S phases (Fe content ~6-

10%) present within all the slag assemblage and chemically between bornite and covellite are also referred as 'covellite'.

Oxidic copper-bearing phases sometimes include delafossite ($CuFeO_2$), although more frequently they appear as prills of cuprite (Cu_2O), and less frequently tenorite (CuO) or phases similar to cupric peroxide (CuO_2, although the high oxygen in the latter is likely due to corrosion). It is not uncommon to find residual S (up to 2.4%) within the metal prills and scant O (~3-4%) within some sulphides. The largest Cu-rich matte particles are frequently attached to a gas void (Figure 4.3). Some of the sulphides attached to voids present an incipient rim of iron oxide, which is consistent with the evolution of gaseous sulphur dioxide (Georgakopoulou et al. 2011, 131).

Matte particles widely predominate among the Cu-rich particles in WY and XY slag; metallic copper prills are even more exceptional than in the other three sites in Daye. Here sulphide droplets are comparatively larger, typically ~50 µm in diameter, and frequently larger than 100 µm. They are, however, scarce overall. Compositionally, practically all the particles from XY are chalcocite whereas WY shows a little more variation, with a few phases of bornite and Cu_2FeS_3.

All the analysed Cu-rich particles were plotted in the ternary diagram Cu–Fe–S (Figure 5.12). The ternary diagram shows that there are no radical differences between sites but three main groups of metal particles: the metal of the first one consists basically of metallic copper, typically with scant sulphur (<1%) and iron (<6%). The second cluster is the largest, and it consists of matte particles with the bulk concentrated between 60-80% Cu, 20-30% S and 1-20% Fe. The third group is a cluster with very similar composition to the second but richer in S (30-40%). These latter two clusters correspond to the microscopically identified chalcocite and covellite minerals respectively. A final, less-defined cluster can be observed with the specimens richer in Fe (>20%) with 40-50% Cu and S respectively. Overall, this last bundle includes only samples from MY, MC and WY which fits with the larger variety of sulphidic phases observed within these three sites.

Turning to metal prills, these are rarely larger than 80 µm, usually ranging 10-30 µm, with very few exceptions where large (200 µm) copper particles are common: HF17, MC2,

MY19, and WY7. As mentioned, copper prills systematically contain iron (~1-4%) (Figure 5.14).

Copper prills	*S*	*Fe*	*Cu*	*Matte particles*	*S*	*Fe*	*Cu*
HF MEAN (26)	0.03	2.26	97.71	***HF MEAN (16)***	22.37	3.96	73.67
MEDIAN	bdl	1.76	98.24	***MEDIAN***	20.84	3.24	73.64
STD	0.45	2.46	2.91	***STD***	3.52	2.59	3.32
MAX	0.90	4.91	100.0	***MAX***	32.23	10.81	77.98
MIN	bdl	bdl	94.19	***MIN***	19.32	0.65	67.12
MY MEAN (25)	0.26	3.58	96.16	***MY MEAN (122)***	37.55	5.76	56.68
MEDIAN	bdl	2.50	97.50	***MEDIAN***	36.37	4.27	59.45
STD	0.69	3.94	4.30	***STD***	6.03	4.86	8.33
MAX	2.87	17.07	100.0	***MAX***	59.33	29.56	83.47
MIN	bdl	bdl	82.93	***MIN***	9.75	bdl	27.91
MC MEAN (14)	0.04	4.78	95.17	***MC MEAN (42)***	39.22	7.34	53.44
MEDIAN	bdl	4.46	95.54	***MEDIAN***	37.41	4.59	53.70
STD	0.16	2.91	2.89	***STD***	9.13	5.18	11.67
MAX	0.62	12.55	100.0	***MAX***	57.18	17.27	89.63
MIN	bdl	bdl	87.45	***MIN***	6.55	0.42	32.23
WY MEAN (15)	0.45	1.29	98.26	***WY MEAN (46)***	36.52	7.19	56.29
MEDIAN	0.25	1.16	98.50	***MEDIAN***	35.41	5.13	60.01
STD	0.51	1.41	1.72	***STD***	9.35	6.79	13.29
MAX	1.63	4.29	100.0	***MAX***	48.97	31.78	90.62
MIN	bdl	bdl	94.49	***MIN***	3.67	bdl	24.60
XY MEAN (2)	1.99	3.74	94.28	***XY MEAN (50)***	34.68	3.81	61.51
MEDIAN	bdl	4.23	95.47	***MEDIAN***	33.70	3.46	62.48
STD	bdl	1.04	1.04	***STD***	6.09	2.04	5.94
MAX	bdl	4.53	97.55	***MAX***	52.73	12.19	89.80
MIN	bdl	2.45	95.47	***MIN***	5.97	1.32	41.48

Table 5.6: Chemical composition of the Cu-rich particles present in the Daye copper smelting slag.
SEM-EDS point analyses. Particles >3 % S content are counted as matte.

WY7 is the only sample in Daye which contains copper silicates (Figure 5.13). These occur as partially reacted agglomerations with compositions of ~33% SiO_2, 27% FeO and 36% CuO, with occasional Al_2O_3 and CaO as minor elements. Within these, an unusually higher

number of large size copper prills can be found, most of them with tiny matte segregates. The area in which these minerals appear has large gas voids and shows significant corrosion, which explains the post-depositional alteration of most of the copper prills to cuprite, and the matte copper sulphates (33.4% SO_3).

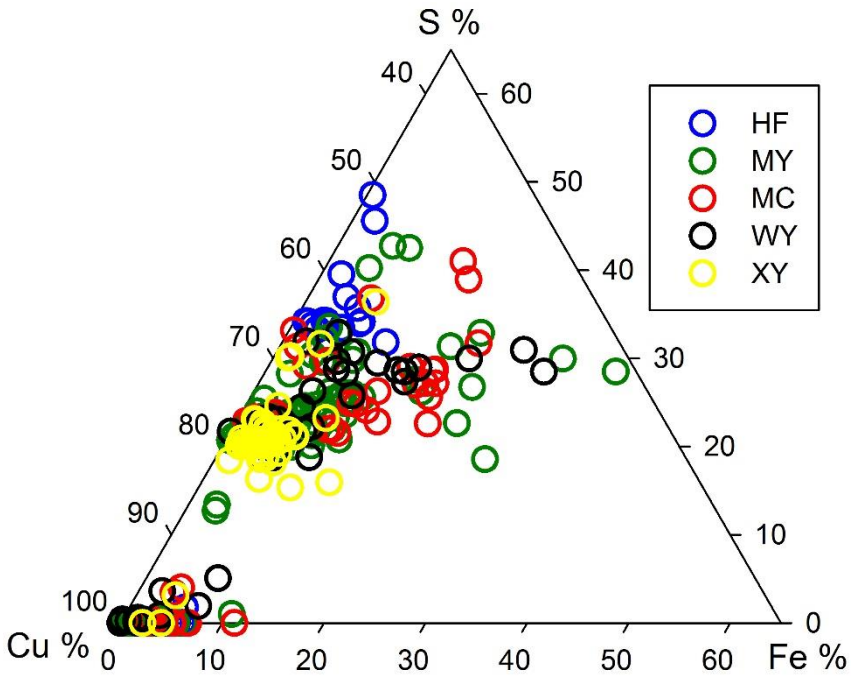

Figure 5.12: Cu–Fe–S ternary diagram in atomic % (EDS-SEM data) with all the Cu-bearing metal particles analysed in the Daye copper slag smelting plotted.

The occurrence of sulphides other than copper sulphides, or metal other than copper is rare and unssystematic; the most recurrent one is barium sulphate – HF15, HF17, MY22, MC3 – which sometimes is associated with Pb – MY10, MY12, MY13, MC2, MC8. Apart from this, MC7 contains one particle rich in As (5.5%) and Sb (15%), and XY5 a tiny (~10 µm) grain of iron-nickel oxide.

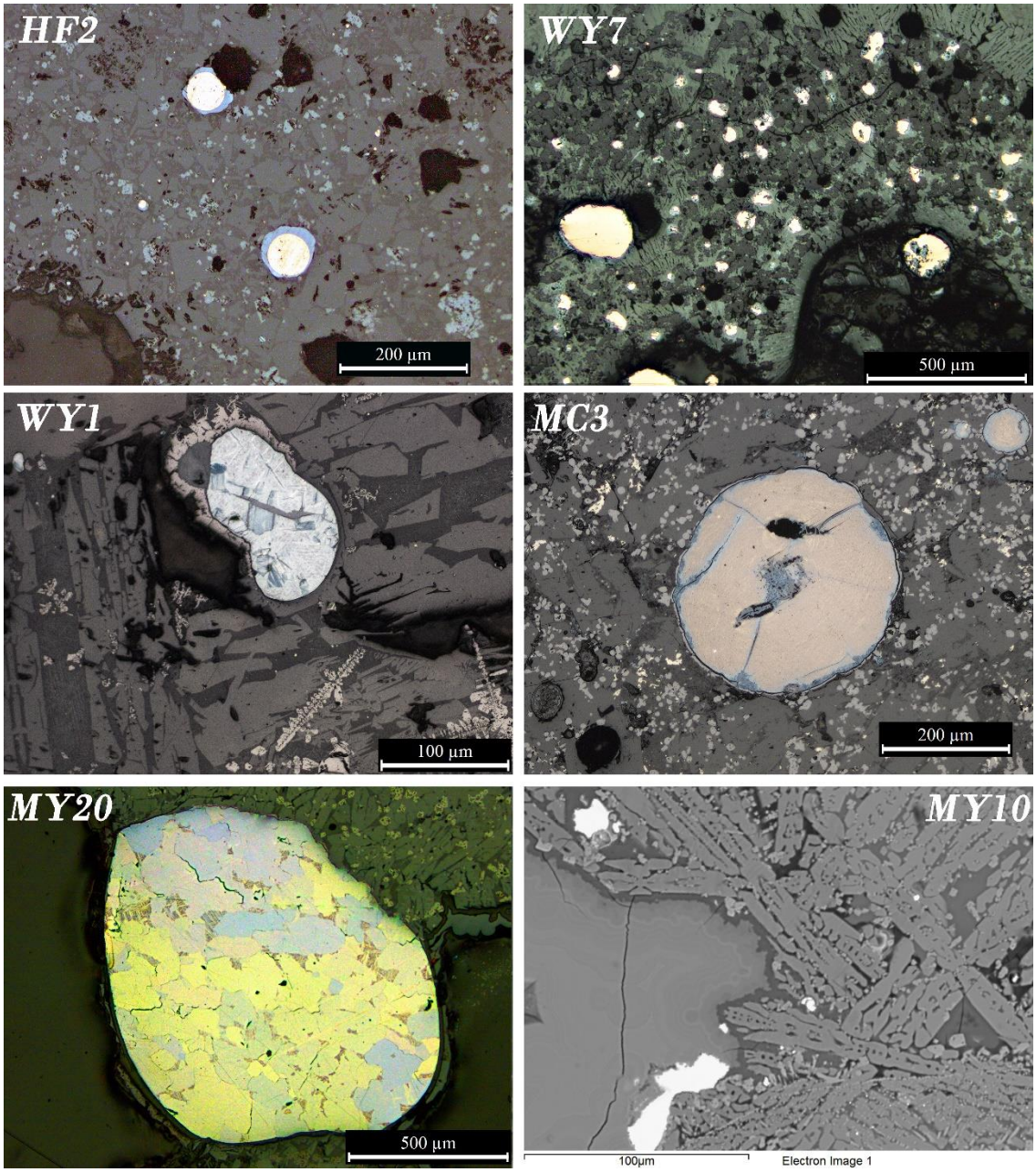

Figure 5.13: OM and SEM micrographs showing matte and copper particles in the Daye copper smelting slag.
(HF2) Copper prills (yellow) with an outer matte envelope (blue), fayalite crystals (dark grey) and magnetite clusters (light grey); **(WY7)** Partly reacted copper silicates (dark grey), fayalite crystals (light grey), abundant copper prills (yellow) and few sulphides (indigo); **(WY1)** Large droplet of chalcocite (lead-grey) with small phases of covellite (pale blue, indigo) surrounded by flakes of magnetite (light grey); **(MC3)** Rounded particles of bornite (yellow pinkish) with veins of covellite (indigo) within a matrix dominated by pseudomorphs of magnetite (light grey) that also contain tiny particles of barium sulphate (white yellowish); **(MY20, OM XPL)** Large matte particle showing crystals of bornite (pink), covellite (brass-yellow) and chalcocite (blue-lead); **(SEM micrograph MY10)**; Elongated particle of barite (white) next to silicates, fayalite laths and CuS particle (white, top).

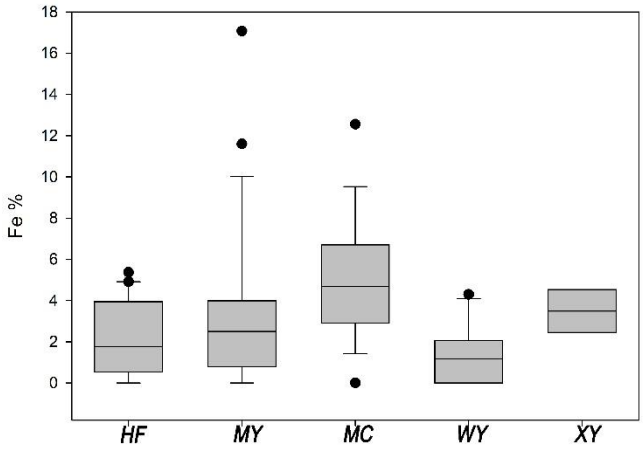

Figure 5.14: Box and whisker plot showing the distribution of the metallic iron dissolved in copper prills.

5.1.6 Atypical by-products

The microstructure of MY26 presents relatively large masses of iron oxides (haematite or magnetite) partially decomposed without well-developed crystals. Occasional melted areas are present within the massive agglomerations of iron oxides that commonly contain iron silicates (fayalite), tiny phases of copper and iron sulphides, and also rare copper prills held together by scant slaggy matrix (Figure 5.15).

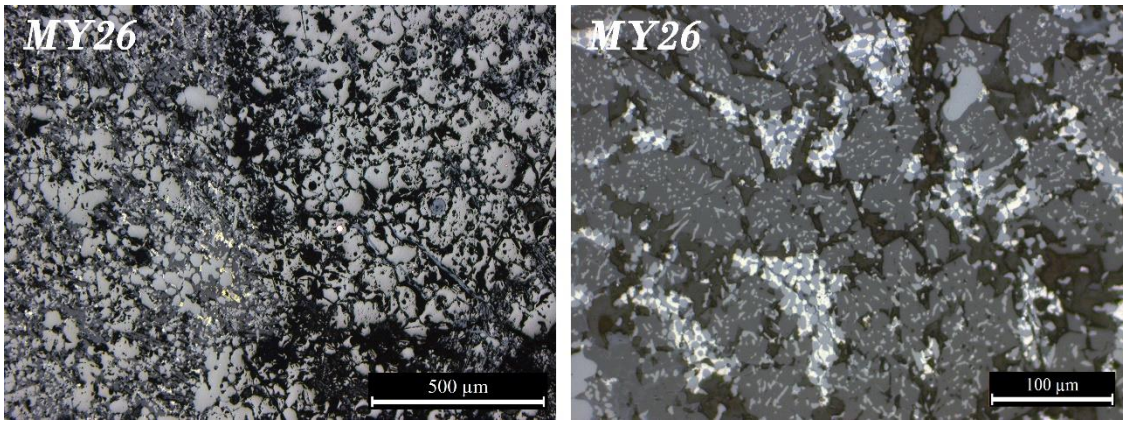

Figure 5.15: OM micrographs showing the microstructure of the atypical by-product MY26. Left: Massive agglomeration of iron oxides (brighter grey) showing small melted areas of iron silicates (dark grey) and metal-rich particles (white yellowish). **Right:** Detail of one melted area showing fayalite crystals (dark grey), iron sulphides (light grey) and copper sulphides with small points of Fe-S rich in Cu (white) held by glassy matrix (dark grey).

The occurrence of complex combinations of copper, iron, oxygen and sulphur within a general absence of molten phases, and the abundant porosity, are consistent with roasting and processing of ores (Marechal 1985; Rehder 2000; Kassianidou 2003; Hauptmann 2014).

It is rather unlikely that MY26 is the result of roasting copper-rich ores since its copper content (less than 1%, Table 5.3) is far too low; however, this bulky anomalous lump consisting mostly of partially reacted iron oxides with a bulk FeO content of 85% could constitute a piece of roasted haematite.

5.2 Copper smelting furnaces and technical ceramics

Except in MY, where no piece of furnace wall was found, furnace fragments were sampled in all sites scattered on surface (Table 5.1). The only well preserved structure is a shaft furnace with tapping hole of approximately 50-60 cm of inner diameter that was located in HF in 2005 (Figure 5.16). Unfortunately, in 2014 this structure was not visible and exact dimensions could not be measured. Two different furnaces were located visible on a natural section (Figure 6.18) but these are related to bloomery iron production rather than copper, and are therefore described in chapter 6.

Figure 5.16: Shaft furnace related to copper smelting located in HF.
Image courtesy of Prof. Li Yanxiang.

Only in one case (HF10) was it possible to conclusively relate a technical ceramic fragment to a specific furnace facility, which corresponds to an already disaggregated fragment of the base of the furnace found inside the chamber of the HF shaft furnace.

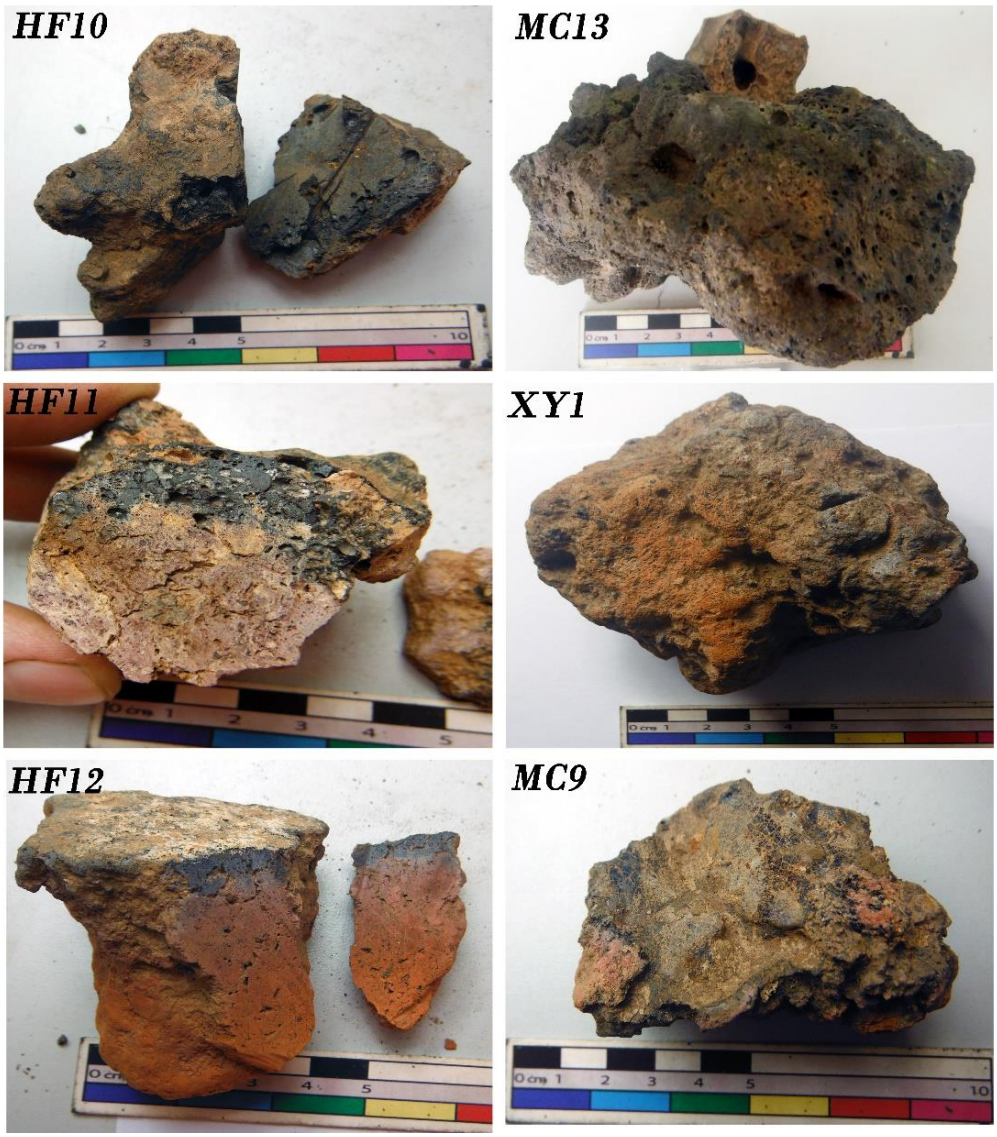

Figure 5.17: Photographs and cross-sections of selected copper furnace wall fragments.
(HF11, HF12) Gradient sections showing thermic-alteration: red-burnt clay and black vitrified clay; **(HF10)** uniquely the blackish ceramic; **(MC13)** Spongy clay materials directly exposed to high temperatures, being appreciable a possible fragment of a brick attached to the upper part; **(XY1)** Undetermined fragment of red-burnt clay furnace wall; **(MC9)** Front view of the ceramic directly exposed to high temperatures.

In general, all samples are visually and compositionally quite similar. The samples display a bulky amorphous morphology, and generally display a gradient in section that is widely recognisable in pyrotechnical ceramics activities (Herdits 1993): a grey-black layer of frequently vitrified ceramic on top of a red-burnt clay with less severe signals of exposure to high temperatures (Figure 5.17). In general, the red-burnt clay is predominant while the black one is thinner, sometimes with a very thin totally vitrified layer 'coating' it; however, the vitrified skin can often be dislodged post-depositionally and thus the predominance of the redder type could be largely due to a sampling bias.

In no case the collected fragments allowed a reconstruction of the furnace diameters or thickness of the original walls. Equally, a possible fragment of a brick (not analysed) is attached to MC13 but no evidence of this constructive material was reported by the local archaeologist who located the shaft furnace of HF.

5.2.1 Analyses of technical ceramics

Seven out of the nine samples associated to copper smelting sites present a ceramic body showing predominantly red-orange colours, occasionally with a reduced black – frequently vitrified – layer on top (Figure 5.17, HF11, HF12, XY1); these are considerably less altered by fire than the other fragments where the darker material is predominant (Figure 5.17, HF10, MC9, MC13). Based on the chemical composition of the samples that appeared less altered by use, the preparation of technical ceramics seems to have followed a very similar recipe at all sites, based on the use of non-calcareous clays. The bulk chemical results of these samples reveal relatively low FeO (~4-6%), moderate Al_2O_3 (~12-18%) and high SiO_2 (~71-77%). Other elements are typically ≤1% excepting K_2O (~2%) (Table 5.7). The composition was obtained by averaging five SEM-EDS area analyses per homogeneous layer, avoiding the temper-rich and the strongly altered areas. Thus it is fair to say that a proper bulk analyses would likely read a higher content of SiO_2.

In section, five samples showed a compacted, black ceramic with some porosity and vitrified areas which indicate that these were the inner parts of the furnace wall subjected to much higher temperatures; this is very clear in the voluminous spongy masses of MC, which also show chemical changes resulting from the interaction with the smelting charge.

The chemical composition of this sample nearly doubles the amount of FeO than in the reddish clay fabric (~8-15%), and is significantly poorer in silica (57-62%), with variable levels of alumina, being noticeable the 25% of alumina in MC9. Another notable difference is the incorporation of heavy metal oxides, namely MnO, CuO, ZnO and PbO that are generally absent within the normal ceramic fabric, and where MC9 stands out again for the high content in PbO (3.6%) (Table 5.7).

		Na_2O	MgO	Al_2O_3	SiO_2	P_2O_5	K_2O	CaO	TiO_2	MnO	FeO	CuO	ZnO	PbO
RED-BURNT FABRIC	**HF11**	bdl	0.9	14.5	74.8	bdl	2.8	bdl	1.2	bdl	4.6	0.9	bdl	bdl
	HF12	bdl	0.7	16.9	73.1	0.7	1.9	bdl	1.1	bdl	5.7	bdl	bdl	bdl
	MC11	bdl	0.9	18.0	71.6	bdl	2.2	bdl	1.4	bdl	5.9	bdl	bdl	bdl
	MC13	bdl	0.8	12.5	73.4	bdl	bdl	2.2	1.3	bdl	6.9	1.4	bdl	bdl
	XY1	bdl	0.3	12.3	77.7	1.1	1.6	0.6	1.0	bdl	5.2	bdl	bdl	bdl
	WY9	0.2	0.4	14.3	75.5	bdl	2.0	bdl	1.3	bdl	6.5	bdl	bdl	bdl
	WY6	bdl	0.6	14.7	75.4	bdl	1.6	bdl	1.2	bdl	6.3	bdl	bdl	bdl
BLACK VITRIFIED	**HF11**	0.3	1.4	11.1	62.2	0.8	4.1	4.5	0.7	0.5	8.4	6.2	bdl	bdl
	MC13	bdl	1.0	17.3	58.3	1.1	2.2	4.7	1.3	bdl	12.3	4.3	bdl	bdl
	MC11	bdl	1.6	11.3	58.2	0.6	2.1	3.1	0.9	0.3	15.7	6.1	bdl	bdl
	HF10	bdl	0.9	12.4	64.1	1.2	2.3	1.0	1.4	0.8	13.5	1.4	0.8	bdl
	MC9	bdl	0.9	25.0	57.3	0.2	1.8	0.3	1.3	bdl	10.1	bdl	bdl	3.6
DP	***HF13***	1.5	1.0	19.1	62.4	4.3	2.6	1.5	0.9	bdl	6.8	bdl	bdl	bdl

Table 5.7: Bulk chemical composition of technical ceramics and domestic pottery (DP).

The copper-smelting ceramics of Daye County were heavily tempered with relatively well sorted finely crushed quartz of sizes typically ranging 100-300 µm – rarely larger than 500 µm – showing angular shapes. Owing to their small size, quartz grains are generally not visible macroscopically in cross-section although these are ubiquitous in all of the samples (Figure 5.18). Due to the high melting temperature of silica (~1600 °C), the addition of this non-plastic temper increases significantly the refractoriness of the clay, which is also increased by the moderately high Al_2O_3 (Freestone 1986; Freestone & Tite 1989). Only in the areas of the ceramic closer to the reaction zone and therefore exposed to higher

temperatures and more aggressive chemical environments does one observe quartz grains partly dissolving in the ceramic matrix, occasionally recrystallising with iron-rich phases or even copper prills similar to those in the slag. Generally, however most of the quartz grains show little reaction with the matrix and retain the original angular shapes.

The use of organic temper such as grass is relatively common in ancient technical ceramics, and it leaves characteristic fibre-shaped voids after the ceramic is fired at high temperature. This kind of temper has the double advantage of increasing the clay plasticity and thus to facilitate the furnace construction on the one hand (Freestone 1986) whereas on the other hand the voids left can increase the heat retention capability of the ceramic and improve thermal shock resistance (Martinón-Torres & Rehren 2014). In this case, however, microscopic observation suggests that organic temper was not widely used since the ceramic fabric generally shows few voids, and these are typically rounded rather than elongated, and they predominate in the black-vitrified layer; voids are less frequent in the less altered red-burnt clays.

Most of the copper smelting samples show only a very thin layer of almost complete vitrification, where the operative temperature of the furnace went well beyond the limit of thermal stability of the ceramic (Chirikure & Rehren 2004). While some specimens suggest that some of the lining certainly collapsed and went into the charge (Figure 5.17, MC13), technical ceramics appear to have coped well with the smelt.

As mentioned in chapter 3, domestic pottery sherds – from Neolithic vessels to Ming porcelain – are very abundant in surface scattered across all the sites. The Daye local archaeologist granted permission to sample only a small sherd found in HF for analyses and comparison with the technical materials. HF13 presents a coarse fabric with visibly large temper, and it is clearly handmade, which indicates a date likely no later than Western Han Dynasty (Prof. Cheng Shuxiang personal communication).

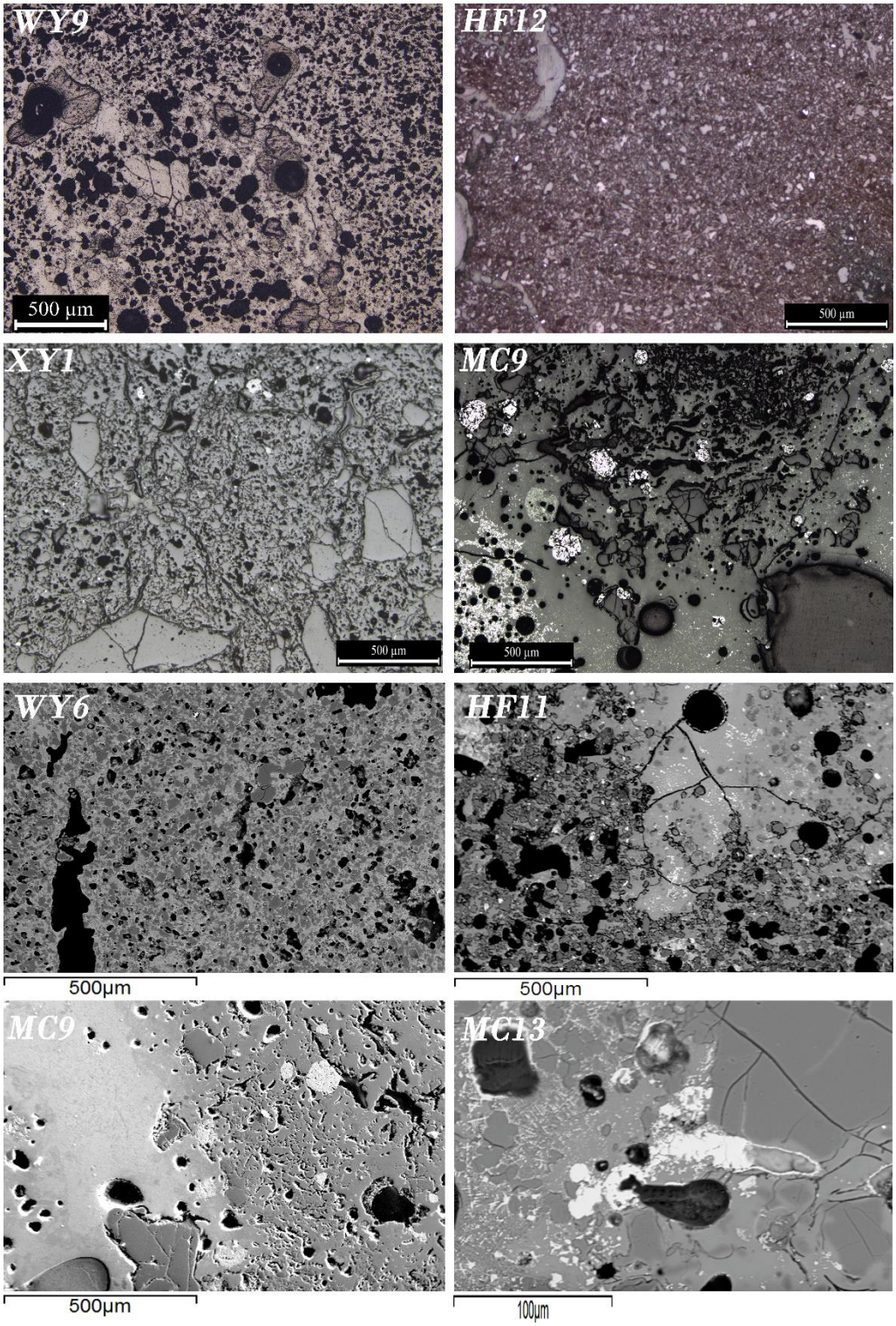

Figure 5.18: OM and SEM micrographs of the copper smelting technical ceramics. **(WY9, HF12)** red-burnt ceramic fabric showing few elongated voids and chunks of quartz; **(XY1, MC9)** chunks of quartz on normal and altered ceramic fabric, the bright particles are zirconium silicates and iron oxides. **SEM micrographs: (WY6)** elongated void in red-burnt ceramic fabric; **(HF11)** agglomeration of quartz (dark grey) stopping the melting of the clay (light grey); **(MC9)** same phenomenon where the quartz grains are partly dissolved in the matrix; **(MC13)** detail of the molten phase (light grey) surrounded by embedded grains of quartz (dark grey) and iron oxides (white) containing few Cu0 (~2%).

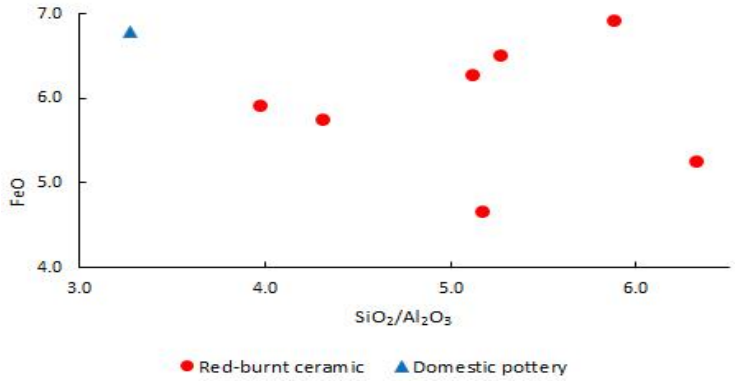

Figure 5.19: FeO to SiO_2/Al_2O_3 ratio values of technical and domestic ceramics.

The bulk chemical composition of this sherd and the analyses of clays of the technical ceramics is relatively consistent (Table 5.7); in general, the domestic pottery is more similar to the red-burnt fabrics than to the vitrified ones. It presents similar levels of FeO, but higher Al_2O_3 (1-7% more depending on the specimen) and clearly lower SiO_2 (9-15% less depending on the specimen) than the red-burnt clays, and lacks any heavy metal oxides which are recurrent in the vitrified ceramics. Since the fluctuations of SiO_2/Al_2O_3 are likely due to the addition of extra silica in the form of quartz temper, this ratio was plotted against FeO to check if the domestic pottery grouped with the furnace wall ceramics, showing that it is broadly within the same line as the less altered clays (Figure 5.19). Figure 5.19 suggests – although not conclusively – that the technical ceramics and the domestic pottery were manufactured using a rather similar clay, and that the differences within the three major components are due to the addition of quartz in the technical ceramics that dilutes the rest of the elements, although the FeO content is not diluted in WY6, WY9 and MC13.

A PCA plot was created in order to investigate the relation between the technical and the domestic ceramics (Figure 5.20).The figure shows that all the red burnt ceramics groups in a relative tight cluster towards the SiO_2 whereas the black vitrified ones plot dispersed in the opposite extreme, dominated by FeO, K_2O, CaO_2, and heavy metals CuO, MgO and Zn. Notably, the domestic pottery plots closer to FeO than to the ceramic-rich cluster, which supports the argument that the natural clay was heavily tempered with quartz. Overall, the domestic pot is broadly similar but bear notable differences too: such as

higher Na and Mg, lower Ti, and exceptionally high P which suggests postdepositional alteration anyway, and makes it hard to offer any meaningful comparison. Thus, it can be argued that technical ceramics were not selected for their particular refractoriness, but at the same time it cannot be claimed that domestic and technical ceramics are the same clay deposit. A fuller petrographic analyses would be useful to further this comparison.

A final noticeable observation is the outlier specimen MC9. Its distinct composition with a high content in Al_2O_3 (Table 5.7) suggests that the ceramic fabric was prepared differently, while the high PbO content may suggest that this ceramic was related to pyrometallurgical activities but not necessarily copper smelting.

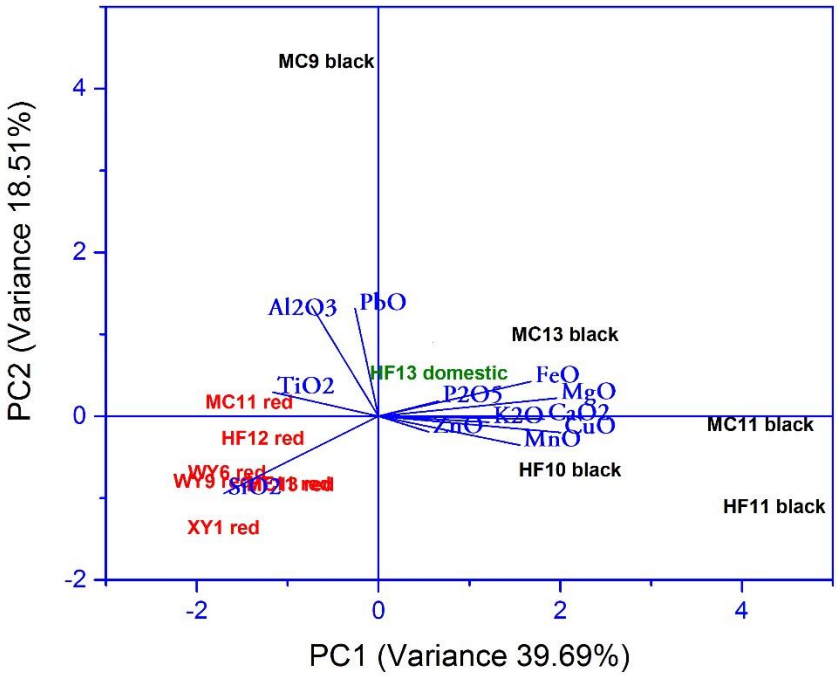

Figure 5.20: PCA plot for the Daye copper technical and domestic ceramics.
First three components explain 74.6% of cumulative variance.

5.3 Ore

Of the four suspected ore pieces analysed (Figure 5.21) none of them corresponds to copper but to iron-rich minerals. Three of the fragments were picked up within a small

heap in physical contact with the flow slag of HF whereas MC17 was randomly recovered from the surface.

Three of them turned out to be very pure haematite, as confirmed by XRD analyses (Figure 5.22) (Appendix VII). Sample HF5 was totally consumed for the XRF and SEM analyses and there is no XRD results to confirm the mineralogy albeit the chemical composition equally points to a high grade iron ore (Table 5.8). Chemical results show low levels of Si and Al, and trace S and Cu, except in MC17, where Al, Mg and Cu are higher. On balance, these minerals are plausibly representative of the iron flux thrown into the copper smelting furnace (section 5.4.1), perhaps after roasting as suggested by the enriched ores HF3-5-6, and also suggested by the atypical by-product MY26.

	MgO	***Al_2O_3***	***SiO_2***	***P_2O_5***	***SO_3***	***K_2O***	***CaO***	***TiO_2***	***MnO***	***FeO***	***Cu****
HF3	0.3	1.6	3.8	0.1	0.1	0.1	0.2	0.1	0.1	93.7	152
HF5	0.2	1.3	3.2	0.03	0.1	0.1	0.1	0.1	0.1	94.9	137
HF6	0.2	1.8	3.5	0.03	0.1	0.1	0.1	0.1	0.1	94.0	128
MC17	6.5	5.9	3.2	0.2	0.1	0.03	0.04	0.1	1.3	82.5	1606

Table 5.8: WD-XRF results of mineral samples.
*All values in % except Cu (ppm).

Polished blocks were mounted for HF3, HF5 and HF6 to check if accessory minerals could be identified, but excepting quartz no crystal whatsoever was identifiable within the agglomeration of iron oxides (Figure 5.23). Typically, the three samples present abundant cracks which is a signal of exposure to high temperatures and consistent with roasting (De Faria & Lopes 2007). The benefits of roasting the flux previously to its addition remain on the one hand in the elimination of the gangue products – silicates mostly – obtaining an enriched content of iron oxides. On the other hand, roasting the flux has the further benefit of facilitating both the crushing and the smelting, since large chunks of pure iron oxide ores are known to be complicate to smelt (Miller, D. et al. 2001; Killick & Miller 2014)

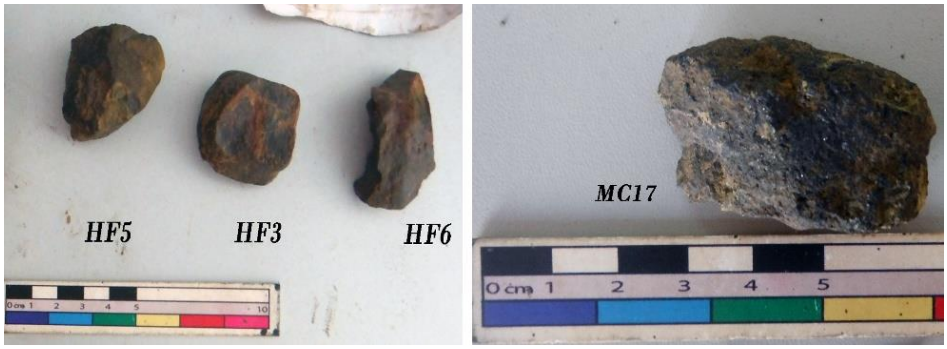

Figure 5.21: Ore fragments recovered in Hongfengshuiku and Maochengnao.

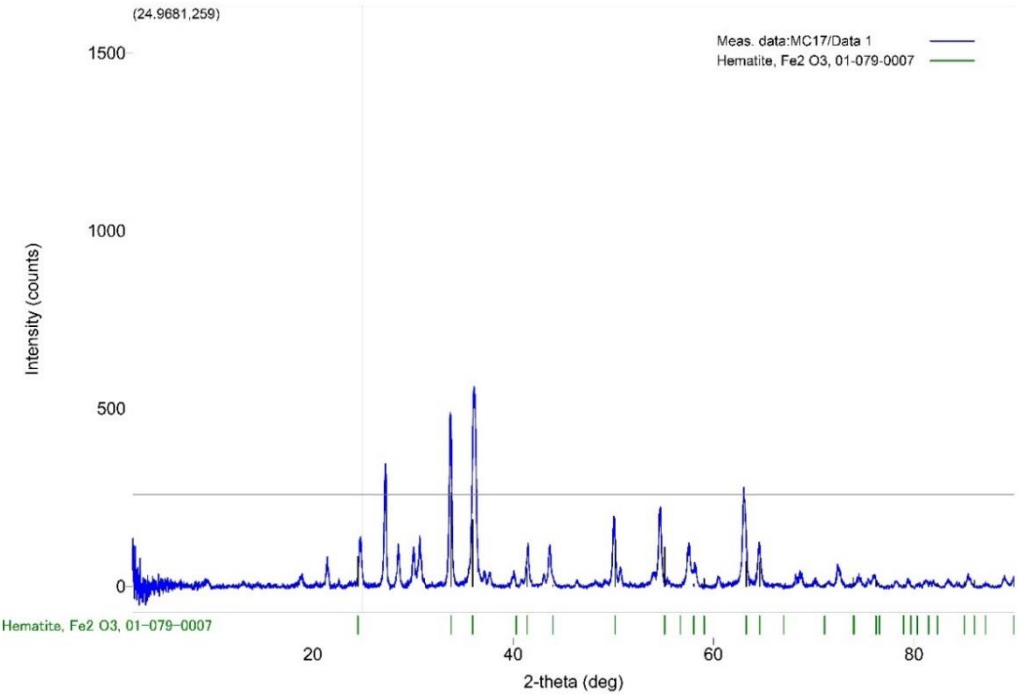

Figure 5.22: XRD spectrum showing the perfect match of the peaks of the sample MC17, and the Fe_2O_3 spectrum from the reference library.

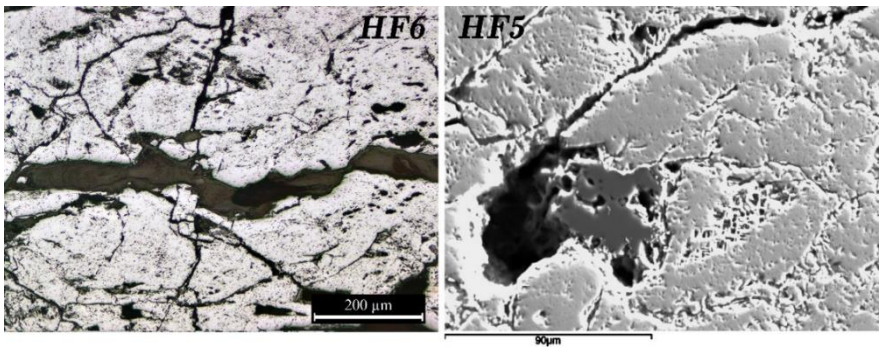

Figure 5.23: OM and SEM (left) micrographs showing microscopic cracking of the ore fragments and a grain of quartz (dark grey).

5.4 Discussion

The Daye slag can be unequivocally identified as a waste product of copper metal reduction, as it presents several well diagnostic characteristics of this type of slag: olivine-dominated microstructure, free iron oxide crystals in the form of magnetite, a variable number of copper prills of different sizes, and droplets of copper sulphides, widely documented throughout different chronologies and geographical locations from the Bronze Age to medieval times in Europe, Asia, the Middle East and America (e.g. Rothenberg et al. 2004; Chiarantini et al. 2009; Maldonado & Rehren 2009; Du et al. 2012).

In addition, there are no other non-ferrous metal particles and the furnace atmosphere was clearly insufficient to reduce iron (Figure 5.34). The iron oxide crystals in the slag are typically magnetite which are clearly not the primary iron oxide phase one would expect in bloomery iron slag, i.e. wüstite (Wingrove 1970), a mineral which is exiguous in these slags.

While all the parameters point to copper production, a main feature to be resolved is the type of ore used – oxidic or sulphidic. This aspect is considered in the following section.

5.4.1 Metal smelting or matte smelting?

Sulphides in copper slag "usually indicate the use of sulphide-rich copper ore during the smelting process" (Shugar 2003, 455). As mentioned before, the use of sulphidic ores entails a much complicated smelting process motivated by the processing of copper rich sulphides. Matte production implies a multi-stage process and better control of the furnace operations; as such, it almost inevitably leads to assumptions about certain status of knowledge and capability on the ancient smelter. Nonetheless, the presence of sulphidic phases in the charge or the smelting remains does not prove the practice of matting activities (Hauptmann 2007, 179; Rehren et al. 2012), and sulphur-bearing metallurgical residues can be open to multiple interpretations, such as inclusions of sulphides that 'contaminate' the oxidic ore, co-smelting of oxidic and sulphidic ores, or proper matte smelting (Rostoker et al. 1989; Li, Yanxiang 1999; Metten 2003). Against this background, the aim of this section is to discern the kind of process that was developed

in Daye by considering several criteria which have been proposed to determine the sulphidic or oxidic nature of the copper ore charge based on slag analysis. This is particularly necessary given the fact that no copper ores were recovered with the sample from any of the sites, and also considering that while most of the works regarding the main mine of Tonglüshan describe the use of oxidic ores (Huangshi Municipal Museum 1980; Wagner 1986; Zhou, B. et al. 1988; Huangshi Municipal Museum 1999), sulphidic ores have also been suggested at one stage during the active period of the mine (Li, Yanxiang 1998a, 1998b, 1999; Li, Yanxiang et al. 1999).

5.4.1.1 Multi-stage production and furnace operation

The reconstruction of metallurgical activities based on the reduction of sulphidic ores has perhaps received more attention in the Alpine region than anywhere else in the world. Abundant efforts have been made in order to reconstruct the industrial activities developed there that in essence involve two main steps: roasting and smelting (Sperl 2003), which were combined in a multi-step process to obtain finally black copper of about 94-6% purity (the balanced being residual Fe and S), successfully separated from the slag (Goldenberg 1998). This process oxidised first some of the iron sulphides of the ore by roasting, then smelted the roasted ore under highly reducing conditions in square furnaces to obtain Cu-rich matte that was roasted and smelted again to obtain the final impure metal (Eibner 1982) (Figure 5.24). This proposal for matte smelting requires very uniform smelting conditions by the combination of strongly reducing atmosphere – pO_2 ~10^{-8} atm or lower (Yazawa 1980 in Moesta & Schlick 1989) – and high temperatures – ~1300 °C (Rosenqvist 1983, 324-331) to succeed in the reduction; as noted below (sections 5.4.2 and 5.4.3), these extremes were not reached in Daye. As a matter of fact, the model has been criticised as being too complex for the Middle Bronze Age periods while this was in use largely in the medieval period and later, and that there were other possibilities of roasting-smelting whose success lied not within the reducing conditions but better in the repetitiveness of technical steps (Moesta 1986; Moesta & Schlick 1989).

A different multi-step process has been suggested by other scholars (e.g. Rostoker 1975) in which the smelting of sulphide ores incorporated more actions with the result that the

copper metal smelted from the ore was not separated from the slag but trapped within it, thus incorporating also beneficiation of the slag as a necessary step to recover the metal prills. The single smelting operation (Rostoker et al. 1989) is based on the gradual liquefaction of Cu–Fe–S minerals that disaggregate from the gangue at low temperatures but leave abundant and massive copper and Cu-rich matte particles in the slag, and thus requires the systematic crushing of the slag cakes – which contain plenty of unreacted quartz materials – to extract mechanically the copper prills (Metten 2003).

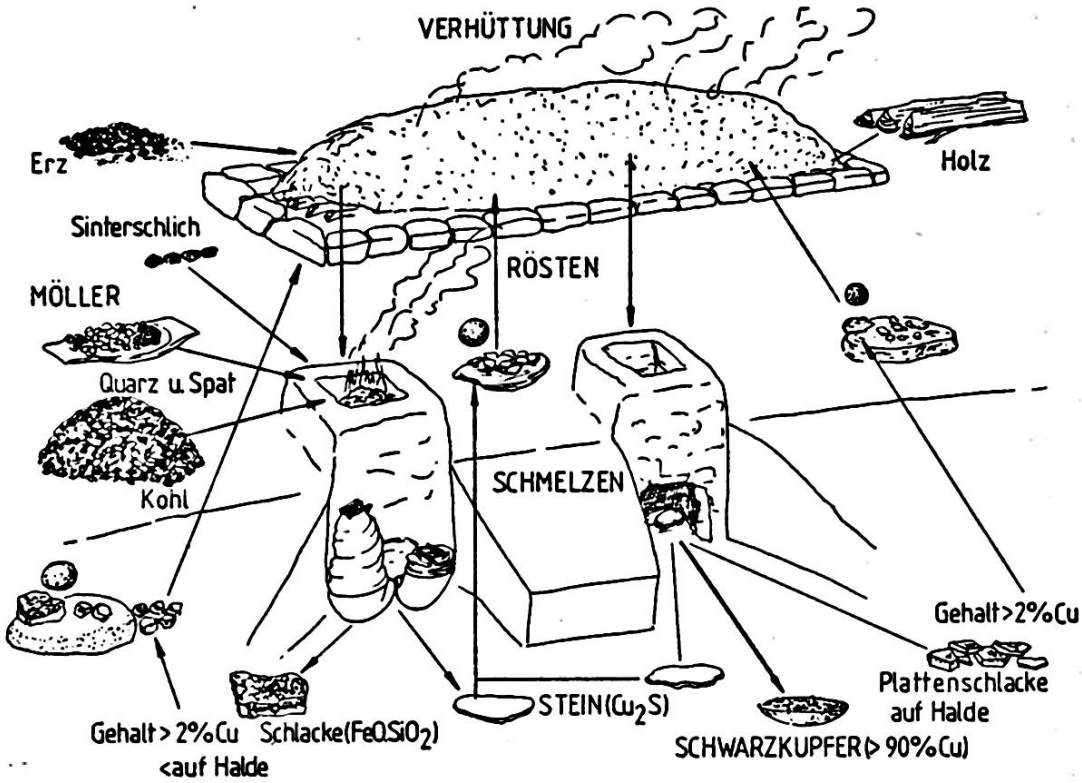

Figure 5.24: Matte smelting structures in the Alps according to Eibner (1982).
The upper part shows a roasting bed and the bottom square twin furnaces. From Metten (2003, Fig. 6).

In Daye, however, the cakes appear naturally broken and mostly complete; the slag is fluid and mostly free of unreacted materials (which, if present, are microscopic and correspond to iron oxides not to silicates); the metal left in the slag is very scarce and in the form of microscopic droplets; and most of the copper in slag is present as sulphide droplets.

A reliable indicator of the matting activities is the existence of a sequence of by-products that follows the reduction of a sulphidic ore, since the mineralogy and microstructure of the slag can be diagnostic of each stage (Figure 5.25). The existence of two main types of slag – coarse and flat – is frequently found in the Italian Alps (Artioli et al. 2007), and occasionally the complete chain slagging–matting–smelting can be distinguished on the basis of chemical, physical and mineralogical parameters of each slag group (e.g. Addis et al. 2015). However, waste products from different processes are often too similar (Erb-Satullo et al. 2015), and in some cases researchers have struggled to identify two different processes out of a single slag assemblage (Van Brempt & Kassianidou 2016).

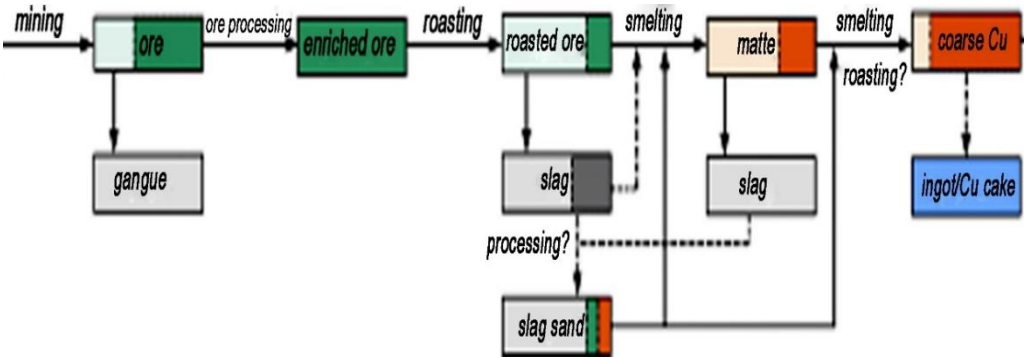

Figure 5.25: Hypothetical reconstruction of the chaîne opératoire of the copper production process during the Bronze Age in the Alps.
After Della Casa et al. (2016, Fig. 4).

In principle, the uniformity of the slag could be used as an argument to defend that a single high-temperature process was taking place, which would be consistent with the smelting of oxidic ores. However, such an assumption might be risky: a slag recycling practice has been proposed for the Chinese copper smelting sites of Jiuhuasan (Li, Yanxiang 1998b) and Sijiawan (Larreina-Garcia et al. 2012), where the by-products of the diverse smelting cycles were recovered and charged back into the furnace along with roasted ore, which led to a single type of by-product left for a multi-stage process. This occasional re-smelting of by-products has been observed in the Alps too – both re-smelting of Cu-rich matte and the use of platy slag as a flux (Larreina-Garcia et al. 2015), and some scholars also argue that two of the diagnostic slags from the Alps – *plate* and

tap slag – could also be the result of one single smelting process (Piel et al. (1992) and Metten (2003) cited in Hauptmann 2007, 37).

Furthermore, in the Early Bronze Age site of Saint Véran (western Alps), a metallurgical process has been reported that involved large-scale production of copper from sulphidic ores (bornite) in a one-step process that did not involve roasting whereas the oxygen was supplied by the tuyere, and that generated mainly one type of slag (Bourgarit et al. 2008). Whereas the Saint Véran's case seems to be unique due to the exceptional circumstances of the ore deposit still documents that smelting copper from sulphidic ores is possible in a single step.

To summarise, the Daye waste-products do not present any evidence of systematic subjection to low pO_2, nor are they suggestive of a combination of different technical steps that successively obtain enriched Cu-matte products and copper metal, which are clear indicators of the use of sulphidic ores. In general, this is a macro and microscopically homogenous well molten slag with a marginal presence of sulphide droplets. Even though these are the main copper-bearing phases in the Daye slag, they are very scant and do not appear to have agglutinated forming thick layers or cakes, as one could expect for sulphidic ores smelted at the temperatures and atmospheres recorded here of ~1100-1200 °C (Rostoker 1975; Rüffler 1996) (section 5.4.2 below). Thus it would seem that the ores smelted were relatively poor in sulphidic minerals. The occasional presence of small amounts of oxidic phases associated to the sulphide particles can be interpreted as the beginning of their desulphurisation during smelting (Hauptmann 2007, 178) but this desulphurisation is quite poor and seems incidental rather than systematic. Overall it seems that the smelters were not too concerned with dealing with any sulphides in the charge, which indicates that they were a minority and not perceived as a problem. As a matter of fact, the presence of some sulphur in the system can facilitate the extraction of copper since sulphides can form at low temperatures ranging the 800-900 °C – thus before the slag formation – acting as a solvent and collection accumulator for copper metal during smelting, as well as a lubricant that considerably enhanced the liquid-liquid separation of the copper from the slag as it solidified (Rostoker 1975; Hauptmann et al. 2003; Metten 2003).

5.4.1.2 Bulk sulphur content

The XRF results show relatively low sulphur values for the Daye slag (0.1-0.7%). However, the bulk sulphur content in the slag cannot be taken as a reliable indicator of the type of ore or smelting activities (Pryce et al. 2010). For example, rather low levels of sulphur (0.1-0.9%) have been recorded in slags where other evidence indicated multi-stage matte smelting with predominantly sulphidic ores (e.g. Chiarantini et al. 2009; Maldonado & Rehren 2009). Here, a substantial amount of sulphur would have been removed through the roasting and/or re-smelting of the sulphur-rich charge. Conversely, small amounts of sulphur (up to 2%) have been noted in smelting slags where geological and archaeometallurgical studies indicated predominantly-oxidic ores, probably containing some residual sulphides (e.g. Wagner 1986; Georgakopoulou et al. 2011).

Figure 5.26 shows the average bulk chemical composition of S and Cu in slag of different matte and oxide smelting sites. On a first impression (upper chart), there seems to be a tendency of the slag to be Cu-rich if the ore is oxidic. However, the lower chart shows a much blurred distribution without clear patterns between the normal content of Cu and S in slag (up to ~2% respectively). Notably, many matte smelting slags plot within the oxidic ore smelting expected area richer in Cu than in S – frequently lower in S than oxidic smelting slags – and viceversa, many oxidic ore smelting slags are richer in S than in Cu, and a large part of the slags contain rather similar levels of both elements. The Daye slag plots clearly within the oxidic-ores smelting cluster, but as observed the bulk composition of S in slag can be a tricky indicator if considered alone to determine the type of ore and smelting activities.

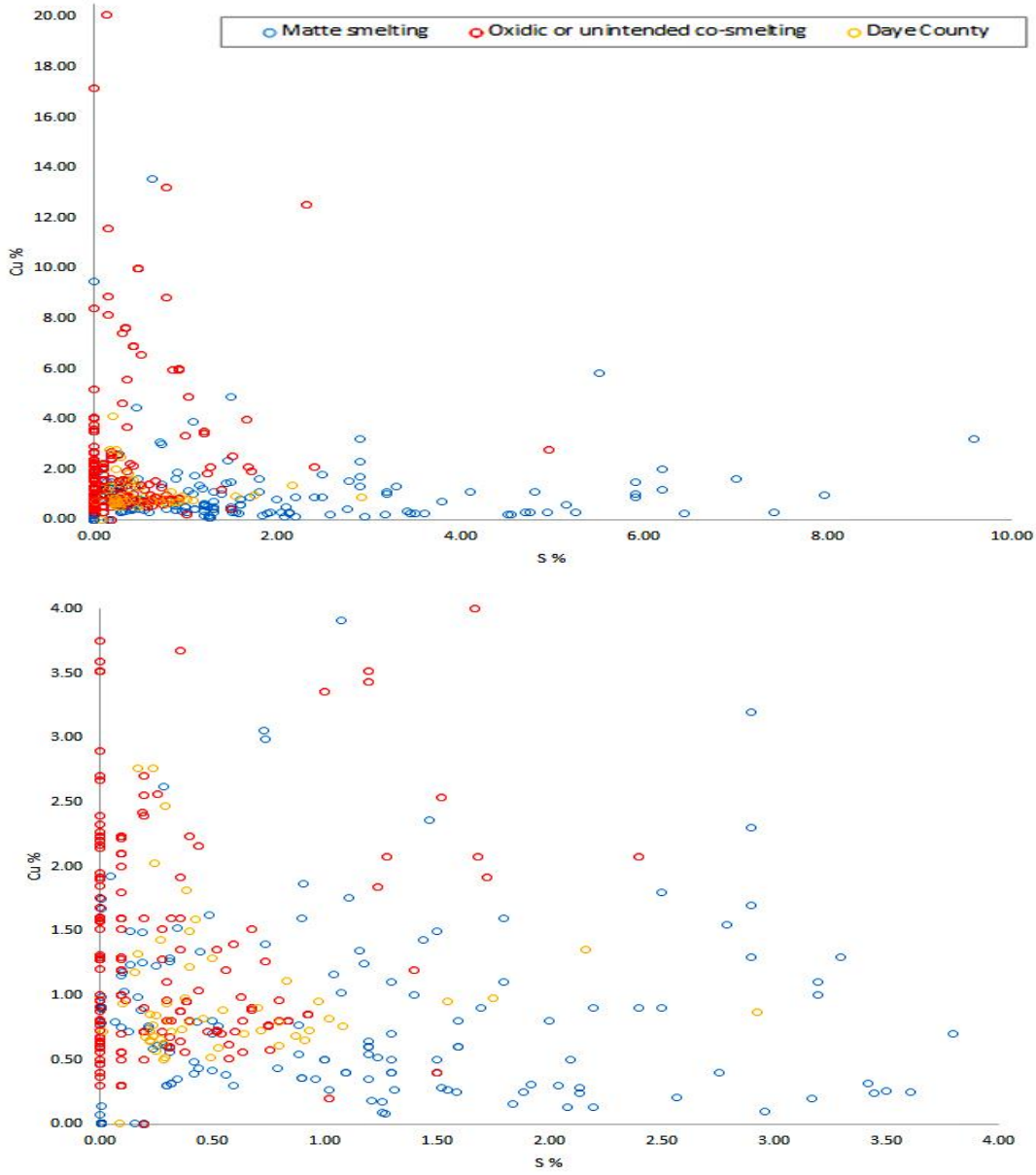

Figure 5.26: Binary plot comparing the bulk sulphur composition of S and Cu (weight %) in slag of different archaeological sites related to matte and oxidic ores smelting, and the Daye copper smelting slag.

Matte smelting slag data: Luserna (Italy) LBA (Addis et al. 2015, Table 3); Kalavasos (Cyprus) LBA (Van Brempt & Kassianidou 2015, Table 2) ; Baratti (Italy) 9th-8th cent BC (Chiarantini et al. 2009, Table 2); Cappatoli (Italy) 7th cent. BC (Manasse et al. 2001, Table 1); Skouriotissa (Cyprus) AD 500-600 (Georgakopoulou & Kassianidou 2013, Table 3.41); Sijiawan (China) AD ~800-1100 (Larreina-Garcia et al. 2012, unpublished data); Tuscany (Italy) AD 1300-1400 (Manasse & Mellini 2002, Table 1); Itziparátzico (Mexico) AD 1450-1530 (Maldonado & Rehren 2009, Table 2).

Oxidic smelting slag data: Timna and Faynan (Israel, Jordan) Chalcolithic and EBA (Rothenberg 1988, 199; Hauptmann 1989, Table 14.12); Peñalosa (Spain) EBA (Rovira et al. 2015, Table 2); Shar-i-Shokta (Iran) EBA (Hauptmann et al. 2003, Table 2); Seriphos (Greece) EBA (Georgakopoulou et al. 2011, Table 2); Kition and Enkomi (Cyprus) LBA (Hauptmann 2011, Table 19.11); Tonglüshan (China) 1st Millennium BC (Wagner 1986, Tables 7-8-9); Khao Wong Prachan (Thailand) 1st Millennium BC (Pryce et al. 2010, Table 7); Shankare (South Africa) early 2nd millennium AD (Thondhlana 2012, Table 6.7).

5.4.1.3 Sulphidic phases suspended in the slag

It appears that the nature of the sulphides and their mineralogical associations, rather than the bulk sulphur content, may be a more reliable technological indicator: sulphide-smelting slags often contain complex sulphides in the form of matte (Figure 5.27), and these tend to be more abundant than copper prills (e.g. Van Brempt & Kassianidou 2016) whereas oxide-smelting slags tend to be dominated by metal prills, with sulphides being simpler and relatively scarcer (e.g. Hauptmann 1989).

The simple sulphides as observed in HF (Figure 5.13) surrounding small copper prills have also been described in Early Bronze Age slags from Faynan (Jordan), and interpreted as deriving from minor amounts of sulphur present in a predominantly oxidic ore; sulphide presence was in fact too low to have any consequence in the kinetics (Hauptmann 1989). However, if the ores contain a larger amount of sulphides – ≥2% sulphur in the charge (Taffel 1953 cited in Kassianidou 1998, 69) – then matte will be formed and retain most of the copper, such that hardly any metal can be found in the slag (Hauptmann 2007, 179). This seems to be the case in the other four sites (Table 5.6 and Figure 5.12).

Similar copper prills 'stained by globules of copper sulphide and copper-iron sulphide inclusions, also surrounded by blue rims rich in sulphur' – were documented in Shankare Hill in South Africa (Thondhlana 2012, 220). As in Faynan, the evidence at Shankare does not seem to suggest predominant use of sulphide ores went into the charge but rather the opposite situation. The sulphide inclusions are interpreted as residual sulphidic cores present within secondary copper carbonates ores (Thondhlana 2012, 262). Moreover, no complete matter prills were documented in the Shankare slag samples, as would have been expected with a sulphur-rich charge (Thondhlana et al. 2016).

Nonetheless, frequently it is difficult to discern between 'complex' and 'simple' sulphides in slag (e.g. Chiarantini et al. 2009) as is as well the case of Daye where several other parameters indicate the same smelting procedure. Figure 5.27 compares the distribution of the composition of matte and copper particles in slag of several oxidic and sulphidic smelting sites. Typically, the distribution of the Cu–Fe–S particles is wider within the matte smelting sites. However, this diagram also reveals that in one occasion the distribution is quite flat (Colchis) since the particles contain very low sulphur (bdl-0.39) while in the

oxidic ore smelting site of Seriphos there is also chalcocite in the plot. Thus, Baratti (~30 particles) shows a moderate variation in comparison with the Trentino area and Sijiawan (>100 particles each) that display a much wider diversity; Daye also shows a relatively wide scatter of composition if is plotted as a single group but if one compares Figure 5.27 with the binary plots Cu/S in Figure 5.6 and Figure 5.12 where each site in Daye is plotted individually, it is possible to appreciate that the variation within sites is generally much more limited, and the spread is mostly corresponding to the same site (MY). In general, the composition of the matte particles is not correlated to a specific type of slag, as is evident in the sites of Baratti and the Trentino area where different types of slag from a multi-stage process were analysed.

As a matter of fact, the analyses of modern slag involved in smelting-converting-refining operations to produce blister copper equally reports a wide variation in size, shape, composition and distribution of the copper matte particles; and neither the bulk sulphur content in slag nor the operational stage in which this was generated seems to have a strong influence on the grade of the matte particles (Fernández-Caliani et al. 2012). The distribution of the matte particles is equivalent in the first two stages of the process – flash and electric furnace respectively – whereas the particles within the granulated slag (final stage) contain more sulphur and show a slightly wider distribution than the converter slag from a previous refining stage (Figure 5.28).

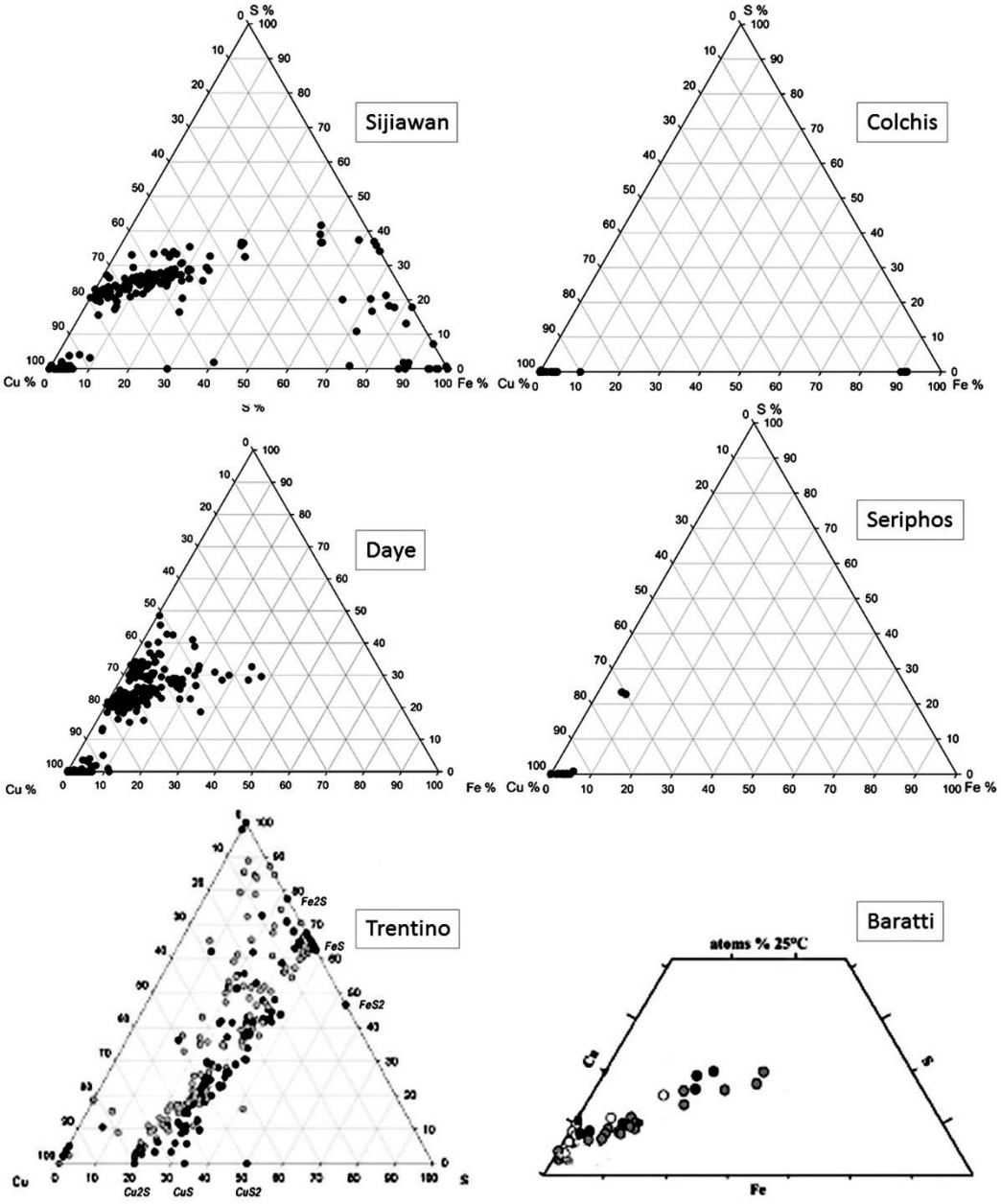

Figure 5.27: Ternary diagrams Cu-Fe-S (weight %) comparing the distribution of matte and metal particles in slag within Daye and different smelting sites that used sulphidic or oxidic ores.

Matte smelting sites: Sijiawan (China); Trentino (Alps, Italy) plotted as Cu-S-Fe, figure modified from (Angelini et al. undated, Fig. 1); Baratti (Italy), diagram in atomic % from (Chiarantini et al. 2009, Fig. 6); Colchis (South Caucasus) (Erb-Satullo et al. 2015, Table 4).

Oxidic ore: Seriphos (Greece, oxidic ore) (Georgakopoulou et al. 2011, Table 3).

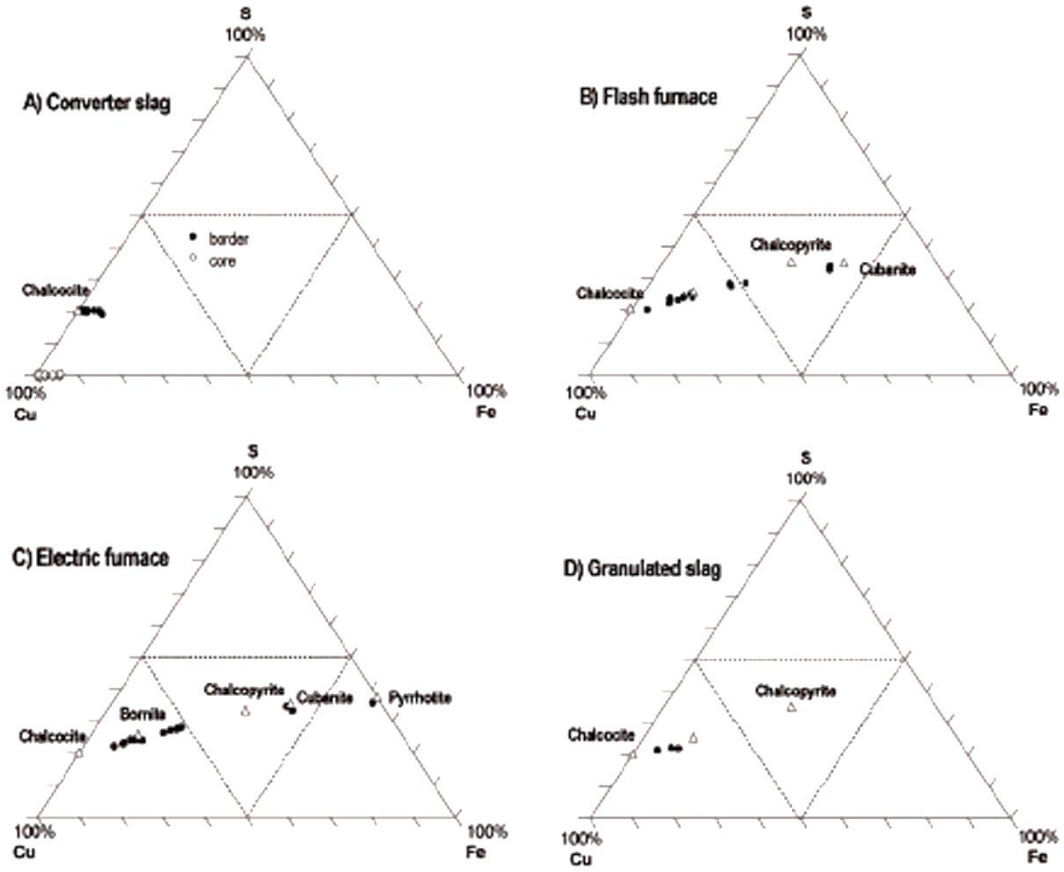

Figure 5.28: Ternary diagrams Cu-Fe-S (in atomic %) showing the composition of copper matte particles in modern copper blister production slag.
Triangles indicate the reference minerals, from Fernández-Caliani et al. (2012, Fig. 6).

5.4.1.4 Cu to S ratio

Tylecote (1987, 303) suggests the calculation of the Cu/S ratios in slag to discern the primary or secondary character of the copper ore: if the ratio is around 1:1 this may denote matte-smelting, while a ratio in the order of 10:1 is expected for oxidic ores. Other scholars (Li, Yanxiang 1998a, 1999) propose a different system based on the same ratio Cu/S but measured in the sulphide droplets instead of in the slag bulk composition: a ratio lower than 4 is indicative of matte smelting, whereas a higher one indicates copper-oxide smelting. Both ratio calculations were applied to the Daye slags with somewhat contradictory results (Table 5.9): the bulk Cu/S in the slag is significantly higher than 1:1 but not as high as the 10:1 expected by Tylecote to be conclusive of oxidic ores except perhaps for HF, where the ratio is 9, and MY, where the ratio is very close to 1. The same ratio in slag was calculated for several oxidic and sulphidic ore smelting sites but the

results are not convincing either: the ratio in some matte smelting sites is lower than 1:1 as expected but in many of them this in an ambiguous intermediated position between 2 and 9.

The Cu/S ratio in slag is in general equivocal. For example, this criterion would lead us to think that oxidic ores or co-smelting were used at Itziparátzico, where in fact matte smelting activities are well documented (Maldonado et al. 2005; Maldonado & Rehren 2009). Equally the calculated ratio of 5 would indicate that Sijiawan was likely co-smelting ores, even though we know that the main ore was chalcopyrite (Larreina-Garcia et al. 2012). Conversely, at sites such as Tonglüshan where we know oxidic ores were used, the Cu/S ratio in slag would indicate sulphidic ores if we were to follow the above criterion.

On the other hand, using the Cu/S ratio in matte particles we would infer that four of the sites in Daye (MY, MC, WY and XY) were smelting sulphidic ores since values for all the sites are below 4, while HF would be smelting secondary ores.

The Cu/S ratio in matte particles applied to other smelting sites is also equivocal, as it yields a ratio of 389 – definitely higher than 4 and thus indicative of oxidic ores smelting – for matte smelting sites in the South Caucasus (Erb-Satullo et al. 2014). The calculation of this ratio is not straightforward since there are unclear explanations concerning its application: for example it is stated that only droplets bigger than 50 µm are suitable for the analyses but attending to the micrographs shown in the publication, smaller particles are also included in the analyses (Li, Yanxiang 1998a, Fig. 1-6); the paper also fails to explain how complex droplets are measured: e.g. the copper prills with matte envelopes or the double prills. Finally, it is not clear either if the method is intended to discern the sulphidic or oxidic nature of the ore smelted or to discern between primary matte smelting slag from refining slag generated in posterior stages.

Consequently, none of the above criteria seem to be particularly determinative, since the Cu/S ratio is a changing variable. As previously detailed, the smelting of sulphidic ores is a complex process that typically entails multiple stages whereby the original ore is transformed into matte products that are progressively Cu-enriched at the expense of

	Site / Slag type	*Cu/S in slag*			*Cu/S in Cu-bearing particles entrapped in slag*					
		S	**Cu**	**Cu/S**			**S**	**Fe**	**Cu**	**Cu/S**
Daye County	**HF**	0.1	0.9	9	**HF (42)**	MEAN	8.5	2.9	88.6	10.4
	MY	0.8	1.0	1.2		STD	11.1	2.3	11.9	
	MC	0.5	1.7	3.4		MAX	32.2	10.8	100.0	
	WY	0.4	0.8	2.0		MIN	bdl	bdl	67.1	
	XY	0.3	0.7	2.3	**MY (147)**	MEAN	31.2	5.1	63.7	2.0
						STD	15.1	4.8	16.6	
Matte smelting	**Baratti matte-rich**	0.6	0.8	1.3		MAX	59.3	29.6	100.0	
	Baratti matte-Cu	0.6	2.5	4.2		MIN	bdl	bdl	27.9	
	Baratti Cu-rich slag	0.3	1.6	5.3	**MC (56)**	MEAN	28.8	6.6	64.5	2.2
	Luserna coarse slag	1.0	1.4	1.4		STD	18.4	4.8	20.4	
	Luserna massive	1.5	1.1	0.7		MAX	57.2	17.3	100.0	
	Luserna flat slag	0.9	0.5	0.5		MIN	bdl	bdl	32.2	
	Itziparátzico platy	0.1	1.2	12	**WY (61)**	MEAN	28.2	5.8	65.9	2.3
	Itziparátzico lumpy	0.2	1.2	6.0		STD	17.2	6.5	21.2	
	Marsiliana	2.5	0.4	0.2		MAX	49.0	31.8	100.0	
	Arialla	2.2	0.4	0.2		MIN	bdl	bdl	24.6	
	Rochette	4.5	0.3	0.1	**XY (52)**	MEAN	32.8	3.8	63.4	1.9
	Cappatoli	3.0	0.3	0.1		STD	8.8	2.0	8.8	
	Kalavasos tap slag	5.6	1.5	0.3		MAX	52.7	12.2	97.5	
	Kalavasos furn. slag	1.8	1.2	0.7		MIN	bdl	1.3	41.5	
	Skouriotisa	1.6	0.7	0.4	**Seriphos**	MEAN	2.5	3.1	93.6	37.5
	Sijiawan	0.1	0.5	5.0		STD	6.9	1.9	8.6	
Oxidic ores smelting	**Seriphos**	0.1	1.6	16.0		MAX	22.9	6.9	98.9	
	Khao Wong Prachan	0.8	2.4	3.0		MIN	bdl	bdl	68.5	
	Shankare	0.2	1.2	6.0	**Colchis**	MEAN	0.2	16.5	77.9	389
	Tonglüshan	0.6	0.8	1.3		STD	0.1	29.3	33.7	
	Faynan	0.5	24.7	49.4		MAX	0.4	84.8	100.0	
	Kition	0.9	9.6	10.6		MIN	bdl	bdl	7.9	
	Shar-i-Shokta	0.5	7.0	14	**Sijiawan**	MEAN	23.5	8.8	67.7	2.9
						STD	5.3	9.2	18.5	
						MAX	37.4	59.1	98.6	
						MIN	2.0	0.8	3.6	

Table 5.9: Cu to S ratios in slag (left) and in matte particles.
References of the sites available in caption of Figure 5.26.

sulphur and iron; this sequence has been recorded in numerous archaeological sites (e.g. Doonan et al. 1994; Ryndina et al. 1999; Manasse & Mellini 2002; Mei & Li 2003; Metten 2003; Knapp & Kassianidou 2008; Anguilano et al. 2009; Chiarantini et al. 2009, etc.). As a result, the slag from the last stages of the process can contain negligible levels of sulphur and copper, and scant sulphur inclusions or copper particles, and thus bear virtually identical features to slag from the smelting of oxide ores. Moreover, single specimens can modify considerably the ratio (e.g. MC3, HF17). As noted above, attending to the Cu/S ratio there should be at least two different ores types in use in Daye – oxidic in HF and sulphidic or mixed ores in the rest of the sites – which seems surprising when other parameters (flux, furnace operating conditions, etc., addressed below) suggest a common technical procedure which would not fit with the processing of different ores.

5.4.1.5 Iron in copper

Copper smelted by the matte process typically renders copper metal of 94-96% purity with a significant number of impurities, primarily S and Fe; as a result of the conversion of sulphidic ores into iron-copper matte products and the gradual enrichment of those matte products into Cu-rich matte and finally into Cu metal. During this process, certain amounts of Fe and S are typically present as resistants in the final ingot that requires refining (Goldenberg 1998). Therefore, determining the origin of the iron in the copper – i.e. iron added as a flux or from iron in oxidised sulphide ores – can yield valuable information concerning the metallurgical process (Cooke & Aschenbrenner 1975, 254). Iron has a relatively low solubility in copper between 1100°C and 1200 °C (~3-6%); however, a mere 2% S in the system can increase dramatically the iron solubility in copper up to a 20% at 1200 °C (Craddock & Meeks 1987) (Figure 5.29).

The iron in the final copper metal ingot can be reduced down to trace element levels after several refining steps (Craddock & Meeks 1987; Merkel 1990, Table 13) but the trapped copper prills in the slag should contain significant levels of Fe – even after the multi-stage reduction – since these were not refined. Figure 5.14 shows that, with a couple of exceptions, the iron content of the copper prills trapped in Daye slag generally ranges between 2-6% or lower.

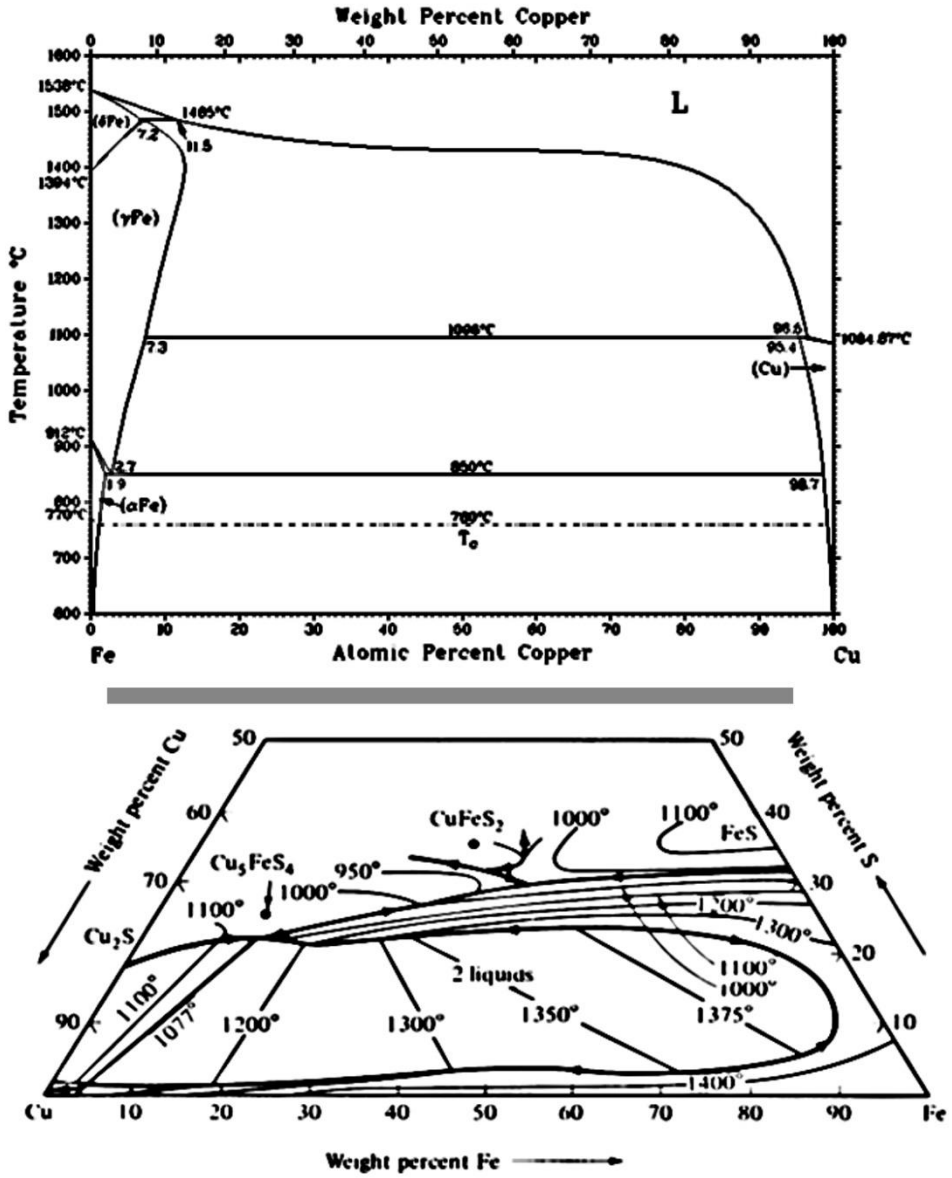

Figure 5.29: Fe-Cu equilibrium diagram and Cu-Fe-S liquidus system.
Fe-Cu diagram courtesy of http://www.himikatus.ru/. Cu-Fe-S diagram after Rosenqvist (1983, Fig. 12-12).

This range is comparable to iron in copper levels in slag prills of both oxidic and sulphidic-ore smelting observed in several smelting sites (Hauptmann 1989, 127; Li, Yanxiang 1998a, Tables 3-4; Hauptmann 2007, 202-203) or even in finished objects (Craddock & Meeks 1987).

Other comparative material is found in several copper smelting sites in South Africa during the second millennium AD (Thondhlana 2012). While there is no evidence for smelting of primary sulphide ore in southern Africa the copper particles in the slag are recurrently

contaminated with residual sulphides and exsolved iron, which can be as high as 30 wt% (Killick et al. 2016). However, these sulphides simply denote the residual presence of sulphides in predominantly oxidic ores whereas the exsolved iron is due to an over-reducing furnace atmosphere, and are not the result of matte smelting (idem). The smelted yield of metal was iron-rich black copper that required refinement to get rid of the impurities in the earlier sites, however, it is also detected a technological improvement through time where balance in redox and temperature together with use of well beneficiated ores seems to solve the problem of the impurities (Thondhlana 2012, 358; Killick et al. 2016; Thondhlana et al. 2016).

These results therefore do not point clearly to either oxidic or matte smelting. There is no correlation between sulphur and iron that might be related to an iron increase facilitated by the presence of sulphur in the system (Figure 5.30). Furthermore, experimental archaeology has demonstrated that even if the reduced ore is oxidic the result after the first smelting can be a very Fe-rich (22%) black copper, and that successive remeltings still can render quantities of 1-6% Fe in copper (Merkel 1990, Tables 13 and 14).

Finally, the iron content measured in the prills can be misleading since these are typically very small particles and therefore, when analysed by SEM-EDS, the electron beam interaction volume may be larger than the prill and cover part of the surrounding iron-rich matrix (Georgakopoulou et al. 2011, 133).

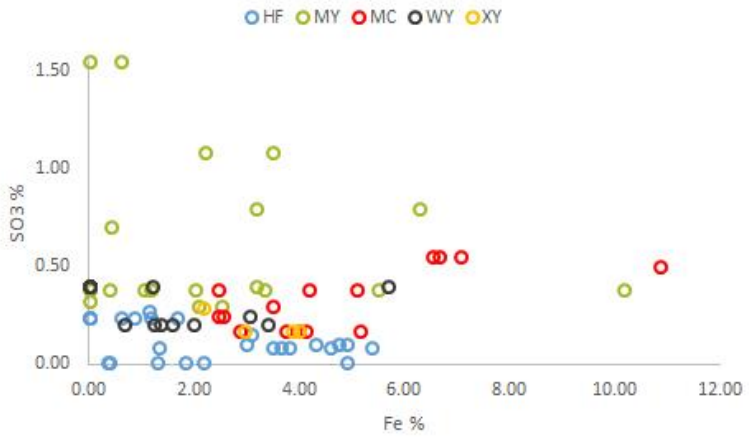

Figure 5.30: Scatterplot of bulk SO_3 % (WD-XRF) content in slag vs Fe weight % (SEM/EDS) in copper prills.

5.4.1.6 Potential ores and fluxes

There are no other mineral phases containing copper in the Daye slag apart from the sulphides and metal particles suspended in the matrix. Since in most of cases sulphur is low or not detected, this could be an indication that the original ore was an oxidic one and that this contained minor amounts of sulphidic minerals. In this view, the copper silicates observed in WY7 could correspond to the hosting ore and the copper prills to the metal reduced from it (Figure 5.13).

The economic geology in the area has been characterised for the nearby mines of Tonglüshan (Figure 5.31). Here, oxidic copper ores (malachite, azurite, chrysocolla, etc.) are so abundant that the area has been described as a *'geological freak*' (Wagner 1996, 129). At the same time, the analyses of one lump of copper found in Tonglüshan reported 1.33% sulphur (Wagner 1986), which again demonstrates the existence of sulphidic minerals mixed with the predominantly oxidic ones.

The geology of Daye is equally rich in high grade iron ores like the fragments analysed in section 5.3. It is significant that the few Fe-rich minerals collected in HF present a regular small rounded size and evidence of roasting – microscopic cracking – which indicate that they were manipulated before deposition, and it is also significant that most of the copper slags in Daye regularly contain residual iron minerals. The recurrent presence of agglomerations of iron oxides in the Daye slag is interpreted as remnants of the flux added to improve the SiO_2/FeO ratio, to obtain a less viscous slag at a relatively low temperature. Especially clear when clusters are formed, sometimes still preserving the shape of the parent rock grain, the dominant phases of magnetite are likely a recrystallization of partly reduced chunks of haematite (Figure 5.11). The very low copper content in them excludes the possibility of these as copper ore relicts – lower than 1% in the pieces analysed in Table 5.8, and typically below detection limits in the SEM analyses of the inclusions present in the slag.

The use of haematite as a flux for copper smelting is a common practice documented in numerous archaeological sites including the nearby principal site of Tonglüshan (Zhou, B. et al. 1988). Significantly, this practice is common in smelting weathered ores (Tylecote 1980, 5) but would not be expected in matte smelting. Cu–Fe–S matte will form below a

certain temperature solid magnetite that coexist with the matte (mostly FeS and CuS), and metallic copper cannot be separated from this equilibrium unless temperatures above 1300°C are reached (Rosenqvist 1983, 327-329). The addition of more solid iron oxides to the burden will defeat the purpose of copper extraction: an increase of the iron concentration in the slag leads to the formation of magnetite crystals, which causes heterogenisation of the silicate melt and an increase of its viscosity thus inhibiting the slag-matte separation and so increasing the mechanical losses of copper to the slag (Fernández-Caliani et al. 2012, 166). Therefore, the addition of iron oxide to the slag is not consistent with matte processing which instead requires a high silica flux (Rehder 2000, 116).

Lastly, the barium sulphates and other elements such as Pb occasionally present in several specimens must have been present in the ore, or in the flux, since associations of barite with both haematite and copper are common in the local geology (Sun, H. et al. 1998). These would serve as an additional connection between the Tonglüshan geology and the Daye slag.

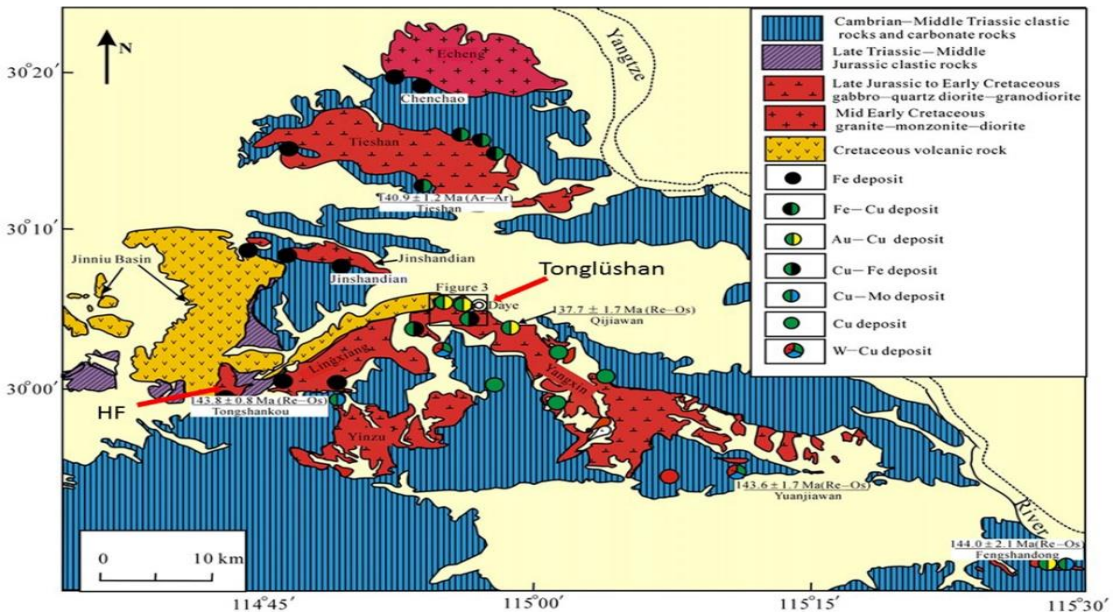

Figure 5.31: Geological map of the south-eastern Hubei province, showing the abundant Cu-Fe deposits available in Daye County.
Tonglüshan and HF (the furthest smelting site to the mine) have been added to the map as reference. Modified from Xie et al. (2011, Fig. 2).

5.4.1.7 Metal smelting, not matte smelting

The previous sections have explored a variety of criteria which have been proposed previously to help discriminate the predominantly oxidic or sulphidic nature of the ores based on the analyses of slag. It has been shown that several of these – such as Cu/S ratios and Fe dissolved in Cu – can yield contradictory or inconclusive results with multiple interpretations. However, the weight of the evidence for the Daye case supports the proposition that the ore employed here would have been an oxide (Table 5.10).

The addition of iron oxide as a flux is perhaps the strongest argument in favour of the use of weathered ores since, as explained, the complete elimination of iron from the sulphide to obtain Cu-rich matte constituted one of the major problems for the ancient smelter (Rostoker et al. 1989, 70). Therefore, further increasing the charge with iron would certainly not facilitate the extraction of copper.

CRITERION		HF	MY	MC	WY	XY
Evidence for a multi-stage process		oxidic	oxidic	oxidic	oxidic	oxidic
Bulk sulphur content in slag		oxidic	oxidic	oxidic	oxidic	oxidic
Nature of the sulphides suspended in the matrix		oxidic	sulphidic	sulphidic	sulphidic	sulphidic
Cu/S ratio in	***slag***	inconclusive	inconclusive	inconclusive	inconclusive	inconclusive
	Cu-rich grains	inconclusive	inconclusive	inconclusive	inconclusive	inconclusive
Iron in copper		inconclusive	inconclusive	inconclusive	inconclusive	inconclusive
Residual minerals in slag		oxidic	oxidic	oxidic	oxidic	oxidic

Table 5.10: Summary of results of the different criteria to discern between metal and matte smelting applied to the copper smelting sites of Daye County.

The relatively small and scarce sulphide particles present in the slag can be explained as resulting from residuals intergrowths of sulphidic minerals within the predominantly weathered deposits. They survived the smelting because there was no attempt by the smelter to remove those by desulphurisation. All these sulphur rich particles were parted in the slag since matte has a specific gravity very close to that of the slag (Figure 2.5), and

therefore were trapped there giving a false impression of predominance when, in fact, these were scarce in the original charge.

Carbonate minerals such as malachite and azurite or other minerals like chrysocolla that contain minor amounts of sulphidic minerals are the predominant in the area (Huangshi Municipal Museum 1980; Wagner 1986; Zhou, B. et al. 1988; Li, Yanxiang 1998b; Xie et al. 2011), and while the nature of the sulphidic mineral charged with the main ore is uncertain the only possible ore relic found within the slag corresponds to copper silicates (section 5.1.5).

The general shortage of matte in the slag and a lack of evidence for any matting activity – roasting, changes in the furnace operation, different by-products, etc. –, support as well the hypothesis of smelting oxidic ores with minor amounts of sulphidic grains. The absence of these evidences suggest that the amount of sulphur was too small to affect the generally quite efficient metal recovery, and therefore did not have a resounding impact on the process or final result or obliged the smelters to take extra actions to remove the sulphur and recover the copper trapped in it.

5.4.2 Slag formation

The main slag compounds were plotted in the phase equilibrium diagram Al_2O_3-SiO_2-FeO as an approximation of the more complex multi-oxide system of the slags (Figure 5.32). As stated all the Daye slag is generally thoroughly molten and homogenised and the bulk composition fairly represents the composition of the molten phase. Since the sum of these oxides ranges 90-94% in the slag, no other elements were added up to the totals of the reduced analyses. The ternary diagram shows that practically all the specimens are within the fayalite area, with melting points between 1100-1200 °C. Regardless of the metal being extracted, the vast majority of ancient slags tend to be chemically and mineralogically dominated by iron silicates, and the copper smelting slag of Daye County is no exception.

More specifically, the predominance of fayalite (Fe_2SiO_4) in the slag reflects the suitable proportions of iron and silica in order to obtain a slag that could be melted at

temperatures within reach of ancient technologies (Maldonado 2006, 151). This aspect was controlled by ancient smelters by manipulating the content of the charge (ore, fuel and flux) loaded into the furnace in each smelting cycle, and to some extent to the adjustment of the redox environment of the furnace by regulating the addition of new batches of charge and the air rate.

Some ores can contain the right proportions of silica and iron oxide in their gangue to be self-fluxing; some silica can also be obtained from the technical ceramics, and additional fluxing elements such as calcium oxide may be supplied by fuel ash. However, especially in large-scale exploitations, deliberate fluxing with additional materials is likely to have been common practice. The flux to be added depends on the nature of the ore; in general, a sulphidic ore is ferruginous and requires silica fluxing, whereas an oxidic ore is silica-rich and requires iron oxide fluxing (Tylecote 1980, 5; Craddock 1995, 138). In any case the result will be an iron silicate-dominated slag, which melts in the temperature range of 1100-1200 °C (Tylecote 1992, 7). Nevertheless, (unusual) cases of carbonates ores fluxed with additional silica and slag dominated by calcium silicates have also been reported (Killick et al. 2016).

On the other hand, it is difficult to determine if the addition of silicates is an intentional action. In most of the slag samples quartz grains are still recognisable embedded within the matrix, yet these could constitute gangue from the ore (Figure 5.8), even in the extreme case of the specimen saturated with chunks of quartz (Figure 5.2).

Rehren et al. (2007) mark two eutectic areas for bloomery iron smelting in the equilibrium diagram $FeO–Al_2O_3–SiO_2$ (Figure 5.32) which maximise the slag fluidity relative to energy inputs at particularly low melting temperatures. The two eutectic points denote different configurational parameters of the furnace and charge – that were manipulated by the smelters –, and therefore may reflect decisions and behaviour of the ancient smelters. Even if their model was suggested as the most suitable engineering solutions for bloomery iron and not for copper smelting, in terms of slag formation the extraction of both metals typically creates rather similar by-products on the $FeO\text{-}SiO_2$ system (Hauptmann 2007, 21) (Figure 5.32); therefore some considerations regarding the dynamics are equally valid. The main aspect which is not comparable between the two productions is the amount of

iron lost into the slag: this is a crucial point in iron reduction since the more iron sacrificed in the slag the lower the metal yield (section 6.4.1).

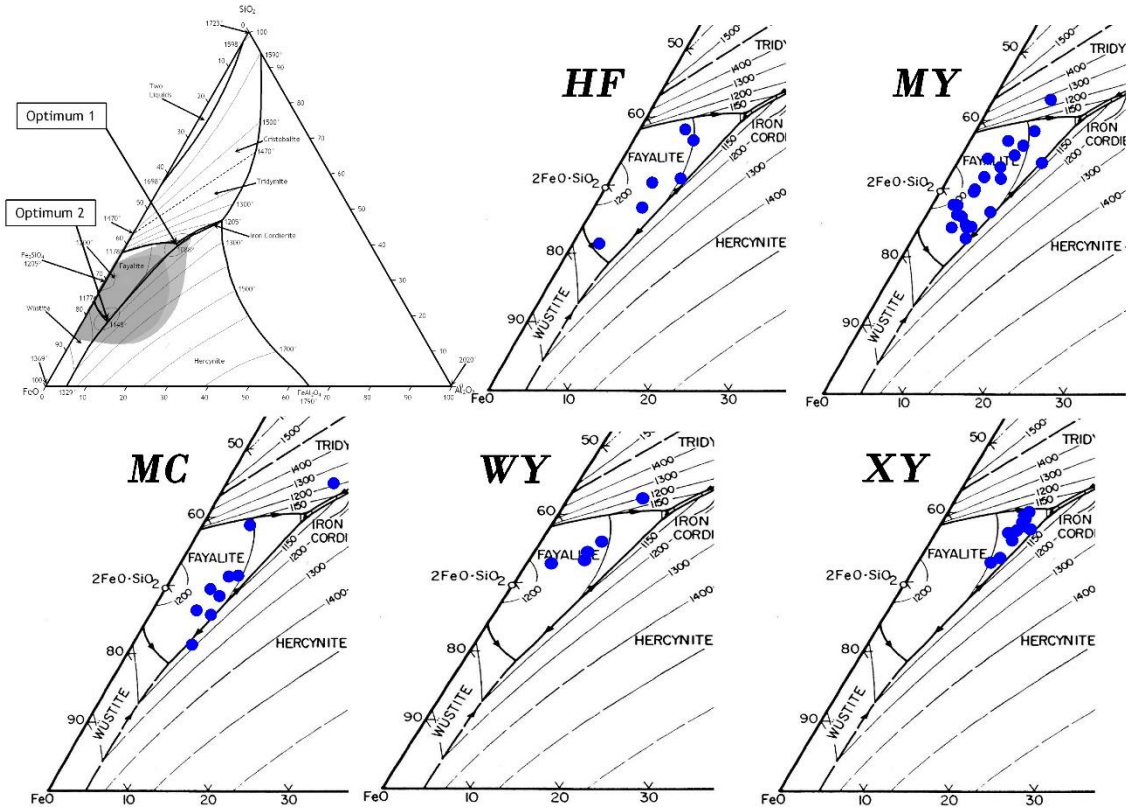

Figure 5.32: Comparison between typical composition of ancient slag and the Daye copper smelting slag.
Average composition of ancient slag from copper smelting (light grey area) and iron smelting (dark grey area) shown in the ternary system FeO–Al_2O_3–SiO_2 (modified after Hauptmann 2007, Fig. 2.2). The two eutectic points in the system are also highlighted (modified after Rehren et al. 2007, Fig. 1), and compared to the Daye copper slag plotted in the same diagram.

In terms of copper smelting, however, the amount of iron that goes into the slag is less relevant economically, since the aim is the extraction of copper. In principle, copper smelting slag can sit anywhere in between the two eutectic points marking the fayalite region and even beyond towards the wüstite region, since an iron-rich composition in slag facilities the melting at manageable temperatures 1100-1200 °C whereas a composition richer in silica closer to eutectic 1 is at a higher risk of freezing the furnace (small variations in the amount of silica in this area of the phase diagram can increase the melting temperature dramatically). This can be appreciated in Figure 5.32 where MC14 and MY11 are plotted within isotherms beyond 1200 °C and sample WY4 on the isotherm marking

1200 °C. Their respective SiO_2 bulk composition (Appendix III) is unusually rich: 37-39% of an average ranging 27-34%. Notably, for specimens MC14 and MY11 – which contain abundant unreacted quartz – it can be argued that the estimated melting temperature was not kept for long enough for the charge to melt, but specimen WY4 is perfectly molten material (Figure 5.8), and shows clearly the risk of a silica-rich composition since a silica increment of 1-2% would be close to melting temperatures higher than 1250 °C, thus harder to maintain in pre-industrial furnaces.

The smelting of copper in most cases entailed some risk of producing iron at the same time, and although the reduction of iron depends upon the furnace temperature and redox conditions, a higher amount of iron in the system increases the risk of producing metallic iron (Gale et al. 1990; Rehder 2000, 117). Furthermore, as seen before, even unreduced iron in slag can then dissolve in copper, which will harden this metal and decrease its workability (Cooke & Aschenbrenner 1975; Craddock & Meeks 1987; Rehder 2000, 114; Pryce et al. 2007, 552). However, in Daye, the average amount of iron dissolved in copper prills is not correlated with the FeO content in slag, and the site with highest bulk FeO composition (MY) shows less iron in copper prills than the site with the lowest bulk FeO in the slag (XY) (Figure 5.4 and Figure 5.14).

A second disadvantage of a high iron concentration in slag is the increment of magnetite which increases the slag viscosity (Fernández-Caliani et al. 2012). The viscosity index for the Daye slag was calculated after Bachmann (1982, 19), which expresses the ratio of the basic oxides against the acid oxides – viscosity-reducing agents/viscosity-increasing agents. The ratio of the two sums provides the index, typically a number between 0.5-1 – the lower the viscosity index, the higher the viscosity.

$$viscosity\ index = \frac{CaO + MgO + FeO + MnO + K_2O}{SiO_2 + Al_2O_3}$$

This is a simple approximation to the otherwise much more complicated calculation; although several other authors have proposed corrections and different formulas (e.g. Manasse & Mellini 2002; Ettler et al. 2009), it remains true that in general viscosity is negatively correlated with basic oxides content, and positively correlated with acidic oxides (Rosenqvist 1983); therefore Bachmann's formula was considered appropriate. The calculated index (Table 5.11) shows that all the Daye slag is fluid and has low viscosity,

and that the magnetite crystals present in the slag have no negative influence on it since XY presents the lowest fluidity and contains the lowest proportion of magnetite crystals. Therefore, none of the shortcomings pointed for an iron-rich slag composition – higher proportion of iron dissolved in copper and increment of viscosity due to higher crystallisation of magnetite – seems to have a significant influence in the Daye slag.

	HF	*MY*	*MC*	*WY*	*XY*
Viscosity index	1.8	1.9	1.7	1.5	1.2
Magnetite content	Frequent	Frequent	Frequent	Common	Few

Table 5.11: Viscosity index in relation with magnetite content in the Daye slag.

5.4.2.1 Cooling rates

The morphology of the fayalite crystals can be used to estimate the cooling rates of the melt (Manasse et al. 2001) and thus to approximate the conditions in which the slag solidified (Figure 5.33). The olivines crystallise progressively depending on the cooling conditions, basically – assuming same composition and temperature when they start solidifying – 'the larger the olivine content of a melt the slower the cooling rate at which a particular olivine shape grows, whereas the lower the melt viscosity, the greater the cooling rate' (Donaldson 1976, 187). Attending to the different crystallisation structures, two groups can be distinguished within the Daye slags: fast cooled lath crystals in WY and XY, and predominance of the more slow cooled skeletons, hopper and euhedral crystals in HF, MC and MY (Figure 5.8).

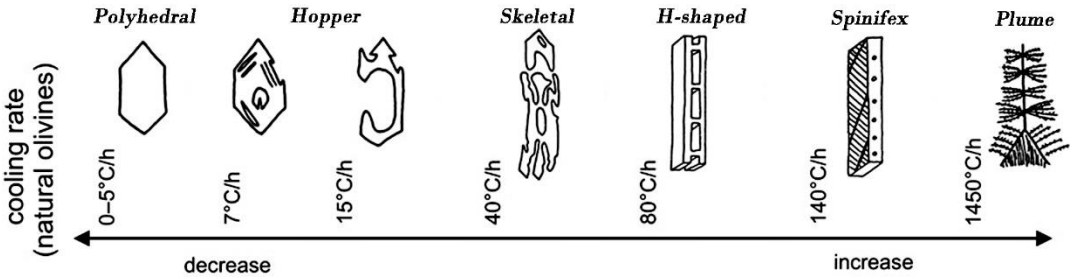

Figure 5.33: Change of shape of olivines in cooling rate from complete to incipient. After Ettler et al. (2009, Fig. 6).

The slow cooling rate evidenced by the euhedral-hopper crystallisation of fayalite indicates that, during the transition from liquid to solid, the slag was not exposed to dramatic temperature changes. Typically this situation occurs when the slags cool down within the furnace or crucible. However, with the exception of the flow slag of HF, the Daye slags are typical examples of tap slag: they a) present a molten phase fluid enough to separate from the metal and tapped from the furnace; b) soil particles attached to the bottom side resulting from the slag dragging on the soil once out of the furnace; c) they recurrently show 'magnetite skins' or slightly more oxidised interfaces that often separate different tap cycles, resulting from exposure to the air, and d) they present elongated morphologies with very clear flowing patterns (Morton & Wingrove 1969; Craddock 1995, 146-147; Herdits 2003; Maldonado & Rehren 2009). Even though some of these diagnostic features are absent in HF, the flow slag is certainly fluid enough to be tapped out of furnace and the same furnaces generated as well tap slag (HF16) that presents a microstructure identical to the other Daye tap slags (Figure 5.5). A likely explanation for the different crystal structures observed in the slags is that these were tapped out at different temperatures and hence some had more time to solidify than others, which is supported by the variable smelting temperatures estimated in Figure 5.32. Conversely, XY, which clusters more tightly in the ternary diagram, also shows the shorter variation in the olivines shape, which crystallise nearly invariable as very thin laths crystals.

5.4.3 Furnace atmosphere

Another important parameter in furnace operation is the redox environment. The slag combination of phases present in the microstructure, notably metallic Cu and magnetite,

indicate that the furnaces were operated in broadly similar ways, reaching a similar range of temperatures in a mildly reducing atmosphere of ~10^{-6} atm (Figure 5.34). This is supported by the nature of free iron oxides in the slag, which crystallised typically as magnetite (Fe_3O_4) instead of wüstite (FeO) which requires considerably lower pressure (~10^{-10}/10^{-12} atm instead of ~10^{-2}/10^{-4}) at the same range of operating temperatures (1100-1200 °C). Despite the relatively common occurrence of pseudomorphs of natural magnetite, this mineral is only rarely reduced to wüstite (FeO) which was only identified in 4 out of 59 specimens, and no free particles of metallic iron were identified in the entire collection – apart from the copper prills which can absorb the iron directly from solid iron oxides (Craddock & Meeks 1987). As noticed, this pressure is definitely insufficient to reduce metallic iron.

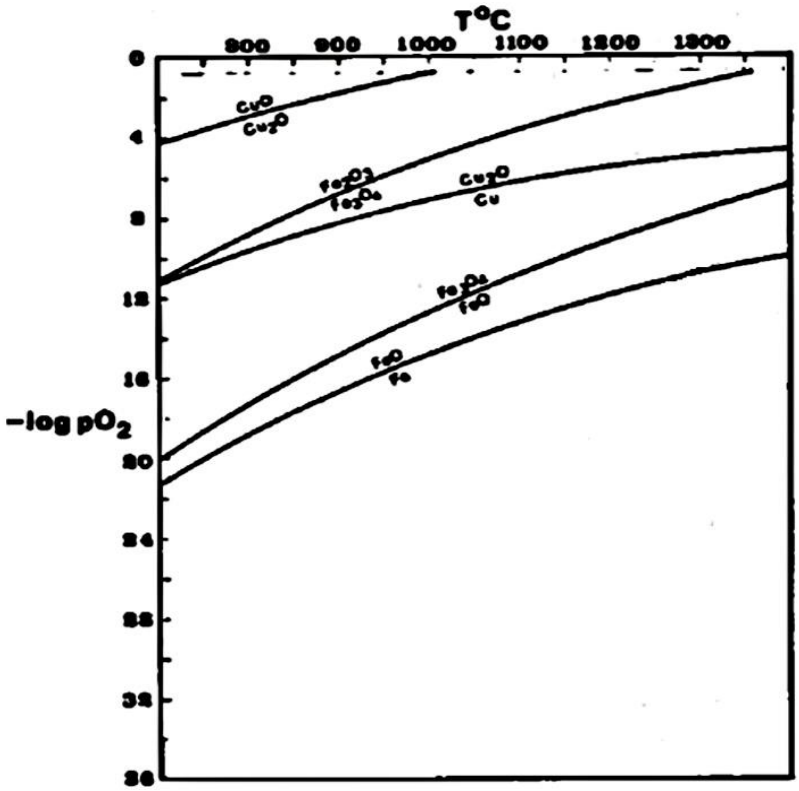

Figure 5.34: Temperature/Oxygen partial pressure relationship for copper and iron oxides.
After Freestone et al. (1985, Fig. 3).

Magnetite is the only iron oxide crystallised as well within the furnace fragments analysed while pseudomorphs and wüstite are totally absent from these. This indicates that the

atmosphere in the furnaces did not reach extremely low pressures either, in agreement with the 10^{-6} atm estimated for the slag. Under these conditions – the expected oxygen partial pressure for copper smelting processes (Yazawa 1980 in Moesta & Schlick 1989, Tab. 1) – and range of temperatures (1100-1200 °C), all the main minerals observed can co-exist: cuprite, delafossite, haematite, magnetite, and copper metal suspended on a fayalitic-molten phase of slag (Figure 5.35). On the other hand, the scant tenorite – only found in MY – indicates high oxygen pressure – but this is a very infrequent and minor occurrence likely due to the localised pockets within the furnace and do not represent standard operation procedures.

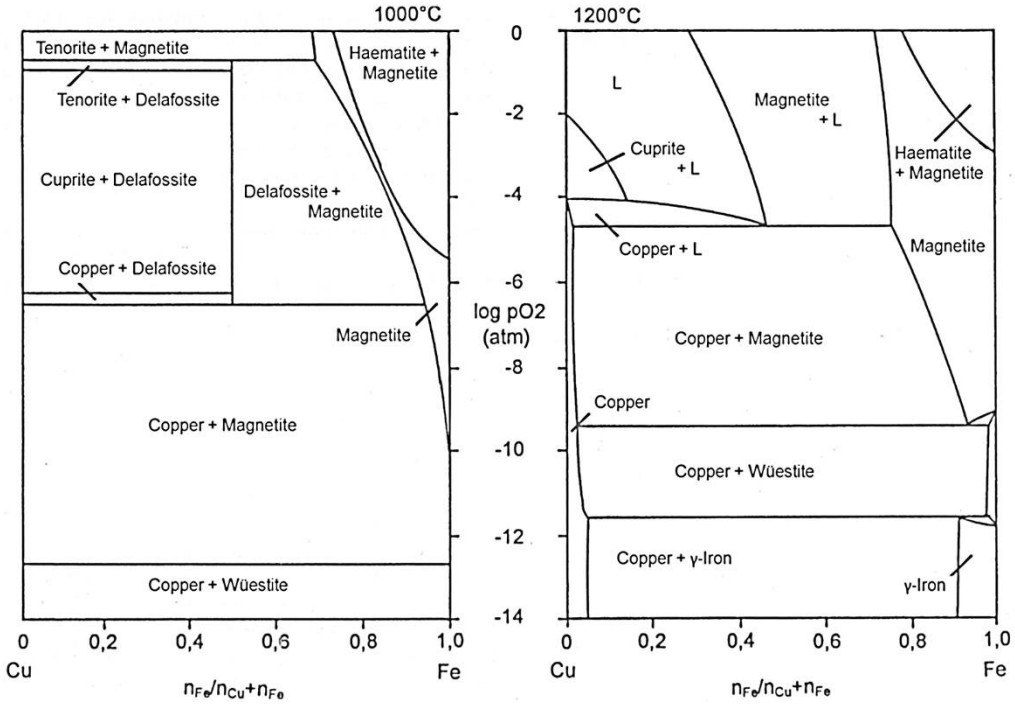

Figure 5.35: Simplified sections of the pO_2/T-diagram of stability of the system Cu-Fe-O for 1000° and 1200 °C.
After Metten (2003, Fig.31).

5.4.4 Process and recipe

In general, the copper slags from Daye are surprisingly similar, particularly if we take into account that they were collected from five different sites and on three occasions – 1993, 2005 and 2014. The analogous morphology of the slag; microstructure and mineralogy; bulk chemical composition; haematite fluxing, furnace operating conditions and nearly identical furnace ceramic fabrics altogether point to a common procedure. Another

remarkable feature is the limited chemical variability of the copper slag from Daye. As displayed in Figure 5.36, the Daye copper slag shows a standardised composition with a maximum fluctuation of 6% within the major compounds Al_2O_3, SiO_2, FeO and CaO (also Figure 5.4). Other compounds below 1.5% – P_2O_5, MgO, K_2O and MnO – show slightly larger variances, with HF notably more variable than the other sites. CuO and SO_3 percentages show a very steady tendency in all sites. In general, the chemical composition supports as well the argument of a common procedure whereas the small variances observed are natural within a standardised process.

Many operating parameters can be modified, resulting in different slag compositions and microstructures: for example, the temperature and atmosphere of the furnaces can change greatly depending on little deviations in the blast of air, or the nature of the charge depending on variations of the ore quality and processing (Humphris et al. 2009). As a result, multiple production events can blur – *cumulative blurring* – the standardisation signature of an overall homogeneous process (Blackman et al. 1993), which in the case of smelting slag can derive in variation in the shape of the slag cakes; different frequency and crystallisation of minerals; or changes in composition. However, several of these variations are explained by the logical deviation consubstantial to any standardised manufactured process (Blackman et al. 1993); furthermore, this deviation is inherent to the smelting process (Tylecote 1992; Craddock 1995). Furthermore, different by-products are generated depending on the stage of the process, as numerous archaeological reconstructions and experimental smelting campaigns demonstrate (e.g. Merkel 1990; Benvenutti et al. 2000), which would potentially add variability to the random sample analysed here. Therefore, the several versions of tapping shapes from a generally recognisable elongated flat cake with evident flowing signals, are in all probability due to the stage in which these were tapped out of the furnace. The different thickness, rounded or elongated shape, volume of material per cake, etc. were likely generated by variations in the furnace operations, charge, cooling temperatures and tapping regime, all possible within a single standard regime.

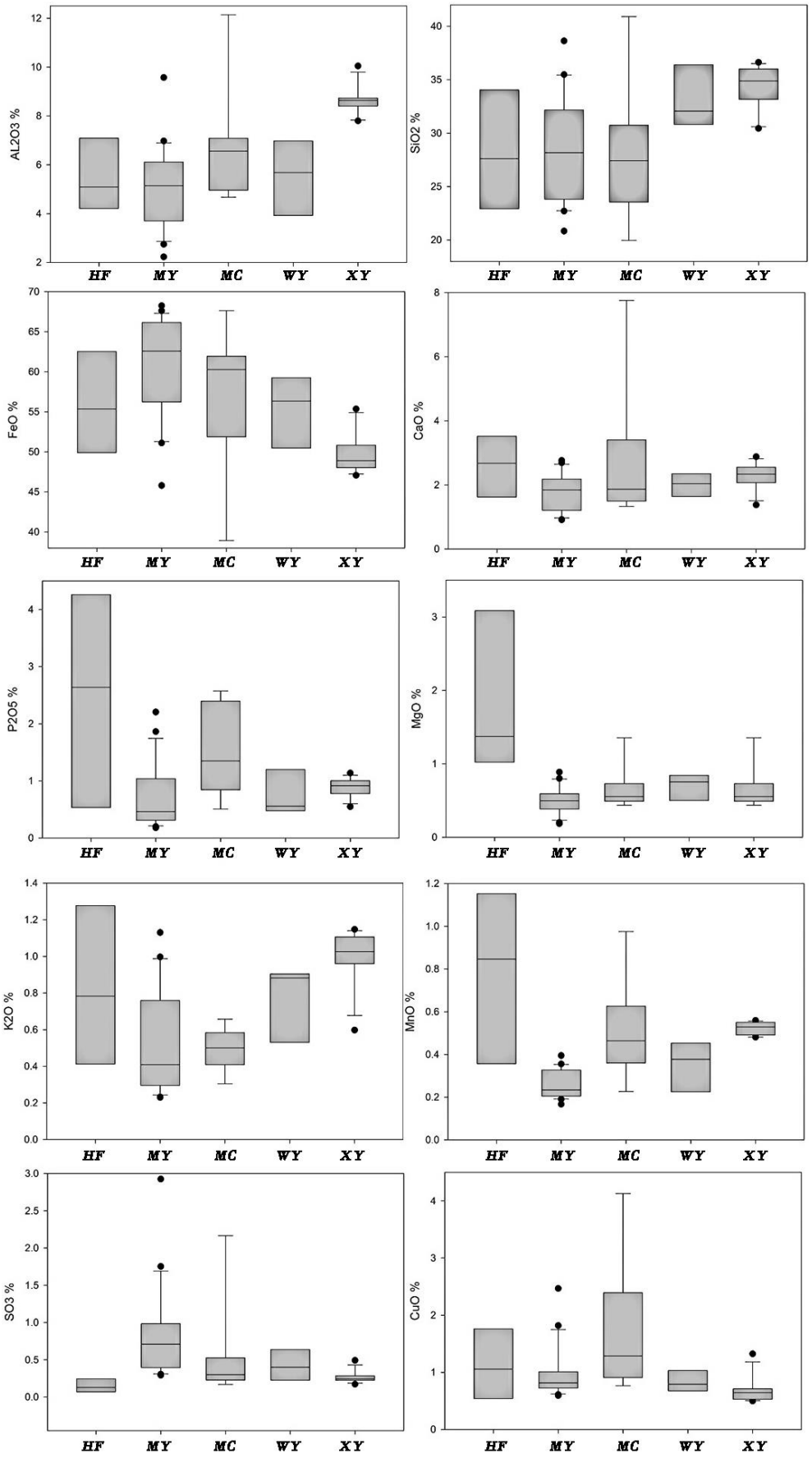

Figure 5.36: Box and whisker plot showing media, minimum and maximum variances (compounds %) of the composition of the Daye copper smelting slag.

Equally, the narrow differences in chemical composition and mineralogy can be explained by little changes in the kinetics of the process. For example, the higher MgO detected in HF could be also a contribution from the flux: while all sites were fluxing with iron oxides, of the possible analysed minerals used as a flux some of them were richer in MgO than others (Table 5.8), and thus this could provide an extra source of MgO that could also have a reflection in the composition of the olivine crystals (Table 5.5). Another explanation for the higher MgO in HF is that this is a contribution of the fuel ash, as well as the CaO, P_2O_5 and K_2O, which also have a tendency to be higher at this site. Perhaps the small pieces of flow slag of HF represent small droplets that solidified inside the furnace rather than being tapped, and thus were longer exposed to the charcoal ash absorbing more of its constituent elements.

Finally, SO_3 and CuO are provided by the ore and flux; the slight variances within all sites most likely derived from punctual internal dynamics such as the position within the furnace and exposure to lower/higher temperatures or to the tapping regime.

The three main compounds Al_2O_3, SiO_2, and FeO are fairly similar in all sites and are mainly provided by ores and flux. As discussed above, the addition of iron oxides as a flux is a consistent practice in Daye; we can further assume (as also discussed above) that similar or identical copper ores were used. Consequently, the increase of 3 wt% Al_2O_3 and 5 wt% SiO_2 in XY slag compared to an average of 5.5 wt% Al_2O_3 and 29 wt% SiO_2 (Figure 5.4) presumably could be due to an intentional addition of silicates although there is no evidence to support the addition of a second flux rich in silica. Albeit this extra amount could be donated by the furnace walls, the homogeneous composition of the technical ceramics in all sites and the narrow range of temperatures reached by the slags do not suggest that the furnaces from XY were particularly prone to collapse. On the other hand, WY presents also a significant increase in SiO_2 although the chemical variation is less apparent here since there is neither an increament in Al_2O_3 nor a notable decrease of FeO. Therefore, three sites in Daye generated slag richer in iron, while one of the sites produced silica-rich slag, and a further site a by-product that is in a midway position between them.

Summing up, since all the parameters point out that the smelters from Daye were following the same recipe and procedure it is more likely that the variations in bulk chemical composition are due to the kinetics of the slag formation, such as the tapping

regime or slight variation in the quantity of added iron oxide flux, and not to an intentional addition of a second flux.

5.4.4.1 Tapping regime

Based on iron smelting experiments, tapping early and often yields slags higher in iron oxides whereas tapping late and sparsely yields slags lower in iron oxides; this regime can be controlled by the smelter by manipulating the air blast and charge (Sauder & Williams 2002). The reasons that may lead a smelter to moderate the tapping regime are essentially that the slag bath prevents the reduced iron from re-oxidation; facilitates the movement of metal particles to coalesce in the bloom; and also avoids drastic thermal fluctuations when new charge is added to the burden or at the last stages of the process (Sauder & Williams 2002, 129). Adapted to copper smelting, these three assets can be presumed to be equally effective: the slag bath is perhaps not so crucial in terms of re-oxidation of reduced copper metal but it certainly can provide a medium for metal prills to coalesce into a copper ingot, as the copper particles have more time to settle at the bottom of the slag pool – thus the slag traps less copper –; and the role of the slag as a thermal reservoir would seem equally positive in copper smelting.

As previously observed, most of the Daye slags are in an intermediate position between the two eutectics of the ternary diagram Al_2O_3-SiO_2-FeO, with a relatively iron-rich bulk composition and abundant free iron oxides. This results in a quite fluid slag (Table 5.11) that was easily tapped out of the furnace, on occasion without allowing time to clean these out by the smelters, and thus accumulating over several cycles (Figure 5.1 and Figure 5.2).

Conversely, the slags of XY contain considerably less free iron oxides (Figure 5.8 and Figure 5.11), and present a much more cryptocrystalline microstructure, and a bulk composition that contains more silica and alumina than any of the other slags in Daye, which plots towards the eutectic 1 of the equilibrium diagram (Figure 5.32). This slag would represent the slag tapped at the very end of the process, once most of the iron oxide added as a flux has been dissolved in the charge and the temperature of the furnace is going down. Therefore, the cakes are smaller and thinner since there is less molten material – more

viscous and dragging slower – left in the furnace. The cakes contain larger size sulphides than the slags of the other sites since there is no attempt in removing those along the entire process so they concentrate as residues, and includes even less copper prills than the other waste-products since these had more time to coalesce into the ingot. The slag cakes of WY also fit into the hypothesis of slag tapped at the last stage of the process although in this case the melt is still very fluid and can occasionally shape flow slags that trap with them relics of the ore and copper prills. In agreement with this hypothesis, a replication experiment of ancient copper smelting reported that the iron content of slag decreased in a 7% from early tapped slag to the slag that stayed on the furnace bottom, which also was enriched in silica and alumina (Izawa 2015).

On the other hand, the thickest cakes of MC and MY would correspond to the earlier tapped iron-rich slags when the furnace is fully operational receiving new charges of burden that affects to the inner temperature and environment. Therefore, since the molten bath is generated within a less stable atmosphere, the tapping cycles are not continual which results in the different morphology of the cakes, which also present more variations in mineralogy – size and shape of the crystallised olivines and iron oxides. The hypothesis of earlier tapping also fits with the presence of occasional unreacted siliceous materials since the chunks did not have the time to react, and the imprints of charcoal presumably are only seen in these slags since the furnace was charged more abundantly with fuel. The diversity of the matte phases responds as well to the early tapping with some of them closer to the original residual sulphidic minerals present in the mainly oxidic ore (chalcopyrite), others partially reduced (cubanite), and the majority as chalcocite or covellite. However, the latter minerals appear typically in smaller concentrations than in the equivalent droplets of WY and XY although occasionally they can reach very large size. These slags also can occasionally trap larger copper prills as in MC2 or HF17 that did not have time to coalesce into the bath of copper metal.

All in all, it may be suggested that the morphological differences detected within the sites are due at least in part to their having formed at different stages of the smelting operation. They are thus not significant enough to be taken as indicative of different smelting traditions. As a matter of fact, similar thin cakes of composition richer in Al_2O_3 and SiO_2, and poorer in FeO were also sampled in HF, MY and MC (Figure 5.1) (exceptions in Table

5.4) (Appendix III). On the other hand, specimen WY7 has a bulk composition more similar to the high iron thick cakes, and also contains unreacted materials and more copper prills, which demonstrates that each site generated the same type and range of by-products suggesting that the observed variation within those respond to the nature of the technological process, and was in all probability influenced by the availability of the materials and the sampling strategy.

Similarly, the flow slag from HF could correspond to small fractions disaggregated from a bigger slag batch during the tapping out. The abundance of this slag type is also strongly influenced by the sampling strategy since most of the tap slag picked up from the surface was thought to be copper smelting slag when in fact it corresponds to bloomery iron reduction (chapter 6). However, still one sample (HF16) fit well into the category of tap slag and presents as well a relatively lean microstructure similar to that of WY or XY (Figure 5.5).

5.5 Summary

On the basis of the analysis of technical materials, it has been possible to identify the copper smelting practice at the five sites of Honfengshuiku (HF), Mianyangdi (MY), Maochengnao (MC), Wangyuecun (WY) and Xiyuqiao (XY). Notwithstanding variability among sites (with XY standing out with a composition richer in silica and alumina, and microstructure much more poor in free iron oxides, and HF recurrently presenting a different morphology), the technical procedure appears to have been broadly similar across Daye: it involved the reduction of copper from the oxidic ores abundant in the region – a tradition that is well documented at other sites in Daye County – by means of slag tapping furnaces operated at mildly reducing conditions and temperatures ranging around 1100-1200 °C. The furnace charge was systematically fluxed with iron oxides – haematite – which was probably roasted in advance.

Based on the sample analysed, the by-products generated at all the sites are agreeably homogeneous in morphology, chemical composition and mineralogy while the variations within them are due to the internal dynamics of the different stages of a common operation. They are characterised by their flow textures and their well-reacted

microstructures, with very scant residual materials and only minor amounts of copper trapped. The fact that most of the copper is present in the slag as Cu-rich sulphides is argued to be not an indication of matte smelting but the result of the presence of minor amounts of sulphur in the ore and/or the flux. It would not have been possible to reduce these at the normal operating conditions but, in any case, their presence was not deleterious for the process.

Judging by the high volume of waste-products visible on the surface and by the degree of standardisation of those, it could be proposed that the sites operated on a relatively large scale. However, it is admitted that the large slag dumps could have resulted from the accumulation of smaller-scale debris over a long period.

Li Kui noted an anvil, hammers, a forge, pincers, awls and pokers.
"Must be a blacksmith" he thought.

(Outlaws of the Marsh, 水浒传)

6 Analytical results II: bloomery iron production in the Daye County

A total of five sites in Daye county yielded remains that could be interpreted as related to bloomery iron production, including Hongfengshuiku (HF) and Maochengnao (MC), which are also copper production sites as seen in the previous chapter. The other three sites are Lidegui (LD), Yanwopu (YW), and Cangxiawu (CX).

Most of the evidence corresponds to tap smelting slag with the exception of a few specimens (8 out of 47) which are bulky slag not tapped out of a furnace, and which are argued to be smithing slag (section 6.4.4). The assemblage is completed by a few fragments of furnace wall and possible fragments of ore that were recovered in some of the sites (Table 6.1).

The interpretation of the bloomery iron slag from Daye is straightforward and unequivocal: the crystalline matrix with olivines; dominant dendritic wüstite; few metallic iron particles; absence of any other relevant metal particle; fayalitic bulk chemical composition of 57-78% FeO and 15-31% SiO_2; and very low levels of any non-ferrous heavy metal; altogether clearly indicate that this is a waste product of bloomery iron smelting activities (Rostoker & Bronson 1990; Pleiner 2000; Buchwald 2005) comparable in morphology, microstructure and composition to bloomery iron slag from Africa, (e.g. Avery et al. 1988), Northern Europe, (e.g. Espelund 2015) or Southeast Asia, (e.g. Chuenpee et al. 2014).

There is only one exception to this picture: one sample of slag from HF was shown to be glassy slag containing round iron metal particles and singular composition of 49% SiO_2, 18% CaO, 8% Al_2O_3 and 15% FeO. Also at this site, a lump of very high carbon steel (~1.5% C) was recovered. These two samples are inconsistent with bloomery iron smelting, as detailed in section 6.1.6.

	HF	*MC*	*LD*	*YW*	*CX*	*Total*
Smelting (tap) slag	5	2	12	8	12	39
Smithing (lumpy) slag	5	2	1	–	–	8
Furnace wall	–	–	2	2	1	5
Ore	4	–	–	2	–	6
Other by-products	2	–	–	–	–	2
Total	16	4	15	12	13	60

Table 6.1: Sampled materials per site associated to bloomery iron production.

6.1 Characterisation of the Daye County iron slag

Morphologically and regardless of site, the bulk of the collection appears as polygonal, relatively thin (20-40 mm) tablets (Figure 6.1). Thick cakes incorporating more than one slag tapping cycle are unusual. Their flat shape, distinct smooth upper face with flowing signals and rough bottom face with occasional soil or imprints of soil particles, and overall flow texture are diagnostic of slag that was tapped out of the furnace, with numerous examples in archaeological contexts regardless of metal and chronology, e.g. copper during the Late Bronze Age (Knapp & Kassianidou 2008), iron during Roman times (Fulford et al. 1992) or lead and silver smelting during medieval times (Ettler et al. 2009), with variations in viscosity, size and shape.

Normally, the Daye tap slag appears fragmented in relatively large pieces (~8-10 cm of length) broken in straight fractures; the size and shape of a complete cake could not be reconstructed through the fragments found (Figure 6.1). It generally shows a dark grey colour with reddish hues and occasional maroon stains, although some samples exhibit a green colour and glossy appearance quite similar to some of the copper waste-products described previously, particularly to the flow slag (Figure 5.3). The fresh cut section shows a dense molten slag with very little porosity although quite occasionally large voids (~1-2 cm) can appear. Unreacted macroscopic materials are absent in the entire collection. Contrary to the copper tap slag, these cakes respond weakly to magnetic test.

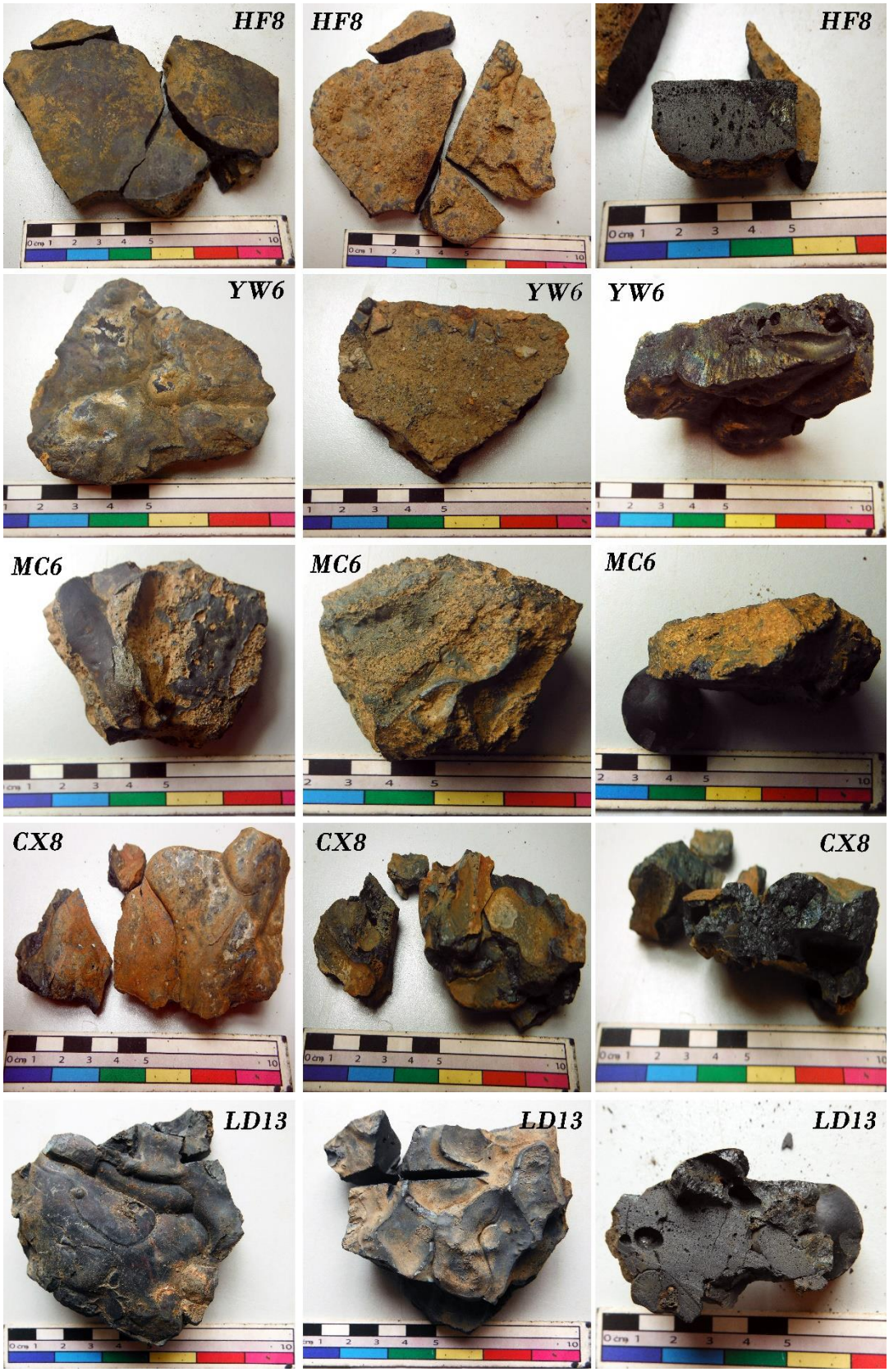

Figure 6.1: Typical appearance of the Daye bloomery iron tap smelting slag.
Top (left), bottom (centre) and section (right) of the typical tap slag cakes recovered in Daye.

A total of eight specimens display different features and are referred as 'lumpy' slag because they are particularly bulky fragments (Figure 6.3). Like the tap slag, the lumpy cakes respond weakly to magnetic test with the exception of sample HF24 that responds strongly. All the lumpy slag show plenty of gas cavities (1-3 cm) in section, evenly distributed, abundant orange-reddish stains, and brittle appearance. The microstructure of these samples is separately discussed in section 6.1.5 below.

Five specimens from HF appear in the form of amorphous bulky cakes uniformly covered by an orange-brown rusty tarnish, showing occasional vitrified points and pieces/imprints of charcoal that are totally absent in the tap slag. Two of these samples (HF23-24) have more recognisable plano-convex shapes and show smooth surfaces mostly or totally free of embedded charcoal.

Two samples from MC (MC18, MC12) appear as amorphous lumps although these samples are not covered by a rusty tarnish or show imprints of charcoal, but present smooth surfaces and contorted textures on the bottom surface.

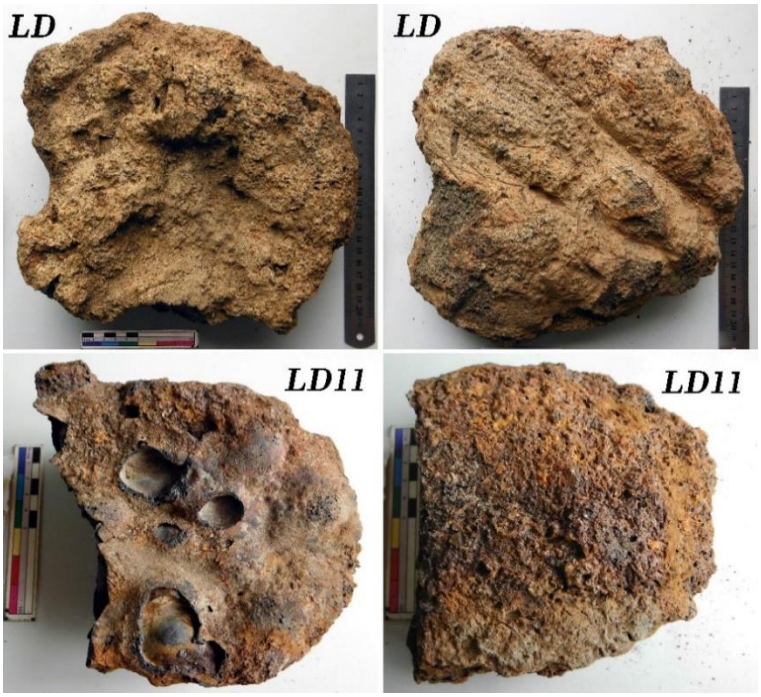

Figure 6.2: Complete cakes related to bloomery iron production.
Top: complete cake (not-sampled) found in Lidegui during the excavation of 2005, and (bottom) sampled cake found on surface also in 2005. Dimensions of the scale are 20 cm (metallic) and 10 cm.

During the archaeological excavation in LD a few complete irregular plano-convex cakes were recovered, approximately 30 cm in maximum diameter and about 8 cm of maximum thickness; their mass could not be measured since it exceeded the capacity of the electronic balance available (1 kg) but around 5 kg seems a reasonable approximation. However, these were not available for sampling; permission was given only to analyse one cake (LD11), which is smaller (~16 cm in diameter and ~2 kg), with the topside vitrified and the underside looking like burnt clay with soil impressions (Figure 6.2).

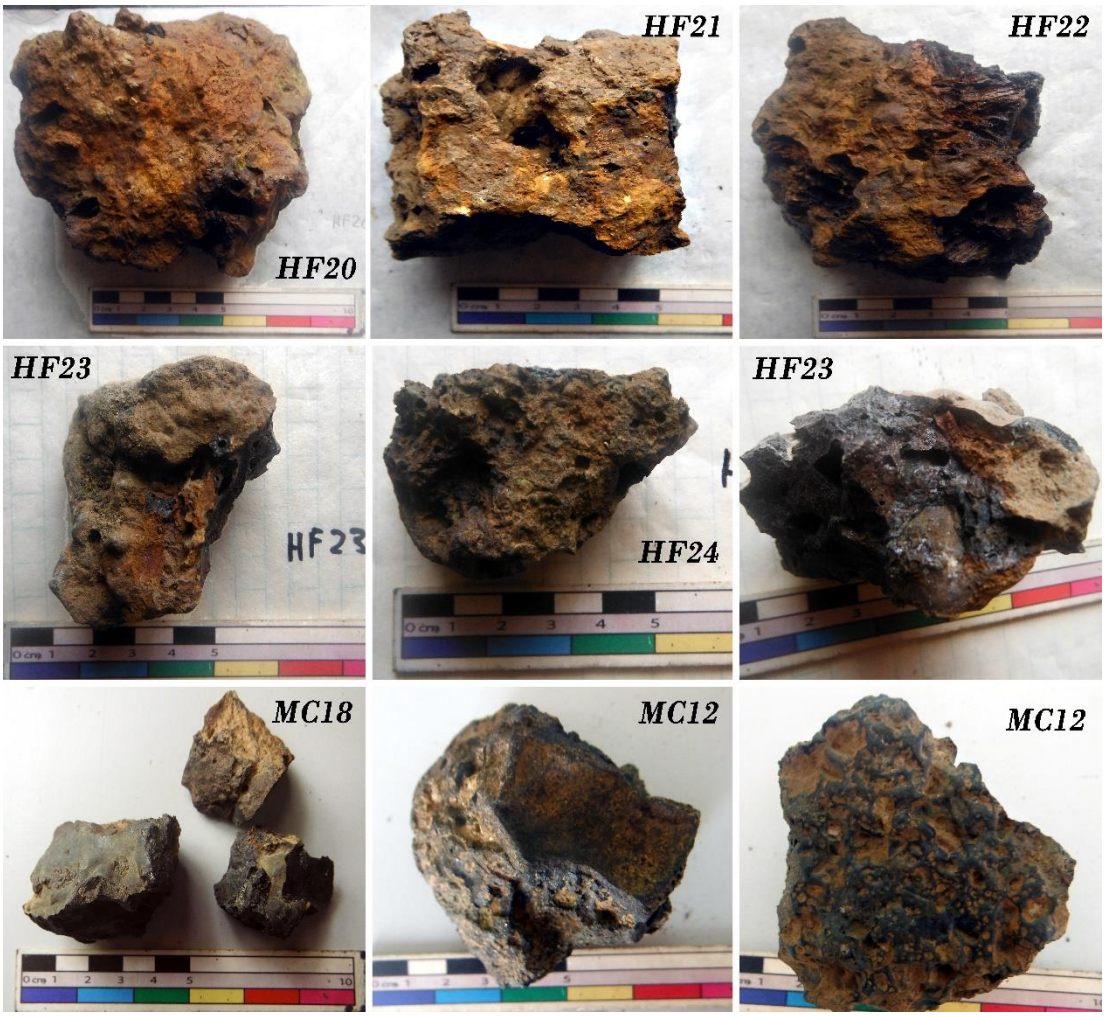

Figure 6.3: Bulky slag cakes related to bloomery iron production.
(HF20, HF21, HF22) Different versions of the bulky cakes found in HF showing heavy rusty tarnish and abundant imprints of charcoal; **(HF23, HF24)** Plano-convex cakes occasionally showing smooth surfaces, and cut section showing heterogeneous textures; **(MC18)** Lumps of slag that correspond to the same broken specimen showing mostly smooth surfaces; **(MC12)** Back and front of an amorphous cake with contorted textures on the bottom face.

6.1.1 Bulk chemical composition

Like the copper slag, the bulk chemical composition of the Daye iron slag is fayalitic, ranging 62-71% FeO and 20-25% SiO_2. Al_2O_3 is the third major oxide (4-6%) in all cases. When SiO_2, FeO and Al_2O_3 are added up, they make up over 95% of the bulk (Table 6.2). All other compounds are present in minor amounts with the exception of CaO that occasionally can reach up to 3-4% in certain specimens.

SO_3 typically ranges 0.05-0.1% whereas Cu typically appears at trace levels and only very rarely reaches more than 100 ppm; in LD and CX, Cu is below the detection limit in the majority of the samples (Appendix IV). The notable exception is sample YW4, with a Cu content of more than 5000 ppm and also higher SO_3 (0.2%). This sample presents identical bloomery iron microstructure to the other specimens of Daye, and the most likely explanation is that the high levels of Cu and S are due to ore contamination.

As in the case of the copper slag, a series of binary plots were generated to explore correlations between the different oxides of the bulk composition (Figure 6.4). Correlation between the major oxides is only evident in the negative correlation between FeO and SiO_2, which is not particularly informative since these are the major compounds in a closed system. On the whole and regardless of whether these are tap or lumpy slag, the different sites show the same tendency and usually overlap with each other as a homogenous group, rather than splitting by site.

6.1.2 Silicates

Fayalite is the only silicate that appears crystallised out of the glassy matrix and, as was the case in most of the copper slag, this olivine contains regularly some MgO (1-2%), which can be higher in YW (up to 30%) crystallising as forsterite, although this is infrequent (Table 6.3). It typically occurs as a massive agglomeration of 'blocky' olivines which are occasionally interrupted by scant areas of glassy matrix (Figure 6.5); the latter with a composition of FeO (~25%) and CaO (~10%), and incorporating minor oxides such as MgO and TiO_2, typically ≤1%. Alternatively, in fewer samples, the olivines are present as lattice

close or single spaced, and containing more second-generation fayalite as tiny feathers between the larger crystals.

	MgO	*Al_2O_3*	*SiO_2*	*P_2O_5*	*SO_3*	*K_2O*	*CaO*	*TiO_2*	*MnO*	*FeO*	*Cu**
HF MEAN (5)	0.5	5.2	21.4	0.2	0.1	0.9	1.0	0.2	0.2	70.3	53
MEDIAN	0.6	5.2	21.1	0.2	0.1	0.8	0.9	0.2	0.1	70.0	68
STD DEV	0.1	0.4	3.0	0.1	0.01	0.2	0.3	0.02	0.03	3.4	37
MAX	0.6	6.0	26.6	0.3	0.1	1.1	1.5	0.2	0.2	75.5	91
MIN	0.4	4.6	17.5	0.1	0.1	0.7	0.7	0.1	0.1	65.1	bdl
MC MEAN (2)	0.6	5.6	19.6	0.2	0.1	1.0	1.9	0.2	0.2	70.7	268
MEDIAN	0.6	5.6	19.6	0.2	0.1	1.0	1.9	0.2	0.2	70.7	268
STD DEV	0.3	1.1	0.3	0.1	0.02	0.1	1.1	0.01	0.1	2.6	268
MAX	0.9	6.7	19.9	0.4	0.1	1.1	3.1	0.2	0.3	73.2	536
MIN	0.3	4.5	19.3	0.1	0.1	0.8	0.8	0.2	0.1	68.1	bdl
LD MEAN (12)	0.4	4.1	20.5	0.3	0.1	1.0	1.6	0.2	0.2	71.6	52
MEDIAN	0.5	3.9	20.3	0.3	0.1	1.1	1.4	0.2	0.1	72.5	8
STD DEV	0.1	0.7	2.8	0.1	0.03	0.3	0.8	0.1	0.1	4.4	88
MAX	0.6	5.7	25.2	0.4	0.13	1.4	2.8	0.3	0.3	78.2	318
MIN	0.2	3.4	16.0	0.2	0.04	0.3	0.4	0.1	0.1	64.8	bdl
YW MEAN (7)	0.5	4.5	20.0	0.2	0.1	0.7	1.0	0.2	0.1	72.5	81
MEDIAN	0.7	4.6	20.4	0.5	0.1	0.7	1.6	0.2	0.2	71.0	806
STD DEV	0.4	0.5	2.8	0.7	0.1	0.1	1.4	0.03	0.3	5.4	1819
MAX	1.7	5.7	24.9	2.1	0.2	0.9	4.9	0.2	0.9	77.3	5260
MIN	0.5	4.1	15.5	0.1	0.1	0.5	0.6	0.2	0.1	59.4	bdl
CX MEAN (12)	0.5	4.4	21.3	0.2	0.1	0.6	0.7	0.2	0.1	71.8	20.0
MEDIAN	0.5	4.3	20.8	0.2	0.1	0.6	0.7	0.2	0.1	72.4	5.0
STD DEV	0.1	0.5	2.3	0.03	0.01	0.1	0.2	0.03	0.03	3.0	28.8
MAX	0.6	5.3	25.7	0.2	0.1	0.7	1.1	0.2	0.2	77.1	81
MIN	0.4	3.5	17.7	0.1	0.03	0.4	0.5	0.2	0.1	67.0	bdl

Table 6.2: WD-XRF chemical composition of Daye bloomery iron tap slag.
*All values in % except Cu (ppm).

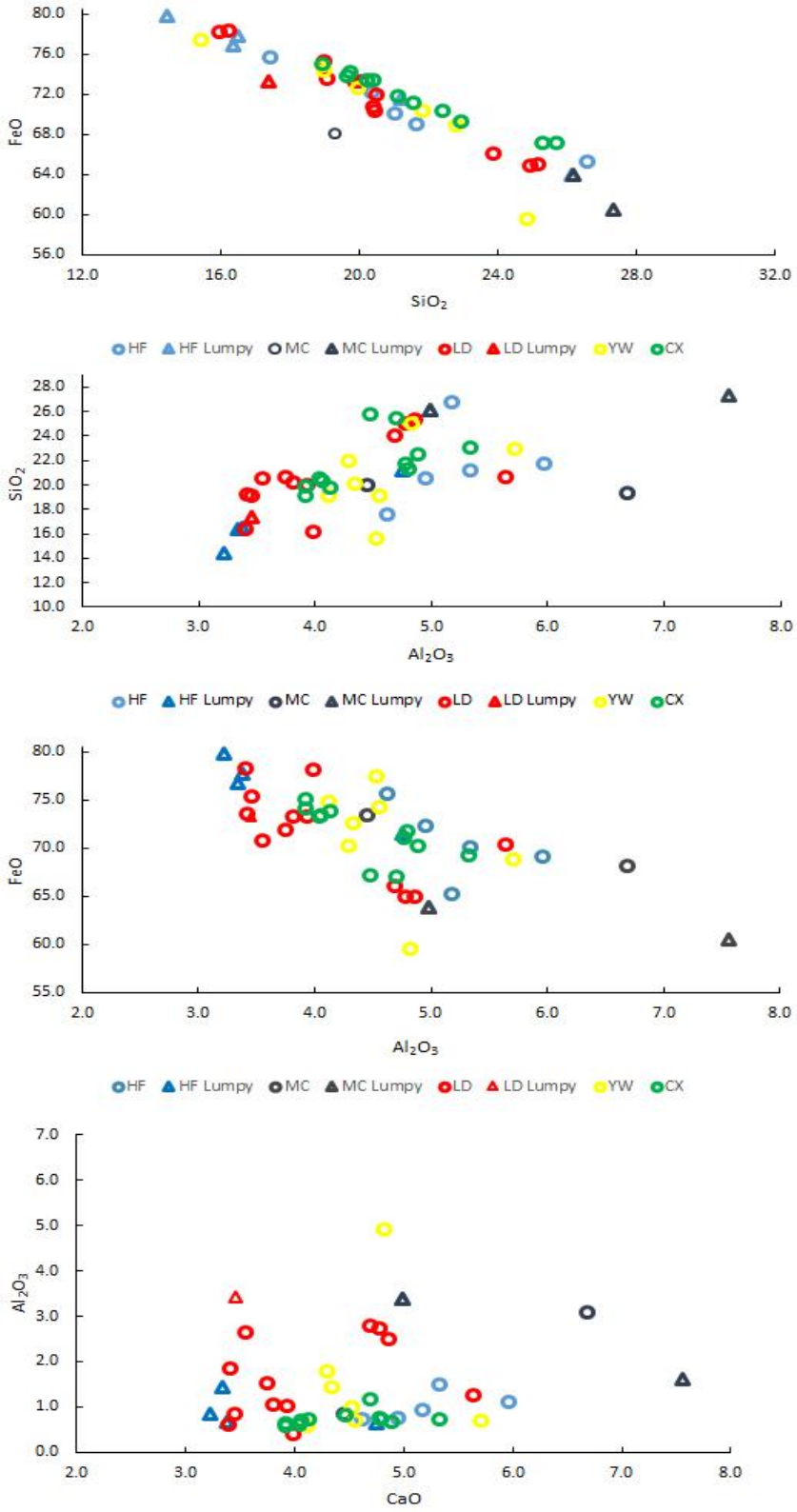

Figure 6.4: Binary plots of the bulk chemical composition of the Daye iron slag. The dots indicate tap slag and the triangles lumpy slag.

		MgO	*SiO_2*	*CaO*	*MnO*	*FeO*			*MgO*	*SiO_2*	*CaO*	*MnO*	*FeO*
HF	**MEAN**	1.4	29.5	0.6	0.4	68.3	***YW***	**MEAN**	6.1	26.1	1.1	1.2	66.1
	STD	0.4	1.1	0.3	0.01	1.7		**STD**	12.0	3.0	0.8	0.5	3.8
	MAX	2.1	31.4	1.6	0.4	73.5		**MAX**	30.8	35.2	3.7	1.6	79.2
	MIN	0.6	25.3	0.3	0.4	63.0		**MIN**	0.6	18.4	0.3	0.5	59.2
MC	**MEAN**	2.1	29.9	1.0	0.6	67.0	***CX***	**MEAN**	1.2	28.7	0.6	0.5	69.7
	STD	0.5	1.0	0.7	0.1	1.6		**STD**	0.3	1.4	0.3	0.01	0.6
	MAX	2.8	32.0	2.2	0.8	69.4		**MAX**	1.9	29.7	1.3	0.5	71.3
	MIN	1.5	28.8	0.4	0.6	64.9		**MIN**	0.6	22.5	0.3	0.5	68.4
LD	**MEAN**	1.1	29.0	1.5	1.5	67.0							
	STD	0.5	1.4	1.5	1.5	7.2							
	MAX	2.3	30.4	5.8	5.8	72.5							
	MIN	0.6	22.3	0.3	0.3	29.9							

Table 6.3: Average composition (SEM-EDS) of olivine crystals in the microstructure of the Daye bloomery smelting slag.
Average of 3-5 crystals per sample.

Phases of hercynite ($FeAl_2O_4$) appear occasionally within the fayalite crystals. Also occasional are few small phases of iron aluminium silicates with variable levels of alumina (1-10 %) typically associated to gas cavities. Finally, few samples present iron-rich silicates phases quite similar to iscorite ($Fe_7[SiO_4]O_6$); the rare transitional phase from wüstite to fayalite identified in some ancient bloomery slags (Rose et al. 1990; Forrières 1987 and Kessmann 1989 in Pleiner 2000, 252; Hauptmann 2014, Fig. 5.5). However iscorite was not confirmed in Daye, as these crystals frequently contain Al_2O_3 (~2-5%, ~80 % FeO, 15-20 % SiO_2) and/or do not occur as needles as typical of this mineral, but in cubic shapes (Figure 6.5). The occurrence of minor silicate phases like the ones described is common in bloomery iron slag (Fluzin 2003; Muralha et al. 2011), particularly if the slag has reached high temperatures and reducing atmospheres (Herbert 2003).

Residual quartz and argillaceous materials are exceptional; only identified in 7 out of 39 specimens: MC1, YW6, YW7, YW8, CX2, HF9 and HF25.

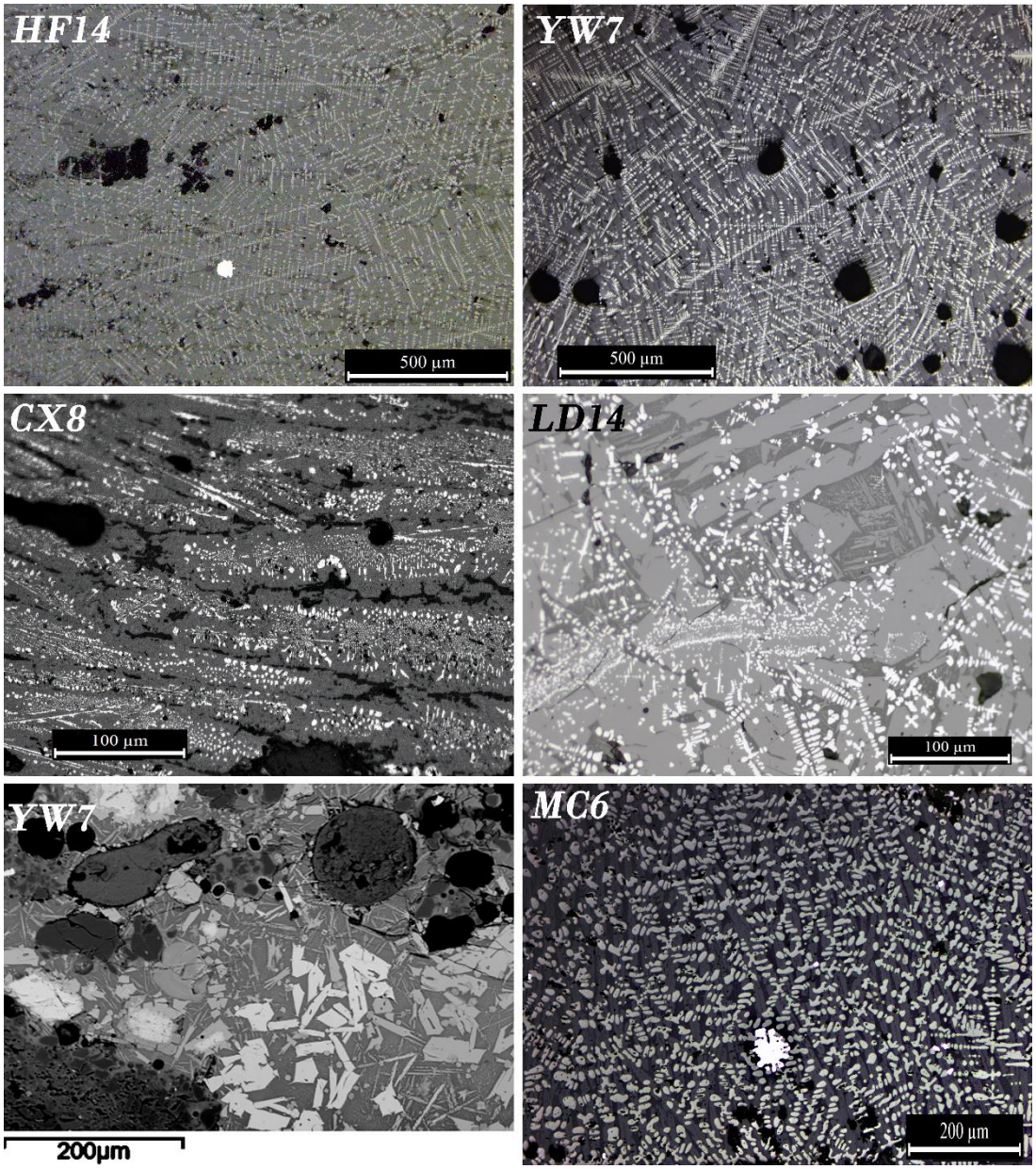

Figure 6.5: OM and SEM micrographs showing the typical microstructure and olivines appearance in the Daye bloomery tap slag.

(HF14, YW7) Normal appearance showing predominant blocky olivines (medium grey) surfaced by dendritic wüstite (light grey or white), with occasional iron metal particles (bright white); **(CX8)** Detail of blocky olivines (dark grey) and tiny dendritic wüstite (white); **(LD14)** Detail of plume olivines growing between larger crystals (light grey) partially covered by dendritic wüstite (white); **(YW7 SEM micrograph)** Possible iscorite crystals (bright light grey) in a glassy matrix with fayalite crystals (medium grey) in between porosity and argillaceous materials (darker greys); **(MC6)** Detail of dendritic wüstite (medium grey) and an iron particle (white) over blocky olivines (dark grey).

6.1.3 Iron oxides

Wüstite is by far the dominant iron oxide within the microstructure of the tap slag and is frequently predominant over the olivines in certain areas where it appears as large (~50 µm) globules (Figure 6.8). Other iron oxides are anecdotal in comparison: cubic shapes or pseudomorphs of magnetite, which were the most common iron oxide phases in the copper slag, are extremely rare here, usually constrained to the oxidised boundary that separates consecutive runs of slag (Figure 6.6).

Eight specimens out of 39 contain chunks of residual haematite normally showing signals of advanced reactions: i.e. embedded in the matrix, with cracks filled by slag, or as agglomerations of re-crystallised iron oxides pseudomorphs of the parent mineral.

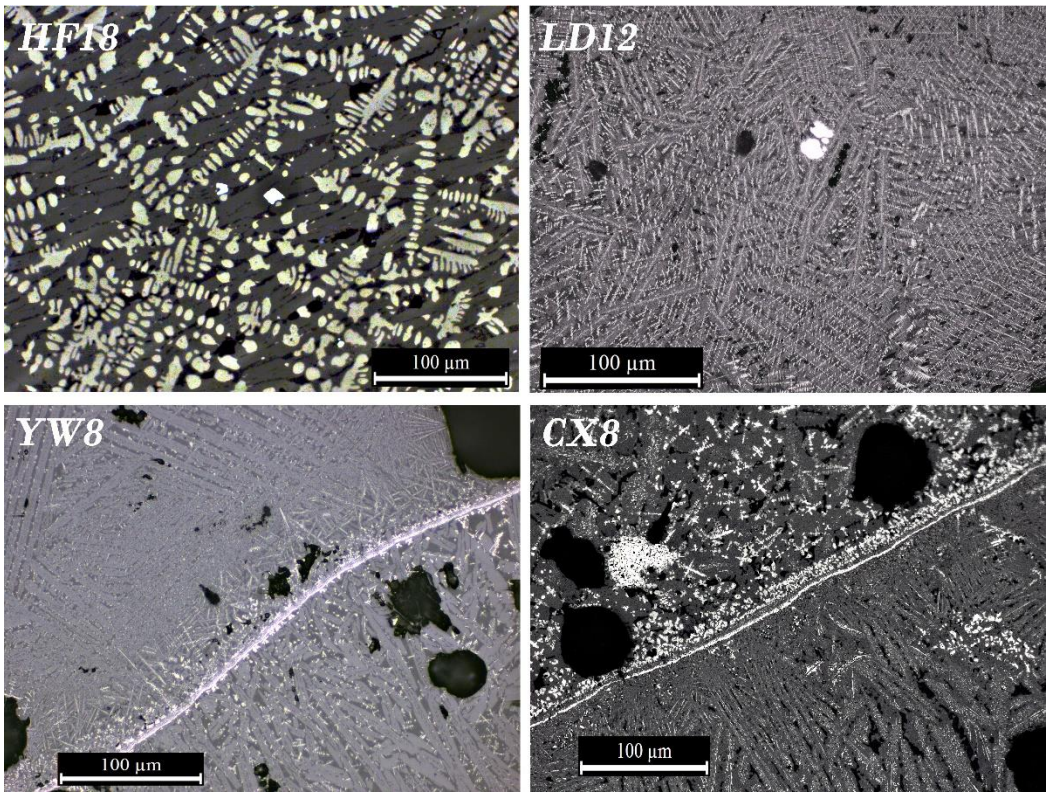

Figure 6.6: OM micrographs of iron oxides in the microstructure of the Daye bloomery iron tap.
(HF18) Detail of predominant large size dendritic wüstite (white grey) and two iron particles (bright white) over blocky olivines; **(LD12)** Same mineralogy showing much finer grain size of wüstite and two particles of iron metal (bright white); **(YW8)** Magnetite skin (white) separating fayalite laths (mid grey) mostly free of wüstite; **(CX8)** Magnetite skin separating blocky olivines and fayalite laths, the blocky olivines area showing dendritic wüstite and a small residual piece of magnetite (bright white).

6.1.4 Metal-rich particles

In general, iron particles are not very abundant in the Daye slag; as a matter of fact these are totally absent in 18 specimens, representing 46% of the tap slag sampled assemblage. The size and morphology of the iron micrograins vary depending on the site (Figure 6.8). These are generally absent in CX, HF and MC, but when present they are sub-angular or sub-rounded small particles (≥10 µm) albeit with larger exceptions. On the other hand, LD and YW are comparatively richer in metallic iron, typically in the form of larger particles (40-50 µm) shaped as rounded globules although still appear abundant irregular shapes.

The great majority of the iron particles analysed by SEM-EDS showed no presence of any other element. Although carbon could not be measured because the samples were carbon coated, in most of the slag the morphology of the metal is indicative of solid-state formation and therefore of low or negligible carbon levels (Tholander 1989). However, the droplet shape in several specimens from LD (7), YW(4) and MC(1) is typical of liquid pig iron that are also occasionally formed in a low bloomery furnace (Blomgren & Tholander 1986; Tholander 1989).

Two samples of slag (LD9, HF24), one of furnace lining (YW9) and the glassy slag HF26 (section 6.1.6) were etched in order to reveal the crystal structure and determine the type of iron alloy; the selection criteria was that these samples contained metal particles >50 µm and thus with more probabilities of revealing grain textures. Unfortunately, although these were etched only for one second, the prills were corroded too aggressively and the damage on the crystal structure could not be reverted not even after re-polishing. In spite of the poor quality of the obtained micrographs, some information was collected (Figure 6.7).

All the angular iron particles do not show any crystal, or show very light grain boundaries corresponding to ferrite; the droplet shape grains show more complex structures richer in carbon (cementite, graphite) although difficult to determine due to the low quality of the micrographs. The iron prill in the glassy slag HF26 shows what seems to be ledeburite – an eutectic phase Fe-Fe_3C typical in cast iron microstructures (Scott 1991, 38-41) – within a network of phosphides and few pearlite colonies, although the sample is too corroded and the 'ledeburite' could be in fact rounded pearlite.

Only a few specimens showed the presence of some impurities, which broadly coincide with those found in the copper slag. Lead-iron particles occur in four specimens – MC1, CX4, CX8 and LD4 –, and barium sulphates in two – LD7 and HF21. Nickel was found alloyed with iron in a few particles of specimens CX2 and CX10, typically at low levels (1-2%), except for one case (CX10) containing 87% Ni. CX2 is the only sample were the ferro-nickel particles are polymetallic, containing quaternary alloys Fe-Ni-Zn-Cu. All the metallic iron particles in specimen MC6 contain some Cu, typically ~1% Cu although occasionally reaching up to 4%.

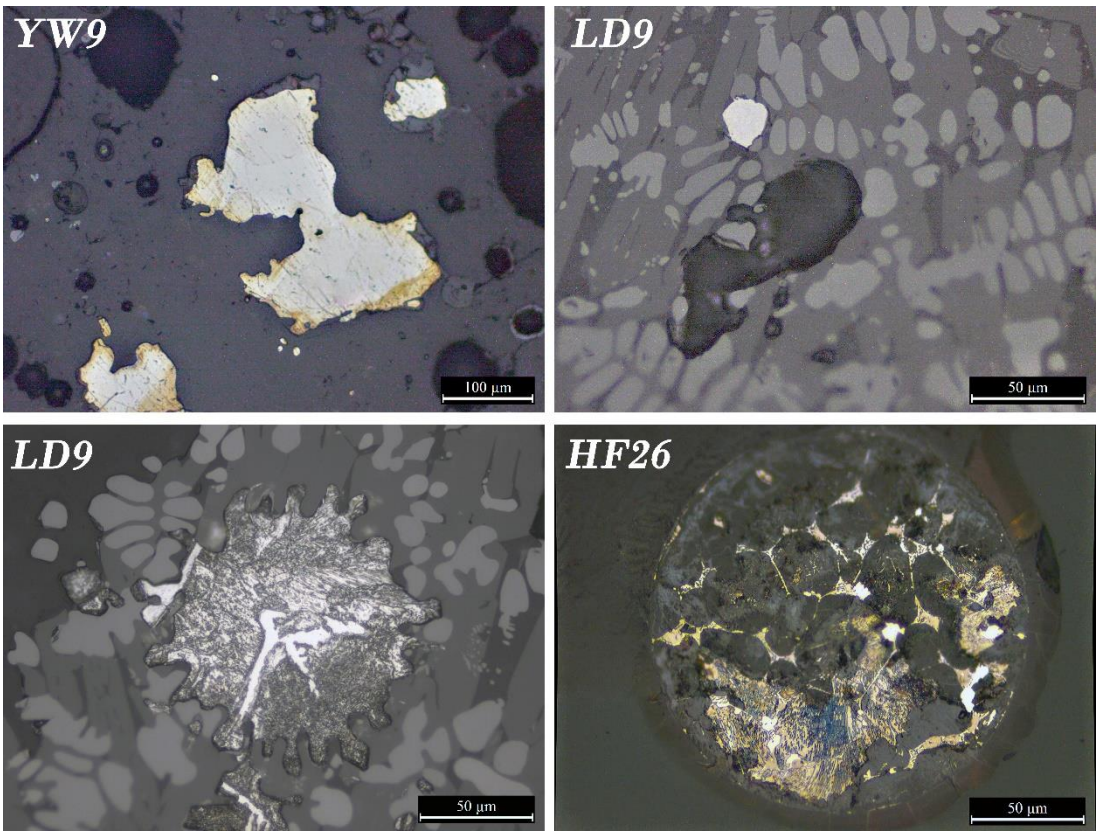

Figure 6.7: Etched iron particles in slag and furnace lining.
(YW9) Large ferrite particle (overetched) in a fragment of furnace lining; **(LD9)** Small sub-angular iron ferrite particle in slag; and large iron droplet showing cementite (white) and graphite flakes in the same specimen; **(HF26)** Iron prill in glassy slag specimen showing pearlite colonies (bottom) and possibly ledeburite (large rounded droplets) surrounded by phosphides; the sample is overetched and thus difficult to characterise conclusively.

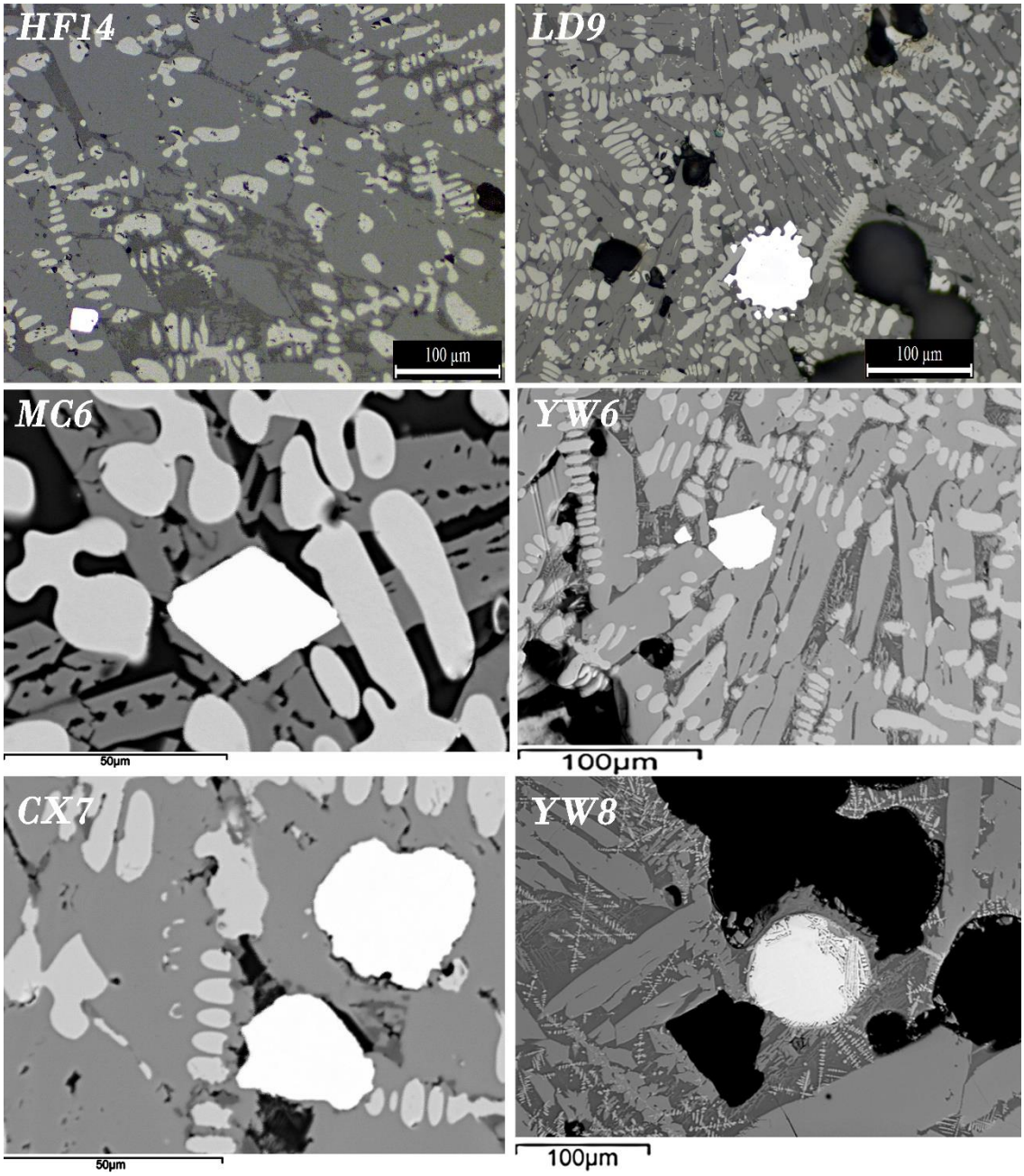

Figure 6.8: OM (HF14, LD9) and SEM (MC6, YW6, CX7, YW8) micrographs of iron metal particles in the Daye bloomery iron tap slag.
(HF14, MC6, CX7, YW6) Typical small sub-angular or sub-rounded iron particles present in the Daye slag; **(LD9, YW8)** Larger size rounded particles, the black material in YW8 is resin and the texture in the prill is due to polishing scratches.

6.1.5 Lumpy slag

In general, the lumpy slag samples show a bulk composition comparable to the tap slag, although typically richer in FeO (73-76% to 70-72%) with a corresponding decrease in SiO_2; Al_2O_3 is still the third major compound although it also decreases (Table 6.4). A higher compositional fluctuation can be noted between the sites, particularly clear in the case of MC, with slag generally richer in SiO_2 (average of 26% *vs* 17% for the other sites) and Al_2O_3 (6% *vs* 3%), and poorer in FeO (62% to an average of 73-76%). CaO is frequently higher in these slag lumps than in the tap slag (2-3% more).

The microstructure of the lumpy slag is dominated by the same phases identified within the tap slag: olivines, wüstite and metallic iron particles, but generally in the lumpy slags the predominant minerals are not the olivines but the wüstite (Figure 6.9). The crystallisation of fayalite is irregular from very thin needles to massive agglomerations within the same sample. MC microstructure is the exception, where the olivines are the predominant mineral that crystallises homogeneously as blocky olivines in MC12 and as laths in MC18. MC12 also presents more hercynite than any of the other samples in Daye.

	MgO	***Al_2O_3***	***SiO_2***	***P_2O_5***	***SO_3***	***K_2O***	***CaO***	***TiO_2***	***MnO***	***FeO***	***Cu****
HF MEAN (4)	0.4	3.7	17.1	0.3	0.1	0.6	0.9	0.1	0.1	76.5	3
MEDIAN	0.4	3.4	16.4	0.3	0.1	0.6	0.8	0.1	0.1	77.3	4
STD DEV	0.1	0.6	2.5	0.1	0.01	0.1	0.3	0.01	0.01	3.1	2
MAX	0.6	4.7	21.2	0.4	0.2	0.8	1.4	0.2	0.2	79.8	5
MIN	0.3	3.2	14.5	0.2	0.1	0.6	0.6	0.1	0.1	71.5	bdl
MC MEAN (2)	0.6	6.3	26.7	0.3	0.0	1.0	2.5	0.2	0.1	62.2	45
MEDIAN	0.6	6.3	26.7	0.3	0.0	1.0	2.5	0.2	0.1	62.2	45
STD DEV	0.1	1.3	0.6	0.0	0.0	0.5	0.9	0.1	0.1	1.7	22.0
MAX	0.7	7.6	27.3	0.3	0.1	1.6	3.4	0.3	0.1	63.9	67
MIN	0.5	5.0	26.1	0.2	0.0	0.5	1.6	0.2	0.0	60.5	bdl
LD (LD11)	0.6	3.5	17.4	0.5	0.1	1.1	3.4	0.2	0.1	73.2	136

Table 6.4: WD-XRF chemical composition of Daye bloomery iron lumpy slag.
*All values in % except Cu (ppm).

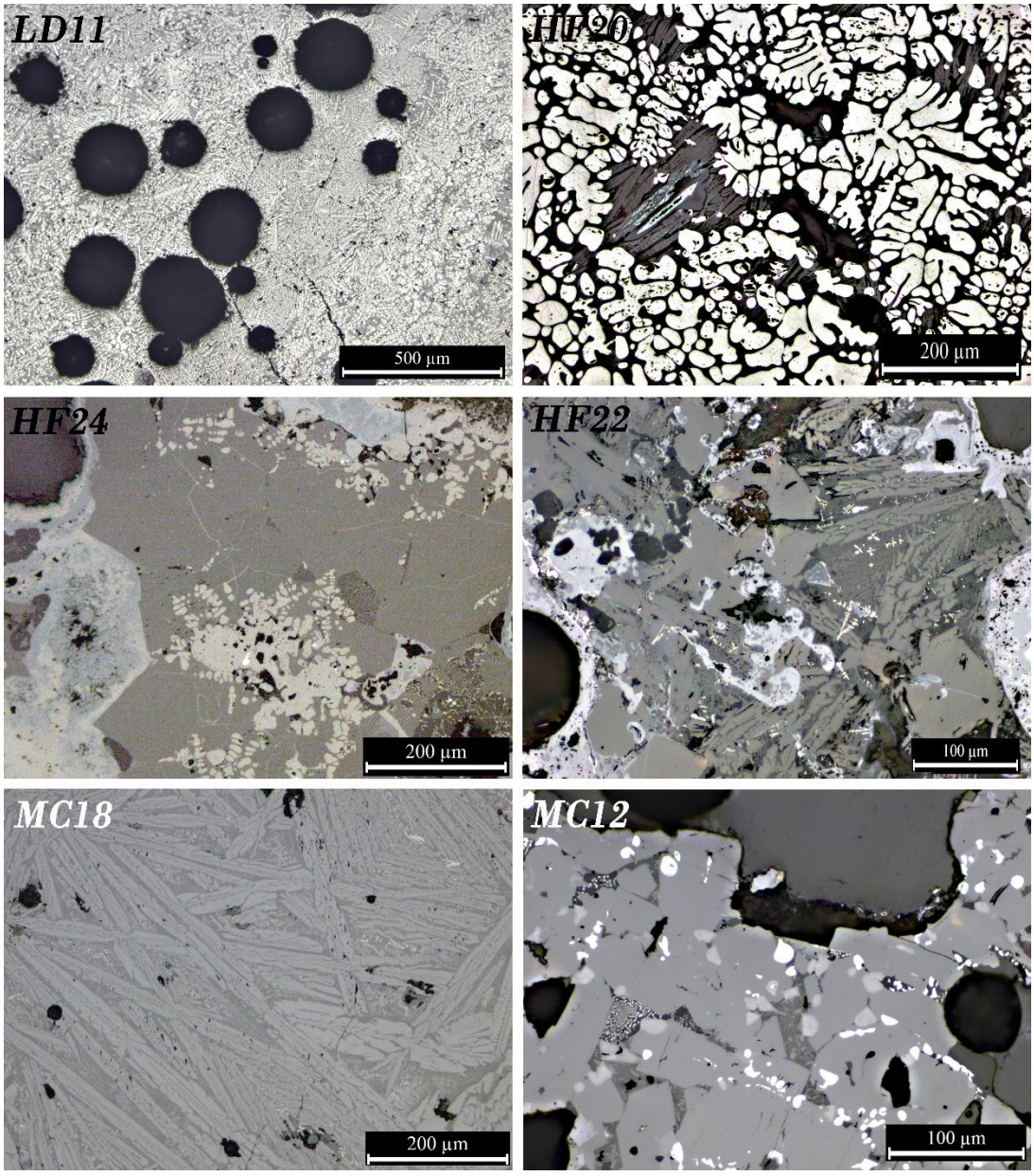

Figure 6.9: OM micrographs showing the typical microstructure and olivines appearance in the Daye bloomery lumpy slag.
(LD11) Typical texture of the lumpy slag showing intergrowns of predominant dendritic wüstite and scant visible areas of olivines, and abundant porosity; **(HF20)** Detail of olivine laths (dark grey) and thick globules of wüstite (white); **(HF24)** Detail of massive olivines (dark grey) between corrosion products (light grey, bluish), and agglomerations of wüstite (light grey) with few iron metal particles (white); **(HF22)** Detail of heterogeneous microstructure of the lumpy slag showing fayalite laths and polygonal crystals (mid grey), iron aluminium silicates (very dark grey, black) and corrosion products (bright light grey); **(MC18)** Lath olivines (light grey) on a glassy matrix (medium grey), and scant magnetite (grey white); **(MC12)** Detail of blocky olivines (medium grey), scattered hercynite (light grey) and wüstite (white).

Another characteristic of the lumpy slag is that most of the samples present partial or severe corrosion that alters strongly the microstructure especially in areas close to any

surface. Silicate phases are of much larger size here, occasionally similar to leucite in composition but typically these are undetermined iron aluminium silicates of highly variable composition. Although rich in newly formed phases, these slags normally lack any unreacted inclusions apart from occasional patches of clay, likely absorbed from the technical ceramics. All of these phases appear distributed differently in each specimen composing a heterogeneous microstructure significantly different to the more uniform texture of the tap slag. As a rule, the typical microstructure olivine-dendritic wüstite-iron particles is only visible occasionally at the core of the samples, which also display abundant corrosion from corroded metal, redeposited around pores, etc.

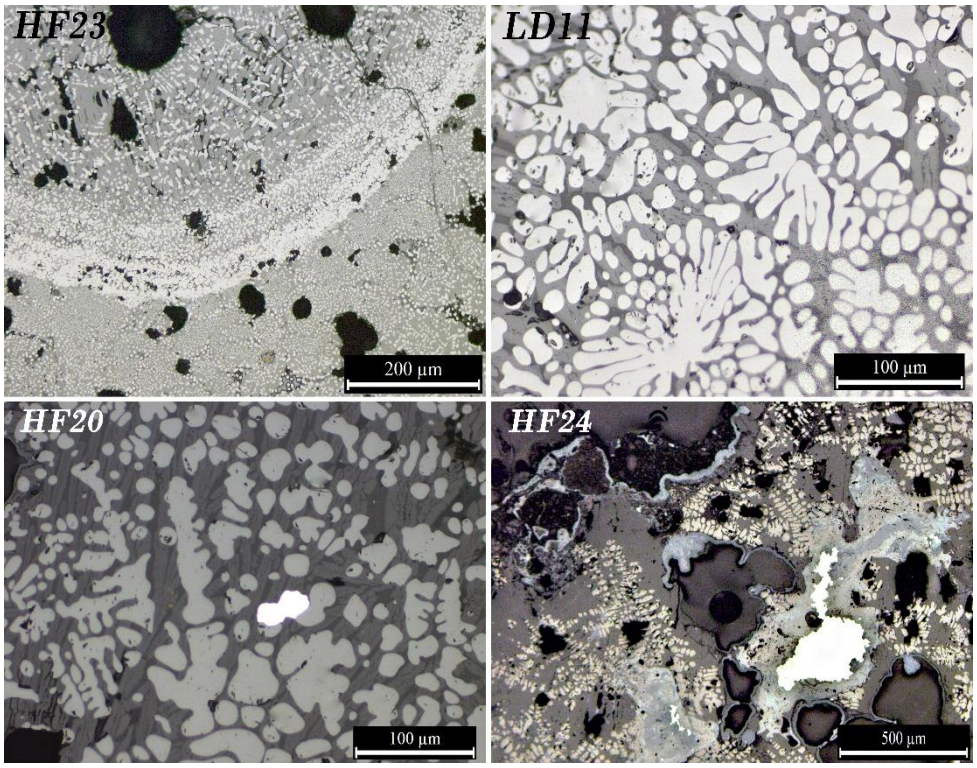

Figure 6.10: OM micrographs of iron oxides and metal particles in the Daye bloomery iron lumpy slag.
(HF23) Thick magnetite-wüstite skin separating blocky olivines and dendritic wüstite of coarse (up) and fine grain (bottom); **(LD11)** Tightly packed grains of wüstite (white grey), note the difference in grain size with the equivalents in tap slag. **(HF20)** Large sub-rounded iron metal particle; **(HF24)** Very large agglomeration of iron metal (bright white) surrounded by abundant corrosion products (light grey-blueish), wüstite (white grey) and iron silicates (dark grey).

In general, the lumpy slag is considerably richer in free iron oxides than the tap slag – as is also reflected in the chemical composition with the two exceptions from MC–, and presents abundant conglomerates of those, frequently arranged imperfectly in dendritic formation of large grain size (~60-100 μm) occasionally exhibiting very tightly packed grains. The wüstite globules are overwhelmingly predominant over the laths of olivines in the lumpy slag (Figure 6.9).

The iron metal particles present in the lumpy slag generally show the sub-angular/sub-rounded shapes like CX or HF described before, but here they tend to be larger, and occasionally occur as clusters (Figure 6.10).

6.1.6 Atypical by-products

Mixed with the lumpy slag of HF, two samples were recovered that do not seem consistent with bloomery iron smelting: a fragment of glassy slag (HF26) and a lump of high carbon steel (HF7).

Glassy slag

The slag is a small (39x32 mm, and 23 g of weight) fragment of cubic shape, dark green-bluish colour and vitrified external surface spotted with clay particles (Figure 6.11). The cut section reveals a very glassy, colourful slag banded in masses of aquamarine and dark green colours. Its microstructure is notably uniform, consisting of glass containing sporadic pyroxenes and very few metallic iron particles (Figure 6.13). Iron particles are always perfectly round and larger (60-100 μm) than those observed within the majority of the other iron slag. All the prills contain phases rich in phosphorus (0.7-3%) and some of them also sulphur (22-32%) whereas carbon could not be quantified since the sample was carbon-coated although the etching reveals that is high carbon steel (Figure 6.7).

HF26 is the only non-fayalitic slag of the entire collection (Table 6.5): instead of iron-rich silicates, the bulk chemical composition corresponds basically to a lime-rich glass notably poorer in FeO than any of the other slag (15% compared to 57-79%). The glass is basically a calcium iron silicate of composition similar to augite [(Ca; Na)(Mg; Fe; Al; Ti)(Si; $Al)_2O_6$] – a pyroxene that crystallised occasionally. The glassy microstructure with rounded iron prills and lime-rich chemical composition suggests that this is a by-product of blast furnace slag. The absence of fayalite (Fe_2SiO_4) or wüstite (FeO), typical in bloomery iron slag, is also consistent with blast furnace slag while the relatively high CaO suggests that lime was

used as a flux (Tylecote 1987, 329-332; Tholander 1989; Rehren & Ganzelewski 1995; Buchwald 2005, 158-159).

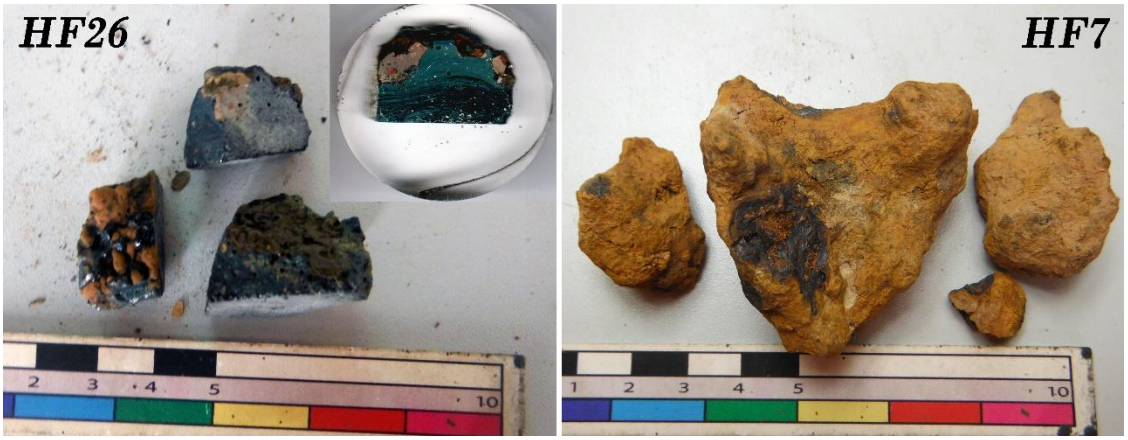

Figure 6.11: Atypical by-products related to the iron production.
HF26 after cutting and mounted on a polished block, and HF7 lump with disaggregated fragments due to corrosion.

The main oxides, when plotted in the CaO-FeO-SiO_2 phase diagram (Figure 6.12) indicate that the glassy slag reached temperatures around 1400°C, considerably higher than those estimated for the rest of the slag (Figure 6.12). Nevertheless, it must be noticed that the temperature is hard to estimate accurately since the specimen plots in an area of the phase diagram with very closely packed isotherms, and hence small changes in composition due to the other oxides not accounted for in the phase diagram – e.g. the 3% K_2O, plus some uncertainties because of MgO, Al_2O_3, etc. – might actually bring down the temperatures in the diagram (Rapp 1998). The presence of well-rounded, molten iron, however, does indicate a high temperature, highly reducing environment (Wingrove 1970). On balance, it seems realistic to state that specimen HF26 reached higher temperatures than any of the other slags, albeit possibly not as high as 1400°C.

	MgO	***Al_2O_3***	***SiO_2***	***P_2O_5***	***SO_3***	***K_2O***	***CaO***	***TiO_2***	***MnO***	***FeO***	***Cu****
Bulk chemical	3.3	8.4	49.6	1.0	0.2	2.8	18.3	0.5	0.5	15.4	19

Table 6.5: Chemical composition of atypical specimen HF26.
All values in % except Cu in ppm.

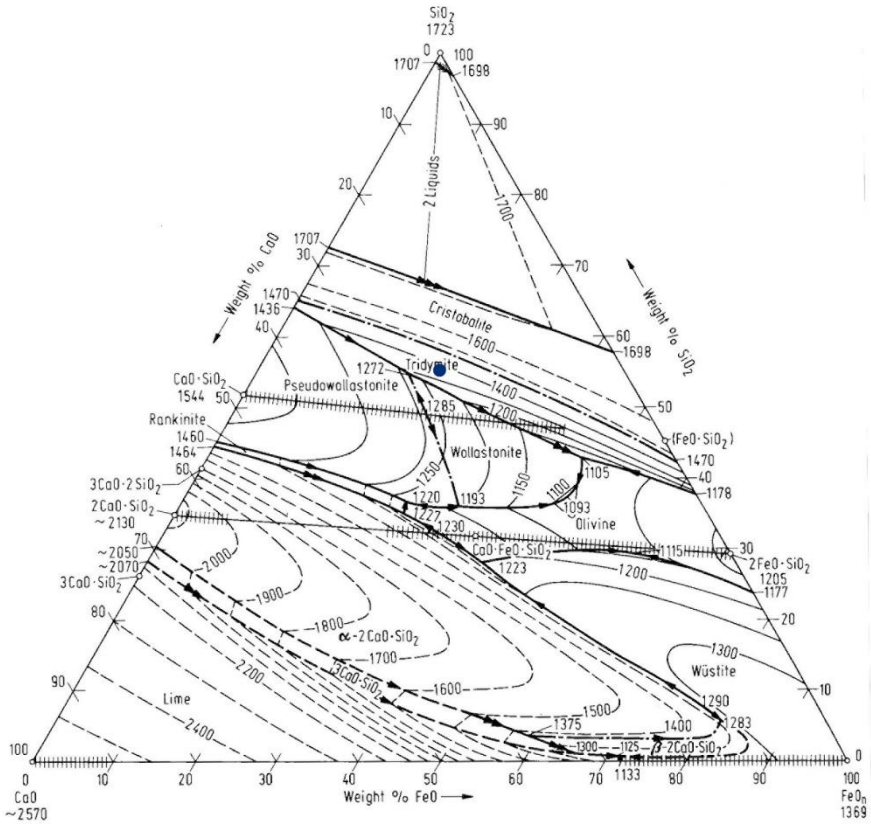

Figure 6.12: Ternary diagram CaO-FeO-SiO_2 with the glassy slag plotted within the Tridymite area.
MgO was added to FeO to make the sum of the reduced elements more realistic.

Metallic iron lump

The other unusual sample was found in physical contact with the glassy slag. This is a small (50x50x21 mm, and 106 g) lump of metallic iron relatively regular in shape and slightly concave, which is affected by severe corrosion (Figure 6.11). The metal is so hard that the sawing blade was broken in several pieces at the first cutting attempt. The metallography revealed that the metal is very high carbon steel with a structure of predominant pearlite with cementite at the grain boundaries that occasionally shows Widmanstätten structures (Figure 6.13). Similar hypereutectoid steels have been estimated to contain carbon levels ranging 1.4-1.6% (Birch 2013), considerably higher than the ranges expected for iron produced by the direct method (0.01-0.4 %) (Rostoker & Bronson 1990, 97).

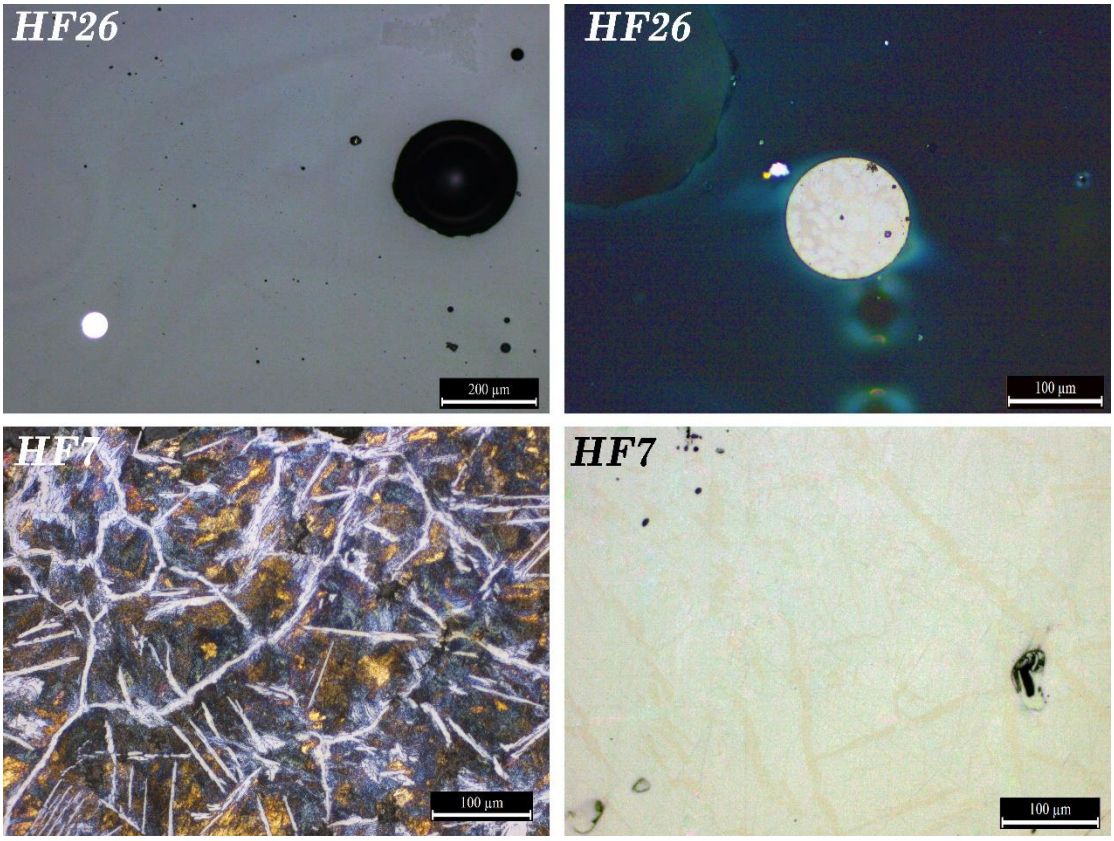

Figure 6.13: OM micrographs showing the microstructure of the atypical by-products. **(HF26)** Glass containing one iron prill; and detail of the same prill (XPL) showing the inner phosphoric phases. **(HF7)** Etched microstructure showing hypereutectoid pearlite and grain boundary cementite (left); and unetched microstructure where only the pale-orange C-rich boundaries are distinguishable (right).

6.1.6.1 Blast furnace-like by-products from a bloomery process

The piece of glassy slag (HF26), as mentioned, incorporates all the diagnostic features of a blast furnace debris: dense and viscous slag showing bright colours (non-matte), glassy (non-crystalline) homogeneous microstructure with very few iron prills and chemical composition poor in FeO (15%) and rich in CaO (18%), which is the type slag expected in cast iron production (White 1980; Rehren & Ganzelewski 1995). The piece of metal (HF7) found in the same site, however, despite of its carbon richness still is below of the ~4-5% C content typical of pig iron, which is the iron-carbon alloy to be expected from a blast furnace (Wagner 1996, 339-351). Furthermore, there is a total lack of evidence at the site for a blast furnace, or for any of the large scale infrastructures typical of a Chinese cast iron production plant (Wagner 2008). Even if HF was only field-walked, it is conceivable that some remains would be at sight, particularly when other remains from different

periods and productions (copper smelting, porcelain, bloomery iron) are evident on surface. The small size – 23 g of slag and 100 g of metal – and rarity of the samples thus suggest that these could be an 'accidental' by-product.

The production of C-rich iron in a bloomery furnace at moderate temperatures of ~1150°C has been reported numerous times (e.g. Maddin 1985; Blomgren & Tholander 1986; Clough 1987). This has been frequently recognised as 'risk' or a 'problem' and tried to prevent from happening since an excessively C-rich iron alloy requires a decarburisation process of the metal to be workable as wrought iron (Pleiner 2000, 139; Rehder 2000, 123; Craddock & Lang 2005, 42). Experimental archaeology (Crew et al. 2011; Wrona 2013) has demonstrated that cast iron can be produced in a bloomery furnace by adjusting the fuel to ore ratio and the air blast.

Moreover, some cast iron is very likely to occur within an ordinary bloomery smelting furnace even if the smelters do not force the conditions to carbon-enrich the bloom (Figure 6.14). This is also demonstrated by the increasing examples of cast iron products formed by the bloomery process and discarded as useless in the archaeological record (e.g. Navasaitis & Selskienė 2007b, 2007a; Crew et al. 2011 and literature therein). Of particular interest is the case of the Roman site of Semlach/Eisner in Austria (Birch 2013; Fillery-Travis 2015, 219-221) where 17 highly carburised iron lumps were produced by the direct reduction method. The lumps present smooth but corroded surfaces, globular morphologies and a microstructure of highly carburised iron classified in three groups: hypereutectoid steel (~1.5% carbon), white or grey cast iron. The six specimens labelled as hypereutectoid steel present a microstructure identical to that of HF7 (Figure 6.15).

The interpretation of these lumps is that they correspond to small amounts of liquid iron generated during the bloomery that coalesced forming globular shapes with smoothed surfaces, which cooled rapidly when the raw iron was extracted from the furnace. Also very significant is that these lumps were recognised and discarded in situ by the smelters as they were considered 'useless' (Birch 2013, 10)

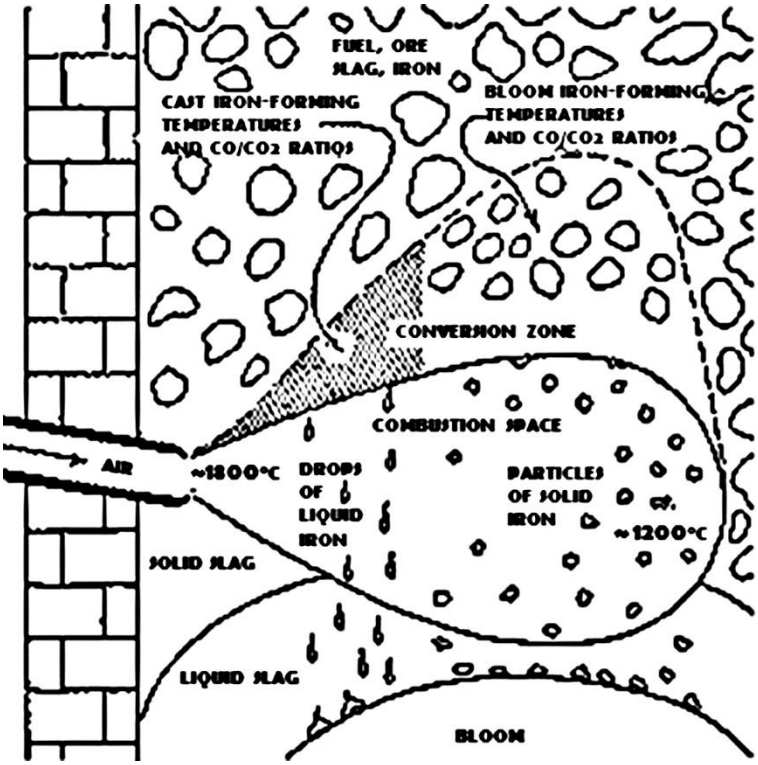

Figure 6.14: Heterogeneous conditions in the combustion zone of a bloomery furnace.
In some circumstances zones of high carbon content can occur in a bloom. The illustration suggests that both the temperature and the CO/CO_2 ratio immediately above the tuyere orifice inside the furnace are higher than elsewhere. According to fuel/ore ratio and air input rate, the conditions for smelting to cast iron could be achieved locally. After Rostoker et al. (1989, Fig. 9.7).

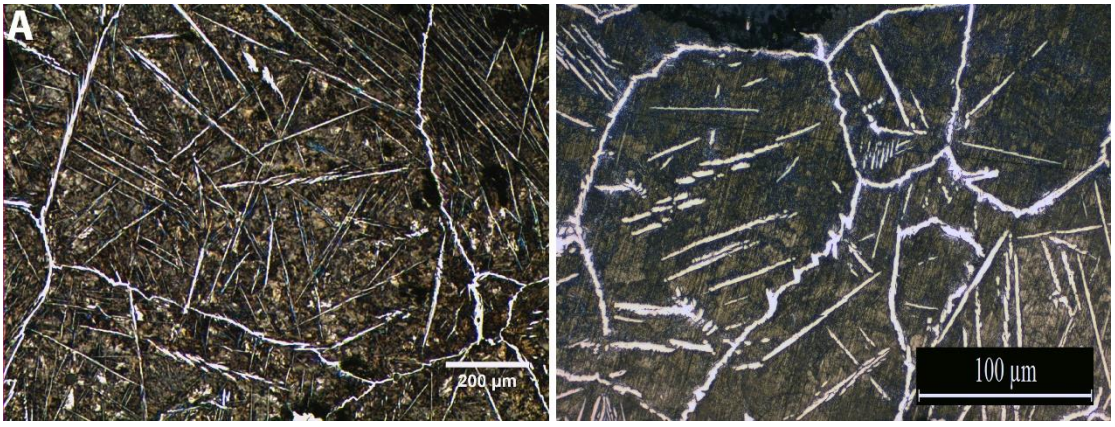

Figure 6.15: OM micrographs of hyper-eutectoid steel.
Left: Pearlite predominates with a network of cementite visible as precipitates on grain boundaries on a lump at Semlach/Eisner (Birch 2013, Fig. 2). Right micrograph shows the same features in HF7. Left picture courtesy of Thomas Birch.

Exactly the same scenario is conceivable for HF: a punctual internal dynamic within a bloomery furnace generated a small amount of highly C-rich iron metal and glassy slag that were discarded by the smelters. This interpretation, however, is considerably less solid than the Semlach/Eisner case since the latter is strongly supported by the archaeological excavation context that, unfortunately, does not exist for HF.

The fact that perfectly rounded C-rich iron prills are only present within the glassy slag and absent in the rest of the collection supports the hypothesis of HF7 and HF26 as fortuitous generation of cast iron by-products within a bloomery iron furnace (Figure 6.7).

6.2 Bloomery iron furnaces and technical ceramics

Furnace fragments were recovered at all sites although some of them were demonstrated to be associated to copper production, as discussed in section 5.2, and not to bloomery iron. All the fragments were recovered from different points scattered on the surface without visible remains of the original furnace foundations. LD is the only site that was excavated and that presented well preserved furnaces (Figure 3.9 and Figure 6.16).

A total of 23 embanked furnaces arranged in battery were discovered at the site of LD: all of them presenting a robust base – in some cases the only preserved part – with two clearly separated features: the furnace chamber and forehearth on the one hand, and a working platform for the bellows at the rear on the other – although the latter is frequently lost or badly preserved; the two features were connected by a tuyere hole of ~4 cm of diameter (Hu et al. 2013) (Figure 6.17). Typically, the complete structure measures 80-90 cm in length, with the furnace shaft smaller than the bellows operating working platform (Figure 6.18). The shaft is hopper-shaped and of small dimensions, typically the diameter at the top ranges 35-60 cm and 20-34 cm at the bottom, the shaft is ~50cm high. The largest dimensions are reached in furnace 22 with a diameter of 60x36 (top and bottom), and 54 cm high for the shaft.

Figure 6.16: LD battery of furnaces during the excavation in 2007.
Picture courtesy of Professor Chen Shuxiang.

The morphology of the LD structures is comparable to those found in 2014 in HF and visible on a natural section. Even though these were largely obscured by vegetation and soil, the position of the shaft was evident since abundant charcoal demarcated an oblong shape perpendicular to the tapping holes, which were perfectly visible (Figure 6.19).

None of the mentioned structures were directly sampled since this action required a special permission that was not granted to the local archaeologists that excavated LD and field-walked HF. Therefore, all the specimens provided for archaeometric analyses correspond to broken pieces of the smelting structures recovered in the course of the archaeological intervention, yet is not possible to relate these to specific furnaces (Figure 6.20).

Finally, for the sake of simplicity, all the analysed technical ceramics are labelled as 'furnace wall'. While no diagnostic remains of other technical ceramics such as tuyeres were found, it should be acknowledged that some of 'furnace walls' recovered at iron smelting remains could actually belong to smithing hearths.

Figure 6.17: LD furnaces during the excavation in 2007.
Forehearth (金门) and furnace hearth (炉缸) of furnaces 8 and 4, and working platform with the shallow pit to accommodate the bellows in furnace number 4 seen from the back. Images courtesy of Professor Chen Shuxiang.

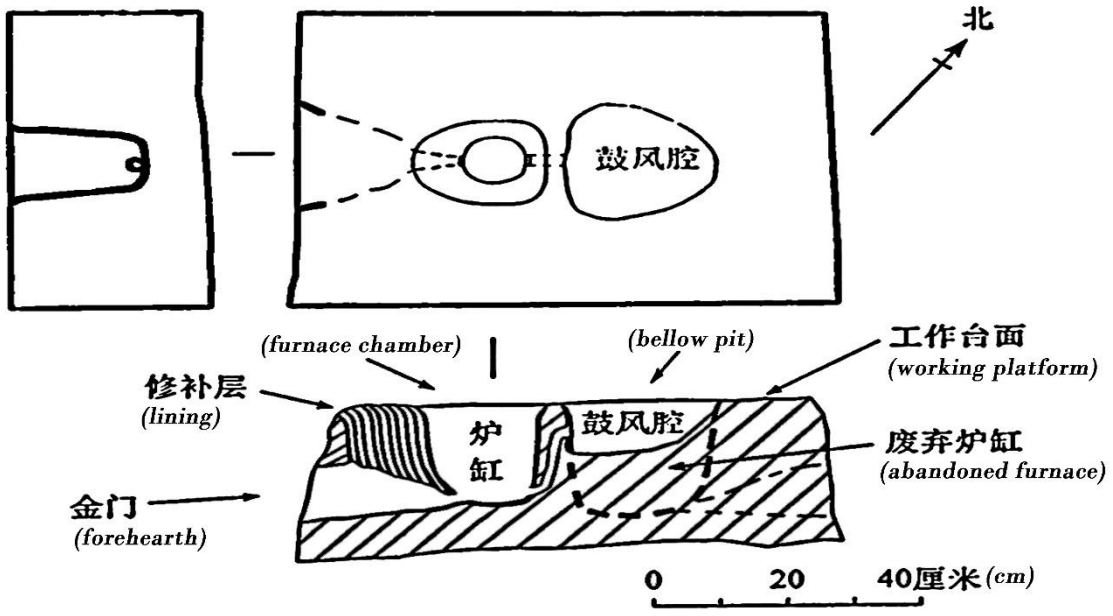

Figure 6.18: Schematic plan of furnace 12.
Bottom: Plan and section of furnace 12 after Hu et al. (2013, Fig. 4).

Figure 6.19: Natural section showing the location of two furnaces in HF (pointed by arrows) and detail of the forehearths.
The pen of the bottom right photograph indicates the estimated position of the charging hole.

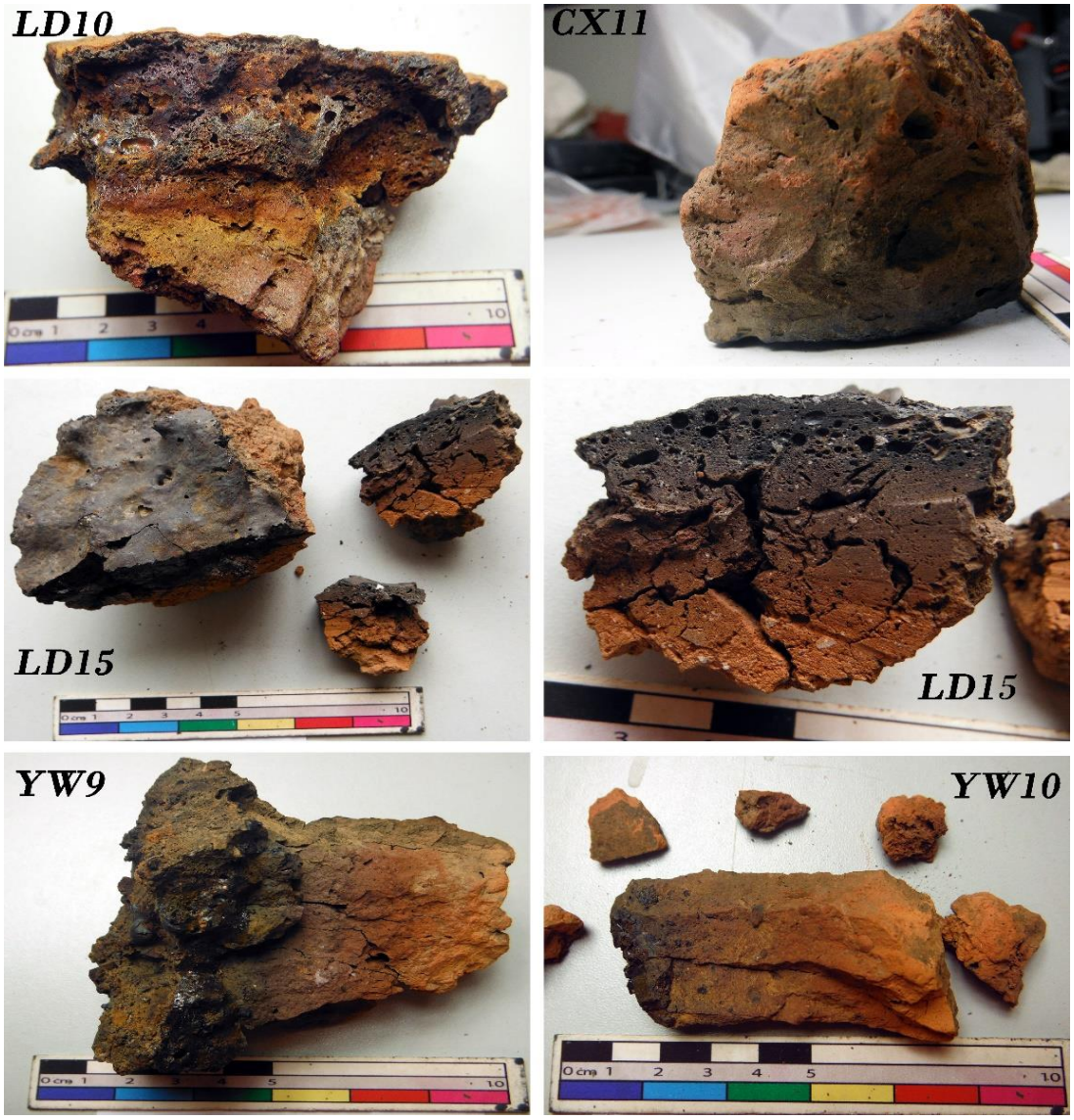

Figure 6.20: Selected fragments of furnace walls related to bloomery iron production. **(LD10)** Section showing gradient of ceramics less (pink) to more severely thermically affected (black and grey colours, and vitrification); **(CX11)** Large block of mostly red-burnt clay showing a slightly more altered surface at one extreme (grey colours); **(LD15)** Front view of the vitrified part and detail (right) of the section showing the black and the red-burnt clays; **(YW9, YW10)** Section of a furnace wall showing predominant altered black ceramics (YW9) and predominantly red-burnt ceramics (YW10).

6.2.1 Characterisation of the technical ceramics

The chemical composition of the technical ceramics associated to iron metallurgy is broadly similar to that of those related to copper with major elements SiO_2, Al_2O_3 totalling ~75-90% and FeO as third major element (Table 6.6). On the whole, in comparison with the copper related ceramics they are higher in SiO_2 (77-84% to 71-77%) and lower in Al_2O_3

(9-10 to 12-18%). A further difference between the copper/iron ceramic fabrics is in the heavy metals MgO, CuO, ZnO and PbO, which are regularly present in the ceramic fabric of the copper furnaces as a result of contamination from the smelting charge (Table 5.7). P_2O_5 is also absent in the bloomery iron technical ceramics.

Contrary to the copper furnace walls, the use of organic temper is more conspicuous in these fabrics (Figure 6.21), with some specimens presenting the diagnostic voids created when organic materials are burnt out during firing (Childs 1989). The red-burned clay, which appears less thermally altered, is rich in fine grain quartz inclusions, and is difficult to determine if these are naturally in the clay or added as temper. Only towards the inner, more vitrified surface of the technical ceramics does one identify more abundant minerals of coarse shapes. These could partly derive from the furnace charge or, perhaps more likely, they indicate that the lining applied to the inner surface of the furnace was richer in minerals. Here, not only quartz but also iron oxide minerals (presumably haematite) appear mixed with the clay. Towards the inner surface, the latter appear frequently partially reduced, with characteristic 'coral' bands (Blomgren & Tholander 1986) of reduced metallic iron on top of iron oxides or silicates and also abundant wüstite globules. This combination of quartz and iron minerals in the tempering of the furnace lining may suggest that they were using ore gangue as temper.

		Na_2O	MgO	Al_2O_3	SiO_2	K_2O	CaO	TiO_2	FeO
RED-BURNT FABRIC	**YW9 red**	bdl	0.9	9.0	77.0	3.4	2.2	0.8	6.8
	YW10	bdl	0.3	9.2	84.2	1.5	0.2	1.1	3.7
	LD10	0.4	0.4	9.8	81.1	2.0	0.2	0.8	5.1
	CX11 red	bdl	0.5	10.2	80.2	1.7	0.5	1.2	5.7
VITRIFIED	**YW9 black**	0.2	0.9	9.4	74.8	2.1	2.1	1.1	10.1
	LD15	2.1	1.1	14.7	68.3	2.3	1.4	1.9	8.3
	CX11 black	bdl	0.5	9.8	76.6	1.7	0.5	1.0	10.0

Table 6.6: Bulk chemical composition of the bloomery iron furnace walls.

The grains of quartz and haematite are poorly sorted – particularly the iron oxides are very large –, and these appear more cracked and shattered due to the thermal stress (Tite et al. 2001).

Finally, glassy areas with a structure that resembles that of tap slag – crystallising olivines, wüstite globules and metallic iron particles – appear much more profusely than in the equivalent slaggy areas of the copper furnace walls. This is likely due to the lower alumina and higher iron content of the clay, which would have rendered it less refractory and thus more prone to interact chemically with the charge.

6.3 Ore

Possible fragments of ore were sampled only in two of the six bloomery sites – HF and YW (Figure 6.22). Concerning the HF samples, three of them – HF3, HF5, HF6 – were confidently related to copper production and described in section 5.3. Of the remaining four samples, HF29 was found associated to bloomery smelting slag but the other three – HF19, HF27, HF36 – were recovered from surface scatters and thus cannot be assigned to any production with certainty. Most of them show a variety of dull to bright red colours, frequently with reddish-brown or blood red reflections that together with friable surfaces can sometimes be taken as indicative of roasting (Fillery-Travis 2015, 268). In this case, the samples were not analysed by microscopy since all the sampled material was consumed in bulk WD-XRF, and therefore it is more difficult to establish whether these samples were roasted prior to deposition. However, it should be noted that similar-looking materials were observed scattered on most of the sites field-walked in Daye County. Thus the purple red colours and friable textures could be due to weathering rather than roasting.

During the excavation of LD, abundant fragments of ore were recovered. Although these were not available for the current study, ED-XRF analyses performed on two of them (Hu et al. 2013, Table II) determined that these are moderately rich in iron (45 and 66% respectively reported as Fe_2O_3), and consist mainly of quartz, haematite and magnetite minerals.

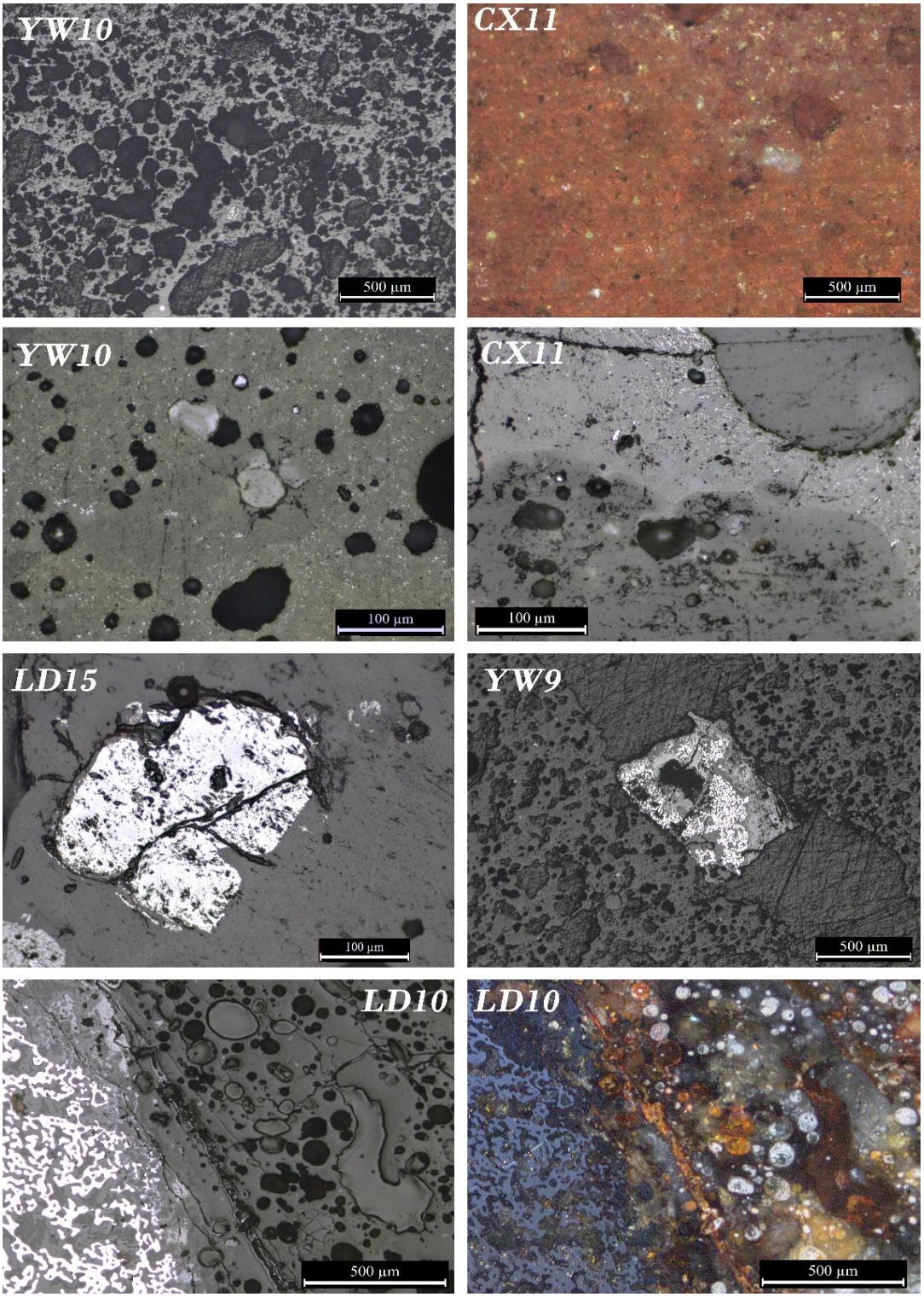

Figure 6.21: OM micrographs of the iron smelting technical ceramics microstructure. **(YW10)** Typical microstructure showing abundant elongated voids (some of them filled by resin) possibly derived from the burning of organic materials; **(CX11)** Red-burnt ceramic showing fine grains of quartz (white); **(YW10, CX11)** Large grain of quartz (dark grey) mostly dissolved into the slaggy matrix; **(LD15)** Detail of a smaller cracked fragment of haematite suspended in a glassy matrix , the bright particle on the left corner at the bottom is a grain of zirconia; **(YW9)** Fragment of iron mineral showing iron corals filling a large void within ceramic fabric with elongated voids; **(LD10)** Transition between the vitrified layer with iron corals and the strongly thermically altered ceramic fabric; and same under XPL.

	MgO	*Al_2O_3*	*SiO_2*	*SO_3*	*K_2O*	*CaO*	*TiO_2*	*FeO*	*Cu**	*XRD analysis*
HF27	bdl	1.0	3.7	bdl	bdl	bdl	bdl	95.0	647	Haematite
HF29	2.4	2.1	5.9	7.0	0.1	1.1	0.1	81.1	832	Magnetite
YW11	0.2	2.3	18.9	bdl	bdl	0.2	bdl	78.1	bdl	Haematite
YW12	0.1	1.8	7.5	0.1	bdl	0.1	0.1	90.2	598	–
HF19	1.1	24.7	65.4	bdl	5.9	0.1	0.7	1.7	229	Phyllosilicate
HF36	0.8	20.8	64.9	bdl	3.5	1.5	1.1	6.3	389	–

Table 6.7: WD-XRF results of mineral samples (relevant oxides only).
*Cu in ppm.

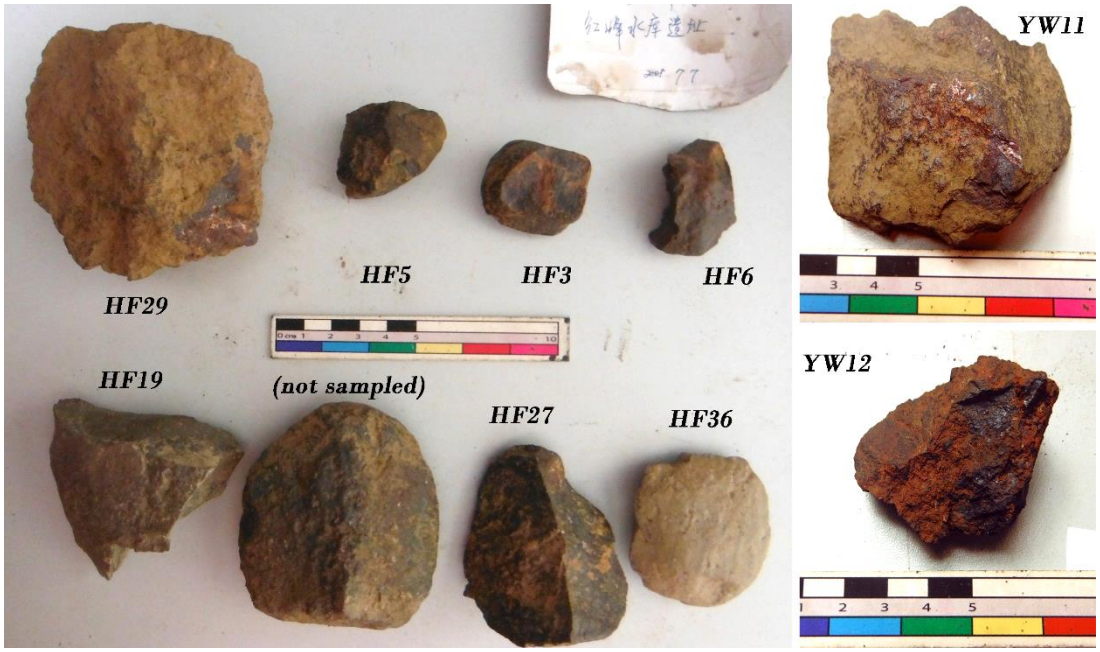

Figure 6.22: Ore fragments recovered in HF and YW.
HF3, HF5 and HF6 analyses in section 5.3.

One fragment from YW (YW11) and two from HF (HF27, HF29) were characterised by X-ray diffraction and found to be dominated by haematite and magnetite, respectively (Figure 6.23) (Appendix VII). Unfortunately, all the available sampled material for specimens HF36 and YW12 was used for WD-XRF analyses and thus XRD could not be performed.

Unlike the published samples from LD, the ores from YW and HF analysed are quite rich in FeO (78-95%). Chemical results show low levels of Si and Al, and traces of S and Cu (Table 6.7). HF29 showed exceptionally high levels of S (7%), although the accuracy of this

value could not be ascertained because sulphur is usually problematic to determine by XRF (Pasitschiniak 1986) and none of the standards available was appropriate to assess data quality for this element.

The other two rock samples collected as possible ore fragments – HF19, HF36 – turned out to be a mixture of silicate minerals and not a metal-rich ore, showing low levels of FeO (up to 6%) and trace Cu (Table 6.7). XRD analysis of HF19 showed that this consists of quartz and alumina-rich minerals; however, in this case the diffractogram is too noisy to attempt a more precise match with diffraction patterns in the library (Appendix VII).

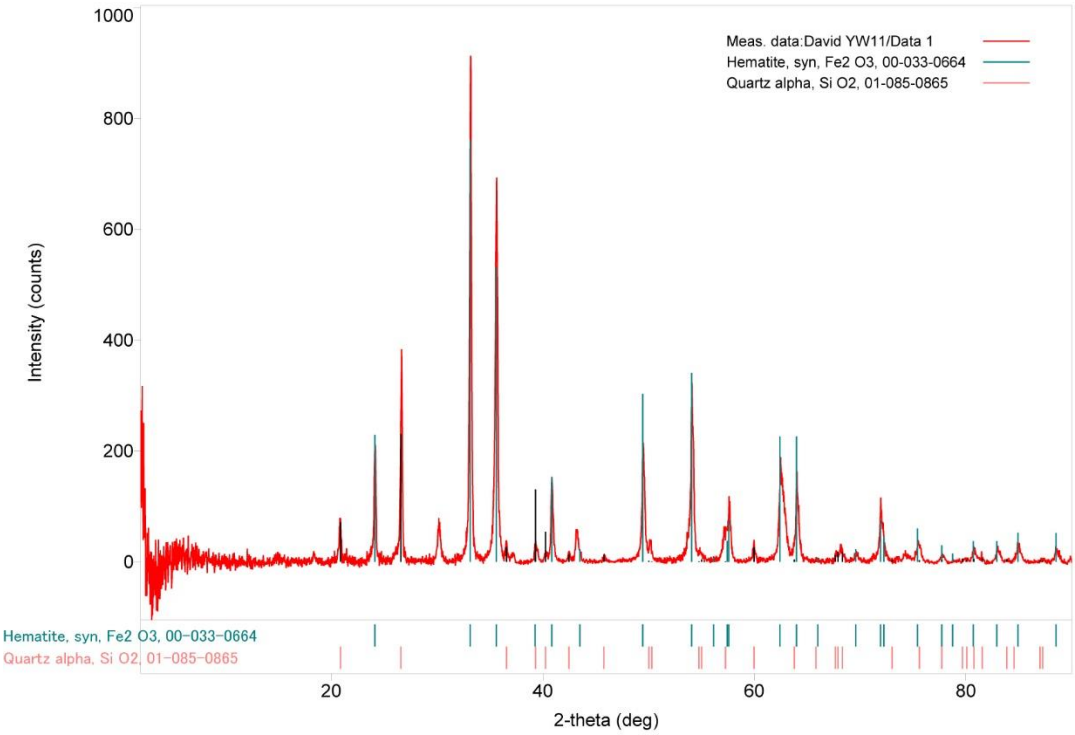

Figure 6.23: XRD diffractograms showing the match of the peaks of the sample YW11 with the haematite diffraction patterns from the reference library.

6.4 Discussion

As introduced before and substantiated by the analytical description, the interpretation of these slag as bloomery iron slag is unequivocal: the crystalline matrix with olivines; dominant dendritic wüstite; few metallic iron particles; and absence of any other relevant metal particle are clear indicators of iron reduction by the direct method (Rostoker &

Bronson 1990; Pleiner 2000; Buchwald 2005). In spite of the differentiation between pre-industrial iron and copper slags is not necessarily straightforward, several mineralogical and chemical indicators allow distinguishing them (Severin et al. 2011, 989).

Therefore, in copper smelting slag free iron oxides are typically present as magnetite not as wüstite, which is indicative of higher reduction environment not required for the extraction of copper (Wingrove 1970; Miller, D. & Killick 2004). This difference is stable in the microstructure of both collections: copper slags present mostly magnetite with very few rare isolated cases of wüstite whereas bloomery slags present the opposite pattern. A second mineralogical distinction is in the metal particles suspended in the matrix: iron particles are exclusively present within the bloomery slag, but this lacks of droplets of copper/copper sulphides that are the typical metal particles within the copper debris. Finally, although both slag types are of fayalitic composition, they are perfectly distinguishable since the bloomery slag is richer in FeO and poorer in SiO_2, and the copper slag contains ~1% of CuO which is consistent with the average copper content (0.5-1%) in archaeological copper smelting slags of Europe and Middle East (Bachmann 1982; Craddock 1995) (section 7.1).

The shape of metallic iron micrograins is a reliable indicator of the furnace reduction conditions. In particular, the angular grains predominant within the Daye slag are indicative of reduction in the solid state in a low bloomery furnace (Tholander 1989), which agrees with the furnace types found at some of the sites (Figure 6.18). As mentioned, in addition to the irregular grains some specimens also present droplets. These are less commonly produced in a low bloomery furnace, yet it is perfectly possible to generate liquid iron punctually using this furnace type, and even C-rich iron as demonstrates the atypical specimen HF7 (Blomgren & Tholander 1986).

6.4.1 Bloomery iron slag formation

The fundamental basis of the direct process is that iron metal is reduced in the solid state as a raw bloom from which the slag drains away , therefore, the formation of fluid slag is essential for a successful smelt (Tylecote 1962, 184; Clough 1987, 19). Although, in exceptional circumstances, a bloom can be produced while generating comparatively little

slag (Killick & Gordon 1989), in the vast majority of cases the formation of a liquid slag was the only way to separate gangue from metal in bloomery smelting. Consequently, the role of the slag in bloomery iron processes is perhaps even more crucial than in copper smelting, where 'slagless smelting' is possible and even a largely unreacted slag can render metallic copper in economically profitable amounts, since this can be retrieved mechanically from the slag (e.g. Metten 2003). Conversely, the bits of reduced iron cannot be retrieved unless that fluid slag is generated and pushes those bits to coalesce into a bloom (Rehder 2000, 103).

The formation of a pool of slag has various positive functions in bloomery smelting apart from the main one of providing a medium for metal particles to move and coalesce in a single mass: slag collects the gangue and non-reducible parts of the fuel ash, and also other impurities (e. g. sulphur); furthermore, it not only protects the already reduced iron from re-oxidation but also helps keeps the amount of carbon in the bloom relatively stable, preventing carburisation and de-carburisation (Clough 1987; Killick & Gordon 1989; Rostoker & Bronson 1990, 81-85; Sauder & Williams 2002).

6.4.1.1 Estimation of smelting temperatures

The moderately higher iron oxide levels have a reflection on the reduced compositions plotted in the equilibrium diagram Al_2O_3-SiO_2-FeO since there is a tendency for the iron slag samples to concentrate towards the iron-rich eutectic in the fayalite area of the diagram (Optimum 2), with a few specimens plotting within the wüstite area (Figure 6.25). The estimated temperature of slag formation, however, is not significantly different from that of the copper slag, pointing to temperatures around 1150-1200 °C.

The cost of producing slag with a relatively low melting temperature, such as the one in Daye, was a loss of potentially reducible iron into the slag (Rostoker & Bronson 1990, 92). Liquid slag is only achieved operating under 1200 °C if an iron-rich silicate melt is created (Figure 6.24), which means that a substantial quantity of the iron oxides present in the charge are not reduced but slagged. As a result, the loss of metal in slag was tolerable by ancient smelters if the ore grade was of 70-80% FeO while contents lower than 60% were hardly smeltable by traditional ancient bloomery (Rostoker & Bronson 1990, 92; Buchwald

2005, 93). The use of much leaner ores reduced by the direct process has been demonstrated or suggested in several places in Africa, India or Thailand (e.g. Rostoker & Bronson 1990, 43; Gordon & Killick 1993; Humphris et al. 2009; Iles & Martinon-Torres 2009; Venunan 2015), but these examples can be regarded as unusual in comparison with the vast majority of cases that used rich ores (Rostoker & Bronson 1990; Tylecote 1992; Pleiner 2000; Buchwald 2005, Humphris & Rehren (Eds) 2013, and literature therein all the cited references).

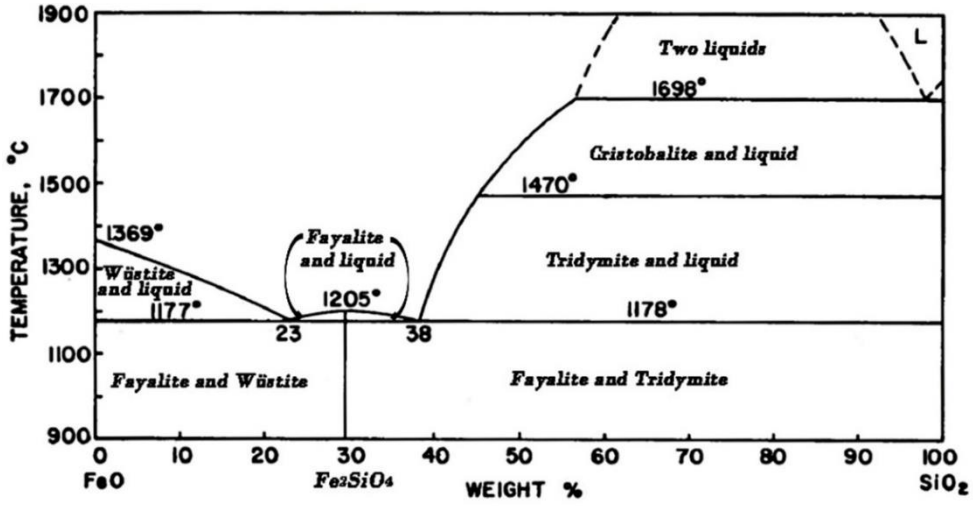

Figure 6.24: FeO-SiO_2 phase diagram showing the limited range of liquefaction of an iron-rich silicate batch.
High amounts of FeO (60-85%) are needed to generate a fayalitic liquid slag at temperatures lower than 1200 °C, and relatively low silica in comparison. Small variations in temperature and charge composition can stop the solid iron particles to settle and aggregate to a bloom obtaining uniquely fayalite rich in wüstite. Modified after (Rostoker & Bronson 1990, Fig. A.8; Buchwald 2005, Fig.85).

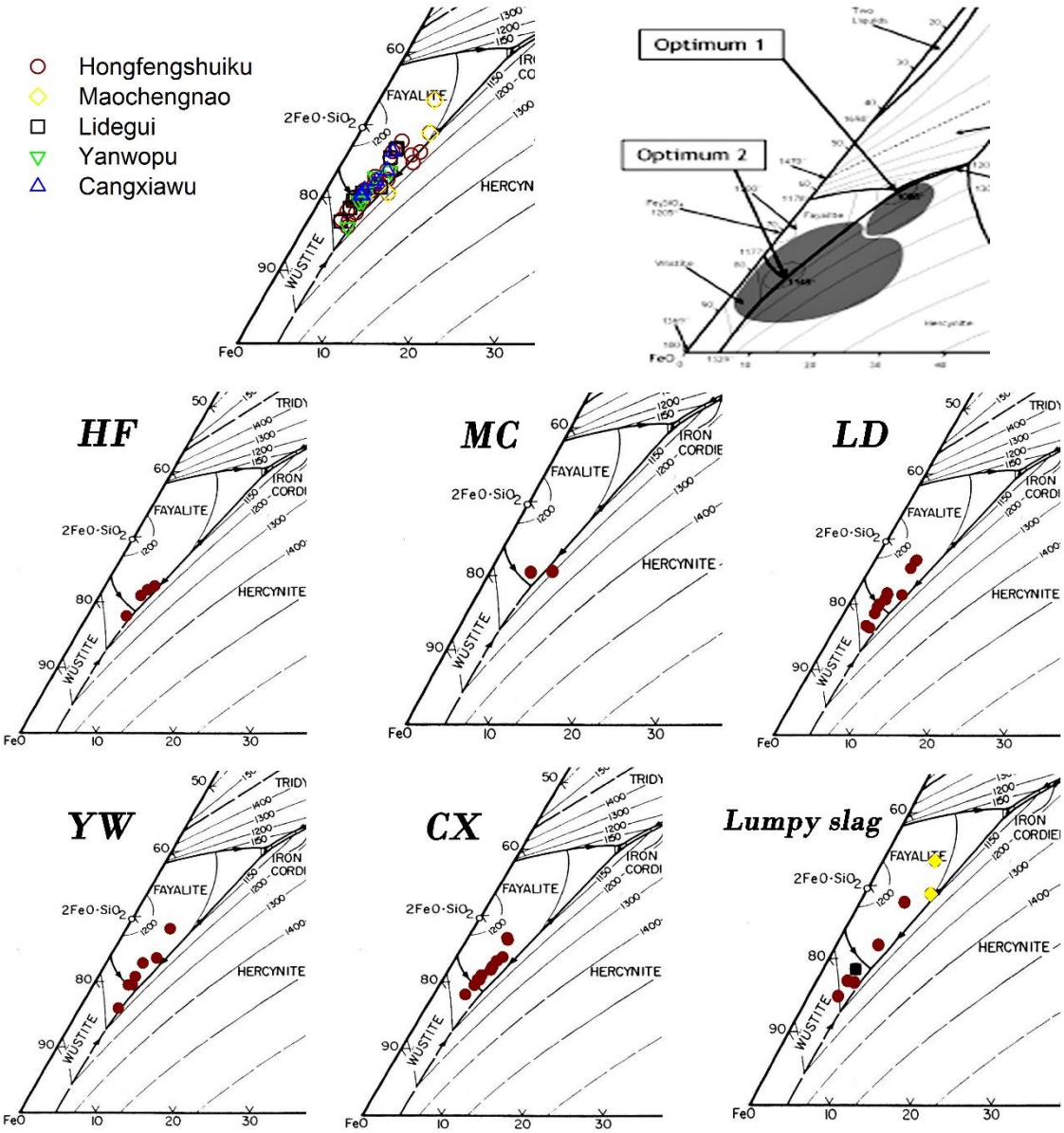

Figure 6.25: Ternary system FeO–Al_2O_3–SiO_2 comparing the typical composition of ancient slag and the Daye bloomery iron slag.
Average composition of ancient slag from bloomery iron smelting (dark shaded area) marking as well the two optimum areas for slag formation (modified after Rehren et al. 2007, Fig. 1) compared to Daye bloomery iron slag plotted in the same diagram. Lumpy slag graph includes the five specimens from HF (red), the two from MC (yellow), and the one from LD (black).

6.4.1.2 Iron loss in slag

One visual indicator of the quantity of iron left in the slag is in the abundance of free iron oxide crystallised out of the matrix. Slags with little or no wüstite indicate a more efficient process since any free FeO in the slag represents iron that could potentially have been

reduced into a bloom but which was not (Tylecote et al. 1971; Pleiner 2000, 253). Charlton et al. (2010, 356) propose the use of a quantitative reducible iron index (RII) to assess the relative proportion of iron oxide that could be reduced into metal but was left in the slag:

$$RII = \frac{2.39 \times SiO_2}{FeO + MnO}$$

Where 2.39 corresponds to the molar ratio of FeO to SiO_2. If the index is higher than 1.0 this indicates that there is SiO_2 in the slag that was not fluxed, whereas a value less than 1.0 indicates that there is an excess of FeO that has not been reduced. Table 6.8 shows that all the bloomery slag from Daye retains FeO, as also observed in the microstructure, which suggests technical inefficiency in terms of metal recovery. Nonetheless, this can be a tricky parameter to calculate efficiency. If the slag is diluted with more gangue or technical ceramics (as for example show some areas in specimens from YW, Figure 6.5) the microstructure will seem leaner, but this is not the product of a more efficient operation, simply of one that produces more slag volume per ore unit.

	HF	*MC*	*LD*	*YW*	*CX*	*Lumpy*
RII	0.7	0.7	0.7	0.7	0.7	0.7

Table 6.8: Reducible iron index of the Daye bloomery slag.

At the same time, the number of reduced iron particles trapped in the slag is very small; when present, iron phases are tiny and scant. Therefore we can assume that virtually all the reduced iron coalesced into a bloom and was gained by the smelter. As such, in terms of cost and benefit, we may consider that at least no fuel and energy were wasted into reducing iron that was not collected. As a matter of fact, one of the benefits of a slag composition towards the excess free iron Optimum 2 – most commonly generated in Daye (Figure 6.25) – is that consumes less fuel than slag with composition towards the Optimum 1 since the latter requires more strongly reduction conditions (Rehren et al. 2007, 214). Further benefits would remain in obtaining a typical yield of ferritic iron (Figure 6.7) avoiding the risk of over-carburising the iron as well as the mentioned higher risk of freezing the furnace caused by an excess of Si-rich materials (section 5.4.2). The major shortcoming of an iron-rich slag is, obviously, a lower yield of iron metal.

The few samples analysed suggest that the ores available in Daye are clearly suitable for bloomery smelting, ranging ~80-90 % of FeO content (Table 6.7). On the other hand, the average FeO content in the tap slag is equally very high; a median of ≥70% of the iron oxide was sacrificed in the slag (Figure 6.26).

In order to estimate the efficiency in the extraction of the iron metal from the ore some mass balance calculation methods are introduced in the following section.

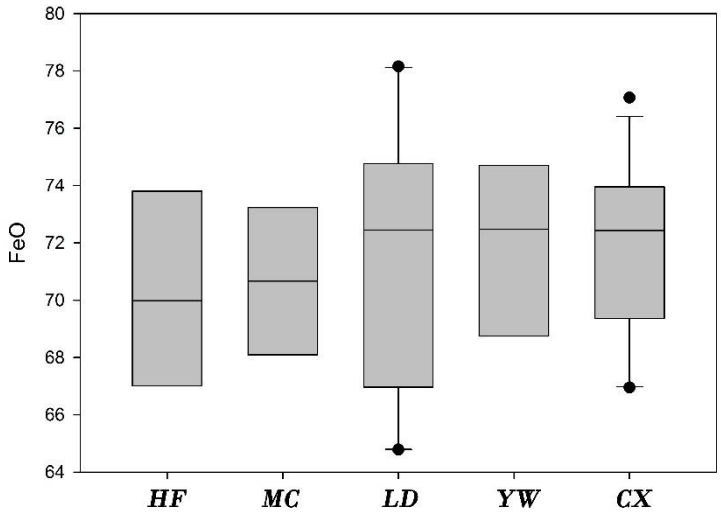

Figure 6.26: Box and whisker plot of FeO content in Daye bloomery tap slag.

6.4.2 Mass balance calculation

Material or mass balances are based on the application of the law of conservation of mass, which states that mass can neither be created nor destroyed. In terms of extractive metallurgy, this means that all the original materials in the furnace charge are transformed into something else and can be accounted for as output:

$$\text{Ore} + \text{Fuel} + \text{Flux} + \text{Furnace lining} \Rightarrow \text{Metal} + \text{Slag} + \text{Gas}$$

Consequently, if the other variables of the equation are known, the yield of metal of a certain production site can be calculated. In practical terms, however, solving the equation is not simple and multiple calculation models have been suggested: from simplified ones that only consider the variables of ore and slag (Tylecote et al. 1971) to

more complicate ones that introduce furnace lining (e.g. Serneels 1993) or charcoal (e.g. Crew 2000), to finally more complete proposals that take into account all the variables, and also introduce a graphical method to determine the contribution of each factor (e.g. Thomas & Young 1999).

The major problem to encounter is that many of these factors can be unknown; typically slag is consistently abundant and often the only remain available of ancient metallurgical activities whereas ore, fuel ash and furnace wall are more exceptional or if present do not necessarily represent those used by the smelters. Frequently, the unknown parameters are ignored or replaced by equivalent materials to get an estimate of the output, at the risk of fabricating the results.

For example, as an alternative to the original fuel, Thomas and Young (1999, 156) suggest that 'charcoal samples, if not forthcoming from excavations, can be produced from wood samples collected from the modern-site', however it seems unlikely that the vegetation of a humanised landscape is going to remain identical after several hundreds of years particularly when strong deforestation has been noticed associated to metallurgical activities (e.g. Hartwell 1967; López-Merino et al. 2014). The replacement of the ore by a modern sample from a nearby outcrop is equally problematic since many ore bodies show major variations in composition and even the ore found in the archaeological register could correspond to the one discarded by the smelter, and thus not representative either (Kresten 1987, 29).

Another possibility is to ignore the missing material as e.g. Venunan (2015) who performs the mass balance calculation without considering the fuel ash, since this is expected to have a small contribution to the total anyway (and no fuel samples were available). As an illustrative example, the contribution of the fuel ash is predicted to be up to 5% (Crew 2000) although it is normally smaller; for example, fuel ash contribution to slag formation is estimated as 0.93% only in the case of the medieval bloomery production of the Lahn–Dill region in Germany (Kronz 2000, Table 1). Having said this, fuel ash may in some cases be a significant source of several minor components such as calcium, potassium, manganese, etc. (Buchwald 2005, 137; Paynter 2006, 272) that under certain conditions can play a crucial role and dominate the chemical signature of the resulting slag (Blakelock et al. 2009, 1755). Thus, the contribution of each variable should not be underestimated.

A further problem concerns the sampling biases and analytical errors associated to the different analytical instruments, which will affect the calculations even when all the parameters are reasonable well known.

Furthermore, there are major uncharted circumstances unlikely to be solved such as for example the active life of a smelting site. Typically, the chronology of an archaeological site is roughly estimated and neither the beginning nor the end of a settlement is known, and thus a mass balance calculation is based on an average for a single site that does not account for diachronic changes.

6.4.2.1 Calculation of the output

Three different models are followed here to estimate the yield: Joosten et al (1998), Serneels (1993), and Crew (2000) with a double aim: to calculate the yield as accurately as possible given all the data limitations; and to assess the quality of the different models. These three models were chosen because they are based on the *enrichment factor (EF)* principle: as iron is removed from the system and reduced as metal, the remaining elements respectively increase in concentration (Thomas & Young 1999, 157), which allows an estimate of the yield of metal throughout this coefficient. The general equation used to calculate the enrichment factor common to the three models is expressed as follows (modified from Fillery-Travis 2015, 82):

$$EF = \frac{C_N^{slag}}{MC_N^{ore} + PC_N^{lining} + C'C_N^{fuel\ ash}}$$

Where C is the concentration of element N except iron, and M, P and C' represent the ore, the furnace lining and the fuel ash respectively. The models differ from each other in the inclusion or not of all the materials, which allows us to compare the mass balances based on the composition of ore and slag (Joosten et al. 1998); ore, slag and furnace lining (Serneels 1993); or these three plus fuel ash (Crew 2000). Excellent explanations and reviews of the three proposals utilised here can be found in Charlton (2006, 149-154) and Fillery-Travis (2015, 81-90).

All the calculations are based on the data from YW since is the only site from where ore, furnace wall, slag and charcoal were recovered. All the materials composition is obtained by WD-XRF except the furnace lining that as explained was analysed by SEM-EDS only. Most of the YW charcoal was consumed in ^{14}C dates so instead it was used equivalent available fuel ash data from Charlton (2006, Table 7.5), which although acknowledging the risk of representativeness, was considered appropriate as both samples correspond to the same family tree (*Fagaceae*) and genus (*Quercus*).

All the data used in the calculations is shown in Table 6.9. The yield was estimated as the result of reducing the rich ore in the three models, except in the third one, where both ore grades were considered.

Method 1:

The enrichment factor is calculated by Joosten et al. (1998) based on the slag:ore ratio and despite of the claim that their model 'makes it possible […] to establish to what extent the furnace lining and fuel ash contributed to the chemistry of the slag' (Joosten & Kars 1999, 243), these factors are not possible to calculate throughout their computations. The first equation figures the EF:

$$EF = \frac{(SiO_2 + Al_2O_3)_{in\ slag}}{(SiO_2 + Al_2O_3)_{in\ ore}} \qquad \frac{(20.1 + 4.0)_{in\ slag}}{(6.8 + 1.6)_{in\ ore}} = 2.86$$

And a second one calculates the metal yield:

$$\%\ yield\ = \frac{(FeO_{ore} \times EF)\ - FeO_{in\ slag}}{(FeO_{ore} \times EF)} \qquad \frac{(90.8 \times 2.86) - 71.6}{(90.8 \times 2.86)} = \ 0.72$$

Therefore, 72% of the FeO in the ore is being turned into metal, thus ~55% Fe.

	MgO	*Al_2O_3*	*SiO_2*	*P_2O_5*	*K_2O*	*CaO*	*TiO_2*	*V_2O_5**	*MnO*	*FeO*	*Cr_2O_3**	*CuO**	*ZnO**	*SrO**	*Y_2O_3**	*ZrO_2**	*PbO**
YW SLAG MEAN (8)	0.6	4.0	20.1	0.5	0.6	1.4	0.2	401	0.2	71.6	188	727	398	10	4	100	2200
MEDIUM GRADE ORE (1)	0.2	2.2	17.4	0.1	0.05	0.2	0.1	460	0.01	79.6	229	482	118	40	1	104	400
RICH GRADE ORE (1)	0.1	1.6	6.8	0.1	0.02	0.1	0.1	276	0.04	90.8	506	542	118	20	2	128	495
BLENDED ORES (2)	0.1	1.9	12.1	0.1	0.04	0.1	0.1	368	0.02	85.2	367	512	118	30	1	116	448
FURNACE WALL CLAY (2)	0.6	9.2	79.9	2.0	1.1	1.0	bdl	bdl	bdl	6.3	bdl	bdl	bdl	bdl	bdl	bdl	bdl
FUEL ASH**	bdl	0.7	2.6	3.6	12.5	46.8	bdl	bdl	1.9	1.0	bdl	bdl	bdl	bdl	bdl	bdl	bdl

Table 6.9: Bulk analyses of YW slag, ores, and fuel ash (WD-XRF) and furnace wall (SEM-EDS).
* ppm
**Fuel ash reported as elements (Charlton 2006, Table 7.5).
SEM-EDS averaging three area analyses of 1 mm by 0.8 mm per sample.
Blended ores is the average of rich and medium grade ores.
Furnace wall average of samples YW9 and YW10.

Method 2:

To calculate the yield (F) Serneels (1993, 17-19) employs a system of equations based on the aliquots of M (ore) and P (clay from the furnace lining) contributing to the average chemistry of 100 units of slag:

$$M \times 100\ units\ ore + P \times 100\ units\ lining = 100\ units\ slag + F\ units\ Fe$$

$$M \times \frac{Si}{100\ units\ ore} + P \times \frac{Si}{100\ units\ lining} = \frac{Si}{100\ units\ slag}$$

$$M \times \frac{Al}{100\ units\ ore} + P \times \frac{Al}{100\ units\ lining} = \frac{Al}{100\ units\ slag}$$

$$M \times \frac{Fe}{100\ units\ ore} + P \times \frac{Fe}{100\ units\ lining} = \frac{Fe}{100\ units\ slag} + F\ units\ Fe$$

In other words to produce 100 g of slag are needed M grams of ore and P grams of furnace lining:

$$M + P = F + 100$$

Thus, the calculation for YW would be as follows:

$$M\ x\ 6.8\% + P\ x\ 79.9\% = 20.1 \qquad (Equation\ 1)$$

$$M\ x\ 1.6\% + P\ x\ 9.2\% = 4.0 \qquad (Equation\ 2)$$

$$0.068M + 0.799P = 20.1 \qquad (Equation\ 3)$$

$$0.016M + 0.092P = 4.0 \qquad (Equation\ 4)$$

Dividing the M of equation 3 by the M in equation 4 is obtained the factor 4.2, which multiplied at both sides of Equation 4 generates Equation 5:

$$0.068/0.016 = 4.2$$

$$0.067M + 0.386P = 16.8 \qquad (Equation\ 5)$$

To isolate the variable P, Equation 5 is divided by Equation 3:

$$0.48P = 0.83$$

$$P = 1.72$$

Thus, variable M can be isolated as well:

$$0.068M + 0.799P = 20.1$$

$$0.068M = 18.7$$

$$M = 275$$

Once M and P are known, it is possible to solve for variable F calculating separately the contributions of FeO donated by the ore and furnace lining:

$$275\ x\ 90.8\ =\ 24.97$$

$$1.72\ x\ 6.3\ =\ 10.83$$

The sum of these two amounts is the total contributed by the ore and the furnace lining that taken out from the 100 units of slag created results in 65.16 FeO in slag. Total FeO in slag minus the total FeO gives 29.36 that presumably has all been turned into Fe metal, therefore the metal created in this process is 22.8 g per 100 g of slag.

$$F = 65.16 - 35.80 = 29.36$$

Method 3:

The last proposal is in fact a modification of the previous one, but applied across the full range of elements and materials involved in the smelting process (Crew 2000, 40):

$$EF = \frac{(SiO_2 + Al_2O_3)_{slag}}{(M\ \times (SiO_2 + Al_2O_3)_{ore}\ \ (P\ \times (SiO_2 + Al_2O_3)_{clay}\ (C\ \times (SiO_2 + Al_2O_3)_{ash})}$$

From which the yield of metal is calculated:

$$yield\ \% = \frac{FeO_{balance\ in\ the\ system} - FeO_{in\ slag}}{EF\ \times (Ore\ Contribution\ \times FeO_{in\ ore})}$$

The fundamentals behind the calculations still remain the same but taking into account the source of each oxide (ash, ore, clay) and possible partitioning of the different elements between slag and metal: e.g. Fe derives mainly from the ore and is removed as the metallic bloom but also as slag; metals such as Co, Ni or Cu are found in the ore and also reduced into the bloom; Si and Al derive from the ore and the furnace lining and are removed as slag; Ca and Mg are mostly a contribution of the fuel ash and

separate in the slag melt; other elements such as C, As or P are expected to leave the system as gases although can also separate into the bloom, etc. (Tylecote et al. 1977; Thomas & Young 1999; Crew 2000; Charlton 2006, 153-154; Paynter 2006).

All the analytical data are introduced in a spreadsheet, normalised to the average slag data and plotted on a log scale generating a spidergraph with a fixed line representing the mean slag and other lines representing the calculated balance per element, which is iteratively adjusted by setting the main variables M, P and C; best-fit materials balance is given when the calculated balance line is as close as possible to the mean slag line. The other materials are also represented in the graph normalised to the slag contribution. The setting of the variables is done intuitively and on this point I agree with Fillery-Travis (2015, 84) that it is 'clumsy' and it requires a good deal of personal judgement to decide which adjustment fits best; minor and trace elements are particularly difficult to balance to less than 10% relative difference, and the graph can seriously overestimate those (Charlton 2006, 153; Venunan 2015, 355). Crew (2000) attempts a mass balance based on 23 elements. In the present case only 17 are considered since some of the trace elements – e.g. Ni – were not detected in the analyses of the Daye material.

In this model, three graphs were retained after several iterations. The first and second calculations estimate the yield of metal using the medium grade ore (Figure 6.27) and the high grade ore (Figure 6.28) respectively. The main difference between them lies in the relative contribution of the different materials: in the case of the rich ore, the significant contribution (18.5%) of acid oxides from the furnace lining is crucial to the slag formation, while the medium grade ore is closer to self-fluxing and the clay contributes only 10.0% of the slag bulk. The metal yield is expressed as % bloom per ore unit, and is – as expected – larger in the case of the Fe-rich ore, with a 9% more of iron metal reduced.

The last graph (Figure 6.29) contemplates the likely possibility of using blended ores. In terms of ore and clay contribution the output of the calculation is rather similar to the best-fit materials solution smelting medium grade ore, with 2% more ore (91 to 89%) and ~2% less clay (8.1 to 10%). However, the yield increases dramatically from 8 to 24%, and is even higher than the yield obtained smelting high grade ore (17%).

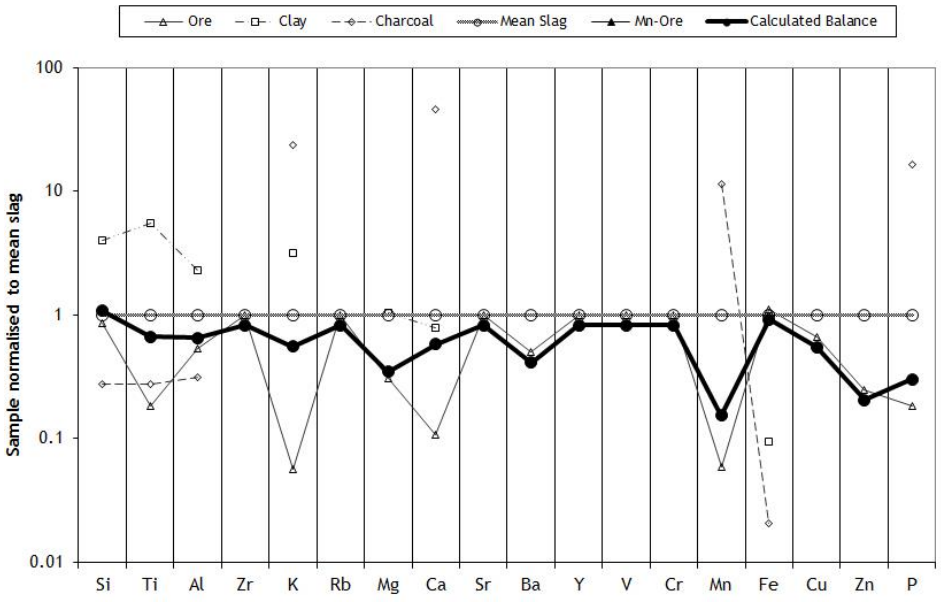

Figure 6.27: Best-fit materials balance solution for YW using the medium grade ore.
EF=0.92; 89.0% ore + 10.0% clay + 1.0% fuel ash = 8.6% iron yield.

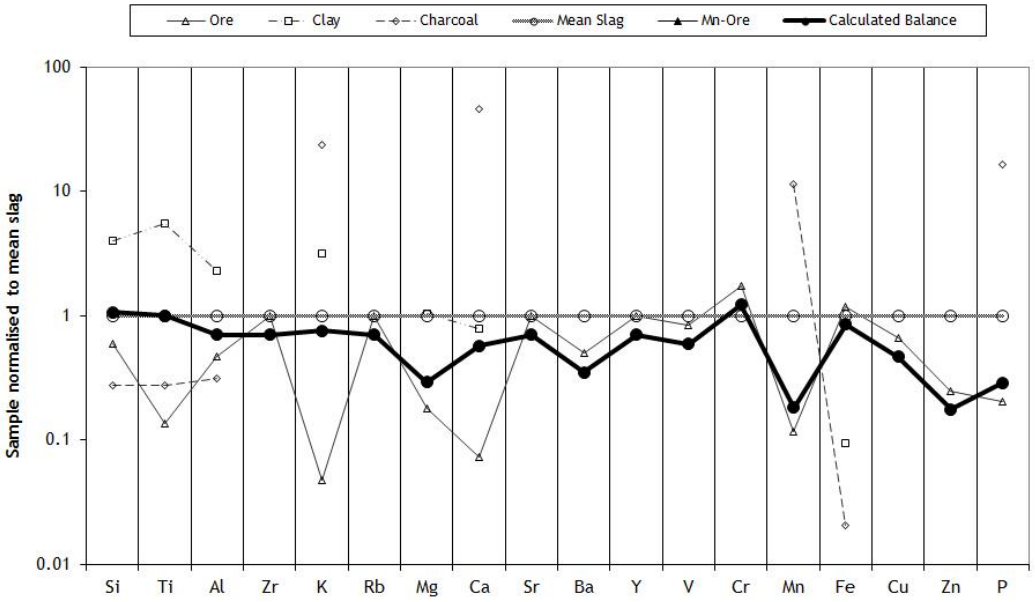

Figure 6.28: Best-fit materials balance solution for YW using the rich grade ore.
EF=0.87; 80.5% ore + 18.5% clay + 1.0% fuel ash = 17.6% iron yield.

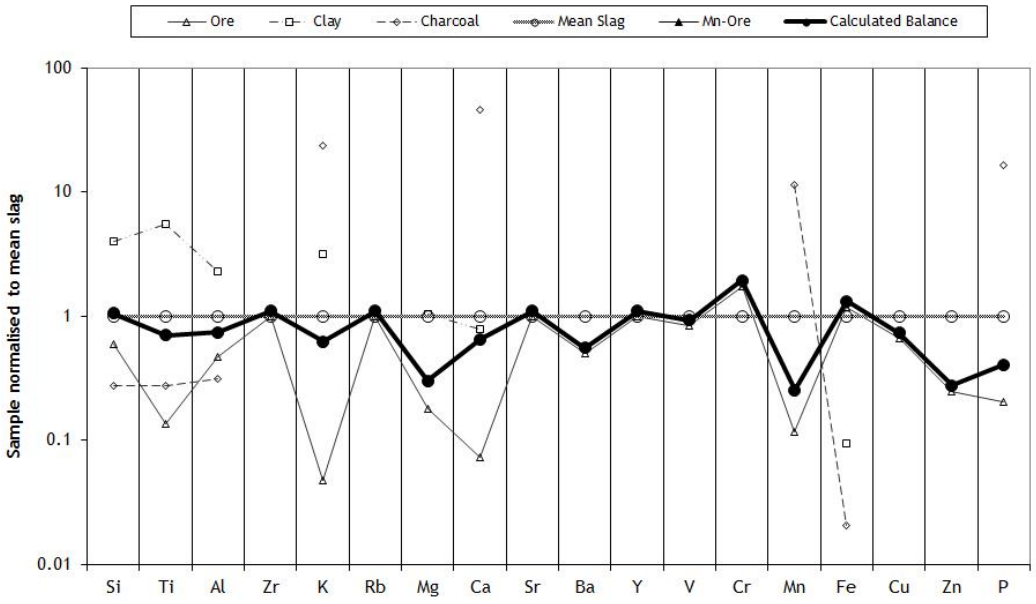

Figure 6.29: Best-fit materials balance for YW using blended ores.
EF=1.21; 91.0% ore + 8.1% clay + 0.9% fuel ash = 24.6% iron yield.

6.4.2.2 Reduction efficiency and iron yield obtained

A comparison of the three mass-balance calculation methods indicates that, the more smelt components included in the calculations, the more realistic the estimation of the yield will be (Thomas & Young 1999, 155; Crew 2000, 38; Charlton 2006, 150). However, in general terms and with the exception of the first model the differences are not so palpable and offer credible numbers (Table 6.10).

Nonetheless, it is observed as well that if data for all the components are known the estimations calculated are more sensible, and it offers more information concerning the contribution of each raw material in the process. Therefore a theoretical calculation of the iron production and yield should take into account the contribution of all the materials.

METHOD	*VARIABLES*	*METAL YIELD*
Joosten et al. 1998	Rich grade ore and slag	72% of FeO in ore
Serneels 1993	Rich grade ore, slag and clay	22.8 g Fe per 100 g of slag
Crew 2000	Medium grade ore, slag, clay and fuel ash	8.6% Fe per 89.0% ore, 10.0% clay and 1.0% fuel ash
Crew 2000	Rich grade ore, slag, clay and fuel ash	17.6% Fe per 80.5% ore, 18.5% clay and 1.0% fuel ash
Crew 2000	Blended grade ores, slag, clay and fuel ash	24.6% Fe per 91.0% ore, 8.1% clay and 0.9% fuel ash

Table 6.10: Estimation of metal yield in YW calculated by the different methods.

The hypothesis of using only rich grade or medium grade ore alone are not very realistic. First, the ancient smelter could not possibly sort and select exclusively one type or the other. Second, the contribution of the clay is considerable in all the solutions but even if the embanked furnaces excavated in LD certainly confirm that the smelter counted with the melting of the walls to create slag (section 6.4.3), a contribution of more than 18% per smelting cycle could likely cause permanent damage to the furnace structure. Such a high contribution is rather unusual in comparable archaeological materials (Table 6.11).

On the other hand, the yield certainly improves when the ore grades are blended whereas the contribution of the ceramics and fuel decreases. Thus in terms of iron reduction efficiency the use of blended ores is the best solution obtaining a better yield with a balanced use of the raw materials. However, a yield of 24% FeO – ~19% iron metal – does not seem to be particularly high, not even when compared to other pre-industrial bloomery smelting sites. Comparative data from multiple periods and bloomery iron smelting sites are given in Table 6.11. Despite of in terms of material contribution YW is within the average of the other sites – ~89% ore, ~10% clay, and ~1% fuel ash (Figure 6.30) –, the yield is significantly lower (24 to an average of 45%), and there is only one site with smaller yield number (5%) which is exceptional since it was smelting very low grade laterite ores (>50% FeO content). In conclusion, assuming that all the sites in Daye obtained a similar yield, which is likely since other parameters such as slag formation or

furnace operating conditions are shared between the sites, the reduction of the iron from the ore was not particularly successful.

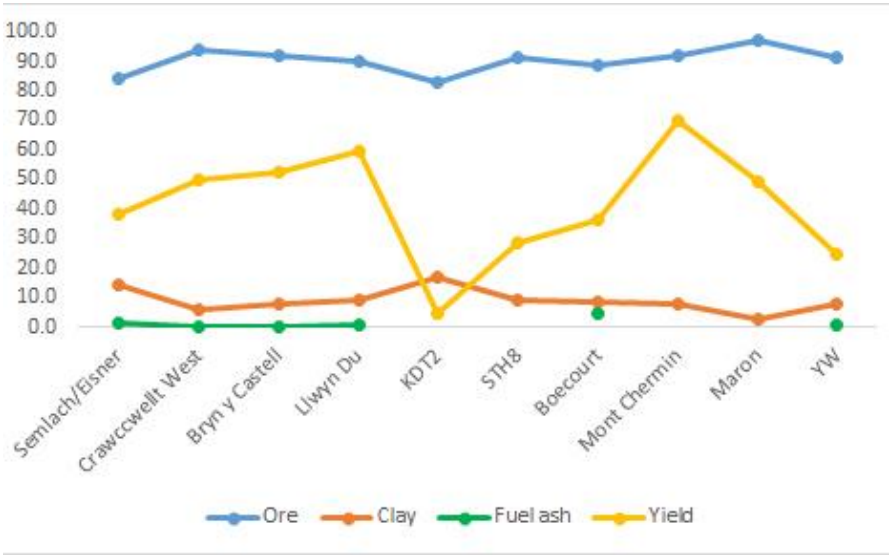

Figure 6.30: Line chart showing the average of yield and raw materials contribution of several pre-industrial smelting sites compared to YW.
References of the sites available in Table 6.11.

Site and chronology	*Calculated weight contribution (%)*			*Yield (%)*	*EF*	*Ore Grade*	*Method and reference*
	Ore	**Ceramic**	**Fuel ash**				
Crawcwellt West (UK), Iron Age	93.5	6.0	0.5	43.8	1.65	Medium	Crew 2000 Charlton 2006, Figures 7.12-7.15
	94.6	5.0	0.4	50.8	1.82	Medium	
	93.5	6.0	0.5	54.7	1.92	Medium	
Bryn y Castell (UK), Late Iron Age to Roman	92.7	7.0	0.3	47.3	2.93	Medium	Crew 2000 Charlton 2006, Figures 8.13-8.14
	90.8	9.0	0.2	57.7	1.94	Medium	
Semlach/Eisner (Austria), AD 100-400	80	18.1	1.9	41	1.40	High-Medium	Thomas and Young 1999* Fillery-Travis 2015, Table 6-18
	84	15.5	0.5	39	1.39	High-Medium	
	87	12.2	0.8	55	1.68	High-Medium	
	84	13.7	2.3	13	1.10	High-Medium	
	84	14	2.0	16	1.12	High-Medium	
	84	15.1	0.9	52	1.60	High-Medium	
	85	13.2	1.8	53	1.64	High-Medium	
KDT2 (Thailand), AD 200-500	83.1	16.9		5.0	1.01	Low	Crew 2000 Venunan 2015, Figure 8.88
STH8 (Thailand), AD 200-500	99.0	1.0		9.0	1.05	Low	Crew 2000 Venunan 2015, Figures 8.90-92

STH8 (Thailand), AD 200-500	91.5	8.5		36.0	1.37	Blended ores	Crew 2000 Venunan 2015, Figures 8.90-92
	82.5	17.5		41.0	1.49	Blended ores	
Boecourt (France), AD 400-700	91.0	9.0		36.5	1.32	Low	Crew 2000, Table 3
	86.5	8.5	5.0	36.7	1.39	Low	
Mont Chemin (France), AD 400-700	92.0	8.0		70.0	2.45	High-medium	
Maron (France), unknown	97.3	2.7		49.5	1.43	Medium	
Llwyn Du (UK), AD 1300-1400	92.2	7.0	0.8	61.8	1.96	Low	Crew 2000 Charlton 2006, Figures 9.8-9.14
	86.7	12	1.3	56.8	1.74	Low	
	92.2	7.0	0.8	67.7	2.12	Low	
	92.4	7.0	0.6	72.1	2.37	Low	
	89.6	10.0	0.4	43.0	1.53	Low	
	89.6	10	0.4	71.1	2.25	Low	
	88.4	11	0.6	42.9	1.53	Low	
Yanwopu (China), AD 1650-1800	80.5	18.5	1.0	17.6	0.87	High	Crew 2000
	89.0	10.0	1.0	8.6	0.92	Medium	
	91.0	8.1	0.9	24.6	1.21	Blended	

Table 6.11: Comparative yield and raw material contribution between diverse chronologies bloomery smelting sites and Yanwopu.
*Thomas and Young method is similar to Crew 2000, uses the same general equation but calculates differently the EF, the output is called 'efficiency' not yield and refers to the weight of iron in bloom/weight of iron in reduced anhydrous ore. Efficiency % given without decimal numbers in the original.
High, medium and low grade ores correspond to ≥80%, 60-80% and <60% FeO content, respectively.

6.4.3 Contribution of the furnace lining

In general, the furnace walls of Daye County seem not to have been made of a particularly refractory material attending to their chemical composition: even accepting that most ancient technical ceramics do not merit the qualification of refractories by modern standards (Freestone 1986; Craddock 2013), and their performance was optimised by tempering and shaping rather than by selecting special clays (Martinón-Torres & Rehren 2014, 108). Specifically, alumina levels seem to be rather low in comparison with other furnaces published in China where the alumina content frequently ranges between 20-30% (Liu, Haifeng et al. 2014b)., and in general ancient pyrotechnological ceramics contain no less than 15 % (Freestone 1986; Freestone & Tite 1989). In contrast, the Daye samples present levels around 10 % in most of the iron smelting ceramics.

However, a comparison between the Daye furnace clays and other archaeological sites technical ceramics shows that the composition of the Daye clays match in general with the composition of other ancient smelting materials, and that certainly most of the smelting ceramics do not merit the qualification of refractory in comparison with both ancient and modern refractory materials (Figure 6.31). Nonetheless, acknowledged this limitation, Figure 6.31 also shows that some of the technical ceramics were more capable to endure a better resistance to high temperatures and were fabricated with clays regarded as suitable for ancient smelting furnaces as in those Semlach/Eisner (Fillery-Travis 2015, 297) and Laikipia (Iles & Martinon-Torres 2009, 2318), and that the copper furnace fabric is plotted in the same region. Note the difference between the technical ceramics of the furnaces of Tonglüshan and the copper sites in Daye: the Tonglüshan fabrics are much more refractory.

As discussed in the previous chapter (section 5.2), the analysis of copper smelting slag does not show a substantial ceramic contribution that one would expect if the furnace wall was heavily degraded during use. The bloomery iron furnaces, on the other hand, compositionally appear more prone to melt into the slag as a result of two factors: low alumina content, and mineral inclusions such as iron oxides that can flux the ceramic body – possibly ore tailings used as temper; the use of ferruginous rocks as temper in technical

ceramics has been reported before (Craddock et al. 2007, 7). Figure 6.31 also shows the copper-related ceramics clustering together more tightly irrespective of their vitrification state (with one exception), whereas iron-related ceramics are slightly more spread, especially because the more thermally altered ones are richer in iron and alkali oxides. The iron ceramic fabric thus seems generally less robust to withstand high temperatures than the copper furnaces.

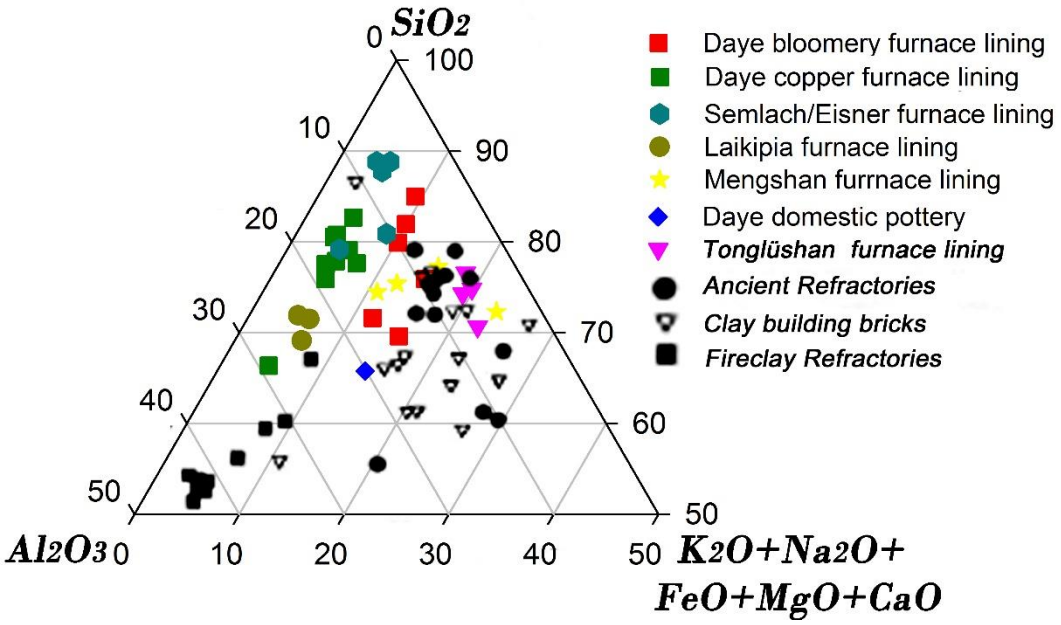

Figure 6.31: Bulk composition of Daye technical ceramics compared to ancient smelting and modern refractories.
Semlach/Eisner (Austria) Roman (1st-4th C. AD) bloomery smelting furnace lining (Fillery-Travis 2015, Table 6.9, samples 173, 175 176 ,194, 179): **Laikipia** (Kenya), bloomery smelting furnace lining dated to the 2nd half of 2nd millennium AD (Iles & Martinon-Torres 2009, Table 1); **Mengshan** (China), Song-Yuan Dynasties lead-silver smelting site (Liu, S. 2015, Table 5.11); **Tonglüshan** copper smelting furnace lining (Wagner 1986, Table 3). **Ancient refractories**, clay building bricks and fireclay refractories from Freestone and Tite (1989, Fig. 21).

This impression is coherent with the suggestion that each of the furnace structures in LD was only used for a short period of time before it needed repairs and relinings (Hu et al. 2013, 294) as is evident in the archaeological remains, with an extreme case of 17 consecutive layers of relining preserved in a furnace (Figure 6.32). It is also obvious that new furnaces were built reutilising parts of the old structures, frequently sharing walls or

even adapting the furnace hearth of a damaged structure into the bellows working platform of a new structure, as in LD furnace number 12 (Figure 6.18).

Figure 6.32: Furnace number 20 showing multiple lining.
Picture courtesy of Professor Chen Shuxiang.

In sum, the ceramic fabric employed in the fabrication of the bloomery iron furnaces was not particularly refractory or strong, and this made it necessary for smelters to continuously refurbish them and even build new facilities. However, this limitation was not catastrophic: for example, none of the excavated structures of LD appeared collapsed to the extent of choking the furnace, and the smelters persisted in the same constructive solution.

The use of less refractory materials for lining is not necessarily interpreted as a failure of the process but rather as a deliberate practice that was understood as essential to allow the slag formation with non-self-fluxing rich ores (Pleiner 2000, 258). Indeed, the type of embanked furnaces used at LD and (possibly) at HF are very suitable for this practice since clay-built shaft furnaces are easy to repair compared to other types of furnaces such as the bowl or sunken-floored furnaces that require replacement better than repairs and are less suitable to be operated on a permanent base (Pleiner 2000, 57-77). To further investigate the ceramic contribution from the furnace walls suggested by the mass balance calculation and by the archaeological features, the composition of technical ceramics, slag and ore was plotted in the ternary diagram Al_2O_3-SiO_2-FeO (Figure 6.33).

The figure shows a relative straight line between ore, which is the richest in iron oxides, and technical ceramics, which are the richest in silica, while the slag plots in between but much closer to the ore. These are the three main elements in all materials typically summing up 90-95% of the composition in a close system where no other material (e.g. silica rich flux) was added attending to the slag microstructural analyses. The estimated contribution of the fuel ash is minimal (~1%) and in any case this does not have any impact in the three major elements. Figure 6.32 shows that even in the case of smelting medium grade ores richer in silica the contribution of the furnace wall was essential, otherwise slag would hardly be generated. The significant role played by the technical ceramics in the slag creation has been pointed before in some archaeological and ethnographic studies. One of the clearest cases is found in the Mafa furnaces of Cameroon in use in the last half of the 20th century (David et al. 1989). Here the smelters build up huge tuyeres weighting ~20 kg and with a much thicker lower part that was consumed during the act of the smelt as it acted as the flux for the forming slag. In a more recent paper it was observed that this practice is not exclusive to the Mafa smelters but that is quite usual and extended throughout the Mandara Mountains as a key technological feature for iron smelting (David 2014). Similar substantial contribution from the furnace wall ceramics to the calculated in YW has been suggested for the Early Iron Age furnaces of Tell Hammeh (Jordan) estimating that ~19 kg of ceramics per 100 kg of ore would be necessary to obtain a low melting slag since there were no evidences of any other flux (Veldhuijzen & Rehren 2007, 194). Lastly, the use of locally available unrefined clays without refractory properties for the technical ceramics has been reported as well for the 1st millennium BC smelting furnaces of West Africa, in which the deliberate addition of clay either as a flux or a significant contribution from the refractories was essential to imbalance the very high grade ore with few gangue in the slag formation (Craddock et al. 2007).

Overall, notwithstanding the macroscopic and compositional similarities between the copper- and iron-related technical ceramics, there are several features that differentiate them, deriving from both different paste preparation and the actual furnace operation parameters. On the one hand, slight differences in chemical composition showing variations in Si and Al derived from clay selection and preparation – e.g. the tempering with iron oxides, perhaps tailings used as temper, in addition to quartz in the case of the

bloomery iron technical ceramics. On the other hand, differences in the microstructure with the occasional presence of wüstite globules and metallic iron in the iron furnaces, compared to magnetite crystals and copper prills in the copper furnaces. These two features not only allow the differentiation of technical ceramics associated to each process, but also point to dissimilar conditions in the charge and furnace operation, with lower oxygen pressure in the bloomery iron technical ceramics (Figure 5.34).

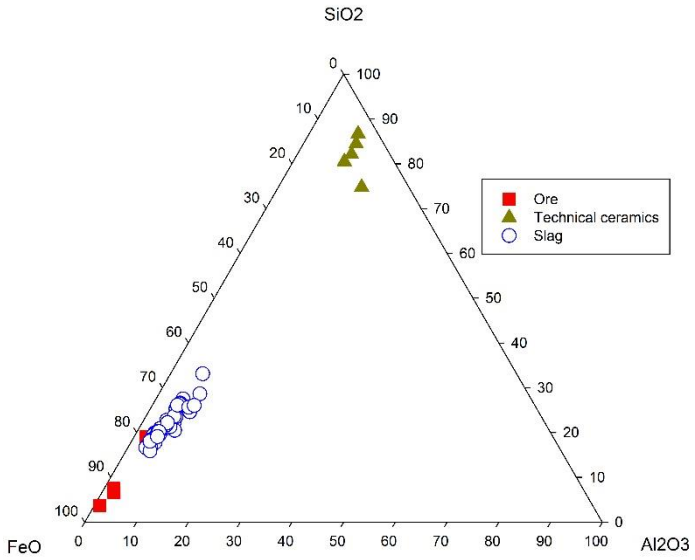

Figure 6.33: Ternary system $FeO–Al_2O_3–SiO_2$ comparing the bulk composition of ores, slag (WD-XRF) and technical ceramics (SEM-EDS) related to bloomery iron production in Daye.

6.4.4 Reduction or post-reduction slag

The term post-reduction slag was proposed by Serneels (1993) to refer to all debris generated after the primary smelting of iron reduced by the direct method, including also activities such as welding or carburisation. In general, post-reduction activities are referred as smithing but this term is understood differently and can be equivocal since many authors understand smithing as the complete process bloom–billet/bar–artefact

and simply label the different stages as *bloom smithing, bar smithing*, etc. (e.g. Crew 1991); others distinguish sharply between *primary* and *secondary* smithing with regard to the refining of the bloom or to the manufacture and repair of artefacts (e.g. McDonnell 1991); while for others smithing concerns the second operation only and use alternative terms such as *reheating* (Pleiner 2000, 215) or *purification* (Buchwald 2005, 88) for the removing of slag from the bloom.

The most diagnostic slag generated during the post-reduction are the so-called smithing hearth bottoms (SHB) – also known as calottes – (Dunster & Dungworth 2012, 1). SHB are typically plano-convex cakes formed after the accumulation and melting of various materials at the base of the hearth – although it need not form at the actual base of the hearth – frequently shaping bulky cakes often with charcoal or charcoal impressions, heterogeneous textures in the microstructure, and iron-rich bulk composition (Figure 6.34). However, their morphology, composition and mineralogy can vary considerably, e.g. occurring as flat cakes or presenting glassy composition (McDonnell 1991; Serneels & Perret 2003; Pleiner 2006, 112-122; Selskienè 2007; Dungworth 2008).

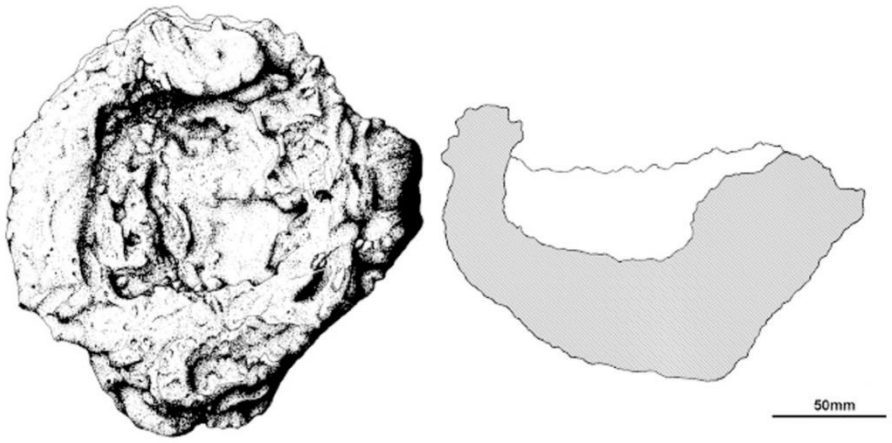

Figure 6.34: Plan and cross-section of a medieval smithing hearth bottom.
After Dunster and Dungworth (2012, Fig. 1)

Nonetheless, very frequently post-reduction slag does not present sufficient characteristics to be categorised and occurs as undiagnostic amorphous lumps of slag less easily recognisable. Slag resulting from the purification of a bloom and non-tapped smelting slag can be quite similar in all aspects – morphology, chemical composition and

microstructure – and discerning one type from the other is not straightforward (McDonnell 1983; Serneels & Perret 2003; Selskienè 2007; Dunster & Dungworth 2012), and even considered 'exceedingly difficult' (Pleiner 2000, 266). These undiagnostic slags are usually referred as smithing slag lumps (SSL), and correspond to materials that failed to incorporate into the SHB. They maintain irregular shapes with occasional smooth upper cooling surfaces and contorted lower surfaces characteristics of cooling in a bed of charcoal, but can also present very different textures simultaneously – rusty tarnish, ceramic materials attached, heavy vitrification, grey ash colours, presence/absence of impressions of charcoal or soil, etc. (McDonnell 1991; Dieudonné-Glad & Conte 2011; Dunster & Dungworth 2012). Most of the lumpy slag of Daye (the five specimens from HF and the two from MC) fit into this category.

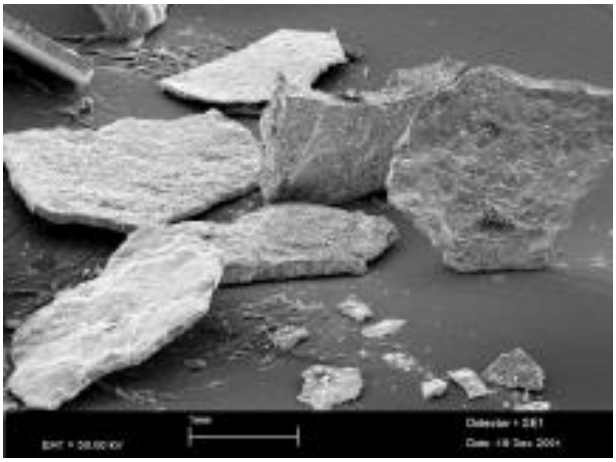

Figure 6.35: SEM micrograph showing flake hammerscale.
After Dungworth and Wilkes (2007, Fig. 1).

Other type of slag characteristic of post-reduction activities is the hammerscale. Flake hammerscale is formed during hammering and consists of the oxidised crust in contact with the air of the hot metal that by contact with the hammer is broken into tiny (1-3 mm) plate or droplet shape particles which are strongly magnetic (Allen, J. R. 1986; Dungworth & Wilkes 2007; Young, T. 2011, 2012) (Figure 6.35). Hammerscale was not detected in Daye but this cannot be taken as evidence of absence, since the sampling strategy employed would not have allowed their recovery since this is a very fine metallurgical debris that is unlikely to recover from surface unless a magnet is used (Bayley et al. 2001).

The excavated site of Lidegui (LD) did not report hammerscale either (Wei et al. 2008; Hu et al. 2013).

6.4.4.1 Furnace bottoms or smithing hearth bottoms

Three specimens from HF (HF20-21-22) are amorphous and porous lumps with much embedded charcoal on their surface whereas HF23 and HF24 present grey colour surface and no charcoal (Figure 6.3). Microscopically they consist of heterogeneous phases of well molten slag usually containing blocky olivines and predominant stubby pseudo-dendritic wüstite but also lath olivines with scant fine dendritic wüstite, as well as abundant corroded phases rich in iron and occasional large iron metal particles; unreacted materials are rare and correspond to patches of clay seemingly eroded from the furnace wall (Figure 6.9 and Figure 6.10). This description and their shape as irregular chunks of lumpy slag with charcoal impressions overall fit well into the characterisation of smelting slag that can be expected at the bottom of a furnace or attached to a furnace wall (Figure 6.37) (Tylecote 1986, 310; Gordon 1997, 13; Pleiner 2000, 262-263; 2006, 119). However, in none of them were identified unreduced or semi-reduced ore grains, which could be seen as more conclusively diagnostics of these by-products.

Their microstructure is consistent with that of furnace slags as described, for example, by Severin et al. (2011) consisting of composite textures of very variable fayalite grains, occasional wüstite globules, and large particles of metallic iron surrounded by abundant corrosion products. In addition, HF slags lack unfused pieces of rock, or sand that are common in smithing slag, and instead present occasional argillaceous materials embedded in the matrix which are more consistent with eroded furnace ceramics not to a deliberate addition; these also lack hammerscale inclusions but contain instead large clusters of reduced metallic iron surrounded by iron corrosion products; finally, the samples are not magnetic with the exception of HF24. The last three features – sand, hammerscale, magnetism –, considered distinctive of smithing slag, are absent here (Unglik 1991).

However, post-reduction slags frequently share identical characteristics to those just described: heterogeneous vesicular cross-section and a microstructure very rich in free

iron oxides similar to hammerscale that also contain crystalline areas free of those, and the hammerscale may present a variety of textures different from the indicative thick layers of wüstite such as subhedral angular pseudo-dendritic structures that can show very close convergence to those preserved in furnace slag (Crew 1991; McDonnell 1991; Buchwald 2005, 99; Paynter 2007; Young, T. 2011; Eliyahu-Behar et al. 2013; Blakelock et al. 2014).

At this stage, the external shape can be taken as a very reliable identification mark (Pleiner 2000, 255). The typical SHB formed during primary or secondary smithing are elliptic dish-shaped cakes ranging 10-16 cm in diameter and 100-1500 g in weight; the top side often displays glazed parts, ridges and sometimes a characteristics depression caused by the blast of air whereas the lower part shows agglomerated textures of slag cooled in a bed of charcoal (McDonnell 1991; Serneels & Perret 2003; Buchwald 2005). Specimen LD11 fits very well into all the parameters of the previous description and can confidently been classified as a SHB (Figure 6.36).

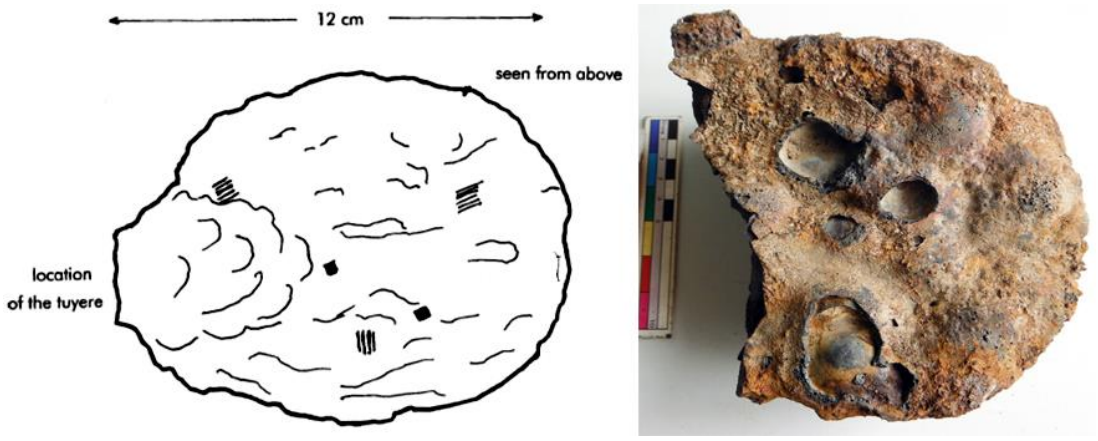

Figure 6.36: Top view of a calotte slag type and top view of specimen LD11.
After Buchwald (2005, Fig. 91).Scale is 10 cm in LD11 picture.

Unfortunately, the shape is only diagnostic in specimen LD11. As mentioned, the plano-convex morphology visible in some of these slag cakes (Figure 6.3) is a recurrent shape within bloomery iron slag assemblages, even where tapping was the predominant method of slag removal. These cakes of slag solidified within the furnace during smelting are known as furnace bottoms and can display large masses (8-13 kg) and dimensions (32-36

cm) (Paynter 2007), although smaller masses (1-3 kg) have also been reported (Dungworth 2008; Iles & Martinon-Torres 2009). With the exception of the non-sampled complete specimen of LD (Figure 6.2) the lumpy slag analysed in this study does not correspond to this morphology. However, even if not shaped as cakes, irregular chunks of lumpy slag with charcoal impressions can be expected at the bottom of a furnace or attached to a furnace wall (Tylecote 1987, 152) (Figure 6.37), but again similar morphologies can be expected in partially preserved SHB and undiagnostic smithing lumps (McDonnell 1991; Serneels & Perret 2003).

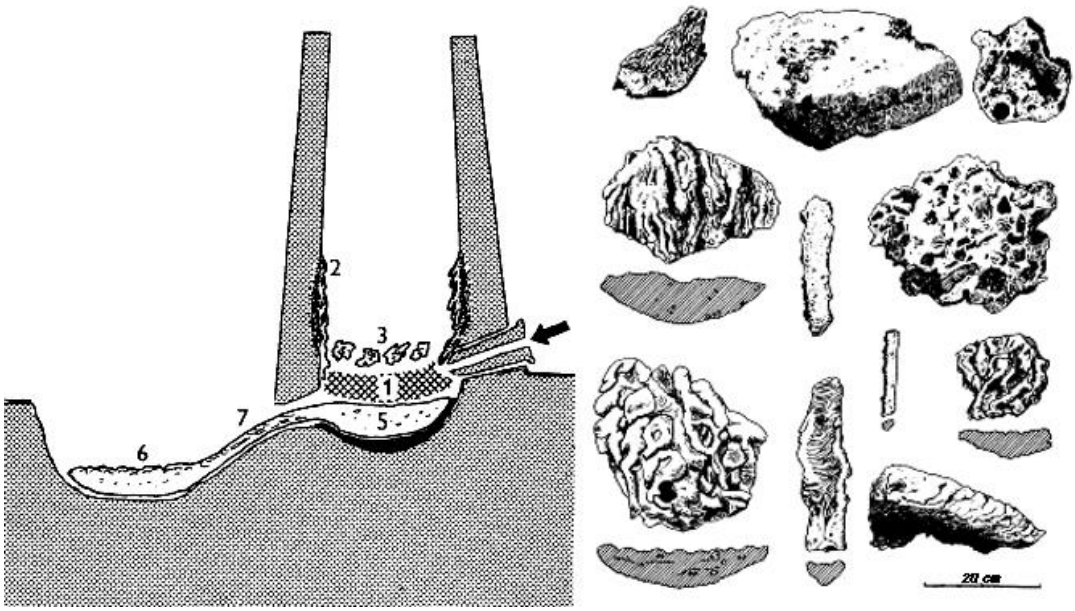

Figure 6.37: Schematic representation of slag formation in a low bloomery furnace and archaeological examples of furnace bottoms and slag found inside the furnace.
1. iron sponge penetrated with slag; **2.** slagged wall or refractory lining; **3.** residual furnace slag with embedded charcoal and unreduced ore pieces; **5.** `furnace bottom' remaining in the hearth of a tapping furnace. **6.** tapped slag cakes in the forepit pool; **7.** last slag flow in the outlet channel, solidified rods (preserved mostly as fragments).
Right figure shows examples of the named slag types generated inside and outside the furnace; scale is 20 cm. After Pleiner (2000, Figures 67 and 71).

On the other hand, specimens HF23 and HF24 consist of plano-convex cakes presenting smooth surfaces generally without charcoal impressions; and the samples from MC are amorphous cakes with contorted lower surfaces characteristic of cooling in a bed of charcoal (Figure 6.3) In general, these two specimens fit well in the category of SGD "scorie grise dense" (dense grey slag) which is one type of SHB of fayalitic composition with a

variable amount of iron oxide very similar to the bloomery smelting slag (Serneels & Perret 2003). However, these characteristics are not sufficient to categorise these fragments as post-reduction slag.

Several authors (e.g. McDonnell 1986) have noticed that variations in the chemical composition of slag can be helpful to discern between smelting and smithing slags. Therefore, the following section consider major, minor and trace elements of the bulk composition as a criteria to discriminate between the slags generated after the different processes.

6.4.4.2 Bulk chemical analyses to distinguish smelting from smithing slags

In general, bloomery iron slags generally share not only a very similar microstructure but also an elemental and mineral composition, and in almost all respects the elements present and their concentrations are within the same range (Dunster & Dungworth 2012), as in fact is the case in Daye (Figure 6.38). The comparison between major and minor elements of the bulk composition shows that these are indeed within the same range, with nearly identical median and distribution. It is observed, however, that the tap slag shows less compositional variation when compared to the lumpy slags. This may well be explained by the process itself: the slag to be fluid and runny to be tapped out it has to have a certain composition, and therefore it is a process-driven phenomenon (Maldonado & Rehren 2009).

However, some slag assemblages have reported variations of certain elements in the composition of smelting and smithing slags, and suggest their use as an indicator to distinguish between both types of slag. Thus, early ironworking British slag can be frequently distinguished from primary smelting slag based on the levels of MnO, which is very low in the former but typically higher (~0.3%) in the latter (McDonnell 1986, 199-208). It was observed that the smithing slags for the Old Iron Age in Lithuania not only contain lower concentrations of MnO but also of P_2O_5 as compared to the smelting slags (Selskienè 2007, 24). This difference was also acknowledged by Buchwald (2005, 137) who also noticed that the smithing slags 'absorb more CaO and K_2O from ashes' (2005, 152).

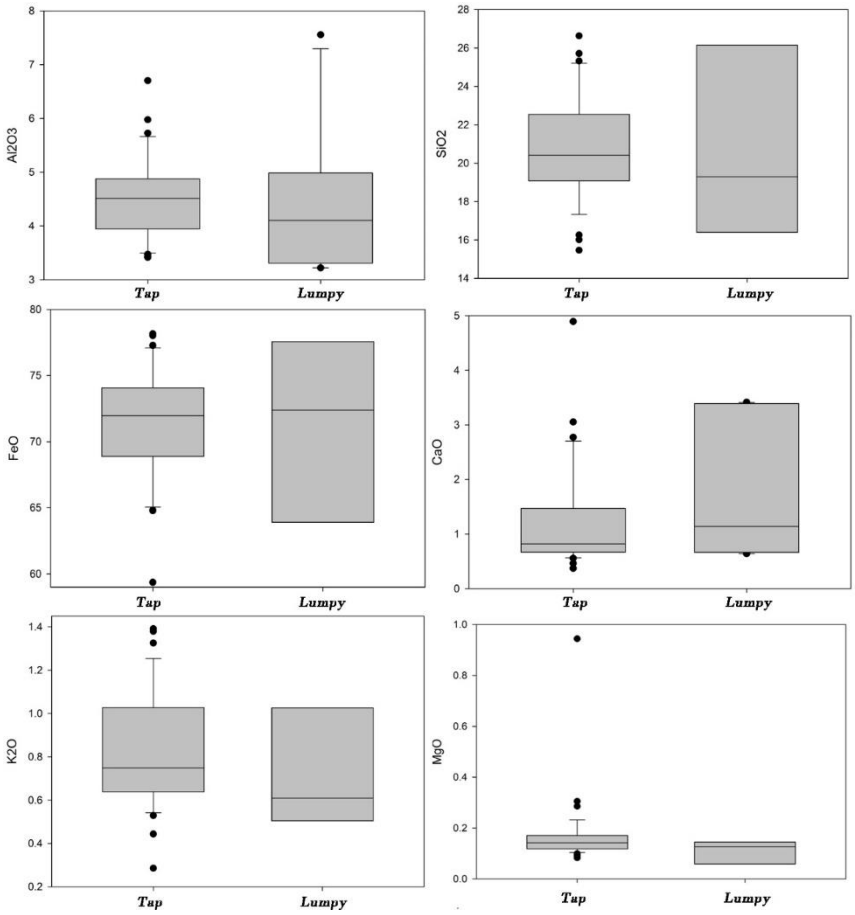

Figure 6.38: Box, median and whiskers comparing the tap and lumpy bulk composition (WD-XRF).

Table 6.12 compares these four oxides between the average of the tap and the lumpy slag of each site. However, the results are not conclusive for none of the four oxides used as indicator in the other assemblages, and frequently would appear to suggest the opposite of the expectation. Thus MnO, which is supposed to be higher in the smelting slag presents mostly identical levels in smelting and smithing slags ranging 0.16 to 0.13%, with only one case of non-tapped slag that is significantly lower in comparison (0.04 to 0.16%), and another case that is actually higher (0.18 to 0.16%). P_2O_5, which is also supposed to be lower in the smithing slag is always higher in the non-tapped slag than the average of the tap slag (0.27 to 0.35%), including some cases than practically contain double the amount. Finally, K_2O and CaO – noticed to increase within the smithing slag – present lower levels to the average of the tap slag in approximately half of the lumpy assemblage, and these two oxides are not correlated. Overall, the use of these oxides to discriminate

within the different productions is not meaningful when applied to the Daye bloomery slag.

	P_2O_5	K_2O	CaO	MnO
Mean bloomery tap slag	0.27	0.81	1.32	0.16
Mean bloomery lumpy slag	0.35	0.87	1.90	0.13

Table 6.12: Comparison between average P_2O_5, K_2O, CaO and MnO (WD-XRF) levels between the different types of bloomery slag.

Since major and minor elements of the bulk composition do not establish a distinction, a comparison was attempted between relevant trace elements present in both the ore and the slag. The assumption is that most lithophile trace elements get into by-products of iron metallurgy from the ore, and thus the generated by product is expected to retain more trace elements from the original ore the closer it is to the former in the chaîne opératoire (Tylecote et al. 1977; Dillmann & L´Héritier 2007; Navasaitis et al. 2010):

Ore ⇨ Primary smelting slag ⇨ Bloom ⇨ Post-reduction slag ⇨ End object

Trace elements found in slag inclusions in bloomery iron artefacts have been frequently used to provide data regarding the provenance of the iron artefacts (e.g. Hedges & Salter 1979; Buchwald & Wivel 1998). Whereas provenancing through the trace elements 'mostly failed to be conclusive', some researches have certainly concluded that the composition of slag inclusions most closely relates to the smelting slag produced (Blakelock et al. 2009, 1745). Therefore, the smelting slag – with an estimated ore contribution ranging 77-91% – should be closer in the composition of trace elements to the ore than the post-reduction slag, which is not formed from the ore but from the oxidation of the iron metal, with contributions of the smelting slag, and the melted clays from the wall of the hearth and/or the possible fluxes added (Serneels & Perret 2003).

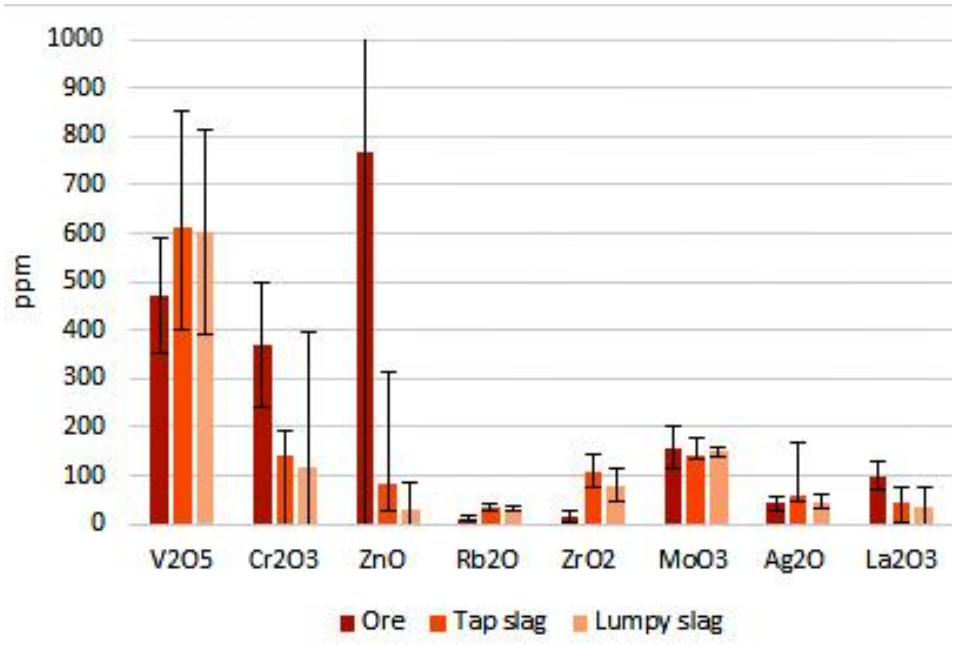

Figure 6.39: Bar with standard deviation error bars showing the average ppm content of relevant trace elements present in the ore, tap and lumpy slag.

Figure 6.39 compares selected trace elements – V, Cr, Zn, Rb, Zr, Mo, Ag, and La –analysed by WD-XRF recurrently present in the iron-rich samples of the ore, in the lumpy slag and in the tap slag (Appendices IV-V); the discarded elements were not present in 90% of the assemblage per material type. The figure is inconclusive and does not show but rarely the expected gradual decrease from the ore to the lumpy slag, with the tap slag marking an intermediate position, and when it does the relative standard variation of each element per assemblage is very high and frequently overlaps. Other important trace elements in bloomery iron such as Cu, Ni and As also failed to be an indicator in the Daye slag (Navasaitis et al. 2010), likely these were reduced into the iron rather than going into the slag.

6.4.4.3 Lumpy slag as smithing slags lumps

Summing up, excepting LD11 with a SHB diagnostic shape, the rest of the lumpy slag assemblage presents undiagnostic features. Their morphology and microstructure clearly rule these out as tap slag, however, these parameters do not allow a positive identification

as furnace or post-reduction slag, and simultaneously present signals characteristic to both waste-products.

Some of the samples fit better in the definition of smithing slag than others: LD11 shape is characteristic, HF24 is magnetic and more brittle, or the largest deviation in chemical composition of MC12 and MC18 to the general composition of tap and lumpy slag (Table 6.2, Table 6.4).

The other specimens, HF20-21-22-23, that are bulky and have charcoal embedded still can have a second possible interpretation as remnants of mixed slag and reduced iron that litter the furnace after a smelt, the so-called '*gromp'* (Sauder & Williams 2002, 124); relevant comparative material is provided by the unconsolidated by-products obtained after two unsuccessful experimental smelts in Poland (Karbowniczek et al. 2006). On both occasions they failed to produce a bloom but instead obtained large masses of a conglomerate of iron and slag phases attached to the shaft walls, which in one case even blocked the taphole. The reduced iron in these masses was strongly contaminated by non-metallic phases, whereas the slag was rather inhomogeneous in terms of microstructure, containing dispersed dendrites and iron particles on a fayalitic matrix (Karbowniczek et al. 2006, 48). Therefore, it is also possible that these are the result of an unsuccessful smelt or bloom fragments, and much of the corrosion/rust could be former bloomery iron that failed to agglomerate properly.

Lastly, in agreement with the identification of LD11 as a calotte, in LD were found two bars of iron (Hu et al. 2013, 295), which is significant since an iron billet or bar is the common kind of useful products obtained by primary smithing, generating the SHB as well (Buchwald 2005, 99). Tentatively, since neither a large stock of iron nor partially complete iron objects were found, and most of all LD is eminently a primary smelting facility as indicate the 23 embanked furnaces and the predominance of smelting over smithing slag, it can be suggested that LD operated as smelting centre that also performed primary smithing activities, consolidating the bloom and transforming this into a bar, but that no objects were manufactured there.

6.5 Summary

In spite of the range of sites, different slag morphology and variations in bulk composition and microstructure, all the Daye ferrous slag is seemingly related to the bloomery production process, and framed within the AD 1650-1800, but most likely within the 18th century according to the radiocarbon dates available.

The reduction of a rich-grade iron oxide ore – haematite – took place in embanked furnaces built of clay operating under reducing conditions with temperatures typically ranging 1100-1200 °C, although higher temperatures were attained occasionally. The contribution of the furnace lining was essential to create a fayalitic molten slag that was tapped out of the furnace, whereas solid iron metal coalesced into a bloom within it. In general, the slag retains an excess of free iron oxides as wüstite globules and the yield of metallic iron is estimated to be modest. The metal produced consisted of ferritic iron and occasional low carbon steel although two isolated by-products indicate that products richer in carbon could be generated as well. In addition, there is evidence of post-reduction activities – likely limited to primary smithing – at three of the sites: LD, HF and MC.

Even more clearly than in the case of the copper smelting by-products, although minor between-site variations can be noted in some cases, overall all the analysed remains are remarkably homogeneous in spite of coming from different sites, which is suggestive of a shared technological tradition.

He led the prosecutor to see the pair of golden hanging bells. They were of matchless workmanship, having made by the most skilful craftsmen in the imperial palace. Only the special craftsmen of the imperial court could have created them.

(Outlaws of the Marsh, 水浒传)

7 Technological traditions, cultural spheres and copper metal smelters on the Yangtze southern margin

The technical analyses reported in chapters 5 and 6 allowed the characterisation of two different production technologies of base metals: copper and bloomery iron. In order to facilitate the rest of the discussion, the first point will be to further examine the copper and bloomery iron technical materials from a comparative perspective. This point is necessary given that the archaeological remains in most of the sites were believed to be the result of copper smelting processes when in fact half of them correspond to bloomery iron production, which, as pointed in chapters 1 and 2, is a rather uncommon production in China. Furthermore, several of these sites present evidence of both types of production, and since all of the analysed assemblage was recovered from surface, it is essential to establish beyond any doubt that the debris is the result of two different processes obtained – as discussed below – by separate methods and chronologies.

This chapter presents more detailed discussion of the copper extractive activities, including a chronological framework as well as in-depth investigations of technical aspects of copper extractive metallurgy that were only highlighted previously; in particular, the variations together with similarities of the archaeometric results are addressed in an attempt to establish discernible patterns at inter-site levels. As the chapter unfolds, the focus will be placed on the adaptation of the technological process in operation in Daye with regards to the management of the available natural resources; the efficiency of copper extraction; and the quality of the smelted metal. Finally, in an attempt to infer aspects of the socio-cultural and political contexts within which the metallurgists operated, a hypothetical model of production is proposed, based on the reconstructed *chaîne opératoire* and the technical parameters. Analysed from a broader perspective that considers copper as the main ingredient of bronze production, the chapter explores the

role of political authorities in the primary production of copper, approaches the social status of the smelters, and challenges long-established historical and archaeological models of the political organisation and the prestigious status of metalworkers in pre-Imperial China.

In spite of this study being only a preliminary stage in constructing such technological histories and despite the scope being necessarily crude, these are important first steps which suggest that regardless of the enormous economic, political and ritual importance of bronze metal in Chinese society, the primary smelting of copper was regarded as an inferior activity with respect to bronze making.

7.1 Technological comparison of copper and iron metallurgies

The distinction between pre-industrial copper and iron slag is not necessarily straightforward since – as seen in chapters 5 and 6 – regardless of the metal smelted both processes frequently create the same type of tap slag debris which forms under the same frame of temperatures, and which have similar iron-silicate fayalitic compositions (Bachmann 1982; Tylecote 1992; Craddock 1995; Pleiner 2000; Hauptmann 2007, 109; Rehren et al. 2007) (Figure 7.1).

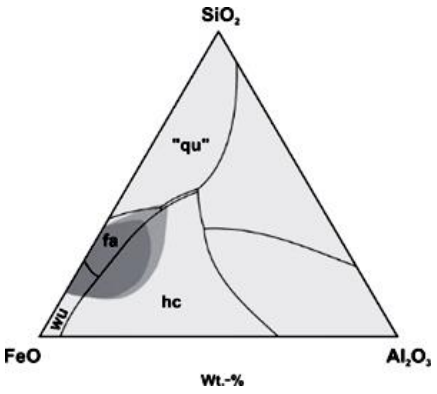

Figure 7.1: Typical composition of ancient slag from copper smelting (medium shaded area) and iron smelting (dark shaded area) shown in the ternary system $FeO–Al_2O_3–SiO_2$.
hc hercynite, *fa* fayalite, *"qu*" quartz, *wu* wüstite. After Hauptmann 2007, Fig. 2.2.

In order to differentiate between them, the most diagnostic criteria are some mineralogical and chemical indicators – mineralogy of free iron oxides, nature of metallic droplets, and copper content in slag – already introduced during the discussion of the previous chapters and summarised in Table 7.1.

	Free iron oxides in microstructure		*Metallic particles in microstructure*		*Cu in slag*
	Magnetite	**Wüstite**	**Copper**	**Iron**	
Copper slag	Frequent, present in all 59 specimens	Very scarce, present in 4 specimens	Present in all 59 specimens	Absent in all 59 specimens	>0.5% excepting 1 specimen (HF1)
Bloomery iron slag	As skins or bands only	Predominant, present in all 47 specimens	Absent in all 47 specimens	Present in 29 specimens	<0.02% excepting 1 specimen (YW4)

Table 7.1: Mineralogical and chemical indicators to discern between copper and bloomery iron slag applied to the Daye assemblage.

In the copper slag from Daye, free iron oxides are in the form of magnetite, whereas in the bloomery iron slag they are wüstite. This difference reflects the corresponding redox conditions required for smelting copper and iron; the reduction of copper oxide to copper metal takes place under conditions where magnetite is stable, while the reduction of iron oxide to iron metal requires much more reducing conditions, where wüstite is the stable free iron oxide (Severin et al. 2011, 989) (Figure 5.34). If wüstite is created during copper smelting, this could be reduced into metallic iron, and thus contaminate the copper metal, therefore over-reducing conditions were avoided as far as possible (Cooke & Aschenbrenner 1975; Craddock & Meeks 1987; Rostoker et al. 1989; Rehder 2000, 114; Pryce et al. 2007; Killick et al. 2016). The absence of metallic iron particles within the copper slag assemblage also reflects that the redox conditions were insufficient to reduce metallic iron (Wingrove 1970; Cavallini 2013), thus it is obvious that the intention of the smelter was to extract a metal different than iron. Lastly, a few droplets of copper metal and Cu-rich sulphides are recurrently present within the copper slag microstructure but

these are absent within the bloomery iron slag. These droplets do not result in a high bulk copper content in the slag, yet this is fifty times higher than the average amount of copper present within the bloomery iron slag (~1.0% vs 0.02% Cu) (Figure 7.2 and Figure 7.4). The bulk copper content in slag is also consistent with the average (0.5-1.0%) concentration of copper in archaeological slags from most of Europe and the Middle East (Pleiner 2000, 254; Severin et al. 2011, 989).

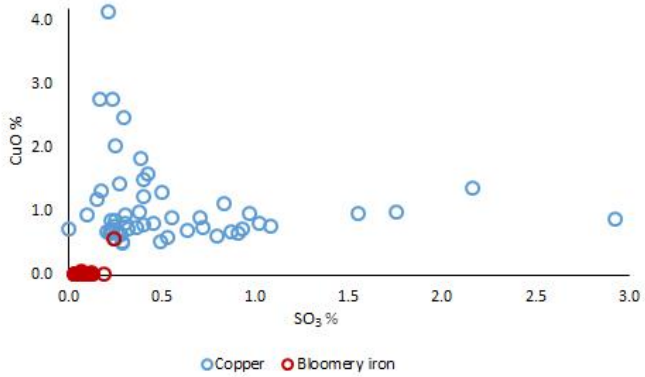

Figure 7.2: Binary plot CuO vs SO_3 (% in slag) plotting the copper and bloomery iron smelting slags.

However, even if these indicators enable a confident identification of copper and bloomery iron slags, they need to be contrasted against other parameters and should not be considered as absolute factors. For example, reducing conditions higher than necessary to extract copper have been frequently observed in ancient copper slags, and it has been pointed out that a copper furnace can be perfectly suitable to reduce iron as well as copper without drastic variations in the operating conditions (e.g. Wagner 1986; Gale et al. 1990; Merkel 1990; Rüffler & Gonser 1992; Rehder 2000, 114-119; Wagner 2008, 112; Rehren et al. 2012; Thondhlana 2012, 357; Izawa 2015; Killick et al. 2016; Van Brempt & Kassianidou 2016). Experimental archaeology has also demonstrated this possibility of obtaining metallic copper and lumps of iron after the same smelting cycle (Izawa 2015). In addition, bloomery iron by-products can be contaminated by copper if the ores occur together, which modifies the fingerprint of the slag obscuring the identification (Killick et al. 2016; Thondhlana et al. 2016).

In Daye County, however, these criteria are highly conclusive within the complete assemblage, allowing a clear distinction between copper and bloomery iron slags with very few borderline cases. Only 4 out of 59 of the copper slag specimens contain wüstite, which is generally scarce, and all of them contain a few copper prills and sulphides but no metallic iron (section 5.1). Conversely, the exceptional bloomery iron slag specimen (YW4) which contains 0.5% CuO only displays metallic iron particles within the microstructure but no copper prills, while all the free iron oxides are dendritic wüstite (Figure 7.3). The copper (~1%) absorbed by the reduced iron particles in MC6 is very likely due to contamination from the haematite ore (section 5.3), since the rest of the characteristics correspond to a standard waste-product of iron smelting by the direct method (section 6.1). Lastly, the specimen HF1 with unusual low Cu content in the slag still displays abundant copper prills but neither wüstite nor metallic iron (Figure 7.3).

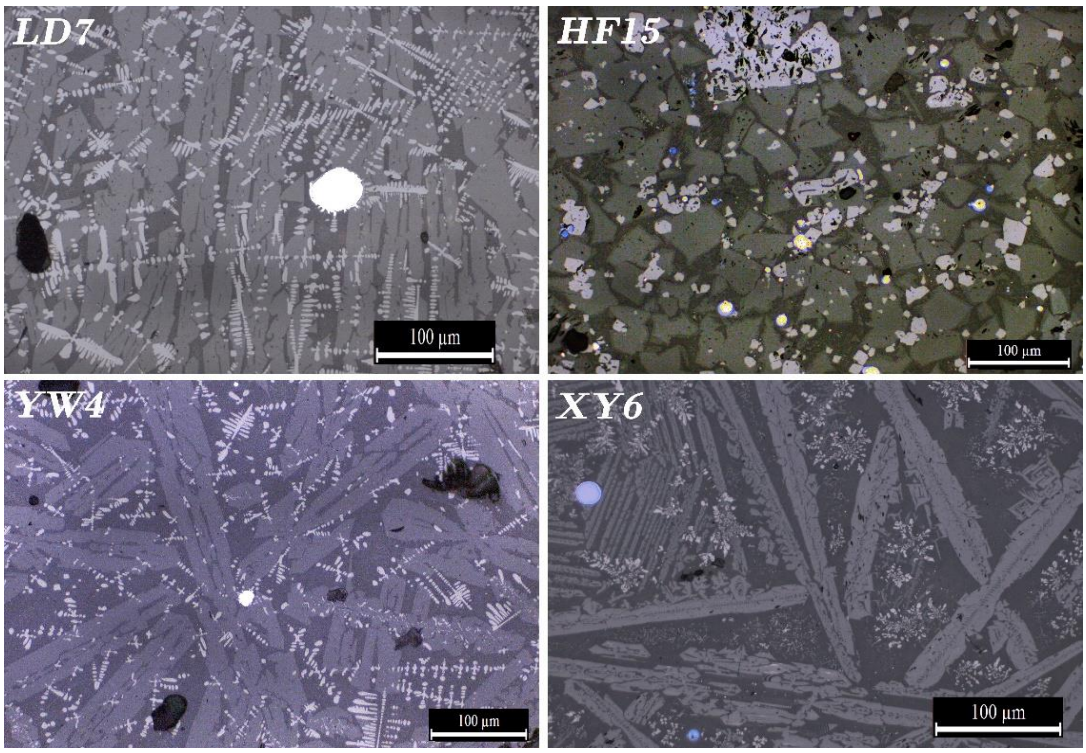

Figure 7.3: OM micrographs comparing the typical microstructures of the Daye copper and bloomery iron slag.
(LD7, YW4) Typical microstructure of bloomery iron slag showing laths of fayalite (medium grey) covered by abundant dendritic wüstite (light grey) and an iron particle (white); compared to the typical microstructure of the copper slag **(HF15, XY6)** showing also fayalite (medium grey), dendrites and flakes of magnetite (light grey), sulphides (blue), and copper prills (yellow).

Notwithstanding the broadly similar fayalitic composition of copper and bloomery slag mentioned above, a more detailed analysis of the slag chemistry can be used to discriminate between both processes if the entire assemblages are compared. Figure 7.4 shows that the bloomery iron tap slag is on average significantly richer (~14%) in iron oxide than the copper slag, and in general poorer in all the other oxides including the mentioned notable difference in copper content. This last difference is most notable in the binary plot CuO vs SO_3 which shows a clear separation between the two by-products (Figure 7.2).

The distinction between the bulk composition of copper and iron waste-products is very evident if these are analysed together in a PCA plot, which shows a sharp difference between both productions even if both of them are dominated by iron oxides (Figure 7.5). The PCA confirms the stronger homogeneity of the bloomery slag, which plots in a tighter group whose composition is dominated almost exclusively by the iron oxide from the ore; the few outliers corresponding mostly to specimens of post-reduction slag that contain more silica and alumina than the average (HF20, MC12, MC18), and to the Cu-rich specimen YW4. On the other hand, the copper slag is dominated by CuO losses, ceramics (SiO_2, TiO_2, K_2O, Al_2O_3), and fuel ash (CaO, MgO, P_2O_5) while FeO (flux) is generally less influential; the diversity of oxides that influence the composition is reflected in a higher variability of the assemblage. This contrast between compositions dominated by the iron ore or by the other materials is also reflected in Figure 7.4 where bloomery iron is richer in FeO but poorer in all the other oxides, except in K_2O.

The longest vectors correspond to FeO on the one hand, and SiO_2 on the other, which point away in opposite directions from the origin, and that separates two well-defined groups of slag created by means of the smelting of different ores – Cu-rich in the upper part and Fe-rich at the bottom – reflected in the plot. The copper slag is better defined by the higher levels of Cu, P and Mn that pull the slag to the top right. This agrees with the suggested use of haematite type ores for the bloomery smelting and copper carbonates or silicates type ores for the copper smelting. Notably, even if the copper ores were fluxed with iron oxides, in relative terms the slag is still dominated by the components of the copper ore.

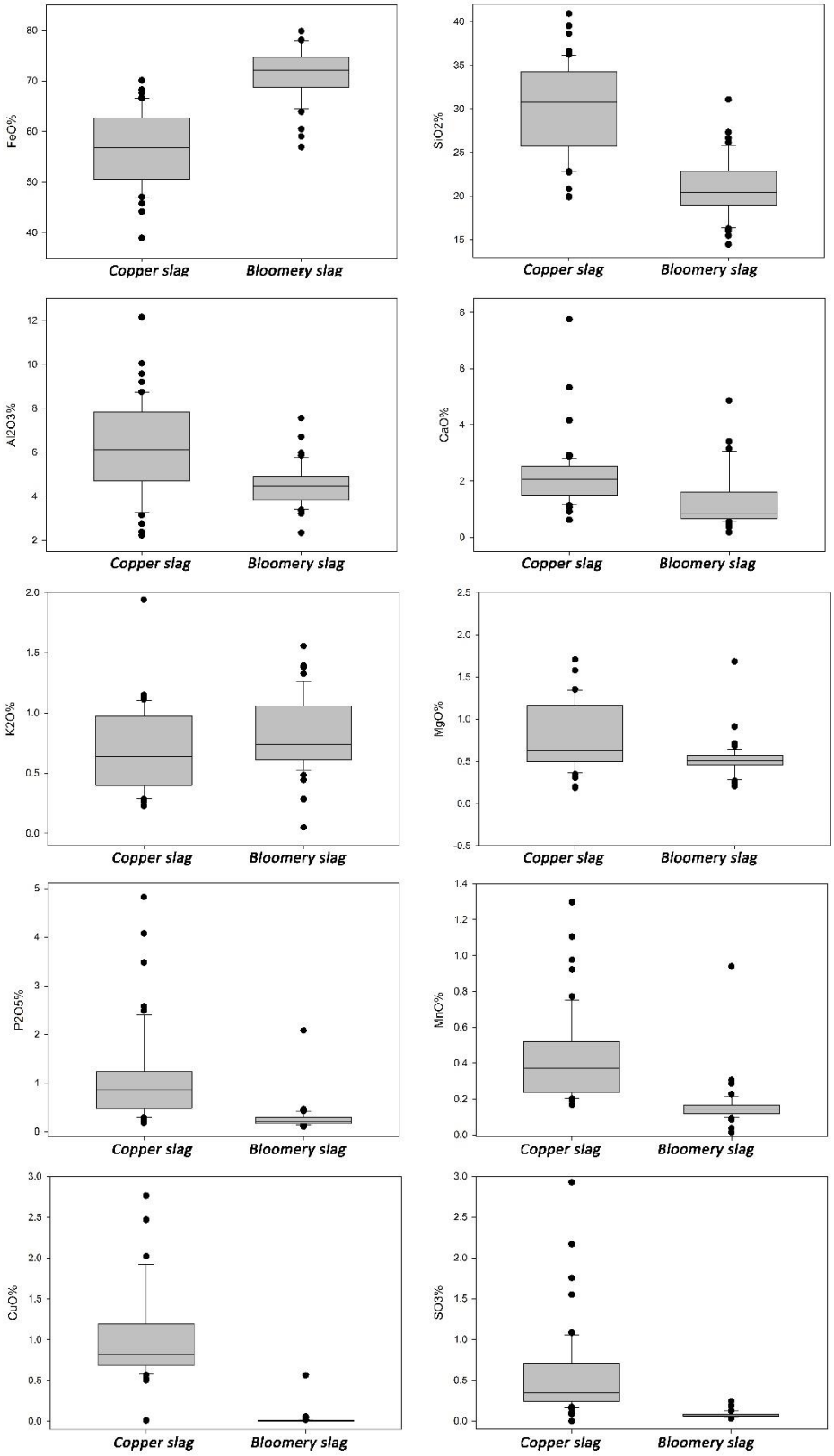

Figure 7.4: Box and whisker plot showing media, minimum and maximum variances (compounds %) comparing the composition of the Daye copper and bloomery iron slag.

Outlier MC4 (4.1% CuO) not included.

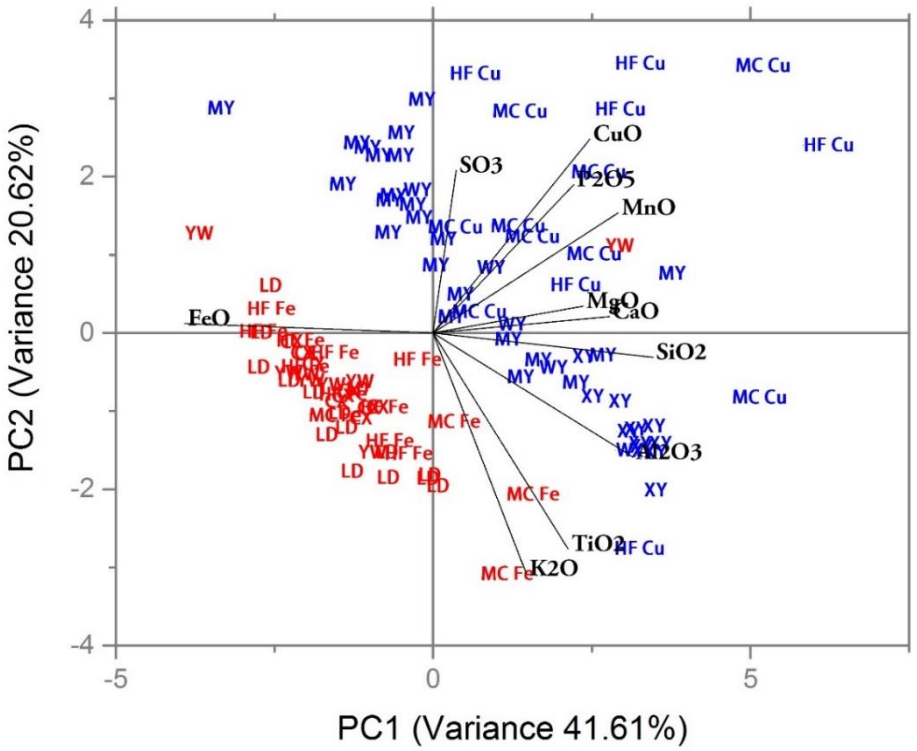

Figure 7.5: PCA plot for the Daye copper and bloomery slag bulk composition. First three components explain 73.2% of cumulative variance. Copper slag is represented in blue colour and bloomery slag in red. To discriminate the sites with both production types, Cu or Fe has been added to the label.

In sum, several technical parameters observed in the studied assemblage enable the distinction between the by-products of copper and bloomery iron smelting. The most diagnostic criteria are reflected in the slag mineralogy and composition: the stable free iron oxide in the slag microstructure of copper slag is magnetite (Fe_3O_4); the slag presents copper prills and/or copper sulphides; and the bulk Cu content in slag ranges 0.5-1%. Conversely in the bloomery iron slag the stable free iron oxide is the more reduced wüstite (FeO); instead of copper droplets the slag can contain metallic iron particles; and the Cu content in slag usually remains at ppm levels.

For the case of the Daye slag, the bulk chemical composition is another reliable indicator to distinguish between copper and bloomery iron slag, with notable variations in the three main oxides of the composition – Al_2O_3, SiO_2 and FeO (Figure 7.4). The other minor oxides generally also mark clear differences between the two assemblages, particularly clear – as mentioned – in CuO and SO_3 levels (Figure 7.2). The PCA indicates unequivocally the

use of a different ore – Fe-rich or Cu-rich – and separates sharply the copper and the iron debris as their compositions are influenced by different factors (Figure 7.5).

Finally, each metal production utilised different furnaces as detailed in sections 5.2 and 6.2. Assuming that the furnace structures excavated in LD and identified in HF are representative of the rest of the bloomery sites – CX, YW, MC – then the iron reduced by the direct method took place in batteries of embanked furnaces. On the other hand, if a similar assumption is made for the copper smelting sites – MY, MC, WY and XY – copper was smelted in shaft furnaces, as indicated by the structure located in HF (Figure 7.6). Therefore, copper and bloomery iron were extracted in clearly distinct structures. Even though none of the furnace wall fragments recovered from the sites allow a reconstruction of the furnace types, their fabric preparation, chemical composition and mineralogy are still distinguishable by their temper as well as heavy metal contamination.

Figure 7.6: Embanked furnaces excavated in LD, and shaft copper smelting furnace found in HF.
LD Furnace picture courtesy of Prof. Chen Shuxiang, shaft furnace of Prof. Li Yanxiang.

A further element to consider to distinguish between copper and bloomery iron debris are the archaeological remains. In all the prospected sites of Daye County the archaeological features are usually conspicuous on the surface as agglomerations of slag, frequently associated with domestic pottery (Figure 7.7). It is noticeable, however, that the bloomery iron slag heaps are much more prominent than the copper ones. Typically,

the former slag heaps appear in sites widely covered by vegetation, in the form of artificial mounds where the slag is always visible on surface but not the domestic pottery. The copper slags, on the other hand, typically are only visible on sections after removal of the natural soil or at the banks of reservoirs, marshes and waterways, and almost always have plenty of ceramics associated.

Figure 7.7: Archaeological evidences visible on surface in Daye County.
a) Massive heap of bloomery iron slag in HF; **b)** detail of the heap in HF showing no other material but slag; **c)** soil removed by excavator exposing abundant archaeological materials in Guohua (郭华), site close to MY no studied in this thesis; and **d)** detail of materials recovered including ceramics, polished stones and slag.

In general it seems that in all the prospected sites the archaeological remains associated with bloomery iron production are much more abundant than the copper ones, and thus it would seem that the bloomery production was of much larger scale than the copper one. Nonetheless, this perception cannot be taken as absolute since at the site of MY, which only presents evidences of copper smelting, large slag deposits that extend approximately 6-8 m in length with no less than 1-2 m of potential depth are visible in

terrace sections (chapter 3). Therefore the volume of slag is not necessarily representative of the scale of the production since this is based on partial data visible on surface, and evidence of large slag deposits associated with copper production is found as well. Lastly, the sites associated with copper production appear considerably more altered by post-depositional activities than the bloomery ones, frequently showing total removal of the soil, breaking the archaeological deposits and destroying almost entirely the original stratigraphy and the archaeological features.

In short, it can be concluded that the copper remains are deposited in lower stratigraphic levels than the bloomery iron evidence, which frequently appears on the current soil level accumulated in heaps and in larger volumes than the copper debris. The copper debris are visible mainly after strong alterations of terrain that have reached the archaeological levels, and that invariably leave scattered pieces of slag associated with fragments of ceramics (Figure 7.7, see also chapter 3). Incidentally, the deeper stratigraphy of the copper remains points to an older date.

7.2 Variability and efficiency in copper production technology

The copper by-products analysed in chapter 5 are argued to be the result of a similar technical procedure in which oxidic ores were smelted in shaft furnaces at mildly reducing conditions of ~10^{-6} atm pO_2 and temperatures around 1100-1200 °C. A key step of the procedure was the addition of iron oxides – haematite – to facilitate the creation of molten fayalitic slag. The small variations in slag morphology, chemical composition and mineralogy were explained by the internal dynamics of the procedure – e.g. variations of the charge composition, temperature and atmosphere of the furnaces, slag tapping ratio, etc.

As previously observed, the copper assemblage presents a broad similarity in bulk composition that allows the recognition of a single chemical group across all the sites (section 5.1). To further investigate any possible subgroups in the smelting slag assemblage, PCA in conjunction with hierarchical cluster analysis were undertaken on the slag chemical data. For the following explorations, key oxides were considered for their correspondence to parent material: MgO, Al_2O_3, SiO_2, P_2O_5, K_2O, CaO, TiO_2, MnO, FeO and

CuO. Some trace elements – e.g. Pb, Ba – were considered since these were sporadically seen in some minerals of the slag microstructure, however, when plotted in the PCA these proved to be irrelevant and were finally discarded.

The dendrogram of variables of Figure 7.8 (top) discriminates two main clusters: FeO and SO_3 on the one hand (red) and all the rest of the oxides on the other. The second main cluster splits into another two subgroups, one including ceramic oxides (dark yellow) and the other minor oxides of the bulk composition (blue).

When the observations are clustered by site, the dendrogram splits also into two groups – separated by the yellow dotted line – that correspond to ceramic-rich on the one hand (brown colours), and Fe-rich, Cu losses and minor oxides on the other (Figure 7.8, bottom). The observations split again at about the same horizontal distance – green dotted line. However, these cluster analyses also show that there is no correlation between groups and sites and all the specimens are scattered along the different sub-clusters, with the exception of XY that almost always groups within the ceramic-rich cluster. The rest of the sites do not follow any clear trend, although they appear more frequently in the iron-rich cluster, perhaps more clearly in the case of MY which plots a substantial number of specimens within the same group (red colour).

The plot of the data on the PCA shows that all the slags are compositionally part of the same system, but also that there is some internal structure on a site by site basis (Figure 7.9). The groups are not perfectly tight but show interesting trends that seem to characterise different sites. Thus, most of the slag from MY is dominated by flux signatures (FeO) whereas all the specimens from XY are grouped in the opposite extreme of the PCA plot, dominated by ceramic oxides (SiO_2, TiO_2, K_2O, Al_2O_3), and WY occupies an intermediate position between them, although it tends to be closer to the ceramic. The MC slag is more problematic since is typically dominated by CuO losses and/or CaO, MgO, P_2O_5, and MnO which can be found in both ore and the fuel ash (Tylecote et al. 1977; Crew 2000). Finally, the remaining site HF does not show a clear pattern since two samples plot within the clay dominated group but the other four are outliers to the general cluster, and plot in the CuO losses area.

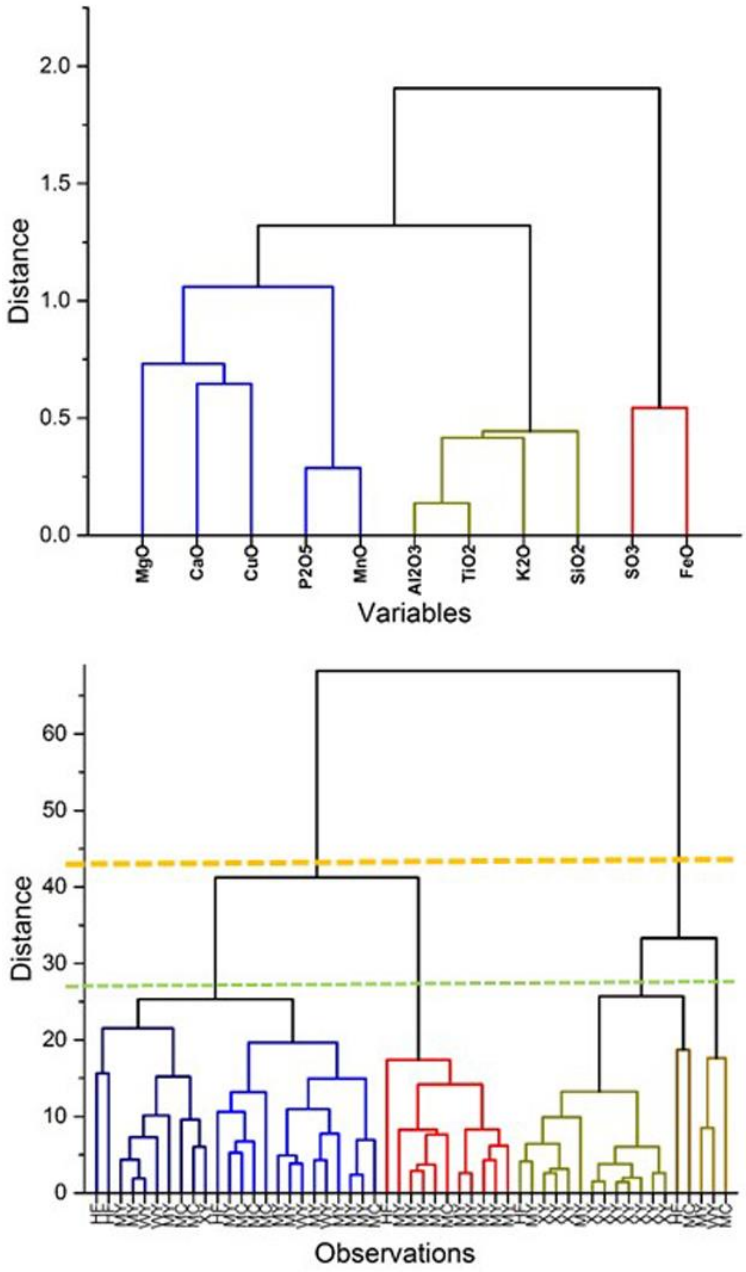

Figure 7.8: Hierarchical clustering analyses carried out by main variables of the chemical composition of the Daye copper slag (top) and by observations (bottom).
The yellow line indicates the first discrimination between clusters and the green line the distance separating the subgroups by site observed in the PCA plot.

The PCA and hierarchical clusters confirm that the Daye copper slag is certainly a homogeneous assemblage and that the variations observed in the sites are related to the internal dynamics of a shared smelting process based on the dominance of metal oxides in the composition provided by ore and flux on the one hand – including most of the slag

from HF, MC, MY and WY –, or based on the dominance of ceramics provided by gangue and furnace wall on the other – including all except one of the specimens from XY and few specimens from the other sites, including the only sample of tap slag from HF.

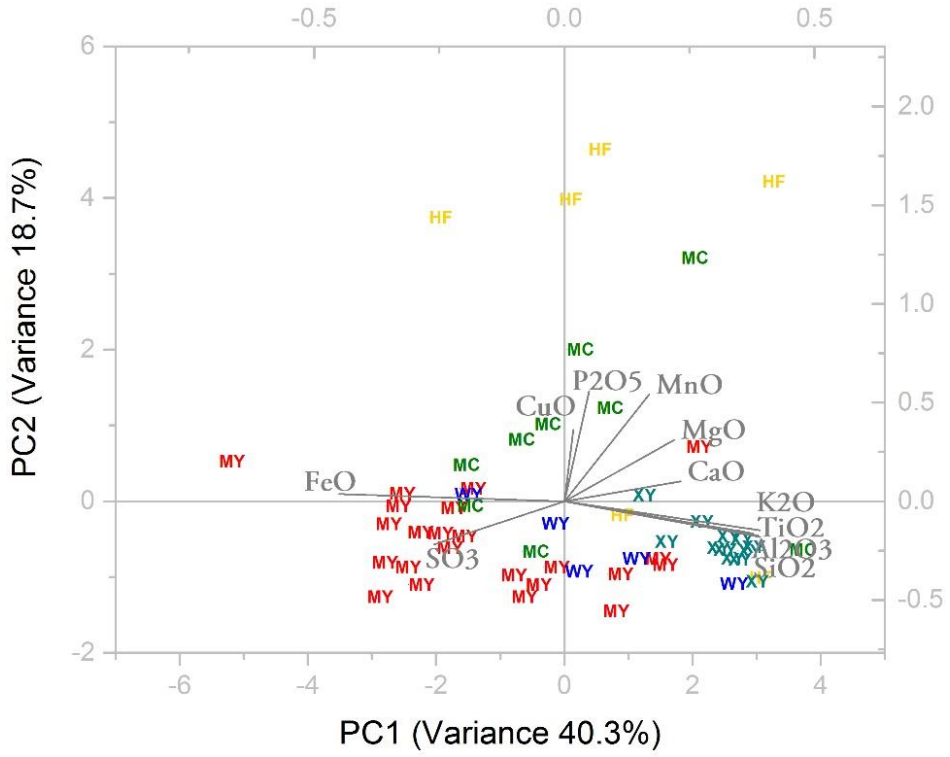

Figure 7.9: PCA plot showing variances in bulk composition of copper slag per site
First three components explain 72.2% of cumulative variance.

Despite the existence of subtly different chemical subgroups, there seems to be no indication of significant changes in technological processes or raw materials within the studied sites, and the smelting practices appear to have been similar across the landscape of Daye County copper production. As discussed, all parameters point to a common procedure visible in the analogous morphology of the slag; microstructure and mineralogy; bulk chemical composition; haematite fluxing, furnace operating conditions and nearly identical furnace ceramic fabrics. The overall narrow differences between these criteria suggest a standardised process to smelt copper from oxidic ores that was followed in all of the 5 sites of Daye studied here.

Incidentally, the PCA plot of Figure 7.9 also supports the hypothesis of ore smelting and not matte smelting in the case of the copper slag, as indicates the distance between S, Fe

and Cu, main elements of the sulphidic ores minerals (Bachmann 1982, 16; Craddock 1995, 149), which should be all pointing in the same direction if they had the same origin.

7.2.1 Technological choices in the *chaîne opératoire*

In Antiquity, the process of smelting copper from weathered ores typically employed bowl and shaft furnaces operating around 1100-1200 °C with charcoal as a reducing agent, and usually the complete process occurred within a single step. The typical furnace charge consisted of copper and iron minerals and silica that, when heating together in a suitably reducing atmosphere, form iron silicates – namely fayalite – with a melting point in the neighbourhood of 1200 °C, separating the copper metal from the gangue (Moesta 1986; Craddock 1992; Tylecote 1992, 7-17; Craddock 1995, 126-127). The key feature is slag formation since the slag is the most 'practical way of completely separating the smelted metal from the gangue contained in the ore charged, and eliminating it from the furnace', which 'also promotes coalescence of molten reduced particles, protects droplets of reduced metal from re-oxidation, and creates some thermal stability between the lower/high-temperature parts within the furnace' (Rehder 2000, 109).

In reality, the creation of slag was greatly constrained by the limited technological capacity of the ancient smelters: e.g. scant control or management of temperature, low attainable temperatures, heat losses, high fluctuations of the oxygen pressure within the furnace gas atmosphere, feeble air supply rates, rudimentary materials of construction, inexact methods to judge the ore quality, smelter actions driven by trial and error with only a basic understanding on the kinetics, etc. (Freestone & Tite 1989; Rostoker et al. 1989; Craddock 1992; Rehder 2000, 3-8; Hauptmann 2003; Miller, D. & Killick 2004; Karbowniczek 2005; Bourgarit 2007; Pryce 2008, 277). Given the interdependence of all these procedural parameters, 'there are only a very few ways in which all the low-melting slags could have been produced throughout the world' (Hauptmann 2014, 100), which is usually manifest in an iron silicate-dominated slag because iron oxides and silica are the primary oxides found in the ores, and because in the right proportions these melt in the temperature range of 1100-1200 °C, i.e. the range attainable for ancient smelters (Tylecote 1980, 5). Therefore, the reason why most of the archaeological slag falls within

the fayalitic area of the ternary diagram in Figure 7.1 is largely explained by the kinetics: slag formation occurs within the lowest temperatures marked by the eutectic points between FeO and SiO_2 because these are the two most abundant oxides in metal rich ores and/or flux, and because temperatures beyond that limit were mostly unreachable in a sustained way by ancient technologies (Elliot 1976; Bambergen & Wincierzt 1990; Tylecote 1992, 7ff; Craddock 1995; Rapp 1998; Hauptmann 2007, 18-31; Schlesinger et al. 2011; Craddock 2013; Hauptmann 2014). The ability of the smelter remains in finding the suitable proportions of iron and silica in order to obtain a slag that could be melted at those temperatures (Maldonado 2006, 151).

As a result, the process is strongly determined by the chemistry and melting behaviour of the materials, the technical limitation in achieving high temperatures, and control of redox conditions. To the extent that some scholars argue that the suitable combination of FeO and SiO_2 'does not reflect the technical skills of the ancient metalworkers' (Hauptmann 2014, 99) but 'merely (reflects) the bounding limits of compositions with suitable liquidus temperature' (Young, T. P. & Poyner 2012, 93), and that ancient metallurgy in general was a 'fortuitum and sordidum opus' (Cavallini 2005, 3) mostly controlled by chemistry that the ancient smelter could hardly understand, and where the accidents were more determinant than the skills (Cavallini 2005; Hauptmann 2007, 20-21; Cavallini 2014). However, while accepting that ancient metallurgy was heavily constrained by natural laws and technical limitations, it is my opinion that in the ancient metallurgical processes there was more serendipity than random fortune, and that the lack of understanding of the otherwise very complex kinetics should not be interpreted as indicative of a lack of skills from the smelter.

Extractive metallurgy demands good planning and strategy, so that by the time that the smelter lights the furnace and introduces the charge, many decisions and actions that influence the smelting outcome have already taken place (Figure 7.11). At that point, the smelter has extracted and processed the ores; decided the morphology of the furnace; provided the constructive materials; built the furnace and accessory features such as pits or roasting structures; assembled the air supply system according to the furnace design; collected and processed the flux; and made charcoal to use as fuel.

Furthermore, producing slag to extract the metal is not easy. It is necessary to maintain temperature and supply of air in a stable way; to be aware of the speed of consumption of the fuel and reduction of the ore to refill the burden conveniently; to add the appropriate flux; to pay attention to the tapping regime; and of course to execute all these actions within the correct timing and with the suitable proportion of materials, with numerous possibilities of ruining the operation because any of these parameters failed (Tylecote 1987; Muhly 1988; Rostoker & Bronson 1990; Tylecote 1992; Craddock 1995; Pleiner 2000; Karbowniczek et al. 2006; Crew 2013). While some of these settings would seem rather difficult to be strictly controlled – e.g. the maintenance of identical temperature and atmosphere within the furnace chamber – the furnace charge is to some extent more easily controllable by the smelter, who can establish how much and how often ore, charcoal, and flux are going to be loaded into the furnace (although natural variability within each of these should be taken into account). The composition of the charge has a strong impact on the process, affecting the tapping regime, temperature, metal extraction or fuel consumption (Craddock 1995, 147; Rehder 2000, 111; Miller, D. et al. 2001; Sauder & Williams 2002; Bourgarit 2007; Rehren et al. 2007). Manipulating the charge, however, requires some abilities since there is only a limited range of compositions that come closest to a fayalitic composition. If too much quartz (SiO_2) is added or too much iron oxide such as magnetite or hematite, then the charge will only be partially liquefied (Figure 7.10). The main risk, would be to freeze the furnace for the partially molten charge to solidify and clog the furnace, or to create a slag rich in unreacted charge materials, which might increase the loss of copper, or create difficulties in recovering metal prills trapped in the slag (Hauptmann 2003; 2007, 25; 2014, 101).

For the case of an iron-rich flux, such as in Daye, there also exists the opposite risk; to generate a large amount of slag not beneficial for the process. If there is an unbalanced high Fe content in the system, then this iron would react with the SiO_2 in the furnace wall, creating large quantities of slag with no benefit to the process since this makes no contribution to the reduction of copper, deteriorates the furnace wall, and merely consumes energy (Bambergen & Wincierzt 1990, 155-156).

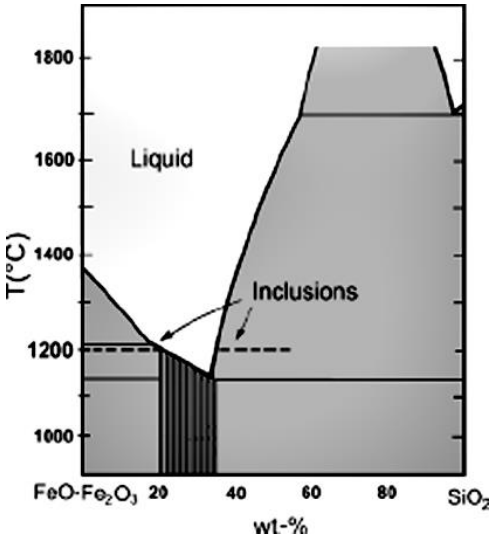

Figure 7.10: Simplified cross-section through the binary system Fe oxide–SiO_2 to demonstrate the liquefaction of an iron-rich silicate melt.
The maximal area of variation (hatched) is shown for a charge that can be liquefied completely at 1200 °C. After Hauptmann (2007, Fig. 2.5).

In sum, while the principal characteristics of the metallurgical process are governed by chemistry and thermodynamics, there is window of opportunity for skill and choice, which is expressive of cultural behaviour and manifest in the slag if we analyse it properly. By means of these technological choices the metalworker may not control all the parameters of the process but certainly influence the dynamics, and this certainly allowed them to control a substantial part of the process, i.e. if they decided to saturate the slag with chunks of quartz to retrieve mechanically the prills instead of generating well molten slag to extract the copper, they were actually conditioning the process and making cost/benefit decisions.

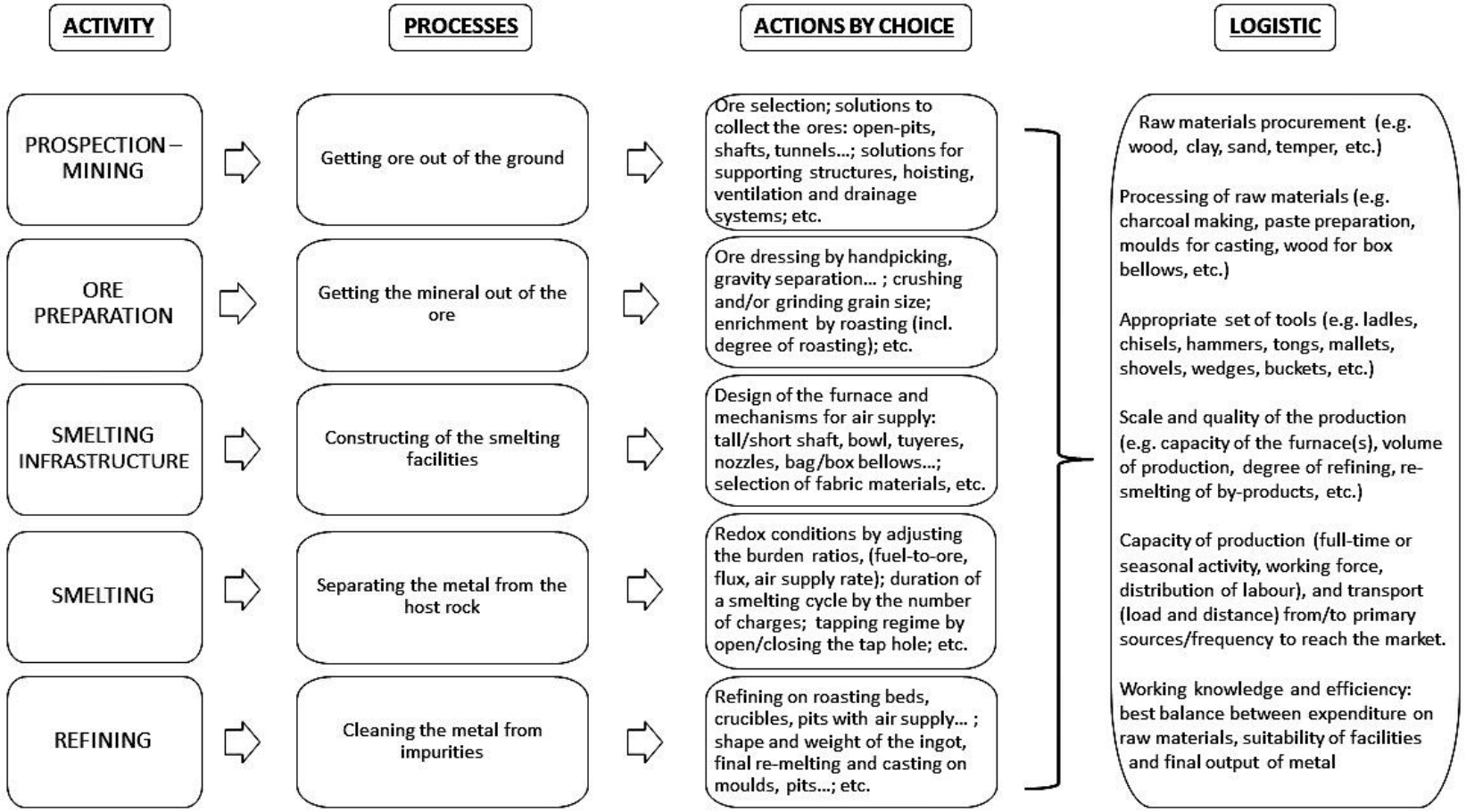

Figure 7.11: Flow chart showing the basics steps in the copper smelting *chaîne* opératoire, the actions in which the smelter can make direct decisions, and the general logistics intrinsic to the process.

7.2.2 Adjustments of the smelting recipe

Based on the very limited and inconsistent variability between sites, the preceding technical discussion (section 5.4) has introduced the idea that there was a common strategy to smelting in the Daye County. The small variations between slag samples are explained as a result of minor changes in the operating parameters – furnace redox atmosphere, composition of the charge, cooling temperatures and tapping regime – all of which can occur within a single smelting system.

This would already suggest that there were no significant site-specific choices, at least not systematically presented. However, it is appropriate to discuss further the extent to which these small differences may be indicative of significantly distinct behavioural patterns or decisions on the part of the smelters.

In this vein, a conceivable hypothesis would be that while there was a relatively uniform 'cultural tradition' between all the smelters of Daye, the smelters of XY altered the recipe by decreasing the amount of haematite added to the furnace burden. This would have the advantage of minimising the risk of reducing iron at the same time as copper, since there would be less iron in the system, as well as to avoid the creation of too much slag that reacts with the furnace wall instead of the gangue (Bambergen & Wincierzt 1990, 155-156; Gale et al. 1990; Rehder 2000, 117; Izawa 2015). Presumably, the slag formation and tapping regime would be slower since there is less iron in the system that takes more time to react with the silicates giving the copper more time to separate from the gangue, and thus benefit the copper recovery.

XY shows less variability and more consistently plots around the Fe-poor eutectic of the phase diagram $FeO–Al_2O_3–SiO_2$, in comparison with the other sites that are more widely distributed within the fayalite area (Figure 7.13). This suggest that some smelting parameters, if not radically different from the rest, were at least more consistently applied since all the other sites show much wider variability.

The internal variability of the sites was also explored by the coefficient of variation (CV), which is a measurable indicator to assess standardisation quantitatively since this

expresses the precision and repeatability of a procedure, an approach which has been frequently applied to archaeological materials (e.g. Blackman et al. 1993; Costin & Hagstrum 1995; Martinón-Torres et al. 2014) (Figure 7.12). It must be noted, however, that slag is a by-product rather than a product, and therefore there is no baseline to establish what is or isn't standardised. The line chart indicates that XY is the most uniform and MC the most variable, and also that with the exception of MC, most of the sites show variation bellow 60%, therefore also supporting the hypothesis of a common process which perhaps evolves with the time towards a standardised product represented by XY.

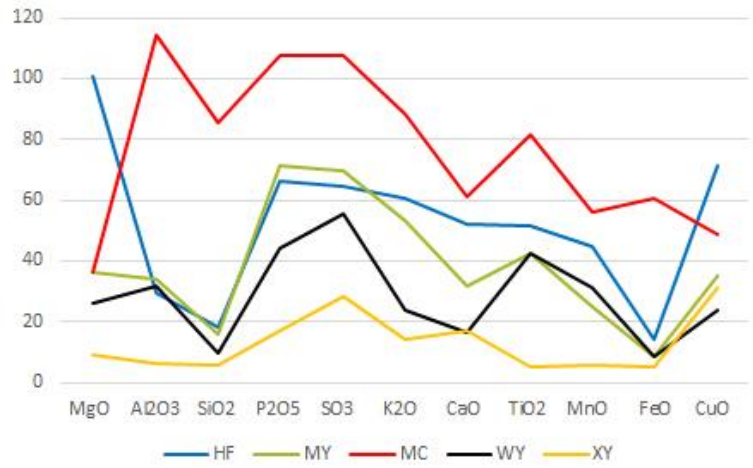

Figure 7.12: Line chart comparing the coefficient of variation of copper slag in Daye.

Therefore, a speculative scenario would be a diachronic evolution of the smelting process where XY improves the recipe, obtaining purer copper metal with less iron contamination, by means of a better control of the smelting process that is reflected in the higher standardisation of the by-products.

Finally, archaeological excavations demonstrate that different traditions can co-exist in the same area, for example, the Sicán mining and metallurgy complex for copper-arsenic production (AD 900-1375) in northern Peru (Shimada & Craig 2013). Here there are described several relatively small-scale production units sharing basic technology and achieving equivalent outputs within an area of 50x50 km. However, the homogeneity and organisational redundancy did not eliminate variation among workshops, which enjoyed

a 'good degree of technical, artistic and perhaps even political, autonomy' visible in minor changes in the *chaîne opératoire*, the number of furnaces per workshop, distinct decoration of tuyères and domestic ceramics, product variability, etc. concluding that 'only in a general sense can we speak of standardized products' (Shimada & Craig 2013, 25). A second illustrative example, is found in African (Mali) ferrous metallurgy where six districts with different metallurgical traditions of bloomery smelting that co-existed in a geographically limited area of 15,000 km^2 during a period of 2-3 centuries (Robion-Brunner et al. 2013). Unlike in Daye County these differences were very evident under all technological, cultural or economic criteria: from the furnace size and shape, metallurgical waste generated, smelting procedure, scale of the production, or distribution and consumption of the end products.

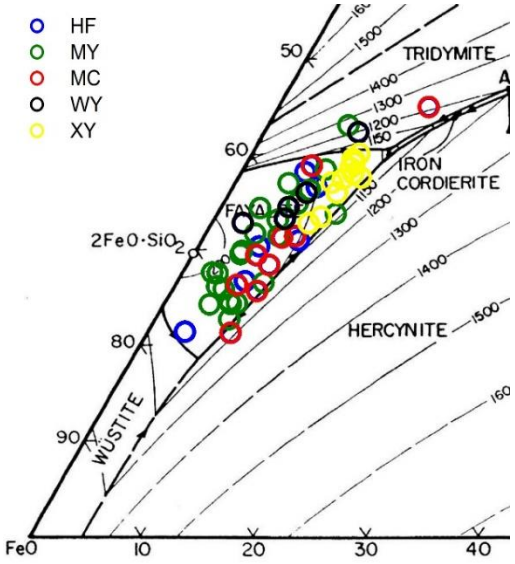

Figure 7.13: Ternary system FeO–Al_2O_3–SiO_2 plotting all the Daye copper smelting slag.

To conclude, there is not enough data to support that the variations detected in the XY slag were due to modifications of a common technical procedure in Daye County. Compared to other metallurgical regions that present clear indicators of the self-sufficient character of workshops within the same cultural sphere, these variations are a weak argument in favour of a particular technological choice distinct from the other sites made in XY. However, it also needs to be considered that the case studies mentioned have

considerably larger archaeological datasets than is currently available for Daye, and thus this statement will possibly change after new archaeological interventions.

7.2.3 Refining of copper

In spite of the fact that raw copper was not identified in our samples from primary smelting sites in Daye, the metal produced was in all probability impure, mainly with residual iron and sulphur, as indicated by the matte envelopes and occasional exsolved iron and sulphide inclusions in the copper prills, as well as the generally high iron content of the metal particles embedded in the slag – often 2-6% Fe and reaching over 10% (section 5.1.5). While it would be risky to draw a direct correlation between the composition of the copper trapped in the slag and that of the bulk metal produced, the evidence does suggest that metallic iron would have been present in the copper, which can lower the quality of the metal affecting its workability (Craddock & Meeks 1987; Romanow 1995; Pryce et al. 2007); thus, the raw copper from Daye likely required secondary processing.

The production of black copper is normally associated with matte production although it is acknowledged that impure copper was commonly the result of smelting oxidic ores as well, with several archaeological examples of copper smelting that rendered highly ferruginous raw copper (e.g. Kelso 1951; Wagner 1986; Roman 1990; Tylecote 1992, 38-39; Izawa 2015; Ben-Yosef et al. 2016; Thondhlana et al. 2016), and also shown by experimental archaeology (Merkel 1990; Pryce et al. 2007; Izawa 2015).

Refining black copper from oxidic ores does not entail a major problem, a simple remelting will improve the copper quality although a more effective way is to refine the copper under oxidising conditions (Merkel 1990). In Merkel's experiments, raw copper from primary smelting placed in a shallow pit under charcoal with an airflow at the rim of the pit decreased the iron content in copper metal from 22% to 6%, and three successive refining iterations lowered the content to 0.014% (Merkel 1990, 107-109).

There is no evidence of any refining practice in the sample from Daye analysed, and such evidence was not recorded for the copper extracted in Tonglüshan either. As a matter of

fact, a bronze axehead and a copper ingot found in the vicinity of Tonglüshan also registered high iron content in the metal – 1 and 5% respectively (Wagner 1986, Table 6). The shifting from 5% Fe in the ingot to 1% in the object does suggest that the raw copper was refined but not thoroughly. This is surprising, especially taking into account the negative influence of iron on the castability of copper, as it provokes large shrinkages during solidification (Konečná & Fintová 2012, 2), and even more surprising when we bear in mind the prevalence of casting in ancient China (Barnard 1961; Fong 1980; Linduff & Mei 2014). Typically, the analysis of bronze artefacts of Shang and Zhou periods show negligible iron levels, even when the raw metal can contain up to 6.8 wt% Fe (Lian & Tan 2003; Chen, K. et al. 2009; Zhou, W. et al. 2009). Overall the refining of iron-rich copper ingots (typically 2-9% Fe) was a common activity in the bronze foundries of the Zhou period, with other raw copper ingots from Tonglüshan reported to contain 3-4% Fe and the extreme case of copper ingots found in Anhui province with 30% Fe content (Zhou, W. et al. 2009). On balance, it would seem that the object reported above is an exception, and that the refining of copper must have been a common practice in Daye County.

This aspect of iron contamination in copper is worthy of further investigation in the future. It has been suggested for a similar case of smelters that had difficulty in controlling the reducing furnace atmosphere that the smelting method was optimised over time to avoid the problem, by refining the redox conditions and temperature together with use of well beneficiated ores (Killick et al. 2016, 24). This would constitute a powerful reason to alter the smelting tradition as in the hypothetical diachronic scenario of XY improving the recipe introduced in the previous section.

7.2.4 Efficiency of the smelting process

Efficiency is a complex concept that can be measured at various scales – management of time, energy, labour, and raw materials input to the work – subject to the limitations of the archaeological data, and which is interpreted differently depending on contextual social needs (Costin 2001; Chirikure & Rehren 2006). For example, a smelting furnace that renders a low metal yield and incompletely molten slag, as is the case with Pre-Columbian *huayrachina* silver smelting furnaces, could easily be labelled as 'inefficient'. However, the

huayrachina is 'exceptionally fuel-efficient' and thus very well adapted to the scarcity of fire-wood at high altitudes where fuel is more inaccessible than ore (Rehren 2009-2011, 82). Therefore, in order to avoid confusion, the term 'efficiency' is used in this dissertation narrowly to refer to the extraction recovery (i.e. amount of metal extracted from ore unit) whereas the cultural or contextual dimensions of efficiency are considered under 'cost/benefit balance'. Unfortunately, the partial data from Daye do not allow a full exploration of the latter, e.g. it is not possible to discuss the technology in terms of labour and time needed to produce the copper (Shennan 1999) – but it is still appropriate to clarify the difference between the two above concepts.

Efficiency is frequently estimated based on the copper content in the slag. It is generally considered that extractive technologies that produced slags which retained high copper content were inefficient, while low copper content in the slag is a sign of efficient extractive technologies (Hauptmann 2007, 160). This statement, however, also needs to be qualified since the type of ore smelted (e.g. sulphidic, oxidic, high or low grade); the smelting method (e.g. crucible, bowl furnace, slag-tapping furnace); or the chronology, are all aspects that need to be considered when labelling the copper content as 'low' or 'high'. To illustrate this point we can compare the statement inspired by the crucible slag from 2nd millennium BC Peñalosa (Spain), described as 'immature slag that retained much copper' (Rovira et al. 2015, 362), to the 1st millennium BC crucible slag from Thailand considered a 'relatively efficient smelting product' (Pryce et al. 2011, 3316). In both cases, the copper levels were generally 1-2% (excluding outliers).

In general, the copper losses in Daye slag are not high, rarely exceeding 1%, with copper content comparable to sites of the same or later chronologies (Figure 7.14). As explained before (section 5.4.1), there is no direct evidence of the type of ore smelted in Daye, but the ores available in the area are medium-high grade copper minerals such as malachite, azurite, chrysocolla, tenorite and cuprite (Wagner 1986; Xie et al. 2011), and we can thus assume that they were using these. Therefore, ~1% Cu in slag in ores with potential copper content of 40-70% seems a very tolerable loss. The relative low amounts of copper in the slag, mainly as tiny grains (10-80 μm) of matte and metal prills indicate that the smelters from Daye had a good understanding of the metallurgical process: after (likely) beneficiating the ores, these were appropriately fluxed with iron oxides to create a fully

molten iron-rich silicate slag that was tapped out of shaft furnaces. The furnaces were operated at relatively stable conditions of moderate temperatures and mild reducing conditions; the entire process was likely achieved with a moderate consumption of fuel, due to the mild atmosphere and the small size of the furnace chamber (Figure 7.15 right).

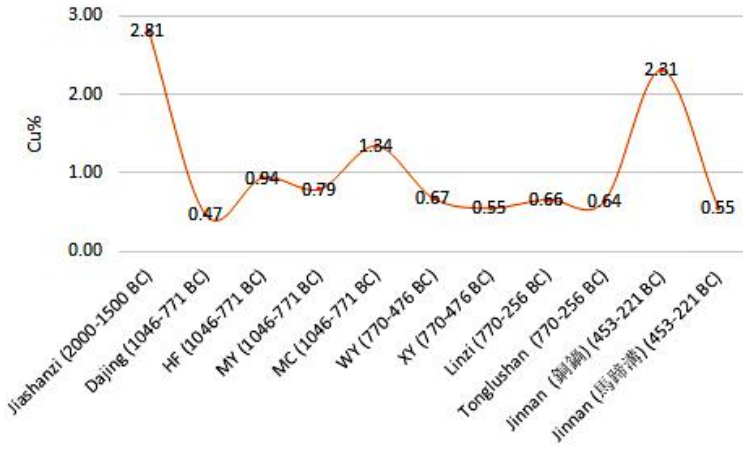

Figure 7.14: Line chart showing a comparative of average copper content in archaeological slag between pre-imperial Chinese copper smelting sites.
The dates within brackets correspond to Chinese historical periods given by the corresponding authors: **Jiasahanzi** (Li, Yanxiang et al. 2011, Table 1), **Dajing** (Li, Yanxiang & Han 2002, Table 3), **Linzi** (Du et al. 2012, Table 1), **Tonglüshan** (Li, Yanxiang et al. 1999, Table 2), **Jinnan** (Li, Yanxiang 1993a, Tables 1 and 2). The chronology of the sites in Daye is explained in section 7.3.

Figure 7.15: Front view of a smelting furnace of Tonglüshan (model), and the copper smelting shaft furnace found in HF to the right.

In sum, the Daye smelters skilfully used the available natural resources to smelt the abundant copper-rich ores: they built suitable furnaces with the local clay that was tempered with quartz to improve its refractoriness; the copper extraction was maximised by fluxing the ore with previously roasted iron oxides, which generated fully molten slag

with scant unreacted materials and trapped very little copper; and the entire process consumed a balanced amount of charcoal.

Finally, it is worthy to note that these are five case studies out of few tens of possible more copper smelting workshops surrounding the Tonglüshan mine (Wagner 1986), and that although the production of metal cannot be estimated with available data, the total volume had necessarily to be very large – estimations between 40,000-120,000 tonnes of copper metal have been suggested for Tonglüshan (section 2.5.2). Therefore, the copper production clearly exceeded the needs of consumption of the local communities, and these must have been exchanging or trading the copper with other consumers.

7.3 Founding of copper smelting traditions in the Daye County: chronological framework of the copper smelting sites

The ancient copper metallurgy of Daye County is to a great extent contemporary to the exploitation of the ancient mine of Tonglüshan. The Tonglüshan metallogenic deposit in the Middle Yangtze River is one of the economically most important Fe and Cu-mineralisation systems in China (Zhao et al. 2012). The deposits have been classified in twelve ore bodies, and except for deposits X and XII, all the ore bodies were already exploited by the end of the 1st millennium BC (Huangshi Municipal Museum 1999, 29-31; Xie et al. 2011).

The mine exploitation was initiated during the Western Zhou Period (1046-771 BC), although the mining activities in the area – vicinity of Tonglüshan if not in the very mine – most likely existed earlier than this date (section 2.5). In fact, bronze metallurgy is documented in the area in the Early Shang Period (~1500 BC) associated to the Yueyang culture and the city of Panlongcheng (Figure 7.16). Panlongcheng was a stronghold of the early Shang culture in southern China with a foundry for bronze casting, and the city played an important role in the Shang state network to deal with other polities in the south in addition to the acquisition of resources, among those the copper from the mine of Tonglüshan – ~70 km as the crow flies, well connected by the Yangtze river (Chang 1980b, 303; Li, X.-J. 1996-97; Flad & Chen 2013, 186; Yuan 2013, 329-335).

The hypothesis of exploitation of the copper resources during the Shang period finds support in the analyses of cores extracted from lake sediments at the Liangzhi lake, some 60 km far from Daye, close to Panlongcheng (Lee et al. 2008). According to this study, before 3000 BC, the pre-Bronze Age, metal levels in the sediments are very low, indicating natural slow leaching from the background mineralisation but no mining. Entering the second half of the 2nd millennium BC, metal in the sediments increased significantly, suggesting the start of organised mining of copper and other metals, with a second important expansion around the 500 BC, a sure indication that copper was extracted on a large scale by that date (Lee et al. 2008, 13; Coulson 2012).

Apparently, the most intense period of activity in Tonglüshan corresponds to the years 500-200 BC, culturally the late Spring and Autumn and Warring States periods (Coulson 2012). This was a time of frequent military conflict within China, with high demand for copper by all the contender Warring States. The smelting furnaces that were associated with Tonglüshan mine correspond roughly to this second period of expansion, with 10 furnace structures of the same type unearthed on the same stratigraphic level of the 6th–5th century BC (Wagner 1986, 2; Zhou, B. et al. 1988, 128; Huangshi Municipal Museum 1999).

As previously described these structures resembled a blast furnace integrating a characteristic hollow base to preserve the heat and insulate the hearth from moisture, two tuyeres, a conical shaft and a wide working platform; the furnace wall fabric notably refractory (Figure 6.31) built up with a mixture of red clays, quartz sand, iron powder and kaolin (Huangshi Municipal Museum 1980; Zhou, B. et al. 1988; Wagner 1996, 44). The morphology and ceramic fabric of these furnaces is clearly different to that of the small shaft copper furnace found in HF (Figure 7.15). The smelting slag, however, is quite similar, consisting of thin (1.5-3 cm) platy shapes of black-grey colour with flowing patterns (Table 7.2). The glassy matrix contains abundant fayalite crystals and few magnetite spinels, very few small grains of sulphides, very rarely pure copper prills, and occasional relics of hematite. The major difference in comparison with Daye is in the bulk composition, which in Tonglüshan is richer in silica (32 to 28%) and alumina (7-8 to 5-6%) and poorer in iron oxides (53 to 62%) (Li, Yanxiang et al. 1999) (Figure 7.17). In terms of efficiency, the copper content of the slag is equivalent in both collections.

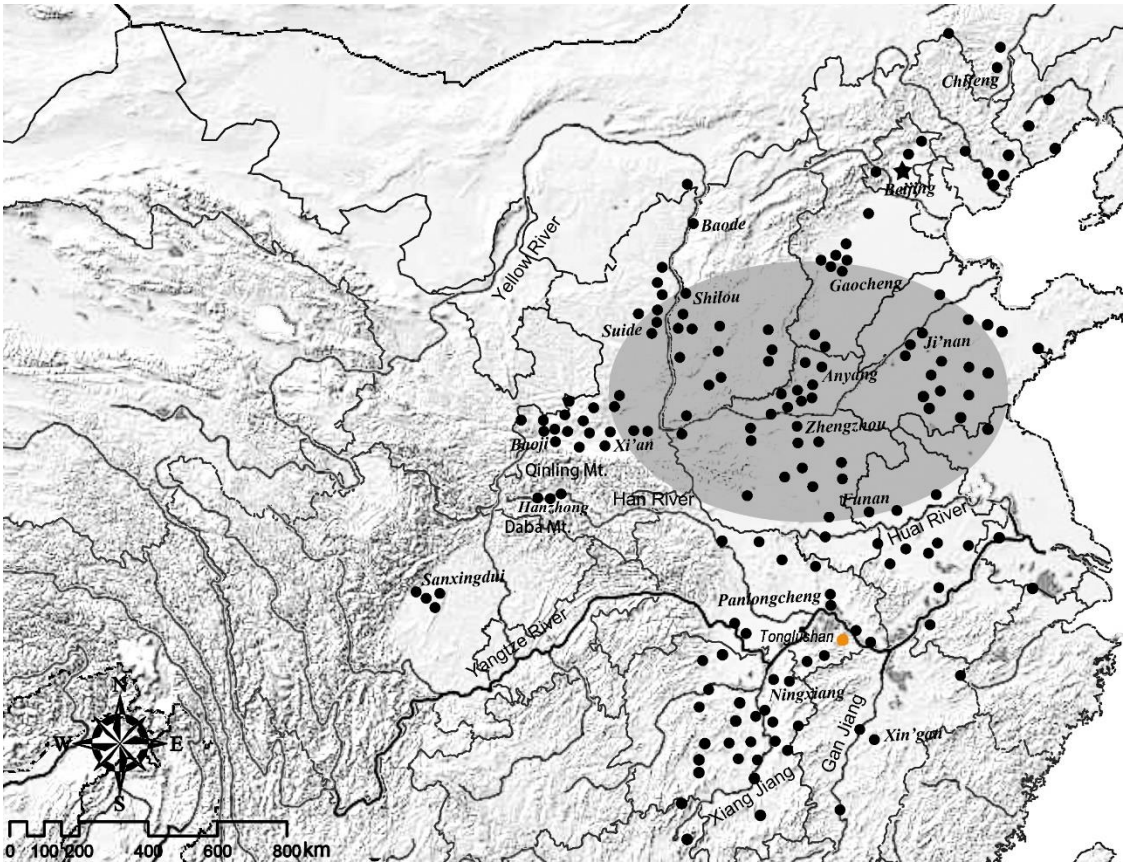

Figure 7.16: Map of the Shang State.
Distribution of the main sites yielding bronzes dating to the late second millennium BC in China. The map shows the natural buffer Shang area (tint) with the nuclear Shang zone. Panlongcheng and Tonglüshan (orange dot, the second in Daye County) are located at the southern boundary of the Shang influence area. Modified from (Chen, K. et al. 2016, Fig. 1).

Overall, the smelting remains of Tonglüshan seem to represent a more sophisticated technological process that utilised larger furnaces with more capacity and incorporating technical innovations such as the hollow base, or the more refractory ceramic fabric. The slag microstructure is fairly similar to the assemblage from Daye, with the same minerals present in the microstructure but slight differences in their occurrence. Thus, in Tonglüshan the free magnetite in the matrix is not so common and the haematite microscopic chunks are much more exceptional than in Daye; copper-rich particles are really tiny particles (~10 µm) in comparison with ~10-80 µm found in Daye; and the bulk composition is richer in silica and alumina in Tonglüshan and richer in iron oxides in Daye.

The plot of slag compositions on the ternary diagram FeO-SiO_2-Al_2O_3 also reflects the potential technological improvement (Figure 7.18). On the one hand the slag from Tonglüshan plots closer to eutectic 1 (silica rich). A subgroup of these plots in the tridymite

area next to the 1200 °C isotherm, hence potentially reflecting higher melting temperatures – but this should not be a problem in the case of Tonglüshan as the furnaces were more powerful, capable of operating at 1200-1300 °C on a permanent basis thanks to their design like blast furnaces (Wagner 1986; 1996, 44; 2008, 25). At the same time, the slag from different sites in Tonglüshan tend to form tighter clusters, thus indicating a more standardised process.

Overall it is tempting to envision copper smelting developing over time as a regional tradition, characterised by the smelting of oxidic ores fluxed with magnetite using shaft furnaces at several workshops near the Tonglüshan mine, which supplied the ore. These workshops were probably in operation until the surge in demand of copper ~500 BC at the beginning of the Warring States period, which stimulated the development of technologically improved furnaces that rapidly doubled or tripled the existing production. Since there was a risk that iron could be easily reduced together with copper in such furnaces (Wagner 1986, 8; 2008, 25), the amount of haematite added as a flux decreased, seeking to minimise the iron contamination and to obtain good quality copper metal, following a steady tendency in the tradition of reducing the amount of iron of the smelting recipe. Other adjustments, such as ore blending or modifications in the shaft furnace towards a blast furnace final design, can be presumed as well.

Significantly, in HF, MY, and MC the domestic pottery associated with the copper metallurgical debris corresponds to the Neolithic (5000-2000 BC), Shang (1600-1046 BC) and Western Zhou periods (1046-771 BC); the ceramics in WY are roughly described as from the Zhou period (Hubei Provincial Bureau of Cultural Heritage 2002, 42-47; HF personal communication of Dr. Qu Yi and Dr. Kunlong Cheng). In MY some ceramic shapes were identified as typical of the Western Zhou, such as shallow *Dou* plates with radiating pattern and inscribed Li (鬲) wares, as well as two bronze artefacts of the same period (Museum of Huangshi City 1984, 8-14). As mentioned, XY is not recorded in any archaeological inventory and the site is currently mostly destroyed, thus there is no support of the ceramic evidence to help establish a chronology.

	TONGLÜSHAN	***DAYE***
SLAG MORPHOLOGY	Platy with flowing patterns Flat (15-30 mm) Black-grey colours Section is dense showing well molten slag	Platy with flowing patterns Typically flat (17-40 mm) Occasional flow slags Common (MY, HF, MC) thicker specimens (40-65mm) Dark greenish grey or black colours Section is dense showing well molten slag
BULK COMPOSITION	Fayalitic (silica-rich)	Fayalitic (iron-rich)
MICROSTRUCTURE	'Lean' glassy matrix containing: - Dominant fayalite crystals - Few magnetite - Rare to very rare relics of haematite - Cu prills and sulphides (chalcocite, covellite) Most of Cu is lost in the glass, the largest particles have 100 µm	'Packed' glassy matrix containing: - Dominant fayalite crystals - Common magnetite (except XY) - Very few to rare relics of haematite - Cu prills and sulphides (chalcocite, covellite) Most of Cu is lost in sulphides, the largest particles have 500 µm

Table 7.2: Comparison between the main characteristics of the tap slag from Tonglüshan and Daye.

In conclusion, the technological evidence indicates that the metallurgical remains at the archaeological sites in Daye of HF, MY, MC, WY and XY were generated before the peak of production in Tonglüshan. The associated domestic pottery suggests that all of these sites were smelting copper during the Western Zhou Period, some of them perhaps earlier than this, dating to the Shang Dynasty. Based on the consistent similarity observed in the by-products, it is conceivable that all of them were producing copper during the same period, and therefore the Western Zhou-and Spring and Autumn periods (1046-475 BC) is proposed as the probable chronological framework since all sites have ceramics of this date.

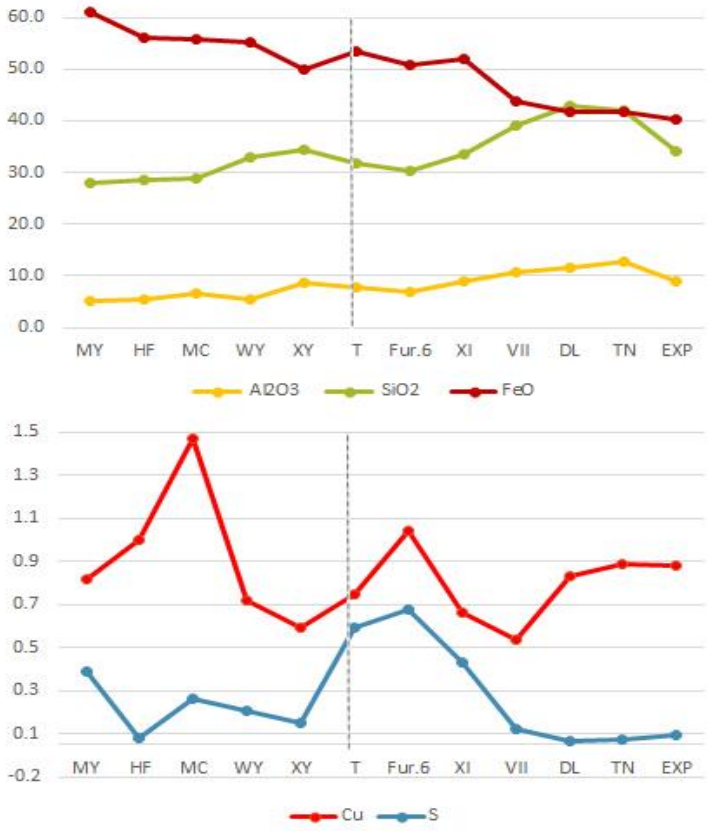

Figure 7.17: Line chart showing the main oxides, Cu and S in slag, of the Daye assemblage compared to the slag from Tonglüshan.
The dashed line separates Daye (left) from Tonglüshan (right). Slag data from Tonglüshan: T(5) slag from a pit; Fur.6 (5) slag from Furnace 6; slag from ore-bodies XI(52) and VII(12), from a warehouse DL(5) and from a stratigraphic section TN(5). EXP(14) is the slag produced after the experimental archaeology (Wagner 1986, Table 7; Li, Yanxiang et al. 1999, Table 9).

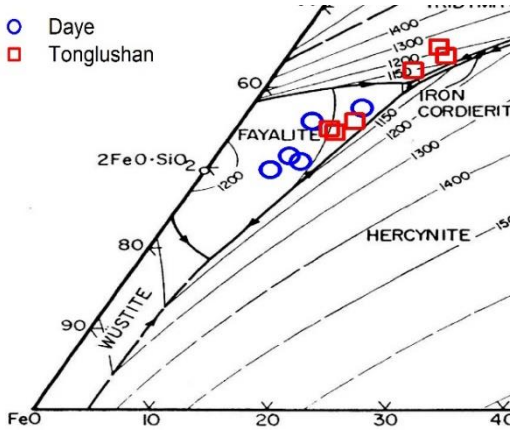

Figure 7.18: Comparison between Tonglüshan and Daye copper slag plotted in the ternary system FeO-SiO_2-Al_2O_3.
Each plot represents the average of the assemblages represented in Figure 7.17 excepting the experimental slag.

Nevertheless, this does not imply that the sites were necessary synchronic. Considering the extended time span, a highly likely scenario is that the studied assemblage corresponds to different moments within the same cultural period. Thus it is tempting to suggest that the bulky slag trapping more copper prills from MY, MC and HF would correspond to an early period – Early Western Zhou or perhaps late Shang –, while the tablet slag from XY and WY with practically no copper prills would correspond to later chronologies – Spring and Autumn (770-476 BC) –, once the smelting technique was more mature and improved, closer in similarity to the large scale production debris of the powerful furnaces of Tonglüshan. In this scenario, the 'cross-over' slag such as HF16 – the only example of platy slag within a collection of flow slag – or YW7 – the only example of flow slag amongst platy slag – would correspond to earlier or later by-products generated in the same site but in different periods, randomly mixed within the assemblage during the surface collection.

Figure 7.19: Map showing the location of the copper smelting sites with respect to the Tonglüshan mine.
Four of the sites (WY, XY, MC and MY) are in a radius of less than 10 km distance from the mine (red dotted line). HF is 28 km away as the crow flies.

Therefore, in Daye indeed there would be a tradition of copper smelting virtually uninterrupted from the 11th to the 1st century BC, and it is conceivable that most of the

smelting sites, if not all, relied on ore mined in Tonglüshan since they are geographically very close to the mine (Figure 7.19).

Finally, it is worth outlining some specific arguments to discard the possibility that copper production was contemporary with the bloomery one, even if two sites present evidence of both metallurgies.

According to radiocarbon dates (section 4.3.7), the iron smelting remains were generated in later chronologies, as recently as 18th century AD. By that moment, the oxidic copper ores used in Daye had long been depleted, ~1600 years before (Huangshi Municipal Museum 1980; Wagner 1986; Zhou, B. et al. 1988; Huangshi Municipal Museum 1999), and copper extraction relied on sulphidic ores, typically involving tall furnaces (dalu 大爐) to smelt and smaller furnaces (xiaotonglu 小銅爐) to convert matte (the same names of dalu and xiaotonglu also refer to blast and puddling furnaces for iron production) (Wagner 1995, 72; Cao 2012, 76-101). From the late 17th century, it seems that the smelting of polymetallic ores rich in copper and lead was a common practice, as well as sophisticated operations such as liquation of copper-silver alloys (Needham 1965; Sung 1966; Tsuna 1983) (Figure 7.20). A final piece of relevant information is found in the historical sources, where Daye is listed in the Yuan, Ming and Qing Dynasties as a source of iron minerals (haematite), but there is no mention to copper mining (Golas 1999, 62-67,153-163). The Qing administration extended a monopoly on copper mines and coinage since copper was considered a natural resource significantly more strategic than iron, essential for the functioning of the economy (Cao 2012, 25). Thus, if copper resources were exploited in Daye during the mid-Qing Dynasty, these would have been registered in the imperial records.

Figure 7.20: Illustrations showing the smelting of copper in China during the 17th-18th centuries according to historical sources.
Left: Smelting of an ore containing both copper and lead; molten lead (left) and copper (right) flowing out from two separate holes, original illustration from AD 1637 (Sung 1966, Fig. 14-16). **Right:** refining of black copper in Japan in the 18th century, based on the Chinese technique, original woodcut illustration from AD 1801 (Tsuna 1983, plate VII).

Thus it is obvious that the analysed assemblage of Daye does not fit into the most common process of smelting copper in the Qing Dynasty: the smelted ore was oxidic, there is no evidence of a multi-stage process, and we would expect for such an important production to appear in the historical sources. Therefore, copper production must predate bloomery iron, as is also suggested by the stratigraphy. Based on archaeological evidence, comparison with Tonglüshan materials, and domestic pottery the most suitable scenario is a long-rooted tradition of smelting oxidic copper ores with iron oxide fluxes during the Western Zhou and Spring and Autumn periods (1046-475 BC).

7.4 Incipient states and organisation of production

Costin (2005, 1064-1069) proposes five dimensions to explore the links between technology and organisation of production, including: standardisation and variation, efficiency and labour investment, control over production, output and specialisation, and technological complexity. Unfortunately, variables such as labour investment, output and specialisation cannot be approached reliably with the available data. To approach the time

or human energy required per smelting cycle, or the degree of competence of the workers, it is necessary to understand e.g. the number and capacity of the furnaces per site as well as the time span of the activities, but none of this information is known. Nonetheless, as seen in section 7.2.4, the efficiency of the process is notable, and the technological complexity seems to be well controlled by the Daye smelters.

Following Costin (2005, 1065-1068), controlling for assemblage size and the size of the consuming population or region is critical to enable an assessment of the organisation of production. In general, production becomes more standardised if there is a low number of producers involved. When the artisans employed a controlled set of tools and materials, fixed and routinised practices; then the produced assemblage will show reduced variation.

This controlling model of production fits well with the ordered political and social structure of the Chinese administration and the character of bronze as a major industry already in place in the Middle Shang, with a small number of bronze makers concentrated in enormous workshops controlled by the administrations of the Shang and Zhou periods (Chang 1980b, 151; Xu & Linduff 1988, 19; Li, X. & Liang 1996; Zhou, W. et al. 2009; Liu, S. et al. 2013). The metallurgy of bronze required an important effort by the administration to coordinate those who procured and converted the raw materials (miners and smelters) with those that processed them (metallurgists and clay workers for the casting moulds). This coordination included the creation of infrastructures that connected the smelting sites – typically closer to the mines – with the large scale foundries closer to the consumers; the establishment of a set of technical and cultural criteria to ensure standards of quality of the final product; the management of skilful labour force to develop the tasks, and a network of merchants and entrepreneurs to trade with the goods (Chang 1980b, 233; 1980a; Fong 1980, 36; Xu & Linduff 1988, 311-318; Liu, L. & Chen 2001; Chang 2005; Falkenhausen 2006, 401-420).

During imperial times, each administration took even closer control of the copper production, establishing offices to regulate mining and smelting, and ultimately monopolised copper mining and the minting of currency (Pirazzoli-t'Sertevenst 1982, 70-74; Ebrey 1986, 608-648; Cao 2012, 25; Watt 2004). Consequently, considering the importance of the bronze industry in ancient China (chapter 1) and specifically the Tonglüshan mine as a major source of copper during the first millennium BC (Huangshi

Municipal Museum 1980; Zhu, S. 1986; Zhou, B. et al. 1988; Golas 1999, 62), the most logical scenario is that the smelters of Daye formed part of this economic structure, and thus the standardised production would be orchestrated by the Zhou administration.

During the early Shang period the political authority radiated outward from a polity's capital, 'petering out fairly quickly as distance from the capital increased' (Falkenhausen 2006, 406). The Shang organisation was characterised by a network of walled towns in hierarchical interrelationship in which the Shang sovereign was responsible for granting the title to the township and land that supported it to the ruling lord, which in return recognised the king as sovereign, contributing with services and grain (Chang 1980b, 210) (Figure 7.21). There was not a centrally administered bounded territory but multi-centered points of development under cultural spheres of influence framed within an exchange network of multiple regional centres (Li, X.-J. 1996-97; Falkenhausen 2006, 406; Chen, K. et al. 2016, 667). This flexible model implied the important concept of *domain* as a territorial unit in which the king was entitled to a share of all its products and labour force (Chang 1980b, 216). In the case of Panloncheng, rank 3 in the four-tier hierarchy of the Shang cities, the key material resources were salt and copper metal, likely at the same level of importance as its political role as an outpost of the Shang territory (Chang 1980b, 303; Flad & Chen 2013, 125; Yuan 2013, 332).

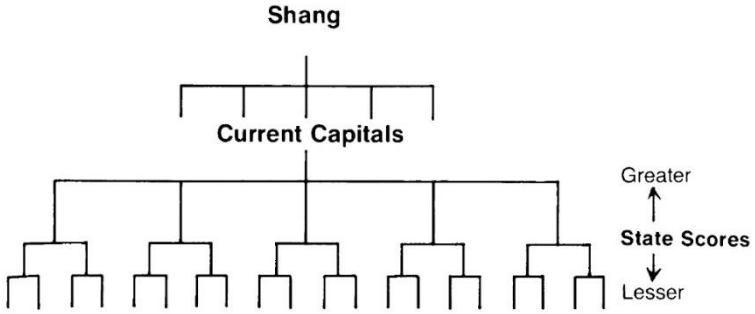

Figure 7.21: The hierarchy of the Shang state network.
After (Chang 1980b, Fig. 53)

During the Western Zhou this upward and centripetal flow of economic resources basically remains the same, except that instead of towns, corporate lineages attached to a polity ruled as feudal lords within their territorial boundaries (Falkenhausen 2006, 406).

The main difference between the Zhou with the Shang in terms of organisation remains in the institutionalisation of the administration – the Shang was an agnatic system whereas the Zhou set into bureaucratisation and 'professional' officers (Xu & Linduff 1988, 227). The appearance of local administrations, however, does not alter the feudal system. On the one hand the bureaucratic organisation consolidates late, during the Eastern Zhou (770-221 BC). On the other, the main obligations of the Zhou officials were to act in sacred functions, as diviners and priests, and also as recorders and historians, but without other specific assignments. There are only vague mentions of supervision of production with references to rice crops and granary management, but there is no specific mention to mining or copper metallurgy, and the only described function of the administrative supervisors of the bronze making foundries was the coordination of the different tasks (Xu & Linduff 1988, 241; Falkenhausen 2006, 415).

The possibility of a tight supervision from the distant Zhou capital in Haojing (now in the southern part of Xi'an, Shaanxi Province, ~900 km from Daye) seems highly improbable and the control – if it indeed existed – was surely limited to an administrative supervisor to ensure quotas of production and standards of quality (Falkenhausen 2006, 416). In all probability the internal organisation of the production, planning and distribution of the tasks, timing, technological features utilised, etc. were formulated by the smelters themselves and not dictated by external civil servants. This statement would seem somehow contradictory, since on the one hand the current data is indicative of a decentralised production system whereas, on the other hand, the limited variation in the smelting assemblages is suggestive of some form of overarching organisation. The likely explanation is that the smelters' communities formed a single unity, in close contact with each other, forced perhaps by geological necessity since they exploited the same ores whose outcrops are in close proximity (Figure 7.19). The scenario suggests that, in Daye, the standardised production was not dictated by a political entity but resulted from 'rational economising' principles and their consequences, as formalised in Ricardo's Law of Comparative Advantage. In essence, Ricardo's Law states that it is not worth producing a certain commodity yourself if you are better off producing another commodity and obtaining it by exchange; in other words, that specialising is generally more economical. Therefore, it may be suggested that people in Daye acted in terms of cost and benefit,

with this balance playing a more important role than the political administration (for discussion of Ricardo's Law in relation to prehistoric smelting communities, see Shennan (1999)).

By the fall of the Western Zhou, the Middle Yangtze became the core area of the Chu polity, one of several bronze-producing peer polities around the Central Plains that would later consolidate as a state and collide with the four other major powers – Qi, Song, Jin and Qin– during the Warring States Period (Zhang & Fan 2003, 37; Flad & Chen 2013, 108). The Chu brings the first real political integration of the territory by means of an expansionist and militaristic approach during the Spring and Autumn period, especially during the 6th century (Figure 7.22). The fortification of the settlements of Ewangcheng and Wulijie close to Tonglüshan during this period seems to be related as well with the intensification of metallurgical activities, with titles such as 'smelter officer' appearing in historical sources, and it is during the Warring States that the individual state governments become also directly involved in the administration of iron production (Peters 1999, 103; Wagner 2001c, 7; Hubei Provincial Institute 2006; Zhu, J. & Xiong; 2006, 310; Flad & Chen 2013, 189-190; Xiao 2014).

The goods deposited at the cemetery of Sifangtang, believed to be the cemetery of the miners that worked in the ore-deposit number VII of Tonglüshan mine, have been taken to suggest that the cemetery was 'majorly influenced by local Yangyue culture and slightly the Chu culture' (IA CASS 2016). The cemetery was in use during the Late Western Zhou and the Spring and Autumn periods. A very likely possibility is that, during this period, the area of Daye was controlled by a small polity which established a system based on 'small scale' autonomous production units, some of them perhaps built upon already pre-existing productions. Later, once the Chu state was firmly consolidated at the beginning of the Warring States period (476-221 BC), the Chu administration would assume a more rigid control over the production, by concentrating the smelting places in the immediate surroundings to the main mine of Tonglüshan, introducing or promoting technological improvements to increase the production, and fortifying the cities surrounding the mining and smelting complex to protect and control the copper wealth.

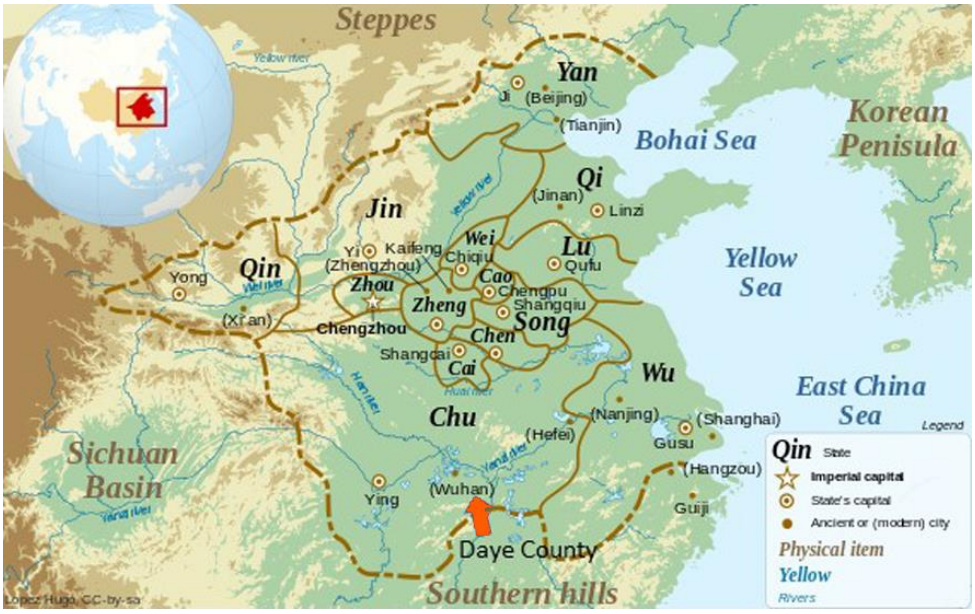

Figure 7.22: Map of the Chinese Plain in the Late Spring and Autumn period showing the location of Daye County (orange arrow) at the south boundary of the state of Chu.
Image courtesy of https://commons.wikimedia.org/w/index.php?curid=15585702

All in all, there is little to suggest any strong political control of the copper metallurgical activities recorded in Daye until the Warring States period. Thus, in all probability, the uniformity observed in the studied assemblage is more likely a by-product of communities of practice than consequence of the organisation of production (Costin 2005, 1065). The technological procedure was employed and repeated in all sites because it was considered the most adequate for the extraction of copper by means of the available resources. In parallel, the standardisation observed at the technological arena suggests that they obviously shared their technology, and formed part of a wider complex community for which they were producing metals. This does not imply necessarily that the smelters were craft-specialists who engaged full-time in order to earn their livelihood, but it can be a case of *site-specialisation* where localisation of production does occur but in simpler circumstances (Muller 1987, 15). This model has been proposed for small size societies who had not reached a true state of political organisation, and where the elites coordinate the exchange between different localities within a society. These localities exploited spatially concentrated resources but held slight social differences where lineages or similar groups within the society probably controlled most production and local distribution of goods (Muller 1987). Applied to Daye, the most likely scenario is that these

were ruled by statelets comprising individual walled towns and a nearby hinterland of dependent households which, regardless of their small sizes, still had multi-directional connections with distant regions, by means of the production of copper – the main ingredient for bronze which had an extraordinary social and political significance – from one of the major mines existing in China (Chengyuan 1980; Huangshi Municipal Museum 1999; Flad & Chen 2013, 109; Chen, K. et al. 2016). Therefore, following the case of Daye, copper extraction during the Shang and Zhou period till the Warring States would be based on a regionalism model of production and not on a centralised one. This is in stark contrast with the case of bronze production that is suggested to be strongly controlled by the political administrations (Chang 1980b, 233; 1980a; Fong 1980, 36; Xu & Linduff 1988, 311-318; Liu, L. & Chen 2001; Chang 2005; Falkenhausen 2006, 401-420).

The existence of indigenous metalworking traditions that worked autonomously but in contact with the Central Plains has been pointed out before for the early stages of Chinese metallurgy (Underhill 1996-97; Chen, K. et al. 2009; Mei et al. 2009; Chen, K. et al. 2012; Chen, K. et al. 2016). It is suggested that the core-periphery expansionist model from the Central Plains oversimplifies the complicated interaction network linking the many different regions, and that in fact this was more likely a net of multi-directional connections with mutual influences (Chen, K. et al. 2016, 672).

Notwithstanding the evidence for the circulation of metalwork, the manufacture of bronze artefacts by the same piece-mould casting technique, and their use to perform comparable rituals, we should be cautious not to overstate these shared traits as synonyms of uniformity, political expansion and cultural assimilation. It is clear that a more complex metallurgical structure existed between different cultural regions within or without the Central Plains; differences that are evident e.g. in the accessibility to raw materials, choice of alloys or performance of specific techniques. This structure based on the existence of multiple centres challenges the traditional model of the spread of the Chinese civilisation from a central core (Li, X.-J. 1996-97; Linduff 2000; Mei 2009a; Mei & Linduff 2009; Linduff & Mei 2014). In this vein, it is perfectly plausible that there was no superstructure of political control from a central administration over the smelters of Daye during the suggested chronology, but rather smaller and more flexible polities that shared

the bronze cultural identity with economic interest in the exploitation of the copper natural resources.

Finally, several scholars point out the existence of a high degree of division of labour within the metallurgical craft in both the Shang and Zhou periods, and also point out the highly specialised workers required by the bronze industry, which agrees with the organisation of the professions by specialities and lineages typical of both kingdoms (e.g. Needham 1958, 11; Barnard 1961; Chang 1980b, 230-234; Chengyuan 1980; Fong 1980; Bagley 1987; Xu & Linduff 1988, 312; Ledderose 1998, 25-50; Sun, S. & Han 2000; Liu, S. et al. 2013). However, this statement is applied nearly exclusively to the *bronze making* industry, i.e. to the manufacture of artefacts and not to the primary smelting. Moreover, although these high rank artisans existed, there was a much larger number of unskilled (i.e. low rank) than of skilled workers, the former underrepresented in the written records (Falkenhausen 2006, 415-416).

The miners of Tonglüshan during the Eastern Zhou period (771-256 BC) are described as ‘the lower end of the commoner class definitely forced into "slave-like" conditions’ (Keightley 1969 in Reinhardt 1997, 59), based on the assumption that these would have a status similar to that of the peasantry. Peasantry is categorised as a ‘very lowly position’ submitted to the ruling bodies, not only performing farming works, but also accomplished any other labour service required by their lords (Chang 1980b, 226-227).

One of the arguments in favour of the introduction of the state monopoly on iron production in the year 117 BC is to relieve the ‘common people’ from ‘ancillary’ labours – smelting and refining of iron – so they have more time for agricultural activities, and convict labourers were employed in the iron plants instead of commoners (Wagner 2001a, 23-25). In spite of the risk of comparing copper and iron productions, especially considering the marked difference in the status of the two metals (chapter 1), it is highly significant that smelting is regarded as ‘ancillary’ and also that the commoners are replaced by criminals to work the furnaces. If copper smelting was at the same level, then the smelters in Daye were most likely fiefs of the lower rank, which perhaps carried out this task temporarily only, with smelting as a secondary enterprise. Lastly, the fact that the technological process was efficiently executed does not necessarily mean that all

workers were qualified or had the relevant *know-how*. A group of unskilled workers well instructed by one or two experienced labourers could obtain satisfactory results.

The grave goods deposited at Sifangtang cemetery confirm that there was a stratified society; in the great majority (116) of the 132 tombs, the bodies were simply deposited inside a coffin or without it, with or without daily objects as grave goods – knifes, mining tools, drinking vessels, and interestingly also pieces of iron ore and malachite. By contrast, the other tombs presented signals of a higher rank; the funerary garments are considerably more varied and sophisticated, including fine ceramics and bronze weapons, and some of the bodies were buried inside double coffins (IA CASS 2016). Therefore, based on the hierarchy observed in the tombs, most of the workers of the mine were lower class, and indeed it does not seem that they possessed a particular series of skills to perform their jobs (crushing, chopping, pumping, etc.); most likely, they were not regarded as a particular social status. We can assume the same low rank for the smelters of Daye since miners and smelters fall into the same category and frequently conducted both tasks (Ledderose 1998; Huangshi Municipal Museum 1999; Li, C. et al. 2004; Barbiery-Low 2007; Cao 2012, 84; IA CASS 2016).

7.5 Summary

The smelting remains from Daye correspond unquestionably to the extraction of two different metals: copper, and bloomery iron. These productions did not take place synchronically, but the bloomery iron was developed during the mid Qing Dynasty (AD ~1700-1800) and the copper much earlier, likely during the Western Zhou period (1046-771 BC) and/or early Spring and Autumn (770-476 BC) before the introduction of blast-type furnaces in Tonglüshan in the 6^{th}-5^{th} centuries BC.

This chronology is proposed for the copper production based on the occurrence of the archaeological remains associated to domestic pottery of the Zhou Period; the comparison with technical materials from well dated nearby sites; and the review of the historical and technical context. These parameters indicate that the assemblage is pre-imperial, with activities perhaps starting during the Shang period in the sphere of the ancient city of Panlongcheng, and predating the emergence of the polity of Chu in the

Middle Yangtze basin, which would bring major technological changes in the copper smelting traditions, most notably the introduction of blast-type furnaces. While all the sites shared a common copper smelting technique, the tradition did not remain immutable but was gradually improved over the centuries, adjusting the amount of iron oxides added as a flux to obtain a yield of copper metal cleaner of impurities.

The smelting sites were part of a complex political and economic organisation in which bronze metal was of vital importance. The extraction of copper occurred in a plurality of smallish workshops altogether producing likely at a large scale, based on the abundance of sites and volume of materials, where all the five neighbouring workshops used the same standardised smelting process, which was quite efficient in terms of metal recovery.

The bronze makers of the Shang and Zhou periods are described as professional lineages of highly specialised workers; it is argued here, however, that the smelters from Daye were, in all probability, members of the lowest social rank. They would be mostly unskilled workers that perhaps combined smelting with other activities, such as agriculture, directed by a smaller number of experienced workers who enjoyed higher social status.

Contrary to the situation described for the massive scale bronze foundries ruled by the administration, the most likely scenario is that the sites were small units, self-managed by local households without direct control or supervision from the royal capitals, and that if these officials existed, their role was limited to collecting the metal output and perhaps to verify its quality. Otherwise, copper in Daye was a regional production which was interregionally exchanged within polities of a complex multi-centered society; all of them sharing the bronze identity.

"We eat iron"

(Population of the town of Yingcheng 蓥成, Shanxi province, to a visitor in 1898)

8 Regionalism and iron production in Qing China

As chapter 6 has demonstrated, this study has revealed important new data on the archaeometallurgy of iron production by the direct method in China. Two archaeological sites catalogued as ancient copper production have been shown to develop copper and iron smelting activities – MC –, and exclusively bloomery iron – YW – (Hubei Provincial Bureau of Cultural Heritage 2002, 43,48); two uncatalogued sites were also proved to reduce both iron and copper – HF –, and exclusively bloomery iron – CX –; and one last site – LD – which was indecisively suggested as a bloomery iron smelting site was proved to be a primary smithing site as well (Wei et al. 2008; Hu et al. 2013).

Before moving on to broader issues such as why bloomery iron and how it fits in the broader picture of the history of iron smelting in china and regional trajectories, this chapter will begin by further discussing the technological production with a focus on the inter-site regularity of the by-products and the efficiency of the process compared to other relevant materials, and a general discussion of bloomery smelting recipes. This first point is necessary in order to analyse all the technological parameters in terms of cost/benefit, contextualise these technologies within the economic history of the Qing Dynasty, and discuss a number of underlying reasons that may justify the choice of the direct method technology instead of the indirect method, the traditional technology for iron reduction in China (Han 1998; Wagner 2008), which is the principal point of the discussion.

The radiocarbon dates (section 4.3.7) indicate that the most likely chronology for the bloomery sites in Daye is the 18th century. This chronology was initially a 'shock' since in that moment the working hypothesis was that the bloomery iron was much more ancient, 8th-6th centuries BC before the generalisation of cast iron in China, or alternatively from the Northern Song Dynasty (AD 960-1127) – as suggested by Prof. Chen Shuxiang and Dr. Qu Yi, from the Institute of Cultural and Historical Relics and Archaeology of Hubei

Province (湖北省文物考古研究所, 湖北武汉). However, the NERC laboratory confirmed that the analyses were perfectly correct and reliable, and that in fact the bulk of the results was very consistent. Even more, another three radiocarbon dates (included at the bottom of Table 4.2) from the bloomery iron excavated site of LD were analysed in China and indicated the same chronology.

It is during this time – 18th century – when the Industrial Revolution takes place in Europe, introducing the puddling process first in 1784, and culminating in 1855 with the Bessemer process – the first inexpensive industrial process for mass-production of steel from molten cast iron (Cipolla 1976, 212ff; Buchwald 2008, 7-8). Notably, by that time the Chinese had more than 2000 years of experience of producing steel from cast iron on an industrial scale at competitive prices (Wagner 2001a; Han 2013). The chapter ends by considering how likely it is for such a drastic technological change from cast to bloomery iron to occur in the 18th century, and explores an alternative scenario.

As in the case of copper production, this study is inevitably limited, nonetheless the available information is robust enough to document the existence of bloomery iron in China and to challenge the monolithic model of mass-production of cast iron orchestrated by the imperial administration.

8.1 Standardisation in the *chaîne opératoire*

The analysed by-products from the bloomery process are remarkably homogeneous, pointing to a common smelting procedure. This consisted in the reduction of high grade iron ores in small embanked furnaces operating at temperatures ranging 1100-1200 °C. The technical ceramics played a significant role in slag formation since the ore was not self-fluxing and no silica-rich flux was added to generate fayalitic slag.

The homogeneity of the assemblage is reflected in the hierarchical cluster analysis (Figure 8.1). In this case, in addition to the key oxides of the bulk composition with correspondence to parent material – MgO, Al_2O_3, SiO_2, P_2O_5, K_2O, CaO, TiO_2, MnO, and FeO –, some trace elements were considered as well – V, Cr, Zn, Rb, Zr, Mo, Ag, and La

– since these were argued to derive predominantly from the ore and used to discriminate between reduction and post-reduction slag. The dendrogram showing the variables (Figure 7.8 top) confirms that all the trace elements except Zn cluster with the ore (blue) while the other oxides of the slag composition cluster separately (red).

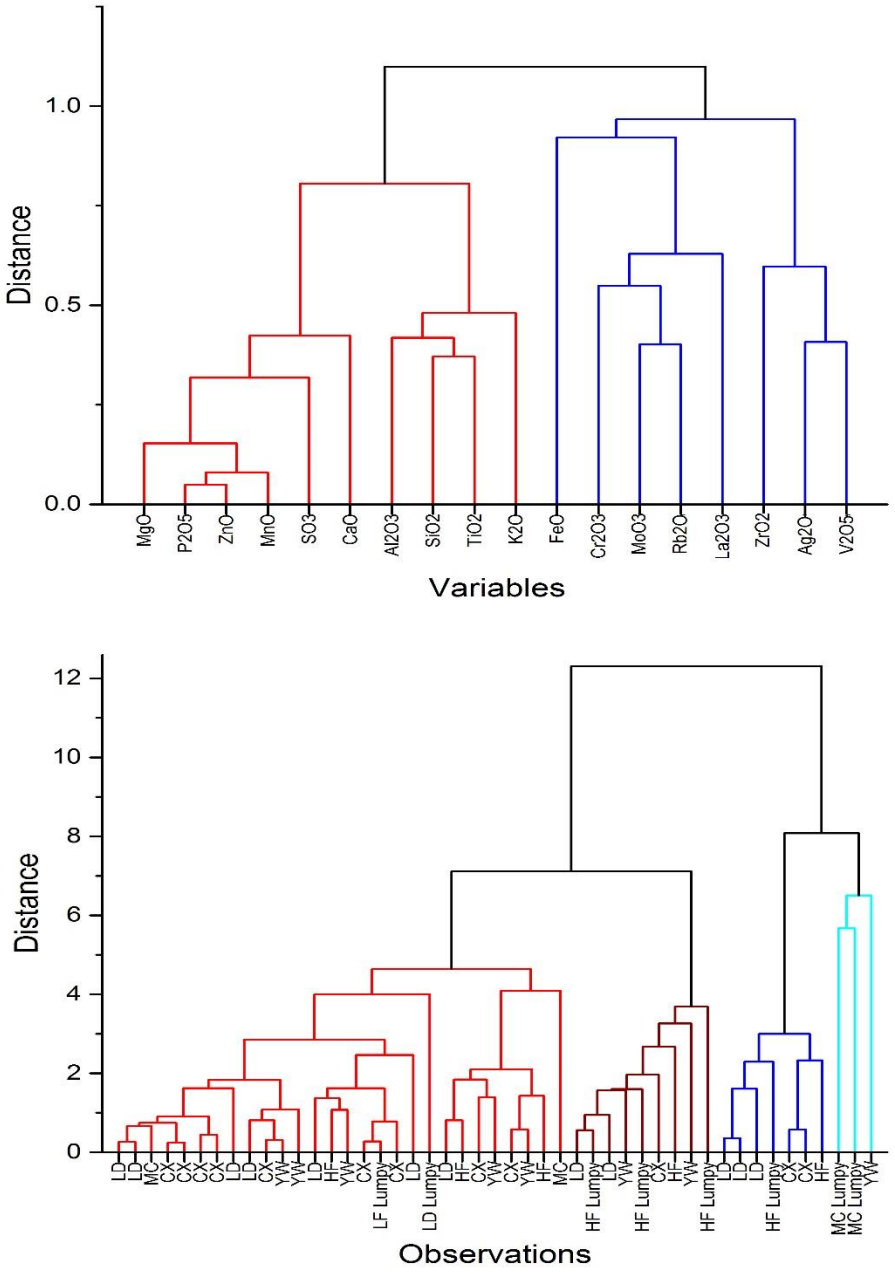

Figure 8.1: Hierarchical clustering analyses carried of the chemical composition of the Daye bloomery slag by variations (top) and observations (bottom).

The dendrogram by site does not show a clear correlation between groups and sites, showing instead high similarities among all the assemblages (Figure 8.1 bottom). This is a simple dendrogram with two main branches separating the slag that is FeO-rich (>68%, red clusters) from the FeO-poor (<67%, blue clusters). The sub-clusters distinguish between the ceramic 'rich' composition (blue) and the iron oxides rich (>73%) (bright red). The burgundy colour represents a relatively better equilibrium in the fayalitic composition with iron oxides ranging 68-71% and silica 19-22%.

As with the copper slag, a PCA was also attempted including the major elements of the chemical composition (Figure 8.2). The loading vectors show nicely the correlations among the four ceramic oxides (K_2O, Al_2O_3, SiO_2, TiO_2), negatively correlated to Fe. So slags are either rich in Fe or rich in ceramic, spreading on that line. None of the slags appear strongly dominated by ore and ash oxides, to the right. The PCA confirms the close similarities among the by-products of the different sites, particularly clear in the sites of CX, LD, HF and YW – excepting the Cu-rich outlier YW4. The variation observed in MC is not really meaningful taking into account the short size of the sample (2 specimens).

Summing up, the hierarchical cluster analysis in conjunction with the PCA confirm the similarity of the by-products that was observed by other parameters such as the analogous morphology of the slag; microstructure and mineralogy; bulk chemical composition, furnace operating conditions and furnace ceramic fabrics. The very narrow differences between these criteria indicate a highly standardised process to smelt iron by the direct method.

In order to ascertain the extent to which smelting was standardised at each site, the coefficient of variation (CV) was calculated for the slag oxides. As explained before this rationale is frequently used in archaeology to reflect the degree of standardisation of a given assemblage (section 7.2.2). The line chart in Figure 8.3 shows that the CV for the three main oxides of the composition remains low, especially the FeO. The oxides showing the most significant variation are MgO, CaO and P_2O_5 while the other minor oxides TiO_2, MnO, K_2O and SO_3 are more constant in comparison. Overall the CVs range between 10 and 40%, frequently under 20% and rarely over 40%.

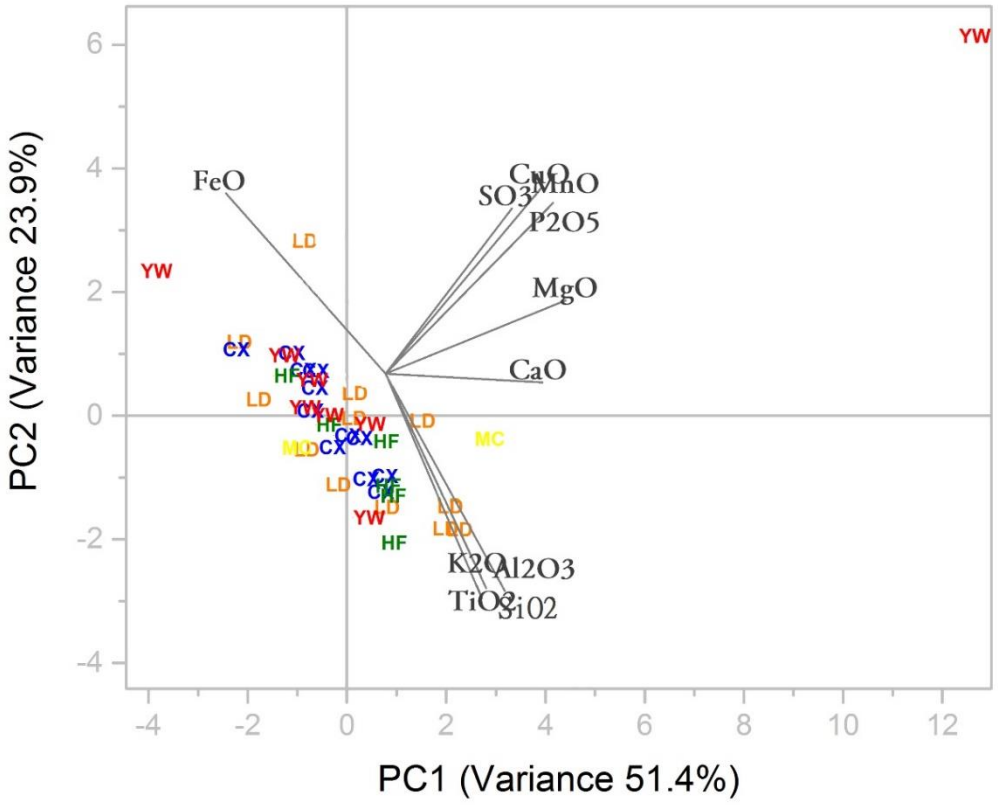

Figure 8.2: PCA plot showing the variances per site in bulk composition of bloomery iron tap slag.
First three components explain 74.1% of cumulative variance. A PCA including trace elements were also carried out but the results are broadly the same, therefore, these are excluded from the figure PCA since the plot remains identical.

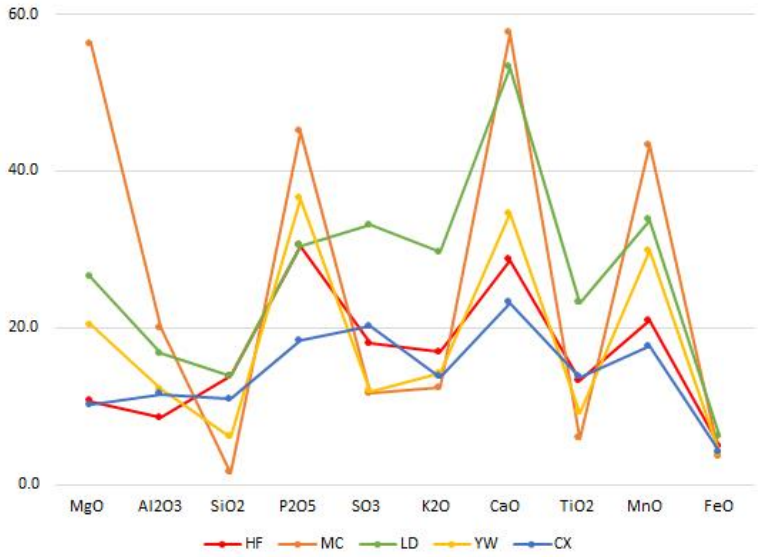

Figure 8.3: Line chart comparing the coefficient of variation of bloomery iron tap slag per site.

The smelters of CX in particular seem to have maintained very constant parameters in their smelts while in MC and LD the fluctuation is much higher. The little variation shown in the chemical composition reflects that the 'chemical lineage' – patterns of slag chemistry in terms of invention, selection, and socially mediated constraint processes – of the slag is strong, pointing out that the smelting recipe was strictly followed and thus that the process was standardised (Charlton et al. 2010, 352).

'Standardisation' is a concept frequently applied to technologies where there is regular and large-scale production, where a technology has been 'routinised' to maximise efficiency and cost/benefit (Rice 1991; Blackman et al. 1993; Costin & Hagstrum 1995). Nonetheless, in comparison with other sites, the efficiency in the reduction of metal is modest in Daye, with a lower yield than smelting sites that used leaner ores and in earlier chronologies (Figure 8.4). Therefore, even if the process was highly standardised, a large yield of iron metal was not obtained. This seems a contradiction since obviously an efficiency in the production was not achieved, and no attempt from the ironmakers to optimise their process and maximise the yield has been detected.

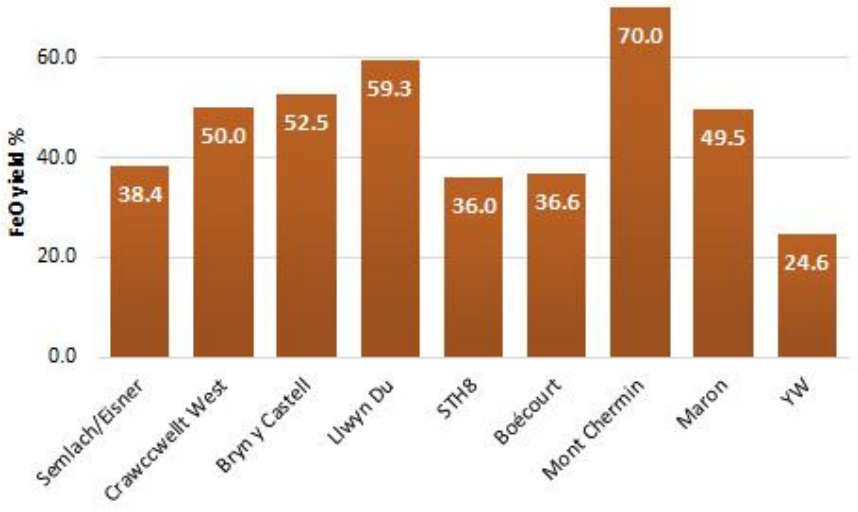

Figure 8.4: Bart chart showing the estimated iron yield of several bloomery iron smelting sites in comparison to Daye (YW).
Crawcwellt West (UK), Iron Age; **Bryn y Castell** (UK), Late Iron Age to Roman; **Semlach/Eisner** (Austria), AD 100-400; **STH8** (Thailand), AD 200-500; **Boécourt** (France), AD 400-700; **Mont Chemin** (France), AD 400-700; **Maron** (France), unknown; **Llwyn Du** (UK), AD 1300-1400; **Yanwopu** (China), AD 1700-1800. References available in Table 6.11. All data is provided by the corresponding authors using the same method of calculation (Crew 2000).

8.1.1 Bloomery iron smelting recipes

Regardless of chronology or location, the formation of a liquid slag was in the vast majority of cases the only way to separate gangue from metal in bloomery smelting (Tylecote 1962, 184; Clough 1987, 19; Rostoker & Bronson 1990, 89-100). As introduced before, since the main oxides of the chemical composition from the parent materials – FeO and SiO_2 –, and the optimum range of attainable temperatures ~1100-1200 °C are the same, typically bloomery iron and copper debris have fayalitic composition (Figure 7.1). However, in bloomery production the ratio FeO to SiO_2 in slag is much more relevant, since a lower proportion of FeO in the slag will mean that potentially more metal can be recovered in the bloom. The main point of this section is to consider that the smelting recipes were not driven exclusively by the metal output, but that other factors were equally determinant.

Rehren et al. (2007) suggest two main bloomery recipes in pre-industrial times visible in the two eutectic areas – so-called Optimum 1 and Optimum 2 – in the equilibrium diagram FeO–Al_2O_3–SiO_2 (Figure 8.5), as the most suitable engineering solutions for bloomery iron production. The key difference between the two eutectic is not in the temperature, which is low in both cases (1088 and 1148 °C) but in the different configurational parameters of the furnace and charge – that were manipulated by the smelters –, each of them marking different strategies of cost, risks and benefit. Thus Optimum 1 lies at ~50% FeO, 40% SiO_2 and 10% Al_2O_3, and has the benefit of allowing a larger yield since less FeO goes into slag, but at the cost of higher fuel consumption necessary to create stronger reducing conditions, and at the double risk of producing a pool of unusable molten high carbon steel or cast iron (if the furnace is too reducing), or of freezing the furnace (giving the steep liquidus gradients in that area of the phase diagram). Optimum 2 is situated at ~75% FeO, 20% SiO_2 and 5% Al_2O_3, which means that the metallic yield is lower than in Optimum 1. However, the cost is also lower because theoretically the slag forms faster and at less reducing conditions and thus using less fuel, which frequently was the most expensive raw material to use in the process (Charlton et al. 2010), and thus the benefit remains in the balance moderate yield/lower cost minimising the risk of producing over-carburised iron whereas the main risk is to produce only molten slag with no reduced iron. Figure 8.5 shows that the second solution was predominant in Daye.

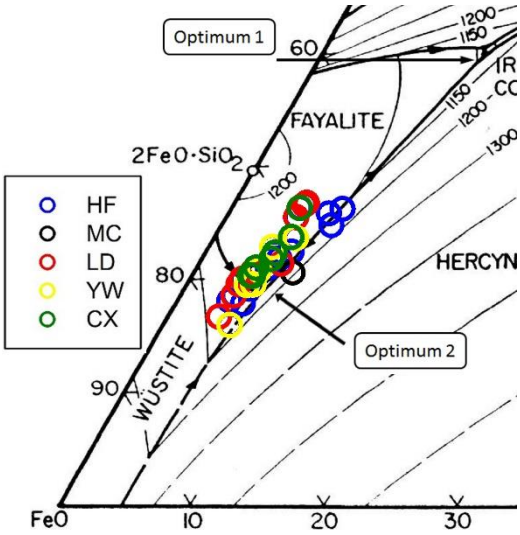

Figure 8.5: Ternary system $FeO–Al_2O_3–SiO_2$ plotting the Daye bloomery iron slag with the two eutectic marked.

A logic assumption would be that efficiency was the most important factor for the smelters to determine the smelting recipe, and that the smelters made efforts to improve their technologies to achieve the maximum metal yield. Figure 8.6 shows that, on a global scale, over time there is a gradual displacement of the slag towards Optimum 1 – the solution rendering the highest yield –, but it also shows that many slags from historical later periods – which supposedly apply more powerful technologies – plot towards Optimum 2. The ternary diagram shows that recipes rendering large metal yields were not necessarily the option systematically chosen by the smelter, and that there were other factors to determine in the election of a suitable recipe (Rehren et al. 2007; Charlton et al. 2012). Charlton et al. (2010, 353-354) define the bloomery recipe as the combination of utilised resources, furnace design, air supply mechanism and operating procedures in order to get over the constraints in iron production – namely a suitable reduction atmosphere, heat energy and adequate lengths of time – associated to a number of costs and benefits in terms of time, energy and resources where the given economic environment and the kinds of inventions and innovations adopted played a crucial role. The following section analyses the bloomery process carried on in Daye under this wider definition in order to understand their choice of bloomery recipe.

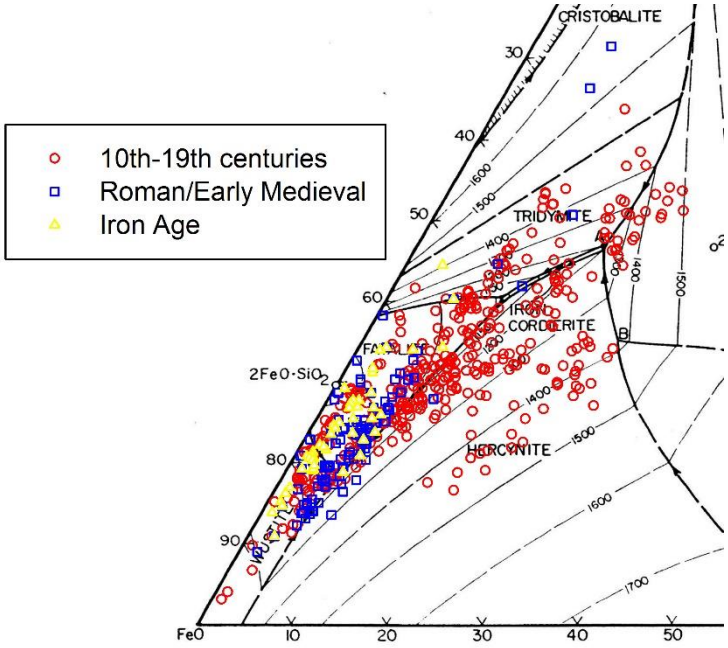

Figure 8.6: Ternary system $FeO–Al_2O_3–SiO_2$ plotting smelting and smithing bloomery iron slag from different chronologies and sites.
Data for the diagram was collected by Dr. Michael Charlton from several sources: (Morton & Wingrove 1969, 1972; Killick et al. 1988; Killick & Gordon 1989; Eschenlohr & Serneels 1991; Serneels 1993; Buchwald & Wivel 1998; Chirikure & Rehren 2004; Joosten 2004; Miller, D. & Killick 2004; Charlton 2006; Paynter 2006, 2007; Iles & Martinon-Torres 2009). The slag from Daye and from Pingnan (Guangxi) (Huang 2008) are also plotted.

8.2 Contextualising efficiency

As detailed in chapter 6 all the main ingredients necessary for bloomery production were available in Daye County: haematite and magnetite are still nowadays widely available in the area (Zhao et al. 2012); the same for local clays for furnace construction (section 6.2); and timber for charcoal was still available in Southern China during Ming and Qing Dynasties (Wright 2007).

The discussion begins summarising the technical findings detailed in chapter 6: utilised resources and facilities necessary for the reduction (ore, fuel, technical ceramics, embanked furnaces, air supply). Secondly, the *châine opératoire* is reconstructed and the technical parameters are analysed in terms of cost/benefit.

8.2.1 Ore

As mentioned, the Tonglüshan metallogenic belt is one of the most important mineral deposits in China, rich not only in Cu and Fe but also in Au, W and Mo, the latter ones exploited only from current times while the exploitation for Cu started most likely during the 2nd millennium BC (Xie et al. 2011; Zhao et al. 2012).

In general, the Fe-rich minerals correspond to high grade ores of magnetite and haematite, and these were exploited during the Song, Ming and Qing Dynasties (AD 960-1912) – if not earlier – as registered in historical sources and also documented archaeologically with several iron smelting bowl furnaces dating to the Song period (Huangshi Municipal Museum 1980; Zhou, B. et al. 1988; Golas 1999, 153-163). The analyses of the ores reveal that these range between 78-95% FeO content (section 6.3), and thus very suitable for bloomery smelting (Rostoker & Bronson 1990, 92; Buchwald 2005, 93).

However, these very pure ores are known to be difficult to smelt, the complication given by the fact that these are less permeable than porous, fine grained ores – such as e.g. laterite or bog ores –, and they do not readily allow carbon monoxide, the reducing agent, to access the inner parts of the typically massive grains (Miller, D. et al. 2001, 414; Killick & Miller 2014). Roasting and crushing the ore is necessary to avoid this complication. Whereas there is no evidence of roasting, iron ore powder was found in abundance during the excavation of Lidegui, and thus it is conceivable that the ore was roasted prior to crushing and powdering (Hu et al. 2013).

8.2.2 Fuel

Extensive use of coal as a substitute of charcoal happened in China during the Song Dynasty (~AD 1100) when deforestation became a serious problem to make charcoal (Needham 1958; Hartwell 1967; Wagner 1996, 317; Golas 1999, 195). Metallographic studies of iron artifacts confirm the use of coal for iron smelting since coal leaves many sulphur impurities (Liu, S. 2015, 321, and literature therein). Coal for other metal productions – copper and zinc – is also documented after the Song Dynasty (Cao 2012, 80; Zhou, W. et al. 2014).

This, however, does not mean that charcoal ceased to be used. As matter of fact, 'coal was rarely used in blast furnaces in Sichuan' (Wagner 2008, 26) to avoid the sulphur contamination, and it has been pointed that the use of coal is a geographic circumstance related to deforestation. Thus, in North China, heavily deforested, coal was the main fuel whereas the forest resources of South China allowed making charcoal and the use of coal was much limited (Golas 1999, 196; Wright 2007). Thus, the use of charcoal in Daye during the late Qing Dynasty is not surprising since this was more desirable than coal or coke in terms of contaminants, and was still the main fuel in some regions of China (Craddock et al. 2003, 46; Wagner 2008, 331-334; Cao 2012, 96). One disadvantage of the charcoal, however, was the high cost: for base metals Cu and Fe in 17th-18th centuries China, charcoal was more costly than the ore (Cao 2012, 91; Liu, S. 2015, 233), and firewood is needed for roasting too, thus adding to the expense.

8.2.3 Technical ceramics

The technical ceramics of the bloomery furnaces are made of local clays, in fact the same local clays that were used for the copper furnace walls some ~2500 years before, although in comparison the paste preparation for the bloomery furnaces seems less careful resulting in poor refractory ceramics with low alumina content, and temper of iron oxides – likely tailings from the ore – that flux the ceramic body. As a result, no less than ~8-10% of the furnace walls of the furnaces were consumed per smelting cycle obliging the smelters to continuously refurbish them and even build new facilities upon old structures (section 6.4.3).

Whereas it is argued that this was an intentional practice necessary to generate molten slag due to the non-self-fluxing ore, it is somehow surprising that the smelters preferred this solution instead of building more robust structures and fluxing the charge with ceramic, as for example has been documented for the Early Iron Age in Rwanda (Craddock et al. 2007), or at least sacrifice only part of it as is the case of the tuyeres of the Mafa furnaces in Cameroon (David et al. 1989; David 2014). These techniques would have likely allowed them for a better control of the process, possibly increasing the yield, since it is

easier to calculate more accurately the amount of silicates necessary to create the slag, and thus sacrificing less iron into it.

As seen in section 7.3 there were examples in the very Daye county of much more solid furnace structures of walls constructed by a mixture of clays including the highly refractory kaolin (Wagner 1986; Zhou, B. et al. 1988) (Figure 6.30), but obviously the iron smelters did not follow that tradition. In fact, the constructive materials are unexpected in this late chronology (~AD 1700) since stone and not clay was generally the main material to construct furnaces after the Tang Dynasty (ending in AD 907), and more carefully selected refractory clays – e.g. lined with finery powdered charcoal, sandstone, etc. – and bricks were the materials to construct blast furnaces in several parts of China during the 18th century (Wagner 2001a, 2001c, 2008; Liu & Yue 2011 in Lam 2014, 524; Huang, X. et al. 2015).

8.2.4 Furnace structures

Similar solutions to the embanked furnaces found in Lidegui were widely in use in Eastern Europe during early medieval times (Pleiner 2000, 75-77). These ironworks were based on batteries of permanent furnaces, set alongside one another with their furnace arches all facing in the same direction (Figure 8.7). Typically they were cut into soil banks so that the natural soil well-protected and insulated the structures. The shafts were cut out of the clay block and their front walls modelled in clay, thus the features were easy to repair by replacing the internal lining. According to Pleiner, such units of bloomeries with embanked furnaces 'give the impression of having been carefully planned enterprises […] they clearly represent an intensive mode of iron production' since the large number of structures allowed to always have furnaces in operation, in waiting, and under repair at any given time (Pleiner 2000, 76). It has been estimated that a bloomery of 20 embanked furnaces would have a minimum capacity of production of 6 or 7 tonnes annually, based

on reasonable numbers of producing 5 kg of iron per smelt and a total of sixty smelts per year (Pleiner 2000, 75)[2].

The embanked furnaces of Lidegui, however, exhibit certain precariousness in comparison with the Slavic complexes. Firstly, the construction perhaps was not so carefully planned in Lidegui since the structures are grouped rather than aligned and frequently have the forehearths opposite to one another instead of facing the same direction and thus precluding a simultaneous operation, which anyway would be quite difficult to achieve in such a confined space (Figure 8.7).

Another weakness of the Lidegui furnaces is the size. The typical thin walled shaft furnaces of Roman and medieval times found in archaeology measure 50-60 cm of diameter or more (Tylecote 1992, 47-94), but 60 is the maximum shaft diameter in Daye, whereas the regular dimensions of the European embanked furnaces of the medieval period range between 1 and 1.5 meters (Pleiner 2000, 75-79). Thus, the furnaces of LD appear to be too small in comparison: the complete structure has a rectangular shape of 80-90 cm long and 60 cm high, with a funnel-shape shaft of ~50 cm high, 35-60 cm diameter at the top and 20-34 cm at the bottom (section 6.2) (Figure 8.8). These dimensions are an obvious limitation for a large capacity of production. Making a rough calculation of the volume of the shaft – the volume calculated as an inverted cone, radius 18-30 and height 50 cm – this ranges between 17,000 and 50,000 cm^3, whereas the volume of an European embanked furnace with cylinder-shape shaft rounds 1,000,000 cm^3 (radius 50 and height of 150 cm).

[2] Note that the descriptions of 'large scale', 'intensive production', etc. are meant for the Early Middle Ages (8^{th}-10^{th}) in the context of the recovery of the European ironworks after the strong contraction of the iron market followed by the collapse of the Roman Empire.

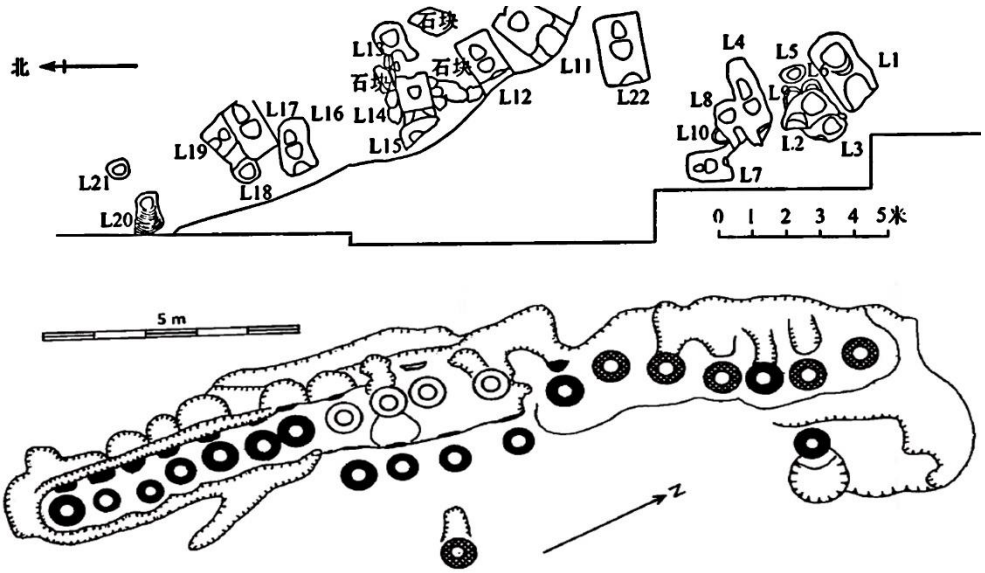

Figure 8.7: Comparison between the plans of the embanked furnaces of Lidegui (top) and Želechoviche (Moravia).
Želechoviche bloomery furnace system of the 9th century AD; empty circles represent furnaces devastated during the function of the plant, replaced by a second line of the furnaces. Želechoviche after Pleiner (2000. Fig. 17), Lidegui after Hu et al. (2013, Fig. 2). (石块 bedrock, 米 meter, 北 north).

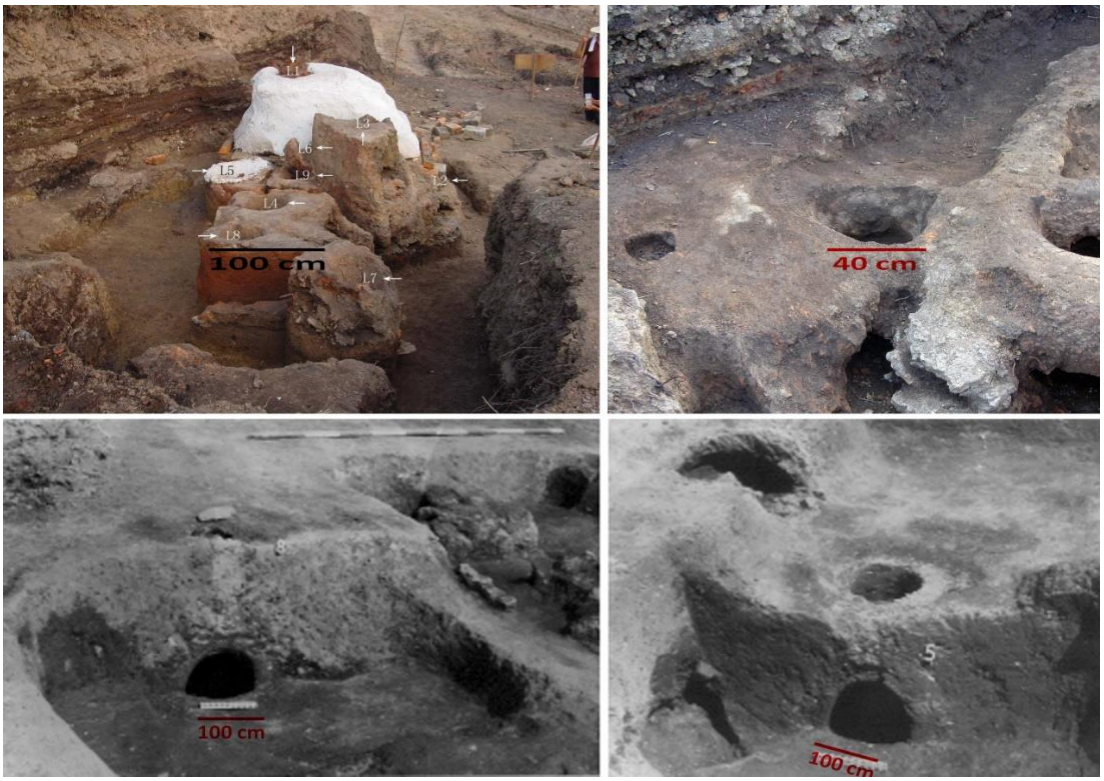

Figure 8.8: Comparison in alignment and dimensions between embanked furnaces from Lidegui and Szákony (Hungary).
LD furnace pictures (top) courtesy of Professor Chen Shuxiang. AD 1000 Hungarian furnaces from Pleiner (2000, Plate XVIII).

8.2.5 Air supply

The rate of air supply to a fuel bed is the primary control over the rate of generation of heat and the performance of the furnace, and thus it is essential for all smelting operations (Craddock 1995, 174; Rehder 2000, 74). A major contribution of China to this matter is the invention of a compelling air supply mechanisms: the double-acting piston bellows in use by the 4th century BC (frequently referred simply as windbox, *fengxiang* 風箱), and also notable is the early application of hydraulic power ~1th century AD (Wang, L. & Robinson 1971 135-155; Wagner 2008, 22-25). The windbox provides a continuous blast in a stable way since at each stroke, while expelling the air on one side of the piston, it draws in an equal amount of air on the other side (Figure 8.10).

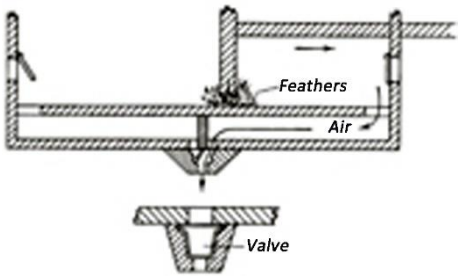

Figure 8.9: Longitudinal section of a Chinese double-acting piston mechanism.
After Wang, L. and Robinson (1971 , Figure 427c).

The significance of the invention is considerable since it allowed the early production of cast iron in blast furnaces, and since then the windbox – both in its double or single-piston version – has been widely utilised in any industry requiring high temperatures, with many examples in written sources (Needham 1958; Sung 1966; Barnard & Tamotsu 1975; Wagner 1999) (Figure 8.10).

The embanked furnaces of Lidegui, however, were designed to host another type of air supply system, most likely small bag bellows accommodated in the bellow pit connected to the tuyere hole and operated by a single person (since there is no space for a larger mechanism) (section 6.2), thus ruling out as well the possibility of a hydraulic blowing-engine.

Figure 8.10: Blast furnace with a box bellow attached operated by two workers.
The cast iron is poured into a pit and from this into a square ditch where other workers throw earthen materials and stir the batch with wooden sticks to burn out the carbon and produce wrought iron. Original illustration from AD 1637 (Sung 1966, Fig. 14-10).

8.2.6 C*hâine opératoire* and efficiency of the technical process

One can assume that the first operation after mining and beneficiating the ore involved the roasting of the ore which was afterwards crushed into fine powdered grain. The charge most likely consisted of blended iron ores (medium and high grade haematite and/or magnetite) and charcoal as reducing agent. The furnace atmosphere was suitably reducing, ranging between $10^{-12}/10^{-14}$ atm, following the range of temperatures in which slag was generated (1100-1200 °C) (section 6.4.2). The latter is iron-rich (>70% FeO) fayalitic and well molten slag, which typically presents abundant dendritic wüstite. The slag also presents very scant and tiny sub-angular or sub-rounded iron particles (≥10 µm) which indicate that the process took place in a low bloomery furnace (section 6.1).

These particles are ferritic iron and thus the result of the smelting was presumably a bloom of ferritic iron. However, occasionally iron with higher carbon content – pearlite – was generated as is visible in the droplet shape particles and crystal structure of a few

specimens (section 6.1.5 and 6.1.6). The appearance of these carburised iron particles is a common phenomenon in bloomery smelting and typically is beneficial for the process since liquid or semi-liquid particles would travel through the slag more easily than in the solid state to coalesce into the bloom, however, occasionally this was a problem generating lumps of unwanted hypereutectoid steel (~1.4-1.6% C). The bloom was refined at the smelting site as demonstrate the presence of a calotte and several smithing slag lumps, and also by the discovery of two bars of iron ready to forge in the excavated site of Lidegui (Hu et al. 2013).

The furnace devices are of the embanked type. Embanked furnaces were frequent in bloomeries of early medieval Europe as devices designed to produce on a large scale, as seems to be as well the intention in Daye, since a battery of 23 furnaces was found in one of the sites. Nonetheless, this large number of structures may not have rendered a large metal yield, with the mass balance calculation estimating a modest maximum yield of 19% iron metal per cycle, thus ~19kg per 100kg ore while the average of the comparative studies is 35kg per 100kg ore (section 6.4.2.1). This low yield was consequence of three main choices: 1) not building a taller furnace with more capacity to hold the batch and more space for the gas to circulate; 2) not controlling more effectively the charge composition by adding silica flux instead of relying exclusively in the contribution of the furnace walls, and 3); not moderating the tapping regime to allow more time for the reduction and facilitate the movement of metal particles to coalesce into the bloom. For the last parameter, however, it can be argued that virtually all the reduced iron coalesced into the bloom since the iron particles trapped into the slag are scant and tiny.

8.2.7 Cost/benefit in the smelting operations

To conclude, a significant labour force and time engaged in the production was required to develop the volume of activities documented in Daye, yet the efficiency was low. For the sake of comparison, a single traditional Chinese small blast furnace was capable of producing ~600-1200 kg of cast iron per day working for 6-7 days without requiring a repair, and it was easily handled by just 2-3 people (Wagner 1997, 18).

The small productivity per site is a conceivable reason to explain the relatively high concentration of bloomeries in Daye (Figure 8.11), and it suggests that there was no technological knowledge or incentive to build more productive facilities; it also suggests that the demand for iron was a relatively small market, likely the immediate local market, i.e. the local community.

Figure 8.11: Location of the bloomery iron smelting sites in Daye County.

Charlton et al (2010, 357) have hypothesised that bloomery slags with low fuel to ore ratios and chemistry close to Optimum 2 'would be favoured in economies where there is little competition and the demand for iron is relatively low'. This could be a possible explanation for the apparently not too efficient process in Daye. During the Qing Dynasty there was a generalised increase in the demand of iron that the imperial production could not satisfy, and to the point that China started to import raw iron from Western producers (Wagner 1997; Broadberry et al. 2014). Therefore, a likely explanation is that in Daye they resolved to produce their own iron, and thus there was no market pressure since they were producing for a small market.

This context also provides a potential argument to explain why iron was produced by the direct method instead of by the indirect method, since the production of cast iron requires large investments, sophisticated facilities, technical knowledge and large markets.

Ironmaking is 'a capital intensive way to make a living and the socioeconomic environment actively selects amongst competing recipes based on the quantity and quality of iron they produce' (Charlton et al. 2010, 354); furthermore, independent workers tend to minimise the cost of production and transaction as well as the risk in the production process (Costin 1991, 17). If these elements of capital, risk, investment and market are considered and contrasted with the model of smelting process and organisation characterised for Daye, the conclusion is that the balance of cost and benefit was unfavourable and that the goods obtained were hardly competitive in an open market.

The impression is that the production system in Daye was more similar to that of a subsistence economy than of a market economy. Other factors that support the hypothesis of people making iron for themselves are the use of the natural resources immediately available in the area – abundant high grade ores, wood for charcoal, and clays – which would help save costs e.g. by making charcoal themselves instead of purchasing. The Qing state established a tax relaxation policy on the land, and did not levy handicraft factories either (see land tax in Rowe 2009), so the smelters probably did not have to pay any amount for the use of the land or permissions to carry out the industrial activity.

Finally, the production of cast iron by-products within a bloomery iron furnace has been suggested in chapter 6 as an undesirable accident, and compared to the case of the Roman smelters of Semlach/Eisner who discarded it (Birch 2013). Unlike the Romans, however, the Chinese had mastered multiple solutions to decarburise cast iron (Taylor & Shell 1988; Wagner 1989; 1996, 339-361; 2008; Han & Chen 2013), and it thus seems more significant that they did not try to recycle those lumps to be converted somewhere else. Fining would require specific installations and investment in fuel and time, and probably was not worth doing it on such a small scale, which again points out to a subsistence economy.

The following section turns to the economic context of the Qing Dynasty, with a specific focus on the situation of ironmaking, with the aim of contextualising the production in

Daye and offering a scenario that may further explain the reasons behind the bloomery model. It is acknowledged, however, that the attempted reconstruction is necessarily very crude and limited, and it is presented only to stimulate further work and discussion. Among other limitations, it only addresses (and partially) the negative aspects of the Qing administration economy but does not offer a balanced contrast with the positive assets such as the outward expansion, consolidation of the Chinese territory, or the introduction of new crops (Gernet 1999; Zhang & Fan 2003; Rowe 2009). In all probability, complete archaeological information and an exhaustive review of historical sources that are beyond the research scope and ability of this writer will reveal a much different scenario.

8.3 Economic framework: iron and famine in AD 1700s China

In 1750 a French ship berthed in the port of Guangzhou with a cargo of 30 tonnes of iron; by 1867 China imported over 7000 tonnes, and in 1891 the figure was 112,000 tonnes from several countries that were selling iron of higher quality and a cheaper price than the Chinese. By the end of the 19th century the competition with the foreign iron had ruined the iron industries of most regions within China (Wagner 1995; 1997, 7-8).

However, the decline in iron production had started before the 1700. As a matter of fact, after the peak in iron production of ~3000 tonnes as early as 1078, metals and mining remained depressed during the following dynasties, before picking up again during the Qing Dynasty (Bain 1933, 82; Hartwell 1967; Broadberry et al. 2014, 16). Despite the increase in production, in the 1700s the iron industry was not a particularly healthy sector due to several factors.

To start with, China had a serious problem of transportation which inhibited a regular supply for long distance (and even local) markets, since this only connected certain parts of the territory while most of the regions of the empire were effectively isolated (Skinner 1985) (Figure 8.12). Overall, transport was ‘dreadful’ (Wagner 1997, 9). Generally costly, unstable and extremely slow, particularly land transport that was dependent on horses, mules and porters since the state of the roads limited considerably the use of vehicles (Wagner 1997, 8; Cao 2012, 121-150), and even during the World War I context the transport was done on the backs of coolies (Wagner 1997, 77). The internal geography

played against an integrated and coherent system of communication and trading throughout the whole empire, where geographic barriers and rivers divided China into physiographic macroregions (Skinner 1977, 1985). In Skinner's model, interaction within each macroregion – e.g. flow of commercial goods, movement of people and information – was much more intensive than the inter-regional communication since most water transportation systems only connected core and periphery of each region rather than between different regions. As a result, many sub-regional systems – basically all the regions without navigable rivers or coastal areas without port facilities (Figure 8.12) – were effectively isolated from the rest of the region, had a primitive infrastructural base and were extremely vulnerable to natural or economic shocks (Skinner 1985, 286-287).

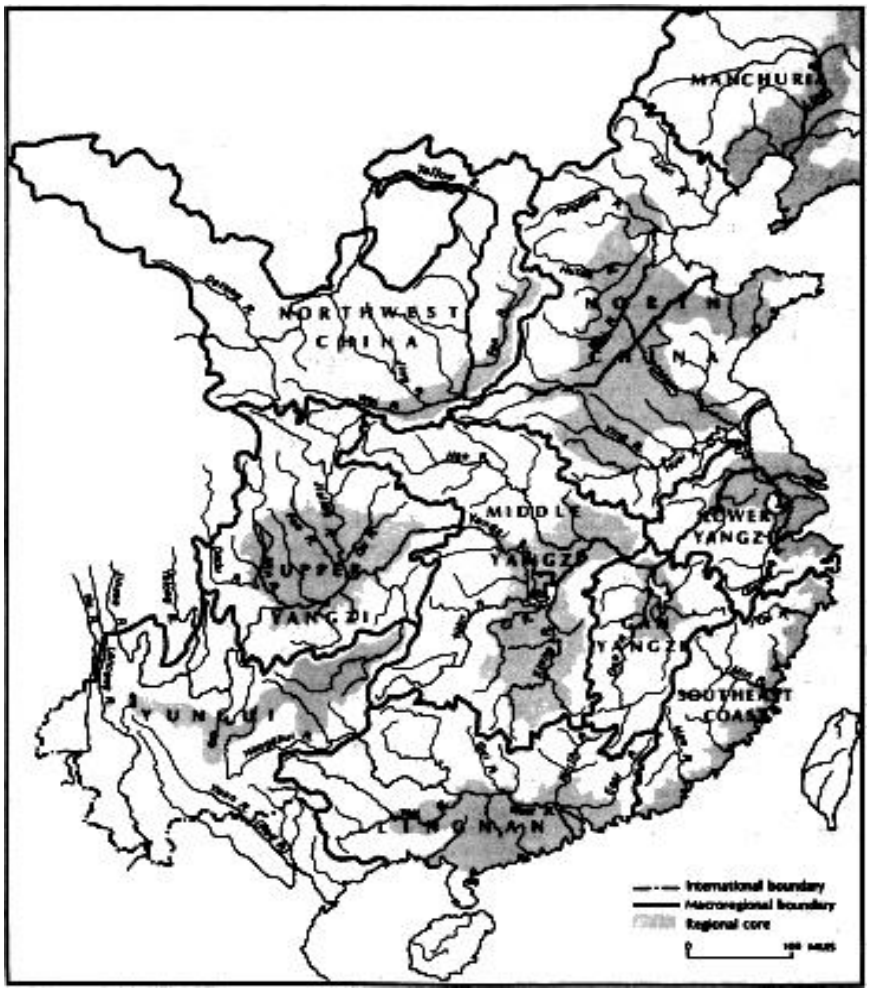

Figure 8.12: China's macroregional systems, ca. 1893, showing major rivers and the extent of regional cores.
The shadow areas are the regions where good transportation and communication is possible. After Skinner (1985, Map 1).

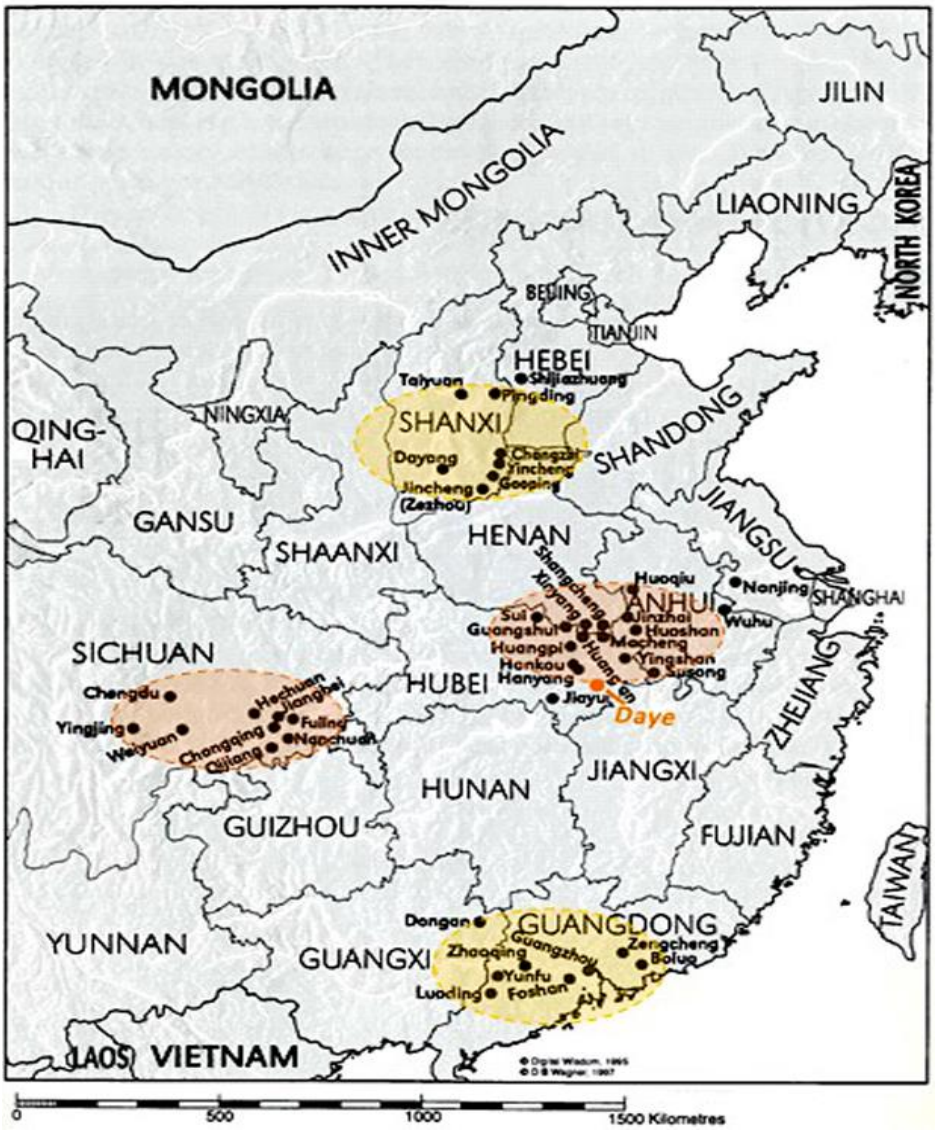

Figure 8.13: Map of China showing four iron producing areas in the 19th/20thcenturies.
After Wagner (1997, Figure 1). Daye has been added to the original figure in orange colour, and the two productions areas of which Daye was likely aware are also marked in orange colours: Sichuan to the west and to the northeast the mountain range of Dabieshan, located between Anhui, Henan and Hubei provinces.

With the exception of Guangdong – province on the South China Sea coast well connected by rivers, and open to Western contact by the ports of Hong Kong and Macao – iron mining and metal industries were located in these secluded areas. These areas produced metal for the region or province, not to export to other provinces since this was difficult, and certainly all these industries were not part of an integrated system producing iron by very

different means: e.g. using large blast furnaces in Sichuan province; small 'dwarf' blast furnaces in Dabieshan (middle-Yangtze basin); both large and small blast furnaces in Guandong; or crucibles in Shanxi province (Wagner 1997) (Figure 8.13).

The other three problems – state of the mining sectors, shortage of capital, and lack of technological innovation – are concatenated. Thus the miners and metal workers were in permanent poverty situation without the possibility to prosper or change the activity, since they were constrained to isolated areas not attractive for the investment which moved to other sectors such as profitable crops of tea, tobacco, opium, etc.; and there was no interest in innovation and search for more cost-effective technologies or initiatives by the state to provide better infrastructures, which could have presumably regenerated the metal industries and stimulated the inversion of new capital (Lin 1995; Wagner 1997; Wu 2015, 18-27). The disinterest to invest and innovate in technology is not a new phenomenon of 18th century China, but in fact goes back to the 14th century when China 'had reached the threshold level for a full-fledged scientific and industrial revolution' (Lin 1995, 271). However, China never made the technological and social shift due to several reasons, among others China had no particular interest in creating labour-saving technology since always had very large populations (Lin 1995). In addition, China had an extremely sophisticated bureaucratic system that look for maintenance and not favourable to the emergence of a mercantile class, which acted as the engine in the search for most cost-effective technologies and advanced in scientific knowledge in Europe (Needham 1964 in Lin 1995, 282). During the Ming and Qing Dynasties (1368-1912) the members of gentry families were much more interested in taking civil service examinations to enter the ruling bureaucracy – which was considered the final goal of social mobility – than to became an entrepreneur or businessman, activities that were left to the less gifted that failed the examinations, and limited their actions to administrate production quotes and salaries – typically increasing the former and decreasing the latter (Lin 1995). Moreover, this situation seems to be endemic in mines in general and in Daye in particular since the scenario described for Tonglüshan in the 1st millennium BC is identical: 'the landowner taking a rent or profit share from the operator but staying well clear of the business of mining […] investing as little capital as possible […] exploited by

rudimentary methods […] based on cheap and plentiful workforce including women and children' (Coulson 2012, 12)

The situation in other economic sectors in the 18th century was also of recession, with general long-term concerns of population pressure and underemployment, aggravated by corruption and maladministration (Rowe 2009, 153). China was substantially behind the leading European economies with significant parts of their population suffering endemic famine; this circumstance was made worse during the first half of the century by incessant natural disasters (Will & Wong 1991; Broadberry et al. 2014). The Qing administration carried out several initiatives to reverse the situation, injecting money in the deprived areas and, most importantly, encouraging migration from depressed areas to most favourable ones where the administration provided free passage, working capital (seeds and tools) and tax holydays (Deng 2015). In the Hubei province, there was a special action in 1713 named 'filling up Sichuan with the population from Hubei' and in the period between 1743-48 alone 250,000 migrants from Hubei were resettled in Sichuan (Deng 2015, 10). Significantly, contrary to other provinces that donated and received migrants, Hubei only donated. The migrant people were mostly agricultural workers that were used as unskilled labourers in construction and helpers in other industries. This group constituted the base of the society still submitted to a master-servant bond, with very low living standards and a necessity of completing their incomes with other activities, generally spinning and weaving of cotton and silk, and leading several rebellions and crises throughout the Qing Dynasty in attempts to improve their situation (Will 1990, 50-62; Gernet 1999, 465-467; Rowe 2009, 96-99, 155-157; Allen, R. C. et al. 2011).

In this context of cyclical crises, the Qing state initiated in the 18th century a timid policy of encouraging private enterprises aimed at arresting the population crises and augmenting the tax income that was frequently negative due to the unbalanced system tax income/expenses, particularly owing to the chain of natural disasters (Will 1990; Rowe 2009, 91-96; Deng 2015; Wu 2015, 25-27). These enterprises typically involved small shareholders focused on the exploitation of local sectors already active, with little or no additional investment. The Qing state had a desperate urgency to increase income in the short-term and thus did not introduce the long-term mechanisms of the capitalistic world economic system until the second half of the 19th century (Feuerwerker 1958; Wu 2015).

As a result, the administration did not try to regulate commerce or production – as had occurred in the preceding Ming dynasty –, but instead they sold rights of monopoly or oligopoly; the concessions for mining and smelting among them (Rowe 2009, 44; Cao 2012, 47ff). Even more, since finding officials with technical knowledge was problematic, most of the iron sector was not regulated and the licenses were simply dispatched (Wagner 1997, 7).

Daye County is particularly well situated from the point of view of communications, and had been exploiting iron for several centuries (Golas 1999, 155). The impoverished population of the mining sector was undermined by this policy since the state showed far more interest in revenues generated by mines than in improving the technology of extraction or the conditions of the miners (Golas 1999, 21; Li, C. et al. 2004, 26). A very likely scenario is that the wages of the miners decreased to increment the benefits of the entrepreneur who was exploiting them (Deng 2015); ores that were likely exported to Sichuan to the west or to Anhui and Jiangxi to the east via Yangtze river since no iron industry is documented in Daye (Wagner 1997; 2001, 2008). Therefore, the miners were forced to look for ways of increasing their income with side activities, turning in this case not to textiles but to transforming the raw material that they had in abundance and that was in increasing demand in the mid-18th century: iron. However, there was no similar pre-existing industry in the County and since miners were mostly unskilled workers, they developed an unusual process conceived to work on a large scale but constrained by their limitations in technical knowledge. Their model of production, however, had the virtue of requiring very small investment since the raw materials were available in the area – ore, wood for charcoal, and clay for constructions –; their furnace solution was quite cheap as well, consisting merely in cutting a furnace from the soil of a bank; and they also enjoyed the tax burden relaxation on the land that allow surpluses to be retained by ordinary households (Deng 2015, 14), being also likely that not only miners but also farmers were involved in the iron production since these would be also immersed in the crisis.

It is quite likely that the iron smelting activities took place for a relatively short period only, until migration was balanced and the growth of population reached Daye. This agrees with the impression of the excavation of Lidegui that the furnaces were in use for a short period of time (Hu et al. 2013), and with the consistency of the ^{14}C dates (section 4.3.7). For sure,

any existing small-scale iron production disappeared with the arrival of the first modern ironwork in 1889 – the *Hanyeping Coal and Iron Company* –, based in Hubei and coordinating resources from the Daye iron mines and the Pingxiang coal mines that were converted in the Hanyang iron foundry (Feuerwerker 1958, 87; Wu 2015, 106), although the most likely scenario is that the bloomery production was abandoned by ~1800, following the radiocarbon dates.

This simple small-scale labour-intense model of production which required little capital investment or training from the operatives is practically the only model of production that could arise given the economic circumstances of Daye in particular and China in general during the 18th century. In fact, this is the only production system that actually survived till the 20th century, whereas the large-scale sophisticated state-controlled processes by the indirect method went under (Wagner 1985, 1995, 1997; Craddock et al. 2003; Wagner 2008, 7-82). As a matter of fact, the Hanyeping company 'never operated successfully, being over-burdened with debt and handicapped by obsolescent machinery' (China Proper 1945, 354-355), the coal mines 'failed to deliver usable coal' due to the high level of sulphur (Wu 2015, 112), and the cartel had to close in 1908 due to the scant profitability (Liu, Y. 2010).

The motivation of mine workers for enlarging their income seems a suitable explanation for the Qing Dynasty iron smelting sites in the Daye County and explains why the smelting process was irregularly developed since it would have been run by unskilled people during a short period of time, and therefore not allowing a significant improvement of the technique via trial and error. Nonetheless, even though there was a large room for improvement in terms of technical dynamics and metal recovery, it is also true that the investment was minimal in terms of raw materials, and that the smelters found an excellent model of production – the embanked furnaces – even if they did not make the best of it, and they managed to coordinate the production in at least three – HF, LD, YW – different workshops as indicate the ^{14}C dates and most likely in five, since the other two sites – CX, MC – present very similar by-products. Moreover, perhaps the short yield per site was not a real problem either, since it was meant for an equally small market. In summary, the process can be regarded as inefficient but with a low cost/benefit balance, and therefore, suitable within the unfavourable context in which it was developed.

An additional question that arises from this investigation is why inexperienced smelters would choose a way of production – direct method – that had supposedly fallen in disuse in China in the 3rd century BC in favour of blast furnaces (Wagner 2001c). This is the subject of the next section.

8.4 Technological change or from bloomery to bloomery?

This last section of the discussion explores the possibilities of an independent 'reinvention' of bloomery iron in the Daye County in the 18th century, against the background of statements such as 'evidence known for the practice of a bloomery iron in ancient China is sparse and far from being conclusive' (Park & Rehren 2011, 1180) and 'cast iron smelting technology was the main technique within China's cultural area' (Huang, Q. & Li 2013, 333). In general, it has been accepted that cast iron was the only type of iron produced in China since the imperial monopoly of iron was established in the year 117 BC. This situation has been considered 'odd' by some scholars since 'the small-scale iron technology would have continued in use virtually indefinitely in numerous parts of the empire' (Wagner 2008, 246). However, the apparent absence of evidence for bloomery iron production would appear to confirm the first statement, and the few cases of bloomery iron documented have typically been explained as marginal productions in peripheral areas under the influence of the empire during early dynasties, when the state administration was not totally consolidated (e.g. Huang, Q. 2008).

Technological change is understood to be cumulative and integrated within a network consisting of both social contexts and the evolutionary selection of traits to be transmitted (Lam 2014, 511). Thus, it is usually distinguishable a 'lineal development' of sequences of changes resulting from rational choices which are often not 'lineal', since the technical means were selected in accordance with different social strategies, meanings, and conditions, which means that although overall there is a development, this is not homogeneously adopted everywhere and different technological solutions co-exist (Lemonnier 1993, 4; Roux 2008). An interesting idea when considering technological change is that this is understood as the result of the transportation and transmission of information and *culture traits*, a process similar to the inheritance of genes in biological

evolution. Cultural traits include the materials required to construct a product, the production tools and facilities employed, the knowledge or practices required for production, and the ways in which final products are used (Schiffer & Skibo 1987).

Applied to the case of Daye, if the tradition in the area was the production of cast iron it is very hard to understand why unskilled non-professional metalworkers would have started to use a technology of which they had no previous knowledge. Even more, 'consumption plays a key role in deciding the condition of production' (Costin 2007, 155), and thus it seems very unlikely that in Daye they started to produce a product – bloomery iron – different to the one that the consumers were expecting – cast iron –, specially taking into account that the smelting of iron was a mean to complement their scant income, and thus experimenting with a new product would seem an undesirable risk. In this view, the remaining scenario is that the bloomery technology was already known in Daye in the 18th century BC, and thus bloomery iron was practiced previously.

As a matter of fact, there is additional evidence for bloomery iron production in Daye. The excavation of Tonglüshan also revealed the presence of bowl furnaces related to iron production but much posterior to the active live of the copper mine which ended in the 1st century BC, while the iron production is dated to the Northern Song Dynasty (AD 960-1127) (Wagner 1986; Huangshi Municipal Museum 1999). As many as 17 bowl furnaces were excavated within a workshop of 320m^2; these furnaces were small (~40 cm of diameter) and the walls were relined with clay several times (Huangshi Municipal Museum 1980, unpaged) (Figure 8.14). The ceramic paste of the furnace wall was prepared by mixing powdered sandstone and charcoal with clay, and the composition is reported as 62.67% SiO_2; 10.29% FeO; 16.94% Fe_2O_3; and 3.57% CaO, although the analytical method is not reported and no specifications are given (note the very high level of iron oxide in the ceramic); it is also noted that 'the degree of relining in the furnaces is significant, meaning a high degree of corrosion during the smelting' (Zhu, S. 1986; Zhu, S. & Zhang 1986). The associated slag is tap slag of fayalitic composition (~65 FeO, 21% SiO_2), and having ruled out the production of copper, gold and silver, researchers suggested that these were by-products of puddling furnaces used to decarburise cast iron in spite of there is no evidence of any production of cast iron in Daye, and the typology of the furnace and volume of slag do not fit into this category and are not comparable to the refining devices

and debris known for the period (Zhu, S. 1986; Zhu, S. & Zhang 1986) (section 2.5.3). The main arguments to support this statement were that the slag was generated under oxidising conditions, contained some prills with high carbon content, and that the iron content in slag was very high to be a cast iron smelting slag (Zhu, S. & Zhang 1986, 473).

However, the characterisation of the slag is rather identical to typical bloomery iron slag as reported in this thesis, with glassy matrix, fayalite laths, and few sub-angular iron particles that correspond to ferrite. The main exception is that the main free iron oxide is reported as magnetite rather than wüstite, although it is acknowledged that the latter is also regularly present in the slag (Zhu, S. & Zhang 1986, 471). In the micrographs of slag provided in the paper, the free iron oxides are systematically dendrites of globular shapes, different from the angular flakes that are typical of magnetite (Zhu, S. & Zhang 1986, Figures 2-5). In addition, since it is tap slag, it wouldn't be surprising to find magnetite, particularly towards the surfaces of the slag, resulting from oxidation during cooling and hence not reflecting the furnace atmosphere. Therefore, it is my opinion that these slags were incorrectly interpreted as fining slags, perhaps based on the misidentification of wüstite as magnetite.

The puddling slag typically presents a complex intergrowth of mineral phases in the matrix in which the magnetite is frequently arranged as clusters, with large agglomerations of fayalite crystals, abundant crystals of hercynite, and – specifically diagnostic features of the puddling slag – large grains of silica and iron sulphides (Killick & Gordon 1987; Buchwald 2003). However, the tap iron slag from the Song Dynasty found in Tonglüshan lack of any of these diagnostic characteristics of the puddling slag, and the characterisation fits comfortably into the description of bloomery slag. Notably, by the Song Dynasty many blast furnaces in China were using coal as fuel (Wagner 2001b), and it would be expected more iron sulphides contamination in the slag, particularly when both local ores and coal present a high content of sulphur that provoked a serious technical complication using modern technology during the 19th century (Wu 2015, 112). The presence of the liquid iron prills can be explained simply as the result of occasional conditions in which over-carburised iron is generated within the bloomery process (section 6.1.6) whereas, in any case, the majority of the iron particles present in the slag

correspond to ferrite reduced in the solid state, as indicate the sub-angular or sub-rounded shapes.

Turning to the bowl furnace structures, these seem more appropriate to create a reducing atmosphere favourable for smelting than an oxidising one as expected for puddling; the tuyere hole is placed at the bottom rear of the structure, while the blast of air in a refining device of these characteristics is supplied from the top, and the general aspect of a fining device is that of an open-hearth that somewhat resembles a smith's forge (Wagner 1997, 24; Buchwald 2008, 559) (Figure 2.12). Notably, the small dimensions, shape of the chamber – an inverted cone –, and the multiple relining of the bowl furnace are evocative of those of the embanked furnaces of Lidegui, characterised above, and these are appropriate to create a reducing atmosphere (Figure 8.14). Consequently, it may be appropriate to suggest that those or similar structures were the cultural trait that links the Song with the Qing smelters: both of them reducing iron in small funnel-shape devices without the addition of flux, but relying on the contribution of the furnace wall, which required frequent relining, as is evident in the furnaces of both chronologies.

There are additional arguments in support of this hypothesis, since Daye county could have chosen between at least two different models of cast iron production developed in areas of which they had close contact or at least had knowledge, yet they carried on iron reduction by the direct method. In the late 18th, 19th and early 20th centuries the iron industrial sector in China was not integrated but this was a regionalism system of production areas which worked independently without a common strategy (Wagner 1997). Two of these production areas – Dabieshan, and Sichuan – were close or well communicated to/with Daye (Figure 8.13).

The mountainous region of Dabieshan in Central China was extremely constrained by geographic isolation; this region produced cast iron in small 'dwarf' blast furnaces – 2-3 m high –, which was consumed in the immediate vicinity (Figure 8.15). Characteristically, the iron in Dabieshan was mostly produced by non-professional metallurgists, indeed it was noted that the 'poorest peasants produced the best iron' (Rewi Alley quoted by Wagner 1997, 11). This seasonal activity survived until the 20th century, enjoying a last moment of splendour during the Great Leap Forward (1958-60) (Wagner 1985, 1997). Sichuan, to the West, had a significant iron economy of scale with large production – a

single furnace could produce ~2.4 tonnes per day – and a very good internal transportation that facilitated the supply to the large demand from the region, even isolated from the rest of China, excepting the areas communicated via the Yangtze river, like Daye (Wagner 1995, 1997; 2008, 5-59).

Figure 8.14: Remains of a bowl furnace of Northern Song Dynasty (AD 960 -1127) found in Tonglüshan with slag stuck to the tap-hole compared to the furnace chamber of furnace 4 of Lidegui.
Tonglüshan picture from Huangshi Municipal Museum (1980, unpaged), Daye picture courtesy of Professor Chen Shuxiang.

It is understandable that the inexperienced smelters from Daye did not choose the large-scale model of production of Sichuan. However, the case of Dabieshan presents some parallels to Daye, even if with a different technology: the small shaft furnaces represented a suitable solution to their needs, as an economic set-up with relatively low investment and large productivity; each furnace required relatively low labour force; and the conversion of cast into wrought iron was uncomplicated: achieved by stirring the iron under a blast of air – provided by a windbox manufactured also by the smelters. Also relevant and similar to Daye, many of these smelters produced iron as a seasonal activity, and they were peasants before metallurgists. Even if Dabieshan is a rather inaccessible region, the people of Daye must have been aware of their cast iron method of production,

since they are geographically quite close. In fact, there is evidence of this connection: the local gazetter of Hubei gives notice of a man from Huangpi (Figure 8.13) who in the late 18th century established 'an iron smelter where iron woks were cast using handicraft methods'; most likely, these woks were made with cast iron from the small furnaces of Dabieshan (Wagner 1995; 1997, 26; 2008).

Iron 'has always been an embedded technology rooted in the cultural beliefs of its producers and the consumer' (Humphris 2010, 289). Furthermore, 'ironmaking was not simply an economic or technical activity, it was a subculture in its own right, with its own traditions, prejudices and hierarchies' (Hayman 2005, 9). In this vein, it seems reasonable that if the Daye smelters did not adopt the cast iron technology from Dabieshan, presumably more efficient and apparently suitable for their necessities, the reason must be in the weight of their own technological tradition and the avoidance of risk: they already had a technological model that worked, which they understood better because that was the traditional smelting technology in the area, and thus they did not venture to change a familiar model for a different one, following their cultural traits. Also in this vein, is significant that they threw away the lump of cast iron, a potential indicator that they were not familiar with the refining technology or lack of the appropriate set up, and considered it as a lost.

A second reason to explain why Daye did not adopt blast furnaces is related to the model of production. The cast iron production – even using the 'simple' Dabieshan type furnace devices –, still requires a considerably set-up of facilities between blast furnaces, fining structures, and powerful air supply systems; and each of them constructed of different specific materials. It also requires substantially more ore and fuel: to produce 1 tonne of pig iron in 24 hours the small Dabieshan furnace consumed ~1400 kg of ore and 2 to 7.5 tonnes of charcoal (Wagner 1985, 12-22; 1997, 14-20). In comparison, a bloom of 13.5 kg can be obtained in 5 hours using 91 kg of charcoal and 41 kg of ore (Sauder & Williams 2002). The bloomery case is much more readily accessible than the indirect method since requires far less investment in facilities – simple structures excavated on the soil in the case of Daye – and procurement of raw materials, and has the advantage that it can be put into practice immediately. Moreover, massive-production is not necessarily an asset if the production largely overwhelms the demand and the producer has no means to

manufacture or trade the surplus, which would ultimately render in a tremendous waste of resources strong enough to provoke a non-reversible collapse in the production.

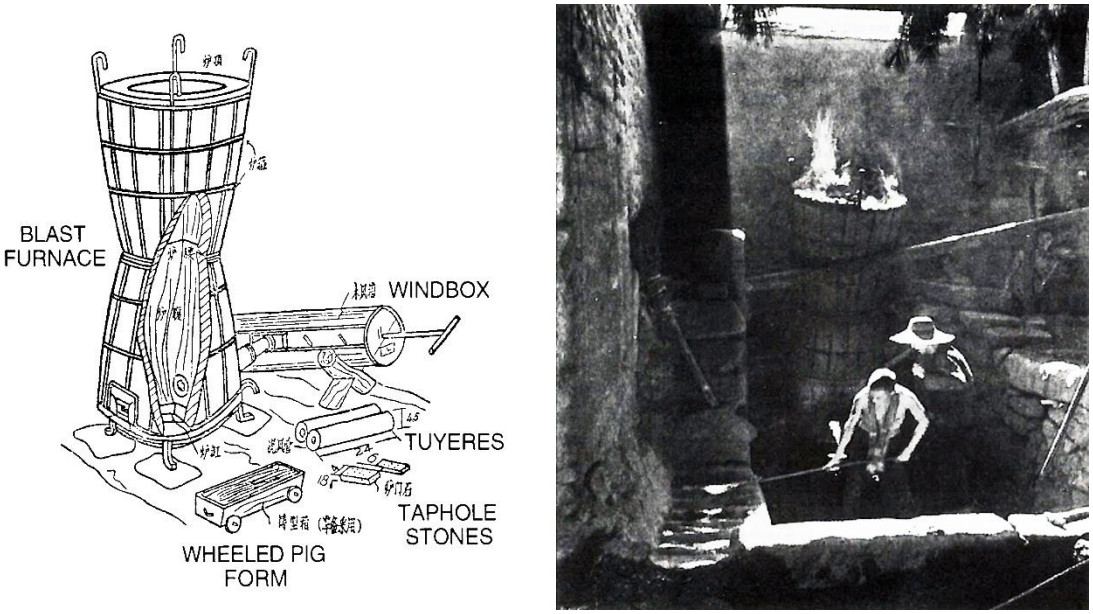

Figure 8.15: Sketch of the Dabieshan small blast furnace as used in the Great Leap Forward period and picture of a blast furnace in operation in 1958.
From Wagner (1997, Figures 4 and 6).

8.4.1 The bloomery disappearance scenario

Traditional accounts of the history of Chinese iron production tend to report that cast iron displaced bloomery iron after the monopoly on iron production during the 1st century BC, with the bloomeries disappearing completely by the early Han Dynasty (e.g. Taylor & Shell 1988; Wagner 2001a; Bai 2005; Wagner 2008; Han 2013; Han & Chen 2013; Huang, Q. & Li 2013). From the monopoly onwards, cast iron production appears as the only, unchanging and unchangeable option, which was directly controlled by the state in large scale industrial plants that employed complex techniques developing the entire *chaîne opératoire* from reduction to refining and manufacturing of objects, with many examples of this type of production (e.g. Huang, K. et al. 1996; Li, J. 1997; Han 1998; Wagner 2001c; Chen, J. & Han 2005; Han & Ke 2007; Wagner 2008). This is a model of economy of scale in which independent producers and regionalism do not exist.

However, it seems unlikely that this model of production would have remained unchanged for 2000 years, and indeed that it would be equally applicable to every context across China. Frequently (e.g. Zhang & Fan 2003), Chinese history is narrated as that of an homogenous package, where historical events occur in a logical smooth line, and new events are immediately absorbed by the system to enrich and perpetuate it, with every change spreading equally throughout the confines of the empire. Other scholars, however, highlight the fact that the Chinese empire was a very complex mixture of ecosystems, ethnic groups, cultural traditions, modes of subsistence, and political regulations, which developed across a colossal territory with changeable borders, periods of strength and stability as well as crisis occurring simultaneously within each dynasty (e.g. Gernet 1999; Loewe 2006).

It is extremely unlikely that a technology and the superstructure that supported it remained immutable for two millennia, operating in identical conditions for centuries among the vast landscape of different natural resources, climate, wealth, changeable borders and political situations of the Chinese empire. This seems even more unlikely when we remember that technology is particularly prone to adapt to, and in turn reflect, different environmental and cultural contexts (Sillar & Tite 2000; Killick 2004).

The occurrence of bloomery smelting in China has typically been explained as a marginal circumstance. The apparent reluctance to accept the importance of bloomery iron in the metallurgical history of China has sometimes led to interpretations of the archaeological evidence that seem unnecessarily convoluted in order to retain the sense of a single cultural package evolving on a single line. Thus ^{14}C dates indicating bloomery smelting during the 5-6th centuries AD are ignored in favour of ceramic typology to propose Western Han chronology (206 BC – AD 9) (Huang, Q. 2008, 117-120); the possibility of bloomery smelting is not even contemplated even when it is acknowledged that the given interpretation of an enormous volume of slag as puddling slag is inconsistent (Zhu 1986; Zhu & Zhang 1986); or the suggestion of bloomery smelting is so tentative that it would seem an extremely unlikely possibility (Wei et al. 2008; Hu et al. 2013). Recently, this uniformity has been questioned for the early Chinese history (e.g. Chen, K. et al. 2016), but this sensitivity for geographic and temporal diversity has not permeated studies of Imperial China. This is in spite of the fact that heterogeneity and multiple natural,

economic, politic and social circumstances are notable (e.g. Gernet 1999), particularly clear in the case of the iron production which is based on independent productive regions developing activities frequently unregulated by the administration and/or carried on by non-professional metallurgists, even if only during the last dynasty (Wagner 1997).

The possible existence of a tradition of bloomery iron in the Daye County since at least the Song Dynasty and in the core of the empire – middle Yangtze river –, challenges the traditional discourse. Firstly, not only bloomery iron survived after the 3rd century BC, but it co-existed with the most splendorous peak of cast iron production during the Song Dynasty, and it was still in use seven centuries later. Secondly, the imperial administration may not have shown excessive interest in dictating and controlling iron production by Iron Offices after the Han monopoly – incidentally their existence has never been documented in Hubei (Wagner 2008, 198-209). The production of bloomery iron in Daye was obviously tolerated; they produced bloomery iron openly on a significant scale (five workshops); and this occurred in one of the richest geological resources of metal in China – known from the 2nd millennium BC and still in exploitation – with multiple mention to the mines in written sources (Golas 1999). Nonetheless, it is difficult to conceive why if indeed a tradition of bloomery iron existed this is not visible in the archaeological record but only in two moments along the centuries, or why this industry was never registered in the imperial records. The available data is insufficient to explain this circumstance although is tempting to make speculations: in this research it has been suggested that the bloomery in Daye is product of a particular contingency around AD 1700. Perhaps the know-how of bloomery making was not forgotten in Daye but this only materialised under specific economic or social circumstances, otherwise they consumed the cast iron produced somewhere else. It is also likely that – as suggested by Wagner (2008, 246) – the bloomery production survived in many parts of the empire, but in such a small scale in comparison with the cast iron production that it remained unnoticed.

Finally, it is worth attempting to explain why bloomery iron was not abandoned in Daye. The main difference between both types of iron is better explained in terms of models of production: cast iron is a large-scale enterprise that guarantees stable production of large quantities of goods, while bloomery iron is a small-scale enterprise that is flexible and where manufacture of items can be immediately adapted to the consumers demand. This

difference of scale is frequently determined by the simplistic view of large equals sophisticated and small equals primitive (e.g Tylecote 1981; Hua 1983), however, a large-scale capital-intensive technology can be unsuitable in many cases. The former requires not only the appropriate 'sophisticated' technology – blast furnaces in this case – but also developments in transportation and in political and commercial institutions capable of reaching large markets regularly, and also requires a large superstructure to regulate prices and qualities, establishments of labour quotas, specialisation of personnel, etc., and thus is a rigid model that is more sensible to system variations and thus requires stability to survive (Becker 1962; Wagner 1995, 155). On the other hand, small-scale models are flexible and more easily adaptable to circumstances. These are frequently rooted in economically rational solutions since e.g. the Han Iron Offices were not merely an administrative office, but 'include the machinery and the living quarters of hundreds of workers', and thus required a considerable investment in terms of management and regulation to administrate the plant, inform the external population, taxation, administrative staff, coordinate the different divisions, etc. (Wagner 2008, 210). As such, bloomery iron would seem a more suitable model of production in areas where production was not concentrated, there was low demand of the standard products, or were isolated from the communication routes (Wagner 2001a, 85-88).

Large-scale production systems were not sustainable in the Qing Dynasty, which had a much more complex reality to manage than the Han Dynasty 2000 years earlier, with the mentioned problems of growing population, food supply, communications, etc. As a matter of fact the large-scale model of cast iron production best worked when the territory of expansion was the smallest during the Han and Northern Song dynasties (Figure 8.16).

'There was from early times an unfilled economic niche for a reasonable efficient small-scale iron production technology in isolate regions in China' (Wagner 1995, 156). Daye was economically isolated and although not particularly efficient in terms of metal yield, presumably it supplied local markets with ordinary products not readily accessible to the large-scale sector, and thus filled the niche.

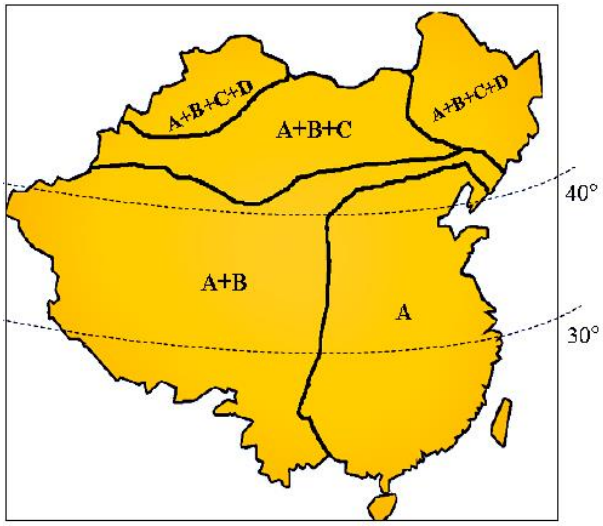

Figure 8.16: Boundaries of the Qing empire in comparison with previous dinasties.
(approx.) **A** = the Qin territory (c. 207 BC) and roughly the Northern Song territory (960–1127); **A+B** = the Western Han territory (c. 24 AD); **A+B+C** = the Tang territory (c. 907); **A+B+C+D** = the Qing territory (c. 1912) and roughly the Yuan territory (1279–1368). All the iron offices found dating to the Han Dynasty are located as well within the A territory. After Deng (2015, Figure 2).

8.5 Summary

Five sites in Daye County close to the Tonglüshan mine were proved to be bloomery smelting workshops, with activities taking place much later than the copper metallurgical activities thought to have developed during the first half of the 1st millennium BC. The study of the assemblage revealed a great deal of uniformity in the production remains, resulting from the same smelting technique of reducing high grade ores in small embanked furnaces without the addition of a flux. Archaeological remains and ^{14}C radiocarbon suggest that the activities were carried during a relatively short period of time, between *ca*. AD 1700-1800.

The chapter has integrated the technological parameters in environmental, political, and socioeconomic settings in order to explore the interaction of technological choices with other historical factors. The conclusion is that the process in Daye was poorly executed in terms of engineering parameters, with several inefficient technological choices visible in the haphazard planification of the working space, the excessively small size of the furnaces or the low efficiency. As a result, the production had a low efficiency, requiring high labour

force and intensity of work but rendering low metal yield. At the same time, the model is economically rational by using the available resources with the minimal investment and the number of sites would balance the low yield per workshop. It is also possible that in the active time of the production there was not a large local demand to supply, and thus the low efficiency was not considered a problem.

It is suggested that this unusual process was run by unskilled workers – such as agricultural workers or miners of the Daye ferrous mine – who smelted iron as a side activity to complete their income in a period of general economic crisis and low living standards, and thus workers from the territory resolved to smelt iron to improve their economic situation. The circumstance of non-professional metal workers producing iron is not new in China and has several historical examples, some of them still active in the 20th century. This was a regionalism type of production, which used different technologies adapted to the local environment, which could produce in large scale, but not within an economy of scale model to supply to all China but only to the local region or province.

The reasons that may explain why Daye appears different from the well-established tradition of cast iron production in China were discussed by engaging the concept of technological change, and revisiting hitherto misidentified evidence for earlier bloomeries in Daye. It was argued that it is unusual for a society to change dramatically the technology and come up with something totally new, since the cultural traits inherent to the technology – including definite parameters such as resources and knowledge – are inherited. Even more, it would have been risky for a group of unskilled people with limited resources to start utilising a different technology of which they did not have previous knowledge to generate a final product which is unexpected in the market. It seems more logical to accept a scenario of unskilled people trying to reproduce a familiar technology and sell easily a product that can help to relieve their impoverished situation. On this basis, it was argued that bloomery iron technology never disappeared from Daye, as suggested by evidence of its use in the Song Dynasty.

Those with ore smelted ore, and those without still found something to smelt.

(A Chinese life)

9 Conclusions and future work

While the manufacture and consumption of copper-alloys and iron artefacts in China has received a lot of attention, the smelting process, which is fundamental to obtaining the raw material necessary to make such artefacts, has been poorly studied. The broader aim of this doctoral thesis was to understand aspects of the technology that underlay the primary production of base metals at one of the most important metallogenic deposits in China. Analysis of the technical materials from Daye County in the Hubei province, exploited from the early 1st millennium BC until the present day, has provided insight into such practices and enabled discussion of issues of broader historical and archaeological significance.

Literary evidence give us the impression that the production of copper and iron in China were enterprises strictly regulated by the political administration, particularly during imperial times, and that this involved the utilisation of highly sophisticated technology in large workshops designed for standardised mass-production. This model of production has been assumed and considered virtually immutable for all the Chinese historical periods, according to the literature (e.g. Tylecote 1981; Xu & Linduff 1988; Li, X. & Liang 1996; Wagner 2008; Huang, Q. & Li 2013; Liu, Haifeng et al. 2014a). However, archaeological evidence confirms the existence of large-scale cast iron production only during certain periods of the Han (206 BC-AD 220) and Song Dynasties (AD 960-1279), and large bronze-making foundries during the late 2nd and 1st millennium BC. Furthermore, it is typically considered that this model is applicable to any part of mainland China – especially within the Central Plains area – regardless of natural, political, socio-cultural or economic factors. Implicitly, this model served to explain the purported abandonment of bloomery iron, which is an inherently small-scale enterprise, in favour of cast iron, which can be produced on an industrial scale. Therefore, a second major aim of this thesis was to test the validity of this model, and to use archaeological information to assess the

extent to which regional perspectives from the periphery might contribute to provide a more complex, diverse and realistic picture.

9.1 Copper smelting traditions in Daye County

Reconstruction of the technical *chaîne opératoire*

Copper smelting was identified at five sites in Daye County: Honfengshuiku (HF), Mianyangdi (MY), Maochengnao (MC), Wangyuecun (WY) and Xiyuqiao (XY). Overall, the technical procedure appears to have been broadly similar across Daye since the analysed specimens of slag and furnace walls were found to be homogeneous, indicating a standardised process with low variability. The ore was mined in any of the copper-rich deposits available in the area, but most likely from the Tonglüshan mine which has outcrops that are visible on the surface and easy to mine, as well as having activity documented from the beginning of the 1st millennium BC and possibly earlier. The Tonglüshan deposits are exceptional since the main ore body is a massive agglomeration of secondary minerals – an abundance of carbonate and silicate copper-bearing ores. The ores were charged into a shaft furnace together with an iron flux (haematite, previously roasted), which was necessary to create an iron-rich silicate slag of fayalitic composition at temperatures ranging 1100-1200 °C, thus separating the metal from the gangue. The slag was fully liquid and tapped out of the furnace, typically trapping small amounts of copper, ~0.7%. The result of the smelting was black copper with an iron content of ~5-6%. Overall, the technical process was well executed both in terms of efficiency and cost/benefit, but it left scope for improvement in the Fe content in the copper as this would have to be refined.

The common smelting procedure, using the same ore type probably mined at Tonglüshan, and the physical proximity between the five sites, are indicators of a shared smelting tradition. Some low variability was documented, however, and this was attributed to two main factors, which are not mutually exclusive: 1) in general, we document the expectable variation present in any standardised process generated during the different stages of a common operation; 2) at two of the sites, however (WY and particularly XY) it was suggested that the variations between these and the other sites in slag morphology,

chemical composition and mineralogy resulted from conscious intervention by the smelters to optimise the process over time in an attempt to obtain cleaner copper metal, predominantly through the manipulation of the furnace charge and (probably) by improving the furnace design to allow better control of redox conditions and temperature. The recipe followed for the ceramic fabric of the furnace walls, however, remained the same.

Chronology and foundations of the copper smelting tradition

By comparing the results of this study to those of previous investigations at Tonglüshan it was possible to identify progressive diachronic improvement in the smelting recipe within a single cultural tradition in metal smelting in Daye spanning from the Western Zhou till the end of the Warring States periods (~11th-3rd centuries BC). Based on indirect evidence from ceramic typology, it is suggested that the five sites were active during the first half of this period (~11th-6rd centuries BC), as evidenced by the less advanced technology when compared to the smelting workshops excavated close to the mine, which have been dated to the 6th-5th centuries BC and where blast-type furnaces were identified. However, this does not necessary imply that the five workshops studied here were operating synchronically – they could have started activities at any time within the aforementioned chronological framework. In principle, three of these sites – Honfengshuiku (HF), Mianyangdi (MY), Maochengnao (MC) – are suggested to be earlier than Wangyuecun (WY) and Xiyuqiao (XY) which would have chronologies much closer to the smelting workshops of Tonglüshan.

Involvement of political entities in the organisation of production

While there is documentary and archaeological evidence for the political control by the emerging state of Chu at the Tonglüshan mine and smelting site by the 6th-5th centuries BC, there is no indication of external authorities in earlier periods. The only possible control over the smelters of Daye could be from the city of Panlongcheng, an outpost of the Shang state network located ~70 km from Daye as both places were well communicated by the Yangtze river. However, the role of Panlongcheng has been described as a negotiator with other polities in order to ensure the supply of certain key resources such as salt and copper. Thus, in harmony with the Shang policy, this role was

more diplomatic and commercial than military or authoritative (Chang 1983; Wang, A. 2000; Flad & Chen 2013; Yuan 2013). On the other hand, titles such as 'smelter official' appear in the written sources only from the Warring States period onwards. In essence, the Shang was not a bureaucratic administration and the officials of the Zhou dynasty did not have specific assignments beyond rituals or recording functions, i.e. tasks quite removed from organising and coordinating the production at smelting sites such as those at Daye.

As such, the standardisation of production is not due to a dictated organisation and control from a political entity but to rational economising. The smelters made a rational choice of specialisation in the production of copper to achieve the best productive usage of the available natural resources, converting these into economic income. The likely scenario is a self-managed community that produced copper – a highly valuable commodity – in exchange for other products. Thus, the *economic agent* – the smelter community – chose from a set of available alternatives (e.g. agriculture, cattle, pottery, textile, etc.) the most desirable from among the feasible alternatives (i.e. mining and smelting), setting a microeconomic model based on *rational* choice (Rubinstein 2006). It is quite likely that communities under the same cultural sphere were running all the smelting sites since these are physically concentrated within a small space and, by logical extension, the standardisation was due to the use of the same natural resources, facilities and smelting recipes. It appears that the Zhou and possibly the Shang were obtaining copper from outside their borders (Chang 1983, 103-104; Reinhardt 1997, 100), and thus there was a secure market for the copper metal with the generally stable political situation of the Shang and Western Zhou periods – especially in comparison with the convulsed Eastern Zhou – favouring the continuation of this model of administration.

Technical procedures would be transmitted to the next generations of smelters thereby establishing the foundation of a technological tradition still alive in the 5th century BC, when technical innovations were introduced to increase the production. The new period also initiated major changes such as the re-arrangement of space, locating the smelting facilities immediately next to the mines, as well as the fortification of the mine vicinal cities to guard the mineral resources.

The conclusion that production of such a key resource for the Shang and Zhou cultural identities was not under their direct supervision contradicts the extended argument that these administrations were closely involved in metal production, to such an extent that it would have resulted in the relocation of their secular capitals to control and ensure access to it. The investigation of the smelting sites in Daye seriously challenges this proposal and it is suggested that control of the metallurgical process was restricted to the bronze-making foundries, i.e. mining and smelting was not under their jurisdiction. This is not a completely new argument. It has been suggested that the rise of the state of Chu was partly enabled because there was no control over the southern mines by the Zhou administration (Reinhardt 1997, 97). However, this is the first time that the model is supported by archaeological evidence and archaeometric analyses, and hence it is hoped that it will gain consideration among archaeologists and archaeometallurgists.

Social status of the smelters

The fact that Daye produced and traded a treasured commodity indispensable for bronze making – and thus vital for the politics, economy and cultural identity of all the cultural spheres connected to the Central Plains area – does not mean that the mining and smelting communities enjoyed a high social status. Mining and smelting were not considered activities for the educated, and a few competent workers were sufficient to direct large populations of unskilled labour. In other words, it was argued in this thesis that the primary smelters of copper in Daye were commoners of the lower classes, and with few choices but to work in the mines or smelting workshops. This is in opposition to the high status and social recognition normally assigned to the bronze making artisans.

9.2 Bloomery smelting traditions in Daye County

Reconstruction and chronology of the *chaîne opératoire*

Five sites of the analysed assemblages have remains of bloomery iron smelting. Two of them, Hongfengshuiku (HF) and Maochengnao (MC), also yielded evidence of copper production during an earlier period, while the other three sites, Lidegui (LD), Yanwopu (YW), and Cangxiawu (CX), only show evidence of the remains of iron reduction by the

direct method. Bloomery production involved the reduction of high grade iron ores – haematite and magnetite – in small embanked furnaces operating at temperatures ranging 1100-1200 °C. The ore was not self-fluxing and no silica-rich flux was added, and thus the contribution of furnace wall ceramics or lining molten into the charge was essential to generate fayalitic slag. The bloom was consolidated and probably shaped into iron bars in the same ironworks, but the end objects were likely manufactured somewhere else.

The production was large-scale, judging by the number of smelting sites and the volume of the metallurgical remains found, i.e. large heaps of slag, and furnaces arranged in batteries containing more than 20 devices. Unlike the long-lasting copper smelting, these activities were developed within a short time during the 18th century AD, as indicated by radiocarbon measurements from three of the sites (HF, LD, YW), the stratigraphy of the only excavated site (LD), and relevant historical documentation.

Cost/benefit and organisation of production

Contrary to copper smelting, the efficiency of iron production was low and the cost/benefit balance deficient, despite employing a significant labour force in an intensive activity. In essence, technical shortcomings limited the final metal yield.

The large-scale production with a relatively low metal yield per smelt is coherent with a picture at Daye of local people, without a previous tradition in metallurgy, struggling to reduce iron with limited knowledge and technological resources. Throughout the entire 18th century, China suffered a strong economic recession aggravated by a nearly permanent famine crisis, an unusual concentration of natural disasters, and an unparalleled – and uncontrollable – growth in population (Will 1990; Rowe 2009; Broadberry et al. 2014). This situation was particularly severe in the mining areas, where the onset of economic stagnation starting earlier, with unskilled metalworkers turning to smelt iron, a product in high demand, in order to make a living. The logic of the rational action of smelting metal in an area with plenty of mineral resources is evident in this case as well. However, the economy of the bloomery smelters is much closer to a subsistence than to a market economy, where the surplus was not abundant and most likely consumed in the immediate local market. It is also possible that they tried to compensate

for the low iron yields per furnace by increasing the number of devices, instead of through technical modification of the furnace design to optimise the output. This, once again, suggests that the smelters were not professional metalworkers.

The tentative scenario presented in this thesis, and which should be contrasted with further archaeological and historical research, is that the smelters were low class unskilled commoners with limited resources that supplemented their lack of economic assets through a large labour force. Their lack of expertise and minimal investment is evident through their digging of furnaces directly into the earth, thus saving the cost of building complex structures such as blast furnaces with multiple parts and different construction materials. They could also make the charcoal themselves – the most expensive raw material – since they had access to forests. Finally, nodules of high grade iron ore can still be easily picked up from surface, so the ore was possibly the most accessible of the necessary raw materials. The tax burden relaxation policy exerted by the Qing Dynasty (i.e. land tax holidays for certain periods) on commoner's households also played to their benefit, since in exchange for the right to use the land's natural resources they likely had had to contribute to the state with a small – if any – burden.

Technological changes and cultural traditions

While the circumstances of impoverished people diversifying activities to complement their incomes is not a novelty – with many examples within China and beyond – a more unexpected finding of this research is the type of iron that was produced, i.e. bloomery iron whose production was supposed to have ceased in China 2000 years earlier. This work has also explored the widely accepted scenario of the almost inevitable abandonment of bloomery iron in favour of cast iron, concluding that this is not a solid hypothesis. The production of cast iron allows mass-production and standardisation of products, which is consistent with the generally accepted technological history of China (Ledderose 1998). However, this is a large-scale model of production strongly constrained by the economic situation and highly dependent on infrastructures connecting producers and consumers. This sophisticated production model requires large investment, abundant forced labour, good transportation, ample markets, and administrative regulation. All these conditions are only possible under favourable political, economic and social situations. These requirements are severely affected during periods of crisis and instability e.g. recession,

war, population decline, etc. and are unlikely to survive unchangeable for a period of 2000 years. This thesis has argued that perhaps the circumstances during the 18th century did not favour this model since transportation was extremely deficient, investment in the metallurgical sector was virtually inexistent and there were no initiatives or legislation by the administration.

Bloomery iron, on the other hand, is flexible and ideally suited for small-scale production. While the yield per smelt is considerably lower, it is also much more economically rational in some contexts, consuming less natural resources. Furthermore, the quality of the artefacts is normally better than in large-productions, and is perfectly capable of satisfying the local demand regardless of economic or political turbulence. Given the precarious general economic situation in 18th century China, and the particular depression in the Hubei province (thus in Daye) plus the stagnation in the mining sector, a model based on small-scale labour-intensive technology is the most logical solution.

Besides the economic arguments, it is posited that bloomery iron existed in Daye since at least the 11th century AD based on the evidence of bowl furnaces similar to the small embanked furnaces of Lidegui, i.e. similar in terms of size, shape, location of (single) tuyere, and multiple relining of the furnace walls. It is argued that these furnaces may have been misinterpreted as fining furnaces but their design is not suitable for this propose – the atmosphere is reducing and the blast of air is provided at the bottom instead of at the top. Moreover, neither the amount of slag associated with the structures nor their microstructure and mineralogy are diagnostic of fining slag. Conversely, these features fit perfectly with bloomery iron production. In addition, the 18th century iron smelters did not choose a model of production based on 'dwarf' blast furnaces, of which in all probability they were aware of, since it was quite extended in the surrounding mountainous area. The latter furnace type would have seemed ideal for the case of Daye, since it was carried out by commoners in isolated regions as a seasonal activity to meet the needs of the population. However, they did not adopt these means of production since blast furnaces were technologically alien to the people in Daye, who produced iron following their established practice rather than changing their technology.

To summarise, it is probable that bloomery existed in Daye as their traditional method of producing iron metal, well embedded in their culture.

9.3 Original contributions and suggestions for future research

The research at a range of archaeometallurgical sites in Daye County provides several original contributions to the characterisation and interpretation of copper and iron smelting technology in China, which will hopefully provide pointers for future work.

Existence of two base metal smelting traditions: copper and bloomery iron

From an archaeological perspective, the existence of two types of production separated by ~2500 years has been positively identified and comprehensively characterised for the first time. The earliest of these productions is copper, which was known in the area from the late 2nd millennium BC. Copper production was supposed to be related with the smelting tradition of Tonglüshan mining and smelting sites, and its chronology loosely described between the Bronze Age and the 1st century BC. This work has demonstrated that the analysed material predates the smelting facilities of Tonglüshan, suggesting that Tonglüshan inherited a technological tradition that would only undergo significant innovations by the 6-5th centuries BC.

The second production operation documented is bloomery iron, which is an extraordinary occurrence in China, with very few archaeological examples associated with pre-imperial times and never earlier than the 3rd-2nd centuries BC. The identification of five sites active in the 18th century AD challenges the long-cherished generalised model of a technological transition from bloomery to cast iron during the 8th-5th centuries BC. Received wisdom suggested a total predominance of the latter but the disappearance of the former by the early Han period, and the introduction of the state monopoly on iron production in the late 2nd century BC. Moreover, based on a reappraisal of comparative material excavated in Tonglüshan, it appears that in Daye there was a technological tradition of bloomery iron smelting in existence from at least since the 11th century AD.

Variability in production models

Another major contribution of this thesis concerns the models of production. Due to the considerable size of the Chinese population and the enormous consumption of metals documented throughout several pre- and historical periods, it has been assumed that metal production took place at equally massive centres of production. These plants would

be rigidly controlled by the political administration, which also regulated and controlled the production. While there is documentary and archaeological evidence for the existence of such large facilities, during pre-imperial times this applies exclusively to secondary production in the case of copper, i.e. bronze making and manufacture of implements. The production described in Daye contradicts this model for rigid control and large-scale workshops in the case of primary smelting of copper. There was a general disinterest by the Shang and Zhou polities to control copper resources, and a change of policy only takes place later, possibly motivated by the rise of the Warring States. Regrettably, the size of the smelting facilities is unknown due to the lack of archaeological excavations. However, taking into account the concentration of sites within walking distance of each other within the same area, it seems more likely that there was not a single large-size production unit but several small ones.

For the case of iron production, massive industrial plants are only documented for certain historical periods rather than throughout the entire Chinese imperial history, i.e. from the 221 BC to the year AD 1912. Moreover, the furnaces in Daye were not blast furnaces and were not operated by professional metallurgists, which again contradicts the supposed monopoly on production and the prohibition of producing iron outside of the state facilities.

As discussed in this thesis, the large-scale capital-intensive model of production is fragile, due to its reliance on the economic, political and social situation, and that this is only operative if both infra- and superstructures (roads, ports, laws, prices, etc.) are functioning harmoniously. Furthermore, to organise and sustain this model, strong investment and high technical expertise are necessary. Nonetheless, these prerequisites were but rarely met throughout the centuries and thus the model was unworkable most of the time. Therefore, the development of small-scale technologies for iron production on a domestic or small scale such as the ‘dwarf’ blast furnaces of Dabieshan and the embanked bloomery furnaces of Daye are indeed a major aspect of the technological progress, reflecting the rational technological choices made by the smelters. The contextualised comparative studies revealed a range of social-economic and environmental factors which precluded the development of state-supervised large-scale production and allowed the evolution of varied technological traditions in the different

regions of China. As such, this thesis begins to reveal the existence of different regional technological traditions and variability in production, and seriously challenges the traditional model of metallurgical production in China, implicitly taken as universal and immutable.

Analysis and methodology of the study of technical materials

From an archaeometallurgical perspective, a key original dimension of this research is that that it has looked into the technical materials of primary production, which have been mostly ignored in China and regarded as of lesser importance compared to finished artefacts. This thesis has also demonstrated that even without an optimal archaeological contextualisation, the archaeometric study of surface collections can provide information that goes beyond the exclusively technical; in combination with archaeological and historical data, such work can lead to social and economic interpretations. Methodologically, this research highlights the utility of applying archaeometric approaches and the need to contrast the different datasets from written sources and archaeology, as well as advising against the extrapolation of historical explanatory models to different contexts.

A further dimension in which it is hoped that this work may stimulate further archaeometallurgical research in China is its comprehensive dual approach: on the one hand, this work considered all the steps of the primary metallurgical process from ore to metal, requiring an understanding of material constraints and thermodynamics; on the other hand, it approached metallurgical technology as part of a myriad of dynamic human activities and relationships in specific and changing social contexts. The study of the whole diversity of the archaeometallurgical, archaeological and historical record is anchored in a concern with how a specific social context shaped metallurgical technology. Specifically, the concept of *technological choice* has been illuminating in this thesis since it was possible to reveal and discuss a clear instance of the choice of a particular technology (and many other chained decisions) over two different options: reducing iron by the direct or by the indirect method.

Suggestions for future work

The archaeological and historical legacy of the metallurgical activities in Daye is rather exceptional and rich, and should be further investigated. Perhaps the most desirable way to follow up this thesis would be a systematic archaeological investigation of the smelting sites at Daye, including accurate data regarding the nature and volume of the remains observed on surface, through mapping and photographic documentation, as well as test pitting and selected excavations in areas accompanied by a series of radiocarbon analyses and stratigraphic descriptions. It would be also desirable to establish a preliminary discrimination between sites depending on the different production, e.g. by analysing a small number of slag samples per site. Furthermore, some of these excavated sites should also be preserved and musealised following the example of the Tonglüshan Ancient Metallurgy Museum. At a time when cultural diversity is increasingly recognised as wealth, archaeometallurgical remains provide an original medium to add time depth to a sense of common heritage whereby different communities adapted to their environments and successfully engaged in productive activities that strengthened their cultural identity.

This work suggested the existence of several polities that produced and traded copper during the 1st millennium BC. However, discussion of the specific kind of political organisation or trade models in operation was necessarily limited. There is not enough information to establish how much and for how long these relationships existed. Equally, more information is needed to ascertain whether the bloomery iron technology was a response activity provoked by unfavourable economic situations, or whether this had a more permanent character spanning throughout extended periods of time. In this vein, the apparent gap of 600-700 years from Song to Qing Dynasties in the production of bloomery iron remains unexplained; whether this simply reflects gaps in the data record or true historical contingencies remains to be investigated.

In addition, it is needed more systematic research on historical documents. A significant obstacle in this thesis has been my own limitation in reading Chinese. I tried to use as many documents in Chinese as possible within the time and material constraints of a doctoral dissertation, but I am sure that there are relevant documents that I did not check or had access to. Specifically, I regret that I was not able to approach historical Qing documents – the local gazettes of Daye in Huangshi city (黄石) – that in all probability

would have contributed useful information in order to establish whether bloomery production was a registered (legal) activity as well as determining the scale of production, the agents involved and the location of the secondary smithies, etc – these are necessarily left for future research.

Notwithstanding many imperfections derived from the nature of the evidence, the typical constraints of a PhD project and those derived from the limitations of the author, this research has revealed technological behaviour that shaped the lives of countless copper and iron smelters in Daye, whose work established the foundations of long-lived metallurgical traditions that are at the heart of one of the most important commodities in the economy and identity of China.

References

Abd El-Rahman, Y., Surour, A. A., El Manawi, A. H. W., Rifai, M., Abdel Motelib, A., Ali, W. K., & El Dougdoug, A. M. (2013). Ancient mining and smelting activities in the Wadi Abu Gerida area, central Eastern desert, Egypt. Preliminary results. *Archaeometry, 55* (6), 1067-1087.

Addis, A., Angelini, I., Nimis, P., & Artioli, G. (2015). Late bronze Age copper smelting slags from Luserna (Trentino, Italy): interpretation of the metallurgical process. *Archaeometry, 58* (1), 96-114.

Allen, J. R. (1986). Interpretation of some Romano-British smithing slag from Awre in Gloucestershire. *Historical Metallurgy, 20* (2), 97-104.

Allen, R. C., Bassino, J.-P., Ma, D., Moll-Murata, C., & van Zanden, J. L. (2011). Wages, Prices, and Living Standards in China, 1738-1925: in Comparison with Europe, Japan and India. *Economic History Review, 64*, 8-38.

Angelini, I., Anguilano, L., Artioli, G., Baumgarten, B., Dugnani, M., Moroni, M., & Pedrotti, A. (undated). Archeometallurgia del rame nelle alpi occidentali. https://www.academia.edu/17100924/ARCHEOMETALLURGIA_DEL_RAME_NELLE_ALPI_ORIENTALI

Anguilano, L., Oberrauch, H., Hauser, H., Rehren, Th., & Artioli, G. (2009). Copper Smelting at Fenhals-Kurtatsch (South Tyrol). In Moreau, Auger, Chabot & Herzog (Eds.), Paper presented at the Proceedings/Acts of the 36th International Symposium of Archaeometry, Quebec City, 02 - 06 May 2006, pp. 375-382.

Artioli, G., Angelini, I., Burger, E., Bourgarit, D., & Colpani, F. (2007). Petrographic and chemical investigations of the earliest copper smelting slags in Italy: towards a reconstruction of the beginning of copper metallurgy. Proceedings of the *2nd Intern. Conference "Archaeometallurgy in Europe 2007, Aquileia, 17-21 June 2007. Proceedings on CD*.

Avery, D. H., Merwe, N. J. v. d., & Saitowitz, S. (1988). The metallurgy of the iron bloomery in Africa. In Maddin (Ed.), *The beginning of the use of metals and alloys : papers from the Second International Conference on the Beginning of the Use of Metals and Alloys, Zhengzhou, China, 21-26 October*. Cambridge, Mass: MIT Press. pp. 261-282.

Bachmann, H. G. (1982). *The identification of slags from archaeological sites.* London: Institute of Archaeology.

Bagley, R. W. (1987). *Shang ritual bronzes in the Arthur M. Sackler collections.* Washington, D.C.: Cambridge: Arthur M. Sackler Foundation, Harvard University.

Bai, Y. X. (2005). *Archaeological Study on Iron Works before 3rd century AD in China （先秦两汉铁器的考古学研究）*. Beijing: Science Press.

Bain, F. H. (1933). *Ores and industry in the far East.* New York: Council on Foreign Relations.

Bambergen, M., & Wincierzt, P. (1990). Ancient smelting of ancient copper ore. In Rothenberg (Ed.), *The Ancient Metallurgy of Copper: Researches in the Arabah*. London: Institute for Archaeo-Metallurgical Studies, University College London. pp. 123-156.

Barbiery-Low, A. (2007). *Artisans in early imperial China.* Seatle; London: University of Washington Press.

Barnard, N. (1961). *Bronze casting and bronze alloys in ancient China.* Canberra: Australia National University.

Barnard, N., & Tamotsu, S. (1975). *Metallurgical remains of ancient China.* Tokyo: Nichiōsha.

Bayley, J., Dungworth, D., & Paynter, S. (2001). *Archaeometallurgy.* English Heritage Guidelines. London: English Heritage.

Becker, G. (1962). Irrational Behavior and Economic Theory. *Journal of Political Economy, 70* (1), 1-13.

Ben-Yosef, E., Giddinga, A., Tauxeb, L., Davidovich, U., Najjare, M., & Levy, T. E. (2016). Early Bronze Age copper production systems in the northern Arabah Valley: New insights from archaeomagnetic study of slag deposits in Jordan and Israel. *Journal of Archaeological Science, 72*, 71-84.

Benn, C. (2004). *China's golden age: Everyday life in the Tang dynasty.* Oxford: Oxford University Press.

Benvenutti, M., Mascaro, I., Costagliola, P., Tanelli, G., & Romualdi, A. (2000). Iron, copper and tin at Baratti, Populonia: smelting processes and metal provenances. *Historical Metallurgy, 34*, 67-76.

Birch, T. (2013). Abandoned or unused? Ultra-high carbon steel and cast iron lumps from Semlach/Eisner. In Cech (Ed.), *The production of ferrum Noricum at the Hüttenberger Erzberg. The results of interdisciplinary research at Semlach/Eisner between 2006-2009. Austria Antiqua, Wien - forthcoming*.

Blackman, M. J., Stein, G. J., & Vandiver, P. B. (1993). The Standardization Hypothesis and Ceramic Mass Production: Technological, Compositional, and Metric Indexes of Craft Specialization at Tell Leilan, Syria. *American Antiquity, 58* (1), 60-80.

Blakelock, E., Martinón-Torres, M., Veldhuijzen, A., & Young, T. (2009). Slag inclusions in iron objects and the quest for provenance: an experiment and a case study. *Journal of Archaeological Science, 36*, 1745-1757.

Blakelock, E., McDonnell, G., Rubinson, S., Chabot, N., Daoust, A. B., & Clark, A. E. (2014). Reconstructing a blacksmithing 'landscape': Saxon smithing at Wharram Percy. *Historical Metallurgy, 48* (parts 1 and 2), 47-54.

Blomgren, S., & Tholander, E. (1986). Influence of the ore smelting course on the slag microestructures at early ironmaking, usable as identification basis for the furnace process employed. *Scandinavian Journal of Metallurgy, 15*, 151-160.

Bourgarit, D., Mille, B., Prange, M., Ambert, P., & Hauptmann, A. (2003). Chalcolithic fahlore smelting at Cabrieres: Reconstruction of smelting processes by archaeometallurgical finds Paper presented at the Archaeometallurgy in Europe Milan 2003: Associacione Italiana di Metallurgia, *1*, pp. 431-440.

Bourgarit, D. (2007). Chalcolithic copper smelting. In La-Niece, Hook & Craddock (Eds.), *Metals and mines: studies in archaeometallurgy*. London: Archetype. pp. 3-11.

Bourgarit, D., Rostan, P., Burger, E., Carozza, L., Mille, B., & Artioli, G. (2008). The beginning of copper mass production in the western Alps: the Saint-Véran mining area reconsidered. *Historical Metallurgy, 42* (1), 1-11.

Broadberry, S., Hanhui, G., & Li, D. D. (2014). China, Europe and the Great Divergence: A Study in Historical National Accounting, 950-1850. *Economic History Department Paper, London School of Economics., 1-52*, www.nuffield.ox.ac.uk.

Bronk-Ramsey, C., & Lee, S. (2013). Recent and planned developments of the program OxCal. *Radiocarbon, 55 (2-3)*, 720-730.

Buchwald, V. F., & Wivel, H. (1998). Slag Analysis as a Method for the Characterization and Provenancing of Ancient Iron Objects. *Materials Characterization, 40*, 73-96.

Buchwald, V. F. (2003). Bloomery Iron, Osmund Iron, Finned Iron and Puddled Iron. In Nørbach (Ed.), *Prehistoric and Medieval Direct Iron Smelting in Scandinavia an Europe*. Aarhus: Aarhus University Press. pp. 171-176.

Buchwald, V. F. (2005). *Iron and steel in ancient times.* Historisk-filosofiske Skrifter 29. Copenhagen Det Kongelige Danske Videnskabernes Selskab.

Buchwald, V. F. (2008). *Iron, steel and cast iron before Bessemer: the slag-analytical method and the role of carbon and phosphorus.* København: Det Kongelige Danske Videnskabernes Selskab.

Cao, J. (2012). *Mint Metal Mining and Minting in Sichuan, 1700-1900: Effects on the Regional Economy and Society.* Doctoral Dissertation. Electronic publication by Tübingen University.

Cavallini, M. (2005). *Fortuitum & sordidum opus. Appunti di storia della metallurgia.* Perugia: Crace.

Cavallini, M. (2013). Thermodynamics applied to iron smelting techniques. *Applied Physics A, 113*, 1049-1053.

Cavallini, M. (2014). https://www.jiscmail.ac.uk/cgi-bin/webadmin?A0=ARCH-METALS. Retrieved 3-6-2014

Cipolla, C. M. (1976). *The industrial revolution, 1700-1914.* London: Barnes & Noble: Fontana.

Clough, R. E. (1987). The Bloomery Process — Observations on the use of rich ores and the production of natural steel. In Scott & Cleere (Eds.), *The crafts of the blacksmith. UISPP Comité pour la Sidérurgie Ancienne and the Ulster Museum, 1984.* Belfast. pp. 19-27.

Cooke, S. R. B., & Aschenbrenner, S. (1975). The occurrence of iron in metallic copper. *Journal of Field Archaeology, 2*, 251-266.

Costin, C. L. (1991). Craft specialization: issues in defining, documenting and explaining the organization of production. *Archaeological Method and Theory, 3*, 1-56.

Costin, C. L., & Hagstrum, M. B. (1995). Standardization, labor investment, skill, and the organization of ceramic production in late Prehispanic highland Peru. *Society of American Archaeology, 60* (4), 619-639.

Costin, C. L. (2001). Craft production systems. In Feinman & Price (Eds.), *Archaeology at the Millennium: A Sourcebook*. New York: Kluwer Academic. pp. 273-327.

Costin, C. L. (2005). Craft production. In Maschner (Ed.), *Handbook of methods in archaeology*. Lanham MD: Altamira Press. pp. 1032-1105.

Costin, C. L. (2007). Thinking about production: Phenomenological classification and lexical semantics. In Hruby & Flad (Eds.), *Rethinking craft specialization in complex societies: Archaeological analyses of the social meaning of production*. Arlington: American Anthropological Association and the University of California Press. pp. 143-162.

Coulson, M. (2012). *The History of Mining: The events, technology and people involved in the industry that forged the modern world.* Hampshire: Harriman House.

Craddock, P., & Meeks, N. D. (1987). Iron in ancient copper. *Archaeometry, 27* (2), 187-204.

Craddock, P. (1992). Copper production in the Bronge Age of the British Isles. *Bulletin of the Metals Museum, 18*, 3-28.

Craddock, P. (1995). *Early metal mining and production* London: 2010 unchanged reprint of the original edition, published in 1995. Archetype.

Craddock, P., Wayman, M. L., Wang, H., & Michaelson, C. (2003). Chinese Cast Iron through Twenty-Five Hundred Years. In Gett (Ed.), *Scientific Research in the Field of Asian Art: Proceedings of the First Forbes Symposium at the Freer Gallery of Art*. London: Archetype. pp. 36-46.

Craddock, P., & Lang, J. (2005). Charles Dawson's cast-iron statuette: the authentication of iron antiquities and possible coalsmelting of iron in Roman Britain. *Historical Metallurgy, 39* (1), 32-44.

Craddock, P., Freestone, I., Middleton, P., & Van Grunderbeek, M.-C. (2007). Early Iron Age iron-smelting debris from Rwanda and Burundi, East Africa. *Journal of Historical Metallurgy Society, 40* (1), 1-14.

Craddock, P. (2013). Refractories: ceramic with a purpose. *The Old Potter's Almanack, 18* (2), 9-20.

Crew, P. (1991). The experimental production of prehistoric bar iron. *Historical Metallurgy, 25* (1), 21-36.

Crew, P. (2000). The influence of clay and charcoal ash on bloomery slags. In Tizzoni & Tizzoni (Eds.), *Il Ferro nelle Apli – iron in the Alps*. Bienno: Comuni di Bienno. pp. 38-48.

Crew, P., Charlton, M., Dillmann, P., Salter, C., & Truffaut, E. (2011). Cast iron from a bloomery furnace *The Archaeometallurgy of Iron: recent developments in archaeological and scientific research*. Praha: Institute of Archaeology of the ASCR. pp. 239-316.

Crew, P. (2013). Twenty-five years of bloomery experiments: perspectives and prospects. In Dungworth & Doonan (Eds.), *Accidental and experimental archaometallurgy*. London: Historical Metallurgy Society Ocassional Publication nº 7. pp. 25-50.

Chang, K.-C. (1980a). The Chinese Bronge Age: A modern synthesis. In Fong (Ed.), *The great bronze age of China: an exhibition from the People's Republic of China*. New York: Metropolitan Museum of Art. pp. 35-50.

Chang, K.-C. (1980b). *Shang civilization.* New Haven, London: Yale University Press.

Chang, K.-C. (1983). *Art, myth and ritual. The path to political authority in ancient China.* Cambridge: Harvard University Press.

Chang, K.-C. (2005). The rise of the kings and formation of the city states. In Allan (Ed.), *The formation of Chinese civilization: an archaeological perspective*. New Haven, London: Yale University Press. pp. 125-140.

Charlton, M. (2006). *Ironworking in Northwest Wales: An evolutionary analysis.* (Unpublished Ph.D dissertation), University College London, UCL Institute of Archaeology.

Charlton, M., Crew, P., Rehren, Th., & Shennan, S. (2010). Explaining the evolution of ironmaking recipes -An example from northwest Wales. *Journal of Anthropological Theory, 29*, 352-367.

Charlton, M., Blakelok, E., Martinón-Torres, M., & Young, T. (2012). Investigating the production provenance of iron artifacts with multivariate methods. *Journal of Archaeological Science, 39*, 2280-2293.

Charlton, M., Rehren, T., Crew, P., & Shennan, S. (2013). Measuring variation in iron smelting slags: an empirical evaluation of group-identification procedures. In Humphris & Rehren (Eds.), *The World of Iron*. London: Archetype. pp. 421-430.

Chen, J., & Han, R. (2005). *The technology study of iron and steel in Central Plains and North China in Han and Jin Dynasties.（汉晋中原及北方地区钢铁技术研究）.* Beijing: Science Press.

Chen, J., Mao, R., Wang, H., Chen, H., Xie, Y., & Qian, Y. (2012). The iron objects unearthed from the Tombs of the Siwa Culture in Mogou, Gansu, and the origin of iron-making technology in China. (甘肃临潭磨沟寺洼文化墓葬出土铁器与中国冶). *Cultural Relics (文物), 8*, 45-53.

Chen, K., Mei, J., Rehren, Th., & Zhao, C. (2009). Special alloys from remote frontiers of the Shang Kingdom: scientific study of the Hanzhong bronzes from southwest Shaanxi, China. *Journal of Archaeological Science, 36*, 2108-2118.

Chen, K., Mei, J., Rehren, Th.., Anding, S., & Larreina-Garcia, D. (2012). *Hanzhong and Guanzhong: Looking through their metallurgy in Shang Period*. Poster presented at the conference Emergence of Bronze Age Societies – A Global Perspective, 7-11 November 2011. Baoji.

Chen, K., Mei, J., Rehren, T., & Zhao, C. (2016). Indigenous production and interregional exchange: late second-millennium BC bronzes from the Hanzhong basin, China. *Antiquity, 90* (351), 665-678.

Chengyuan, M. (1980). The splendor of ancient chinese bronzes. In Fong (Ed.), *The great bronze age of China: an exhibition from the People's Republic of China*. New York: Metropolitan Museum of Art. pp. 1-19.

Chernykh, E. (2009). Ancient metallurgy in the Eurasian steppes and China. In Mei & Rehren (Eds.), *Metallurgy and civilisation, Eurasia and Beyond. International Conference on the Beginnings of the Use of Metals and Alloys VI: 2006: Beijing, China.* London: Archetype. pp. 3-9.

Chiarantini, L., Benvenutti, M., Costagliola, P., Fedi, M. E., Guideri, S., & Romualdi, A. (2009). Copper production at Baratti (Populonia, southern Tuscany) in the early Etruscan period (9th-8th centuries BC). *Journal of Archaeological Science, 36*, 1629-1636.

Childs, S. T. (1989). Clays to Artifacts: resource selection in African Early Iron Age iron-making technologies. In Bronitsky (Ed.), *Pottery Technology: ideas and approaches*. London: Westview Press. pp. 139-144.

China Proper. (1945). *Economic geography, ports and communications.* China Proper: B.R. 530 (Restricted) Geographical Handbook Series, Vol. III: Naval Intellingence Division.

Chirikure, S., & Rehren, Th. (2004). Ores, Furnaces, Slags, and Prehistoric Societies: Aspects of IronWorking in the Nyanga Agricultural Complex, AD 1300–1900. *African Archaeological Review, 21* (3), 135-152.

Chirikure, S., & Rehren, Th. (2006). Iron Smelting In Pre-Colonial Zimbabwe: Evidence for Diachronic Change from Swart Village and Baranda, Northern Zimbabwe. *Journal of African Archaeology, 4* (1), 37-54.

Chuenpee, T., Won-In, K., Natapintu, S., & Takashima, I. (2014). Archaeometallurgical Studies of Ancient Iron Smelting Slags from Ban Khao Din Tai Archaeological Site, Northeastern Thailand. *Journal of Applied Sciences, 14* (9), 938-943.

Dai, Z., & Zhou, W. (1995). A comparative study on early metal currency (7th-3rd Centuries B.C.) in China and the West. *Bulletin of the Metals Museum, 24*, 33-42.

David, N., Heimann, R. B., Killick, D., & Ayman, M. W. (1989). Between bloomery and blast furnace: Mafa iron-smelting technology in North Cameroon. *The African Archaeological Review, 7*, 183-208.

David, N. (2014). Identification of a slag-draining bloomery furnace in the Mandora Mountains. *Historical Metallurgy, 44* (1), 36-47.

De Faria, D. L. A., & Lopes, F. N. (2007). Heated goethite and natural hematite: Can Raman spectroscopy be used to differentiate them? *Vibrational Spectroscopy, 45*, 117-121.

Della Casa, P., Naef, L., & Turck, R. (2016). Prehistoric copper pyrotechnology in the Swiss Alps: Approaches to site detection and chaîne opératoire. *Quaternary International, 402*, 26-34.

Deng, K. (2015). China's Population Expansion and its causes during the Qing Period, 1644–1911. *Economic History Working Papers, 219*, 1-55.

Dieudonné-Glad, N., & Conte, P. (2011). Smithing at the priory of Lavinadiére, Corréze, France, 13th and 16th centuries. *Historical Metallurgy, 45* (1), 1-7.

Dillmann, P., & L´Héritier, M. (2007). Slag inclusion analyses for studying ferrous alloys employed in French medieval buildings: supply of materials and diffusion of smelting processes. *Journal of Archaeological Science, 34*, 1810-1823.

Dobres, M.-A. (2000). *Technology and social agency: oulining a practice framework for archaeology.* Oxford: Blackwell Publishers Ltd.

Donaldson, C. H. (1976). An experimental investigation of olivine morphology *Contributions to Mineralogy and Petrology, 57*, 187-213.

Doonan, R. C. P., Klemm, S., Ottaway, B. S., Sperl, G., & Weinek, H. (1994). The east Alpine Bronze Age copper smelting process: evidence from the Ramsau valley, Eisenerz, Austria. In Demirci, Özer & Summers (Eds.), *Proceedings of the 29th International Symposium of Archaeometry*. Ankara 9-14 May 1994. pp. 17-22.

Du, N., Wang, X., Li, Y., & Li, J. (2012). Investigation on the copper slag of Linzi city in Shandong Province (山东临淄齐国故城城圈地铜渣的调查与研究). *Journal of Jiangxi University of Science and Technology (江西理工大学学报), 33* (2), 14-17.

Dungworth, D., & Wilkes, R. (2007). *An investigation on hammerscale.* Research Department Report Series no. 26. Porsmouth: English Heritage.

Dungworth, D. (2008). *Redcliff, Welton, East Yorkshire: an examination of the slag.* Research Department Report Series 58. Porsmouth: English Heritage.

Dunster, J., & Dungworth, D. (2012). Blacksmith's fuel, the analysis of slags from archaeological and contemporary iron-working. *English Heritage Technology Report, research report series no. 16-2012*.

Ebrey, P. (1986). The economic and social history of Later Han. In Twichett & Fairbank (Eds.), *The Cambridge history of China v. 1. The Ch'in and Han Empires, 221 B.C.-A.D. 220*. Cambridge: Cambridge University Press. pp. 608-648.

Eibner, C. (1982). Kupfererzbergbau in Österreichs Alpen. In Hänsel (Ed.), *Südosteuropa zwischen 1600 und 1000 v. Chr. Prähist. Arch. in Südosteuropa 1*. Berlin. pp. 399-408.

Eliyahu-Behar, A., Yahalom-Macka, N., Gadota, Y., & Finkelstein, I. (2013). Iron smelting and smithing in major urban centers in Israel during the Iron Age. *Journal of Archaeological Science, 40*, 4319-4330.

Elliot, J. F. (1976). Phase Relationship in the Pyrometallurgy of Copper. *Metallurgical Transactions B, 7B*, 17-33.

Erb-Satullo, N. L., Gilmour, B. J. J., & Khakhutaishvili, N. (2014). Late Bronze and Early Iron Age copper smelting technologies in the South Caucasus: the view from ancient Colchis c. 1500-600 BC. *Journal of Archaeological Science, 49*, 147-159.

Erb-Satullo, N. L., Gilmour, B. J. J., & Khakhutaishvili, N. (2015). Crucible technologies in the Late Bronze Early Iron Age South Caucasus: copper processing, tin bronze production, and the possibility of local tin ores. *Journal of Archaeological Science, 61*, 260-276.

Eschenlohr, L., & Serneels, V. (1991). *Les Bas Fourneaux Mérovingiens de Boécourt, Les Boulies (Ju, Suisse).* Porrentruy: Office du Patrimoine Historique Société Jurassienne d'Émulation.

Espelund, A. (1997). An attempt to define Archaeo-Metallurgy. In Nørbacht (Ed.), *Early Iron Production -Archaeology, Technology and Experiments*. Technical Reports nº 3. Denmark. pp. 7-14.

Espelund, A. (2015). Bloomery ironmaking during the Roman period in mid-Norway. *Historical Metallurgy, 48* (1), 16-24.

Ettler, V., Cervinka, R., & Johan, Z. (2009). Mineralogy of medieval slags from lead and silver smelting (Bohutín, Příbam district, Czech Republic): towards estimation of historical smelting conditions. *Archaeometry, 51* (6), 987-1007.

Falkenhausen, L., von,. (2006). *Chinese society in the age of confucius (1000-250 BC).* University of California, Los Angeles: Cotsen Institute of Archaeology.

Fernández-Caliani, J. C., Ríos, G., Martínez, J., & Jiménez, F. (2012). Occurrence and speciation of copper in slags obtained during the pyrometallurgical processing of chalcopyrite concentrates at the Huelva smelter (Spain). *Journal of Mining and Metallurgy, Section B: Metallurgy, 48* (2B), 161-171.

Feuerwerker, A. (1958). *China's Early Industrialization: Sheng Hsuan-huai (1844-1916) and Mandarin Enterprise.* Cambridge; Massachusetts: Harvard University Press.

Fillery-Travis, R. (2015). *Iron production in the Western Roman Empire: A diachronic study of technology and society based on two archaeological sites.* (unpublished Ph.D dissertation), University College London, UCL Institute of Archaeology.

Flad, R. K., & Chen, P. (2013). *Ancient Central China: centers and peripheries along the Yangzi river.* Cambridge University Press.

Fluzin, P. (2003). Synthèse des études métallographiques d'Échantillons de la forge de Ponte di Val Gabbia III (Bienno V-VI century AD). In Nørbach (Ed.), *Prehistoric and Medieval Direct Iron Smelting in Scandinavia an Europe*: Aarhus University Press. pp. 139-147.

Fong, W. (1980). *The great bronze age of China: an exhibition from the People's Republic of China.* New York: Metropolitan Museum of Art.

Freestone, I., Craddock, P., Hegde, K., Hughes, M. J., & Paliwal, H. V. (1985). Zinc production at Zawar, Rajasthan. In Craddock & Hughes (Eds.), *Furnaces and Smelting Technology in Antiquity*. London: British Museum. pp. 229-244.

Freestone, I. (1986). Refractory materials and their procurement. In Hauptmann, Pernicka & Wagner (Eds.), *Old World Archaeometallurgy – Archäometallurgie der alten Welt. Der Anschnitt, Beiheft 7.* Bochum: Deutsches Bergbau-Museum. pp. 155-162.

Freestone, I., & Tite, M. S. (1989). Refractories in the ancient and preindustrial world. In Kingery (Ed.), *High-technology ceramics past, present, and future: the nature of innovation and change in ceramic technology*. Westerville, OH: The American Ceramic Society, Inc. pp. 35-63.

Fulford, M. G., Allen, J., Gaffney, C., Gater, J., Boon, G. C., & Figueira, I. (1992). Iron-making at the Chesters Villa, Woolaston, Gloucestershire:Survey and Excavation 1987-91. *Britannia, 23*, 159-215.

Gale, N. H., Bachmann, H. G., Rothenberg, B., Stos-Gale, Z. A., & Tylecote, R. F. (1990). The adventitious production of iron in the smelting of copper. In Rothenberg (Ed.), *The Ancient Metallurgy of Copper: Researches in the Arabah*. London: Institute for Archaeo-Metallurgical Studies, University College London. pp. 182-191.

Georgakopoulou, M., Bassiakos, Y., & Philaniotou, O. (2011). Seriphos surfaces: A study of copper slag heaps and copper sources in the context of early Bronze Age Aegean metal production. *Archaeometry, 53* (1), 123-145.

Georgakopoulou, M., & Kassianidou, V. (2013). Archaeometallurgical finds and analytical results. In Given, Knapp, Noller, Sollars & Kassianidou (Eds.), *Landscape and interaction: The Troodos archaeological and environmental survey project, Cyprus*. Oxford and Oakville: Oxbow Books. Volume 1 Methodology, Analysis and Interpretation.

Gernet, J. (1999). *El Mundo Chino.* Barcelona: Crítica.

Golas, P. J. (1999). *Science and Civilisation in China, Part XIII: Mining.* Cambridge: Cambridge University Press.

Goldenberg, G. (1998). L'exploitation du cuivre dans les Alpes Austrichiennes á L'âge du Bronze. L'Atelier du bronzier en Europe du XX au VIII siècle avant notre ere. Proceedings of the *Actes du colloque International Bronze '96. Neuchatel et Dijon.Tomme II: Du mineral au métal â l'objet.*, Paris CTHS.

Gordon, R. B., & Killick, D. (1993). Adaptation of Technology to Culture and Environment: Bloomery Iron Smelting in America and Africa. *Technology and Culture, 34* (2), 243-270.

Gordon, R. B. (1997). Process Deduced From Ironmaking Wastes and Artefacts. *Journal of Archaeological Science, 24*, 9-18.

Han, R. (1998). Iron and steel making and it's features in ancient China. *Bulletin of the Metals Museum, 30*, 23-37.

Han, R., & Sun, S. (2004). Preliminary studies on the bronzes excavated from the Tianshanbeilu cemetery, Hami, Xinjiang. In Linduff (Ed.), *Metallurgy in Ancient Eastern Eurasia from the Urals to the Yellow river*. Lampeter, Ceredigion, Wales: The Edwin Mellen Press. pp. 157-172.

Han, R., & Ke, J. (2007). *A History of Science and Technology in China - Metallurgy.（版本中国科学技术史•矿冶卷）*. Beijing: Science Press.

Han, R., & Duan, H. (2009). An early iron-using centre in the ancient Jin state region (8th-3rd century BC). In Mei & Rehren (Eds.), *Metallurgy and Civilisation: Proceedings of the 6th International Conference on the Beginnings of the Use of Metals and Alloys (BUMA VI)*. London: Archetype. pp. 99-106.

Han, R., & Li, X. (2009). The bronze-using cultures in the northern frontier of ancient China and the metallurgies of ancient Dian area in Yunnan province. In Hanks & Linduff (Eds.), *Social complexity in prehistoric Eurasia*. Cambridge: Cambridge University Press. pp. 168-186.

Han, R. (2013). The East Asia Section. In Humphris & Rehren (Eds.), *The World of Iron*. London: Archetype. pp. 331-332.

Han, R., & Chen, J. (2013). Manufacturing techniques and dates of iron objects at Chinese archaeological sites. In Humphris & Rehren (Eds.), *The world of iron*. London: Archetype. pp. 345-354.

Hanning, E., Gauß, R., & Goldenberg, G. (2010). Metal for Zambujal: experimentally reconstructing a 5000-year-old technology. *Trabajos de Prehistoria, 67* (2), 287-304.

Hartwell, R. (1966). Markets, Technology and the structure of Enterprise in the development of the eleventh-century Chinese iron and steel industry. *The Journal of Economic History, 26*, 29-58.

Hartwell, R. (1967). A cycle of economic change in Imperial China: Coal and Iron in Northeast China, 750-1350. *Journal of the Economic and Social History of the Orient, 10 (1)*, 102-159.

Hauptmann, A. (1989). The Earliest Periods of Copper Metallurgy in Feinan/Jordan. In Hauptmann, Pernicka & Wagner (Eds.), *Archäometallurgie der Alten Welt/Old World*. Archaeometallurgy. Der Anschnitt, Beiheft 7, Deutsches Bergbau-Museum Bochum. pp. 119-135.

Hauptmann, A. (2003). Rationales of liquefaction and metal separation in earliest copper smelting: basic for reconstructing Chalcolithic and Early Bronze Age smelting processes Paper presented at the Archaeometallurgy in Europe (International Conference) vol. 1 Milano: Associacione Italiana di Metallurgia, pp. 459-468.

Hauptmann, A., Rehren, Th., & Schmitt-Strecker, S. (2003). Early Bronze Age copper metallurgy at Shahr-i Sokhta (Iran), reconsidered. In Stöllner, Körlin, Steffens & Cierny (Eds.), *Man and mining*. Bochum: Deutsches Bergbau-Museum. Anschnitt, Beiheft 16, pp. 197-213.

Hauptmann, A. (2007). *The archaeometallurgy of copper: evidence from Faynan, Jordan.* Berlin: Springer.

Hauptmann, A. (2011). Slags from the Late Bronze Age metal workshops at Kition and Enkomi, Cyprus. In Betancourt & Ferrence (Eds.), *Metallurgy: Understanding How, Learning Why. Studies in honor of James D. Muhly*. Philadelphia, Pennsylvania: INSTAP Academic Press. pp. 189-202.

Hauptmann, A. (2014). The investigation of Archaeometallurgical slag. In Roberts & Thornton (Eds.), *Archaeometallurgy in Global Perspective: Methods and Syntheses*. New York; London: Springer. pp. 91-106.

Hayman, R. (2005). *Ironmaking : the history and archaeology of the iron industry.* Stroud: Tempus.

Hedges, R. E. M., & Salter, C. J. (1979). Source Determination of Iron Currency Bars through Analysis of the Slag Inclusions. *Archaeometry, 21* (2), 161-175.

Herbert, B. (2003). Experimental bloomery ironworking in the Weald of Southern England in the 21st Century. *www.wealdeniron.org.uk.* Retrieved Acess to the web in November 2014, WEALDEN IRON RESEARCH GROUP (WIRG) 2000-2012

Herdits, H. (1993). Zum Beginn experimentalarchäologicher Untersuchungen einer bronzezeitlichen Kupferverhöttungsanlage in Mülbach, Salzburg. *Archaeologia Austriaca, 77*, 31-38.

Herdits, H. (2003). Bronze Age smelting site in the Mitterberg mining area in Austria. In Craddock & Lang (Eds.), *Mining and metal production through the ages* London: British Museum pp. 69-75.

Hoover, H. C., & Hoover, L. H. (1912). *Georgious Agricola De Re Metallica.* Reprinted by Forgotten Books in 2012.

Hu, X., Qu, Y., Han, C., Wei, G., & Qin, Y. (2013). The analysis of the middle Qing Dynasty iron smelting furnace at Hualushan (化炉山), Lidegui (李德贵) village in Hubei province. In The cultural Heritage committee of the Tonglushan ancient copper mining and smelting site in Daye city (大冶市铜绿山古铜矿冶遗址保护管理委员会) (Ed.), *The Discovery and Study of the Tonglushan Ancient Copper Mining and Smelting Site (铜绿山古铜矿遗址考古发现与研究)*. Beijing: Science Press (科学出版社). pp. 294-306.

Hua, J. (1983). The Mass Production of Iron Castings in Ancient China. *Scientific American, 248* (1), 121-129.

Hua, J. (1996-97). Technical and social characteristics of Pre-Qin bronze culture. In Bulbeck (Ed.), *Ancient Chinese and Southeast Asian bronze age cultures : the proceedings of a conference held at the Edith and Joy London Foundation property, Kioloa, NSW, 8-12 February, 1988* Taipei: SMC Publishing Inc. Vol. 2, pp. 731-748.

Huang, K., Li, J., Miao, C., & Zuo, C. (1996). The investigation and preliminary study of iron smelting sites in Damiofan and Jiehe in Xinyang county, Henan province, China. *Bulletin of the Metals Museum, 26* (2), 53-59.

Huang, Q. (2008). *Studies on the Ancient Iron Smelting Sites and Slag in Guigang District of Guangxi (广西贵港地区古代冶铁遗址调查与炉渣研究).* Doctoral Dissertation. University of Science and Technology Beijing.

Huang, Q., & Li, Y. (2013). Preliminary studies on Western Han Dynasty iron smelting sites and slag found in Pignan County, Guangxi Province, China. In Humphris & Rehren (Eds.), *The World of Iron*. London: Archetype. pp. 333-342.

Huang, R. (1981). *1587, a year of no significance : The Ming dynasty in decline.* New Haven ; London: Yale University Press.

Huang, X., Qian, W., Wei, W., Guo, J., & Liu, N. (2015). 3D numerical simulation on the flow field of single tuyere blast furnaces: A case study of the Shuiquangou iron smelting site dated from the 9th to 13th century in China. *Journal of Archaeological Science, 63*, 44-58.

Huangshi Municipal Museum. (1980). *Tonglüshan (Mt. Verdigris Daye)- A pearl among ancient mines （铜录山， 中国古矿冶遗址）*. Beijing: Cultural Relics Publishing House.

Huangshi Municipal Museum. (1999). *Ancient Mining and smelting site at Tonglushan (with an English abstract) (铜录山古矿冶遗址).* Beijing: Cultural relics Publishing House.

Hubei Provincial Bureau of Cultural Heritage. (2002). *Atlas of Chinese Cultural Heritage: Hubei 2 (中国文物地图集：湖北分册下册).* Xi'an Xi'an Atlas Press (西安地图出版社).

Hubei Provincial Institute. (2006). *Memory of the excavation of the Spring and Autumn Period site of Wulijie City, Daye (大冶五里界: 春秋城址与周围遗址考古报告).* Hubei Provincial Institute of Cultural Remains and Archaeology: Science Press.

Hughes, T. P. (1986). The seamless web: technology, science, etcetera, etcetera. *Social Studies of Science, 16* (2), 281-292.

Hughes, T. P. (1987). The Evolution of Large Technological Systems. In Bijker, Hughes & Pinch (Eds.), *The Social Construction of Technological Systems: New Directions in the Sociology and History of Technology*. Cambridge: MA: MIT Press. pp. 51-82.

Humphris & Rehren (Eds). (2013). *The World of Iron.* Humphris and Rehren (Eds.). London: Archetype.

Humphris, J., Martinón-Torres, M., Rehren, Th., & Reid, A. (2009). Variability in single smelting episodes – a pilot study using iron slag from Uganda. *Journal of Archaeological Science, 36*, 359-369.

Humphris, J. (2010). *An Archaeometallurgical Investigation of Iron Smelting Traditions in Southern Rwanda.* (Unpublished Ph.D dissertation), University College London, UCL Institute of Archaeology.

IA CASS. (2016). Miners' cemetery of the Zhou Dynasty found at Tonglushan, Hubei. *translated by Dong Ningning* Retrieved 7/2016, from http://www.kaogu.cn/en/Special_Events/en/Special_Events/Top_10_Archaeological_Discoveries_in_China_2015/2016/0517/53955.html

Iles, L., & Martinon-Torres, M. (2009). Pastoralist iron production on the Laikipia Plateau, Kenya: wider implications for archaeometallurgical studies. *Journal of Archaeological Science, 36*, 2314–2326.

Izawa, E. (2015). Iron lumps formed from the ancient copper smelting: an example from Naganobori, Japan. In Srinivasan, Ranganathan & Giumlia-Mair (Eds.), *Metals and Civilizations: Proceedings of the Seventh International Conference on the Beginnings of the Use of Metals and Alloys (BUMA VII)*. Bangalore: National Institute of Advanced Studies. pp. 55-61.

Jiang, Y.-Q., Ruan, S.-X., Tang, S., & Shuai, Z.-G. (2011). Chemistry Progress and Civilization in Ancient China. *Bulletin of the Chinese Academy of Sciences, 25* (1), 29-34.

Joosten, I., Jansen, J. B. H., & Kars, H. (1998). Geochemistry and the Past: Estimation of the Output of a Germanic Iron Production Site in the Netherlands. *Journal of Geochemical Exploration, 62*, 129-137.

Joosten, I., & Kars, H. (1999). Early historical iron production in the Netherlands: estimation of the output. In Young, Pollard, Budd & Ixer (Eds.), *Metals in antiquity*. Oxford: British Archaeological Reports. pp. 243-251.

Joosten, I. (2004). *Technology of Early Historical Iron Production in the Netherlands.* Amsterdam: Institute for Geo- and Bioarchaeology, Vrije Universiteit.

Jost, A. (2014). *From secret knowledge to mass production: the wet copper industry of Song China (960-1279).* Doctoral Dissertation. Electronic publication by Tübingen University.

Karbowniczek, M. (2005). Metallurgical process in ancient shaft furnace, theoretical consideration. *Association of metallurgical engineers of Serbia, 5*, 145-155.

Karbowniczek, M., Weker, W., & Suliga, I. (2006). Experimental metallurgical process in a slag pit bloomery furnace. *EuroREA, 6*, 45-49.

Kassianidou, V. (1998). Was silver actually recovered from speiss in antiquity? . In Rehren, Hauptmann & Muhly (Eds.), *Metallurgica Antiqua* Der Anschnitt, Beiheft 8. Bochum: Deutsches Bergbau-Museum. pp. 69-76.

Kassianidou, V. (2003). Early extraction of Silver from complex polymetallic ores. In Craddock & Lang (Eds.), *Mining and metal production through the ages* London: British Museum pp. 198-206.

Kelso, L. J. (1951). Ancient Copper Refining. *Bulletin of the American Schools of Oriental Research, 122*, 26-28.

Killick, D., & Gordon, R. B. (1987). Microstructures of puddling slags from Fontley, England and Roxbury, Connecticut, USA. *Journal of Historical Metallurgy Society, 21* (1), 28-36.

Killick, D., van der Merwe, N. J., Gordon, R. B., & Grébénart, D. (1988). Reassessment of the Evidence for Early Metallurgy in Niger, West Africa. *Journal of Archaeological Science* (15), 367-394.

Killick, D., & Gordon, R. B. (1989). The mechanism of iron production in the bloomery furnace. In Farquhar, Hancock & Pavlish (Eds.), *Proceedings of the 26th International Archaeometry Symposium, held at University of Toronto, Toronto, Canada, May 16th to May 20th 1988. Toronto: University of Toronto*. pp. 120-123.

Killick, D. (2004). Social Constructionist Approaches to the Study of Technology. *World Archaeology, 36*, 571-578.

Killick, D. (2014). From ores to metals. In Roberts & Thornton (Eds.), *Archaeometallurgy in Global Perspective: Methods and Syntheses*. New York; London: Springer. pp. 11-46.

Killick, D., & Miller, D. (2014). Smelting of magnetite and magnetite-ilmenite iron ores in the northern Lowveld, South Africa, ca. 1000 CE to ca. 1880 CE. *Journal of Archaeological Science, 43*, 239-255.

Killick, D., Miller, D., Thondhlana, T. P., & Martinón-Torres, M. (2016). Copper mining and smelting technology in the northern Lowveld, South Africa, ca.1000 CE to ca. 1880 CE. *Journal of Archaeological Science, 75*, 10-26.

Knapp, B., & Kassianidou, V. (2008). The Archaeology of Late Bronze Age copper Production: Politiko Phorades on cyprus. In Yançil (Ed.), *Anatolian Metal IV*: Der Anschnitt, Beiheft 21, Deutches Bergbau-Museum Bochum. pp. 135-147.

Ko, T. (2000). Preface. In Linduff, Han & Sun (Eds.), *The beginnings of metallurgy in China*. Lewiston: N.Y.: Edwin Mellen Press. pp. vii-xi.

Konečná, R., & Fintová, S. (2012). Copper and Copper Alloys: Casting, Classification and Characteristic Microstructures, Copper Alloys - Early Applications and Current Performance - Enhancing Processes. In Collini (Ed.), *Interdisciplinary Science Reviews* (pp. 1-30). ISBN: 978-953-51-0160-4, InTech open science: http://www.intechopen.com/books/.

Kresten, P. (1987). The Ore-Slag-Technology Link: Examples from Bloomery and Blast Fumace Sites in Dalarna, Sweden. In Scott & Cleere (Eds.), *The crafts of the blacksmith*. Belfast: UISPP Comité pour la Sidérurgie Ancienne and the Ulster Museum, 1984. pp. 29-33.

Kronz, A. (2000). Self-mixing melt compositions in fayalitic slags - a key in understanding early metal production? In Rammlmair, Mederer, Oberthür, Heimann & Pentinghaus (Eds.). Proceedings of the *Applied Mineralogy in Research, Economy, Technology, Ecology and Culture. Proceedings of the Sixth International Congress on Applied Mineralogy, ICAM, Gottingen 17-19 July 2000* Balkema, Rotterdam, *3*, pp. 1005-1008.

Lam, W. (2014). Everything old is new again? Rethinking the Transition to Cast Iron Production in the Central Plains of China. *Journal of Anthropological Research, 70*, 511-542.

Larreina-Garcia, D., Chen, K., Li, Y., & Rehren, Th. (2012). *Oodles of copper for the Chinese Emperors: The case of Sijiawan plant.* 39th International Symposium on Archaeometry 28 May-1 June 2012. Leuven, Belgium: Centre for Archaeological Sciences, KU Leuven.

Larreina-Garcia, D., Cech, B., & Rehren, Th. (2015). Copper smelting in the Raxgebiet (Austria): an Alpine industrial landscape during the Late Bronze Age. In Suchowska-Ducke, Scott Reiter & Vandkilde (Eds.), *Forging Identities. The Mobility of Culture in Bronze*. Oxford: BAR S2771 1, pp. 207-2013.

Lechtman, H., & Klein, S. (1999). The production of Copper-Arsenic alloys (Arsenic Bronze) by Cosmelting: Modern Experiment, Ancient Practice. *Journal of Archaeological Science, 26*, 497-526.

Ledderose, L. (1998). *Ten thousand things: module and mass production in Chinese art* Princeton, N.J.: Princeton University Press.

Lee, C. L., Qi, S.-H., Gan, C., Chun, L.-L., Zhao, L., & Li, X.-D. (2008). Seven Thousand Years of Records on the Mining and Utilization of Metals from Lake Sediments in Central China. *Environmental Science and Technology, 42*, 4732-4738.

Lemonnier, P. (1989). Bark capes, arrowheads and concorde: on social representations of technology. In hodder (Ed.), *The meaning of things. material culture and symbolic expression*. Boston, Massasuchets: Unwin Hyman. pp. 156-171.

Lemonnier, P. (1992). *Elements for an anthropology of technology.* University of Michigan; Anthropological Paper 88. Michigan: Ann Arbor.

Lemonnier, P. (1993). *Technological choices: transformation in material cultures since the Neolithic.* London: Routledge.

Levy, T. E., Adams, R. B., Hauptmann, A., Prange, M., Schmitt-Strecker, S., & Najjar, M. (2002). Early Bronze Age Metallurgy: A Newly Discovered Copper Manufactory in Southern Jordan. *Antiquity, 76*, 425-437.

Li, C., Zhou, Y., Ma, J., Wu, L., & Lia, H. (2004). *Catálogo de la exposición de los bronces de China.* Museo de Shanghai. Beijing: China Intercontinental Press.

Li, J. (1994). Inquiring into the ruins of iron smelting in ancient Xiping, China -Tracing the manufacturing places of the famous swords in the Eastern Zhou Dynasty-. *Bulletin of the Metals Museum, 22* (2), 8-15.

Li, J. (1996). The excavation and study of iron smelting sites in Henan of Han Dynasty, China. *Bulletin of the Metals Museum, 25*, 14-25.

Li, J. (1997). The excavation and study of iron-smelting ruins in the Warring States period in Henan province, China. *Bulletin of the Metals Museum, 27*, 26-45.

Li, X.-J. (1996-97). The cultural spheres of the bronze age in China. In Bulbeck (Ed.), *Ancient Chinese and Southeast Asian bronze age cultures : the proceedings of a conference held at the Edith and Joy London Foundation property, Kioloa, NSW, 8-12 February, 1988* Taipei: SMS Publishing Inc. Vol. 2, pp. 603-614.

Li, X., & Liang, Z. (1996). *Art of the Houma foundry / Institute of Archaeology of Shanxi Province = [Hou-ma t'ao fan i shu / Shan-hsi sheng k'ao ku yen chiu so], edited by Noel Barnard.* Princeton, N.J.: Princeton University Press

Li, Y. (1993a). A Preliminary Study on Ancient Mining and Metallurgy （中条山古铜矿冶遗址初步考察研究）. *World of Antiquity （文物世界）, 2*, 63-68.

Li, Y. (1993b). Ancient China Copper Pyrometallurgy in the lower and middle reaches of the Chanjiang river according to documents from Tang to Ming Dynasty (从古文

献看长江中下游地区火法炼铜技术). *China Historical Materials of Science and Technology (中国 羁技曼料), 14* (4), 83-90.

Li, Y. (1998a). Ancient matte slags in Tonglushan （铜绿山 X I 矿体古代炉渣冶炼冰铜说）. *Nonferrous Metals, 50* (3), 120-128.

Li, Y. (1998b). *Studies on the Ancient Copper Smelting Slag in Tonglushan and Jiuhuashan （铜录山，九华山古代炼铜炉渣矿穷）.* (Unpublished Ph.D dissertation), University of Science and Technology Beijing.

Li, Y. (1999). Study on smelting of ancient matte in Tonglushan （矿体古代冰铜渣的熔炼过程）. *Nonferrous Metals, 51* (4), 93-96.

Li, Y., Han, R., & Ko, T. (1999). The investigation on the ancient copper smelting slag from vein XI, Tonglushan (铜绿山 XI 号矿体古代炼铜炉渣研究). In Museum (Ed.), *The ancient mining and smelting site at Tonglushan (铜绿山古矿冶遗址)*. Beijing: Cultural Relics Press (文物出版社）. pp. 215-233.

Li, Y. (2000). Study on copper smelting technology at Jiuhuashan site (九华山唐代铜矿冶遗址冶炼技术研究). *Nonferrous Metals, 52* (4), 95-99.

Li, Y., & Han, R. (2002). The Smelting Technology of Dajing, an Ancient Copper Mining and Smelting Site in Chifeng District, Inner Mongolia. *Research of China's Frontier Archaeology, 00*, 204-213.

Li, Y. (2009). *Studies on the Ancient Smelting Sites in Beiliu Tongshiling and Ronxian Xishan of Guangxi (广西北流铜石岭、容县西山冶炼遗址调查研究).* Master Dissertation. University of Science and Technology Beijing.

Li, Y., Dong, L., Li, L., & Yang, J. (2011). Investigation on Jianshanzi Smelting Site in Wengniuteqi of Chifeng of Inner Mongolia （内蒙赤峰翁牛特旗尖山子冶炼遗址考察）. *Nonferrous Metals (extractive metallurgy) （有色金属 冶炼部分）, 7*, 66-72.

Lian, H., & Tan, D. (2003). A study of the making of bronze weapons in the Wu and Yue states during the Eastern Zhun period in China. In Jett (Ed.), *Scientific research in the field of Asian art*. London: Archetype. pp. 47-52.

Lin, J. Y. (1995). The Needham puzzle: Why the Industrial Revolution did not originate in China. *Economic Development and Cultural Change, 43* (2), 269-292.

Linduff, K. M. (2000). Metallurgist in ancient Chinese Asia: the Chinese and Who else? In Linduff, Han & Sun (Eds.), *The beginnings of metallurgy in China*. Lewiston: N.Y.: Edwin Mellen Press. pp. 1-28.

Linduff, K. M., & Mei, J. (2014). Metallurgy in Ancient Eastern Asia: Retrospect and Prospects. In Roberts & Thornton (Eds.), *Archaeometallurgy in Global Perspective: Methods and Syntheses*. New York; London: Springer. pp. 785-804.

Liu, H., Chen, J., Mei, J., Jia, J., & Shi, L. (2014a). A view of iron and steel making technology in the Yan region during the Warring States period and the Han dynasty: scientific study of iron objects excavated from Dongheishan site, Hebei province, China. *Journal of Archaeological Science, 47*, 53-63.

Liu, H., Qian, W., Chen, J., Li, Y., Guo, J., & Liu, N. (2014b). A preliminary study of furnace materials from Shuiquangou iron smelting site of Liao and Jin period in Beijing. *ISIJ International, 54* (5), 1159-1166.

Liu, L., & Chen, X. (2001). Cities and towns: the control of natural resources in early states, China. *Bulletin of the Museum of Far Eastern Antiquity, 73*, 5-47.

Liu, S. (2002). *The archaological report of the Laoniupo site. (in Chinese)* Shaanxi People's Publishing House, Xi'an.

Liu, S., Wang, K., Cai, Q., & Chen, J. (2013). Microscopic study of Chinese bronze casting moulds from the Eastern Zhou period. *Journal of Archaeological Science, 40* (1), 2402-2414.

Liu, S. (2015). *Gold and silver production in imperial China: Technological choices in their social-economic and environmental settings.* (Unpublished Ph.D dissertation), University College London.

Liu, Y. (2010). Revisiting Hanyeping Company (1889–1908): A case study of China's early industrialisation and corporate history. *Business History, 52* (1), 62-73. doi: 10.1080/00076790903469612

Loewe, M. (2006). *The government of the Qin and Han empires 221 BCE-220 CE.* Indianapolis/Cambridge: Hacket Publishing Company, Inc.

López-Merino, L., Martínez Cortizas, A., Reher, G. S., López-Sáez, J., M. Mighalle, T., & Bindlerf, R. (2014). Reconstructing the impact of human activities in a NW Iberian Roman mining landscape for the last 2500 years. *Journal of Archaeological Science, 50*, 208-218.

Lu, L., & Yan, W. (2005). Society during the Three Dynasties. In Allan (Ed.), *The formation of Chinese civilization: an archaeological perspective*. New Haven, London: Yale University Press. pp. 141-200.

Maddin, R. (1985). The technology of iron making. Proceedings of the *Medieval iron in society*, Norberg May 6-10, 1985: The Historical Metallurgical Group of Jernkontoret, pp. 127-157.

Maldonado, B., Rehren, Th., & Howell, P. (2005). Archaeological copper smelting at Itziparátzico. In Vandiver, Mass & Murray (Eds.), *Material issues in Art and Archaeology VII*. Michoacan, Mexico: Warrendale. MRS Proceedings 852, pp. 231-240.

Maldonado, B. (2006). *Preindustrial Copper Production at the Archaeological Zone of Itziparatzico.* (Unpublished Ph.D dissertation), The Pennsylvania State University, University Park.

Maldonado, B., & Rehren, Th. (2009). Early copper smelting at Itziparátzico, Mexico. *Journal of Archaeological Science, 36*, 1998-2006.

Manasse, A., Mellini, M., & Viti, C. (2001). The copper slags of the Capattoli Valley, Campiglia Marittima, Italy. *European Journal of Mineralogy, 13*, 949-960.

Manasse, A., & Mellini, M. (2002). Chemical and textural characterisation of Medieval slag from the Massa Marittima smelting sites (Tuscany, Italy). *Journal of Cultural Heritage, 3*, 187-198.

Marechal, J. R. (1985). Methods of ore roasting and the furnaces used. Furnaces and smelting technology in antiquity. *British Museum occasional paper, 48*, 29-41.

Marshak, B. I. (2004). Central Asian metalwork in China. In Watt & Prudence (Eds.), *China: dawn of a golden age, 200-750 AD*. New Haven; London: New York Metropolitan Museum of Art; Yale University Press. pp. 47-55.

Martinón-Torres, M. (2008). Why Should Archaeologist Take History and Science Seriously? In Martinón-Torres & Rehren (Eds.), *Archaeology, History and Science : Integrating Approaches to Ancient Materials*. Walnut Creek, CA Left Coast Press.

Martinón-Torres, M., Li, X. J., Bevan, A., Xia, Y., Zhao, K., & Rehren, Th. (2014). Forty Thousand Arms for a Single Emperor: From Chemical Data to the Labor

Organization Behind the Bronze Arrows of the Terracotta Army. *Journal of Archaeological method and theory, 21*, 534-562.

Martinón-Torres, M., & Rehren, Th. (2014). Technical Ceramics. In Roberts & Thornton (Eds.), *Archaeometallurgy in Global Perspective: Methods and Syntheses*. New York; London: Springer. pp. 107-131.

Martinón-Torres, M., & Killick, D. (2015). Archaeological Theories and Archaeological Sciences. In Gardner, Lajke & Sommer (Eds.), *The Oxford Handbook of Archaeological Theory (Forthcoming)*.

McDonnell, G. (1983). Tap slags and Hearth bottoms, or how to identify slags. *Current Archaeology, 86*, 81-83.

McDonnell, G. (1986). *The classification of early ironworking slags.* Birmingham, University of Aston, Unpublished PhD thesis.

McDonnell, G. (1991). A model for the formation of smithing slags. *Materialy Archeologiczne, XXVI*, 23-27.

Mei, J., & Li, Y. (2003). Early copper technology in Xinjiang, China: the evidence so far. In Craddock & Lang (Eds.), *Mining and metal production through the ages*. London: British Museum. pp. 111-121.

Mei, J. (2004). Metallurgy in Bronze Age Xinjiang and its cultural context. In Linduff (Ed.), *Metallurgy in Ancient Eastern Eurasia from the Urals to the Yellow river*. Lampeter, Ceredigion, Wales: The Edwin Mellen Press. pp. 173-186.

Mei, J. (2009a). Early Metallurgy in China: some challenging issues in current studies. In Mei & Rehren (Eds.), *Metallurgy and Civilisation: Proceedings of the 6th International Conference on the Beginnings of the Use of Metals and Alloys (BUMA VI)*. London: Archetype. pp. 9-16.

Mei, J. (2009b). Early metallurgy and socio-cultural complexity: archaeological discoveries in Northwest China. In Hanks & Linduff (Eds.), *Social complexity in prehistoric Eurasia*: Cambridge University Press. pp. 215-232.

Mei, J., Chen, K., & Cao, W. (2009). Scientific examination of Shang-dynasty bronzes from Hanzhong, Shaanxi Province, China. *Journal of Archaeological Science, 36* (9), 1881-1891.

Mei, J., & Linduff, K. M. (2009). Metallurgy in Ancient Eastern Asia: Retrospect and Prospects. *Journal of World Metallurgy, 22*, 265-281.

Mei, J., Wang, P., Chen, K., Wang, L., Wang, Y., & Liu, Y. (2015). Archaeometallurgical studies in China: some recent developments and challenging issues. *Journal of Archaeological Science, 56*, 221-232.

Merkel, J. (1990). Experimental reconstruction of Bronze Age copper smelting based on archaeological evidence from Timna. In Rothenberg (Ed.), *The Ancient Metallurgy of Copper: Researches in the Arabah*. London: Institute for Archaeo-Metallurgical Studies, University College London. pp. 78-112.

Merkel, J., & Rothenberg, B. (1999). The earliest steps to copper metallurgy in the western Arabah. In Andreas, Pernicka, Thilo & Yalçin (Eds.), *The Beginnings of metallurgy, Proceedings of the international conference "The Beginnings of Metallurgy", Bochum 1995*. Bochum: Der Anschnitt, Beiheft 9, Deutches Bergbau-Museum Bochum. pp. 149-166.

Merwe, N. J. v. d., & Avery, D. H. (1982). Pathways to Steel: Three different methods of making steel from iron were developed by ancient peoples of the Mediterranean, China, and Africa. *American Scientist, 70* (2), 146-155.

Metten, B. (2003). Beitrag zur spätbronzezeitlichen Kupfermetallurgie im Trentino (Südalpen) im Vergleich mit anderen prähistorischen Kupferschlacken aus dem Alpenraum. *Metalla (Bochum), 10*.

Miller, D., Killick, D., & Merwe, N. J. v. d. (2001). Metal Working in the Northern Lowveld, South Africa, A.D. 1000-1890. *Journal of Field Archaeology, 28* (3/4), 401-417.

Miller, D., & Killick, D. (2004). Slag identification at southern african archaeological sites. *Journal of African Archaeology, 2* (1), 23-47.

Miller, M.-L. (2007). Archaeological approaches to technology. Amsterdam; London: Elsevier/Academic Press.

Moesta, H. (1986). Bronze Age Copper Smelting. *Interdisciplinary Science Reviews, 11* (1), 73-87.

Moesta, H., & Schlick, G. (1989). The furnace of Mitterberg: An oxidizing Bronze Age copper process. *Bulletin of the Metals Museum, 14*, 5-16.

Morton, G. R., & Wingrove, J. (1969). Constitution of bloomery slags. Part I: Roman. *Journal of the Iron and Steel Institute, 207*, 1556-1564.

Morton, G. R., & Wingrove, J. (1972). Constitution of bloomery slags. Part II: Medieval. *Journal of the Iron and Steel Institute, 210*, 478-488.

Muhly, J. (1988). The beginnings of metallurgy in the Old World. In Maddin (Ed.), *The beginning of the use of metals and alloys: papers from the Second International Conference on the Beginning of the Use of Metals and Alloys, Zhengzhou, China, 21-26 October*. Cambridge: MIT Press. pp. 2-20.

Muller, J. (1987). Salt, chert, and shell: Mississippian exchange and economy. In Brumfiel (Ed.), *Specialization, exchange, and complex societies* Cambridge: Cambridge University Press. pp. 10-21.

Muralha, V. S. F., Rehren, Th., & Clarka, R. J. H. (2011). Characterization of an iron smelting slag from Zimbabwe by Raman microscopy and electron beam analysis. *Journal of Raman spectroscopy, 42*, 2077–2084.

Museum of Huangshi City. (1984). *The archaeological investigation of ancient sites in Daye (大冶古文化遗址考古调查).* Jianghan Archaeology (江汉考古).

Navasaitis, J., & Selskienė, A. (2007a). Iron smelting techniques in the Virbaliūnai ancient settlement. *Archaeologia Baltica, 8*, 387-394.

Navasaitis, J., & Selskienė, A. (2007b). Metallographic examination of Cast Iron Lump Produced in the Bloomery Iron Making Process. *Materials Science (Medžiagotyra), 13* (2), 167-173.

Navasaitis, J., Selskienė, A., & Žaldarys, G. (2010). The study of trace elements in bloomery iron. *Materials Science (Medžiagotyra), 16* (2), 113-118.

Needham, J. (1958). *The development of iron and steel technology in China.* Cambridge: Newcomen Society.

Needham, J. (1965). Valves, bellows, pumps and fans *Science and civilisation in China*. London: Cambridge University Press. IV, pt. 2, pp. 135-150.

Needham, J. (1970). *Clerks and craftsmen in China and the West: lectures and addresses on the history of science and technology.* London: Cambridge University Press.

O'Brien, W. (2015). *Prehistoric copper mining in Europe: 5500-500 BC.* Oxford: Oxford University Press.

Ottaway, B. S. (2001). Innovation, Production and Specialization in Early Prehistoric Copper Metallurgy. *European Journal of Archaeology, 4* (1), 87-112.

Park, J.-S., & Rehren, Th. (2011). Large-scale 2nd to 3rd century AD bloomery iron smelting in Korea. *Journal of Archaeological Science, 38*, 1180-1190.

Pasitschiniak, A. (1986). Determination of Sulfur Content by X-Ray Fluorescence in Samples Containing a Single Sulfide Phase. *X-Ray Spectrometry, 15*, 197-199.

Paynter, S. (2006). Regional variations in bloomery smelting slag of the Iron Age and Romano-British Periods. *Archaeometry, 48* (2), 271-292.

Paynter, S. (2007). Romano-British workshops for iron smelting and smithing at Westhawk Farm, Kent. *Historical Metallurgy, 41*, 15-31.

Peters, H. A. (1999). Towns and Trade: Cultural Diversity and Chu Daily Life. In Cook & Major (Eds.), *Defining Chu: Images and Reality in Ancient China*. Honolulu: University of Hawai'i Press. Project MUSE. pp. 99-119.

Pfaffenberger, B. (1992). Social Anthropology of Technology. *Annual Review of Anthropology, 21*, 491-516.

Pirazzoli-t'Sertevenst, M. (1982). *The Han civilization of China.* Oxford: Phaidon Press.

Pleiner, R. (2000). *Iron in Archaeology: the European bloomery smelters.* Prague: Archeologigky Ustav Avcr.

Pleiner, R. (2006). *Iron in Archaeology: early European blacksmiths.* Prague: Archeologigky Ustav Avcr.

Pryce, T. O., Bassiakos, Y., Catapotis, M., & Doonan, R. C. (2007). 'De caerimoniae' technological choices in copper-smelting furnace design at Early Bronze Age Chrysokamino, Crete. *Archeometry, 49* (3), 543–557.

Pryce, T. O. (2008). *Prehistoric Copper Production and Technological Reproduction in the Khao Wong Prachan Valley of central Thailand.* (Unpublished Ph.D dissertation), University College London, UCL Institute of Archaeology.

Pryce, T. O., Piggot, V. C., Martinón-Torres, M., & Rehren, Th. (2010). Prehistoric copper production and technological reproduction in the Khao Wong Prachan Valley of Central Thailand. *Archaeological Anthropological Science, 2*, 237-264.

Pryce, T. O., Brauns, M., Chang, N., Pernicka, E., Pollard, A. M., Ramsey, C., Rehren, Th., Souksavatdy, V., & Souksavatdy, C. (2011). Isotopic and technological variation in prehistoric Southeast Asian primary copper production. *Journal of Archaeological Science, 38*, 3309-3322.

Rapp, G. (1998). Composition and softening/fluid temperatures of some Cypriots slags. In Rehren, Hauptmann & Muhly (Eds.), *Metallurgia Antiqua*: Der Anschnitt, Beiheft 8, Deutches Bergbau-Museum Bochum. pp. 177-182.

Rehder, J. E. (2000). *The mastery and uses of fire in antiquity.* Quebec: McGill-Queen's University Press.

Rehren, Th., & Ganzelewski, M. (1995). Early blast furnace and finery slags from the Jubach, Germany. In Magnusson (Ed.), *The importance of ironmaking, Technological innovation and social change*. Stockholm. pp. 172-179.

Rehren, Th., Charlton, M., Chirikure, S., Humphris, J., Ige, A., & Veldhuijzen, A. (2007). Decisions set in slag: the human factor in African iron smelting. In La-Niece, Hook & Craddock (Eds.), *Metals and mines: studies in archaeometallurgy*. London: Archetype. pp. 211-218.

Rehren, Th. (2009-2011). The production of silver in South America. *Archaeology International, 13/14*, 76-83.

Rehren, Th., Boscher, L., & Pernicka, E. (2012). Large scale smelting of speiss and arsenical copper at Early Bronze Ager Arisman, Iran. *Journal of Archaeological Science, 39*, 1717-1727.

Reinhardt, K. (1997). *Mining and Smelting Technology and the Politics of Bronze in Shang and Western Zhou China: An Inquiry into the Bronze Age Interaction Sphere.* (MA dissertation), McGill University, Montreal.

Rice, P. M. (1991). Specialization, Standardization, and Diversity: a retrospective In Lange (Ed.), *The Ceramic Legacy of Anna O. Shepard*. Colorado: University of Colorado Press. pp. 257-273.

Robion-Brunner, C., Serneels, V., & Perret, S. (2013). Variability in iron smelting practices: assestmen of technical, cultural and economic critera to explain the metallurgical diversity in the Dogon area (Mali). In Humphris & Rehren (Eds.), *The world of iron*. London: Archetype. pp. 257-265.

Roman, I. (1990). The Copper ingots. In Rothenberg (Ed.), *The Ancient Metallurgy of Copper: Researches in the Arabah*. London: Institute for Archaeo-Metallurgical Studies, University College London. pp. 176-181.

Romanow, H. P. (1995). Archaeometallurgical investigations of casting-cake and a copper ore sample from the Klinglberg excavations. Bronze Age copper producers of the Eastern Alps, excavations at the St. Veit-Klinglberg. *Universitätsforschungen zur prähistorischen Archäologie, 27*, 263-266.

Rose, D., Endlicher, G., & Mücke, A. (1990). The occurrence of 'iscorite' in Medieval iron slags. *Historical Metallurgy, 24*, 27-32.

Rosenqvist, T. (1983). *Principles of extractive metallurgy.* 2nd ed. New York; London: McGraw-Hill

Rostoker, W. (1975). Some experiments in prehistoric copper smelting. *Paleorient, 3*, 311-315.

Rostoker, W., Pigott, V., & Dvorak, J. R. (1989). Direct reduction to copper metal by oxide-sulfide mineral interaction. *Archaeomaterials, 3*, 69-87.

Rostoker, W., & Bronson, B. (1990). *Pre-Industrial Iron: its technology and ethnology.* Archaeomaterials Monograph No. 1. Philadelphia: Pennsylvania University Press.

Rothenberg, B. (1988). *The Egyptian mining temple at Timna.* London: Institute for Archaeo-Metallurgical Studies: Institute of Archaeology University College London.

Rothenberg, B. (1990). *The Ancient Metallurgy of Copper: Researches in the Arabah.* London: Institute for Archaeo-Metallurgical Studies, University College London.

Rothenberg, B., Segal, I., & Khalaily, H. (2004). Late Neolithic and Chalcolithic copper smelting at the Yotvata oasis (south-west Arabah). *IAMS Newsletter, 24*, 17-28.

Roux, V. (2008). Evolutionary trajectories of technological traits and cultural transmission. In M. T. Stark (Ed.), *Cultural transmission and material culture: Breaking down boundaries*. Tucson: University of Arizona Press. pp. 82-105.

Rovira, S., Renzi, M., Moreno, A., & Contreras, F. (2015). Copper slags and crucibles of copper metallurgy in the Middle Bronze Age site (El Argar Culture) of Peñalosa (Baños de la Encina, Jaen, Spain). In Hauptmann & Modarressi-Tehrani (Eds.). Proceedings of the *Archaeometallurgy in Europe III , June 29-July 1, 2011*, Bochum: Deutsches Bergbau-Museum Bochum, pp. 355-362.

Rowe, T. W. (2009). *China's last empire, the Great Qing.* Massachusetts, London: Belknap Press of Harvard University Press.

Rubinstein, A. (2006). *Lecture notes in microeconomic theory, The economic agent.* Priceton and Oxford: Priceton University Press.

Rüffler, R., & Gonser, U. (1992). Three thousand years of copper metallurgy seen through the eyes of Mössbauer spectroscopy: a Bronze Age copper process in the alpine region. *Hyperfine Interactions, 70*, 1005-1008.

Rüffler, R. (1996). Three thousand years of copper metallurgy - seen through the eyes of Mössbauer spectroscopy. Part III: copper losses in bronze age slags. *Hyperfine Interactions, 99*, 401-407.

Ryndina, N., Indenbaum, G., & Kolosova, V. (1999). Copper production from polymetallic sulphide ores in the northeastern Balkan Eneolithic culture. *Journal of Archaeological Science, 26*, 1059-1068.

Sadao, N. (1986). The economic and social history of Former Han. In Twichett & Fairbank (Eds.), *The Cambridge history of China v. 1. The Ch'in and Han Empires, 221 B.C.-A.D. 220*. Cambridge: Cambridge University Press. pp. 551-607.

Sauder, L., & Williams, S. (2002). A practical treatise on the smelting and smithing of bloomery iron. *Historical Metallurgy, 36* (2), 122-131.

Scott, D. A. (1991). *Metallography and microstructure of ancient and historic metals.* Marina del Rey, CA: Getty Conservation Institute.

Scott, D. A., & Ma, Q. (2006). Metallographic examination of iron artefacts from Gansu Province, China. *Historical Metallurgy, 40* (2), 105-114.

Schiffer, M. B., & Skibo, J. M. (1987). Theory and experiment in the study of technological change. *Current Archaeology, 28* (5), 595-622.

Schlesinger, M. E., King, M. J., Sole, K. C., & Davenport, W. G. (2011). *Extractive metallurgy of Copper.* Oxford: Elsevier-5th Edition.

Selskienè, A. (2007). Examination of smelting and smithing slags formed in bloomery iron-making process. *Chemija, 18* (2), 22-28.

Serneels, V. (1993). Archéometrie des scories de fer. Recherches sur la sidérurgie ancienne en Suisse romande. *Cahiers d'Archéologie Romande, 61. Lausanne*.

Serneels, V., & Perret, S. (2003). Quantification of smithing activities based on the investigation of slag and other material remains. Proceedings of the *Archaoeometallurgy in Europe*, Milano: Associacione Italiana di Metallurgia, pp. 469-478.

Severin, T., Rehren, Th., & Schleicher, H. (2011). Early metal smelting in Aksum, Ethiopia: copper or iron? *European Journal of Mineralogy, 23*, 981-992.

Shennan, S. (1999). Cost, benefit and value in the organization of early European copper production. *Antiquity, 73*, 352-362.

Shimada, I., & Craig, K. A. (2013). The style, technology, and organization of Sicán mining and metallurgy, northen Peru: insights from holistic study. *Chungara, Revista de Antropología Chilena, 45*, 3-31.

Shugar, A. N. (2003). Reconstructing the Chalcolithic metallurgical process at Abu Matar, Israel. Proceedings of the *Archaeometallurgy in Europe*, Milan 2003: Associacione Italiana di Metallurgia, *1*, pp. 449-458.

Sillar, B., & Tite, M. (2000). The challenge of 'technological choices' for material science approaches in archaeology. *Archaeometry, 42*, 2-20.

Skinner, G. W. (1977). Cities and the hierarchy of local systems. In Skinner (Ed.), *The City in Late Imperial China*. Taipei: SMC Publishing INC. pp. 257-352.

Skinner, G. W. (1985). The Structure of Chinese history. *The Journal of Asian Studies, 44* (2), 271-292.

Sperl, G. (2003). Scientific research on remains of the Late Bronze Age: copper production in the Alps. *Microscopy and Microanalysis, 9 (Suppl. 2)*, 654-655.

Sun, H., Wu, J., Yu, P., & Li, J. (1998). Geology, geochemistry and sulfur isotope composition of the Late Proterozoic Jingtieshan (Superior-type) hematite-jasper-barite iron ore deposits associated with stratabound Cu mineralization in the Gansu Province, China. *Mineralium deposita, 34*, 102-112.

Sun, S., & Han, R. (2000). A study of casting and manufacturing techniques of early copper and bronze artefacts found in Gansu. In Linduff, Han & Sun (Eds.), *The beginnings of metallurgy in China*. Lewiston: N.Y.: Edwin Mellen Press. pp. 175-194.

Sung, Y.-H. (1966). *Chinese technology in the seventeenth century. T'ien-Kung K'ai-Wu (translated from the chinese and annotated by E-Tu Zen Sun and Shiou-Chuan Sun).* Mineola, New york: Dover publications.

Taylor, S. J., & Shell, C. A. (1988). Social and Historical Implications of Early Chinese Iron Technology. In Maddin (Ed.), *The beginning of the use of metals and alloys : papers from the Second International Conference on the Beginning of the Use of Metals and Alloys, Zhengzhou, China, 21-26 October*. Cambridge: MIT Press. pp. 205-221.

Tholander, E. (1989). Microstructure examination of slags as an instrument for identification of ancient-iron making processes. In Pleiner (Ed.), *Archaeometallurgy of iron: International symposium of the Comité pour la sidérurgie ancienne de l'UISPP: Liblice, 5-9 October 1987* Prague pp. 35-42.

Thomas, G. R., & Young, T. P. (1999). The determination of bloomery furnace mass balance and efficiency. In Pollard (Ed.), *Geoarchaeology: exploration, environments, resources*. Geological Society, London, Special Publications 165. pp. 155-164.

Thondhlana, T. P. (2012). *Metalworkers and Smelting Precincts: Technological Reconstructions of Second Millennium Copper Production around Phalaborwa, Northern Lowveld of South Africa.* (Unpublished Ph.D dissertation), University College London, UCL Institute of Archaeology.

Thondhlana, T. P., Martinón-Torres, M., & Chirikure, S. (2016). The archaeometallurgical reconstruction of early second-millennium AD metal production activities at Shankare Hill, northern Lowveld, South Africa. *Azania: Archaeological Research in Africa*, 1-35.

Thornton, C. P., Rehren, Th., & Pigott, V. (2009). The production of speiss (iron arsenide) during the Early Bronze Age in Iran. *Journal of Archaeological Science, 36* (2), 308-316.

Tite, M., Kilikoglou, V., & Vekinis, G. (2001). Strength, toughness and thermal shock resistance of ancient ceramics, and their influence on technological choice. *Archaeometry, 34*, 301-324.

Tsuna, M. (1983). *Kodo Zuroku. Illustrated Book on the Smelting of Copper.* (A facsimile of the original edition ca. 1801, edited by Cyril Stanley Smith). Norwalk, Connecticat: Burndy Library.

Tylecote, R. F. (1962). *Metallurgy in archaeology: A prehistory of metallurgy in the British isles.* London: Edward Arnold.

Tylecote, R. F., Austen, J. N., & Wrath, A. E. (1971). The mechanism of the bloomery process in shaft furnaces. *Journal of the Iron and Steel Institute, 209*, 342-263.

Tylecote, R. F., Ghaznavia, H. A., & Boydell, P. J. (1977). Partitioning of Trace Elements Between the Ores, Fluxes, Slags and Metal During the Smelting of Copper. *Journal of Archaeological Science, 4*, 305-333.

Tylecote, R. F. (1980). Summary of results of experimental work on early copper smelting. In Oddy (Ed.), *Aspects of Early Metallurgy*. London: British Museum British Museum Occasional Paper nº 17, pp. 5-12.

Tylecote, R. F. (1981). Comparison between Western and Eastern metallurgical technologies as deduced from traditional Japanese and Chinese illustrations. *Bulletin of the Metals Museum, 6*, 1-14.

Tylecote, R. F. (1986). *The prehistory of metallurgy in the British isles.* London: Institute of Metals.

Tylecote, R. F. (1987). *The early history of metallurgy in Europe.* London: Longman.

Tylecote, R. F. (1992). *A history of metallurgy (2nd ed).* London: Institute of Metals.

Underhill, A. P. (1996-97). The Lung-Shan period in the Yellow river Valley: communities at the treshold of the bronze age. In Bulbeck (Ed.), *Ancient Chinese and Southeast Asian bronze age cultures: the proceedings of a conference held at the Edith and Joy London Foundation property, Kioloa, NSW, 8-12 February, 1988* Taipei: SMS Publishing Inc. Vol. 2, pp. 615-633.

Unglik, H. (1991). Observations on the structures and formation of microscopic smithing residues from Bixby Blacksmith Shop at Barre Four Corners, Massachussets 1824-55. *Historical Metallurgy, 25* (2), 92-98.

Van Brempt, L., & Kassianidou, V. (2016). Facing the complexity of copper-sulphide ore smelting and assessing the role of copper in south-central Cyprus: A comparative study of the slag assemblage from Late Bronze Age Kalavasos-Ayios Dhimitrios. *Journal of Archaeological Science: Reports, 7*, 539-553.

Veldhuijzen, A. (2005). *Early iron production in the Levant: smelting and smithing at early 1st millennium BC Tell Hammeh, Jordan, and Tel Beth-Shemesh, Israel.* (Unpublished Ph.D dissertation), University College London.

Veldhuijzen, A., & Rehren, Th. (2007). Slags and the city: early iron production at Tell Hammeh, Jordan, and Tel Beth-Shemesh, Israel. In La-Niece, Hook & Craddock (Eds.), *Metals and mines: studies in archaeometallurgy*. London: Archetype. pp. 189-201.

Venunan, P. (2015). *An archaeometallurgical study of iron production in Ban Kruat, lower Northeast Thailand: Technology and social development from the Iron Age to the imperial Angkorian Khmer period (fifth century BC – fifteenth century AD).* (Unpublished Ph.D dissertation), University College London, UCL Institute of Archaeology.

Wagner, D. B. (1985). *Dabieshan: Traditional Chinese Iron-production Techniques Practised in Southern Henan in the Twentieth Century.* London and Malmö: Curzon.

Wagner, D. B. (1986). Ancient Chinese copper smelting, sixth century BC: recent excavation and simulation experiments. *Journal of Historical Metallurgy Society, 20* (1), 1-16.

Wagner, D. B. (1989). *Toward the Reconstruction of Ancient Chinese Technique for the Production of Malleable Cast Iron.* East Asian Institute Occasional Papers 4. Copenhagen: University of Copenhagen.

Wagner, D. B. (1995). The traditional Chinese iron industry and its modern fate. *Chinese Science, 12*, 138-161.

Wagner, D. B. (1996). *Iron and steel in ancient China.* Leiden: E.J. Brill (2nd edition with corrections).

Wagner, D. B. (1997). *The traditional Chinese iron industry and its modern fate.* Nordic Institute of Asian Studies 32. Richmond: Curzon.

Wagner, D. B. (1999). The earliest use of iron in China. In Young, Pollard, Bodel & Ixer (Eds.), *Metals in antiquity*. Oxford: BAR International Series 792. pp. 1-9.

Wagner, D. B. (2000). Chinese monumental iron castings. *Journal of East Asian Archaeology, 2* (3/4), 199-244.

Wagner, D. B. (2001a). *The state and the iron industry in Han China.* Copenhagen: Nordic Institute of Asian Studies.

Wagner, D. B. (2001b). Blast furnaces in Song-Yuan China. *East Asian Science, Technology, and Medicine, 18*, 41-74.

Wagner, D. B. (2001c). Technology as seen through the case of ferrous metallurgy in Han China In Chemla (Ed.), *Enciclopedia Italiana: Storia della scienza: Scienza in Cina*. Roma: Instituto della Enciclopedia Italiana.

Wagner, D. B. (2005). The State Ironworks in Zunhua, Hebei, 1403–1581. *Late Imperial China, 26* (2), 68-88.

Wagner, D. B. (2008). *Science and Civilisation in China, Part XI: Ferrous metallurgy.* Vol. 5. Cambridge University Press.

Wang, A. (2000). *Cosmology and political culture in Early China.* Cambridge: Cambridge University Press.

Wang, L., & Robinson, K. (1971). Science and civilisation in China. Volume 4, Physics and physical technology. Cambridge: Cambridge University Press.

Wang, Q. (2002). *Metalworking technology and deterioration of Jin bronzes from the Tianma-Qucun site, Shanxi, China.*, BAR international series 1023. Oxford: Archaeopress.

Wang, Z. (1982). *Han civilization.* New Haven: Yale University Press.

Watt, J. (2004). *China: dawn of a golden age, 200-750 AD.* New York: Metropolitan Museum of Art.

Wayman, M. L., & Michaelson, C. (2006). The metallurgy of early Chinese wrought-iron and steel objects from the British Museum *Historical Metallurgy, 40* (2), 95-104.

Wei, G., Qin, Y., Han, C., Qu, Y., Wang, C., & Dong, Y. (2008). Analysis of Smelting Relics from Lidegui Site of Daye City （大冶李德贵冶炼遗址矿冶遗物分析）. *Rock and Mineral Analysis, 27* (2), 99-102.

Whitbread, I. K. (1995). *Greek transport anphorae, a petrological and archaeological study.* Occasional paper 4. The British School at Athens: Ficth laboratory, Athens.

White, J. R. (1980). Historic blast furnace slag: Archaeological and metallurgical analysis. *Journal of Historical Metallurgy Society, 14*, 55-64.

Will, P.-E. (1990). *Bureaucracy and Famine in Eighteenth-Century China.* Stanford: Stanford University Press.

Will, P.-E., & Wong, R. B. (1991). *Nourish the People: the State Civilian Granary System in China, 1650-1850.* Ann Arbor: University of Michigan Center for Chinese Studies.

Wingrove, J. (1970). Identification of iron oxides. *Journal of Iron and Steel Institute, 208* (3), 258-264.

Wright, T. (2007). An economic cycle in Imperial China? Revisiting Robert Hartwell on iron and coal. *Journal of the Economic and Social History of the Orient, 50*, 398-423.

Wrona, A. (2013). The Production of High Carbon Steel Directly in Bloomery Process: Theoretical Bases and Metallographic Analyses of the Experiments Results. *EXARC, 2013/2*. doi: http://journal.exarc.net/

Wu, S. X. (2015). *Empires of Coal: Fueling China's Entry into the Modern World Order, 1860–1920.* Standford, California: Stanford University Press.

Xia, N., & Yin, W. (1982). The ancient copper mine at Tonglüshan, Hubei （湖北铜绿山古铜矿）. *Kaogu Xuebao （考古学报）, 1*, 1-14.

Xiao, C. (2014). The Underground Kingdom of Chu. *China Scenic*. Retrieved from http://www.chinascenic.com/ website:

Xie, G., Mao, J., Zhao, H., Wei, K., Jin, S., Pan, H., & Ke, Y. (2011). Timing of skarn deposit formation of the Tonglushan ore district, southeastern Hubei Province, Middle–Lower Yangtze River Valley metallogenic belt and its implications. *Ore Geology reviews, 43*, 62-77.

Xu, Z., & Linduff, K. M. (1988). *Western Chou civilization.* New Haven: Yale University Press.

Yan, W. (2000). A discussion of the Chalcolithic Age in China. In Linduff, Han & Sun (Eds.), *The beginnings of metallurgy in China*. Lewiston: Edwin Mellen Press. pp. 99-116.

Young, T. (2011). Some preliminary observations on hammerscale and its implications for understanding welding. *Historical Metallurgy, 45* (1), 26-41.

Young, T. (2012). Iron: hand blacksmithing. *The Historical Metallurgy Society: Archaeology Datasheet No 303, hist-met.org*.

Young, T. P., & Poyner, D. (2012). Two medieval bloomery sites in Shropshire: the adoption of water power for iron smelting. *Historical Metallurgy, 46*, 78-97.

Yuan, G. (2013). The Discovery and Study of the Early Shang Culture. In Underhill (Ed.), *A companion to Chinese archaeology*. Hoboken, NJ: Wiley-Blackwell. pp. 323-342.

Zhang, Y., & Fan, W. (2003). *The History and Civilization of China.* Beijing: Central Party Literature Publishing House.

Zhao, H., Xie, G., Wei, K., & Ke, Y. (2012). Mineral compositions and fluid evolution of the Tonglushan skarn Cu–Fe deposit, SE Hubei, east-central China. *International Geology Review, 54* (7), 737-764.

Zhou, B., Hu, Y., & Lu, B. (1988). Ancient copper mining and smelting at Tonglushan, Daye. In Maddin (Ed.), *The beginning of the use of metals and alloys : papers from the Second International Conference on the Beginning of the Use of Metals and Alloys, Zhengzhou, China, 21-26 October*. Cambridge, Mass: MIT Press. pp. 125-129.

Zhou, W., Chen, J., Lei, X., Xu, T., Chong, J., & Wang, Z. (2009). Three Western Zhou bronze foundry sites in the Zhouyuan area, Shaanxi province, China. In Mei & Rehren (Eds.), *Metallurgy and Civilisation: Eurasia and Beyond, BUMA VI*. London: Archetype. pp. 62-72.

Zhou, W., Martinón-Torres, M., Chen, J., & Li, y. (2014). Not so efficient, but still distilled: the technology of Qing Dynasty zinc production at Dafengmen, Chongqing, southwest China. *Journal of Archaeological Science, 43*, 278-288.

Zhu, J., & Xiong;, B. (2006). *The Spring and Autumn period walled city of Wulijie in Daye （大冶五里界：春秋城址与周围遗址考古报告）*. Beijing: Science Press.

Zhu, S. (1986). Ancient metallurgy of non-ferrous metals in China. *Bulletin of the Metals Museum, 11*, 1-13.

Zhu, S., & Zhang, W. (1986). A study of the Song period metallurgical furnaces at Tonglüshan in Daye County, Hubei (in Chinese). *Kaogu, 1*, 469-476.

Appendices

Appendix I Chinese history timeline

***ca.* 5000-2000 BC**	**Neolithic cultures (in the middle-Yangtze river)**	**Daxi (5000-3000) Qujialing (3400-2600) Shijiahe (2500-2000) Yangyue (3000-1800)**
***ca.* 1600-1050 BC**	**Shang Dynasty**	
***ca.* 1046-256 BC**	**Zhou Dynasty**	
	Western Zhou (*ca.* 1046-771 BC)	
	Eastern Zhou (*ca.* 771-221 BC)	**Spring and Autumn Period (*ca.* 770-475 BC) Warring States Period (*ca.* 475-221 BC)**
221-206 BC	**Qin Dynasty**	
206 BC-AD 220	**Han Dynasty**	
	Western Han (206 BC-AD 9)	
	Eastern Han (AD 25-220)	
AD 220-589	**Six Dynasties Period**	
AD 581-618	**Sui Dynasty**	
AD 618-906	**Tang Dynasty**	
AD 907-960	**Five Dynasties Period**	
AD 960-1279	**Song Dynasty**	
	Northern Song (960-1127)	
	Southern Song (1127-1279)	
AD 1279-1368	**Yuan Dynasty**	
AD 1368-1644	**Ming Dynasty**	
AD 1644-1912	**Qing Dynasty**	

Appendix II SEM-EDS analysis of CRMs

BHVO-2, BCS-2 CRMs and NIST 1412 are polished blocks. The rest of CRMs are pressed powder pellets, which is reflected in higher errors and lower analytical totals due to mineralogical effects and porosity. Trace elements are below detection limits in all cases and thus the tables only report values higher than 0.1%.

Swedish Slag

	Na_2O	Al_2O_3	SiO_2	K_2O	CaO	TiO_2	MnO	FeO	Total
	wt%	wt%	wt%	wt%	wt%	wt%	wt%	wt%	wt%
Normalised reference values	0.64	7.76	25.82	1.03	1.52	0.32	3.27	59.63	95.76
Measurements (normalised)									
09/06/2013	0.9	7.6	24.6	1.3	1.7	0.3	3.1	60.5	88.8
03/06/2014	1.1	8.3	24.0	1.4	1.8	0.4	3.2	59.9	88.9
14/07/2014	1.0	7.5	23.4	1.3	1.6	0.3	3.5	61.3	86.0
08/12/2014	1.0	7.4	23.9	1.3	1.5	0.3	3.1	61.5	86.5
03/03/2015	1.2	7.6	24.4	1.2	1.6	0.4	3.5	60.1	91.1
22/06/2015	1.0	7.6	24.8	1.2	1.7	0.2	2.9	60.7	90.0
Mean	1.0	7.7	24.2	1.3	1.6	0.3	3.2	60.6	
Precision									
Standard deviation	0.1	0.3	0.5	0.1	0.1	0.1	0.2	0.6	
Coefficient of variation (%)	17	4	2	8	6	17	7	1	
Accuracy									
Absolute error	0.4	-0.1	-1.6	0.2	0.1	0.0	1.0	0.4	
Relative error	62	-1	-6	24	8	-1	2	1	

Kresten, P., & Hjärthener-Holdar, E. (2001). Analysis of the Swedish ancient iron reference slag W-25:R. *Historical Metallurgy*, 35 (48-51).

BHVO-2 Basalt, Hawaiian Volcanic Observatory

	Na_2O	MgO	Al_2O_3	SiO_2	P_2O_5	K_2O	CaO	TiO_2	MnO	FeO	*Total*
	wt%	wt%	wt%	wt%	wt%	wt%	wt%	wt%	wt%	wt%	wt%
Normalised reference values	2.25	7.33	13.69	50.61	0.27	0.53	11.56	2.77	0.17	11.26	98.60
Measurements (normalised)											
09/06/2013	2.1	6.7	13.0	49.7	1.1	0.5	11.5	2.6	0.5	11.1	98.8
03/06/2014	2.3	6.8	12.5	49.0	1.0	0.5	11.6	2.9	0.4	11.3	98.4
14/07/2014	2.3	7.0	12.7	49.6	0.9	0.6	11.4	2.5	0.4	10.8	98.1
08/12/2014	2.2	6.9	12.6	49.2	1.1	0.6	11.3	2.4	0.3	11.2	97.9
03/03/2015	2.6	6.8	12.6	49.7	1.0	0.5	11.5	2.6	0.4	11.9	99.6
22/06/2015	2.3	7.3	12.7	49.6	1.2	0.5	11.1	2.7	0.6	11.5	99.4
Mean	2.3	6.9	12.7	49.5	1.0	0.5	11.4	2.6	0.4	11.3	98.7
Precision											
Standard deviation	0.1	0.2	0.2	0.3	0.1	0.0	0.2	0.2	0.1	0.3	
Coefficient of variation (%)	6	3	1	1	11	9	2	6	22	3	
Accuracy											
Absolute error	0.1	-0.4	-1.0	-1.2	0.8	0.0	-0.2	-0.1		0.0	
Relative error	4	-6	-7	-2	285	-2	-1	-5		0.2	

United States Geological Survey (USGS), 1998. Certificate of Analysis: Basalt, Hawaiian Volcanic Observatory, BHVO-2.

http://crustal.usgs.gov/geochemical_reference_standards/basaltbhvo2.html#bibliography

BCR-2

	Na_2O	MgO	Al_2O_3	SiO_2	P_2O_5	K_2O	CaO	TiO_2	FeO	*Total*
	wt%	wt%	wt%	wt%	wt%	wt%	wt%	wt%	wt%	wt%
Norm. ref. values	3.22	3.65	13.74	55.05	0.36	1.82	7.24	2.30	12.63	98.28
Measurements										
09/06/2013	3.3	3.5	13.0	55.6	0.4	1.8	7.4	2.3	12.6	99.1
03/06/2014	3.3	3.7	13.1	55.7	0.3	1.9	7.2	2.3	12.7	99.6
14/07/2014	3.3	3.3	13.0	55.4	0.4	1.9	7.4	2.5	12.7	98.5
08/12/2014	3.2	3.6	12.9	55.9	0.4	1.7	7.4	2.3	12.6	98.5
03/03/2015	3.3	3.7	13.1	55.2	0.6	1.8	7.4	2.2	12.8	99.5
22/06/2015	3.6	3.6	12.8	55.9	0.5	1.7	7.2	2.4	12.2	99.4
Mean	3.3	3.6	13.0	55.6	0.4	1.8	7.3	2.4	12.6	
Precision										
Standard deviation	0.1	0.1	0.1	0.3	0.1	0.1	0.1	0.1	0.2	
Coefficient of var. (%)	4	4	1	1	26	4	2	5	2	
Accuracy										
Absolute error	0.1	-0.1	-0.8	0.6	0.1	0.0	0.1	0.1	0.0	
Relative error	3	-2	-5	1	15	-1	1	2	-0.2	

United States Geological Survey (USGS), 1998. Certificate of Analysis: Basalt, Columbia River, BCR-2.

http://crustal.usgs.gov/geochemical_reference_standards/pdfs/basaltbcr2.pdf

NCS Clay DC60105

	Na_2O	MgO	Al_2O_3	SiO_2	K_2O	CaO	TiO_2	FeO	*Total*
	wt%	wt%	wt%	wt%	wt%	wt%	wt%	wt%	wt%
Normalised reference values	1.92	1.95	14.08	70.67	2.82	3.43	0.70	4.43	94.30
Measurements (normalised)									
09/06/2013	1.9	2.5	16.6	64.9	3.2	3.9	0.9	6.3	82.7
03/06/2014	2.0	2.5	16.2	65.2	3.2	4.1	0.9	6.0	81.7
14/07/2014	1.7	2.7	16.3	64.4	3.3	4.3	0.8	6.4	82.8
08/12/2014	1.9	2.5	16.2	65.3	3.2	4.0	0.6	6.4	81.3
03/03/2015	2.0	2.5	17.0	65.3	3.2	3.8	0.7	5.5	83.0
22/06/2015	1.9	2.5	16.5	64.9	3.3	4.4	0.8	5.9	82.2
22/06/2015	1.8	2.6	16.7	64.2	3.3	4.2	0.8	6.4	83.5
Mean	1.9	2.5	16.5	64.9	3.2	4.1	0.8	6.1	
Precision									
Standard deviation	0.1	0.1	0.3	0.4	0.1	0.2	0.1	0.3	
Coefficient of variation (%)	6	4	2	1	2	5	13	6	
Accuracy									
Absolute error	-0.1	0.6	2.4	-5.9	0.6	0.7	0.1	1.7	
Relative error	-4	29	17	-8	22	19	10	38	

https://www.labmix24.com/extern/downloadpdfdetails/32203/

NIST 76a Burnt Refractory

	MgO	*Al_2O_3*	*SiO_2*	*K_2O*	*TiO_2*	*FeO*	*Total*
	wt%	wt%	wt%	wt%	wt%	wt%	wt%
Normalised reference values	0.53	39.13	55.51	1.34	2.05	1.46	98.90
Measurements (normalised)							
09/06/2013	0.5	37.8	55.8	1.5	2.3	2.2	84.8
03/06/2014	0.3	37.6	56.0	1.5	2.5	2.1	85.7
14/07/2014	0.5	37.7	56.1	1.4	2.3	1.9	87.7
08/12/2014	0.4	38.0	56.5	1.3	2.0	1.8	86.8
03/03/2015	0.5	38.0	56.1	1.5	2.3	1.6	86.9
22/06/2015	0.6	38.4	55.7	1.4	2.1	1.9	85.7
Mean	0.5	37.9	56.0	1.4	2.3	1.9	
Precision							
Standard deviation	0.1	0.3	0.3	0.1	0.2	0.2	
Coefficient of variation (%)	19	1	1	6	9	10	
Accuracy							
Absolute error	-0.1	-1.2	0.5	0.1	0.2	0.5	
Relative error	-12	-3	1	6	10	32	

National Institute of Standards & Technology (NIST), 1992. Certificate of Analysis – Standard Reference Materials 76a, 77a, and 78a Burnt Refractories. Gaithersberg, Maryland: ASTM/NIST.

https://www-s.nist.gov/srmors/view_det0.120ail.cfm?srm=76a

NIST 1412, multi-component glass

The certified composition also includes Li_2O (4.53%) and B_2O_3 (4.50%), but these light oxides cannot be detected by EDS.

	Na_2O	*MgO*	*Al_2O_3*	*SiO_2*	*K_2O*	*CaO*	*ZnO*	*SrO*	*CdO*	*BaO*	*PbO*	*Total*
	wt%	wt%	wt%	wt%	wt%	wt%	wt%	wt%	wt%	wt%	wt%	wt%
Norm. ref.	5.18	5.18	8.31	46.85	4.58	5.01	4.95	5.03	4.84	5.16	4.86	
Measurem.												
09/06/2013	6.0	5.0	7.8	47.2	4.0	5.1	4.9	4.6	5.2	5.1	5.2	89.0
03/06/2014	5.9	4.5	8.0	47.5	4.4	4.9	4.7	4.9	4.9	5.2	4.9	90.5
14/07/2014	5.5	4.8	8.0	46.4	4.1	5.3	5.6	4.8	5.2	5.0	5.3	92.2
08/09/2014	6.1	4.6	8.0	47.1	4.5	5.0	5.1	4.3	5.0	5.2	5.2	91.4
10/10/2014	6.0	4.9	7.9	46.2	5.0	5.0	4.9	5.0	4.7	5.4	4.9	90.3
08/12/2014	5.9	4.8	8.0	47.4	4.3	4.9	5.1	4.7	4.6	5.2	4.9	91.4
03/03/2015	5.5	4.7	7.5	47.4	4.4	5.2	4.7	5.1	5.0	5.5	4.9	90.6
01/04/2015	5.4	4.9	8.1	46.8	4.9	5.0	4.9	4.5	5.0	5.5	5.1	91.7
22/06/2015	5.9	4.9	8.0	46.5	4.5	5.0	4.7	5.0	5.2	5.3	5.1	91.9
Mean	5.8	4.8	7.9	46.9	4.5	5.0	5.0	4.8	5.0	5.3	5.0	
Precision												
Standard dev.	0.3	0.1	0.2	0.5	0.3	0.1	0.3	0.3	0.2	0.2	0.1	
Coeff. of var.	5	3	2	1	7	2	6	6	4	3	3	
Accuracy												
Absolute error	-0.6	0.4	0.4	-0.1	0.1	0.0	0.0	0.2	-0.1	-0.1	-0.2	
Relative error	-12	8	5	0	2	-1	0	5	-3	-2	-4	

https://www-s.nist.gov/srmors/certificates/1412.pdf

WD-XRF analysis of CRMs

Swedish slag

	Na_2O	MgO	Al_2O_3	SiO_2	P_2O_5	SO_3	K_2O	CaO	TiO_2	V_2O_5	Cr_2O_3	MnO	FeO	SrO	ZrO_2	BaO	La_2O_3	CeO_2	Total
	wt%	wt%	wt%	wt%	wt%	wt%	wt%	wt%	wt%	wt%	wt%	wt%	wt%	wt%	wt%	wt%	wt%	wt%	wt%
Normalised reference values	0.63	0.42	7.67	25.53	0.27	0.10	1.02	1.51	0.32	0.03	0.01	3.23	59.12	0.01	0.01	0.08	0.01	0.03	96.89
Measurements (normalised)																			
10/04/2014	0.86	0.28	7.95	22.73	0.25	0.14	1.02	1.29	0.25	0.03	0.02	3.19	61.78	0.01	0.02	0.11	0.02	0.05	90.20
18/11/2014	0.85	0.27	7.88	22.82	0.24	0.13	1.03	1.32	0.25	0.02	0.01	3.14	61.86	0.01	0.02	0.12	0.01	0.03	90.20
Mean	0.86	0.27	7.91	22.78	0.24	0.13	1.03	1.31	0.25	0.03	0.01	3.16	61.82	0.01	0.02	0.12	0.01	0.04	
Precision																			
Standard deviation	0.0	0.0	0.1	0.1	0.0	0.0	0.0	0.0	0.0	0.0	0.0	0.0	0.1	0.0	0.0	0.0	0.0	0.0	
Coefficient of variation (%)	2	0	1	0	4	5	1	1	0	24	30	1	0	4	0	2	18	39	
Accuracy																			
Absolute error	0.23	-0.15	0.24	-2.75	-0.02	0.03	0.00	-0.20	-0.07	0.00	0.00	-0.07	2.70	0.00	0.00	0.04	0.00	0.01	
Relative error	36	-35	3	-11	-9	30	0	-13	-22	-11	29	-2	5	46	23	51	47	16	

BHVO-2 Basalt, Hawaiian Volcanic Observatory

	Na_2O	MgO	Al_2O_3	SiO_2	P_2O_5	K_2O	CaO	TiO_2	V_2O_5	Cr_2O_3	MnO	Fe_2O_3	*Total*
	wt%	wt%	wt%	wt%	wt%	wt%	wt%	wt%	wt%	wt%	wt%	wt%	wt%
Normalised reference values	2.21	7.21	13.46	49.73	0.27	0.52	11.36	2.72	0.06	0.04	0.17	12.26	100.33
Measurement (normalised)													
10/04/2014	2.48	5.40	16.45	48.77	0.26	0.51	10.69	2.24	0.08	0.06	0.18	12.88	86.80
Accuracy													
Absolute error	0.26	-1.81	2.99	-0.97	-0.01	0.00	-0.67	-0.48	0.03	0.02	0.01	0.62	
Relative error	12	-25	22	-2	-2	-1	-6	-18	48	50	9	5	

NIST76a Burnt Refractory

	Na_2O	MgO	Al_2O_3	SiO_2	P_2O_5	K_2O	CaO	TiO_2	Fe_2O_3	SrO	*Total*
	wt%	wt%	wt%	wt%	wt%	wt%	wt%	wt%	wt%	wt%	wt%
Normalised reference values	0.07	0.52	38.88	55.16	0.13	1.34	0.22	2.04	1.61	0.04	99.58
Measurement(normalised)											
10/04/2014	0.06	0.63	39.22	54.83	0.12	1.34	0.21	1.73	1.81	0.05	86.90
18/11/2014	0.06	0.65	39.17	54.91	0.12	1.34	0.21	1.73	1.78	0.05	87.00
Mean	0.06	0.64	39.20	54.87	0.12	1.34	0.21	1.73	1.79	0.05	
Precision											
Standard deviation	0.00	0.01	0.04	0.06	0.00	0.00	0.00	0.00	0.02	0.00	
Coefficient of variation (%)	2	1	0	0	2	0	1	0	1	2	
Accuracy											
Absolute error	-0.01	0.12	0.31	-0.29	-0.01	0.01	-0.01	-0.31	0.18	0.01	
Relative error	-17	22	1	-1	-6	1	-5	-15	11	25	

Appendix III Normalised WD-XRF data for copper slag samples

(as given by Department of Geociences, University of Fribourg)

Sample	Na_2O	MgO	Al_2O_3	SiO_2	P_2O_5	SO_3	K_2O	CaO	TiO_2	MnO	Fe_2O_3	CuO
HF1	0.16	1.48	7.26	26.36	0.50	0.08	1.82	5.00	0.22	0.34	56.41	0.01
HF2	0.05	0.58	5.10	29.96	1.15	0.23	0.50	2.16	0.13	0.20	58.52	0.79
HF4	0.02	0.56	2.55	18.35	3.21	0.09	0.27	0.57	0.14	1.02	71.95	0.86
HF15	0.02	1.08	4.83	22.29	4.49	0.15	0.42	1.82	0.20	0.86	62.09	1.10
HF16	0.10	1.10	6.45	31.89	0.50	0.26	0.68	2.55	0.12	0.31	54.07	1.34
HF17	0.06	6.84	4.72	32.37	1.70	0.22	1.00	2.49	0.14	0.73	46.42	2.61
MC2	0.06	0.46	4.72	25.55	0.47	0.36	0.59	2.47	0.19	0.21	63.57	0.91
MC3	0.05	0.78	4.36	21.83	0.70	2.02	0.49	3.88	0.14	0.39	63.74	1.26
MC4	0.01	1.28	4.59	30.58	0.89	0.21	0.44	7.33	0.15	0.69	49.37	3.90
MC5	0.02	0.41	5.82	26.52	2.41	0.16	0.50	1.40	0.21	0.49	59.09	2.59
MC7	0.05	0.52	6.32	22.06	2.15	0.47	0.41	1.39	0.20	0.36	64.57	1.20
MC8	0.04	0.45	6.12	24.49	2.32	0.23	0.35	1.74	0.20	0.47	62.50	0.72
MC14	0.04	0.51	11.59	39.05	1.29	0.24	0.63	2.41	0.33	0.32	41.30	1.93
MC15	0.07	0.59	6.92	27.25	1.16	0.28	0.47	1.68	0.21	0.91	59.21	0.87
MY1	0.06	0.42	5.66	27.64	0.36	0.85	0.64	1.60	0.15	0.24	61.50	0.61
MY2	0.08	0.76	6.32	33.41	0.68	0.29	0.91	2.39	0.22	0.33	53.50	0.76
MY3	0.14	0.73	5.60	30.09	0.50	0.60	1.06	2.59	0.17	0.32	57.19	0.66
MY4	0.11	0.17	3.75	27.93	0.17	0.40	0.33	1.39	0.10	0.20	63.64	1.48
MY5	0.02	0.28	5.39	19.36	0.57	2.72	0.39	1.96	0.12	0.29	67.85	0.81
MY6	0.04	0.57	6.20	18.49	1.28	0.51	0.28	1.23	0.18	0.43	69.62	0.82
MY7	0.04	0.55	2.07	24.11	0.23	0.78	0.25	1.77	0.05	0.19	68.72	1.03
MY8	0.10	0.55	6.03	31.79	0.34	0.50	0.94	2.27	0.17	0.21	56.27	0.56
MY9	0.06	0.48	4.90	29.23	0.30	0.35	0.69	1.74	0.12	0.18	61.01	0.69
MY10	0.02	0.37	4.69	21.57	1.03	0.95	0.33	0.99	0.12	0.22	68.64	0.76
MY11	0.04	0.51	5.97	36.61	2.09	0.28	0.61	2.32	0.31	0.33	48.23	2.34
MY12	0.07	0.57	4.92	21.02	0.95	0.65	0.41	1.69	0.12	0.26	67.97	0.84
MY13	0.19	0.83	8.97	28.88	1.38	0.75	0.81	2.52	0.22	0.30	53.85	0.57
MY14	0.04	0.61	6.50	22.84	1.00	1.01	0.76	1.84	0.27	0.28	63.79	0.71
MY18	0.03	0.29	3.30	21.15	0.43	0.90	0.21	1.79	0.10	0.37	70.26	0.88
MY19	0.02	0.46	5.40	21.21	1.73	0.67	0.37	0.85	0.20	0.33	67.75	0.68

Sample	Na_2O	MgO	Al_2O_3	SiO_2	P_2O_5	SO_3	K_2O	CaO	TiO_2	MnO	Fe_2O_3	CuO
MY20	0.02	0.39	2.55	24.15	0.27	0.36	0.22	1.34	0.06	0.18	68.57	1.69
MY21	0.02	0.42	2.94	30.29	0.25	1.45	0.27	1.12	0.07	0.20	61.87	0.89
MY22	0.03	0.32	3.13	23.08	0.36	0.86	0.26	1.12	0.08	0.16	69.69	0.67
MY23	0.05	0.47	3.49	26.48	0.39	0.43	0.32	1.06	0.11	0.21	65.99	0.76
MY24	0.04	0.41	4.15	33.12	0.47	0.30	0.32	0.86	0.13	0.19	59.10	0.67
MY25	0.04	0.49	3.68	22.30	0.43	1.63	0.46	1.93	0.10	0.21	67.55	0.91
MY26	0.02	0.45	2.08	8.51	0.51	0.73	0.05	0.46	0.06	0.31	85.87	0.73
WY1	0.19	0.84	5.86	31.26	0.52	0.38	0.84	2.24	0.22	0.35	56.23	0.75
WY2	0.18	0.71	5.32	28.91	0.41	0.82	0.83	1.91	0.20	0.37	59.43	0.64
WY4	0.27	0.75	7.29	37.30	0.49	0.20	0.86	1.67	0.33	0.48	49.40	0.64
WY7	0.03	0.35	2.23	28.64	1.09	0.38	0.49	1.41	0.09	0.22	63.56	1.14
WY8	0.08	0.67	5.49	29.09	0.43	0.11	1.14	2.95	0.27	0.17	59.24	0.79
XY2	0.13	1.00	8.26	33.97	0.86	0.21	1.00	2.21	0.30	0.46	50.62	0.61
XY3	0.17	1.10	7.99	34.02	0.96	0.22	0.98	2.72	0.28	0.47	50.03	0.68
XY4	0.15	0.98	8.08	32.44	0.87	0.22	0.95	2.25	0.29	0.47	52.30	0.65
XY5	0.11	1.12	7.41	28.52	0.68	0.16	0.56	1.29	0.30	0.52	57.64	1.24
XY6	0.11	0.99	8.68	33.03	0.77	0.21	0.95	1.95	0.31	0.46	51.28	0.81
XY7	0.16	1.14	8.20	34.61	0.95	0.24	1.05	2.52	0.29	0.50	49.44	0.54
XY8	0.18	1.04	7.34	32.00	1.07	0.26	0.95	2.20	0.27	0.52	53.20	0.62
XY9	0.16	1.27	8.17	30.97	0.87	0.27	1.08	2.32	0.29	0.52	53.11	0.59
XY10	0.14	0.97	8.21	33.58	0.85	0.21	0.89	2.15	0.29	0.45	51.29	0.61
XY11	0.17	1.02	7.92	34.21	0.94	0.27	1.06	2.44	0.31	0.50	50.33	0.47
XY12	0.18	1.18	9.48	32.78	0.52	0.27	1.03	1.97	0.33	0.50	50.93	0.49

Sample	Cl	V_2O_5	Cr_2O_3	Co_3O_4	NiO	ZnO	Ga_2O_3	GeO_2	As_2O_3	SeO_2	Br	Rb_2O	SrO	Y_2O_3	ZrO_2	Nb_2O_5	MoO_3	Ag_2O	CdO	In_2O_3	SnO_2
HF1	bdl	726	294	452	bdl	56	33	bdl	bdl	bdl	bdl	51	223	14	133	bdl	151	47	27	bdl	bdl
HF2	bdl	195	160	5200	bdl	664	41	bdl	bdl	bdl	1	20	105	10	75	bdl	249	37	16	bdl	89
HF4	41	308	180	690	bdl	1410	20	bdl	bdl	bdl	bdl	10	45	13	39	bdl	334	14	36	bdl	bdl
HF15	98	261	101	679	bdl	3000	47	bdl	bdl	bdl	bdl	19	119	11	91	bdl	837	31	20	bdl	bdl
HF16	139	354	145	420	bdl	2900	52	bdl	bdl	bdl	2	26	124	13	66	bdl	576	30	15	bdl	bdl
HF17	7	211	309	396	bdl	2850	11	4	bdl	bdl	bdl	45	106	19	71	bdl	723	53	21	bdl	bdl
MC2	bdl	459	203	454	bdl	1570	16	bdl	bdl	bdl	bdl	12	81	24	92	bdl	173	45	33	3	bdl
MC3	bdl	349	78	563	bdl	651	38	bdl	bdl	bdl	bdl	15	154	19	55	bdl	245	36	27	bdl	bdl
MC4	146	284	61	495	bdl	2390	24	bdl	bdl	bdl	bdl	22	54	33	62	bdl	671	35	2	bdl	bdl
MC5	bdl	275	108	600	bdl	784	39	bdl	bdl	bdl	bdl	18	68	29	130	6	227	61	46	21	bdl
MC7	19	321	136	496	bdl	619	13	bdl	bdl	bdl	bdl	21	52	14	113	7	180	16	22	bdl	bdl
MC8	22	468	59	509	bdl	1100	13	6	bdl	bdl	bdl	18	75	52	86	3	159	71	41	12	bdl
MC14	62	315	387	423	bdl	569	17	bdl	bdl	bdl	bdl	14	111	35	227	13	162	42	26	19	bdl
MC15	bdl	252	186	856	bdl	501	23	bdl	bdl	bdl	bdl	15	91	12	109	bdl	244	31	35	bdl	bdl
MY1	bdl	256	117	487	bdl	403	38	bdl	bdl	bdl	bdl	24	91	17	80	bdl	131	64	36	bdl	bdl
MY2	10	288	178	460	bdl	548	26	bdl	bdl	bdl	bdl	34	109	24	127	3	193	26	34	bdl	24
MY3	156	281	177	452	bdl	467	25	bdl	bdl	bdl	bdl	39	168	19	106	bdl	188	37	30	bdl	bdl
MY4	157	246	217	552	bdl	490	15	bdl	bdl	bdl	bdl	13	106	35	47	bdl	267	34	11	bdl	bdl
MY5	bdl	373	39	519	bdl	330	36	bdl	bdl	15	bdl	9	194	32	69	bdl	140	25	29	bdl	1
MY6	17	311	123	589	bdl	628	20	bdl	bdl	bdl	bdl	12	37	14	63	bdl	189	56	22	2	bdl

Sample	Cl	V_2O_5	Cr_2O_3	Co_3O_4	NiO	ZnO	Ga_2O_3	GeO_2	As_2O_3	SeO_2	Br	Rb_2O	SrO	Y_2O_3	ZrO_2	Nb_2O_5	MoO_3	Ag_2O	CdO	In_2O_3	SnO_2
MY7	13	225	52	506	bdl	317	12	bdl	bdl	bdl	bdl	13	48	7	29	bdl	209	70	26	1	bdl
MY8	9	248	151	479	bdl	365	19	bdl	bdl	bdl	bdl	32	128	20	110	1	159	19	24	bdl	bdl
MY9	30	210	121	526	bdl	267	20	bdl	bdl	bdl	bdl	27	104	8	81	6	203	39	28	2	bdl
MY10	5	289	113	524	bdl	845	5	bdl	bdl	27	bdl	25	46	8	55	bdl	314	51	25	9	bdl
MY11	30	344	314	505	bdl	394	28	bdl	bdl	bdl	bdl	15	163	16	153	3	166	31	20	bdl	bdl
MY12	17	271	115	582	bdl	772	25	bdl	bdl	bdl	bdl	18	70	5	75	2	304	42	24	bdl	42
MY13	17	298	220	535	bdl	1080	37	bdl	bdl	bdl	bdl	41	111	11	129	bdl	331	30	bdl	5	303
MY14	11	470	194	527	bdl	759	35	bdl	bdl	bdl	bdl	24	110	17	100	7	181	53	32	1	bdl
MY18	58	256	136	520	bdl	519	21	bdl	bdl	bdl	bdl	11	18	bdl	38	8	177	35	32	bdl	bdl
MY19	bdl	344	131	518	bdl	599	27	bdl	bdl	bdl	bdl	5	43	22	125	bdl	198	44	18	bdl	bdl
MY20	bdl	147	125	496	bdl	300	15	bdl	bdl	bdl	bdl	10	68	bdl	34	bdl	170	19	12	6	bdl
MY21	21	189	167	457	bdl	321	3	bdl	bdl	bdl	bdl	11	48	bdl	26	bdl	308	45	54	18	bdl
MY22	14	175	101	550	bdl	257	3	bdl	bdl	bdl	bdl	12	52	bdl	53	bdl	208	48	31	bdl	bdl
MY23	17	312	152	474	bdl	365	9	bdl	bdl	bdl	bdl	3	35	19	50	bdl	154	26	13	bdl	16
MY24	28	273	176	532	bdl	317	27	10	bdl	bdl	bdl	17	35	11	52	bdl	172	56	20	5	bdl
MY25	28	201	109	526	bdl	305	25	bdl	bdl	bdl	bdl	21	77	3	56	bdl	190	36	5	bdl	bdl
MY26	bdl	329	74	452	bdl	177	10	bdl	bdl	bdl	bdl	11	4	bdl	35	bdl	150	30	20	bdl	bdl
WY1	bdl	243	272	554	bdl	526	7	9	bdl	bdl	bdl	41	177	21	152	5	187	39	41	bdl	2
WY2	bdl	295	149	501	bdl	488	23	3	bdl	bdl	bdl	35	165	17	122	2	152	43	9	bdl	bdl
WY4	18	302	304	490	bdl	578	9	bdl	bdl	bdl	bdl	43	143	23	205	bdl	174	56	28	bdl	bdl
WY7	15	299	149	515	bdl	1270	8	bdl	bdl	11	bdl	17	71	14	37	bdl	229	38	28	5	bdl
WY8	bdl	1670	206	bdl	52	16	26	bdl	bdl	bdl	32	107	21	129	8	100	41	48	24	bdl	5

Sample	Cl	V_2O_5	Cr_2O_3	Co_3O_4	NiO	ZnO	Ga_2O_3	GeO_2	As_2O_3	SeO_2	Br	Rb_2O	SrO	Y_2O_3	ZrO_2	Nb_2O_5	MoO_3	Ag_2O	CdO	In_2O_3	SnO_2
XY2	12	289	237	471	bdl	688	24	bdl	bdl	bdl	bdl	44	126	13	178	2	213	53	30	bdl	bdl
XY3	14	249	227	461	bdl	740	16	9	3	bdl	bdl	45	151	21	159	bdl	195	47	24	bdl	13
XY4	12	271	173	430	bdl	785	4	7	bdl	bdl	bdl	39	135	24	161	bdl	158	30	51	bdl	bdl
XY5	162	312	281	636	bdl	1740	31	bdl	bdl	bdl	1	31	69	18	152	11	113	43	1	bdl	11
XY6	7	323	223	500	bdl	890	39	bdl	bdl	bdl	bdl	49	119	23	171	2	194	43	42	bdl	bdl
XY7	bdl	310	162	477	bdl	711	31	2	bdl	bdl	bdl	41	131	19	148	7	126	29	45	bdl	bdl
XY8	58	268	180	511	bdl	829	13	bdl	bdl	bdl	2	45	135	15	153	10	194	11	15	bdl	bdl
XY9	bdl	242	193	501	bdl	828	38	bdl	bdl	bdl	bdl	35	136	18	155	8	219	26	19	bdl	bdl
XY10	26	302	238	437	bdl	744	26	6	bdl	bdl	bdl	41	125	21	162	5	189	55	18	3	bdl
XY11	bdl	303	235	482	bdl	708	36	bdl	bdl	bdl	bdl	45	140	25	166	4	138	51	31	bdl	bdl
XY12	68	308	233	451	bdl	596	35	bdl	bdl	bdl	bdl	46	111	23	186	4	113	33	19	bdl	bdl
XY13	52	291	179	484	bdl	781	32	bdl	bdl	bdl	bdl	36	109	17	137	bdl	201	35	33	bdl	4

Sample	Sb_2O_3	Cs_2O	BaO	La_2O_3	CeO_2	Nd_2O_3	HfO_2	Ta_2O_5	WO_3	PtO_2	Au	HgO	PbO	Bi_2O_3	ThO_2	U_3O_8
HF1	bdl	bdl	625	21	135	61	30	103	298	bdl	bdl	bdl	bdl	bdl	bdl	bdl
HF2	bdl	41	257	41	93	bdl	89	163	447	26	bdl	bdl	3010	bdl	bdl	bdl
HF4	bdl	bdl	169	131	125	62	27	114	172	bdl	bdl	1	133	bdl	bdl	bdl
HF15	bdl	41	424	44	bdl	13	60	185	313	20	bdl	bdl	106	bdl	bdl	18
HF16	bdl	43	284	bdl	54	bdl	24	192	488	8	bdl	bdl	576	bdl	bdl	bdl
HF17	bdl	19	645	15	bdl	bdl	bdl	127	477	bdl	1	bdl	841	bdl	bdl	bdl
MC2	bdl	41	245	69	272	102	75	108	199	20	bdl	bdl	92	bdl	bdl	bdl

Sample	Sb_2O_3	Cs_2O	BaO	La_2O_3	CeO_2	Nd_2O_3	HfO_2	Ta_2O_5	WO_3	PtO_2	Au	HgO	PbO	Bi_2O_3	ThO_2	U_3O_8
MC3	bdl	bdl	290	45	81	bdl	53	318	524	24	6	bdl	60	bdl	bdl	bdl
MC4	2	bdl	205	bdl	144	7	1	117	649	13	bdl	bdl	402	bdl	bdl	bdl
MC5	21	bdl	296	128	71	20	31	144	553	10	bdl	bdl	112	bdl	bdl	8
MC7	bdl	bdl	223	61	bdl	42	62	173	389	10	5	bdl	64	bdl	bdl	bdl
MC8	bdl	bdl	392	51	bdl	bdl	bdl	136	511	bdl	bdl	bdl	68	bdl	bdl	5
MC14	bdl	5	386	57	115	27	bdl	122	302	bdl	bdl	bdl	33	bdl	bdl	bdl
MC15	bdl	bdl	624	52	bdl	1	79	35	61	26	16	23	426	bdl	bdl	bdl
MY1	bdl	bdl	133	40	75	29	22	124	393	13	bdl	bdl	211	bdl	bdl	bdl
MY2	11	bdl	315	75	88	15	61	109	423	17	bdl	bdl	605	bdl	bdl	bdl
MY3	bdl	bdl	278	59	212	86	bdl	120	379	bdl	bdl	bdl	444	bdl	bdl	bdl
MY4	bdl	bdl	47	62	356	98	bdl	206	532	bdl	bdl	bdl	4	bdl	bdl	bdl
MY5	bdl	bdl	136	30	90	bdl	38	198	271	52	2	2	1	8	6	bdl
MY6	bdl	bdl	206	34	82	7	82	179	297	22	bdl	bdl	596	9	bdl	bdl
MY7	bdl	16	76	60	bdl	bdl	bdl	158	408	bdl	bdl	bdl	28	bdl	bdl	bdl
MY8	bdl	10	217	25	79	11	bdl	119	489	bdl	bdl	bdl	67	bdl	2	bdl
MY9	bdl	bdl	202	bdl	bdl	bdl	16	201	540	bdl	bdl	bdl	24	bdl	bdl	bdl
MY10	bdl	16	142	43	13	4	bdl	201	314	bdl	bdl	bdl	42	bdl	bdl	bdl
MY11	bdl	19	587	bdl	123	4	bdl	206	380	bdl	bdl	bdl	115	1	bdl	bdl
MY12	bdl	bdl	141	54	71	37	71	244	444	13	bdl	bdl	2000	bdl	bdl	bdl
MY13	bdl	17	398	17	154	12	44	151	333	12	3	bdl	3020	bdl	bdl	bdl
MY14	bdl	17	342	72	29	58	bdl	165	308	bdl	bdl	3	225	bdl	bdl	bdl
MY18	bdl	bdl	bdl	108	134	100	5	140	441	9	bdl	bdl	35	bdl	bdl	bdl

Sample	Sb_2O_3	Cs_2O	BaO	La_2O_3	CeO_2	Nd_2O_3	HfO_2	Ta_2O_5	WO_3	PtO_2	Au	HgO	PbO	Bi_2O_3	ThO_2	U_3O_8
MY19	bdl	7	260	115	bdl	bdl	60	130	480	49	8	bdl	175	bdl	bdl	bdl
MY20	bdl	30	187	47	bdl	bdl	bdl	181	308	bdl	3	bdl	22	bdl	bdl	bdl
MY21	bdl	33	84	89	55	4	bdl	100	136	bdl	bdl	bdl	30	bdl	bdl	bdl
MY22	bdl	bdl	42	66	bdl	bdl	8	174	510	bdl	bdl	bdl	12	bdl	bdl	bdl
MY23	18	bdl	92	110	87	75	30	137	395	bdl	bdl	bdl	bdl	bdl	bdl	bdl
MY24	bdl	4	62	61	23	17	bdl	171	431	11	bdl	20	bdl	10	bdl	bdl
MY25	bdl	10	144	46	84	1	24	195	739	18	bdl	bdl	53	bdl	bdl	bdl
MY26	bdl	bdl	9	bdl	135	26	bdl	220	509	9	bdl	bdl	bdl	bdl	bdl	bdl
WY1	bdl	bdl	379	22	57	10	8	140	311	bdl	bdl	bdl	69	bdl	bdl	bdl
WY2	bdl	2	261	67	55	bdl	bdl	165	357	8	10	3	8	bdl	bdl	bdl
WY4	bdl	bdl	360	57	47	bdl	bdl	160	329	bdl	bdl	bdl	163	bdl	bdl	bdl
WY7	bdl	bdl	161	89	65	79	41	208	303	34	3	bdl	92	bdl	bdl	bdl
WY8	bdl	3	149	77	124	bdl	bdl	60	116	bdl	bdl	bdl	3	bdl	bdl	bdl
XY2	bdl	5	493	54	32	28	bdl	167	384	19	bdl	bdl	257	bdl	bdl	bdl
XY3	bdl	30	469	85	101	38	bdl	93	327	bdl	bdl	4	415	bdl	bdl	bdl
XY4	bdl	66	473	15	73	bdl	bdl	77	306	bdl	bdl	bdl	369	bdl	bdl	bdl
XY5	bdl	87	391	53	86	12	12	73	158	bdl	bdl	bdl	75	bdl	bdl	bdl
XY6	bdl	35	550	50	106	56	50	165	352	34	3	bdl	472	4	bdl	bdl
XY7	bdl	20	657	34	24	bdl	36	154	338	bdl	bdl	bdl	205	4	bdl	bdl
XY8	bdl	42	506	62	92	30	12	102	303	bdl	5	bdl	278	bdl	bdl	bdl
XY9	bdl	40	612	49	bdl	9	52	210	338	6	7	bdl	175	bdl	bdl	bdl
XY10	bdl	12	377	36	15	44	bdl	128	319	bdl	bdl	17	292	11	bdl	bdl

Sample	Sb_2O_3	Cs_2O	BaO	La_2O_3	CeO_2	Nd_2O_3	HfO_2	Ta_2O_5	WO_3	PtO_2	Au	HgO	PbO	Bi_2O_3	ThO_2	U_3O_8
XY11	bdl	bdl	555	14	49	16	65	148	338	30	bdl	1	256	bdl	bdl	bdl
XY12	bdl	bdl	447	41	bdl	bdl	36	129	330	14	bdl	bdl	207	bdl	bdl	bdl
XY13	bdl	bdl	385	71	45	28	39	155	417	6	bdl	bdl	166	bdl	bdl	bdl

Appendix IV Normalised WD-XRF data for bloomery slag samples

(as given by Department of Geociences, University of Fribourg)

Sample	Na_2O	MgO	Al_2O_3	SiO_2	P_2O_5	SO_3	K_2O	CaO	TiO_2	MnO	Fe_2O_3
CX1	0.11	0.35	3.21	16.28	0.09	0.03	0.41	0.43	0.14	0.11	78.60
CX2	0.10	0.46	4.94	21.24	0.20	0.07	0.68	0.64	0.21	0.12	71.01
CX3	0.14	0.53	4.37	23.48	0.17	0.06	0.62	1.06	0.22	0.14	68.99
CX4	0.16	0.42	4.44	19.53	0.13	0.07	0.58	0.64	0.22	0.14	73.49
CX5	0.10	0.46	3.74	18.83	0.15	0.06	0.56	0.54	0.17	0.18	75.02
CX6	0.09	0.45	3.62	17.48	0.17	0.06	0.49	0.51	0.15	0.15	76.64
CX7	0.09	0.46	3.62	18.22	0.15	0.07	0.51	0.57	0.16	0.16	75.79
CX8	0.13	0.46	4.42	19.96	0.19	0.07	0.66	0.68	0.19	0.16	72.84
CX9	0.11	0.50	4.53	20.75	0.19	0.08	0.61	0.59	0.20	0.17	72.08
CX10	0.08	0.43	3.82	18.16	0.16	0.06	0.63	0.66	0.20	0.11	75.48
CX12	0.14	0.55	4.16	23.84	0.20	0.08	0.66	0.75	0.21	0.11	69.07
CX13	0.17	0.49	3.75	18.65	0.20	0.08	0.50	0.63	0.16	0.12	75.03
HF8	0.09	0.52	4.94	19.47	0.22	0.08	0.78	1.35	0.19	0.19	71.89
HF9	0.08	0.39	4.58	18.82	0.15	0.07	0.70	0.68	0.17	0.14	73.92
HF14	0.17	0.53	5.53	20.05	0.29	0.06	0.98	1.00	0.18	0.12	70.89
HF18	0.10	0.52	4.26	16.06	0.13	0.05	0.66	0.64	0.13	0.11	77.18
HF21	0.03	0.25	3.10	15.14	0.35	0.18	0.52	0.62	0.11	0.12	79.44
HF22	0.04	0.40	3.07	15.05	0.37	0.07	0.75	1.32	0.11	0.14	78.48
HF23	0.19	0.54	4.38	19.56	0.29	0.09	0.54	0.59	0.14	0.12	73.35
HF24	0.06	0.40	2.95	13.24	0.21	0.07	0.58	0.77	0.12	0.12	81.29
HF25	0.11	0.48	4.82	24.74	0.16	0.05	1.00	0.84	0.20	0.13	67.20
LD1	0.24	0.26	3.52	18.49	0.15	0.05	0.94	0.94	0.21	0.12	74.89
LD2	0.22	0.27	3.13	14.90	0.16	0.06	0.77	0.53	0.13	0.08	79.60
LD3	0.14	0.44	3.16	17.60	0.33	0.09	0.84	1.69	0.22	0.11	75.18
LD4	0.18	0.43	3.47	18.95	0.25	0.08	1.15	1.38	0.16	0.15	73.61
LD5	0.27	0.54	4.52	23.39	0.28	0.07	1.23	2.29	0.21	0.13	66.84
LD6	0.26	0.52	4.36	22.18	0.27	0.10	1.29	2.57	0.21	0.14	67.88
LD7	0.28	0.56	4.45	23.16	0.28	0.09	1.28	2.50	0.22	0.14	66.82
LD8	0.26	0.43	5.22	18.92	0.19	0.06	1.09	1.14	0.24	0.21	72.03
LD9	0.26	0.23	3.19	17.47	0.15	0.04	0.68	0.75	0.17	0.10	76.77

Sample	Na_2O	MgO	Al_2O_3	SiO_2	P_2O_5	SO_3	K_2O	CaO	TiO_2	MnO	Fe_2O_3
LD11	0.30	0.58	3.18	15.99	0.42	0.05	1.01	3.14	0.14	0.12	74.84
LD12	0.13	0.52	3.29	18.87	0.39	0.12	1.12	2.41	0.24	0.13	72.54
LD13	0.25	0.32	3.63	18.32	0.17	0.05	0.88	0.91	0.30	0.16	74.71
LD14	0.04	0.46	3.67	14.69	0.23	0.12	0.26	0.34	0.13	0.26	79.56
MC1	0.25	0.24	4.11	18.27	0.12	0.05	0.77	0.76	0.19	0.11	74.88
MC6	0.31	0.84	6.19	17.78	0.33	0.06	0.99	2.82	0.17	0.28	69.89
MC12	0.26	0.64	7.04	25.46	0.23	0.06	1.45	1.51	0.28	0.14	62.65
MC18	0.86	0.50	4.60	24.13	0.28	0.03	0.45	3.13	0.16	0.03	65.54
YW1	0.14	0.54	3.98	20.21	0.23	0.07	0.59	1.63	0.20	0.13	72.02
YW2	0.10	0.47	4.20	17.49	0.15	0.06	0.52	0.62	0.19	0.09	75.86
YW3	0.08	0.47	3.80	17.46	0.14	0.08	0.50	0.52	0.20	0.12	76.43
YW4	0.05	1.57	4.49	23.08	1.94	0.23	0.78	4.54	0.21	0.88	61.21
YW5	0.11	0.43	4.01	18.44	0.24	0.06	0.63	1.30	0.18	0.09	74.28
YW6	0.12	0.46	5.30	21.15	0.16	0.06	0.87	0.62	0.22	0.10	70.73
YW7	0.11	0.46	4.17	14.20	0.14	0.06	0.71	0.88	0.14	0.10	78.86

Sample	CuO	Cl	V_2O_5	Cr_2O_3	Co_3O_4	NiO	ZnO	Ga_2O_3	GeO_2	As_2O_3	Br	Rb_2O	SrO	Y_2O_3	ZrO_2	Nb_2O_5	MoO_3	Ag_2O	CdO	In_2O_3
CX1	81	bdl	712	141	499	bdl	25	17	11	bdl	bdl	23	22	13	94	bdl	131	42	49	bdl
CX2	61	14	1160	155	448	bdl	105	9	bdl	bdl	bdl	32	48	13	134	2	204	54	48	17
CX3	10	bdl	781	171	427	bdl	18	18	bdl	bdl	bdl	28	47	11	145	bdl	157	42	11	1
CX4	bdl	bdl	595	151	277	bdl	12	57	bdl	bdl	bdl	30	42	7	126	1	182	59	47	63
CX5	bdl	bdl	693	146	238	bdl	21	17	11	bdl	bdl	37	35	8	118	bdl	130	23	18	11
CX6	bdl	bdl	798	131	286	bdl	bdl	37	15	bdl	bdl	33	34	15	91	bdl	125	27	25	bdl
CX7	bdl	bdl	732	79	444	bdl	16	41	bdl	bdl	bdl	29	42	10	98	bdl	134	41	31	18
CX8	bdl	10	871	199	288	bdl	10	16	bdl	bdl	bdl	28	41	13	126	bdl	110	40	55	bdl
CX9	14	38	721	128	462	bdl	12	34	9	bdl	bdl	38	40	11	120	bdl	148	46	46	17
CX10	bdl	bdl	1150	138	233	bdl	bdl	16	bdl	bdl	bdl	34	44	8	127	2	143	62	54	13
CX12	64	118	463	157	420	bdl	78	bdl	bdl	bdl	bdl	36	39	11	138	3	138	45	43	10
CX13	10	94	769	171	482	bdl	22	21	bdl	bdl	bdl	25	28	2	87	bdl	163	53	24	3
HF8	18	32	689	222	503	bdl	14	10	bdl	bdl	bdl	36	82	5	114	1	155	55	29	bdl
HF9	89	bdl	579	234	474	bdl	95	1	bdl	bdl	bdl	33	48	12	103	bdl	152	25	9	1
HF14	91	38	224	132	461	bdl	109	bdl	9	bdl	2	35	44	bdl	97	bdl	94	28	bdl	bdl
HF18	bdl	21	457	104	461	bdl	19	22	15	bdl	bdl	28	44	2	80	bdl	164	37	36	bdl
HF21	3	57	183	40	338	138	3	bdl	bdl	212	bdl	28	23	bdl	73	bdl	155	58	40	3
HF22	5	61	186	64	485	bdl	bdl	23	bdl	bdl	bdl	27	69	5	78	4	180	47	52	bdl
HF23	5	141	576	142	500	bdl	36	9	13	bdl	bdl	26	34	7	88	bdl	169	26	3	11
HF24	bdl	185	610	81	248	bdl	13	22	bdl	43	bdl	30	36	6	70	bdl	175	47	5	bdl

Sample	CuO	Cl	V_2O_5	Cr_2O_3	Co_3O_4	NiO	ZnO	Ga_2O_3	GeO_2	As_2O_3	Br	Rb_2O	SrO	Y_2O_3	ZrO_2	Nb_2O_5	MoO_3	Ag_2O	CdO	In_2O_3
HF25	68	39	885	128	491	bdl	93	16	bdl	bdl	bdl	50	50	7	100	bdl	129	27	25	bdl
LD1	bdl	bdl	462	103	458	bdl	54	bdl	bdl	bdl	bdl	32	72	bdl	162	bdl	157	44	13	bdl
LD2	bdl	bdl	592	68	419	bdl	41	19	bdl	bdl	bdl	20	28	bdl	63	bdl	124	42	21	bdl
LD3	bdl	30	559	56	481	bdl	bdl	19	14	bdl	bdl	32	90	13	78	bdl	115	47	42	bdl
LD4	bdl	bdl	470	87	356	bdl	33	29	bdl	bdl	bdl	37	82	17	111	bdl	160	47	15	bdl
LD5	95	bdl	452	119	485	bdl	77	bdl	bdl	bdl	bdl	36	96	bdl	165	bdl	172	16	bdl	bdl
LD6	89	bdl	425	85	490	bdl	87	11	bdl	bdl	bdl	33	98	13	171	bdl	140	43	36	bdl
LD7	29	bdl	461	119	476	bdl	bdl	23	bdl	bdl	bdl	37	105	14	173	bdl	156	55	44	bdl
LD8	16	bdl	746	87	485	bdl	29	45	bdl	bdl	bdl	42	77	14	140	bdl	108	50	56	bdl
LD9	bdl	59	396	63	479	bdl	29	43	bdl	bdl	bdl	34	39	bdl	92	bdl	176	27	79	bdl
LD11	136	bdl	266	44	479	bdl	75	42	bdl	bdl	bdl	30	224	bdl	78	bdl	111	34	21	bdl
LD12	78	bdl	668	72	435	bdl	88	15	9	bdl	bdl	44	128	11	84	1	123	61	35	29
LD13	bdl	23	1260	108	429	bdl	14	21	3	bdl	bdl	34	62	11	115	bdl	179	29	72	12
LD14	318	167	271	146	518	bdl	48	8	bdl	5	bdl	14	17	2	49	bdl	161	39	16	bdl
MC1	bdl	28	804	133	432	bdl	11	31	bdl	bdl	bdl	27	41	5	117	bdl	185	41	49	bdl
MC6	536	116	443	164	478	bdl	26	33	bdl	bdl	2	39	166	6	79	bdl	147	51	27	bdl
MC12	67	bdl	970	181	425	bdl	77	10	bdl	bdl	bdl	49	60	12	150	bdl	130	61	48	21
MC18	23	24	1430	262	482	bdl	1	25	bdl	bdl	bdl	29	177	10	21	bdl	120	47	32	bdl
YW1	81	44	474	268	466	bdl	104	2	5	bdl	bdl	35	61	bdl	109	4	126	45	32	bdl
YW2	61	34	508	272	466	bdl	87	31	bdl	bdl	bdl	32	48	5	117	3	139	66	49	bdl
YW3	107	20	210	128	487	bdl	93	bdl	bdl	bdl	bdl	30	33	5	126	bdl	118	48	46	16
YW4	5260	bdl	295	165	354	588	1480	35	bdl	bdl	bdl	bdl	19	332	5	109	bdl	722	26	bdl

Sample	CuO	Cl	V_2O_5	Cr_2O_3	Co_3O_4	NiO	ZnO	Ga_2O_3	GeO_2	As_2O_3	Br	Rb_2O	SrO	Y_2O_3	ZrO_2	Nb_2O_5	MoO_3	Ag_2O	CdO	In_2O_3
YW5	bdl	bdl	536	243	345	bdl	51	45	bdl	bdl	bdl	28	62	2	99	bdl	164	29	86	3
YW6	97	bdl	406	168	449	bdl	85	6	11	bdl	bdl	44	41	11	124	bdl	136	39	14	4
YW7	36	bdl	483	107	487	bdl	16	9	6	bdl	2	39	37	3	80	bdl	158	24	14	bdl

Sample	SnO_2	Sb_2O_3	TeO_2	Cs_2O	BaO	La_2O_3	CeO_2	Nd_2O_3	HfO_2	Ta_2O_5	WO_3	PtO_2	Au	HgO	PbO	Bi_2O_3	ThO_2
CX1	bdl	bdl	bdl	bdl	152	39	68	bdl	55	39	184	bdl	bdl	bdl	bdl	bdl	bdl
CX2	bdl	bdl	bdl	10	176	64	80	22	bdl	141	185	8	bdl	21	bdl	bdl	bdl
CX3	bdl	bdl	bdl	4	173	43	bdl	bdl	bdl	14	114	3	bdl	11	5	3	bdl
CX4	bdl	4	bdl	bdl	127	58	9	bdl	55	bdl	88	55	18	2	2	bdl	bdl
CX5	bdl	bdl	bdl	bdl	158	92	64	bdl	bdl	bdl	72	16	5	10	bdl	7	bdl
CX6	bdl	bdl	bdl	bdl	97	68	bdl	bdl	46	26	79	bdl	3	3	bdl	bdl	bdl
CX7	bdl	bdl	bdl	bdl	85	41	bdl	bdl	127	19	bdl	45	22	19	bdl	bdl	bdl
CX8	bdl	bdl	bdl	1	125	105	257	133	bdl	bdl	13	bdl	bdl	bdl	7	bdl	bdl
CX9	bdl	bdl	bdl	bdl	149	44	64	10	bdl	17	87	15	13	5	bdl	bdl	bdl
CX10	bdl	bdl	bdl	11	133	bdl	27	bdl	44	15	47	bdl	19	5	5	bdl	bdl
CX12	bdl	bdl	bdl	bdl	89	86	164	36	bdl	120	184	bdl	bdl	3	bdl	bdl	bdl
CX13	bdl	8	bdl	16	124	95	bdl	bdl	12	48	103	bdl	bdl	bdl	bdl	bdl	bdl
HF8	bdl	bdl	bdl	bdl	181	94	169	89	51	76	229	bdl	21	bdl	bdl	bdl	bdl
HF9	bdl	bdl	bdl	bdl	138	56	221	74	65	130	283	bdl	bdl	bdl	9	bdl	bdl
HF14	bdl	bdl	bdl	bdl	93	7	85	bdl	bdl	193	226	bdl	bdl	bdl	bdl	4	bdl

Sample	SnO_2	Sb_2O_3	TeO_2	Cs_2O	BaO	La_2O_3	CeO_2	Nd_2O_3	HfO_2	Ta_2O_5	WO_3	PtO_2	Au	HgO	PbO	Bi_2O_3	ThO_2
HF18	1	bdl	bdl	bdl	62	18	157	17	bdl	33	29	11	7	bdl	2	9	bdl
HF21	bdl	bdl	bdl	27	151	22	16	4	bdl	bdl	bdl	bdl	bdl	bdl	5	13	bdl
HF22	bdl	bdl	bdl	bdl	300	3	72	bdl	142	bdl	bdl	26	21	13	bdl	bdl	bdl
HF23	bdl	bdl	bdl	bdl	118	75	66	32	bdl	68	66	3	bdl	21	bdl	bdl	bdl
HF24	bdl	bdl	20	47	145	80	bdl	bdl	bdl	bdl	bdl	bdl	8	15	bdl	12	bdl
HF25	bdl	bdl	bdl	6	149	73	bdl	bdl	bdl	133	282	bdl	bdl	bdl	3	bdl	bdl
LD1	bdl	bdl	bdl	bdl	217	21	67	bdl	bdl	59	130	bdl	bdl	bdl	12	bdl	bdl
LD2	bdl	bdl	bdl	bdl	70	13	21	bdl	77	17	bdl	bdl	12	16	bdl	bdl	bdl
LD3	bdl	bdl	bdl	bdl	148	89	50	bdl	bdl	bdl	17	56	45	30	bdl	bdl	bdl
LD4	bdl	bdl	bdl	bdl	118	24	bdl	bdl	124	88	146	49	34	bdl	18	bdl	bdl
LD5	bdl	bdl	bdl	bdl	231	bdl	86	13	bdl	125	229	bdl	bdl	bdl	bdl	20	bdl
LD6	bdl	bdl	bdl	14	213	bdl	38	38	bdl	165	280	bdl	bdl	bdl	bdl	bdl	bdl
LD7	bdl	bdl	bdl	35	212	46	116	15	29	14	92	bdl	bdl	bdl	27	bdl	bdl
LD8	bdl	bdl	bdl	31	306	21	32	bdl	70	54	46	28	bdl	bdl	bdl	bdl	bdl
LD9	bdl	bdl	bdl	bdl	160	29	101	bdl	79	88	87	bdl	bdl	bdl	bdl	bdl	bdl
LD11	bdl	bdl	bdl	bdl	213	bdl	bdl	bdl	111	145	191	34	bdl	bdl	bdl	bdl	bdl
LD12	bdl	bdl	bdl	bdl	148	31	bdl	12	bdl	123	271	7	3	bdl	bdl	bdl	bdl
LD13	bdl	1	bdl	bdl	259	67	176	30	62	77	72	bdl	bdl	28	4	2	bdl
LD14	bdl	bdl	bdl	bdl	101	93	472	61	31	14	11	bdl	bdl	6	bdl	1	bdl
MC1	bdl	bdl	bdl	bdl	82	54	192	24	102	bdl	107	9	bdl	24	9	bdl	bdl
MC6	bdl	bdl	bdl	bdl	330	bdl	114	75	109	83	200	17	7	bdl	bdl	bdl	bdl
MC12	bdl	bdl	bdl	bdl	179	35	bdl	bdl	bdl	141	211	bdl	bdl	bdl	3	1	bdl

Sample	SnO_2	Sb_2O_3	TeO_2	Cs_2O	BaO	La_2O_3	CeO_2	Nd_2O_3	HfO_2	Ta_2O_5	WO_3	PtO_2	Au	HgO	PbO	Bi_2O_3	ThO_2
MC18	bdl	bdl	bdl	bdl	32	20	8	bdl	bdl	17	95	8	3	5	7	bdl	bdl
YW1	bdl	bdl	bdl	bdl	144	47	144	48	bdl	141	251	1	bdl	bdl	bdl	bdl	bdl
YW2	bdl	12	bdl	bdl	35	22	96	12	85	130	261	36	20	bdl	bdl	bdl	bdl
YW3	bdl	bdl	bdl	bdl	133	53	bdl	bdl	bdl	145	258	bdl	bdl	11	bdl	4	bdl
YW4	bdl	27	bdl	bdl	554	16	bdl	70	76	157	457	14	bdl	bdl	139	bdl	bdl
YW5	bdl	bdl	bdl	bdl	180	64	202	84	99	51	83	15	21	bdl	bdl	bdl	bdl
YW6	bdl	1	bdl	24	200	9	16	bdl	44	128	226	bdl	bdl	bdl	bdl	bdl	12
YW7	bdl	bdl	bdl	bdl	110	bdl	bdl	bdl	bdl	109	109	bdl	11	18	1	4	bdl

Appendix V Normalised WD-XRF data for ore samples

(as given by Department of Geociences, University of Fribourg)

Sample	Na_2O	MgO	Al_2O_3	SiO_2	P_2O_5	SO_3	K_2O	CaO	TiO_2	MnO	Fe_2O_3
HF3	0.07	0.27	1.46	3.47	0.05	0.08	0.11	0.15	0.02	0.07	93.94
HF5	0.05	0.21	1.19	2.86	0.04	0.06	0.03	0.07	0.04	0.06	95.07
HF6	0.04	0.18	1.61	3.13	0.03	0.06	0.09	0.09	0.10	0.09	94.23
HF19	0.14	1.10	24.53	64.99	0.36	0.03	5.88	0.11	0.7	0.02	1.83
HF36	5.13	0.79	19.50	60.80	0.91	0.02	3.24	1.44	1.00	0.06	6.52
HF27	0.01	0.03	0.88	3.33	0.08	0.01	0.02	0.04	0.03	0.05	95.27
HF29	0.04	2.17	1.91	5.37	0.08	6.36	0.09	1.03	0.06	0.15	82.40
MC17	0.05	5.88	5.38	2.93	0.19	0.05	0.03	0.02	0.1	1.19	83.32
YW11	0.06	0.19	2.15	17.38	0.10	0.03	0.05	0.17	0.05	0.01	79.64
YW12	0.04	0.05	1.60	6.77	0.13	0.13	0.02	0.06	0.05	0.04	90.81

Sample	Cl	V_2O_5	Cr_2O_3	Co_3O_4	NiO	CuO	ZnO	Ga2O3	GeO_2	Br	Rb_2O	SrO	Y_2O_3	ZrO_2	Nb_2O_5	MoO_3	Ag_2O	CdO
HF3	101	685	503	464	bdl	138	142	bdl	bdl	bdl	21	49	8	9	bdl	180	70	11
HF5	40	641	786	419	bdl	124	107	12	bdl	bdl	12	28	6	9	bdl	175	50	45
HF6	48	966	366	471	bdl	116	184	8	bdl	bdl	19	24	bdl	7	bdl	213	37	32

Sample	Cl	V_2O_5	Cr_2O_3	Co_3O_4	NiO	CuO	ZnO	Ga2O3	GeO_2	Br	Rb_2O	SrO	Y_2O_3	ZrO_2	Nb_2O_5	MoO_3	Ag_2O	CdO
HF19	111	269	0.05	38	21	229	44	40	12	bdl	259	38	42	412	22	21	bdl	13
HF36	85	206	0.01	90	15	389	141	29	3	bdl	124	1040	44	691	48	21	bdl	17
HF27	bdl	83	0.01	459	bdl	584	203	9	28	bdl	4	bdl	3	13	bdl	39	bdl	bdl
HF29	52	470	0.02	596	39	761	334	58	3	bdl	13	50	bdl	21	bdl	155	63	25
MC17	bdl	192	0.03	585	bdl	1460	5060	27	3	2	10	bdl	bdl	18	1	237	28	11
YW11	77	460	0.02	440	bdl	bdl	bdl	bdl	2	bdl	4	8	bdl	35	bdl	126	54	36
YW12	44	269	0.05	575	bdl	542	118	4	13	bdl	15	bdl	bdl	7	bdl	136	39	bdl

Sample	In_2O_3	SnO_2	Sb_2O_3	TeO_2	Cs_2O	BaO	La_2O_3	Nd_2O_3	HfO_2	Ta_2O_5	WO_3	PtO_2	Au	HgO	PbO	Bi_2O_3	ThO_2
HF3	13	bdl	bdl	bdl	bdl	bdl	120	6	bdl	90	138	bdl	bdl	bdl	275	bdl	bdl
HF5	17	bdl	bdl	bdl	4	bdl	89	101	51	175	377	bdl	bdl	bdl	145	bdl	bdl
HF6	bdl	bdl	bdl	bdl	bdl	22	142	67	bdl	260	392	6	7	bdl	169	26	bdl
HF19	bdl	bdl	bdl	bdl	163	1110	bdl	bdl	17	bdl	53	bdl	1	12	22	6	1
HF36	bdl	bdl	bdl	13	161	2170	44	38	44	bdl	90	bdl	bdl	11	28	bdl	bdl
HF27	bdl	bdl	bdl	bdl	186	205	21	bdl	53	144	513	bdl	bdl	bdl	38	bdl	bdl
HF29	bdl	bdl	bdl	bdl	bdl	bdl	59	17	147	bdl	bdl	34	13	bdl	429	bdl	bdl
MC17	bdl	76	bdl	bdl	30	bdl	139	41	bdl	209	352	bdl	bdl	bdl	147	34	bdl
YW11	8	bdl	17	bdl	1	32	116	95	bdl	bdl	23	bdl	6	29	10	15	bdl
YW12	bdl	bdl	bdl	bdl	bdl	bdl	110	46	bdl	170	349	bdl	2	bdl	14	5	bdl

Appendix VI Composition of Cu-rich particles in the Daye copper slag

SEM-EDS point analyses. Weight % normalised results.

HF	1	2	3	4	5	6	7	8	9	10	11	12	13	14	15	16	17	18	19	20	21
S	bdl	bdl	bdl	bdl	bdl	bdl	bdl	bdl	bdl	bdl	bdl	bdl	bdl	bdl	bdl	bdl	bdl	bdl	bdl	bdl	32.2
Fe	bdl	4.9	1.2	1.7	0.6	bdl	0.4	3.6	1.3	1.8	0.4	bdl	3.8	4.6	1.3	3.5	2.2	5.4	0.8	3.1	0.7
Cu	100.0	95.1	98.8	98.3	99.4	100.0	99.6	96.4	98.7	98.2	99.6	100.0	96.2	95.4	98.7	96.5	97.8	94.6	99.2	96.9	67.1
S	bdl	bdl	bdl	bdl	bdl	0.9	19.3	20.2	20.4	20.5	20.6	20.8	20.8	20.8	20.9	20.9	20.9	22.1	22.9	24.9	29.8
Fe	1.1	bdl	3.0	4.7	4.3	4.9	10.8	2.9	5.4	2.2	3.5	7.0	1.5	1.2	3.4	3.1	7.1	5.9	4.1	2.2	2.5
Cu	98.9	100.0	97.0	95.3	95.7	94.2	69.9	76.9	74.3	77.3	75.9	72.2	77.7	78.0	75.8	76.0	71.9	72.1	73.0	73.0	67.6

MY	1	2	3	4	5	6	7	8	9	10	11	12	13	14	15	16	17	18	19	20	21
S	bdl	bdl	bdl	bdl	bdl	bdl	bdl	bdl	bdl	bdl	bdl	bdl	bdl	bdl	bdl	bdl	bdl	bdl	bdl	bdl	bdl
Fe	2.4	3.0	0.5	2.5	4.1	6.2	2.5	1.5	bdl	1.3	0.5	bdl	0.8	bdl	7.1	3.6	3.6	1.2	0.8	2.8	17.1
Cu	97.6	97.0	99.5	97.5	95.9	93.8	97.5	98.5	100.0	98.7	99.5	100.0	99.2	100.0	92.9	96.4	96.4	98.8	99.2	97.2	82.9
S	bdl	0.6	1.1	1.9	2.9	9.7	22.3	23.4	30.2	32.6	32.7	32.9	33.3	33.5	33.5	33.5	33.7	33.8	33.8	33.9	33.9
Fe	17.1	3.9	3.8	11.6	9.0	6.8	3.0	2.8	24.8	5.7	6.4	8.2	2.5	3.1	1.3	1.7	1.0	5.0	10.4	3.5	5.5
Cu	82.9	95.4	95.1	86.5	88.2	83.5	74.7	73.8	45.0	61.7	60.8	58.8	64.3	63.4	65.2	64.8	65.3	61.2	55.9	62.6	60.6
S	34.1	34.1	34.1	34.2	34.2	34.3	34.3	34.4	34.5	34.5	34.5	34.5	34.7	34.7	34.7	34.7	34.7	34.7	34.7	34.8	34.9
Fe	0.4	4.3	1.7	3.4	2.3	2.7	4.3	1.1	bdl	5.2	bdl	7.6	2.2	0.6	bdl	1.7	4.9	3.2	4.6	7.2	4.2
Cu	65.6	61.6	64.2	62.4	63.5	63.1	61.3	64.5	65.5	60.3	65.5	57.8	63.2	64.8	65.3	63.6	60.4	62.1	60.7	58.0	60.9
S	35.0	35.0	35.1	35.4	35.4	35.4	35.5	35.5	35.6	35.7	35.8	35.8	35.8	35.9	35.9	35.9	36.0	36.0	36.1	36.1	36.3

Fe	5.6	4.8	3.0	9.1	7.6	7.5	2.6	6.7	0.9	2.0	19.8	7.3	4.8	3.0	4.9	3.4	2.2	3.3	1.9	4.8	2.5
Cu	59.4	60.2	61.9	55.5	57.0	57.1	61.9	57.8	63.5	62.3	44.4	56.9	59.3	61.1	59.2	60.7	61.8	60.7	62.0	59.1	61.2
S	36.3	36.4	36.4	36.4	36.4	36.5	36.5	36.6	36.6	36.6	36.6	36.7	36.7	36.8	36.9	36.9	37.1	37.2	37.5	37.5	37.7
Fe	2.8	5.7	2.6	3.7	2.4	4.4	1.1	3.1	3.2	2.0	3.1	4.0	2.7	3.3	2.6	2.7	8.8	3.4	3.0	9.4	2.4
Cu	60.9	58.0	61.0	59.9	61.2	59.1	62.4	60.3	60.3	61.4	60.2	59.3	60.7	59.8	60.6	60.4	54.1	59.4	59.5	53.1	59.9
S	37.8	37.8	37.8	37.9	38.0	38.1	38.2	38.3	38.7	39.0	39.1	39.2	39.7	39.8	4bdl	40.2	40.3	40.4	40.5	40.6	40.6
Fe	5.3	2.6	2.8	4.7	4.9	4.3	5.2	1.4	5.7	5.3	6.2	8.7	9.1	7.3	9.9	1.3	7.8	8.1	14.7	8.8	8.7
Cu	57.0	59.6	59.4	57.4	57.1	57.5	56.6	60.3	55.6	55.7	54.7	52.1	51.3	52.9	50.1	58.5	51.8	51.5	44.8	50.6	50.7
S	40.7	40.9	41.0	42.2	42.5	43.7	44.5	45.2	45.3	45.4	46.2	46.4	46.7	48.3	48.3	49.1	49.8	51.3	56.9	59.0	59.3
Fe	8.5	6.8	18.7	13.4	29.6	2.3	24.4	4.5	7.0	4.5	3.3	6.9	14.4	16.1	3.4	4.2	3.2	1.4	3.5	5.7	4.3
Cu	50.8	52.3	40.3	44.3	27.9	54.0	31.1	50.4	47.8	50.2	50.6	46.7	38.9	35.6	48.2	46.7	47.0	47.3	39.6	35.3	36.3

MC	**1**	**2**	**3**	**4**	**5**	**6**	**7**	**8**	**9**	**10**	**11**	**12**	**13**	**14**	**15**	**16**	**17**	**18**	**19**	**20**	**21**
S	bdl	bdl	bdl	bdl	bdl	bdl	bdl	bdl	bdl	bdl	bdl	bdl	bdl	0.6	6.5	7.6	33.6	33.8	34.0	34.1	34.4
Fe	2.8	4.7	5.7	12.6	4.2	4.7	5.8	bdl	2.4	3.0	2.9	7.4	7.5	3.4	3.8	4.3	4.2	2.5	3.2	4.0	3.4
Cu	97.2	95.3	94.3	87.4	95.8	95.3	94.2	100.0	97.6	97.0	97.1	92.6	92.5	96.0	89.6	88.1	62.2	63.8	62.8	61.9	62.2
S	34.6	34.6	34.8	34.9	35.4	35.5	35.9	36.2	36.3	36.3	36.8	37.0	37.2	37.4	37.5	38.1	38.1	39.1	39.2	39.8	40.8
Fe	1.7	2.7	9.9	3.4	8.7	9.1	17.3	2.8	3.7	12.7	1.8	0.8	1.3	3.4	1.5	3.1	11.0	9.8	9.2	15.7	10.9
Cu	63.7	62.7	55.4	61.7	55.9	55.4	46.8	61.0	6bdl	51.0	61.5	62.2	61.5	59.2	61.0	58.8	50.8	51.2	51.6	44.6	48.3
S	41.6	41.7	41.8	43.5	43.6	44.1	44.7	45.3	46.9	47.4	49.5	53.2	55.0	57.2							
Fe	13.8	15.4	14.5	14.4	14.5	12.2	3.3	4.8	16.5	1.5	0.4	5.2	12.0	10.6							
Cu	44.7	43.0	43.8	42.2	41.9	43.7	52.0	49.9	36.6	51.1	5bdl	41.6	33.0	32.2							

WY	1	2	3	4	5	6	7	8	9	10	11	12	13	14	15	16	17	18	19	20	21
S	bdl	bdl	bdl	bdl	bdl	bdl	0.1	0.4	0.7	0.7	0.7	0.9	1.1	1.6	3.7	6.8	9.5	31.1	31.1	31.4	32.0
Fe	4.3	bdl	bdl	bdl	bdl	bdl	1.7	0.8	bdl	1.6	2.2	2.0	1.6	3.9	7.4	2.5	7.6	8.7	5.3	4.3	5.4
Cu	95.7	100.0	100.0	100.0	100.0	100.0	98.2	98.8	99.3	97.7	97.0	97.1	97.3	94.5	88.9	90.6	82.9	60.2	63.5	64.4	62.6
S	33.5	33.6	33.7	33.8	33.8	34.1	34.2	34.2	34.3	34.5	34.5	34.5	34.9	35.0	35.3	35.4	35.4	35.8	37.1	37.2	37.4
Fe	2.1	2.1	2.7	2.6	4.9	2.1	3.6	3.6	4.9	2.0	1.5	1.4	5.1	2.9	3.4	6.6	bdl	7.1	3.6	2.0	2.8
Cu	64.4	64.3	63.6	63.7	61.3	63.8	62.2	62.2	60.8	63.6	64.0	64.1	6bdl	62.1	61.3	58.0	64.6	57.0	59.3	60.7	59.8
S	38.8	40.3	41.1	42.0	42.8	43.5	43.5	43.6	43.7	43.9	44.1	44.8	44.9	45.2	45.8	46.4	47.3	48.1	49.0		
Fe	5.1	8.9	5.2	12.7	23.7	12.0	7.1	31.8	11.3	13.0	6.1	9.2	16.7	5.7	20.6	6.4	27.8	2.0	4.3		
Cu	56.1	50.8	53.7	45.3	33.5	44.5	49.4	24.6	45.0	43.1	49.8	46.0	38.4	49.1	33.6	47.2	24.9	49.9	46.7		

XY	1	2	3	4	5	6	7	8	9	10	11	12	13	14	15	16	17	18	19	20	21
S	bdl	bdl	6.0	26.1	26.9	27.7	30.4	30.8	31.0	31.1	31.9	31.9	33.0	33.1	33.1	33.1	33.1	33.2	33.2	33.2	33.4
Fe	2.5	4.5	4.2	8.9	12.2	5.3	5.7	1.4	4.2	4.7	4.0	5.6	3.7	2.1	1.6	4.0	3.2	2.4	1.5	2.6	3.1
Cu	97.5	95.5	89.8	65.0	60.9	67.0	64.0	67.7	64.8	64.2	64.1	62.5	63.2	64.8	65.3	62.9	63.7	64.4	65.3	64.2	63.5
S	33.4	33.5	33.6	33.6	33.6	33.7	33.7	33.8	34.0	34.0	34.0	34.1	34.1	34.2	34.3	34.4	34.4	34.6	34.8	35.2	35.4
Fe	3.5	4.8	1.8	2.7	1.9	2.3	4.2	4.3	4.8	3.7	3.0	3.3	5.2	4.1	1.3	6.3	4.2	6.1	4.2	3.3	5.3
Cu	63.2	61.8	64.6	63.7	64.4	64.0	62.1	61.9	61.2	62.2	63.0	62.6	60.7	61.7	64.4	59.3	61.4	59.3	61.0	61.5	59.4
S	35.6	36.1	36.6	37.0	37.1	37.3	39.1	45.9	46.1	47.6	52.7										
Fe	3.2	2.6	2.5	1.7	7.9	1.5	2.9	1.3	1.4	3.3	5.8										
Cu	61.2	61.3	60.9	61.2	55.0	61.2	58.0	52.8	52.5	49.1	41.5										

Appendix VII XRD diffractograms

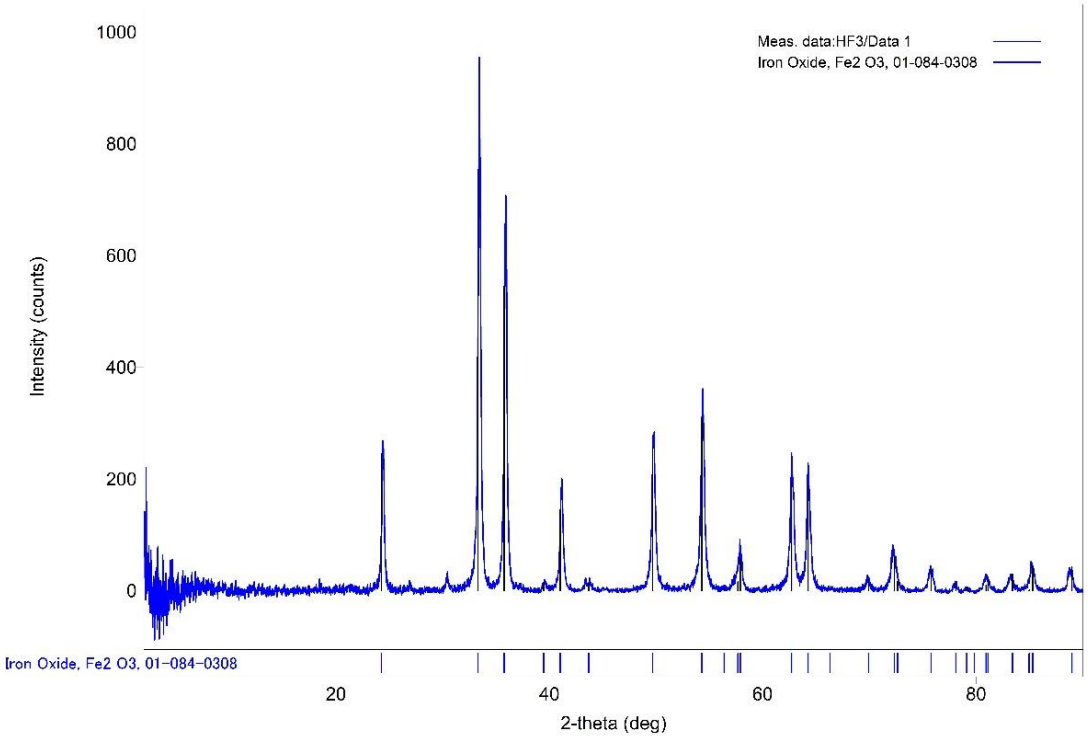

XRD diffractogram showing the match of the peaks of the sample HF3 with the haematite diffraction patterns from the reference library.

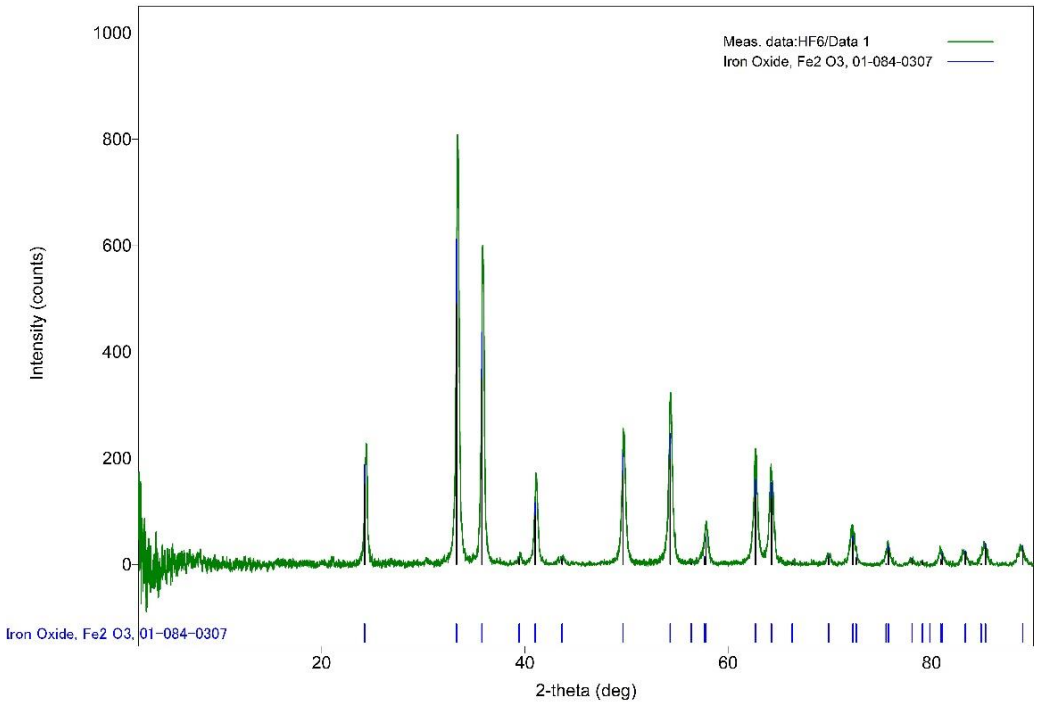

XRD diffractogram showing the match of the peaks of the sample HF6 with the haematite diffraction patterns from the reference library.

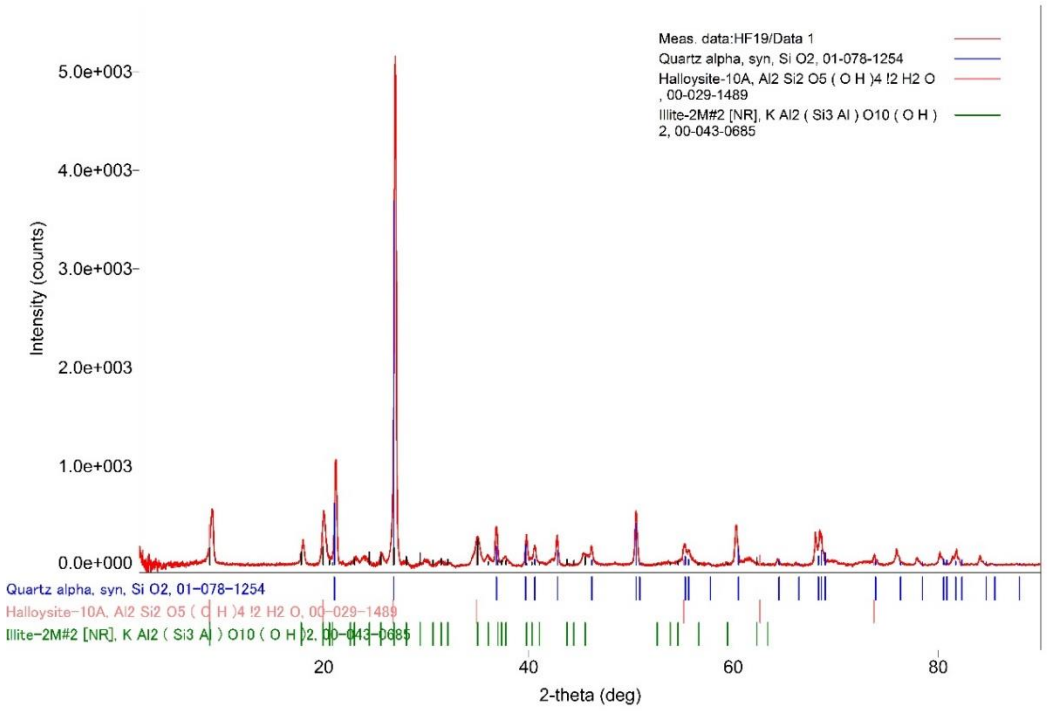

XRD diffractogram showing the match of the peaks of the sample HF19 with phyllosilicate minerals diffraction patterns from the reference library.

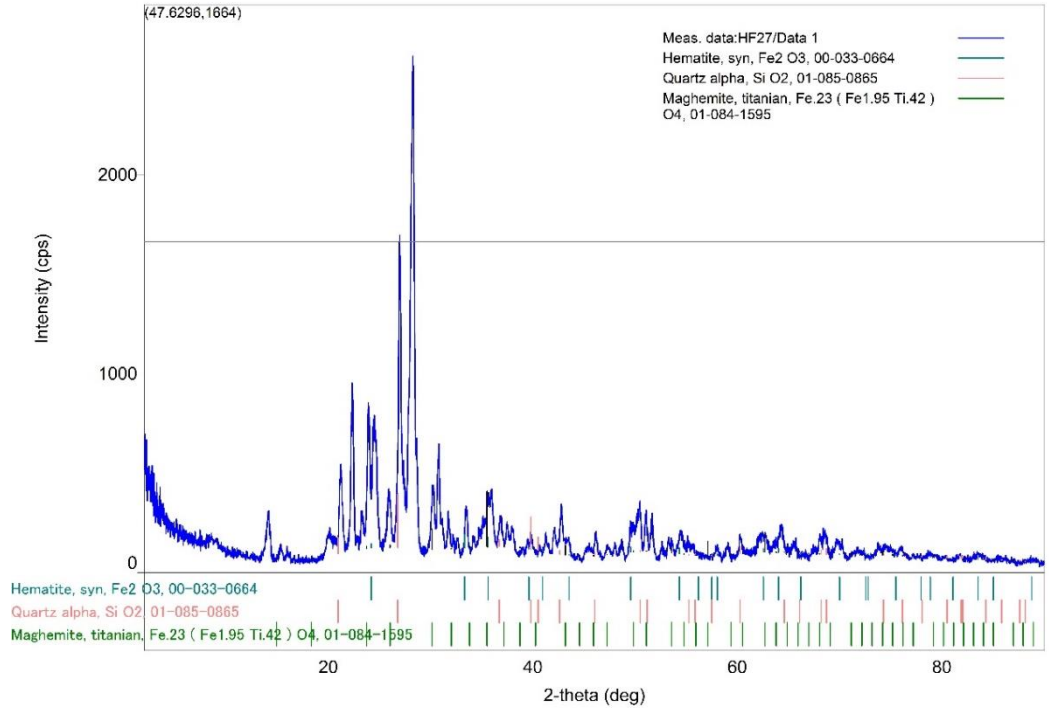

XRD diffractogram showing the match of the peaks of the sample HF27 with the haematite diffraction patterns from the reference library.

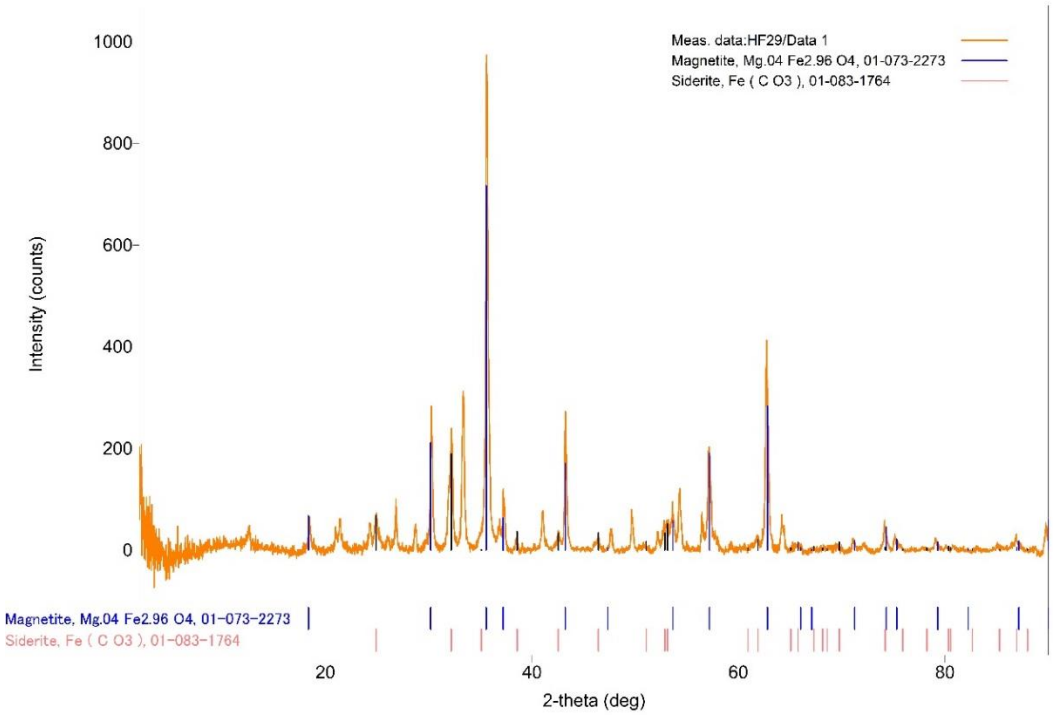

XRD diffractogram showing the match of the peaks of the sample HF29 with the magnetite diffraction patterns from the reference library.